Università degli Studi di Roma "La Sapienza"
Facoltà di Scienze Matematiche, Fisiche e Naturali
Dipartimento di Scienze della Terra

Dottorato di Ricerca in Scienze della Terra

XVIII ciclo

PHOSPHATE-INDUCED HEAVY METALS IMMOBILIZATION IN AQUEOUS SOLUTIONS AND SOILS.

Dottoranda: Dott.ssa Alessia Corami

Docente guida: Prof. Vincenzo Ferrini

Università degli Studi di Roma "La Sapienza"
Facoltà di Scienze Matematiche, Fisiche e Naturali
Dipartimento di Scienze della Terra

Dottorato di Ricerca in Scienze della Terra

XVIII ciclo

Dottorando: Dott.ssa A. Corami Docente guida: Prof. V. Ferrini

L'utilizzo dei fosfati, naturali e sintetici, per l'immobilzzazione di metalli pesanti: Pb, Zn, Cu e Cd in soluzioni acquose e nei suoli

Relazione sull'attività svolta nel corso del Dottorato di Ricerca

La tossicità, anche in minime quantità, dei metalli pesanti, la loro ampia distribuzione e la loro tendenza ad accumularsi nella catena alimentare, rendono indispensabile lo sviluppo di tecnologie in grado di ridurre la "biodisponibilità" di questi elementi nell'ambiente naturale. È noto infatti che i metalli pesanti hanno un notevole impatto sull'ambiente, sulla salute dell'uomo e sulla qualità delle riserve idriche sotterranee e superficiali.

La riduzione della mobilità dei metalli pesanti nell'ambiente attraverso processi di adsorbimento, scambio ionico e precipitazione per mezzo di prodotti chimici naturali o di sintesi (tecniche di stabilizzazione/solidificazione) che limitino la solubilità dei contaminanti è una soluzione poco costosa e che fornisce ottimi risultati (es. Ma et al., 1993, 1994 a e b, 1995).

L'attività di ricerca è stata finalizzata a verificare la stabilità dell'immobilizzazione di Pb, Zn, Cu e Cd ad opera di fosfati sintetici e naturali nelle condizioni chimico-fisiche dell'ambiente supergenico in soluzioni acquose e in suoli.

Inoltre, sono stati condotti esperimenti per definire i processi che determinano l'immobilizzazione dei metalli da parte dei fosfati, quali l'adsorbimento/assorbimento, lo scambio ionico e la precipitazione di fasi minerali dei metalli. In particolare, sono stati studiati gli effetti di combinazioni dei quattro metalli in soluzione acquosa sull'efficienza del processo di immobillizzazione.

Durante i tre anni del corso di dottorato sono stati eseguiti esperimenti di interazione tra un fosfato sintetico (idrossiapatite, HA) e due rocce fosfatiche naturali (fluoroapatite, $Ca_{10}(PO_4)_6(F)_2$) e soluzioni contenenti diverse concentrazioni dei metalli pesanti suddetti, come pure suoli di aree minerarie della Toscana meridionale e della Sardegna sudoccidentale raccolti durante il primo anno di attività di ricerca.

La caratterizzazione dei fosfati originari è stata eseguita mediante analisi XRD, SEM-EDS, FTIR, AFM e ICP-AES.

La HA ($Ca_{10}(PO_4)_6(OH)_2$) è prodotta dall'Alfa Aesar per reazione tra $Ca(OH)_2$ e H_3PO_4 ed ha tenore medio di Ca pari al 30-40 %. I granuli hanno morfologia sferica e/o tabulare con dimensioni medie 170 nm (Fig. 1A). Le analisi EDS hanno confermato la composizione caratteristica dell'idrossiapatite, come anche l'analisi ai raggi X.

Le due rocce fosfatiche provengono, rispettivamente, dalla Florida (FAP, Fig. 1B) e dal Marocco (MAP, Fig. 1C). La FAP proviene dall'Hardee Phosphate Complex (Florida, USA) ed è stata fornita dalla CF Industries; la MAP è stata campionata nel "Plateau dei Fosfati" (Youssufia, Marocco centrale). Lo studio morfologico tramite SEM ha evidenziato che le particelle dei due fosfati naturali hanno spigoli vivi. La FAP, sottoposta anche ad analisi tramite AFM ha evidenziato che le particelle in realtà hanno forma sferica e non spigoli vivi e presenta dimensioni medie di 300-500 nm. Tale discrepanza tra i risultati delle due metodologie analitiche è dovuta alla capacità dell'AFM di eseguire osservazioni più dettagliate e con maggiori ingrandimenti rispetto al SEM.

Le prove di immobilizzazione dei metalli in soluzione acquosa sono state eseguite facendo interagire a temperatura costante (25 $\pm$ 1°C) 0,1 e 0,2 g di HA e 1 g di FAP e MAP con soluzioni acquose a metallo singolo e multi-metal. Nel primo caso la soluzione conteneva un solo metallo mentre nel secondo caso erano presenti tutti e quattro i metalli a diversa concentrazione; la concentrazione dei metalli pesanti in soluzione è stata fatta variare tra 0,05 a 7,87 mmol/L. Questi esperimenti sono stati finalizzati a determinare l'efficienza dell'immobilizzazione da parte dei fosfati in presenza di più elementi nella

soluzione a la realizzazione di fenomeni di "competitive sorption", cioè una competizione per i siti di assorbimento tra gli ioni dei singoli metalli e gli ioni H^+ presenti in soluzione. Il termine sorption viene utilizzato in senso generale per indicare l'assorbimento dei metalli, presenti in soluzione, sulla superficie dei fosfati (Xu et al., 1994b).

Al fine di valutare l'influenza del fattore tempo di contatto fosfato/soluzione sul processo di immobilizzazione dei metalli da parte dei tre fosfati, gli esperimenti sono stati condotti per 2, 4, 24 e 48 ore. Al termine del periodo stabilito le soluzioni sono state filtrate mediante filtri Nucleopore di 0,2 μm e la frazione precipitata è stata raccolta per la successiva fase di indagine analitica. Gli esperimenti sono stati eseguiti senza imporre un controllo del pH delle soluzioni. I valori di tale parametro sono stati solamente misurati prima e dopo le interazioni con i fosfati nei sistemi multi-metal. In tal modo si è tentato di riprodurre in laboratorio condizioni prossime a quelle di applicazione della metodologia *in situ*, nelle quali il controllo del pH delle acque inquinate da metalli pesanti può essere di difficile realizzazione tecnica o risultare antieconomico.

Le soluzioni residue sono state analizzate mediante ICP-AES per determinare le concentrazioni di Cd, Cu, Pb, Zn, Ca e P al fine di valutare, quindi, l'entità della rimozione dei metalli da parte dei fosfati.

I materiali solidi sono stati caratterizzati mediante analisi XRD, FTIR, SEM-EDS presso il dipartimento Scienze della Terra dell'Università La Sapienza e AFM (Atomic Force Microscope) presso il Geology Department of Oxford, Miami University (Ohio, USA) sotto la guida del responsabile del laboratorio, Prof. J. Rakovan.

Le prove di interazione tra suoli contaminati (5 g) da metalli pesanti e fosfati sono state eseguite sia con la FAP che con la HA (1 g). I suoli utilizzati erano stati raccolti dalle aree (piazzali di stazionamento, discariche, stream, ecc.) di alcune miniere di solfuri (principalmente pirite, calcopirite, arsenopirite, blenda e galena) ormai dismesse della Toscana meridionale (Boccheggiano, Gavorrano, Niccioleta e Valle del Temperino) e della Sardegna sudoccidentale (Campo Pisano, San Giovanni, Monteponi e Monte Agruxiau). Sulla base dei risultati di studi precedenti (es. Zhang and Ryan, 1999), queste prove sono state condotte per 20 minuti, misurando il valore del pH dopo 10 minuti ed al termine del periodo di interazione e mantenendo tale valore prossimo a 5 mediante l'aggiunta di HNO_3 o NaOH. Dopo il periodo di interazione previsto, le sospensioni sono state filtrate con le modalità giá descritte e le soluzioni analizzate tramite ICP-AES per determinarne il

contenuto di metalli pesanti. Il materiale solido e' stato studiato mediante diffrattometria ai raggi X.

I risultati delle analisi XRD eseguite sui materiali solidi estratti dagli esperimenti di immobilizzazione non hanno mai evidenziato la presenza di nuove fasi minerali cristalline dopo l'interazione con le soluzioni contenenti i metalli pesanti. Inoltre per alcuni di questi materiali solidi è stato eseguito uno studio tramite spettroscopia IR, che ha ulteriormente evidenziato la buona sovvrapposizione dello spettro FTIR dell'HA con gli spettri dei materiali solidi.

Tutti i materiali solidi sono stati osservati tramite SEM-EDS per studiare la morfologia delle particelle. Non sono state riscontrate sostanziali differenze morfologiche tra le particelle dei fosfati prima e dopo l'interazione con le soluzioni. Al contrario, l'analisi EDS ha evidenziato la presenza dei metalli pesanti sulla superficie dei granuli dei fosfati. I risultati delle analisi eseguite mediante ICP-AES delle soluzioni a metallo singolo che hanno interagito con la HA indicano che generalmente l'entità dell'immobilizzazione dei metalli varia tra il 90 e il 99% (Fig. 2) ed è massima entro le 24 ore di interazione. In particolare, si osserva una correlazione diretta tra il quantitativo di HA utilizzato e l'entità dell'immobilizzazione. Per entrambi i quantitativi di HA utilizzati (0,1 e 0,2 g) le concentrazioni dei metalli al termine del periodo di interazione sono ben al di sotto dei valori limite definiti dalla normativa italiana (D.L. 477/91). Un caso particolare è rappresentato dallo Zn che risulta meglio immobilizzato dal quantitativo maggiore di HA e per un tempo maggiore di interazione (48h).

Per quanto concerne i risultati degli esperimenti eseguiti con la FAP si osserva che l'efficienza dell'immobilizzazione migliora con il tempo di sperimentazione, ed appare indipendente dalla concentrazione iniziale del metallo nella soluzione. Unica eccezione è costituita dallo Zn, per il quale l'entità della immobilizzazione diminuisce all'aumentare della concentrazione iniziale (Fig. 3).

I risultati degli esperimenti eseguiti con le soluzioni multi-metal indicano che nel caso della HA le singole concentrazioni dei metalli pesanti e il tempo di interazione non influenzano l'efficienza di immobilizzazione. La sua entità è, infatti, elevata come nel sistema a metallo singolo, con valori che variano dal 90 al 99%. In alcuni casi si osserva come la presenza di alcuni elementi riduca l'entità dell'immobilizzazione degli altri (Fig. 4).

Nel caso degli esperimenti eseguiti con la FAP, l'efficienza di immobilizzazione migliore è stata raggiunta con un tempo di contatto tra le 24h e le 48h, in funzione della concentrazione iniziale dei quattro metalli pesanti e dei fenomeni di competitive sorption (Fig. 5). Si sono osservati casi in cui l'immobilizzazione è stata molto bassa, prevalentemente per il minore tempo di contatto (2h). In particolare, lo Zn risulta meno immobilizzato rispetto agli altri elementi in funzione delle concentrazioni e quindi della competitive sorption.

Per quanto concerne la MAP, i risultati ottenuti indicano che il miglior tempo di immobilizzazione è variabile in funzione del sistema elementare ed è difficile anche stabilire un ordine di immobilizzazione, per cui sia la concentrazione iniziale dei metalli pesanti, sia la contemporanea presenza delle diverse specie elementari e il tempo di contatto risultano avere influenza sull'efficacia dell'immobilizzazione (Fig. 6).In particolare, quando i quattro elementi sono presenti nella soluzione tutti alla massima concentrazione (500 mg/L), i valori di immobilizzazione sono comunque superiori al 45%, confermando la capacità della roccia fosfatica di ridurre i livelli di questi elementi pesanti in soluzione acquosa. Informazioni sui meccanismi che hanno determinato la sorption dei metalli da parte dei fosfati sono state ottenute dai risultati delle analisi XRD, FTIR, SEM-EDS ed in particolare dai valori dei rapporti molari (Q_S) tra i cationi immobilizzati dai fosfati e il Ca^{2+} rilasciato in soluzione (es. Peld et al., 2004 a e b).

Se il valore di $Q_S = 1$ le quantità di cationi adsorbiti e rilasciati sono uguali, suggerendo come meccanismo più probabile della sorption lo scambio ionico tra la soluzione e i fosfati. Quando il valore di $Q_S > 1$ il quantitativo di cationi adsorbiti è maggiore di quelli rilasciati, indicando che la complessazione superficiale potrebbe essere il principale meccanismo di sorption dei metalli. Infine, valori di $Q_S < 1$ indicano fenomeni di dissoluzione dei fosfati originari e successiva precipitazione di nuove fasi fosfatiche dei metalli.

In generale, i sistemi studiati, sia a metallo singolo che multi-metal, indicano valori del rapporto molare che variano da $Q_S < 1$ a $Q_S >> 1$. I valori del Qs più elevati sono caratteristici dei sistemi in cui l'ammendante utilizzato è stata la roccia fosfatica naturale ed indicano una minore solubilità sia della FAP che della MAP rispetto all'HA. I valori del Qs suggeriscono come principali meccanismi della sorption i fenomeni di precipitazione, di complessazione superficiale e di scambio ionico. In questa ottica, anche le relazioni

esistenti tra le concentrazioni del Ca e del P e quelle dei metalli pesanti indicano i suddetti meccanismi come i più probabili. Ulteriori indicazioni a sostegno dei meccanismi di sorption proposti sono state ottenute dall'analisi delle curve isoterme di sorption (Giles et al., 1960; Bilali et al., 2001; Echeverria et al., 1998), che mettono in relazione il quantitativo di metallo pesante adsorbito dal fosfato e di quello presente in soluzione all'equilibrio. L'andamento delle curve suggerisce un comportamento di tipo Langmuir e tale modello è stato utilizzato per la definizione quantitativa dei fenomeni di sorption. Generalmente le curve dei sistemi presentano un andamento definito di tipo L2 (Fig. 7), in cui si osserva un breve tratto rettilineo seguito da un flesso e un plateau, nel caso della complessazione superficiale. Al contrario, nel caso dei sistemi contenenti Pb, le curve isoterme sono praticamente linee verticali che riflettono un meccanismo di immobilizzazione attraverso la precipitazione.

La stabilità dell'immobilizzazione dei metalli pesanti da parte dei fosfati è stata verificata mediante esperimenti di desorption. Alcuni campioni dei materiali solidi estratti dagli esperimenti di sorption sono stati fatti interagire a temperatura costante (25 ± 1 °C) con soluzioni con pH variabile da 4 a 6. I risultati ottenuti hanno indicato che indipendentemente dalla concentrazione del metallo adsorbito e dal tempo di contatto, la frazione dei metalli rilasciata dai fosfati era generalmente inferiore allo 0,5 % ed in alcuni casi inferiore al limite di rilevabilità dello spettrofotometro ICP-AES.

I risultati degli esperimenti condotti sui suoli delle aree minerarie indicano che la concentrazione dei metalli pesanti biodisponibilie viene immobilizzata quasi totalmente (≈ 99%) (Fig. 8). I materiali solidi sono stati analizzati mediante XRD ed in nessun caso è stata determinata la formazione di nuove fasi minerali cristalline.

I risultati ottenuti dall'attività di ricerca durante il triennio confermano la validità della metodologia di immobilizzazione dei metalli in soluzione acquosa e nei suoli attraverso l'interazione con fosfati sintetici e naturali.

In particolare, l'utilizzo dei fosfati naturali consente di coniugare all'efficienza della metodologia una procedura di "remediation" a costi relativamente bassi rispetto ad altre metodologie note.

Il confronto tra i risultati ottenuti utilizzando le tre tipologie di fosfati, conferma la possibilità di utilizzare materiale naturale e a basso costo per l'applicazione della metodologie di immobilizzazione dei metalli pesanti in acque e suoli.

I risultati dell'attività sperimentale hanno evidenziato che i fattori fondamentali che determinano l'efficienza dell'immobilizzazione dei metalli sono il tempo di contatto fosfati/mezzo inquinato ed i fenomeni di "competitive sorption" nel caso di più elementi metallici. Tale determinazione è di fondamentale importanza per una efficace applicazione della metodologia a situazioni in situ.

Per quanto concerne il tempo di contatto, i risultati ottenuti hanno dimostrato che la cinetica della reazione di immobilizzazione è molto elevata nel caso di sistema a metallo singolo con contestaulmente l'azione dell'HA. Al contrario in un sistema più complesso come quello multi-metal, il tempo di contatto necessario al raggiungimento della reazione di sorption aumenta arrivando in media a 24-48h.

Informazioni sui probabili meccanismi dell'immobilizzazione dei metalli da parte dei fosfati sono state ottenute tramite le analisi XRD, FTIR, SEM-EDS e AFM dei materiali solidi. Queste non hanno evidenziato in nessun caso la formazione di nuove fasi fosfatiche cristalline, nonostante l'analisi mdiante EDS abbia sempre rivelato la presenza dei metalli sulle superfici dei granuli dei fosfati. Tali risultati sono parzialmente in contrasto con quelli di studi precedenti (es. Ma et al., 1993) che, in particolare per l'immobilizzazione del Pb, indicano come meccanismo principale la dissoluzione degli originari fosfati e la conseguente precipitazione di HP. Tuttavia, lo studio dei valori di Q_S e delle curve isotermiche di sorption suggerisce che in alcuni casi si verifichi il processo di dissoluzione/precipitazione di una nuova fase fosfatica. In questa ottica, i preliminari risultati dello studio EXAFS eseguito suggeriscono che la fase sia un fosfato che però non mostra le caratteristiche strutturali della HP.

Oltre al meccanismo di immobilizzazione suddetto, i risultati ottenuti indicano che altri processi hanno determinato la sorption dei metalli. In particolare, un ruolo fondamentale nell'immobilizzazione del Cd è stato svolto dallo scambio ionico tra il Ca e l'elemento sudetto.

Sulla base dei risultati ottenuti il meccanismo dello scambio ionico risulta meno probabile per Cu e Zn. Per questi ultimi due elementi si ritiene che il principale processo sia un meccanismo di complessazione superficiale con i gruppi superficiali del fosfato, ≡POH e ≡CaOH.

In conclusione lo studio effettuato dimostra la validità della metodologia per l'eventuale applicazione in situ per futuri risanamenti ambientali, dimostrando anche il vantaggio economico nell'utilizzazione di rocce fosfatiche in relazione al loro basso costo.

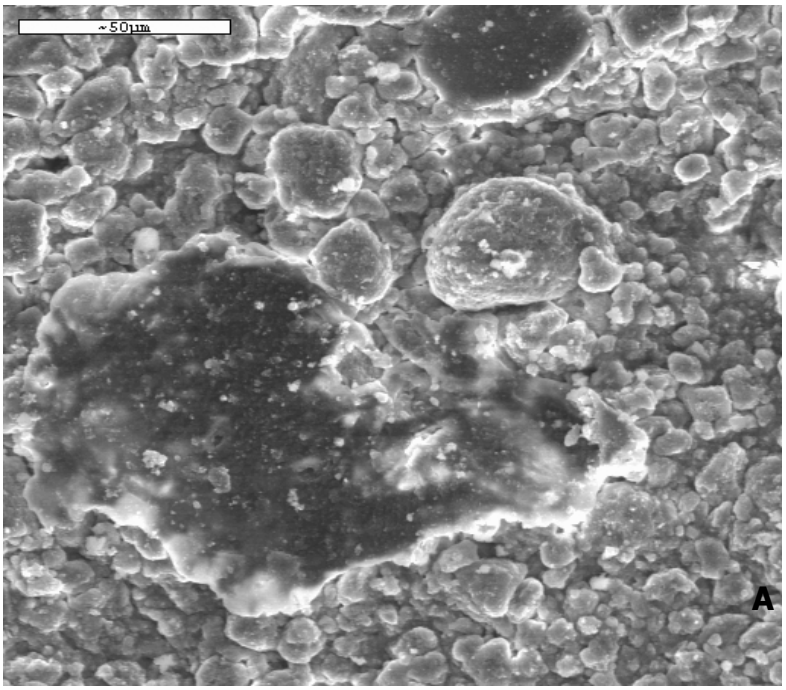

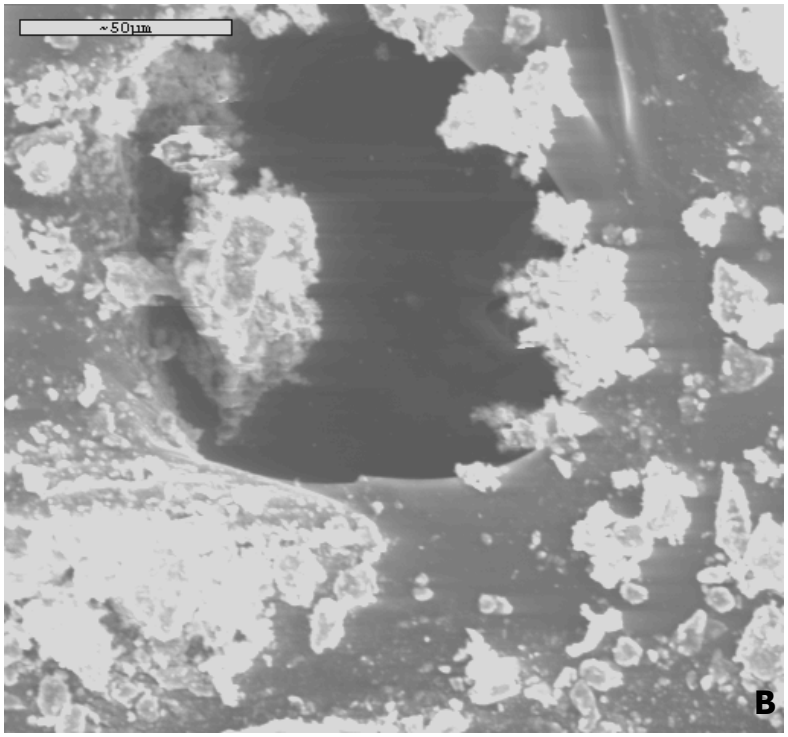

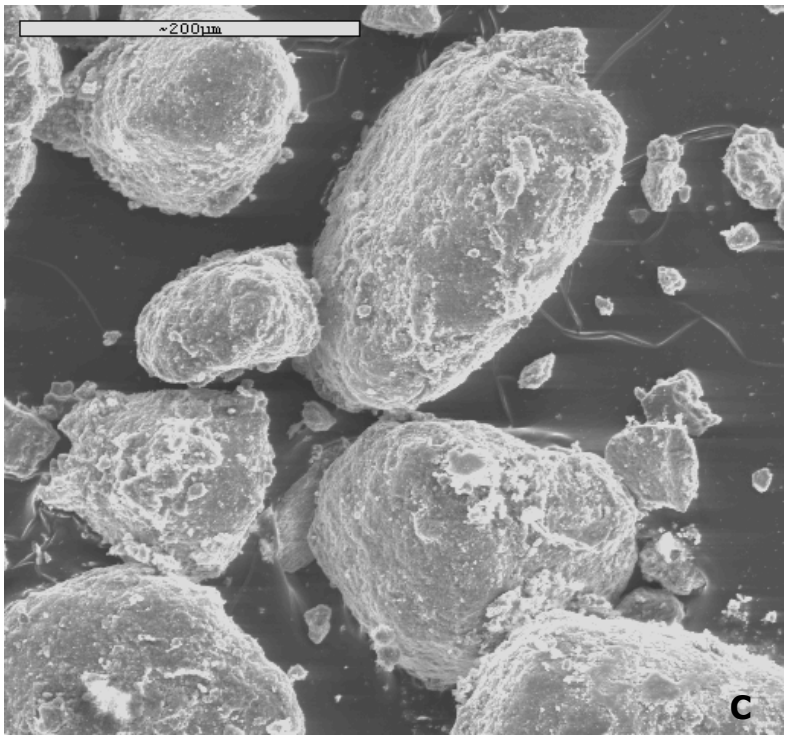

Fig. 1 : Microfotografie al SEM dei tre tipi di fosfato utilizzato. A = Idrossiapatite sintetica (HA)(Alfa Aesar); B = Fluoroapatite della Florida (FAP) e C = Fluoroapatite del Marocco (MAP).

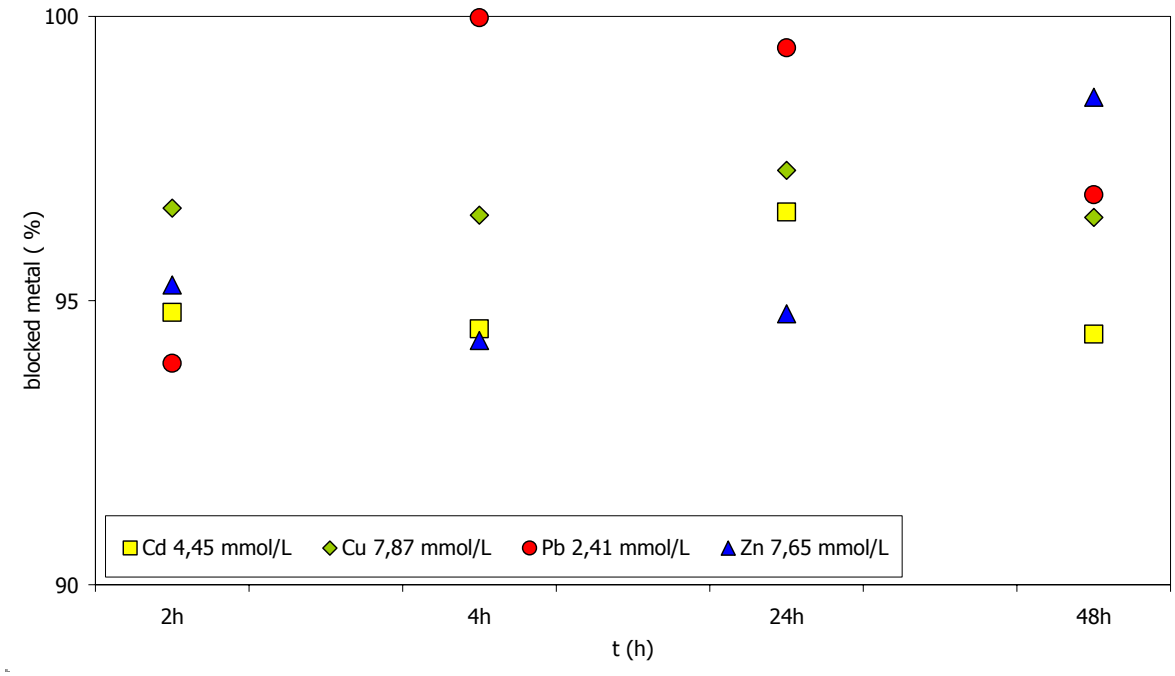

Fig. 2: Esempio dell'efficienza di immobilizzazione dell'HA nel sistema a metallo singolo alle massime concentrazione dei quattro metalli pesanti in soluzione acquosa.

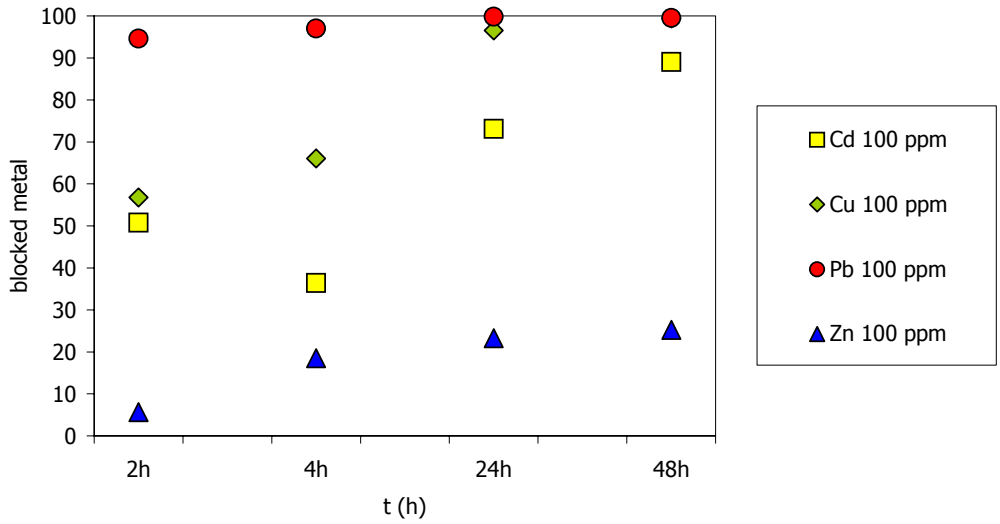

Fig. 3: Esempio dell'efficienza di immobilizzazione della FAP nel sistema a metallo singolo alle massime concentrazione dei quattro metalli pesanti in soluzione acquosa.

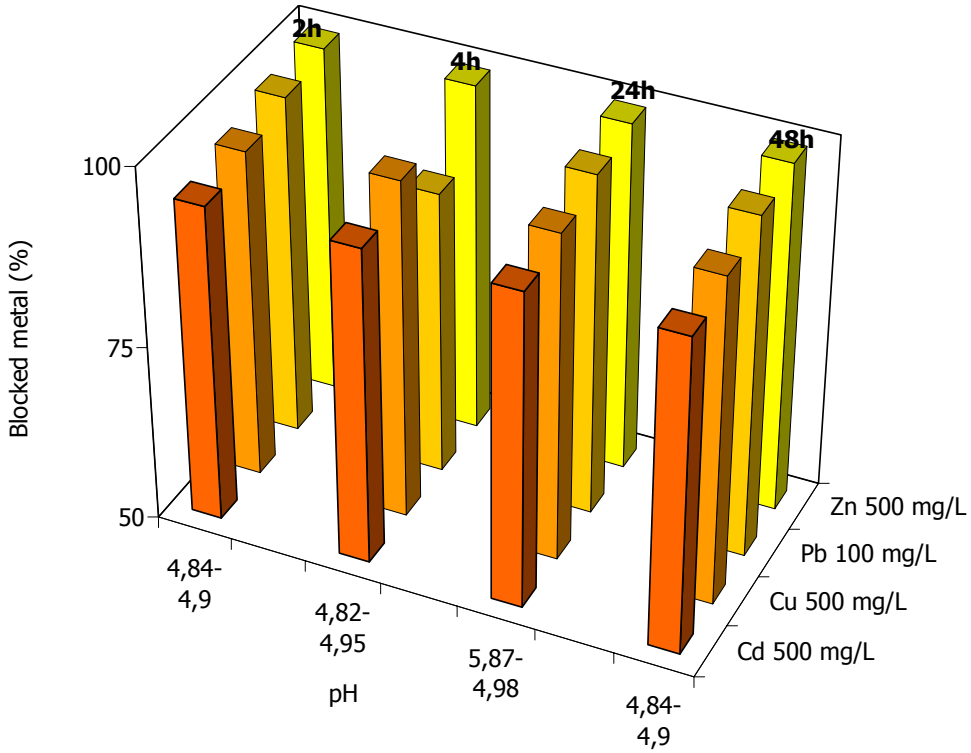

Fig. 4: Esempio dell'efficienza di immobilizzazione dell'HA per il sistema multi-metal. Le concentrazioni in soluzione acquosa sono: Pb = 100 mg/L e Cd,Cu e Zn = 500 mg/L. Si osserva come per alcuni elementi l'immobilizzazione sia minore a causa della competitive sorption.

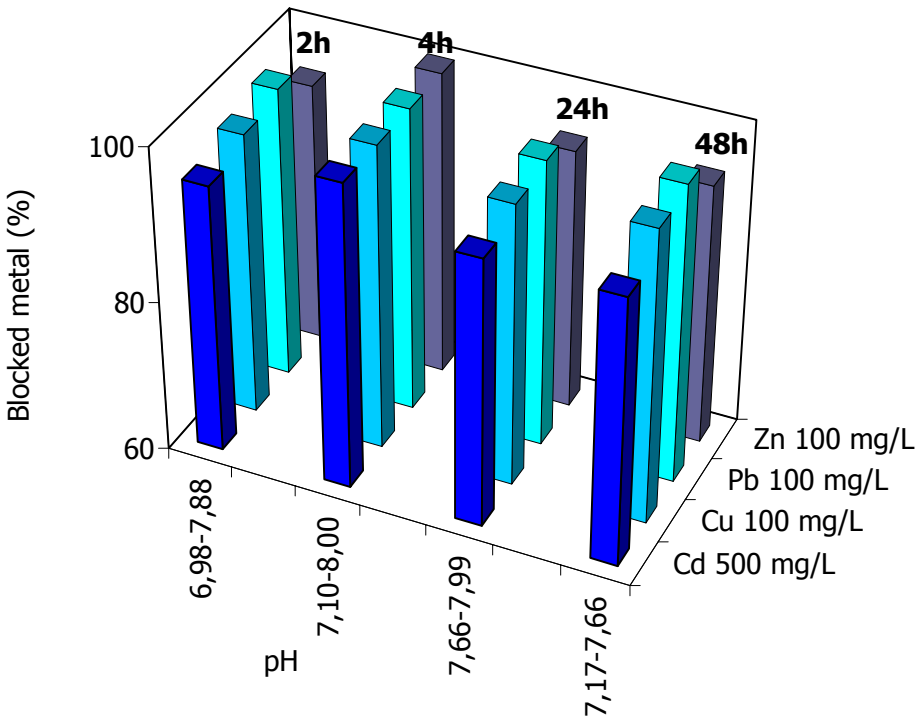

Fig. 5: Esempio dell'efficienza di immobilizzazione della FAP per il sistema multi-metal in cui Cd è l'elemento costante. Le concentrazioni in soluzione acquosa sono:Cd = 500 mg/L; Cu, Pb e Zn = 100 mg/L.

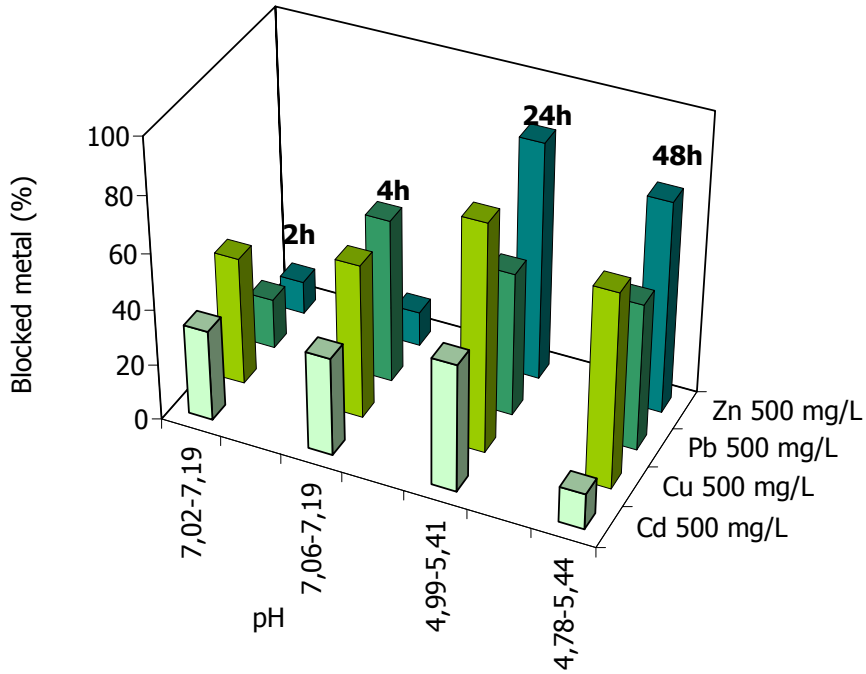

Fig. 6: Esempio dell'efficienza di immobilizzazione della MAP per il sistema multi-metal in cui Pb è l'elemento costante. Le concentrazioni in soluzione acquosa sono: Cd; Cu, Pb e Zn = 500 mg/L.

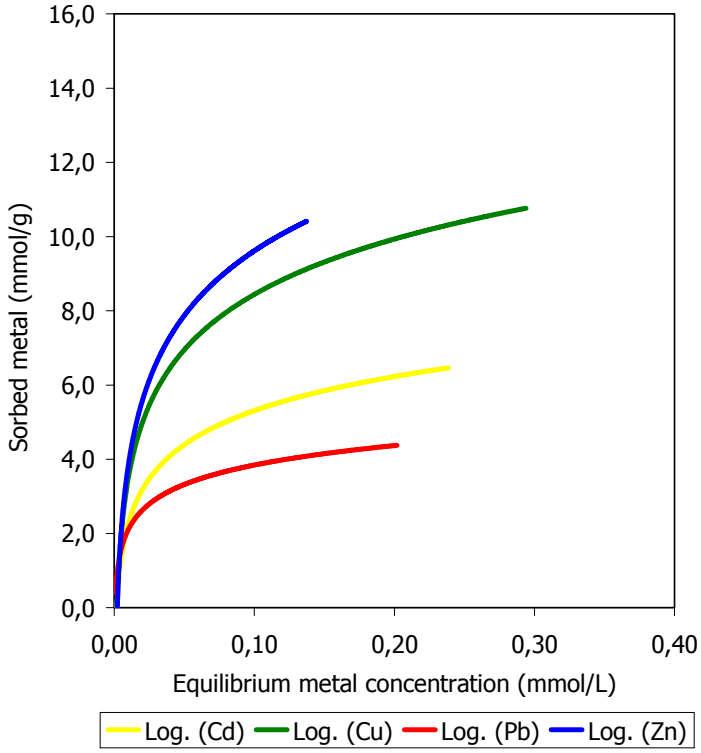

Fig. 7: Esempio di curve isoterme per il sistema a metallo singolo, t = 4h e HA = 0,1g.

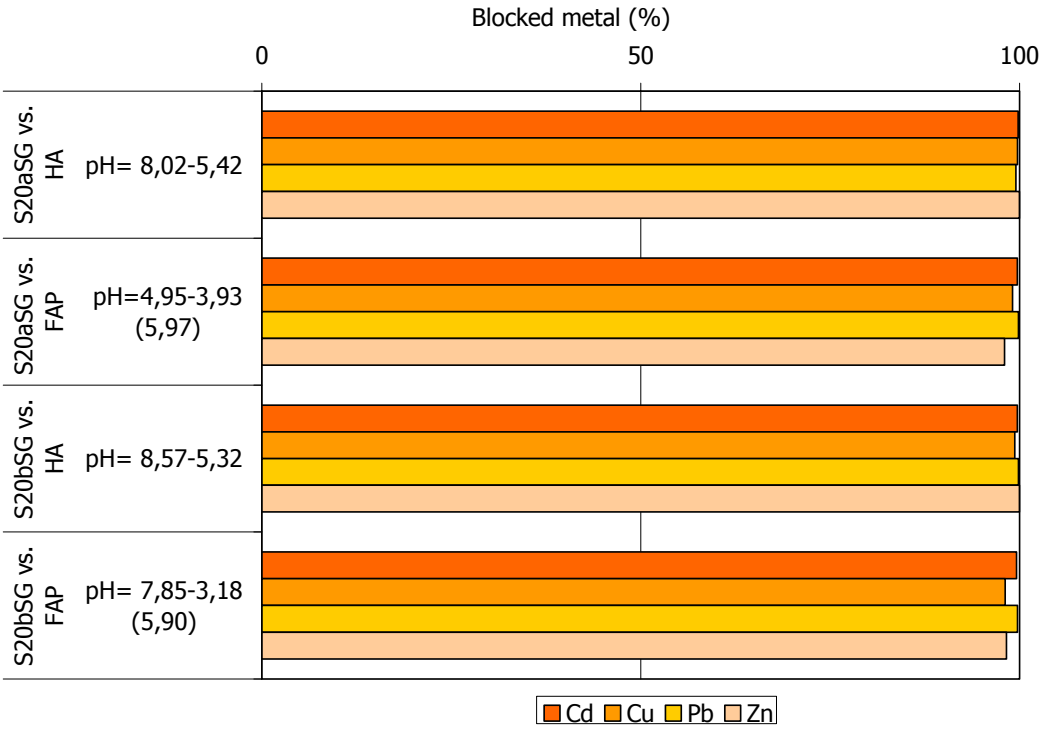

Fig. 8: Esempio dell'efficienza di immobilizzazione sia dell'HA che della FAP per i suoli provenienti dalla miniera di San Giovanni (Sardegna sud-occidentale).

Breve selezione della bibliografia

1. L. Bilali, M. Kouhila, M. Benchanaa, A. Mokhlisse and A. Belghit "Experimental study and modelling of isotherm of sorption of humid natural phosphate" Energy conversion and management 4 2 (2001) 467-481
2. S. Brückner, G. Lusvardi, L. Menabue and M. Saladini "Crystal structure of lead hydroxyapatite from powder X-ray diffraction data" Inorganica Chimica Acta 236 1995 209-212
3. R. X. Cao, L. Q. Ma, M. Chen, S. P. Singh and W. G. Harris "Phosphate – induced metal immobilization in a contaminated site" Environmental Poll. 122 (2003) 19-28
4. X. Cao, L. Q. Ma, D. R. Rhue, C. S. Appel "Mechanism of lead, copper, and zinc retention by phosphate rock" Environmental pollution 131, (2004) 435-444
5. X. Chen, J. V. Conca and J.L. Peurrung "Effects of pH on heavy metal sorption on mineral apatite " Environ. Sci. Technol. (1997) 31 624-631
6. J.C. Echeverría, M. T. Morera, C. Mazkiará, J.J. Garrido "Competitive sorption of heavy metal by soils. Isotherm and fractional factorial experiments" Environmental pollution 101 (1998) 275-284
7. M. Fedoroff, J. Jeanjean, J. C. Rouchaud, L. Mazerolles, P. Trocellier, P. Maireles-Torres and D. J. Jones "Sorption kinetics and diffusion of cadmium in calcium hydroxyapatite" Solid State Sciences (1999) 71-84
8. C. H. Giles, T.H. McEwan, S.N. Nakhawa, D. Smith "Studies in adsorption. Part XI. A system of classification of solution adsorption isotherm, and its use in diagnosis of adsorption mechanism and in measurements of specific surface areas solids" Journal of the Chemical Society (1960) , 3973-3993
9. M. E. Hodson, E. Valsami-Jones, J. D. Cotter-Howells, W. E. Dubbin, A. J. Kemp, I. Thornton and A. Warren "Effect of bone meal (calcium phosphate) amendments on metal release from contaminated soils – a leaching column study" Environment Pollution 112 (2001) 233-243
10. S. K. Lower, P. A. Maurice, S. J. Traina and E. H. Carlson "Aqueous Pb sorption by hydroxylapatite: applications of atomic force microscopy to dissolution, nucleation and growth studies." American Mineralogist Vol. 83 p. 147-158 (1998)
11. Q. Y. Ma, S. J.Traina, T. J.Logan and J. A.Ryan "In situ lead immobilization by apatite" Environ. Sci. Technol. (1993), 27, p. 1803-1810
12. Q. Y.Ma, S. J.Traina, T. J.Logan, J. A. Ryan "Effects of aqueous Al, Cd, Cu, Fe (II), Ni and Zn on Pb immobilization by hydroxyapatite" Environ, Sci. Technol., (1994), 28, 1219-1228

13. Q. Y. Ma, T. J. Logan, S. J. Traina, J. A. Ryan "Effects of NO^{3-}, Cl^{-}, F^{-}, SO_4^{2-}, and CO_3^{2-} on Pb^{2+} immobilization by hydroxyapatite" Environ. Sci. Technol. (1994), 28, 408-418
14. Q. Y. Ma, T. J. Logan, S. J. Traina " Lead immmobilization from aqueous solutions and contaminated soils using phosphate rocks" Environ. Sci. Technol. (1995), 29, 1118-1126
15. M. Manecki, P. A. Maurice and S. J. Traina "Uptake of aqueous Pb by Cl^{-},F^{-}, and OH^{-} apatites: mineralogic evidence for nucleation mechanism" American Mineralogist vol 85 932-942 (2000)
16. S. McGrellis, J-N. Serafini, J. JeanJean, J-L. Pastol and M. Fedoroff "Influence of the sorption protocol on the uptake of cadmium ions in calcium hydroxyapatite" Separation and Purification technology 24 (2001) 129-138
17. J. J. Middelburg and R. N. J. Comans "Sorption of cadmium on hyroxyapatite" Chemical geology 90 (1991) 45-53
18. J. O. Nriagu "Lead orthophosphates-II. Stability of cloropyromorphite at 25°C Geochimica et Cosmochimica Acta (1973) vol37 p. 367-377
19. J. O. Nriagu "Lead orthophosphates-III. Stability of fluoropyromorphite and bromopyromophite at 25°C Geochimica et Cosmochimica Acta (1973) vol 37 p. 1735-1743
20. J. O. Nriagu "Lead orthophosphates-IV. Formation and stability in the environment Geochimica et Cosmochimica Acta (1974) vol38 p. 887-898
21. J. O. Nriagu and P. B. Moore "Phosphate minerals" Springer–Verlag Berlin Heidelberg 1984
22. M. Peld, K. Tõnsuaadu,and V. Bender "Natural and synthetic apatites as sorbents for Cd^{2+} and Cr^{3+} ions from aqueous solutions" Proc. Estonian Acad. Sci. chem., (2004), 53, 2, 75-90.
23. M. Peld, K. Tõnsuaadu, V.Bender " Sorption and desorption of Cd^{2+} and Zn^{2+} ions in apatite-aqueous system" Environ. Sci. Technol. (2004), 38, 5626-5631
24. M. Pujari and P. N. Patel " Strontium – copper – calcium hydroxyapatite solid solutions: preparation, infrared, and lattice constant measurements" Journal of Solid state Chemistry83 100-104 (1989)
25. S. Raicevic, T. Kaludjerovic-Radoicic and A.I. Zouboulis "In situ stabilization of toxic metals in polluted soils using phosphates: theoretical prediction and experimental verification" Journal of Hazardous Materials B117 (2005) 41-53
26. S. P. Singh, L. Q. Ma and W. G. Harris "Heavy metal interaction with phosphatic clay: sorption and desorption beahaviour" Journal of Environmental Quality vol 30 n. 6 (2001) 1961-1968

27. T. Suzuki, T. Hatsushika and Y. Hayakawa "Synthetic hydroxyapatites employed as inorganic cation-exchanger" J. Chem. Soc. Faraday Trans. I. (1981) 77 1059-1062
28. T. Suzuki, T. Hatsushika and Y. M. Miyake "Synthetic hydroxyapatites employed as inorganic cation-exchanger part 2" J. Chem. Soc. Faraday Trans. I. (1982) 78 3065-3611
29. T. Suzuki, K. Ishigaki and M. Miyake "Synthetic hydroxyapatites employd as inorganic cation-exchanger part 3._Exchange characteristics of lead ions (Pb^{2+})" J. Chem. Soc. Faraday Trans. I. (1984) 80 3157-3165
30. E. Valsami-Jones, K. V. Ragnarsdottir, A. Putnis, D. Bosbach, A. J. Kemp and G. Cressey "The dissolution of apatite in the presence of aqueous metal cations at pH 2-7" Chemical Geology 151 (1998) 215-233
31. Xu, Y., Schwartz, F.W.,. "Lead immobilization by hydroxyapatite in aqueous solutions" J. Contam. Hydrol. 15, 187-206 (1994)
32. Y. Xu, F. W. Schwartz, S. J. Traina "Sorption of Zn^{2+} and Cd^{2+} on hydroxyapatite surfaces" Environ. Sci. Technol. (1994), 28, 1472-1480

- **I wish to acknowledge Prof. V. Ferrini for his suggestions during the Ph.D. time.**
- **The kind help of Prof. J. Rakovan and Prof. S. J. Traina is gratefully acknowledge for their useful help during my american term, giving me the opportunity to use their instruments.**
- **In particular I thanks Angelo for his closeness and Jacopo for his birth.**
- **The last thanks goes to all of the Ph.D. students for their friendship.**

INTRODUCTION

Rapid industrialization and urbanization has resulted in the deterioration of water, air and land quality. The increase in the use of heavy metals over the past few decades has resulted in an increase flux of metallic substances in the environment. The heavy metals are of special concern because they are non-degradable.

Moreover, the problem of pollution caused by heavy metals such as: lead (Pb), zinc (Zn), copper (Cu) and cadmium (Cd) is very important, in fact these heavy metals may adversely affect soil ecology, agricultural production and water quality. Contaminated soils and waters often present an unacceptable risk to human and ecological health and must be remediate. In the last years the awareness of the relationship between the human health and the high concentration of these chemical substances is becoming important. It can be considered a public health hazard due to their long residence time in soil and their high toxicity bio-accumulating and being bio-available to animals, humans and especially children ("hand to mouth"), they can enter in the food chain (dietary response) or can be breath (respiratory response). The origin of this pollution can be anthropic, industrial and also it can be caused by the atmosphere or the lithosphere. Mostly, these heavy metals are found in objects commonly used as paint, batteries gasoline, industrial activities, agricultural and urban activities. Among these heavy metals, cadmium, copper, lead and zinc are considered the most toxic and according to EPA (environmental protection agency) they are in a list of the main pollution agent.

These four heavy metals are also found in mine wastes causing a problem of disposal. The soil where the wastes are found with an high concentration can be considered polluted, the real problem is their mobility, so that they can enter in the ground water. The most important problem is their bio-availability, so that it is better to understand if these heavy metals can be available in a soil or water, understand their physicochemical forms and their solubility so that to evaluate the potential environmental and health effects.

During these years many technologies were developed to solve this kind of pollution such as solidification or vitrification, electtrokinetics or microbiological, chemical or physical treatment, either for soils or waters. Generally these methods are expensive and

sometimes the problem is not completely solved, or in case of a soil the method doesn't leave the soil in place for a future use and in this case it must be find a place where to stock the polluted soils. Among these methods the immobilization *in situ* seems the suitable one, it means to transform these heavy metals in more stable and less soluble compounds. The use of phosphate seems to have these characteristics and in particular the apatite shows the most suitable characteristics of immobilization for these heavy metals. The immobilization is through the dissolution of apatite and precipitation of pyromorphite.

Apatite is a mineral which forms also bones and teeth, it has been idealized as calcium hydroxyapatite but some differences in composition and other properties make biological apatite different from pure calcium hydroxyapatite and it is referred as "impure hydroxyapatite". Biological apatite is microcrystalline and has a heterogeneous composition containing carbonate in varying amount as a substituent for phosphate in the apatite structure. Inorganic apatite is generally an accessory mineral in igneous rocks and occurs in regionally metamorphosed rocks ranging from low grade talc and chlorite schists to high grade biotite hornblende gneiss. They are in association with alkaline intrusive plutonic rocks. Weathering and especially the leaching of calcium carbonate are additional factors in the formation of igneous phospate deposits. A little number of deposits occur in caves formed by the accumulation of bat dropping, much less from bird dropping or accumulation of small vertebrate remains. This type of deposit is found primarily on low latitude humid areas to produce large cave systems. Insular phosphate deposit are formed by the accumulation of bird dropping and in part by the secondary phosphatization of the bedrock. Commonly found on warm-arid or semi-arid areas with a large bird population, either at the present days or in the fairly recent past. Phosporites, sedimentary phopshate deposits, are the most important source of phosphate rock. Commonly they occur as beds composed of grains, many of them were originally of biochemical carbonate which were diagenetically phosphatized *(118)*.

Generally, apatite and pyromorphite show a greater stability than the oxides, hydroxides, sulfates and carbonates at earth surface condition, in particular pyromorphite is stable from a pH 2 to a pH 11 and can resist the high temperature, it is stable also in reducing conditions *(118)*.

Particularly hydroxyapatite $Ca_{10}(PO_4)_6(OH)_2$ has the possibility to immobilize bivalent ions like such as: Pb, Zn, Cd, Cu, Cr and Ni and so on (Suzuki et al. *(140 and 142)*; Xu et al. *(152)*; Peld et al. *(122)* and Corami et al. *(33)*).

The mechanism for the immobilization are ion exchange, precipitation of a complex ion-phosphate , dissolution and precipitation of a new mineral. This means heavy metals are well immobilized and for a long time. For this reason many tests are carried on to understand how these heavy metals behaved in different condition and concentration.

Our aim is to demonstrate the efficacy of *in situ* immobilization of toxic metals in waters and soils using synthetic and natural phosphates, secondly to determine a suitable and cost-effectively amendment to reduce the bio-availability and mobility of them. Consequently another purpose will be to characterize the reaction products of phosphates with Pb, Cu, Zn and Cd and to examine the effects of dissolved foreign ions on the attenuation of heavy metals by phosphates.

1 CHARACTERISTICS OF HEAVY METALS

The term heavy metal refers to any metallic chemical element that has a relatively high density (>5 g/cm^3) and it is toxic or poisonous at low concentrations *(85)*.

Metals exist in water and soil either as free (uncomplexed) metal ions, in various soluble complexes with inorganic or organic ligands or associated with mobile inorganic and organic colloidal material. All soils and water naturally contain trace levels of metals. The concentration of metals in uncontaminated soil is primarily related to the geology of the parent material from which soil is formed *(87)*.

Among many metals, those which are commonly encountered in high amounts in waters, soils and wastes are: Pb, Zn, Cu and Cd. As they are included in they are included in the ASTD'S (US Agency for toxic substances and Disease Registry) "Top 20 Hazardous substances " list, they have been chosen for this study.

The limit levels for the four heavy metals are different considering water or soils; in particular, for soil the limit level depend on the use of the soils. Industrial exposure accounts for a common route of exposure for adults and because of all the maladies caused by the accumulation of heavy metals in soil or water, the legislation is

progressively becoming more stringent. According for the Italian law in force, in case of water the limits are: Pb 10 μg/l; Cu 1 mg/l; Cd 5 μg/l and Zn 3 mg\L *(43)*; for soils are Pb 100-1000 mg/kg; Zn 150-1500 mg/kg; Cu 120-600 mg/kg and Cd 2-15 mg/kg *(44)*.

Even though some adverse health effects of heavy metals have been known for a long time, exposure to heavy metals continues and in the less developed countries is increasing (Fig. 1). On the contrary in most developed countries their emissions have declined (fig. 2 A and B).

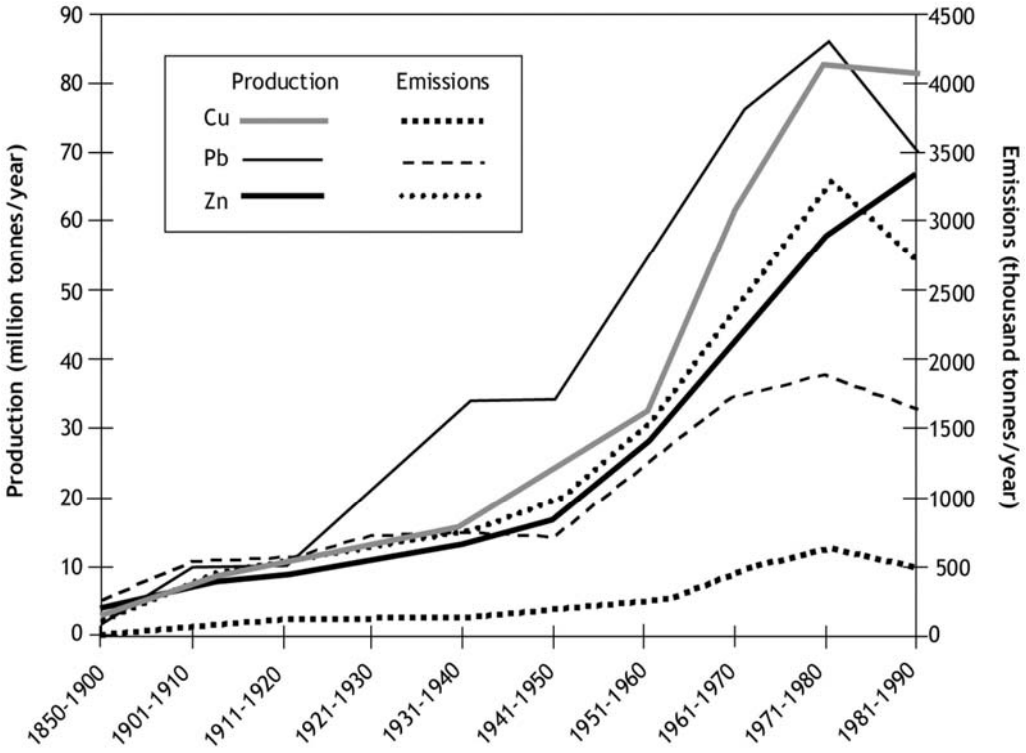

Fig. 1 Global production and consumption of selected toxic metals, 1850-1990 (Järup *(74)*).- Fig.1 Produzione globale e consumo di una serie di elementi metallici tossici (Järup *(74)*).

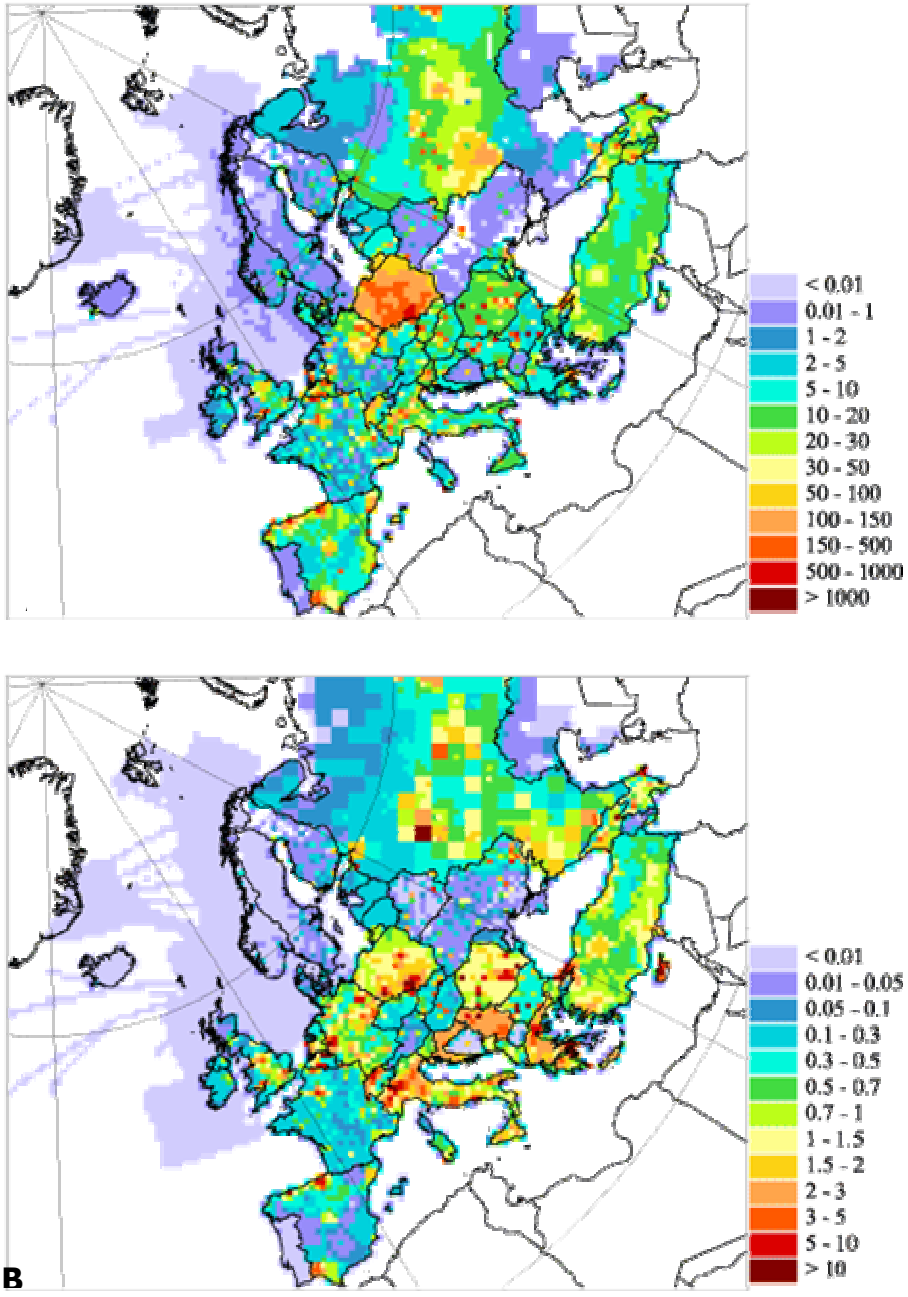

Fig. 5 Spatial distribution of cadmium (A) (g/km2/y) and lead (B) (kg/km2/y) antropogenic emission in 2002 ***(102)***. - Fig. 5 Distribuzione spaziale del cadmio (A) (g/km2/y) e del piombo (B) (kg/km2/y) di origine antropogenica ***(102)***.

1.1 HEAVY METALS AND THEIR USE

1.1.1 Cadmium

Cadmium was discovered in 1817 by F. Stromeyer who named it *cadmium* after cadmeia, the ancient greek name for zinc ore. It is the 63rd element in order of crustal

abundance and its abundace is close to those of antimony and bismuth. It is a soft, ductile, silver-white metal with many industrial uses. Chemically, it is a divalent 4d transition element, atomic number 48, atomic weight 112,41, electron configuration $[Kr]4d^{10}5s^2$, located in period 5 and group IIB. It crystallizes in a distorted hexagonal close-packed structure. It has 43 isotopes and only 8 occur naturally *(54)*, 106 (1.2 atomic abundance %), 108 (0.9 atomic abundance %), 110 (12.4 atomic abundance %), 111 (12.7 atomic abundance %), 112 (24.1 atomic abundance %), 113 (12.3 atomic abundance %), 114 (28.6 atomic abundance %) and 116 (7.6 atomic abundance %). Generally it is not found as a native metal and only three minerals are known: greenockite and hawleyte (CdS) and otavite ($CdCO_3$). The two sulfides are hexagonal and isometric polymorphic of the cadmium sulfide whereas the carbonate crystallizes in the trigonal sytsem. The abundance of the three minerals in the crust are very low to be mined as an ore and they can be found occluded in the analogs of the zinc mineral (wurtzite, sphalerite and smithsonite).

The first use of Cd was in the 19th century as a yellow pigment, commercially produced in Germany in the 1880s as a by-product of the smelting of zinc ore from Upper Silesia (now Poland). Until World War I, Germany was the first world producer, while after the war USA accounted the entire world production of cadmium. Production was spurred by the development of the cadmium electroplating process in 1919, which was applied mainly to the coating of iron and steel, and by the extensive use of cadmium alloy sleeve bearings in automobile engines for several years in the 1930s *(85)*.

In ore deposits cadmium is generally associated with zinc and less closely with lead and copper, and it is a by-product of the mining and processing of zinc. The main world producers of cadmium are Japan, Cina and USA (Tab. 1).

The most significant use of cadmium is in nickel/cadmium batteries which grew for more than 15 years, as rechargeable or secondary power sources exhibiting high output, long life, low maintenance and high tolerance to physical and electrical stress. Cadmium coatings provide good corrosion resistance, particularly in high stress environments such as marine and aerospace applications where high safety or reliability is required. Other uses of cadmium are as pigments, stabilisers for PVC, in alloys and electronic compounds. These other cadmium markets will continue to decline because of the increasingly stringent environmental regulations, concerns of manufacturers about long-term liability,

and the development of less toxic substances. Cadmium is also present as an impurity in several products, including phosphate fertilisers, detergents and refined petroleum products. It is also added to other non-ferrous alloys to improve properties such as strength, hardness, wear resistance, castability and electrochemical behaviour.

Country	Refinery production		Reserves[b]	Reserves base[c]
	2003	2004[a]		
United States	670	600	90.000	270.000
Australia	350	350	110.000	300.000
Belgium	120	100	-	-
Canada	1.400	1.400	55.000	100.000
China	2.500	2.600	90.000	380.000
Germany	450	450	6.000	8.000
India	480	490	3.000	5.000
Japan	2.500	2.600	10.000	15.000
Kazakhsthan	1.350	2.000	50.000	100.000
Korea, Republic of	1.850	2.200	-	-
Mexico	1.400	1.400	35.000	40.000
Russia	950	1.000	16.000	30.000
Other countries	2.880	2.010	140.000	550.000
World total (rounded)	16.900	17.200	600.000	1.800.000

[a] estimated.
[b] it is refer to the in-place cadmium content of ores that can be mined and processed at profit.
[c] it is encompassed the reserves proper, marginally economic reserves and a discretionary part of subeconomic resources.

Tab. 1 Worldwide refinery production of Cd, Reserves and Reserves Base *(108)* – Tab.1 Produzione mondiale di Cd, riserve e riserve sub -economiche *(108)*.

Cadmium-containing products are rarely recycled and sometimes dumped in the household waste *(124)*.

Cadmium phosphates are sparse in the geological record. In particular the ionic ray suggests it could form several phosphates with a composition analogous to Ca and Zn phospate, respectively *(117)*. The dearth of Cd phosphate is related to the low ion activity in subaqueous and supergene environments. Moreover many Ca and Al phosphates show an high concentrations of Cd *(120)*.

The International Cadmium association (ICdA) made an estimation of the cadmium consumption for the 2003: batteries, 79%; pigments, 12%; coatings and plating, 7.5%;

stabilizers for plastics and similar synthetic products, 1%; and non ferrous alloys and other uses 0.5%.

The production was about 16.900 t in 2003 (Fig. 3-4), the primary cadmium production is decreasing, on the contrary the secondary one is increasing and there are three major industry collection and recycling programs: the Rechargeable Battery Recycling corp. (RBRC) in the USA and Canada. The Battery association of Japan and the CollectNiCd programme in EU, but to estimate the amount of Cd recyled is very difficult *(108)*.

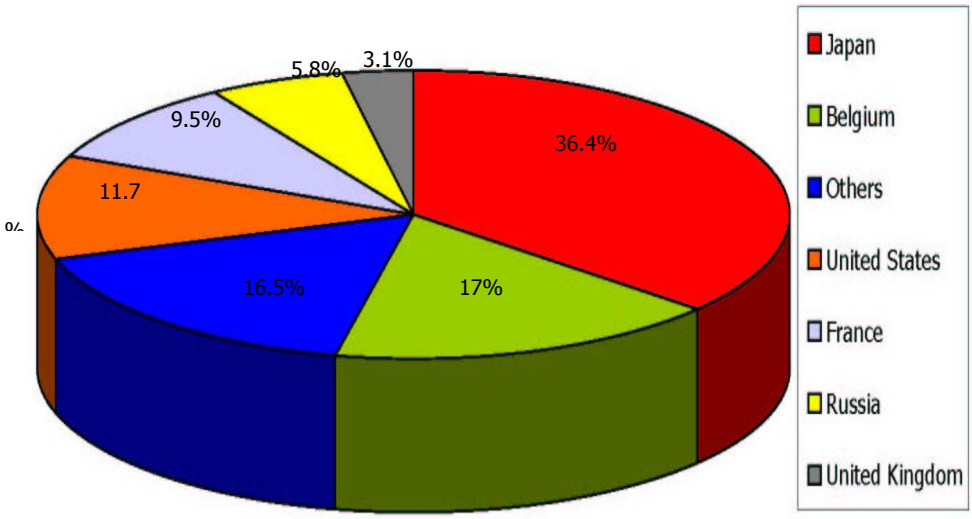

Fig. 3 World cadmium consumption, 2000 *(108)*. – Fig. 3 Consumo mondiale di Cd *(108)*.

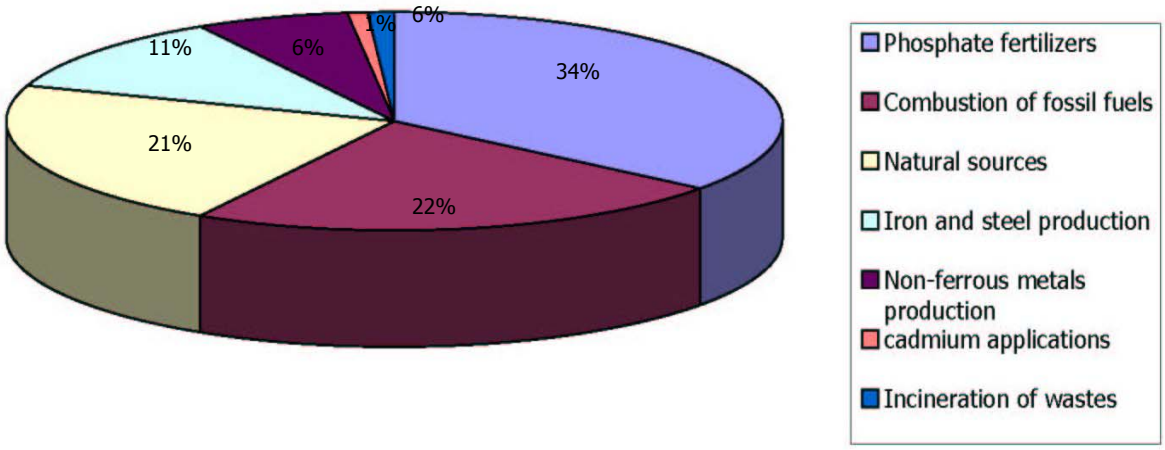

Fig. 4 Relative contribution of the different sources of cadmium to human exposure, in percent *(108)*. – Fig. 4 Indicazione delle differenti origini del cadmio rispetto all'esposizione antropologica, in percentuale *(108)*.

1.1.2 Copper

In Greek times was named *chalkos* and in Roman times was *aes Cyprium* because a huge quantity was mined in Cyprus. It is used from 10000 years ago and by 5000 BC there are the first sign of smelting. The crustance abundace is 5.5 $+10^{-3}$% *(54)*. Its atomic number 29, atomic weight 63.546, electron configuration $[Kr]3d^{10}4s^{1}$and located in period 4 and group IB.

It is a reddish-coloured metal with a high electrical and thermal conductivity. There are two stable isotopes ^{63}Cu (69.1 atomic abundance %) and ^{65}Cu (30.1 atomic abundace %) and a dozen of radioisotopes *(54)*. It multiple oxidation states, the less stable is Cu^{+1} and the more stable is Cu^{+2}. It can form carbonates: $Cu_3(CO_3)_2(OH)_2$ (azurite) and $Cu_2CO_3(OH)_2$ (malachite); sulfates: $CuSO_4$ and $CuSO_4*5H_2O$ (chalcanthite); sulfides: $CuFeS_2$ (chalcopyrite), Cu_5FeS_4 (bornite), CuS (covellite), Cu_2S (chalcocite) and oxides: Cu_2O (cuprite) and CuO (tenorite) *(48)*.

Copper is usually found in association with sulfur. Pure copper metal is generally produced from a multistage process, beginning with the mining and concentrating of low-grade ores containing copper sulfide minerals, and followed by smelting and electrolytic refining to produce a pure copper cathode.

Copper is one of the oldest metals ever used and has been one of the most important materials in the development of civilization. Because of its properties, high ductility, malleability and thermal and electrical conductivity, and its resistance to corrosion, it has become a major industrial metal, third for importance after iron and aluminium *(107)*.

Smelting is the pyrometallurgical process used to produce copper metal. Recently, the trend to recover copper directly from ores through leaching processes has been on the increase. Nowadays the technology to refine the copper production is improved thanked to the use of the solvent extraction-electrowinnig (SX-EW) technology.

Copper is the best non-precious metal conductor of electricity because it can resist to creeping and corrosion. Electrical uses of copper are: power transmission and

generation, building wiring, telecommunication, electrical and electronic products. Such technologies will contribute to improving energy efficiency, reducing greenhouse gas emission and increasing living standards in rural areas.

It is used in the optical fibre for the communications, especially for personal computers and local area networks. Semiconductor manufacturers recently launched revolutionary "copper chip". By using copper for circuitry in silicon chips, microprocessors are able to operate at higher speeds, using less energy. Moreover, it is used for the building roofing because of its resistance to extreme weather conditions. Copper is also used for plumbing, taps, valves and fittings *(72)*.

In nature copper phosphates occurs as torbenite $Cu(UO_2)_2(PO_4)_2*10H_2O$, and metatorbenite $Cu(UO_2)_2(PO_4)_2*8H_2O$, which are usually found in gossans of veins carrying Cu sulfides and uraninite. Moreover these two phosphates are also found with secondary uranium minerals. In acidic environments libethenite $Cu_2(PO_4)OH$, tagilite $Cu_2(PO_4)OH*H_2O$ and nissonite $CuMg(PO_4)OH_21/2H_2O$ are the probable phosphates. In alkaline environments the stable phosphate are pseudomalachite $Cu_5(PO_4)(OH)_4$, cornetite $Cu_3(PO_4)(OH)_3$ and vesezelyte $CuZn_2(PO_4)(OH)_3*2H_2O$ *(113)*.

In less than 30 years, South America and in particular Chile, has emerged as one of the world's major suppliers of refined copper metal, at the same way Asia increased its production of 800% in the same period, mostly in Japan (Tab. 2).

Country	Refinery production		Reserves[b]	Reserves base[c]
	2003	2004[a]		
United States	1.120	1.160	35.000	70.000
Australia	830	850	24.000	43.000
Canada	558	560	7.000	20.000
Chile	5	5.380	140.000	360.000
China	610	620	26.000	63.000
Indonesia	979	860	35.000	38.000
Kazakhsthan	485	485	14.000	20.000
Mexico	361	400	27.000	40.000
Peru	831	1.000	30.000	60.000
Poland	495	500	30.000	48.000
Russia	675	675	20.000	30.000
Zambia	330	400	19.000	35.000
Other countries	1.400	1.600	60.000	110.000
World total (rounded)	13.600	14.500	470.000	940.000

[a] estimated.
[b] it is refer to the in-place copper content of ores that can be mined and processed at profit.
[c] it is encompassed the reserves proper, marginally economic reserves and a discretionary part of subeconomic resources.

Tab. 2 Worldwide refinery production of Cu, Reserves and Reserves Base *(108)* – Tab. 2 Produzione mondiale di Cu, riserve e riserve sub - economiche *(108)*.

1.1.3 Lead

Lead is one of the oldest metal used by mankind and its abundant in the crust is about 1.3 $*10^{-3}$ % *(47)*. Chemically its atomic number is 82, atomic weight 207.19, electron configuration $[Kr]4f^{14}5d^{10}6s^{2}6p^{2}$, located in period 6 and group IVA. It is the most corrosion resistant of the common metals; buildings built in Europe for centuries ago still stand under their original lead roof. It is very dense, ductile, malleable, corrosion resistant blue-gray metal that has been used for at least 5000 years. It is a poor conductor of electricity.

It has four stable isotopes: ^{204}Pb, ^{206}Pb, $^{207}Pb$and ^{208} Pb from ^{238}U, ^{235}U and ^{232}Th; radioactive precursor is not known for ^{204}Pb *(54)*.

Lead occurs in the sulfide mineral galena (PbS) and occurs with vanadium, called vanadinite. Anglesite ($PbSO_4$) is sometimes a mineral with gem quality.

White lead is a basic carbonate, $Pb_3(OH)_2(CO_3)_2$, used as a white pigment in paint until concerns about lead toxicity brought a halt to most such uses, called Cerrusite. Crocoite, $PbCrO_4$, is used (chrome yellow) as a pigment *(87)*. Another form of carbonate is the phosgenite, $PbCO_3$.

The organic lead compound tetraethyl lead, $Pb(C_2H_5)_4$ was widely used as a gasoline additive to prevent knock in the car. Lead forms a thin surface layer of oxide in air, which slowly changes to a basic carbonate. Lead monoxide, PbO, called litharge is made by heating lead in air. It is a yellow powder or yellowish-red crystalline material which is used in making lead glass. Red lead, Pb_3O_4, can be made by heating lead in oxygen and it is used for glass and red paint for protecting iron and steel structure. The Plattnerite, PbO_2, is widely used in lead storage batteries.

Lead emissions are most uniformly distributed over space, because they are associated with the input of road transportation, whereas emission in Europe is connected with non ferrous metallurgy and fuel combustion. Lead in gasoline has been virtually phased out to eliminate the health hazard. The annual production of lead is decreasing (Tab. 3) *(108)*.

Country	Refinery productio		Reserves[b]	Reserves base[c]
	2003	2004[a]		
United States	460	440	8.100	20.000
Australia	694	680	15.000	28.000
Canada	150	80	2.000	9.000
China	660	950	11.000	36.000
Kazakhsthan	40	44	5.000	7.000
Mexico	140	150	1.500	2.000
Morocco	38	41	500	1.000
Peru	308	300	3.500	4.000
South Africa	40	36	400	700
Sweden	50	61	500	1.000
Other countries	370	370	19.000	30.000
World total (rounded)	2.950	3	67.000	140.000

[a] estimated.
[b] it is refer to the in-place lead content of ores that can be mined and processed at profit.
[c] it is encompassed the reserves proper, marginally economic reserves and a discretionary part of subeconomic resources.

Tab. 3 Worldwide refinery production of Pb, Reserves and Reserves Base (www.minerals.usgs.gov/minerals/pubs/mcs/) – Tab. 3 Produzione mondiale di Pb, riserve e riserve sub - economiche *(108)*.

The major use of lead is in lead-acid storage batteries. There are eight broad categories of use: batteries, petrol additives (no longer allowed in the EU), rolled and extruded products, alloys, pigments and compounds, cable sheathing, shot and ammunition *(102)*. The electrical system of vehicles, ships, and aircraft depend on such batteries for start-up, and in some cases, batteries provide the actual motive power. Other batteries provide standby electrical power for emergencies, and very large lead-acid systems are designed to provide "peaking" power in such applications as commercial power networks and subway systems. Non-transportation uses for lead include increasing use for soundproofing in office buildings, schools and hotels. It is widely used in hospital to block X-ray and gamma radiation and is employed to shield against nuclear radiation both in permanent installations and when nuclear material is being transported.

Lead is among the most recycled non-ferrous metals and its secondary production has therefore grown steadily in spite of declining lead prices *(70)*.

Pyromorphite $Pb_5(PO_4)_3(OH)$ is the most stable minerals in neutral to acid environments and it is the one most encountered in supergene environments. His great stability explains his widespread geological occurrence. On the contrary a decrease in Pb

concentration lead to the formation of hindsalite $PbAl_3(PO_4)(OH)_6SO_4$, corkite $PbFe_3^{3+}(PO_4)(OH)_6$-SO_4 or plumbogummite $PbAl_3(PO_4)_2(OH)_5*H_2O$. Corkite and hindsalite are the stable association in alkaline environments, in particular at low P concentrations. Plumbogommite is formed in alkaline environments with an high concentration of Al, expected in weathering environments where Al is a mobile component. Plumbogummite and pyromorphite are found in association with cerrusite $PbCO_3$ and anglesite $PbSO_4$ *(117)*.

1.1.4 Zinc

Zinc is the 23rd most common elements in the earth's crust (0.02%), found in the air, soil and water. Chemically: atomic number 30, atomic weight 65.38, electron configuration $[Kr]3d^{10}4s^2$, located in period 4 and group IIB. In its pure elemental form, it is a bluish – white shiny metal. Most zinc ore found naturally in the environments is in the form of zinc sulfide. It is an essential element for life when present in trace amounts.

Generally zinc is not found as elemental form and it has as stable isotopes: 64 (48.9 atomic abundance %), 66 (27.8 atomic abundance %), 67 (4.1 atomic abundance %), 68 (18.6 atomic abundance %) and 70 (0.6 atomic abundance %) *(54)*. Its electron configuration is $3d^{10}4s^2$ forming tetraedric complex *(134)*. Zinc occurs in ores as sulfide: its main compound are: Sphalerite (ZnS) which is the typical mineral for the extraction with the Smithsonite $ZnCO_3$ and Hemimorphite (Calamine) $Zn_4[(OH)_2Si_2O_7]…H_2O$ *(47)*.

Its major uses are for galvanizing steel, producing alloys, and for serving as an ingredient in rubber, ceramics and paints. Zinc compounds are also used to preserve wood and in manufacturing and dyeing fabrics. They are used also by the drug industry as ingredients in some common products, such as sun blocks, diaper rash ornaments, deodorants, athlete's foot preparations, acne and poison ivy preparations and anti-dandruff shampoos.

Most zinc enters the environment as the result of human activities, such as mining, purifying of zinc, lead, and cadmium ores, steel production, coal burning, and burning of wastes. Zinc is mined in more than 50 countries and is produced as metal and compound in about 40 countries (Tab. 4 and Fig. 5) *(108)*.

Country	Refinery production		Reserves[b]	Reserves base[c]
	2003	2004[a]		
United States	738	770	30.000	90.000
Australia	1.480	1.300	33.000	80.000
Canada	1.000	1.000	11.000	31.000
China	1.650	2.000	33.000	92.000
Kazakhsthan	395	400	30.000	35.000
Mexico	460	420	8.000	25.000
Peru	1.250	1.400	16.000	20.000
Other countries	2.040	1.810	59.000	87.000
World total (rounded)	9.010	9.100	220.000	460.000

[a] estimated.

[b] it is refer to the in-place zinc content of ores that can be mined and processed at profit.

[c] it is encompassed the reserves proper, marginally economic reserves and a discretionary part of subeconomic resources.

Tab. 4 Worldwide refinery production of Zn, Reserves and Reserves Base *(108)* – Tab. 4 Produzione mondiale di Zn, riserve e riserve sub - economiche *(108)*.

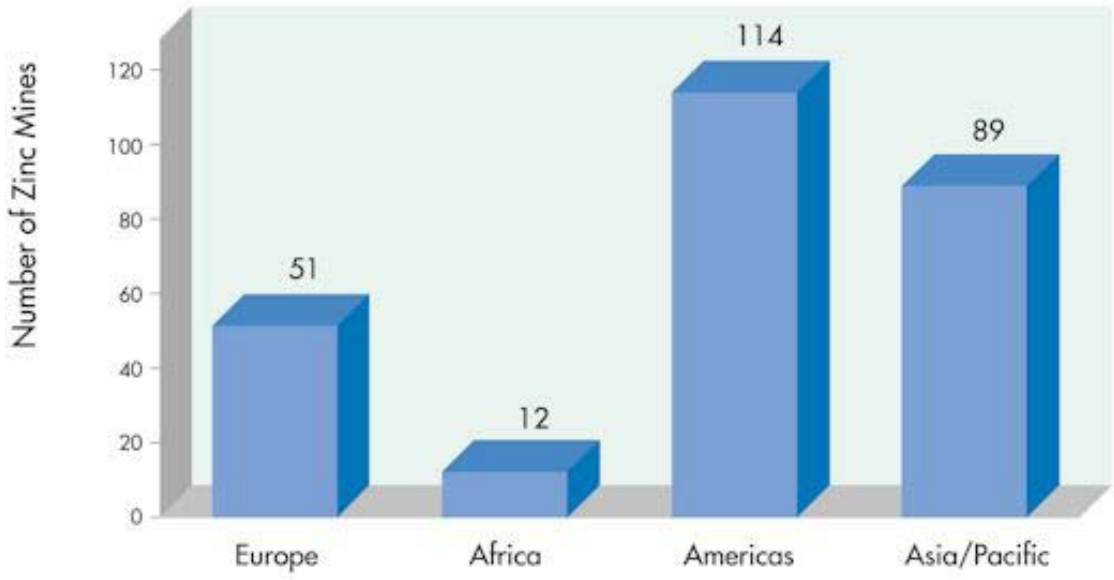

Fig. 5 Zn mines in the world (2003) *(108)*. – Fig. 5 Miniere di Zn nel mondo (2003) *(108)*.

1.2 HEAVY METALS AND THEIR TOXICITY

The emissions of heavy metals to the environment occur via many processes and pathways like combustion, extraction and runoff. Moreover atmospheric emissions tend to

be of greatest concern in terms of human health, the quantities and the widespread dispersion and potential for exposure.

The concentration of metals is not indicative of contamination and small amount of these elements are actually necessary for good health, but large amount of them may cause acute or chronic toxicity. Metals associated with the aqueous phase soils are subject to movement with soil, water and maybe transported through the vadose zone to ground water. Metals cannot be degraded but some of them can be transformed to other oxidation states in soil, reducing their mobility and toxicity.

People may be exposed to potentially harmful chemical, physical and biological agents in air, food, water or soil. Heavy metals become toxic when they are not metabolized by the body and accumulate in the soft tissues.

Heavy metal toxicity can result in damage or reduced mental and central nervous function, lower energy levels and damage to blood composition, lungs, kidneys, liver and other vital organs. Long-term exposure may result in slowly progressing physical, muscular dystrophy, and multiple sclerosis.

The main treats to human health from heavy metals are associated with exposure to lead, cadmium, mercury, arsenic and so on. These metals and others have been regularly studied and their effects on the human health and consequently reviewed by international structures like WHO (World Health Organization).

1.2.1 Cadmium

Cadmium derives its toxicological properties from its chemical similarity to zinc, an - essential micronutrient for plants, animals and humans. Cadmium is bio-persistent and, once absorbed by an organism, remains resident for many years (over decades for humans) although it is eventually excreted.

The United Nations ratified a treat (2003) to protect the quality of the air reducing the emission of cadmium, lead, and mercury and it was signed by 18 countries (EU, USA and ecc.). FAO (Food and Agriculture Organization)/WHO recommend the human weekly intake for cadmium in food remains at 7 μg/Kg of body weight *(124)*.

In general, the major exposure pathway is through food, via the addition of cadmium to agricultural soil from various sources (mainly atmospheric deposition and

fertiliser application) and uptake by food and fodder crops. Additional exposure to humans arises through cadmium in ambient air and drinking water *(74)*.

In humans, cadmium long-term exposure is associated with renal dysfunction. High exposure can lead to obstructive lung disease, kidney damage and has been linked to lung cancer, although data concerning the latter are difficult to interpret due to compounding factors. A first sign of the renal lesion is a tumural dysfunction with the increased excretion of low molecular weight protein or enzymes. Long-term exposure may also produce bone defects (osteomalacia, osteoporosis) in humans and animals. A first case was reported from Japan, where the Itai-Itai (ouch-ouch) disease was discovered in 1950s *(74)*. The malady was caused by the cadmium-contaminated water used for the local irrigation of rice fields. In addition, the metal can be linked to increased blood pressure and effects on the myocardium in animals, although most human data do not support these findings *(88)*.

1.2.2 Copper

Copper is an essential nutrient, his low and high quantity can cause a variety of symptoms and maladies. It is involved in the absorption, storage and metabolism of iron. It can be absorbed by the stomach and small intestinal mucosa. The excess of copper is rare but can occur and its toxicity has been the subject of great concern in recent years and it normally occurs in drinking water from copper pipes *(65)*.

High copper levels, especially associated with low zinc levels produce problems are stress and anxiety states, joint and muscle pains, psychological depression, mental fatigue, poor memory, lack of concentration, insomnia, manic depression, epilepsy, hypertension, preeclampsia of pregnancy *(119)*.

In particular, copper excess builds up in the liver and consequently can invade other tissues and organs. Clinical manifestations of copper excess are: cirrhosis of the liver, hemolytic anemia, neurological abnormalities and corneal opacities. The excess in the eye could cause a genetic disorder, the "Wilson's disease" *(66)*. Generally, copper accumulates if the metabolism slows down. In pregnant woman the excess can be transferred to the foetus and the baby might have bowel problems, allergies, asthma and skin problem.

Gastrointestinal disturbances and liver toxicity have also resulted from long-term exposure to contaminated drinking water *(67)*.

1.2.3 Lead

High lead levels in the environment arises from both natural and anthropogenic sources in roughly equal proportion. Exposure can occur through drinking water, food, air, soil and dust from old paint containing lead. Earlier lead exposure was due to the use the pots used for cooking and storage. Lead has been used for at least 5000 years in building materials, pigments for glazing ceramics and pipes for transporting waters. In ancient Rome lead acetate was used for sweetening old wine and perhaps the amount could have be a gram of lead per day. During the last century lead emission was mainly petrol.

Human exposure to lead can result in a wide range of biological effects depending on the level and duration of exposure. In general, in adult population the major exposure pathway is from food and water. Food, air, water and dust/soil are the major potential exposure pathways for infants and young children. For infants up to 4 or 5 months of age, air, milk formulae and water are the significant sources. In adult people lead can accumulate in lungs, whereas in the children the absorption is via the gastrointestinal tract and can penetrate the barrier blood-brain which is more permeable than in the adults. Half-life of lead in blood is 1 month and in the skeleton is about 20-30 years.

Various effects occur over a broad range of doses, with the developing foetus and infant being more sensitive than the adult. First symptoms are headache, irritability, abdominal pain and other symptoms related to the nervous system. High levels of exposure may result in toxic biochemical effects in humans which in turn cause problems in the synthesis of haemoglobin, effects on the kidneys, gastrointestinal tract, joints and reproductive system, and acute or chronic damage to the nervous system. Lead encephalopathy is characterized by sleeplessness and restlessness. Long time exposure may people suffer memory deterioration, prolonged reaction time and reduce ability to understand. An average level of about 3 μmol/L in the blood can show peripheral nerve symptoms with reduction of the nerve conduction velocity and reduced dermal sensibility. Moreover blood lead level in children below 10 μmg/dl have been considered acceptable for long time, but recently some data indicate that there may be toxicological effects of lead at lower levels of exposure *(74)*.

Lead poisoning, which is so severe as to cause evident illness, is now very rare indeed. At intermediate concentrations, however, there is persuasive evidence that lead can have small, subtle, sub-clinical effects, particularly on neuropsychological developments in children.

Although most people receive the bulk of their lead intake from food, in specific populations other sources may be more important, such as water in areas with lead piping and plumbosolvent water, air near point of source emissions, soil, dust, paint flakes in old houses or contaminated land. Lead in the air contributes to lead levels in food through deposition of dust and rain containing the metal, on crops and the soil *(87)*.

1.2.4 Zinc

Zinc is an important trace element and in the human body is nearly as abundant as iron (1.5-2.5 g). It is concentrated in specialized areas of the brain, pancreas and adrenal gland and it is also present in all cells. It is an antioxidant, necessary for protein synthesis and wound healing. It is useful for the development of the reproductive organs, prostate functions and it governs the contractility of muscles; so that it results less dangerous compared the previous heavy metal. It is used in topical medication. Moreover it is useful to contrast the absorption of other metals It is recommended to ingest about 10 (male) – 12 (female) mg/day, emetic effect occurs at > 150 mg/day. The toxicity is very rare, but it is characterized by gastric distress, dizziness and nausea. Symptoms of chronic toxicity include gastric problems, decreased serum ceruloplasmin activity and hypocupremia, decreased lymphocyte stimulation to LDL (low density lipoprotein) and reduced HDL (high density lipoprotein) cholesterol *(45)*.

2 MATERIALS

2.1 SYNTHETIC PHOSPHATES

2.1.1 Hydroxyapatite

The used synthetic hyroxyapatite (HA) named from Alfa Aesar as a "Calcium phosphate tribasic" has formula $Ca_{10}(OH)_2(PO_4)_6$ with an amount of Ca about 34-40%. This material is typically made by neutralizing slaked lime [Ca(OH)2] with phosporic acid.

HA was analyzed by XRD, SEM-EDS, FTIR and AFM (Atomic Force Microscopy).

The XRD shows the usual peaks, characteristic of hydroxyapatite (Fig. 1). An extra XRD analysis was made at the Earth Science Department of Miami University (Oxford, OH-USA) and comparing the HA from Alfa Aesar and the one from Biorad. The former's diffraction peaks are broader and less intense than the latter one, meaning an HA less crystallized and it may react in a different way from other apatites like BioRad.

The SEM micrographs always show two kind of morphology: a spherical shape (Fig. 2A) and sometimes a flat sheet, not the characteristic hexagonal plate-like (Lower et al. *(90)*). EDS analysis (Fig. 2B) confirms the composition of HA (Ca, P and O), unfortunately it is not possible to define if it is monoclinic *($P2_1/b$)* or hexagonal *($P6_3/m$)*.

Generally, the FTIR band for OH and PO_4 correspond well with peak position of a synthetic HA (Fig. 3).

Studying HA through AFM it was possible to study in detail the particles with a major magnification and to measure their dimensions (Fig. 4 A and B). HA shows a spherical shape with a standard dimension of about 170 nm.

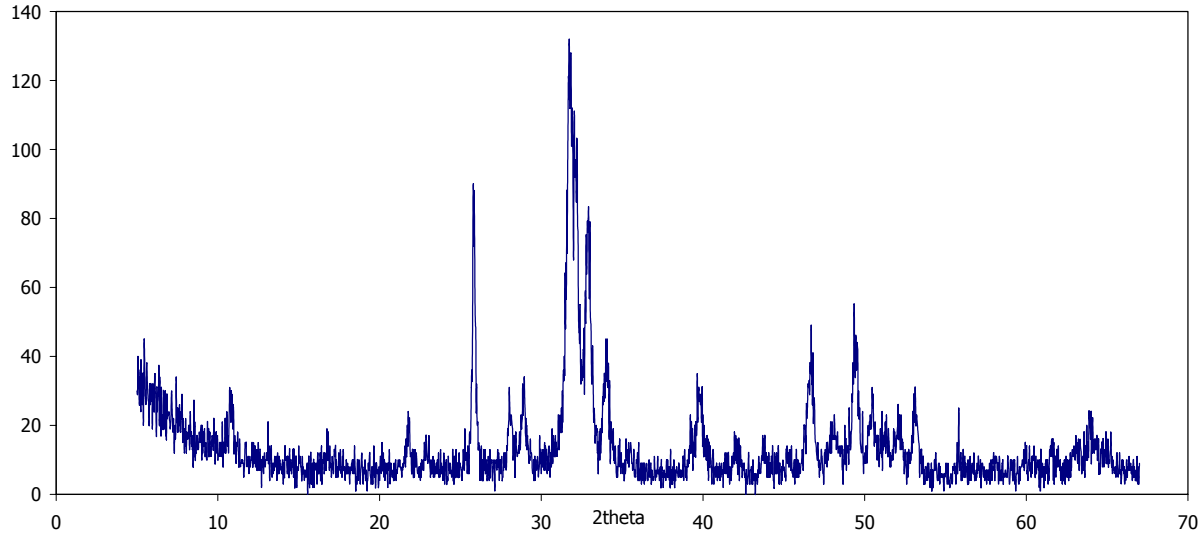

Fig. 1: XRD of synthetic HA from Alfa Aesar. – Fig. 1: Raggi X sull'HA prodotta dall' Alfa Aesar.

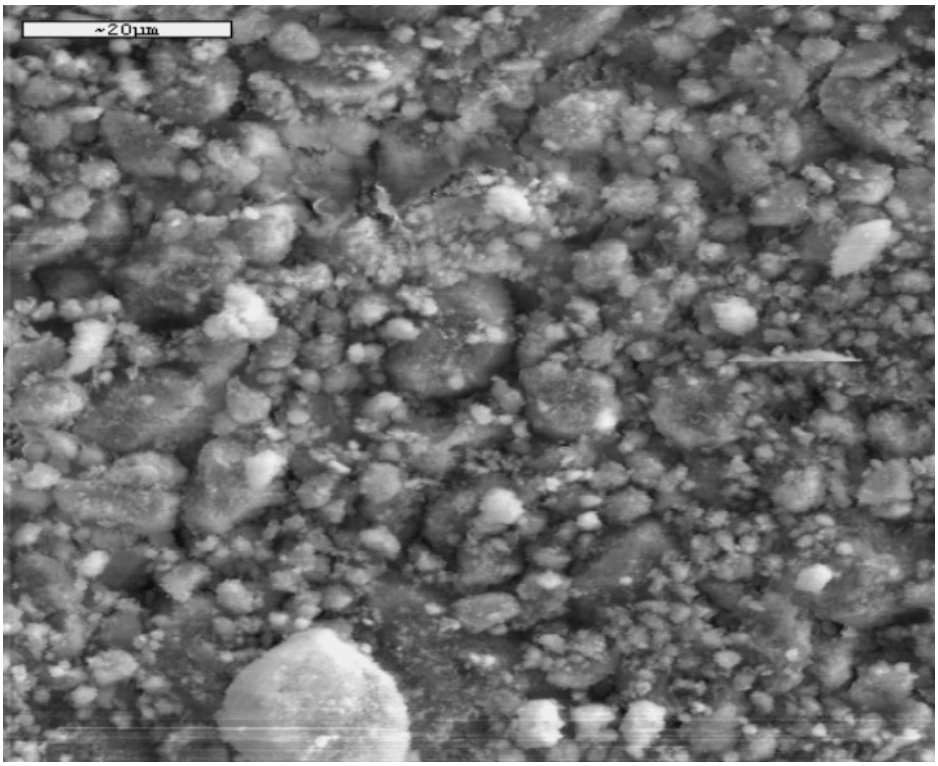

A

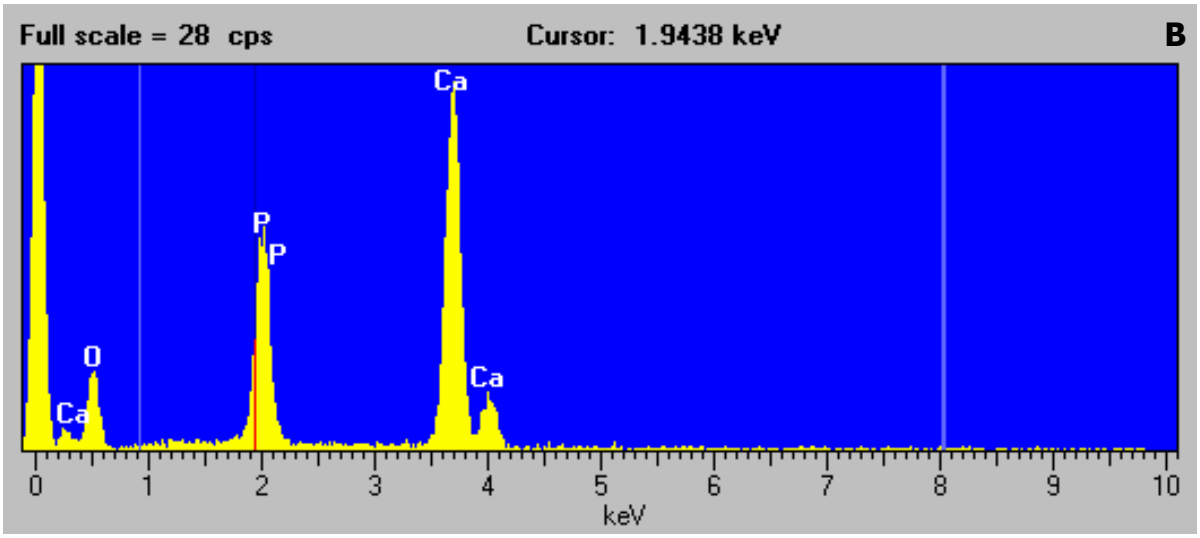

Fig. 2 A: SEM micrograph of the synthetic HA. B: EDS analysis. – Fig. 2 A: Immagine al SEM dell'HA. B: analisi EDS.

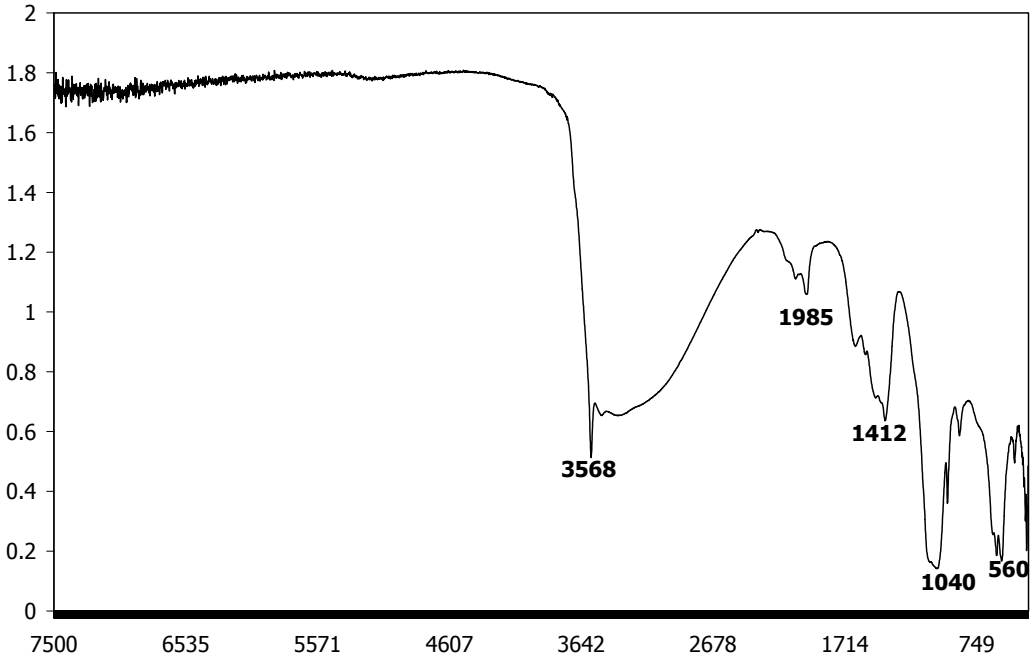

Fig. 3 FTIR spectrum of HA. – Fig. 3 Spettro FTIR dell'HA

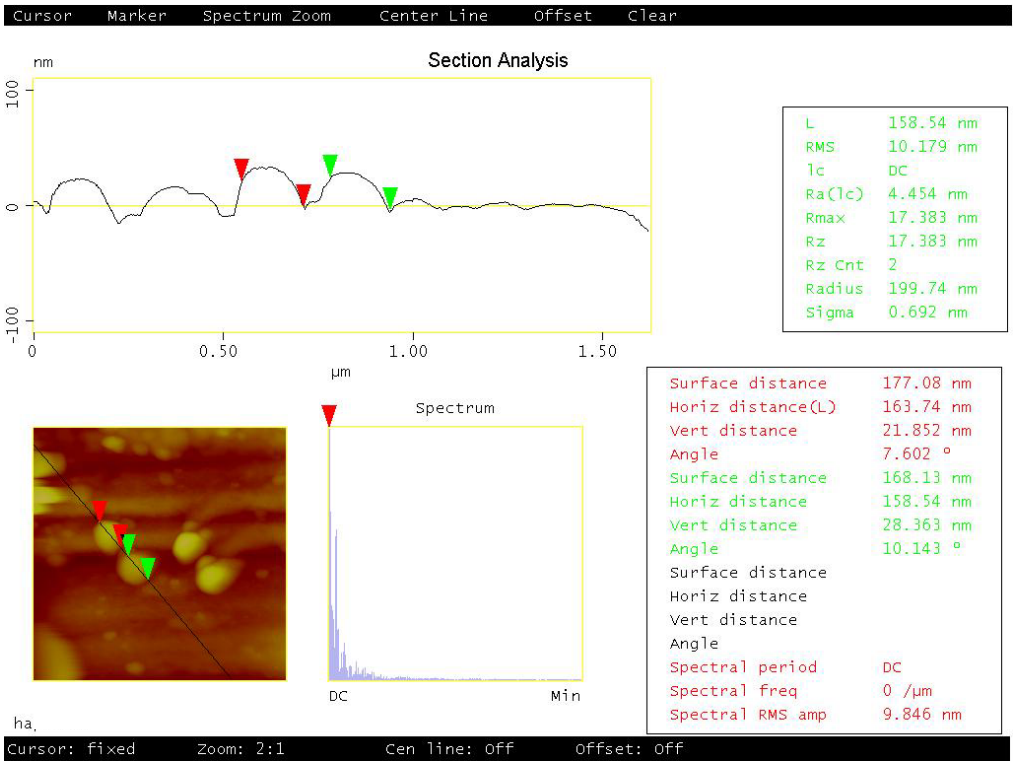

A

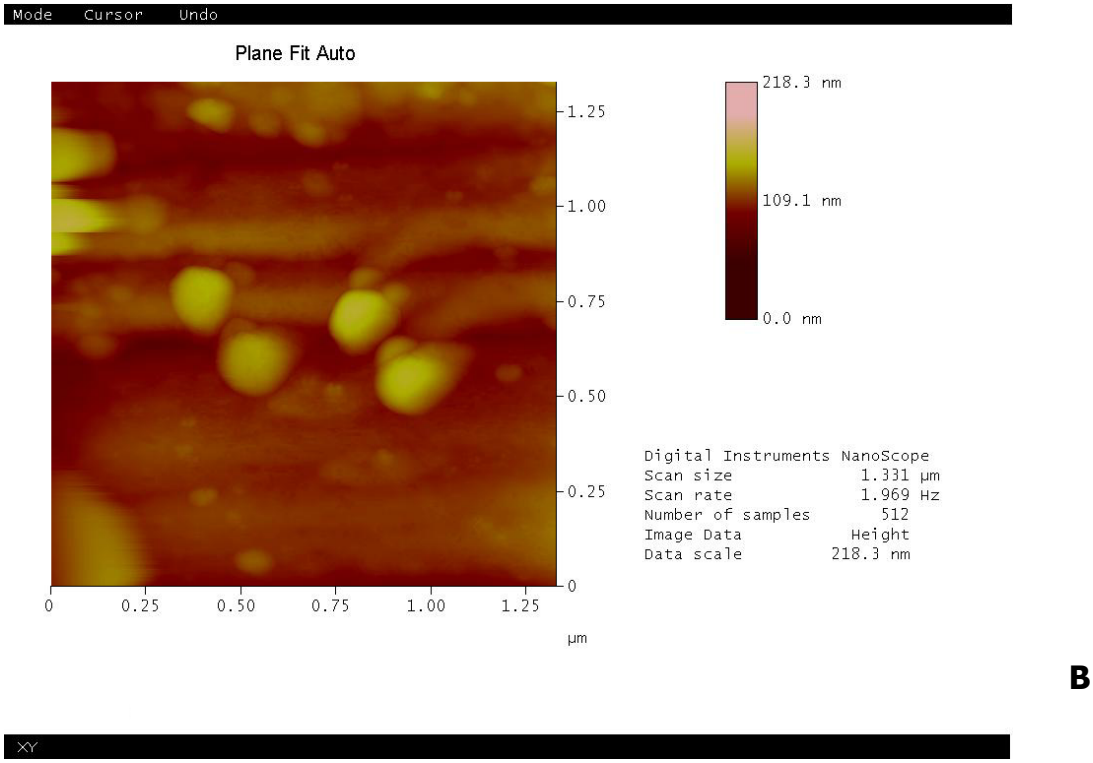

Fig. 4 A: AFM Measure of the HA particles. B: AFM Imagine of HA particles. – Fig 4 A: Misura della dimensione di una particella di HA tramite AFM. B: Immagine di una particella di HA tramite AFM.

2.2 NATURAL PHOSPHATES

As natural phosphate two natural phosphate rocks were used, a fluoroapatite from Florida and one from Morocco. Generally, natural material is less crystalline than synthetic one.

2.2.1 Fluroapatite from Florida

The phosphate rock from Florida is from CF Industries, Inc (Plant city, FL-USA). The chemical analyses from the Company says it is a carbonate-fluoroapatite, an additional chemical analysis was made at Activation Laboratories LTD. (Tab. 1). SEM micrographs shows always semi-rounded particles and EDS confirms the presence of element like F, Ca and P (Fig. 5 A and B). On the contrary AFM analyses show a more rounded particle, because of the magnification, with a dimension of about 500 nm (Fig. 6 A and B).

Analyte symbol (ppm)		Analyte symbol (ppm)		Analyte symbol (ppm)		Analyte symbol (%)	
Cd	2.7	Sc	<1	Nd	68.3	Cl	<0.01
Cu	7	Be	<1	Sm	14.1	F	0.01
Ni	12	V	63	Eu	3.3	Hg	44
Zn	23	Cr	40	Gd	15.5	SO_4	0.95
S	0.63	Co	<1	Tb	2.43	SiO_2	11.61
Ag	<0.3	Ga	3	Dy	14.9	Al_2O_3	1.35
Pb	14	Ge	< 0.5	Ho	3.19	Fe_2O_3	0.99
		As	7	Er	9.57	MnO	0.027
		Rb	11	Tm	1.39	MgO	0.81
		Sr	999	Yb	8.4	CaO	42.12
		Y	139	Lu	1.3	Na_2O	0.63
		Zr	117	Hf	2.4	K_2O	0.27
		Nb	2.1	Ta	0.06	TiO_2	0.144
		Mo	5	W	<0.5	P_2O_5	27.81
		In	<0.1	Tl	0.93		
		Sn	<1	Bi	0.1		
		Sb	1.1	Th	6.64		
		Cs	0.8	U	89.2		
		Ba	81				
		La	83.5				
		Ce	124				
		Pr	16.1				

Table 1: Chemical composition of the fluoroapatite from Florida (USA)[1]. – Tabella 1: Composizione chimica della fluroapatite proveniente dalla Florida (USA).

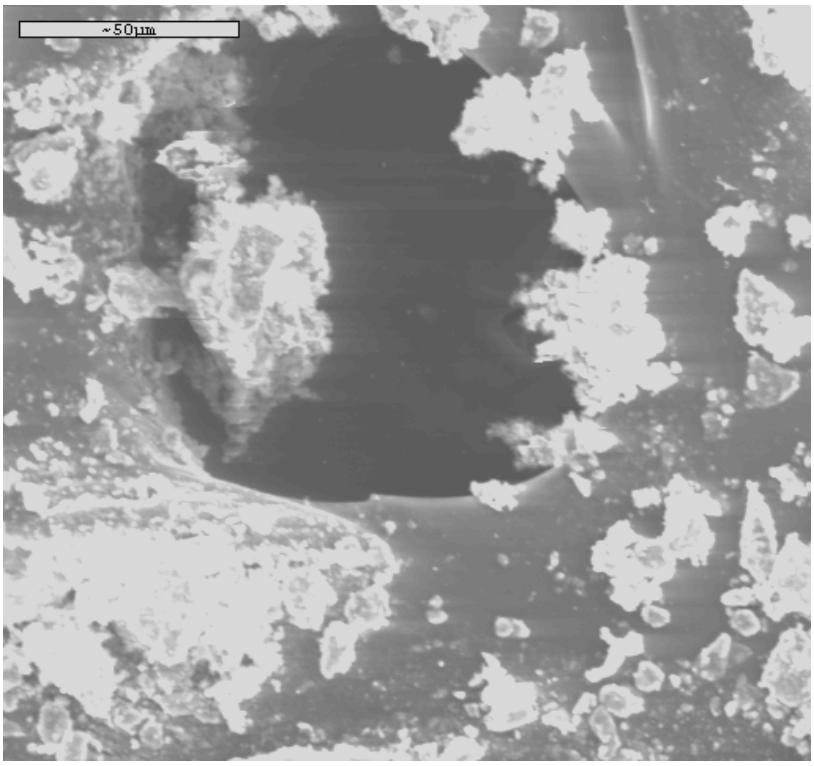

[1] The author wishes to thank Actlabs for their analyses on the fluoropyromorphite from Florida.

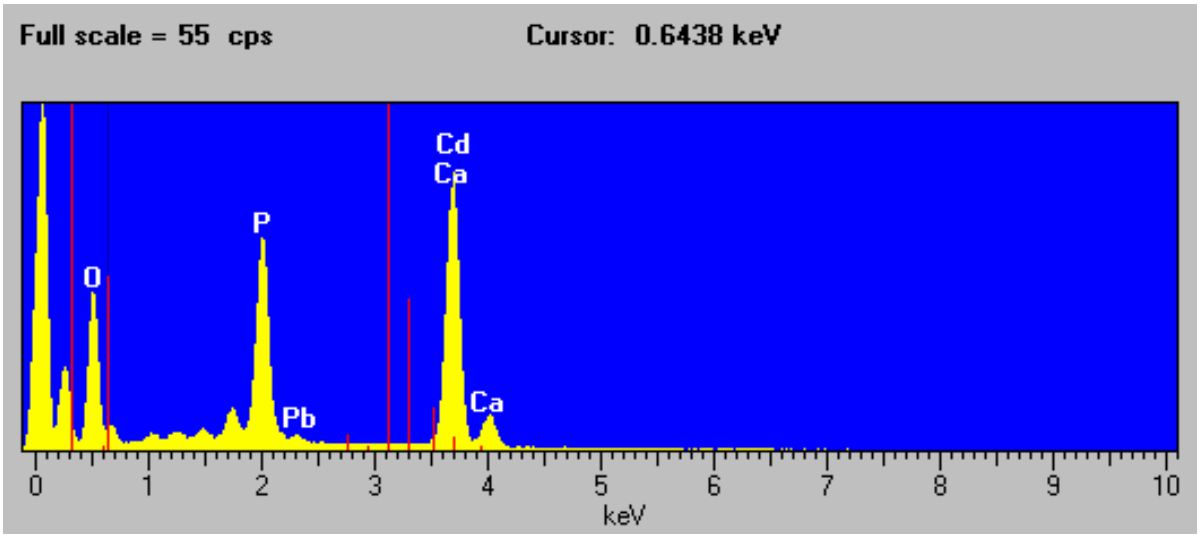

Fig. 5 A: SEM micrographs of FAP. B: EDS of FAP. – Fig. 5 A: Immagine al SEM di una particella di FAP. B: EDS di una particella di FAP

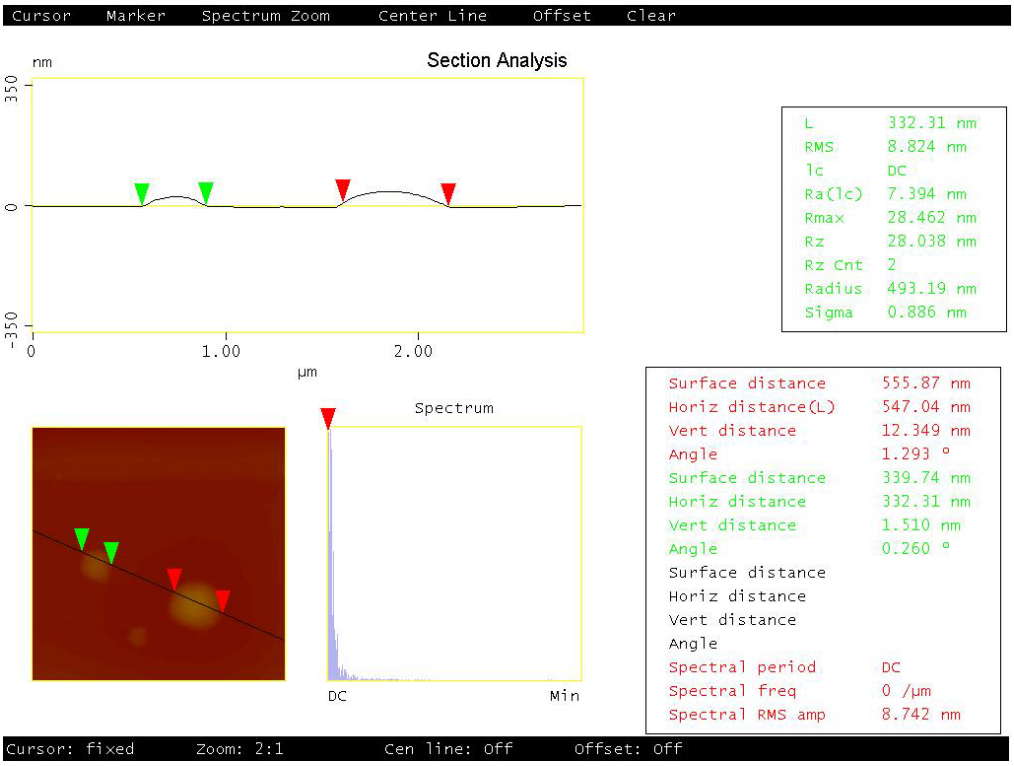

A

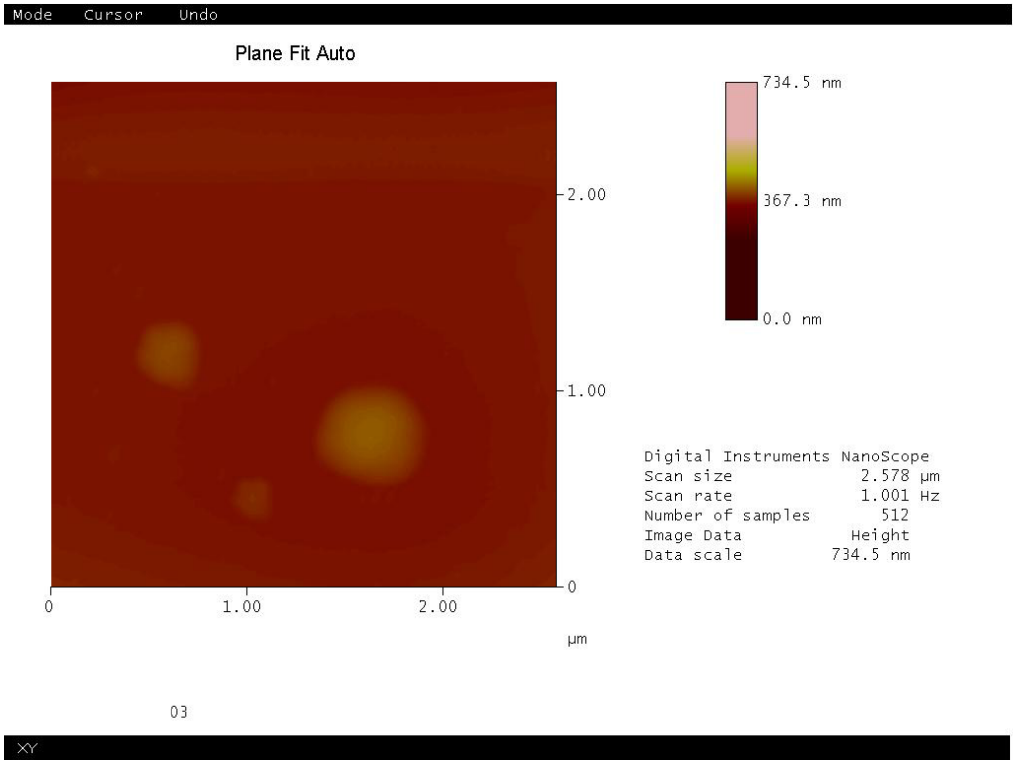

Fig. 6 A: AFM Measure of the FAP particles. B: AFM Imagine of FAP particles. – Fig 6 A: Misura della dimensione di una particella di FAP tramite AFM. B: Immagine di una particella di FAP tramite AFM.

The most significant tectonic feature in the district is a graben that developed in the Triassic. The graben, striking northeast across what is now the panhandle of Florida and South Georgia, connected the Gulf of Mexico with the Atlantic Ocean. The graben separated the crystalline rocks of the Piedmont from the carbonate Florida platform. Sediment began to fill the graben in the Jurassic, and had completely filled it by the early Cretaceous. Reactivation in the Palaeocene created the Gulf Trough. By the early Miocene, the sediments blocked the permanent circulation through the Gulf Trough and separated it from the Apalachicola Embayment. Eustatic sea-level rises may have reconnected it periodically but temporarily throughout the lower Miocene, and eventually the Gulf Trough ceased to exist. The most significant sedimentary section relating to Fullers Earth is the Hawthorne. The Hawthorne is considered a formation only in Florida and it measure more than 30 m in the Fellers Earth district and lies apparently conformably on top of the Tampa limestone. The Miccosukee Formation of upper Pliocene age overlies the Hawthorne unconformably. The origin of the rock is a sedimentary one, in particular it is called a land-pebble type of phosphate rock. Generally the bedrock is a mixture of a

limestone and dolomite, sand and clay, all with phosphate nodules. The bedrock comprise the Hawthorne Formation, lower and middle Miocene epoch which consists of fine to medium grained quartz sand, silt, calcareous sand and dolomite beds, phosphate materials and clay (Moll *(109)*).

The phosphate particles were organically and inorganically precipitated in a shallow sea. Probably the phosphate were carried by cool, near - shore currents and turbulently mixed with the warmer waters of the northward flowing Gulf stream. The cool waters were diverted into the warmer waters by anticlines or domes which were formed during the phosphate deposition process. Phosphate was deposited in the basin adjacent to the domes when the cool and warm waters mixed, thus promoting the deposition. The Bone valley formation of Late Miocene and early Pliocene epoch was deposited on the eroded surface of the underlying phosphatic Hawthorne formation by a transgressing sea which reworked and sorted the phosphatic residual mantle on the Hawthorne. Part of unleached limestone boulders were also phosphatized and formed a basal conglomerate, called "driftrock", which rested on or close to the surface of the Hawthorne formation. Meanwhile the upper Bone valley is deeply leached combining with clay, forming the aluminium phosphate and at the same tie the acid solutions attacked the bedrock, removing the carbonate and leaving behind a residuum enriched in phosphate. This residuum contained finer-sized phosphate and P_2O_5 can be mined if the concentration is cost-effective. The material in use is from the lower part of the Bone valley formation as well as the upper residual part of the Hawthorne formation[2].

2.2.2 Fluroapatite from Morocco

The two Moroccan phosphate rocks were sampled in 2004 near the Youssofia town.

The main constituent of Youssofia ore is apatite associated with clayey and siliceous minerals, sulphates and organic matter. This phosphate has an hexagonal structure ($P6_3/m$) (Laghzizil et al. *(81)*) in particular, the apatite is a fluoroapatite which is the most stable and insoluble of the calcium phosphates of B-type $Ca_{10-z}(PO_4)_{6-x}(CO_3)_xF_{2+x-2z}$. Numerous substitutions reactions are associated with the existence of tunnels which are a favoured paths, infact the ions in the tunnels are weakly bound to the rest of the lattice

[2] CF Industries (Florida)

(Bilali et al. *(14)*). chemical analysis for the two kind of rocks was made at Activation Laboratories LTD. (Tab. 2). The two sampled phosphate rocks are different in colour, one is dark because of the amount of organic material and the second is white. For the experiments, the dark fluoroapatite was used, which contains the highest amount of P. SEM micrographs show rounded particles and EDS analysis show the presence of F, P and Ca (Fig. 7).

Analyte symbol (ppm)		Analyte symbol (ppm)		Analyte symbol (ppm)		Analyte symbol (%)	
Cd	50.3	Sc	9	Nd	31.9	Cl	0.05
Cu	26	Be	<1	Sm	6.73	F	7.91
Ni	61	V	207	Eu	1.83	Hg	33
Zn	568	Cr	270	Gd	8.74	SO_4	1.23
S	1.05	Co	<1	Tb	1.45	SiO_2	2.61
Ag	1.8	Ga	2	Dy	9.68	Al_2O_3	0.36
Pb	<5	Ge	< 0.5	Ho	2.42	Fe_2O_3	0.09
		As	<5	Er	7.87	MnO	<0.001
		Rb	2	Tm	1.19	MgO	1.17
		Sr	1494	Yb	7.45	CaO	46.53
		Y	143	Lu	1.26	Na_2O	0.72
		Zr	18	Hf	0.6	K_2O	0.09
		Nb	0.5	Ta	<0.01	TiO_2	0.027
		Mo	19	W	0.5	P_2O_5	28.35
		In	<0.1	Tl	2.21		
		Sn	<1	Bi	<0.1		
		Sb	0.8	Th	2.04		
		Cs	0.3	U	91.1		
		Ba	54				
		La	51.5				
		Ce	24.6				
		Pr	7.09				

Table 2: Chemical composition of the fluoroapatite from Morocco[3]. – Tabella 1: Composizione chimica della fluroapatite proveniente dal Marocco.

[3] The author wishes to thank the Actlabs for theyr analyses on the fluoropyromorphite from Florida.

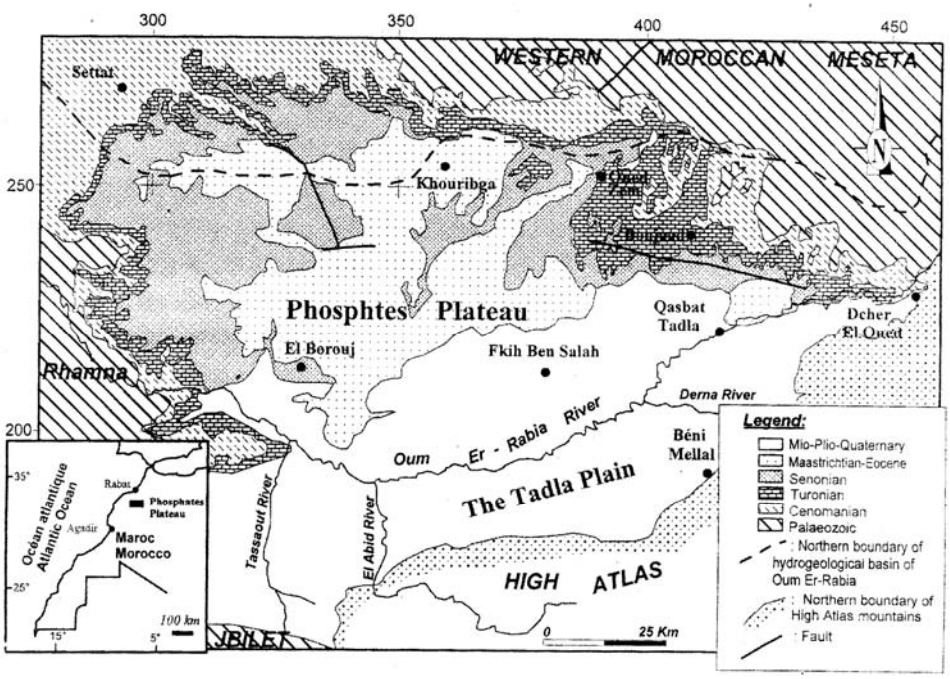

Fig. 7 Location and geological maps of the Phosphates plateau (Ettazzarini and El Mahamouhi, *(51)*). – Fig. 7 Schema geologico del Plateau dei fosfati (Ettazzarini and El Mahamouhi, *(51)*).

The Phosphate plateau is part of the central Moroccan Meseta and it outcrops in four basins, which are from NE to SW: Oulad Abdoun, Ganntour, Meskala and Bu - Craa. Their ages extend from Late Cretaceous (Maastrichtian) to the Middle Eocene (Lutetian) (Bardet et al. *(7)*).

The Phosphate basin of Oulad Abdoun, aged Cretacic – Eocene with well developed phosphogenesis phenomenon is limited to north and east from the Central Morocco Massif, to south from the High Atlas and to west from the Rehamna Massif. To S-E there is the Tadla basin the prolongation of the Ouled Abdoun basin.

The Phosphate plateau has an extension of about 80 Km (Khouribga), it shows an homogeneous facies but the stratigraphy is different. Close to Oued-Zem phosphates are more reddish and rich in clay, they are called "pozdolic phosphates" which means a meteoric alteration (Lucas et al. *(91)*).

In the north of the basin the Cretacic formation, attributed to the Cenomanian and Turonian, overlapped from the formation of the lower Senonian (yellowish marls). Maastrichtian seems to be in continuity with the Campanian and lower Senonian and it is constituted by carbonatic rocks, phosphatic marne and sand phosphates (Rahhali *(128)*).

In the plateau the phosphatic series, aged Maastrichtian from a bentic microfauna (*Siphogenerinoides idkysenis* Colom, *Flabelinella colomi* Rahhali and *Gavellinella* aff. Supracretacea Hofker), is made of bituminous marls and phosphatic marls; the series, aged Paleocene, is made of bituminous marls intercalated with phospatic bed (0.20 m) and rich of bone debris and coprolithes *(81)*.

The Youssofia basin is a platform basin, close to the flat continent and characterized by detritic deposits and biochemical deposits. The succession is a ritmique one and showing the eustatic variation and the deposits typical of an epi-continental sea. The facies are generally clay-marl during the Maastrichtian and the development of this level is opposite to the biochemical facies and to the Eocene facies, so that it seems the basin is filled up. The suitable conditions for the phosphate deposition were the cold water or light hot and a shallow sea (Bardet et al. *(7)*).

The series in Youssoufia is the biggest one (180 m), in particular the high amount of organic matter makes the phosphates black, this level is over the hydrostatic level. This phenomenon doesn't modify the series but it is considered a particular phenomenon. The colour is caused by the amount of organic matter trapped inside during the burying period (Montian and Maastrichtian eras). The total amount of organic matter is 3-4 wt% (Khaddor et al. *(78)*). This part of the series is considered the more richer, probably because of the anoxic conditions which has led the formation of pyrite and water helps to maintain this particular conditions and consequently the black colour (Boujo *(21)*). This black level is the medium one (W-E) and the contact with the white facies is not so well visible according to the piezometric level (fig. 8).

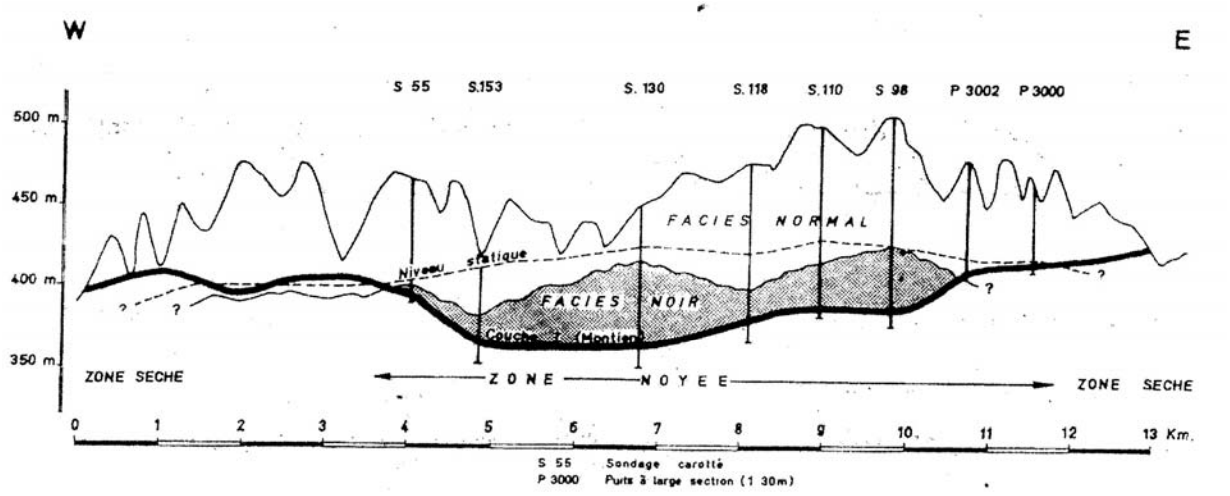

Fig. 8 Profile of the two series (black and white) near Youssoufia (Boujo, *(21)*). – Fig. 8 Profilo mostrante le due serie (bianca e nera) dei fosfati vicino Youssoufia (Boujo, *(21)*).

2.3 SOILS

Heavy metals-contaminated soils have been sampled in sulphide mines areas (tailing dumps, ore stocking areas, streams etc.) in Sardinia and Tuscany where the contamination source was the mining activity.

In south-western Sardinia the soils were collected from the area of the mines of S. Giovanni, Campo Pisano, Monteponi and Mt. Agruxau (southern Iglesiente). In southern Tuscany soils of the mining areas of the mines of Gavorrano, Boccheggiano, Campiano and Niccioleta were sampled.

2.3.1 Soil sampling

The soil sampling was carried out in two different ways. In Tuscany the sampling was aereal, the sampling interested the first centimetres (0 - 30 cm) of the soil whereas in Sardinia some cores were sampled (0 – 4 m and 60 m) and only for the red muds the sampling was aerial. The two different ways of sampling were aimed at determining if there is a difference of pollution and the successive heavy metal immobilization going from the first centimetres of the soil to the depth.

Bulk samples were sieved using a 63-μm mesh to separate the silt-clay (< 63 μm) size particles from the sand fraction. According to David, *(38)* only the silt-clay fraction was analyzed for metals, because in this fraction it is concentrated the highest amount of the heavy metals.

All the samples were analyzed by XRD to determine mineralogical composition and an aliquot (0.5 g) of soil was digested with HF and $HClO_4$ on an hot-plate. The obtained solution was analyzed by ICP-AES to determine chemical composition (Table 3).

	Cd (mg/L)	Cu (mg/L)	Pb (mg/L)	Zn (mg/L)
S1G vs. HA	33	277	14	664
S1G vs. FAP	33	277	14	664
S2G vs. HA	33	358	25	157
S3G vs. HA	458	2013	236	5731
S5Gc vs. HA	35	310	235	603
S5Gc vs. FAP	35	310	235	603
S6Gc vs. HA	4	8	24	31
S6Gc vs. FAP	4	8	24	31
S7N vs. HA	32	154	47	48
S7N vs. FAP	32	154	47	48
S10N vs. HA	27	32	185	14
S11N vs. HA	23	292	277	350
S11N vs. FAP	23	292	277	350
S12N vs. HA	19	34	53	11
S13N vs. HA	37	33	83	45
S14B vs. HA	40	9	177	15
S14B vs. FAP	40	9	177	15
S18aCP vs. HA	53	101	16	63
S18aCP vs. FAP	53	101	16	63
S18bCP vs. HA	7	35	356	454
S18bCP vs. FAP	7	35	356	454
S19aMP vs. HA	18	6	551	285
S19aMP vs. FAP	18	6	551	285
S19bMP vs. HA	119	100	53	2136
S19bMP vs. HA	119	100	53	2136
S20aSG vs. HA	78	12	17	1454
S20aSG vs. FAP	78	12	17	1454
S20bSG vs. HA	48	7	13	895
S20bSG vs. FAP	48	7	13	895
S21FG vs. HA	221	124	52	6984
S21FG vs. FAP	221	124	52	6984
S22MA vs. HA	232	303	28	2865
S22MA vs. FAP	232	303	28	2865

Table. 3: In the table are reported the amount of the four heavy metals in the sampled soils. G= Gavorrano mine; Gc= Campiano mine; N = Niccioleta mine; CP = Campo Pisano mine; MP = Monte Poni mine; SG = San Giovanni mine; FG = Red Muds and MA = Monte Agruxau mine; a= top of the core and b = end of the core. – Tabella. 3: Nella tavola sono elencate le quantità dei quattro elementi pesanti determinate tramite ICP-AES. G= Gavorrano mine; Gc= miniera di Campiano; N = miniera di Niccioleta; CP = miniera di Campo Pisano; MP = miniera di Monte Poni; SG = miniera di San Giovanni; FG = Fanghi rossi e MA = miniera di Monte Agruxau; a= tetto della carota e b = letto della carota.

2.4 TUSCANY

In the southern Tuscan district mining of base metals (mainly Hg and Sb), Fe oxides and pyrite deposits dates back to Etruscan age (e.g. Cipriani and Tanelli *(32)*). Such a protracted and extensive mining activity has left behind many abandoned mines

and mine wastes. Some pyrite deposits and polymetallic mineralizations are hosted in the "Filladi di Boccheggiano Fm" (Triassic (?) – Palaeozoic) and/or located at the contact between this formation and the overlying Calcare Cavernoso formation (late Triassic) of the Tuscan Nappe or at the contact with Pliocenic granitic bodies (e.g. Tanelli and Lattanzi *(144)*).

The Filladi di Boccheggiano consist of a number of tectonic slices, including Triassic (Anidriti di Burano, Formazione di Tocchi) and Paleozoic terrains, detached and piled up during the Appeninic orogeny.

In southern Tuscany the Tuscan Nappe stratigraphic sequence is locally omitted and subject to a strong tectonic elision during the Neogene time, with the juxtaposition of the Ligurian units on the basal Triassic evaporites and/or the Basement units, (*Serie Toscana Ridotta*).

The complete Tuscan Nappe sequence is exposed completely in the Gavorrano Ridge. Neogene clastic sequence border this sector and range in age from the upper Miocene to Lower Pleistocene.

Within the Gavorrano Ridge, the Tuscan Nappe outline a SSW-dipping bedding attitude, defining a monoclinal setting. The ridge is delimited by N-S striking, steeply dipping fault zones, which bring the Tuscan Nappe formations into contact with the allocthonous Cretaceous to Paleocene and Ligurian sediments with Neogene clastic deposits.

The metallic minerals are mainly pyrite with minor chalcopyrite, sphalerite and galena. General agreement exists about late Cenozoic, hydrothermal origin of copper-rich polymetallic mineralizations. However, for the genesis of the pyrite deposits some authors (e.g. Tanelli and Lattanzi *(133)*; Lattanzi et al. *(84)*) suggest a multistage process in which Palaeozoic (?) – Triassic (?) pyritic protores would have undergone strong remobilization during the tectonometamorphic Apenninic event.

2.4.1 Boccheggiano

Boccheggiano mining activity have taken place from the 19th century in lens enriched of pyrite at the contact between the "Filladi di Boccheggiano Fm" and the "Calcare Cavernoso". The Filladi Fm and Quarziti of Mersino represents part of the outcropping of the Filladica di Boccheggiano Fm and three main lithological associations

are distinguished: Gray to black phyllites and quartzites, Green quartzites and phyllites and Quartzitic metaconglomerates. These lithological associations show transitional contacts. The Alpine tectono-metamorphic events obliterated most of the pristine textures of these rocks (Fig. 9) (Costantini et al. *(34)*).

Deposits are constituted of massive pyrite and subordinately sphalerite with galena and chalcopyrite (Gregorio et al. *(63)*).

2.4.2 Campiano

This pyrite deposit occurs in Boccheggiano area. Campiano deposit is associated with a major tectonic lineament, the Boccheggiano fault, a normal fault with a NW-SE trend and extending dip-slip 45°NE (Fig. 10) (Benvenuti et al. *(10)*).

The footwall rocks belong to the Filladi di Boccheggiano formation, a phyllitic complex with interlayered sulphato-carbonatic masses, locally metasomatised to skarn.

The deposit is mainly formed of massive pyrite with less amount of Fe oxides important local amount of Cu – Pb – Zn sulfides in carbonatic, cloritic and quartzose gangue. The mineralogical association is: sphalerite, pyrite, pyrrothine, less amount of chalcopyrite and galena *(41)*.

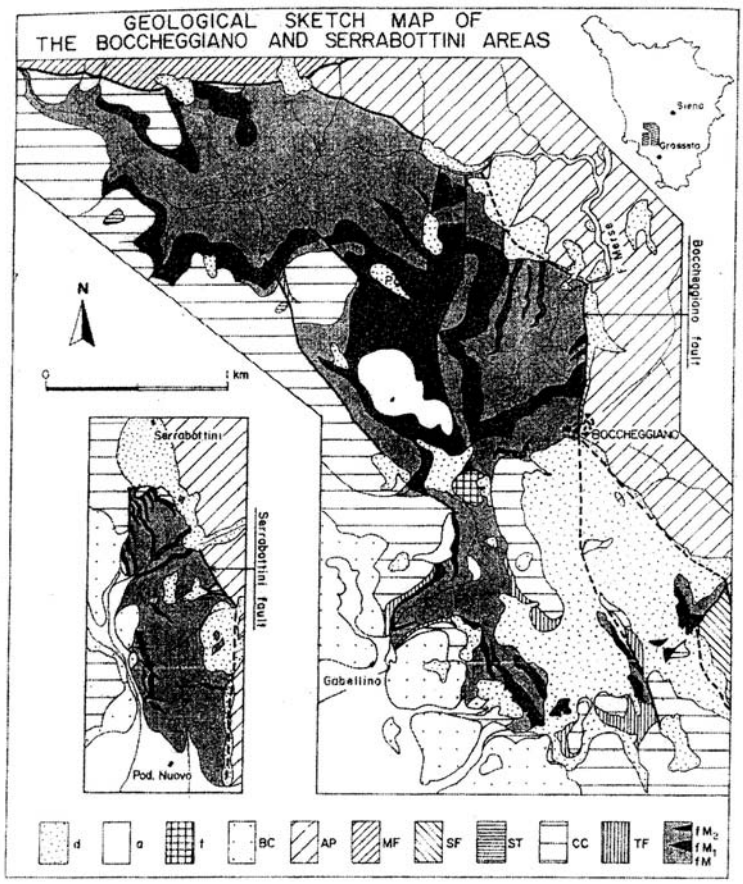

Fig. 9: d:Debris, dumps and oxidation zones, a: Alluvium and alluvial terraces, t: Travertines, BC: Neogene breccias, conglomerates and sands, AP: Argille con Calcari Palombini Formation (Early Cretaceous), MF: Monteverdi Marittimo Formation (Late Cretaceous), SF: St. Fiora Formation (Late Cretaceous), ST: Scaglia Toscana (Cretaceous-Early Oligocene), TF: Tocchi Formation (Carnian), Filladi and Quarziti del T. Mersino, fM: grey to black phyllites and quartzites, fM_1: green quartzites and phyllites, fM_2: quartzitic metaconglomerats (Costantini et al. *(34)*). - Fig. 9: d: Detrito, discariche e zone di ossidazione, a: Zone ad alluvium e terrazze alluvionali, t: Travertini, BC: Brecce neogeniche, conglomerati e sabbia, AP: Formazione argille con Calcari Palombini (Cretaceo inf.), MF: Formazione Monteverdi Marittimo (Cretaceo sup.), SF: Formazione S. Fiora (Cretaceo sup.), ST: Scaglia Toscana (Cretaceo-Oligocene inf.), TF: Formazione Tocchi (Carnico), Filladi e Quarziti del T. Mersino, fM: filladi e quarziti grigio-nere, fM_1: quarziti e filladi verdi, fM_2: metaconglomerati quarzitici (Costantini et al. *(34)*).

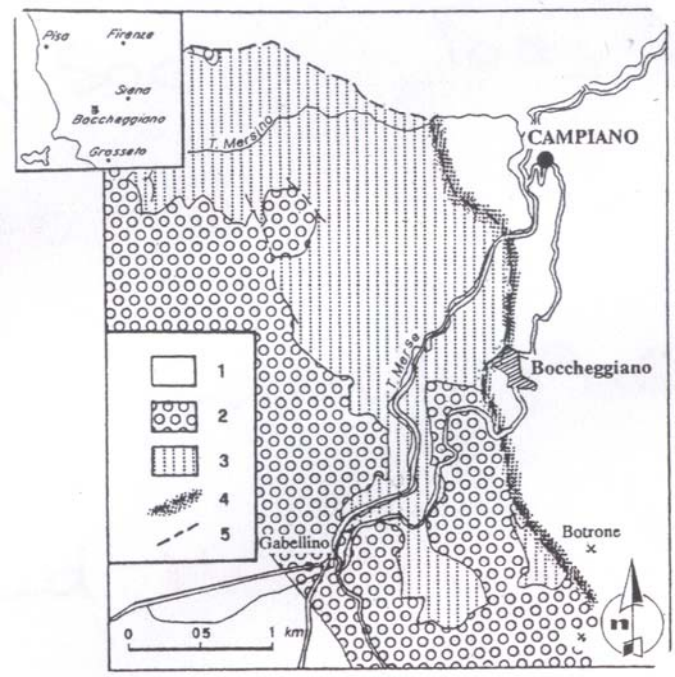

Fig. 10: Simplified geological map of Campiano area. 1 = Ligurids s.l., 2 = Calcare Cavernoso / Anidriti di burano Fms, 3 = Formazione di Boccheggiano auctt. (p.p.), 4 = Filone quarzoso-cuprifero di boccheggiano, 5 = Boccheggiano fault (Benvenuti et al. *(10)*). - Fig. 10: Schema geologico semplificato dell'area di Boccheggiano. 1 = Liguridi s.l., 2 = Calcare Cavernoso / Anidriti di burano Fms, 3 = Formazione di Boccheggiano auctt. (p.p.), 4 = Filone quarzoso-cuprifero di Boccheggiano, 5 = Faglia di Boccheggiano (Benvenuti et al. *(10)*).

2.4.3 Gavorrano

Gavorrano mine is located in the Colline Metallifere region in southern Tuscany (Fig. 11). The original thrust-nappe complex, mainly structured during Late Oligocene-Early Miocene, is composed by the tectono-stratigraphic units: Ligurian units (Jurassic magmatic mafic and low-grade metabasic rocks), Tuscan units (Upper Triassic-Cretaceous shallow-marine to pelagic carbonaceous/carbonaceous siliceous and Late Creataceous –Tertiary pelagic terrigenous formations) and the substratum Tuscan Metamorphic complex (Rossetti et al. *(131)*).

The Gavorrano intrusive monzo/syenogranitic body (Pliocene) crops out at the northern border of the ridge. The contact with the country rocks is marked by two normal faults: NW-SE Gavorrano fault and N-S Monticello fault. The northern termination is bordered by a SSW-ENE trending normal fault, not exposed because of detritic and alluvial cover. The main ore bodies are pyrite and other sulfides localized along these fault zones.

The deposit, close to the mine body called "Massa Boccheggiano", consists of massive pyrite with a gangue of quartz, calcite and clorite, low amount of sphalerite *(101)*.

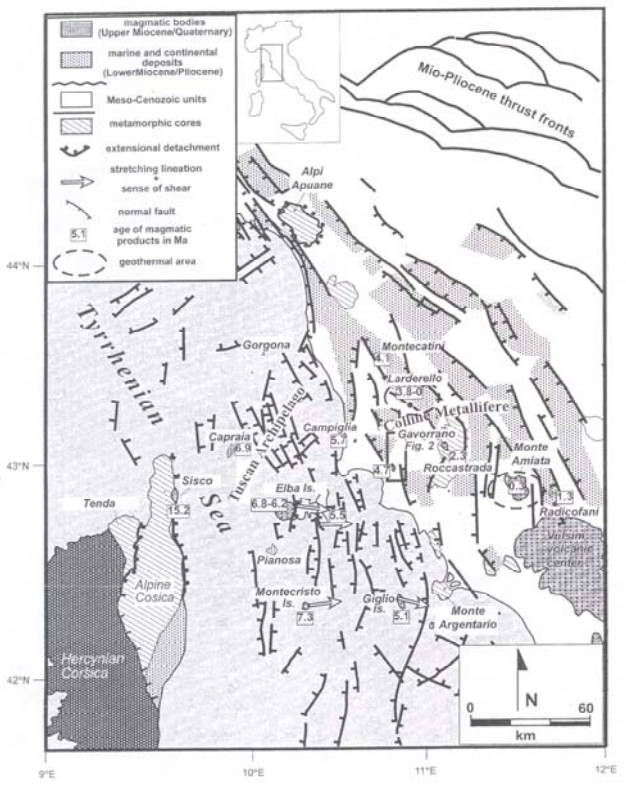

Fig. 11: Tectonic map of the northern Tyrrenian area (Rossetti et al. *(130)*). – Fig. 11 Mappa tettonica dell'area settentrionale del Tirreno (Rossetti et al. *(130)*).

2.4.4 Niccioleta

Niccioleta has been classified as a sediment-hosted massive sulfide deposits according Innocenti et al. *(73)*. Ore genesis involve a Paleozoic–Triassic (?) volcano – sedimentary genesis of large massive pyritic bodies, metamorphosed and remobilized during the Appeninc event (Mid-Tertiary to recent). This event emplaced a mineral concentration (Ag, Sb, As) of minor economic value discordant respect to the massive pyrite. Niccioleta's metabasalts are simply altered metatufs with a huge amount of sedimentary material mixed with volcanic material (Déchomets *(39)*).

The two pyrite bodies are concordant and traced for a lateral extent of 2.5 Km. There are two main generation of pyrite, the first one consists of pyrrhotite and magnetite showing signs of porphyroblastic and porphyroblastic recrystallization of strong deformation. The second generation is undeformed and it is interpreted as the result of

partial remobilization by late - Appenine hydrothermal fluids (Lattanzi et al. *(83)*). Massive pyrite is associated with very low amount of haematite and magnetite. Locally it is found pyrrothina and in geodes or lens inside the massive pyrite it is found chalcopyrite, sphalerite and galena.

2.4.5 Valle del Temperino

The polymetallic deposit of Valle del Temperino (Fig. 12) was a major Cu deposity in peninsular Italy (Martarelli et al. *(101)*). It represents a typical skarn deposit of the southern Tuscan Autochtonous series in the Pliocene. The skarn is composed by two elongated masses, NW-SE and dipping about 80° towards NE, associated with a magmatic body knonw as the green porphyry.

At the lower levels of the porphyry contact the deposit shows a band of magnetite and hematite passing to ilvaite, pyrite, pyrrothite and chalcopyrite in the inner zone and to hedembergite, galena, sphalerite, chalcopyrite and pyrite in the outer zone. In the upper levels of the deposit the inner zone lays directly at the contact with the porphyry because of the absence of the hematite-magnetite zone. According Martarelli et al. *(101)* in the paragenetic sequence three stages have been distinguished: I) Fe oxide stage with crystallization of magnetite and hematite, II) Fe sulfide and silicate stage with the cristallization pyrite, pyrrhotite, ilvaite and hedembergite., III) Cu-Zn-Pb sulfide stage with the deposition of chalcopyrite, sphalerite and galena.

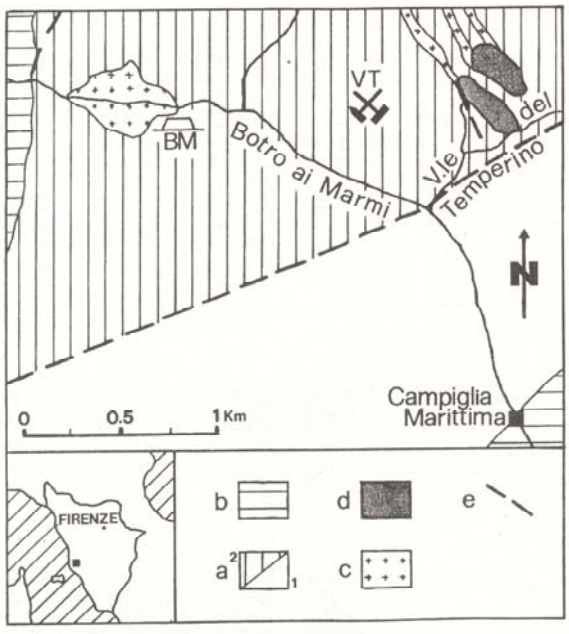

Fig. 12: Geological sketch map of Campiglia Marittima are showing the location of the deposit of Valle del Temperino. a) Tuscan Series (1) and marble (2) (Hettangian), b) Ligurian flysch (Upper Jurrasic - Eocene), c) magmatic rocks (Miocene - Pliocene), d) skarn mineralization, e) faults (Martarelli et al. *(101)*). – Fig. 12: Carta geologica della zona di Campiglia Marittima, è mostrata la localizzazione del deposito della Valle del Temperino. a) Serie toscana (1) e marmo (2) (Hettangiano), b) Flysch Liguride (Giurassico sup. - Eocene), c) rocce magmatiche (Miocene - Pliocene), d) mineralizzazione dello skarn , e) faglie (Martarelli et al. *(101)*).

2.5 SARDINIA

The geology of Sardinia island is largely dominated by Paleozoic lithotypes, of sedimentary, igneous and metamorphic origin (Fig. 13) (De Vivo et al. *(40)*). Paleozoic basement is characterised by the highest grade of industrial mineral deposits and the most important ore bodies are contained in the lower Paleozoic lithotypes.

In the Iglesiente area (SW Sardinia) the Cambro-Ordovician "authochthonous sequence from the so called "External Zones" of the Hercynian orogen predominate. And this area corresponds to the most important mining district in Italy (De Vivo et al. *(41)*).

The Lower Cambrian autochtonous of southwest Sardinia is constituted by the basal Nebida Group (clastic shallow-water sediments) which are intercalated toward the top with carbonates layers increasing, overlained by thick platform carbonates of the Gonnesa Group (300-600 m of shallow water platform carbonates) and by Middle Cambrian nodular limestone (Campo Pisano Fm, Iglesias Group, 50-80 m). From the Upper Cambrian to Lower Ordovician there is a deepening of the sedimentary basin into which clastic material was again deposited (Cabiza Fm, Iglesias Group, 400 m) (Boni et al. *(17)*). Allochthonous succession, together with Upper Cambrian-Ordovician volcanic sequence from the "External Nappes" are tectonically thrust onto the autochthonous sequence (Boni et al. *(17)*).

The Cambrian to Lower Ordovician sediments underwent extensive deformation during the intraOrdovician "Sardic" tectonic phase. This phase was followed by both the Gonnessa and Iglesias Groups deposits characterised by erosion and deposition of Upper Ordovician sediments in angular unconformity, consisting of thick succession of continental conglomerates and sandstones ("Puddinga" AUCT.) followed by marine slates, lasting until Late-Ordovician – Silurian time.

The Variscan orogeny produced at least two compressional phases and one extensional phase of deformation (Carmignani et al. *(27)*). The deformation also produced low-grade metamorphism and several phases of magmatic intrusion, which effected the deformed Paleozoic successions. During the Permian and the Mesozoic, several pulses of extensional tectonics caused repeated opening of fractures, as well as the circulation of hydrothermal fluids (Boni et al. *(19)*).

In this sector of the Iglesiente the biggest mines of the district occur (Fig. 7); in particular, the deposits are defines as: a) stratiform and stratabound consisting of sphalerite-galena-barite bodies, partly classified as Sedex (Sedimentary Exhalative), and partly as MVT (Mississippi Valley type); b) Stratabound ores (Ba-Pb) along the Cambrian – Ordovician unconformity and c) stratabound mineralisation in Ordovician-Silurian shaly and volcano-sedimentary succesion consisting of scheelite, arsenopyrite, antimonite bodies and massive sulphides (Cu-Pb-Zn) (Boni et al. *(18)*).

The main orebodies Zn-Pb and Ba deposits are generally hosted by the carbonate of the Lower Cambrian Gonnessa Group as well as in the upper part of the Nebida Group.

From Cambrian to Lower Ordovician metasediments and their ore deposits were deformed during the Sardic transpressive phase of the Caledonian orogeny. This phase was followed by erosion and deposition of alluvial sediments in unconformity and along this uncoformity concentration of Ba, Pb and Fe occur (Boni et al. *(17)*).

The mines were exploited until recently and produced about a hundred million tons of Pb-Zn-Ag and Ba ores (e.g. Bechstädt and Boni *(9)*; Boni et al. *(18)*), mainly hosted in Lower Cambrian carbonates. They consist partly of massive sulphides (Sedex) hosted in slaty dolomites, and partly of lower-grade sulphide concentrations (MVT) occurring in limestones (Boni et al. *(19)*). The ore minerals are sphalerite and galena with less abundant barite and variable pyrite amounts. Sphalerite contains Fe and Cd-Ge, whereas stratabound galena hosts low grades of Ag; As-rich pyrite is dominant in the massive sulphides. These base metal ores ascribed partly to Sedex and partly to MVT deposits, the former type is located in the stratigraphically lower part of the Cambrian sequence, and the latter at the top of the carbonates (Boni et al. *(17)*). Post-Variscan, low-temperature (< 200°C) base metal-barite veins also occur on the S. Giovanni-S. Giorgio and Barega

Hills (e.g. Boni et al. *(17)*), representing the filling of vein- and paleokarst-structures, with association of Ag-rich galena and barite.

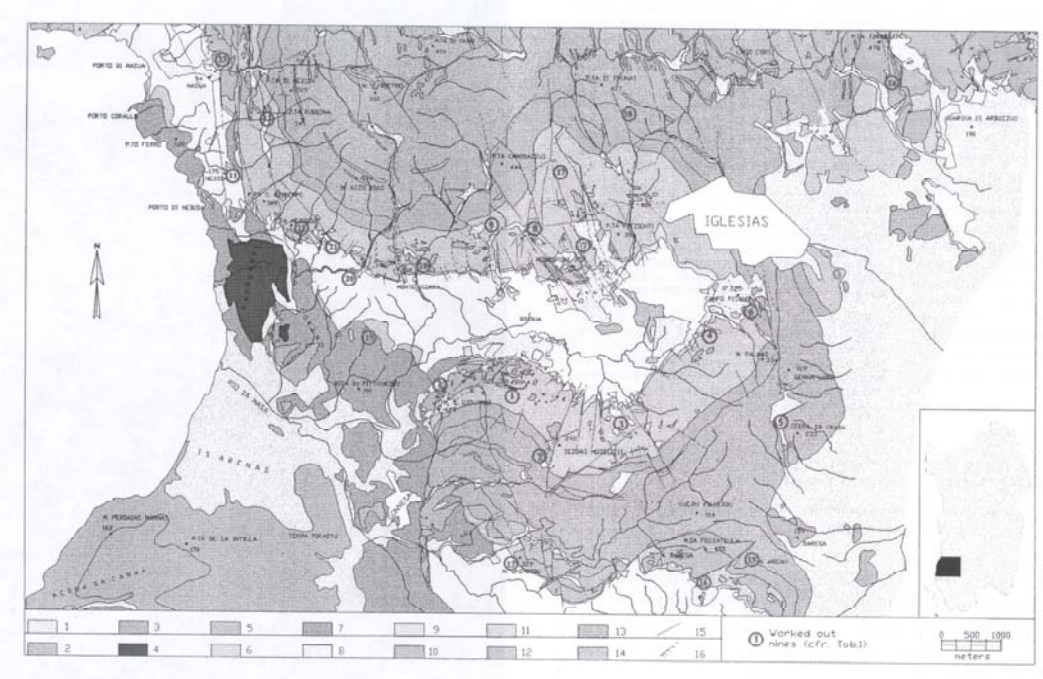

Fig. 13 List of the mineralized site sampled in southern Iglesiente (Boni et al.*(19)*). – Fig. 13 Elenco dei siti mineralizzati campionati nell'Iglesiente meridionale (Boni et al. *(19)*).

2.6 SOLUTIONS

All the aqueous solutions were prepared with deionized water and the nitrate salts as it is known they don't interfere during the reaction *(93)*. The salts were from Sigma-Aldrich and Alfa Aesar. The nitrate used in this study were: cadmium nitrate tetrahydrate [Cd $(NO_3)_2 \cdot 4H_2O$]; copper (II) nitrate [CuN_2O_6]; lead (II) nitrate [$Pb(NO_3)_2$] and zinc nitrate [Zn $(NO_3)_2 \cdot 6H_2O$] from Alfa Aesar.

In single-metal system solution contains only one of the four heavy metals for each experiment (Tab.3). This type of experiment was carried out to test the effects of HA and FAP in immobilizing Pb, Zn, Cu and Cd. The amount of HA used during the experiment was 0.1 and 0.2 g., and the FAP amount was 1 g. pH was not controlled to recreate a real *in situ* situation where it could be difficult to adjust the pH and/or it can be expensive.

In multi-metal system the solution contains all of the four heavy metal for each experiment, maintaining one constant and varying the other three (Tab. 4). This type of

experiment was carried out to test the effects of HA and natural phosphates (FAP and MAP) in immobilizing Cd, Cu, Pb and Zn as a real *in situ* situation, where more than one heavy metal can be present each time. The phosphate amount used during the experiment was HA = 0.2 g; FAP and MAP = 1g . pH was measured at the beginning and at the end of the interaction to determine the variation, but not adjusted because it could be hard to do it *in situ*.

Single metal solutions (mmol\L)			
Cd	0.09	0.89	4.45
Cu	0.16	1.57	7.87
Pb	0.05	0.48	2.41
Zn	0.15	1.50	7.65

Table 3: In the table are listed the values of each metal for the single metal system. – Tabella 1: In tabella sono riportati i valori di ciascun metallo pesante per le soluzioni del metallo a sistema singolo.

Multi metal solutions (mmol\L)		
Cd	0.09	Cu = 1.57; Pb = 0.48; Zn = 1.50
Cd	0.09	Cu = 7.87; Pb = 2.41; Zn = 7.65
Cd	0.89	Cu = 0.16; Pb = 0.05; Zn = 0.15
Cd	0.89	Cu = 7.87; Pb = 2.41; Zn = 7.65
Cd	4.45	Cu = 0.16; Pb = 0.05; Zn = 0.15
Cd	4.45	Cu = 1.57; Pb = 0.48; Zn = 1.50
Cu	0.16	Cd = 0.89; Pb = 0.48; Zn = 1.50
Cu	0.16	Cd = 4.45; Pb = 2.41; Zn = 7.65
Cu	1.57	Cd = 0.09; Pb = 0.05; Zn = 0.15
Cu	1.57	Cd = 4.45; Pb = 2.41; Zn = 7.65
Cu	7.87	Cd = 0.09; Pb = 0.05; Zn = 0.15
Cu	7.87	Cd = 0.89; Pb = 0.48; Zn = 1.50
Pb	0.05	Cd = 0.09; Cu = 0.16; Zn = 0.15
Pb	0.05	Cd = 0.89; Cu = 1.57; Zn = 1.50
Pb	0.05	Cd = 4.45; Cu = 7.87; Zn = 7.65
Pb	0.48	Cd = 0.09; Cu = 0.16; Zn = 0.15
Pb	0.48	Cd = 0.89; Cu = 1.57; Zn = 1.50
Pb	0.48	Cd = 4.45; Cu = 7.87; Zn = 7.65
Pb	2.41	Cd = 0.09; Cu = 0.16; Zn = 0.15
Pb	2.41	Cd = 0.89; Cu = 1.57; Zn = 1.50
Pb	2.41	Cd = 4.45; Cu = 7.87; Zn = 7.65
Zn	0.15	Cd = 0.89; Cu = 1.57; Pb = 0.48
Zn	0.15	Cd = 4.45; Cu = 7.87; Pb = 2.41
Zn	1.50	Cd = 0.09; Cu = 0.16; Pb = 0.05
Zn	1.50	Cd = 4.45; Cu = 7.87; Pb = 2.41
Zn	7.65	Cd = 0.09; Cu = 0.16; Pb = 0.05
Zn	7.65	Cd = 0.89; Cu = 1.57; Pb = 0.48

Table 4: In the table are listed the values of each metal for the multi-metal system. – Tabella 4: In tabella sono riportati i valori di ciascun metallo pesante per le soluzioni del sistema multi-metal.

3 METHODS

3.1 SORPTION EXPERIMENTS

Sorption experiments were performed in batch at room temperature (25°C ± 2). Batch experiment were conducted in double and were mechanically shaken at 500 ± 1 rpm (Fig.1) for 2, 4, 24 and 48 hours. In single-metal sorption tests the HA (0.1 and 0.2 g) and FAP (1 g) were equilibrated in Nalgene beakers with 200 mL of single metal solutions containing initial heavy metal concentrations.

Fig. 1: Example of a batch experiment. – Fig. 1: Esempio di un prova di sorption

In multi-metal sorption experiments the individually prepared solutions of Cd, Cu, Zn and Pb were mixed in the following way: constant concentration of one heavy metal and varying concentrations of the others. Similar procedure as the single-metal sorption experiments was used with the exception that all metals were added simultaneously to each reaction vessel. The amount of phosphates were: HA = 0.2 g; FAP = 1 g and MAP = 1g.

In single metal systems pH was not controlled and in multi-metal systems pH was measured at the beginning and at the end but not adjusted. The reason for this was to

mimic real *in situ* conditions where it could be difficult to adjusted the pH or/and it can be expensive too.

All the suspensions were filtered through 0.2 μm Nucleopore polycarbonate membrane filters (Fig. 2 and 3).

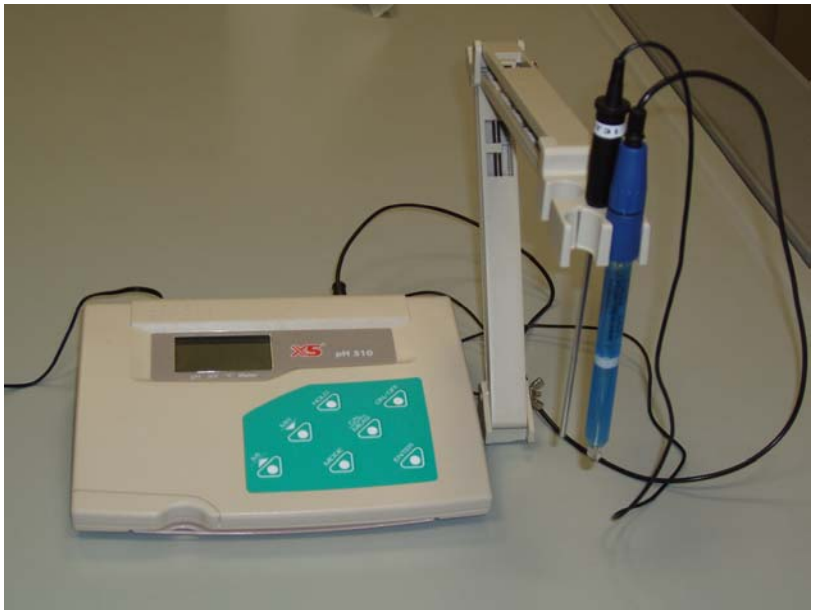

Fig. 2: pHmeter used for the measures either for aqueous solutions and soils. – Fig. 2: pHmetro usato per le misure sia in soluzione acquosa che nei suoli.

Fig. 3: Filter system. – Fig. 3: Sistema di filtraggio

The suspensions were analysed for total Ca, Cd, Cu, P, Pb and Zn by a ICP-AES. The solid materials were analysed by XRD, SEM-EDS, AFM and FTIR .

Soil sorption tests were carried out as batch experiments and were mechanically shaken at 500 ± 1 rpm. For the soil sorption tests 5 g were interacted with 1 g of HA and FAP; they were equilibrated in Nalgene beakers with 100 mL of bidistilled water. The suspensions were filtered through 0.2 μm Nucleopore polycarbonate membrane filters.

Soils are usually composed of sulphur and sulphate minerals, so the reaction among the soils and the HA or FAP was faster and then there is the precipitation phenomenon *(153)*. The most suitable method for the immobilization of heavy metals in this kind of samples is a method based on an interaction time of 20 minutes in aqueous solution; where pH was measured and adjusted at 5 using HNO_3 or NaOH at the beginning of the interaction, after 10 minutes and at the end of the 20 minutes. The fraction of soil heavy metals undissolved can be considered stable and not bio-accessible that is may be encapsulated inside soil particles or other insoluble minerals.

The mineralogical composition of the soils was determined by XRD analyses.

3.2 DESORPTION EXPERIMENTS

These type of experiments were performed in batch at room temperature (25°C ± 2), conducted in double and were mechanically shaken at 500 ± 1 rpm for 24 hours. The prepared solutions were at controlled pH = 4, 5 and 6. Two type of solutions were prepared, the first where pH was adjusted by HNO_3 and NaOH; a second type where pH was adjusted by HCl and NaOH. Random samples were interacted with the solutions, the solid materials were from the sorption experiments and were chosen the filtrates which had interacted for 24hours. After the interaction time the samples were filtrated through 0.2 μm Nucleopore polycarbonate membrane filters. The suspensions were analysed for total Ca, Cd, Cu, P, Pb and Zn by a ICP-AES. The solid materials were analysed by SEM-EDS.

3.3 ICP-AES

All the suspension obtained from the sorption and desorption tests were analyzed by Vista Varian ICP-AES. The detection limits are for Cd 0.1 μmol/L, for Cu 0.3 μmol/L, for

Zn 0.6 μmol/L, for Pb 1.4 μmol/L, for Ca 0.3 μmol/L and for P 6.4 μmol/L. Analytical errors were estimated to be on the order of 3%.

They were prepared regularly and acidified as well as each suspensions with the 2% of HNO_3 as requested to carry on the analyses by an ICP-AES[4]. HNO_3 is from Sigma-Aldrich and the purity is about 69%.

The amount of adsorption per unit mass of HA, FAP and MAP were evaluated using the following expression:

$$q = (C_0 - C)\ V/m$$

where q (mg/g) is the amount of adsorption per unit mass of the amendant; C_0 and C are the concentrations (mg/L) of the heavy metals in the initial solution and in the aqueous phase after the treatment for the interaction time, V (mL) is the volume of the aqueous phase and m (g) is the amount of the amendant *(3)*.

3.4 XRD

XRD analysis was carried on to determine the mineralogical composition. The difractometer was a Seifert MZ IV operated at 35 kV and 20 mA using Cu K-α radiation. Measurements were made using a step-scanning technique with a fixed time of 2 s/0.05° 2θ from 5 to 60° 2θ. All XRD analyses were performed using back-filled and randomly oriented mounts.

XRD analyses were carried on the sampled soils before and after the sorption tests, some of the solid materials obtained from the filtration of the aqueous solutions were randomly chosen and analyzed to determine the lattice parameters using Lsuscripc software[5].

3.5 SEM-EDS

The solid phases were observed with a Zeiss MD 940 scanning electron microscope operating at 25 kV equipped with a EDS Link system microanalysis. The samples were mounted on stainless steel stubs and coated with carbon.

[4] The author wish to thanks Mr. T. Coppola for carrying on the analyses.

[5] The author wish to thanks Mr. S. Stellino and Mr. V. Fiori for carrying on the analyses.

3.6 FTIR

FTIR analyses were carried out on selected samples after being dispersed in KBr excess (sample/Kbr ratio about 1/100) at ambient temperature (25°C) using the DRIFT (Diffuse Reflectance Infrared Fourier Transform) technique with an Interferometer Equinox 55 Bruker having the sample compartment carefully purged. Spectra were taken at a resolution of 1 cm^{-1} or better, cumulating at least 200 scans. FTIR absorption spectra of samples were recorded in the 400-4000 cm^{-1} range[6].

3.7 AFM

The atomic force microscope is substantially a laser microprobe which allows the morphologic analysis of the sample surface. It is possible to observe the defects of the surface and in some cases also to determine the atomic structure for simple and periodic structures (es. FeS_2). The analysis used a "tip" which is in contanct (or at a close distance) of the sample, allowing the study of the surface of little area; the maximum area of observation is of approximately 100 μm^2. In particular, using the AFM in "tapping" mode the tip it goes back and forth on the sample surface, measuring the height and at the same time maintaining the amplitude of oscillation of the tip constant. In this way the tip is't directly in contact with the sample like in "contact-mode". The tip used for this modality is made of silicon.

Analyzing the sample through the tapping mode avoided the presence of lateral forces which disturb the image acquisition. After the acquisition, the image is elaborated with an appropriated software "Nanoscope (r) III" version 5.12b49 in equipment with the instrument. The obtained image after the elaboration there is a chromatic scale which indicates the height regarding the plane of reference (0 nm). Increasing the height the color varied from the dark brown to the white man. Moreover, the data about acquisition are also brought back: the scansion area, the speed of acquisition, the acronym of the sample, the scale and the height or the amplitude.

Sample is put in a ultrasounds bath with bidistilled water and NaCl to avoid flocculation phenomena improving the imagine quality.

[6] The author wish to thanks Msr. S. Nunziante –Cesaro for her help during the analyses.

The obtained solution is put on a mica stub through a pipette. Every time a new sample must be analized a mica stratum is removed. Mica mineral is used because of his sheet habit and avoid any kind of intereferences during the acquisition. The analyses were carried on using the Tapping mode.

4 REMEDIATION TECHNOLOGIES

Heavy metals contamination is one of the most common problems constraining the cleanup of hazardous waste sites across the world. Leachate and run-off from soils contaminated with heavy metals potentially degrade groundwater and surface water; additionally, wind erosion tends to spread contamination over large areas. Contamination exists in mixed water, surface soils, subsurface soils.

Concern over contamination of water and soils by heavy metals from previously abandoned sites or operating sites have generated many remediation technologies to treat contaminated soils, leachate, wastewater, and groundwater contaminated by various pollutants, including *in situ* and *ex situ* methods. The existing remediation technologies are considered expensive and often ineffective. Development of *in situ* treatment technologies or effective volume reduction technologies, will provide a significant cost saving.

A potential method to determine if the heavy metals con be removed by remediation techniques or to predict removal efficiencies is to determine speciation with selective extractive techniques, so that a particular contaminated site may require a combination of procedures to allow the optimum remediation for the prevailing conditions. Many technologies are available for the treatment of contaminated site, their selection depends on the contaminant and site characteristics, regulatory requirements, costs and time constraints. Therefore, the successful treatment of a contaminated site depends on proper selection, design, and adjustment of the remediation technology's operation based on the properties of the contaminants and soil and on the performance of the system.

4.1 SOIL TECHNOLOGIES

Site soil conditions frequently limits the selection of a treatment process. Generally, soil is inherently variable in its physical and chemical characteristics. Usually the variability is much greater vertically than horizontally, resulting from the variability in the process which originally formed the soils.

An important factor in many soil treatment technologies is the soil particle - size distribution. In general, coarse, unconsolidated materials, such as sands and fine gravels, are easiest to treat. Soil washing (see below) may not be effective where the soil is composed of large percentages of silt and clay because of the difficulty of separating the adsorbed contaminants from fine particles and wash from fluids. Moreover, larger particles, such as coarse gravel or cobbles, are undesirable for vitrification and chemical extraction processes and also may not be suitable for the stabilization/solidification.

In situ treatment is usually preferred because the soil may be treated without being excavated; on the other hand, this kind of treatment requires longer time periods. *Ex situ* treatment requires shorter time periods but it needs excavations of soils, which increases the costs and engineering for equipment. Moreover, bioremediation is not applicable for inorganic contaminants.

4.1.1 Soil washing

It combines liquid and mechanical process to scrub soils. Generally, the liquid is water, but occasionally it can be combined with solvents which are chosen on the basis of their ability to solubilize specific contaminants, and on their health effects. Sometimes it is combined with other technologies. As it reduces the quantity of material which would require further treatment by another technology.

The target contaminant groups include semi-volatile organic compounds (SVOCs), petroleum and fuel residuals, heavy metals, PCBs (PolyChlorinated Biphenyls), PAHs (Polycyclic Aromatic Hydrocarbon) and pesticides.

The disadvantage of this technique is that the resulting soil must be disposed carefully and pre-treatment is required if the soil contains humic acids, infact an high content of these acids will act to bind the soil, inhibiting the soil washing. Finally, soil washing is most effective if soil doesn’t contain a large amount of silt and clay.

4.1.2 Solidification/Stabilization (s/s)

It reduces the mobility if hazardous substances and contaminants in the environments through both physical and chemical means. The process is based on reducing the risk posed by a waste by converting the contaminant into a less soluble, immobile and less toxic form. In particular solidification refers to the encapsulation of the waste materials in a monolithic solid of high structural integrity. The process involves three main components: a) mixing the contaminated soil in place; b) a reagent storage, preparation, and feed system; and c) a means to deliver the reagents to the soil mixing zone.

In situ and *ex situ* stabilization/solidification is usually applied to soils contaminated by heavy metals and other inorganic compounds.

Most of these technologies have limited effectiveness against organic and pesticides, except for asphalt batching and vitrification, which destroys most organic contaminants.

Auger/caisson systems and injector head systems are techniques used in soil S/S. They apply S/S agents to soil to trap or immobilize contaminants (Fig. 1).

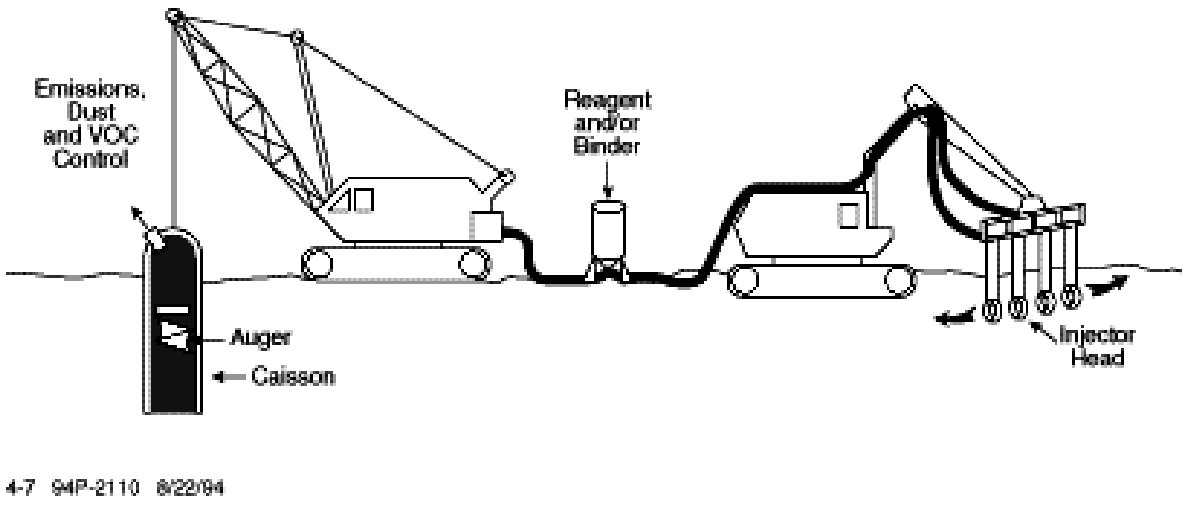

Fig. 1 Model of the Auger/caisson system and injector head *(59)*. - Fig.1 Esempio del sistema Auger/caisson e dell'iniettore *(59)*.

4.1.3 Vitrification

It is a particular case of S/S and it uses a powerful source of energy to melt soil at high temperatures (1600 - 2000°C), immobilizing most inorganics and destroying organic

pollutants by pyrolisis. Most of the contaminants are volatilized, whereas the remainders are converted into a chemically, inert, stable glass and crystalline product. Heavy metals are actually incorporated into a glass structure which is generally strong, durable and resistant to leaching. There are three main types of vitrification process: a) *electrical processes* an in situ application of electrical energy through graphite electrodes inserted into the ground; b) *thermal processes* which requires external heat source and a typical reactor and c) *plasma processes* with temperature up to 5000°C via electrical discharges.

Sometimes the depth of the contaminants in the soil may limit the effectiveness of the process. It is important a long term monitoring to ensure the contaminants are actually immobilized.

4.1.4 Phytoremediation

It consists in using the plants to remove pollutants from the environment. Five subgroups of techniques exist:

Phytoextraction = plants remove metals and concetrate them in the harvestable parts of the plants;

Phytodegradation = plants and microbes degrade organic pollutants;

Rhizofiltration = plant roots absorb metals from waste streams;

Phytostabilization = plants reduce the mobility and bioavailability of contaminants by immobilization or by prevention of migration;

Phytovolatilization = plants volatilizes pollutants in the atmosphere (Fig. 2).

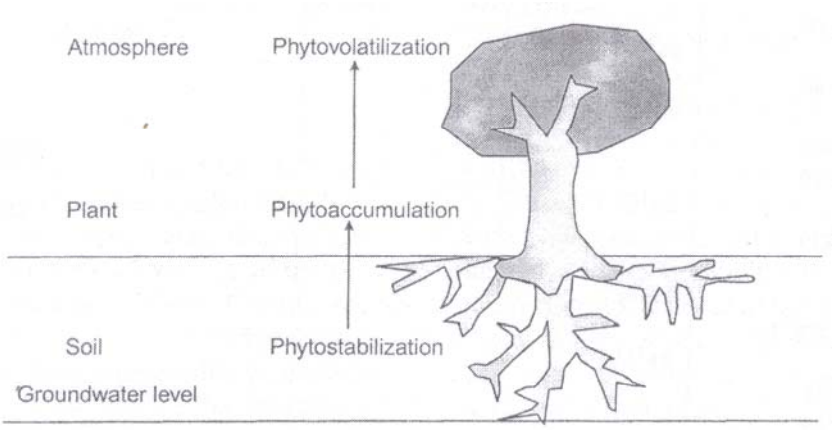

Mechanisms for phytoremediation of metals

Fig. 2 Schematic diagramme showing the mechanism of the phytoremediation process for metal uptake (Mulligan et al. *(111)*). – Fig 2 schema del meccanismo del processo di phytoremediation per l'assorbimento dei metalli da parte delle piante (Mulligan et al. *(111)*).

The best plant species to clean-up a heavy metal-contaminated soil would be a plant with a high biomass producing crop that can tolerate and accumulate the contaminants of interest. Furthermore, the crop from a contaminated land may result in a potentially hazardous biomass. However, the lack of reported toxicity symptoms in trees indicates that their tolerance mechanism allow them to withstand higher heavy metal concentration than agricultural crops.

Moreover, trees species are generally not able to adapt to high concentrations of heavy metals in the soil, resulting in the evolution of only a few metal-tolerant ecotypes. Trees that are not selected for metal tolerance can generally survive in metal-contaminated soil, albeit usually with a much reduced growth rate.

Benefits from phytoremediation are the stabilization of the soil or waste, although in some cases phytoextraction may be sufficient to provide clean up of the soil. On highly contaminated soils, or on mining wastes, tree establishments may be inhibited by high concentrations of heavy metals. Anyway, once the trees have become established, the vegetation cover can promote physical stabilisation of a substrate, especially on sloping ground. Long term stability of the land surface can be achieved as the standing trees decrease erosion of the substrate by wind and water. Uptake and metal accumulation were not related to tolerance, and there was evidence of both general tolerance to a number of different metals and specific tolerance to one heavy metal.

Finally, lead and copper tend to be immobilized in the roots, whereas cadmium and zinc concentrate in aerial tissues.

4.2 WATER TECHNOLOGIES

In situ treatments allow ground water to be treated without being brought to the surface but, as in the soil treatments, they require longer time periods and there is less certainty about the uniformity of treatment; but they are cost-saving methods. On the contrary, *ex situ* treatments require shorter time, and there is more certainty about the uniformity of the treatment; on the other hand they require pumping of groundwater which increases the costs. Bioremediation are not useful in cases of inorganic pollution, as

in the soils. To choose the suitable treatment it is important to determine a major parameter like pH and often pH must be adjusted before or during a treatment process.

4.2.1 Groundwater pump-and-treat technology

In case of contaminated aquifer it is one of the most used technology is this one. The extraction wells are introduced at different location in the contaminated aquifer, consequently the contaminants are removed with the pumped water. The water is treated with different technologies and then re-injected into the aquifer or discharged into a surface water body (lake, river or municipal sewage plants). The aim of this technology is to prevent the contaminant from spreading or to remove the contaminant mass. Nowadays it is not so popular because of the time required to achieve cleanup goals and the ineffectiveness of the system. It treats all the mobile contaminants but it requires a long time, about 5-50 years and it is a very cost method.

4.2.2 Passive/reactive treatments walls

It is an emerging technology, developed and implemented within the last few years.

A permeable reaction wall is installed across the flow path of a contaminant plume so that the water can move through the wall. The barriers allow the passage of water and, at the same time, prohibiting the movements of contaminants by employing agents like zero-valent metals, chelators, sorbent and others. Contaminants will be degraded or retained in a concentrated form by the barrier material. The wall could provide a permanent containment or provide a decreased volume of the more toxic contaminants for a subsequent treatment (Fig. 3). One disadvantage of this technology is that the passive treatment walls have a tendency to lose the reactive capacity over time and require the replacement of the reactive medium. Moreover large and deep plumes are more difficult to remediate than small and shallow plumes.

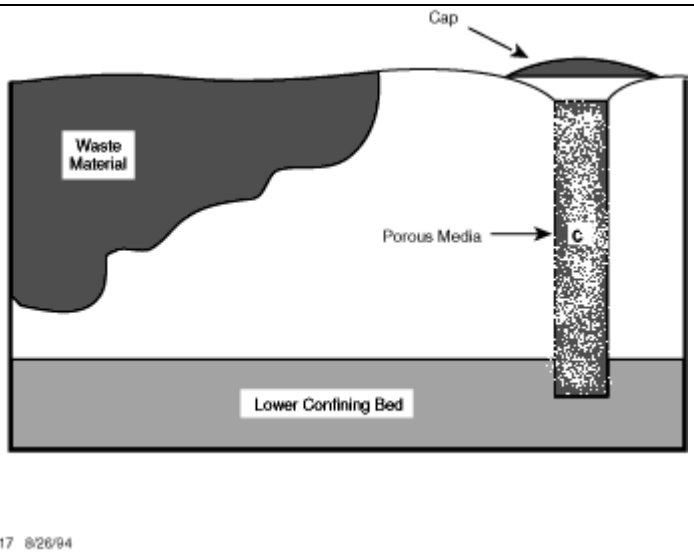

Fig. 3 Typical passive treatment wall (cross-section) *(60)*. – Fig. 3 Esempio di un muro a trattamento passivo (sezione longitudinale) *(60)*.

4.3 SORPTION-BASED TECHNOLOGY

The extensive use in industry and in agriculture of metals such as cadmium, copper, lead and zinc have led to their diffusion in soil or water with danger for human health, so that it has been carried out extensive research on the way of cleanup like the use of adsorbents to remove these metal ions. Generally factors, affecting the heavy metal retention are: pH and the inorganic contaminants, but regarding soils other factors are also important like the soil type and horizon, CEC (cation exchange capacity) and content of natural organic matter. Generally in soils the finest fractions like silt and clays contain the highest concentration of contaminants.

The aim is to isolate contaminants, to minimize further movements and reduce their solubility, as the more mobile is the metal and the more risk associated with it.

The general term sorption includes both adsorption, the process by which a solute clings to a solid surface, and absorption, the process by which the solute diffuse into a porous solid and clings to interior surfaces. Sorption, through a cation exchanger, of heavy metals may be one of the suitable *in situ* remediation technologies.

The sorption theory was applied to predicting the multisolute adsorption capacity using only data for single solute adsorption from dilute liquid solution. The assumption is that the adsorbed phase can be treated as an ideal solution of the adsorbed components.

The difference in sorption capacity for different metal ions may be due to the selectivity of ion exchange in multi-metal system and also the smaller the ionic radius and the greater the valence, the more closely and strongly the ion is adsorbed.

In a binary system there are two reaction fronts moving inside the particle at different speeds, the two species in the outer layer and a single metal in the middle layer and the unreacted core of sorbent in the inner layer. As the middle layer contains a single metal, the sorption capacity can be predict from the single component isotherm (Fig. 4).

The adsorption theory explains the attachment of solute molecules to the adsorbate surface by weak electrical forces. The bonds are physical rather than chemical, attachment can occur over multiple layers in a field near the adsorbent surface. Of course, adsorption is concentrated at the higher-energy site on the surface, and the concentration decreases toward the bulk solution.

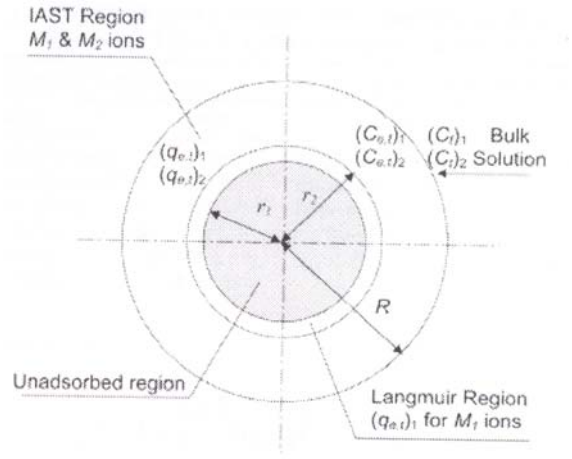

Fig. 4 Mass transport of metal ions M_1 and M_2 at different speed in the sorbent (Cheung et al. *(31)*).
– Fig. 4 Trasporto degli ioni metallici M_1 e M_2 a diverse velocità nel sistema assorbente (Cheung et al. *(31)*).

For example, to maintain the electroneutrality among copper ions and a strong acid like the sulfate ion, during the ion exchange process, a Lewis base/Lewis acid interaction occurs and the anion exchangers may undergo coordination bonding with Lewis acids such heavy metals this is why a weakly basic anion exchangers are normally used for removing strong acids.

In particular, cation exchange and specific adsorption are two mechanisms that control metal adsorption. Heavy metals can also be immobilized by other mechanism such

as: solid-state diffusion and precipitation reactions, metal sorption at surface site and adsorption of metal – ligand complexes. These interactions occur at the solid – solution interface and are controlled by pH, ionic strength, nature of metal and ligands ions.

Heavy metal can be considered partitioned into two fractions: irreversibly and reversibly bound metal phases, so that irreversibly and reversibly kinetic reactions describe the release of metal from these two fractions. It must be considered the intraparticle transport of chemical species by molecular diffusion.

Ion exchange may be a mass transport controlled process so that the heavy metal ion will be transferred along the pore to the sorption site inside the sorbent. The mechanisms are: pore diffusion and surface diffusion. In the first mechanism the heavy metal ion move within the pores of the adsorbent before being adsorbed onto the surface of the pores. The surface diffusion occurs along the pore surface of the adsorbent. Surface diffusion depends on the sorptive affinity between the heavy metal ion and the adsorbent, while pore diffusion is always operating. The prevailing one of these two type of diffusions is dependent upon the adsorbate-adsorbent system.

The ion exchanger is like a plane surface across which the functional groups are distributed and the surface charge are generated because of the dissociation or protonation of surface groups. Protons are adsorbed on the surface, heavy metals in more layers further away and of different distance from the surface. The heavy metal ions are localized in a particular sorption layer called Stern layer (Fig. 5). The fixed groups are charged and they generate an electrical field. The ligand possess high metal complexing abilities towards heavy metals as opposed to hard sphere cations like Ca.

Finally the sorption dynamics is determined by the total cation concentration, the ratio between the cation concentrations and the nature of the ion exchanger. During the sorption processes of heavy metals onto apatites, ion exchange, physical sorption and other mechanism can occur at the same time. The mechanism of sorption of metal ions on HA can proceed via many mechanisms like, surface complexation, adsorption (accumulation of sorbate on the external surface of a solid), absorption is diffusion into the solid, dissolution-precipitation and ion exchange. Probably many of these mechanisms happen at the same time and in fact it is difficult to distinguish which one is the most suitable, one or more could be the right mechanisms at the same time. The predominance of one on the others is difficult to distinguish, on the other hand identifying the right

sorption mechanism of metal on hydroxyapatite can be helpful in indicating the mobilities of the metals in their environments.

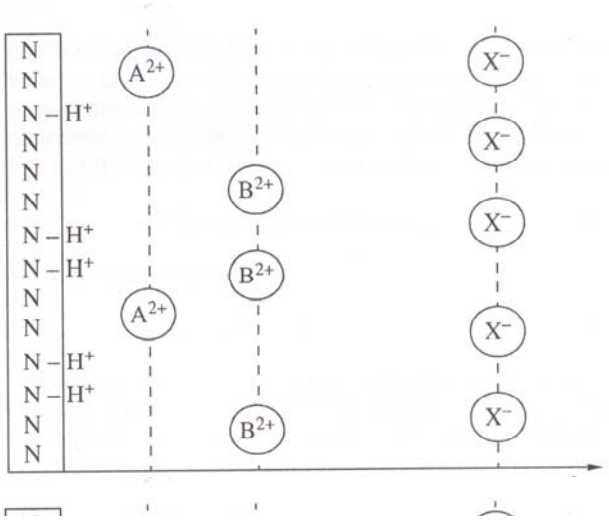

Fig. 5: Stern layers for the sorption of divalent cations and anions (Kalinichev et Hoell *(77)*). – Fig. 5: Strato di Stern per la teoria dell'assorbimento di cationi divalenti e anioni (Kalinichev et Hoell *(77)*).

4.4 STATE OF THE ART

In situ immobilization of heavy metals using inexpensive sequestering agents, such as minerals (e.g. apatite, zeolite (Scott et al. *(133)*) and clay minerals (Celis et al. *(28)*) or waste by-products (e.g. rice bran, crab shell; An et al. *(4)*) and sawdust (Taty-Costodes et al. *(144)*) is an attractive alternative to many current remediation methods.

The use of mineral amendments to immobilize metals has the advantage that it reduces the risk of workers exposure during remediation and is typically less expensive and really less disruptive to ecosystems than conventional ex situ methods involving excavation and treatment, followed by disposal.

Recent works have recognized the importance of phosphate minerals in a variety of areas. Phosphate minerals are the principal constituent of bones and teeth and hydroxyapatite (HA) is the most abundant mineral constituent in human tissues and their sufficient abundance make them usable in industrial processes. Besides phosphates can be useful in the environment for the immobilization of divalent heavy metals forming compounds with a low solubilities at earth surface condition. Another ore of apatite family is pyromorphite which can be formed in the final step of lead cycle in the road ecosystem (Brückner et al. *(23)*).

Nriagu and Moore *(117)* wrote that phosphates of Pb and Zn are generally several orders of magnitude less soluble than the analogous of carbonates and sulphates, moreover phosphates of Pb, Cu and Zn are also more stable (Fig. 6, 7 and 8).

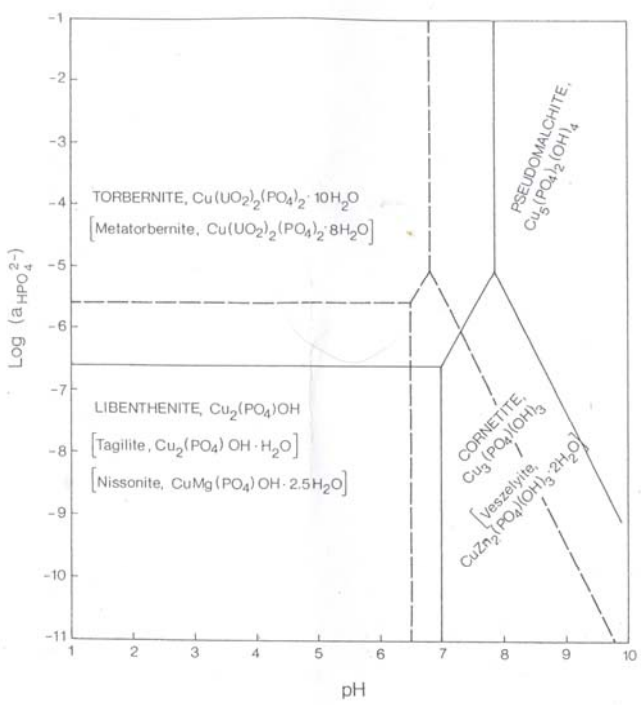

Fig. 6. Phase relations for low temperature copper phosphate minerals, assuming $a_{Mg2+} = 10^{-3}$. For solid lines $a_{Cu}^{2+} = 10^{-6}$; $a_{UO_2}^{2+} = 10^{-7}$; for broken lines $a_{Cu}^{2+} = 10^{-3}$ and $a_{UO_2}^{2+} = 10_{-6,5}$. Minerals with closed related compositions have been assigned the same stability fields (Nriagu and Moore *(117)*). – Fig. 6: Relazioni di fase a basse temperature per i fosfati di rame, assumendo $a_{Mg2+} = 10^{-3}$. Per le linee chiuse $a_{Cu}^{2+} = 10^{-6}$; $a_{UO_2}^{2+} = 10^{-7}$; per le linee spezzate $a_{Cu}^{2+} = 10^{-3}$ and $a_{UO_2}^{2+} = 10_{-6,5}$. I minerali con composizione chiusa sono stati assegnati allo stesso campo di stabilità (Nriagu and Moore *(117)*).

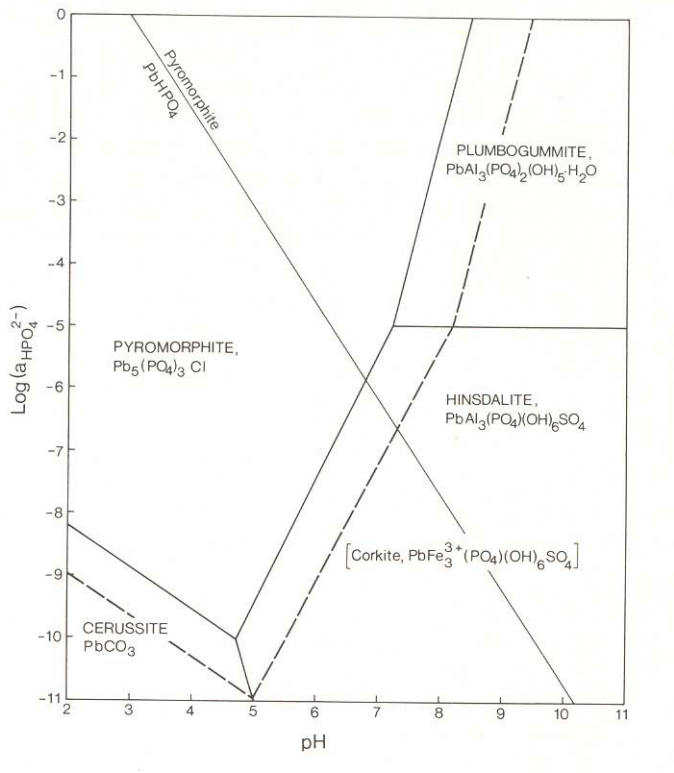

Fig. 7: Stability fields of secondary lead phosphates. The constrains on the ionic activities are: $a_{SO_4}^{2-} = a_{HCO}^{3-} = 10^{-3}$; $a_{Al}^{3+} = 10^{-6}$; $a_{Pb}^{2+} = 10^{-6}$ (solid lines) and $a_{Pb}^{2+} = 10^{-5}$ (broken lines). The broken lines show the direction of change of "solubility" with increasing lead concentration. Minerals with closely related composition and stabilities are assigned the same stability fields (Nriagu and Moore *(117)*). – Fig. 7: Campi di stabilità per fosfati di piombo secondari. Le indicazioni per le attività ioniche sono: $a_{SO_4}^{2-} = a_{HCO}^{3-} = 10^{-3}$; $a_{Al}^{3+} = 10^{-6}$; $a_{Pb}^{2+} = 10^{-6}$ (linee piene) and $a_{Pb}^{2+} = 10^{-5}$ (linee spezzate). Le linee spezzate mostrano la direzione del cambio di solubilità con l'aumento della concentrazione del piombo. Ai minerali con una composizione e stabilità relativamente simile gli è stato assegnato uno stesso campo di stabilità (Nriagu and Moore, *(117)*).

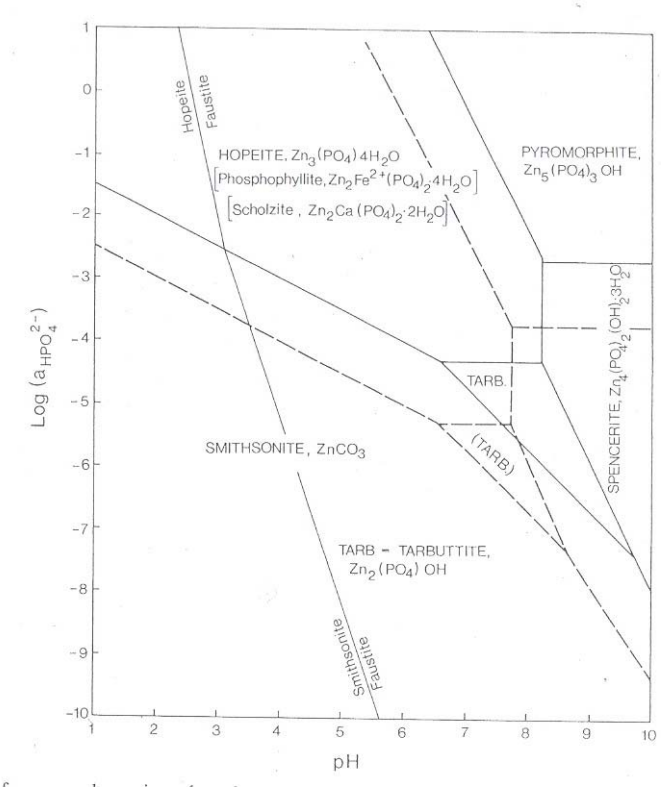

Fig. 8: Stability relationship for secondary zinc phosphate minerals assuming $a_{Zn}^{2+} = a_{Fe}^{2+} = 10^{-6}$; $a_{Ca}^{2+} = a_{HCO}^{3-} = 10^{-3}$ for the solid lines. For the broken lines the activity of Zn^{2+} ions has been assigned a value of 10^{-5}. Minerals with similar compositions and stabilities occupy the same domain in the diagramme (Nriagu and Moore *(117)*). - Fig. 8: Campi di stabilità per i fosfati di zinco secondari assumendo $a_{Zn}^{2+} = a_{Fe}^{2+} = 10^{-6}$; $a_{Ca}^{2+} = a_{HCO}^{3-} = 10^{-3}$ per le linee complete. Per le linee spezzate l'attività dello ione zinco è di 10^{-5}. i minerali con composizione e stabilità simile occupano lo stesso dominio nel diagramma (Nriagu and Moore *(117)*).

Later Suzuki et al. *(140)* examined the feasibility of synthetic hydroxyapatite (HA) $Ca_{10}(PO_4)_6(OH)_2$ as a cation exchanger to treat metals in solution such as Cd^{2+} and Zn^{2+}. They found Cd and Zn are sorbed from apatite trough ionic exchange mechanism with Ca. Successively Suzuki et al. *(141)* carried out sorption batch experiments on Pb, Mn, Co and Cu cations, suggesting for all of the ions the ion exchange mechanism and the uptake was related to the apatite specific surface area. According to their results the uptake of heavy metals depends on the ionic radius and the electronegativity of the cations, so that Pb show a similar characterists to Ca ion and Pb can substitute Ca(2) whereas the other cations have different behaviours and are less removed than Pb. Suzuki et al. *(141)* stated that Pb can occupy M1 and M2 sites of apatite thanks to the strong selectivity for Pb^{2+} ions. In 1984 Suzuky et al. *(142)* demonstrated that increasing the reaction time from 2

hours to 20 days the amount of immobilized Pb increased from 10% to 63% even in high-pH regions. According to the pH values the exchange reaction rate between Ca and Pb ions are slowly (pH = 5) and at pH = 3 the reaction is influenced by H^+ and anions such as Cl^- and NO_3^-.

Pujari and Patel *(126)* observed that apatite undergoes a series of cationic replacement $Ca^{2+} \rightarrow Cu^{2+}$ with a contraction in the cell parameters. This could be explained as an evidence for solid solution in the Sr – Cu – Ca hydroxyapatite series. Also Middelburg and Comans *(106)* found that Cd-apatites are isostructural with Ca-apatites. In particular, an increase in dissolved Ca concentration makes hydroxyapatite more positevely charged, whereas an increase in P concentration makes the mineral more negatively charged, but generally in most natural solutions the surface has a positive charge. In case of Cd uptake they describe a rapid sorption and the adsorption/ion-exchange processes dominate and when the uptake slows down the recrystallization processes dominates.

Ma et al. *(93)* hypothesized HA dissolution and hydroxypyromorphite ($Pb_{10}(PO_4)_6(OH)_2$, HP precipitation as the main Pb immobilization mechanism in wastewater or soils. In particular the process of dissolution\precipitation is based on the assumption that pyromorphite is stable in neutral to acid environments, in particular the products of the sorption must be stable in contaminated environment and the reaction should be rapid. These authors carried out experiments at constant pH and the sorption process resulted as dissolution/precipitation mechanism, being pH a major parameter determining HA solubility and controlling HP precipitation for low pH values.

In addition Nriagu *(114)* demonstrated the greater stability of chloropyromorphite (CP) compared to hydroxypyromorphite (HP), this reaction occurs under most natural environments, in fact $Pb_5(PO_4)_3Cl$ is found as a mineral unlike $Pb(PO_4)_3OH$. On the contrary fluorpyromorphite $Pb_5(PO_4)_3F$ (FP) is the least stable mineral (Nriagu, *(115)*) and no natural occurrence is known.

Nriagu *(116)* suggested also the formation of Pb-phosphates according to Pb and Ca concentration in many sub-aqueous environments.

The effects of interfering ions such as NO^{3-}, Cl^-, F^-, SO_4^{2-} and CO_3^2 on Pb immobilization by HA were determined by (Ma et al., *(94)*). Generally, the presence of Cl- and F- ions lead to the formation of chloropyromorphite (CP) and fluoropyromorphite (FP)

through a precipitation mechanism and the crystallinity of the products decreased with the increasing of pH. On the contrary CO_3^{2-} ion reduced the effectiveness of HA in immobilizing Pb^{2+} whereas SO_4^{2-} had a little effect on final Pb^{2+} immobilization. Ma et al, *(95)* carried out also some tests on the effects of some cations on the Pb immobilization by HA. Added metals such as Al, Cu, Fe (II), Ni and Zn reduced the effectiveness of hydroxyapatite in immobilizing Pb. In particular, Ni has a little effect, but Al, Cd and Zn caused a decrease if Pb concentrations is higher and the ratio between the metal and lead is bigger than one (M/Pb>1); Cu and Fe (II) show the greatest influence on Pb immobilization and this occurs at each Pb concentration and M/Pb>1. In particular, in case of M/Pb = 7 the mechanism dissolution/precipitation didn't occur and consequently other mechanisms must occur. From SEM micrographs it is possible to deduce the ions incorporation into a new solid phase and/or amorphous – poorly crystalline mixed metal phosphates.

In case of other divalent ions like Cd^{2+} and Zn^{2+}, the proposed immobilization mechanism isn't the dissolution/precipitation but the adsorption through surface complexation via hydroxyapatite surface functional group, coprecipitation and ion exchange (Xu et al., *(152)*). Generally, coprecipitation occurs at the end of the sorption reaction and it is more significant for Cd^{2+} than Zn^{2+}, but the three mechanisms usually works together. This was proved observing the increasing $[Ca]_T$ in solution during the sorption of Zn^{2+} and Cd^{2+} onto HA surface. At the same moment pH changes and this makes difficult to determine whether the $[Ca]_T$ increasing is a consequence of ion exchange of Cd^{2+} or Zn^{2+}, or the HA dissolution is due to the decreasing pH or other mechanisms. In particular $[PO_4]_T$ is almost constant in case of Zn^{2+}sorption and decreases in Cd^{2+} sorption. This means a non-stoichiometric dissolution of HA, inferring the ion exchange mechanism is not predominant, because in this case $[Ca]_T$ must be proportional to the sorbed metal. Furthermore, from the isotherm shape Xu et al. *(152)* stated that ion exchange occur but it is not a dominant mechanism in removing Zn and\or Cd, so that other reactions may exist, in particular coprecipitation during the initial uptake stage concurrently with other adsorption processes like the surface complexation with functional groups. High amount of H^+ are in solution which are partially displaced from Ha surface by the sorbed Zn and Cd.

Moreover, Ma et al. *(96)* have proved that also phosphate rocks can immobilize Pb ion and the effectiveness depends on the interaction time and the amount of P in the solution. The percentage of Pb removed ranged from 38.8% to almost 100%. The lower Pb removal efficiency can be attributed to lower solubility and purity of phosphate rocks than synthetic HA. They stated four variables ruled the immobilization: solubility of the phosphate, pH, specific surface area and the amount of Ca and P in the solution. pH seems to be the most important parameter followed by [Ca] and [P] and specific surface area.

Chen et al., *(30)* confirmed the importance of pH in a system containing a single metal. In fact they studied the effects of pH during the sorption of Pb, stating that the solubility of apatite decreases with the increase of pH like the crystallinity of the pyromorphite decreases with the increase of pH. In the case of Cd, the sorption increases with the increasing pH and the formation of otavite ($CdCO_3$) occurs. Unlike Cd, Zn sorption decreased with the increase of pH, till pH > 6.5 resulting an almost complete sorption.

They didn't exclude for lead immobilization, in addition to the main mechanism: precipitation/dissolution, other mechanism such as adsorption and ion exchange. For cadmium immobilization they proposed the precipitation of solid phase and as main mechanism the ion exchange with Ca with Cd which preferentially occupied Ca (2) sites while the concentration of Ca (1) remained unchanged. Furthermore the sorption of aqueous Zn was similar to that of aqueous Cd, so that ion exchange mechanism and, at the same time, the surface complexation with HA surface functional groups are the main mechanism as suggested from Xu et al. *(152)*. Moreover, the competitive effects among heavy metal, like the competition for adsorption sites and for precipitation onto HA, may alter the sorption behaviour. In case of a single – metal system the competition is solely between ions of the same metal (internal competition) and with H^+ for adsorption sites. The situation is more complicated passing from the single system to the multi - metal system where the competitive sorption includes more phenomena: internal competition, competition with H^+ and competition with each element for precipitation and for adsorption sites.

Valsami-Jones et al. *(147)* confirmed that during the sorption of Cd pH increases whereas during Pb sorption pH decreases. Moreover, during Pb sorption the HA dissolution is stoichiometric, being the amount of Ca in solution the same of the loss Pb due to the

precipitation of a Pb-hydroxyapatite which has a larger cell because the Pb ionic radius is larger than that of Ca. In case of Cd sorption, in general, at low pH values hydroxyapatite dissolution is stoichiometric, if pH > 3 the dissolution becomes non-stoichiometric forming a calcium-poor surface layer if the hydroxyapatite is synthetic, in case of natural apatite, the dissolution produced measurable phosphate concentration in solution. In the case of Pb sorption the mechanisms proposed are cation exchange ($Ca^{2+} \rightarrow Pb^{2+}$) and dissolution/precipitation and the precipitation of Pb-hydroxyapatite can be terminated before apatite is completely consumed if Pb-hydroxyapatite isolated un-reacted apatite core.

For Cd sorption the proposed mechanisms are solid state diffusion, adsorption, precipitation of Cd-phosphate and precipitation of Ca-Cd phosphate. According to McGrellis et al., *(103)* the most probable sorption mechanism for Cd is the ion exchange ($Ca^{2+} \rightarrow Cd^{2+}$). In batch experiments Cd^{2+} cation can substitute Ca (2) at 20°C, increasing the temperature to 72°C Cd can occupy both sites Ca (1) and Ca (2). Cadmium slow introduction in the system HA solution allows a more effective diffusion on the metal in the apatitic network with a decrease of the concentration gradient and a larger occupation of Ca (1) site.

In case of double sorption process with slow introduction it is observed a lower occupancy of Ca (1) site and cell parameters is less for comparable Cd contents. One reason for the limitation of cadmium uptake may be an intrinsic property of cadmium not to occupy a site close to another already occupied by the same cation.

The prevailing heavy metal sorption mechanism can be individuated by the shape of the sorption isotherms relating the amount of sorbed metal to the equilibrium metal concentration in the solution [Metal sorbed (mmol/kg) vs. Equilibrium concentration (mM)] as stated in Echeverria et al. *(49)*. For example Pb usually shows a vertical isotherm (type C) reflecting a precipitation mechanism. Cu and Cd isotherms are type L subtype 2 indicating adsorption mechanism and surface precipitation, whereas the sorption isotherm of Zn is a type L subtype 4, meaning ion sorption due to new site or development of a fresh surface where retention take place. Echeverria et al. *(49)* suggested that internal competition affects heavy metals sorption either in single-metal either in multi-metal system, in particular, the presence of other cations decreased the sorption of all metals. The shape of a multi-metal isotherm showed an initial linear part shorter and a knee

sharper than the single-metal isotherm. Furthermore, if the attachment of sorbates to the amendant is strong (Pb and Cu) ions tend to spread out on the surface. In case of lowest equilibrium concentration the competitive ions were retained, whereas for higher equilibrium concentration isotherm showed a major affinity for Pb and Cu than for Cd and Zn.

In case of mono-metal sorption HA dissolution is stoichiometric, Ca desorbed was a linear function of the metal sorbed suggesting an ion exchange mechanism. In case of competitive sorption, even though the relationship among Ca desorbed and the heavy metals sorbed is linear, the slope is lower than one indicating other sorption processes, in particular for Cu, Pb and Zn.

According to them, the increase of pH increased the sorption due to the formation of pH-dependent sites on colloids, reducing competition with H-ions and a change in the hydrolysis state of ions in solution. Moreover Pb and Cu are more retained than Cd and Zn because of less interferences in the competitive sorption process. In particular in soils Pb and Cu would prefer organic site to occupy during the sorption whereas Cd and Zn would prefer inorganic sites.

According to Peld et al. *(122)* a main factor which rules the apatite sorption is the specific surface area, secondly solution composition, contact time, temperature and so on. To discern the predominant sorption mechanism Q_s (molar ratios of cations bound by apatite to Ca^{2+} released from apatite) is helpful. When Qs = 1, the quantities of the bound and released cations are equal indicating an ion-exchange mechanism between the apatite and solution. If $Q_s > 1$, a quantity of bound metal ions is more than the released ones, indicating a non-stoichiometric sorption and mechanisms such as surface-complexation or the filled cationic vacancies in the apatite crystal lattice. When $Q_s < 1$, apatite dissolution and precipitation of new phosphate phase having lower cation to phosphate molar ratio occurs. Determining of the main sorption mechanism is complicated by the fact that these different processes may also occur simultaneously. Peld et al. *(122)* proposed as sorption mechanism for Cd and Zn the ion exchange because there was no evidence of formation of new phases. The opposite process, desorption, of Cd and Zn mainly depend on the amount of cations bound at sorption, so that desorption increased with the increasing of the sorption level.

Concerning soils, Cao et al. *(25)* write that heavy metal immobilization using P as amendment was successful in laboratory study, so that the next step was the implementation of this technology in the field. They experimented with different kinds of amendment and phosphate rock is more effective than phosphoric acid in immobilizing Pb *in situ* because more P was available for formation of Pb-phosphate. They proposed as sorption process the dissolution\precipitation mechanism. In case of Zn immobilization they proposed the surface complexation mechanism of Zn with functional groups and coprecipitation. They also noted that P amendment was less effective in case of Zn and Cu immobilization than for Pb.

In a multi-metal system, like a soil, mineral with a lower solubility form first and unfortunately zinc and copper phosphate have a greater solubility than Pb-phosphate so that the former is formed prior to copper and zinc. In fact hopeite ($Zn_3(PO_4)_2 4H_2O$) is more soluble than HP, so that the retention mechanism might be the sorption onto phosphate mineral rather than the precipitation of hopeite. In particular P amendments is efficient in transforming lead from non residual to residual forms, which is less available than the former. Lead immobilization is trough the formation of insoluble pyromorphite-like minerals after P application.

The effectiveness of immobilization is maximum for Pb and less for Zn and Cu. P amendments is helpful in reducing metal translocation from roots to shoots via formation and/or co-precipitation of insoluble metal phosphates in the roots in case of Pb and Zn, instead Cu concentration in the grass shoot is not affected by P amendments and it is unclear why P was not effective in reducing Cu translocation from root to shoot.

Another theory about *in situ* Cd sorption is proposed by Raicevic et al. *(127)*, who suggested a two step mechanism. The first step is characterized by the dissolution of HA and formation of new stable Cd-apatite phase on its surface. In the second step there is the diffusion of Cd ions inside HA crystal lattice, improving the stability of Cd-apatite. They also explained that the direct incorporation of Pb into HA crystal lattice is not probable because this would decrease the stability of the system. For Pb they proposed the dissolution/precipitation mechanism, with the formation of a new and more stable pyromorphite phase precipitated on the HA surface. This one step mechanism is in agreement with many researchers, HA dissolution provides phosphate anions available for the subsequent pyromorphite precipitation from aqueous solution containing lead cations.

They preferred to distinguish a two co-current process: HA dissolution, HP precipitation and its subsequent deposition on HA surface. If whole HA surface is covered from HP the process may terminate and therefore the Pb immobilization depends on the available HA surface, as previously showed by by Valsami-Jones et al. *(147)*.

Recently some studies were carried out to find suitable economic phosphate sources like natural apatite from phosphate rocks or other natural sources like bones.

Admassu et Breese *(2)* quoted fishbone behave in a similar manner as hydroxyapatite in the sequestration process. The metals contacted with fishbone were: Pb^{2+}, Zn^{2+}, Cd^{2+}, Cu^{2+}, Mg^{2+} and Ni^{2+}. Zinc appears to be sorbed to the surface of the apatite in addition to precipitating. Cu^{2+}, Pb^{2+} and Ni^{2+} seem to be sorbed for low concentration, but increasing the concentration the sorption decreases and a possible explanation is that the metal phosphate precipitates coating the surface of the apatite, preventing further dissolution/precipitation mechanism. The reaction is complete after 15 minutes and this fast reaction support the use of fishbone apatite in either a column or in a barrier form for heavy metal containment or sequestration.

An et al. *(4)* demonstrated the ability of raw crab shell to remove heavy metals like Pb, Cd, Cu and Cr from aqueous solutions, comparing the results with a cation exchange resin (CER), zeolite, granular activated carbon (GAC) and powdered activated carbon (PAC). Lead was better removed with the crab shell rather than with CER, zeolite, PAC and GAC. Cadmium and Cromium show a similar trend of Pb. In case of Cd the removal capacity of crab shell was higher than those of any other sorbents. In case of Cr the removal was not accomplished well comparing to the cases of other metals and no removal by zeolite, PAC and GAC. According to their results the maximum efficiency in removing heavy metal is achieved in 12 hours but it depends on the initial concentration of the heavy metals. The heavy metal removal rate was Cd > Pb > Cr $\geq$ Cu using the crab shell, whereas the order of sorption effectiveness is: crab shell > CER > zeolite > PAC $\geq$ GAC.

Another suitable phosphate source is represented by the ground up bone meal (Hodson et al. *(71)*) for the remediation of contaminated soils with heavy metal. The bone meal was identical to that used as a garden fertilizer and it was used despite its metal contaminants content. The bone meal dissolution was proportional to the amount of bone meal surface area per unit volume of soil and the metal immobilization should increase

with the increase of bone meal surface area per unit volume of soil. It was observed no significant change in metal immobilization with varying bone meal grain size. This might due to low differences between the surface area of the different bone meal grain size and the increase in bone meal crystallinity with incineration. Additional evidence that the reduction in metal release with increasing bone meal concentration was not due to adsorption of metal ions comes from the fact that the CEC (cation exchange capacity) of the bone meal and soil were very similar so that the small addition of bone meal to the soil were unlikely to have caused a change the bulk CEC of the soil: bone meal mix.

Bone meal seemed to be a P source of suitable solubility that dissolves over a reasonable time scale but it doesn't dissolve sufficiently rapidly to release large amount of P into soil drainage water. Its addition generally resulted in increased soil and leachate pH and metal immobilization in the soils. Notwisthanding bone meal can be a potential treatment for metal-contaminated soils.

5 RESULTS SINGLE METAL SYSTEM

5.1 SINGLE-METAL SYSTEM SORBED ON SYNTHETIC HYDROXYAPATITE (HA)

5.1.1 XRD analyses

XRD analyses of solid residues from the filtered supernatants don't show the presence of HP but only HA, peaks and their intensities don't increase with the increasing of heavy metal concentration on the solution (Fig. 1). In addition the intensity of the diffraction patterns don't increase with the increase of reaction time as previously observed in Manecki et al. *(100)*. Comparing XRD patterns between the original HA and the solid materials (Fig. 2 A, B, C, and D), they are almost well overlapped, suggesting that the solid residues are quite similar to the original HA and there is no precipitation of any new phosphate minerals or HP (Fig. 3).

Lattice parameters (*a* and *c*) were calculated for random samples to determine if a new phosphate phase (e.g. Pb – HP) precipitated during the sorption tests. Comparing the lattice parameters of HA, HP and experimental solid materials, the values obtained for the

filtered materials are close to those of HA ones and not to those of HP, whose values are very different (Fig 4).

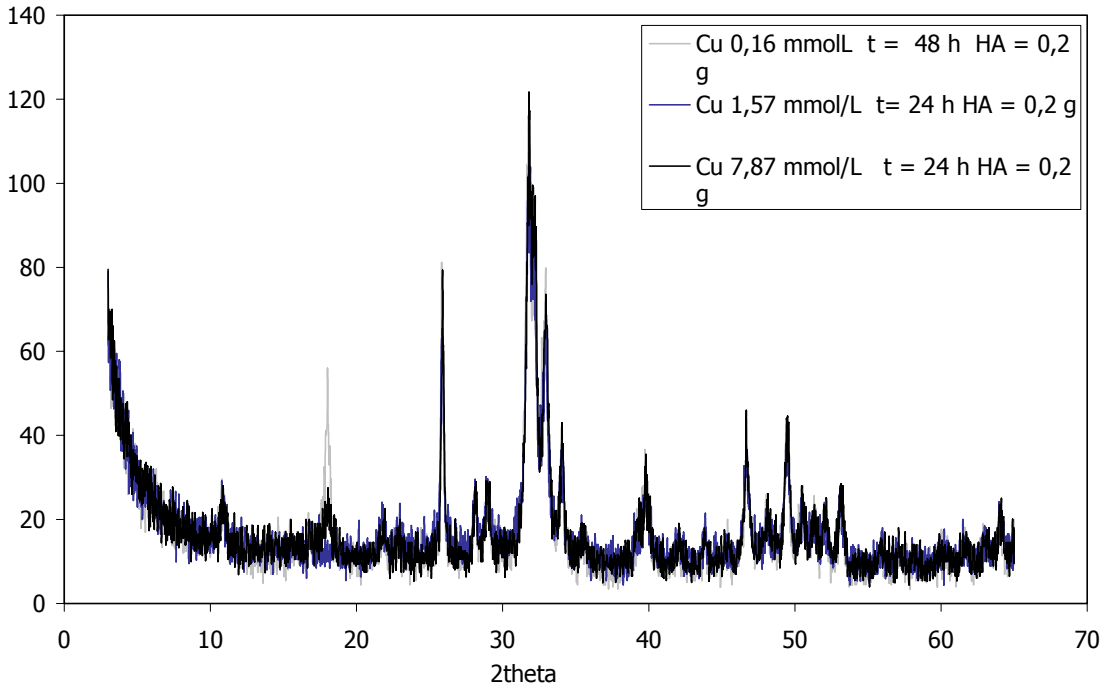

Fig. 1: Example of XRD patterns of the solid residue from a Cu single-metal system. Neither the increase of metal concentration nor the increase of contact time have an influence on the peak intensities. – Fig. 1: Esempio di un diffrattogramma dei materiali solidi estratti da un esperimento con Cu metallo-singolo. Appare evidente che né la concentrazione né il tempo di interazione hanno influenza sull'intensità dei picchi.

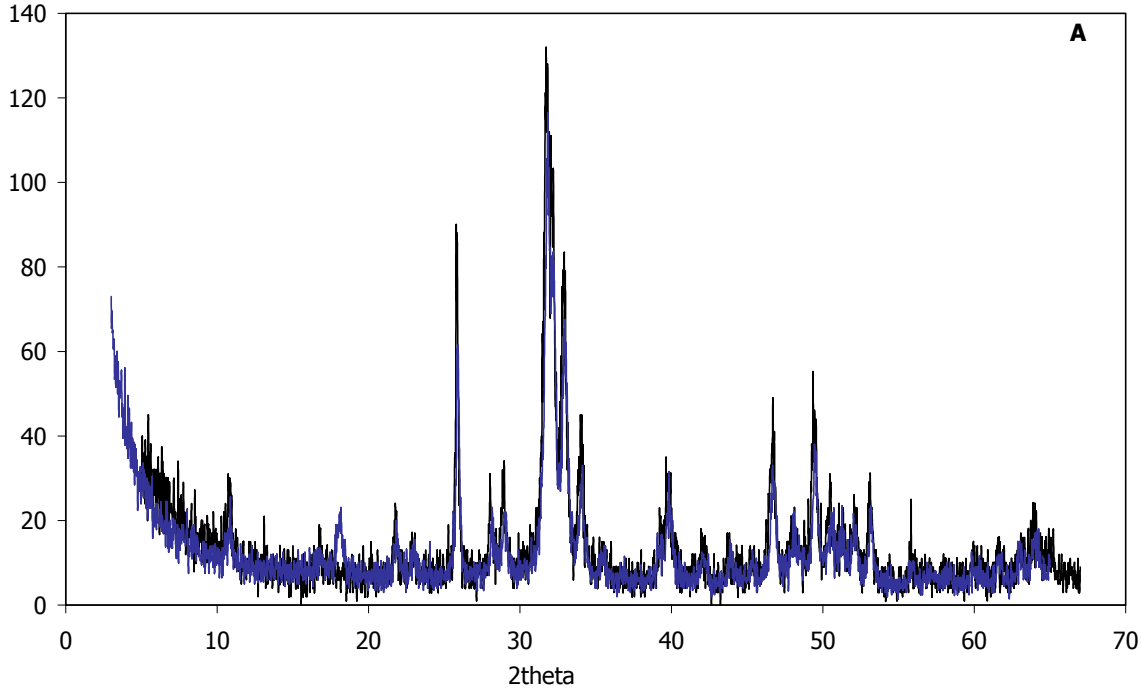

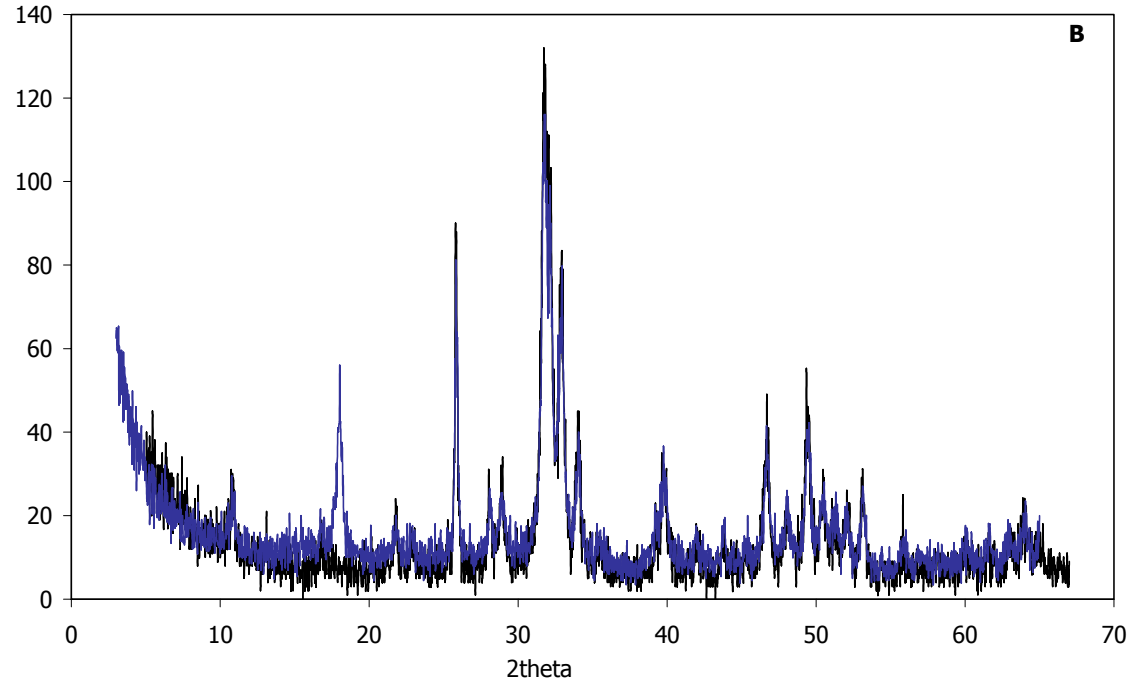
B
140
120
100
80
60
40
20
0
0
10
20
30
40
50
60
70
2theta

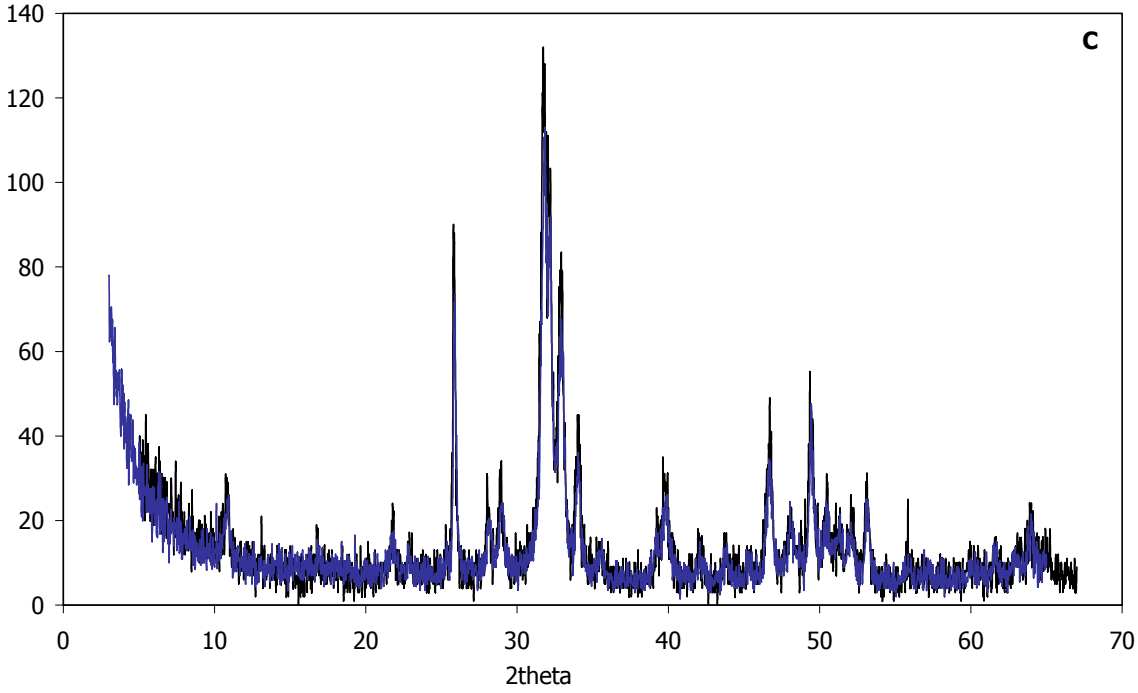
C
140
120
100
80
60
40
20
0
0
10
20
30
40
50
60
70
2theta

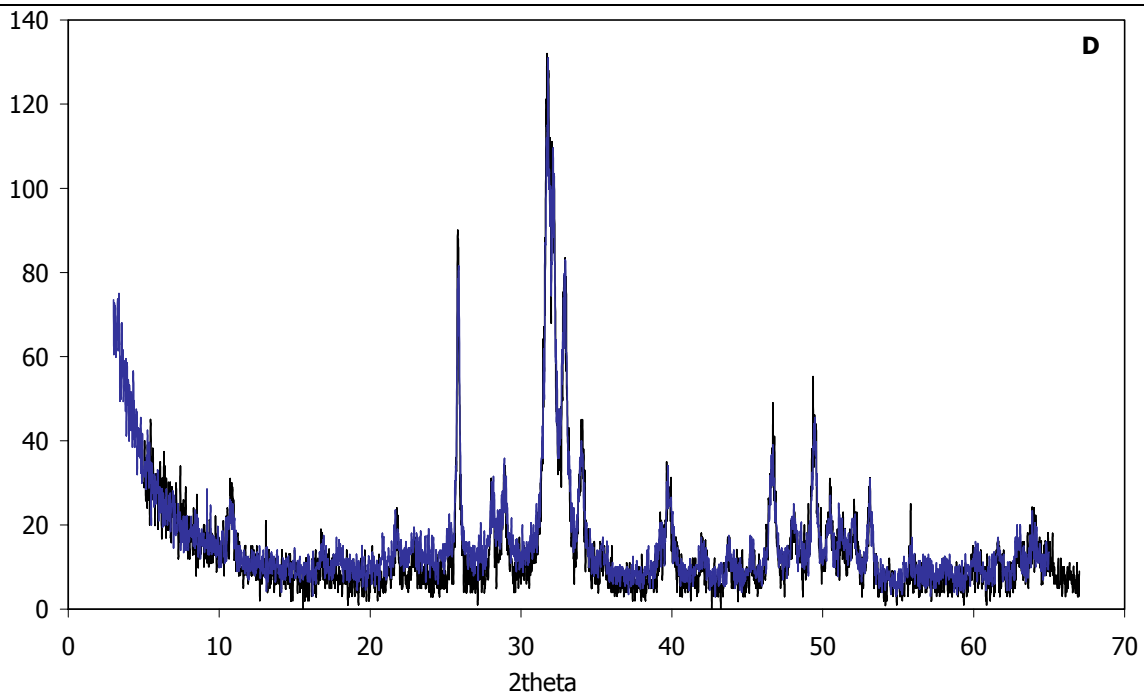

Fig. 2: XRD patterns of some solid materials from single metal system; in black the synthetic HA. A: Cd= 0.09 mmol/L, t= 24h, HA= 0.2 g; B: Cu= 0.16 mmol/L, t= 24h, HA= 0.2g; C: Pb= 0.48 mmol/L, t= 4h, HA= 0.2g; D: Zn= 0.15 mmol/L, t= 2h, HA= 0.2g. – Fig. 2: Risultati dell' analisi diffrattometrica di alcuni materiali solidi del sistema a metallo singolo; in nero è rappresentata l'idrossiapatite sintetica. A: Cd= 0.09 mmol/L, t= 24h, HA= 0.2 g; B: Cu= 0.16 mmol/L, t= 24h, HA= 0.2g; C: Pb= 0.48 mmol/L, t= 4h, HA= 0.2g; D: Zn= 0.15 mmol/L, t= 2h, HA= 0.2g.

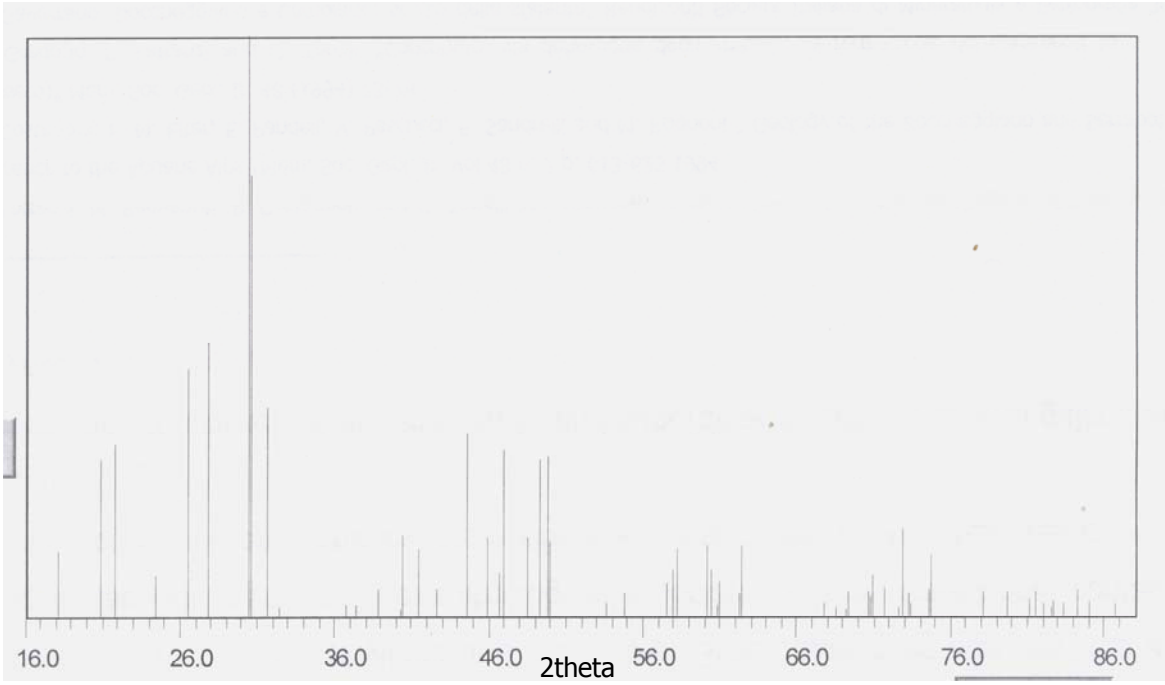

Fig. 3: Example of an HP pattern *(36)*. – Fig. 3: Esempio di diffrattogramma dell'HP *(36)*.

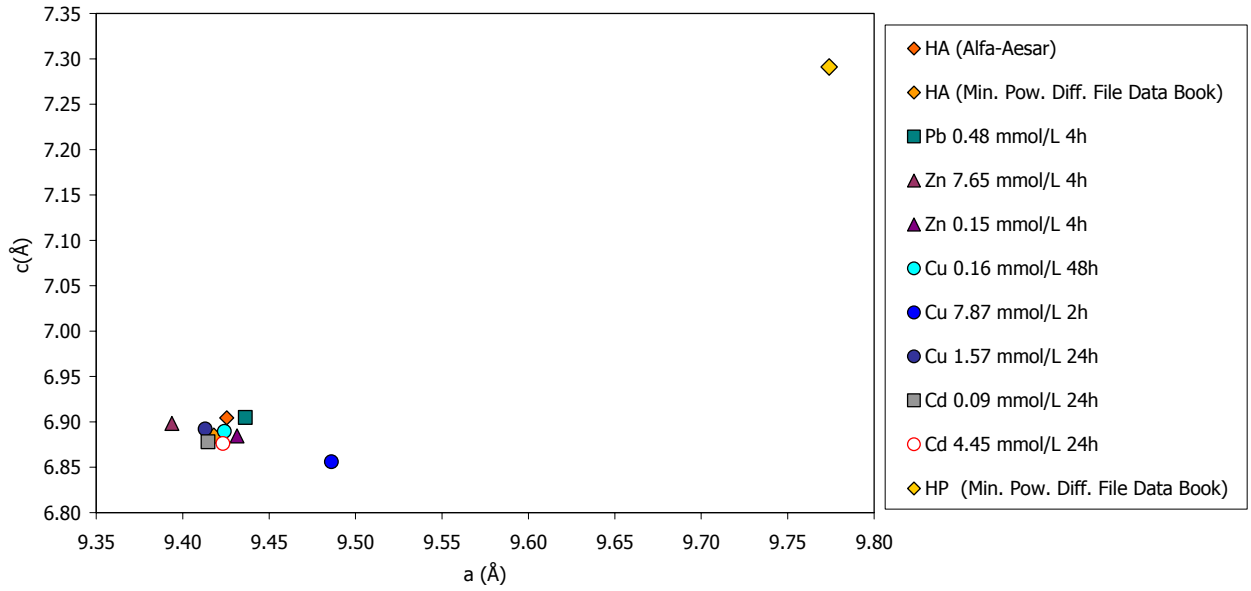

Fig. 4: Lattice parameters for some solid materials from single metal systems. Concentration for the heavy metals and contact time are different, HA concentration is always 0.2 g. - Fig. 4: Parametri di cella per alcuni materiali solidi del sistema a metallo singolo. La concentrazione dei metalli pesanti e i tempi di contatto sono diversi, la concentrazione dell'HA è sempre 0.2g.

5.1.2 FTIR analyses

Infrared spectroscopy was used for studying structural sites occupied by water molecules and hydroxyl groups and in particular to determine if some differences exist among the HA and the solid material after the sorption, because even low levels of substitution induce modifications on the HA spectrum. Each specimen, chosen randomly, used for FTIR analysis was prepared according to standard procedure by mixing about 2.50 mg of powdered sample with 250 mg of KBr and then pressed into a pellet. The water content in KBr was avoid by storaging KBr in a oven at a standard temperature (110°C).

Our solid residues have absorption bands of the synthetic phase comparable with the bands of the starting HA (Fig. 5), without any displacements and magnitude differences in the peaks.

In our samples the tetrahedral PO_4^{3-} ion has only two of the four infrared vibration modes: the band ν_3 is at 1026.9 cm^{-1} and ν_4 575.2 cm^{-1}, these vibration modes are characteristichs of phosphate compounds in the region 1200-900 cm^{-1} and 650-550 cm^{-1} *(136)*.

Generally, the ν_3 phosphate band (1200-900 cm^{-1}) is made of an overlapping components, the first one is in the high wave number (1200-1050 cm^{-1}) and the second one in the low wave number region (1050-900 cm^{-1}). In this case the overlapping doesn't occur, only the second band in the low wave number region is present. The strong band at 1030 cm^{-1} is attribuited to asymmetric stretching of P-O-P groups *(146)*. Besides, the ν_3 band is indicative of a Ca-deficient apatite (1088 cm^{-1} and 1030 cm^{-1}) *(61)*. This band is more sensitive to structural variation of phosphate ions. In particular the shoulder at 1112 cm^{-1}, attribuited to phosphate environments in poorly crystalline apatitic crystals, is absent *(61)*. The band at 1485.4 cm^{-1} represents the ν_3 antisymmetric component *(20)*.

The ν_4 band is described as O=P-O bending vibration *(111)* and the band at 584.4 cm^{-1} attributed to OH^- and not associated with ν_4 band; it was suggested to be the splitting fraction of the ν_4 band indicative of the crystal content of the associate compound in the sample *(146)*. The band at 3566.2 cm^{-1} is due to free and hydrogen bondes surface P-OH group *(98)*. The band at 1634.6 cm^{-1} could be assigned to water *(129)*. Moreover, another quite weak band was found located around 2916 cm^{-1}, it could be due to a stretching mode of the P-O-H group participating in the hydrogen bonding *(50)*.

The band at 469.6 cm^{-1} is assigned to the bending vibration of O-P-O units. In the region 700-830 cm^{-1}, resolved to two components 740 cm^{-1} and 866.9 cm^{-1}, and the band at 866.9 cm^{-1} with a small area is attribuited to the symmetric streching vibration of P-O-P rings. The region 850-1200 cm^{-1} is sensitive for the metaphosphate groups as chains-, ring- and terminal groups *(61)*. The series of weak bands between 1850 and 2000 cm^{-1} correspond to overtones and combinations ($2\nu_3$, $\nu_3 + \nu_1$, $2\nu_1$). Generally they occur at lower wavenumbers than those of Ca-apatite concomitant with the lower wavenumber of the main bands for the pyromorphite *(111)*.

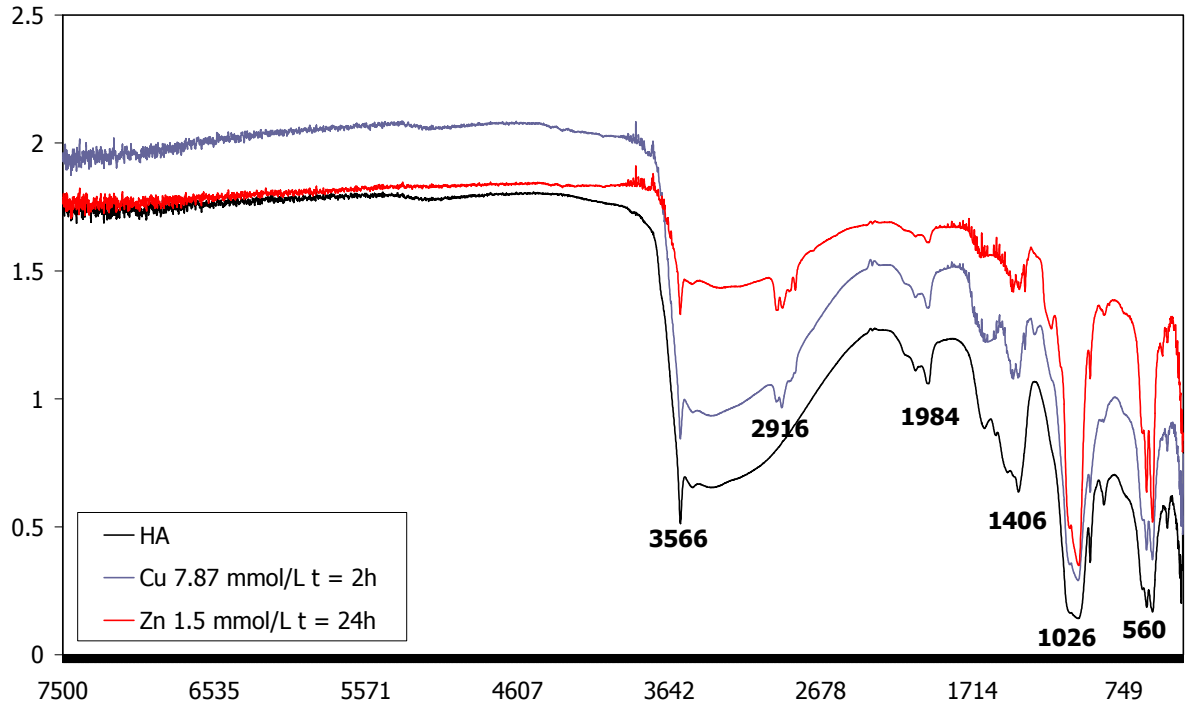

Fig. 5: FTIR spectra of random samples from the single metal system. – Fig. 5: Spettri FTIR di alcuni campioni del sistema a metallo singolo.

5.1.3 SEM analyses

SEM micrographs of the solid materials, before and after the sorption experiments with solutions at increasing concentrations, do not reveal obvious differences (Fig. 6 A, B, C, D and E) and neither significant morphological variations or orientation were found in HA particles, probably, because of their small size and/or SEM was unable to achieve high enough resolution to detect the shape of the particles. EDS studies on the treated HA do not identify new solid phases on the surfaces of HA (Fig. 7 A, B, C, D and E), however the presence of Pb, Zn, Cu and Cd was detected.

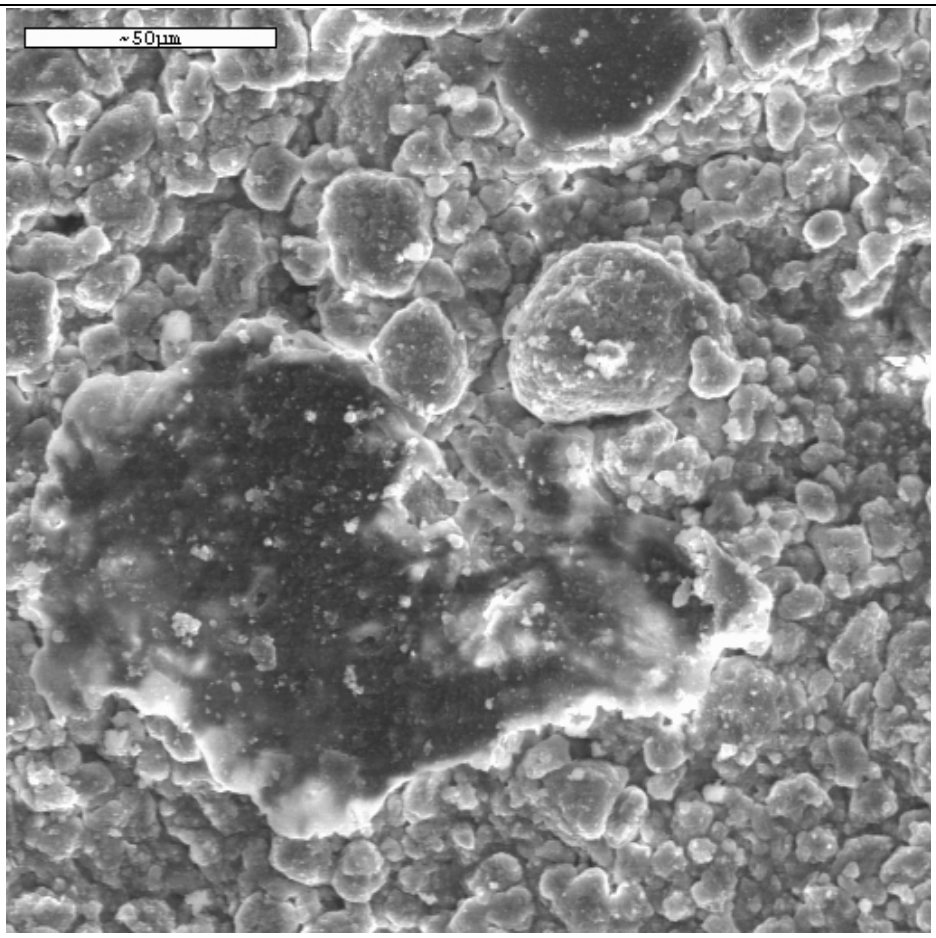

A

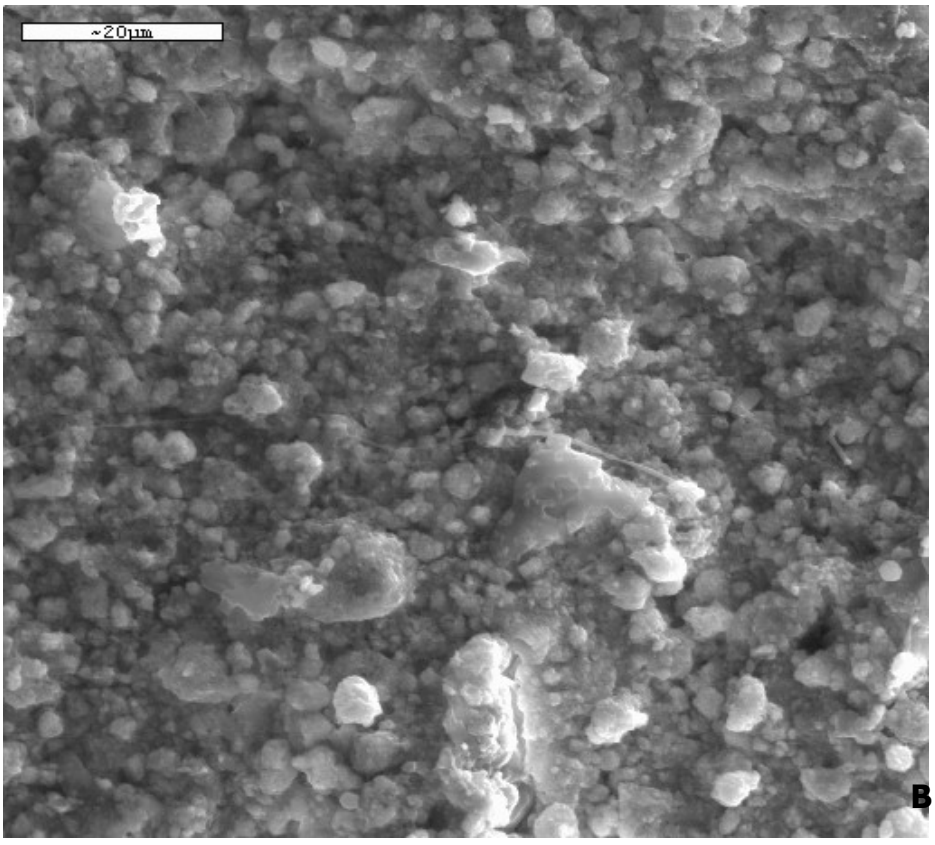

B

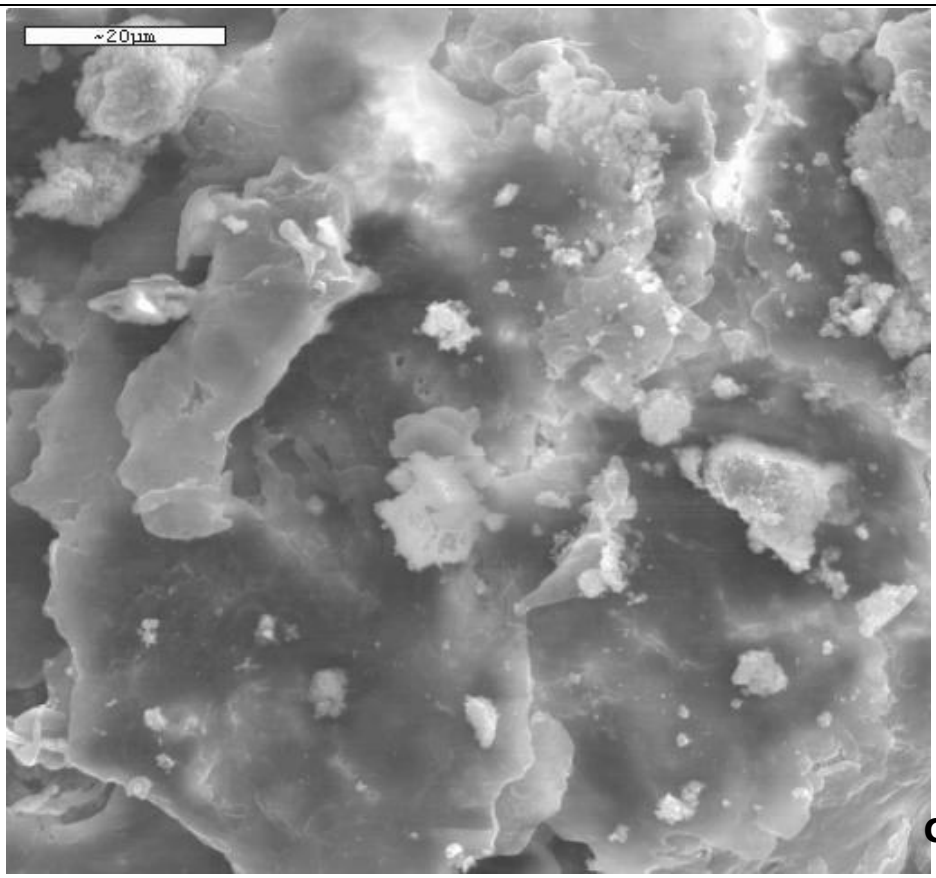

C

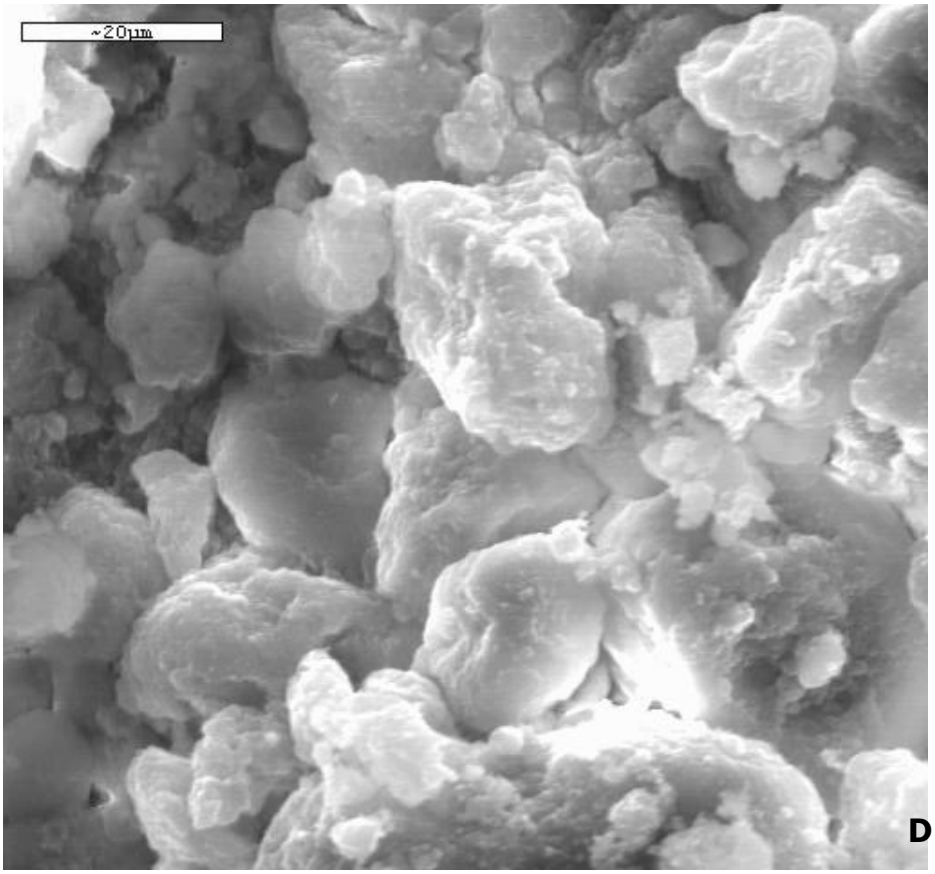

D

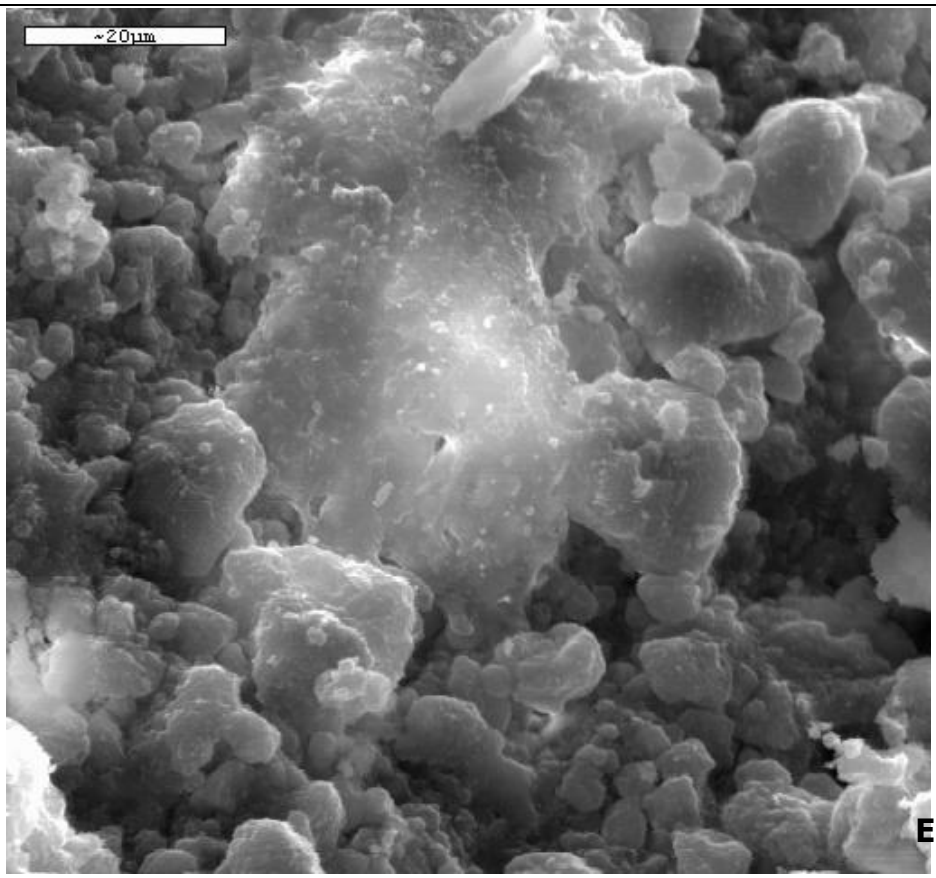

Fig. 6: Examples of SEM micrographs of solid residues: A = blank t = 24h HA = 0.2g; B = Cd 0.89 mmol/L t = 48h HA = 0.2 g; C = Cu 1.57 mmol/L t = 48h HA = 0.2 g; D = Pb 0.05 mmol/L t = 2h HA = 0.2 g; E = Zn 0.15 mmol/L t = 4h HA = 0.2 g. Although the concentrations of each heavy metals are different, the shape of HA grains before and after the reaction is similar. Generally, the grains appear to be both spherical and flat. - Fig. 6: Esempi di immagini al SEM dei residui solidi: A = blank t = 24h HA = 0.2g; B = Cd 0.89 mmol/L t = 48h HA = 0.2 g; C = Cu 1.57 mmol/L t = 48h HA = 0.2 g; D = Pb 0.05 mmol/L t = 2h HA = 0.2 g; E = Zn 0.15 mmol/L t = 4h HA = 0.2 g. Nonostante le concentrazioni di ciascun metallo siano state differenti negli esperimenti, l'abito dei granuli di HA prima e dopo gli esperimenti è simile. Generalmente essi hanno sia forma sferica che tabulare.

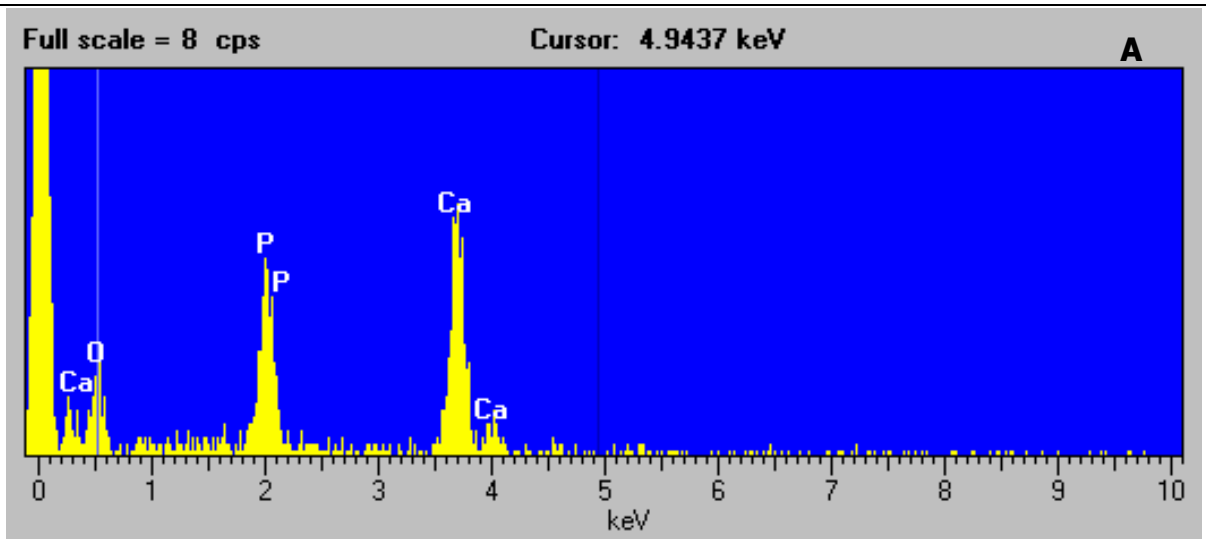
Full scale = 8 cps
Cursor: 4.9437 keV
A
Ca
P
P
O
Ca
Ca
0 1 2 3 4 5 6 7 8 9 10
keV

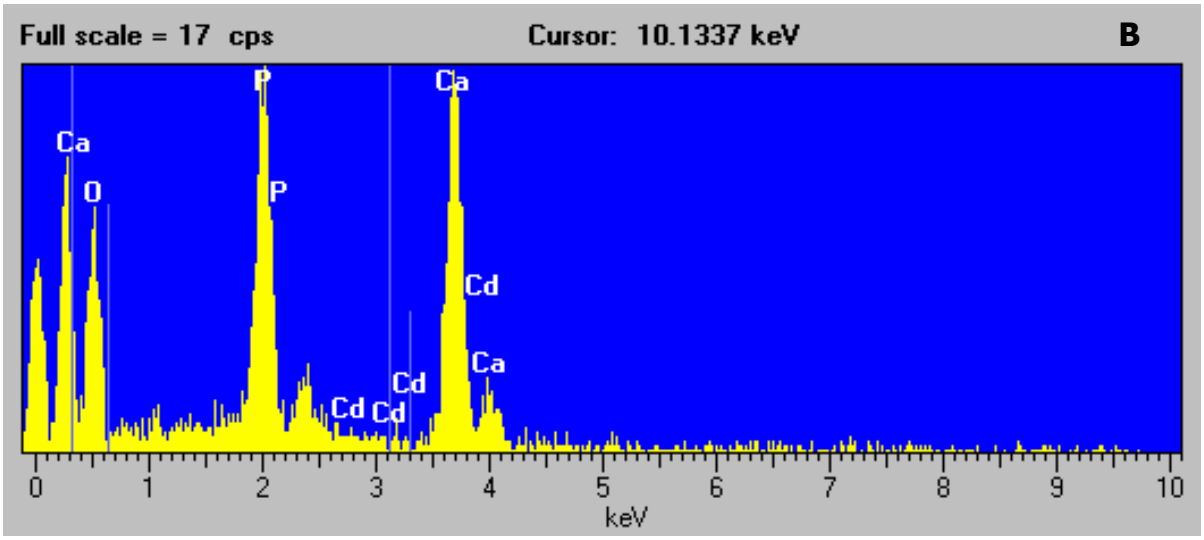
Full scale = 17 cps
Cursor: 10.1337 keV
B
Ca
O
P
P
Ca
Cd
Ca
Cd
Cd
0 1 2 3 4 5 6 7 8 9 10
keV

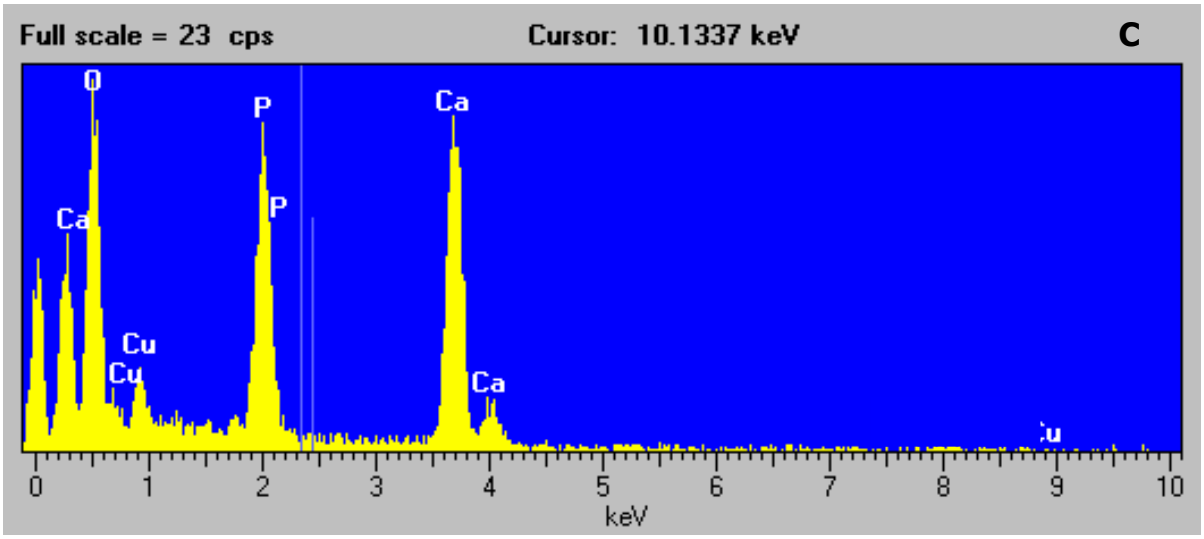
Full scale = 23 cps
Cursor: 10.1337 keV
C
O
Ca
P
P
Ca
Cu
Cu
Ca
0 1 2 3 4 5 6 7 8 9 10
keV

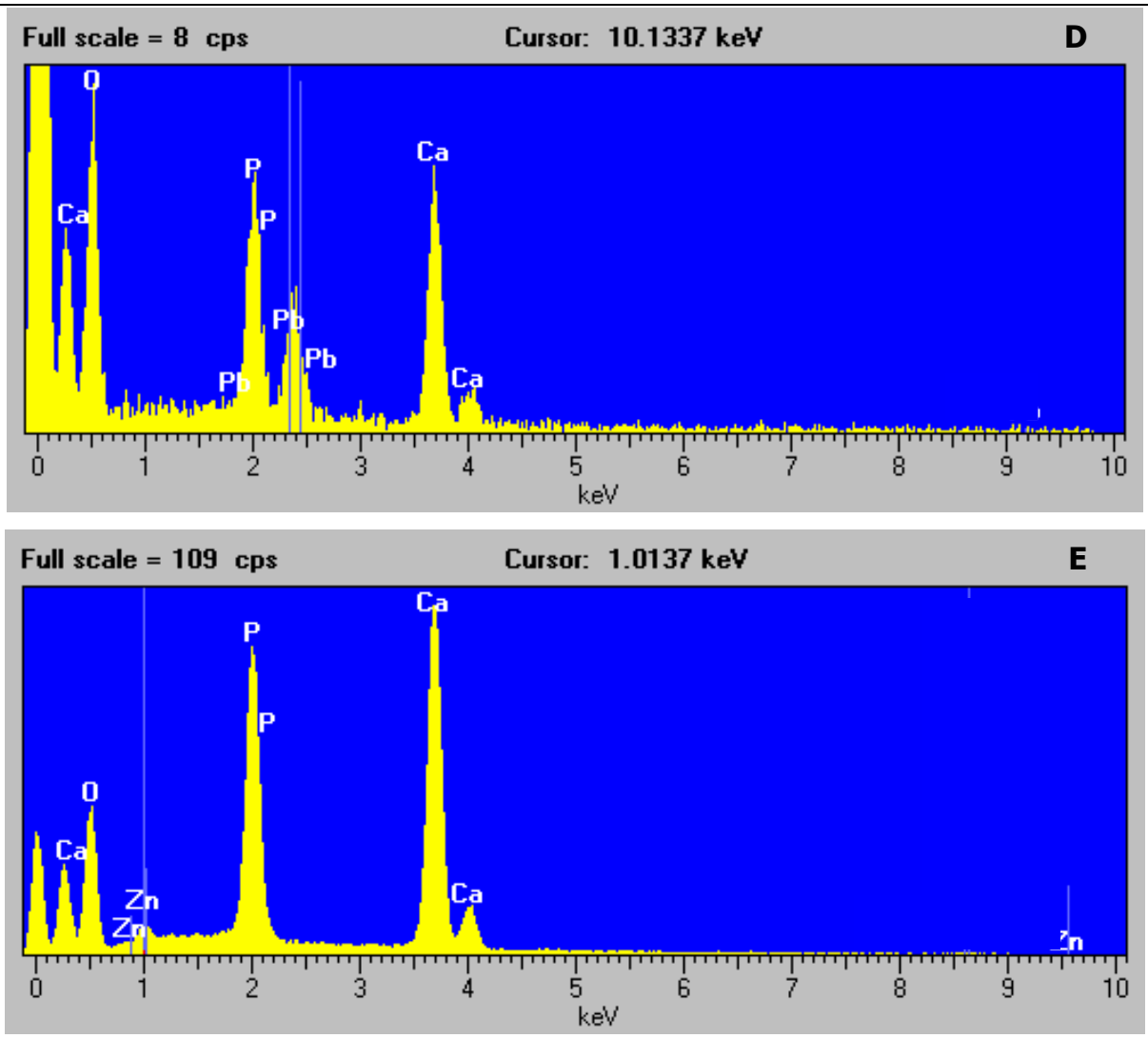

Fig. 7: EDS spectra of the SEM micrographs in Fig. 6 - Fig. 7: Spettri EDS delle precedenti immagini al SEM di Fig. 6.

5.1.4 AFM analyses

The SEM-EDS studies of the reacted HA showed that its morphology was similar to the unreacted one. It could be possible that the dissolution and reprecipitation process affected the morphology of the HA particles at a scale invisible to the SEM technique. Therefore, the solid materials were analysed through AFM (Atomic Force Microscope). The study was carried on with the help of Prof. J. Rakovan at the Geology Department of Miami University (Oxford, OH, USA).

The analyzed samples are generally of 100 mg/L and 500 mg/L for the four interaction times (2, 4, 24 and 48h) and show spherical shape (Fig. 8 A, B, C and D) with an average diameter of about 100 nm, (horizontal distance) (Fig. 9 A, B and C). The

particles don't show any different features from the original HA (Fig. 4b in materials) neither from blank samples (Fig. 10 A and B) and nor from each different single-metal system with various contact time.

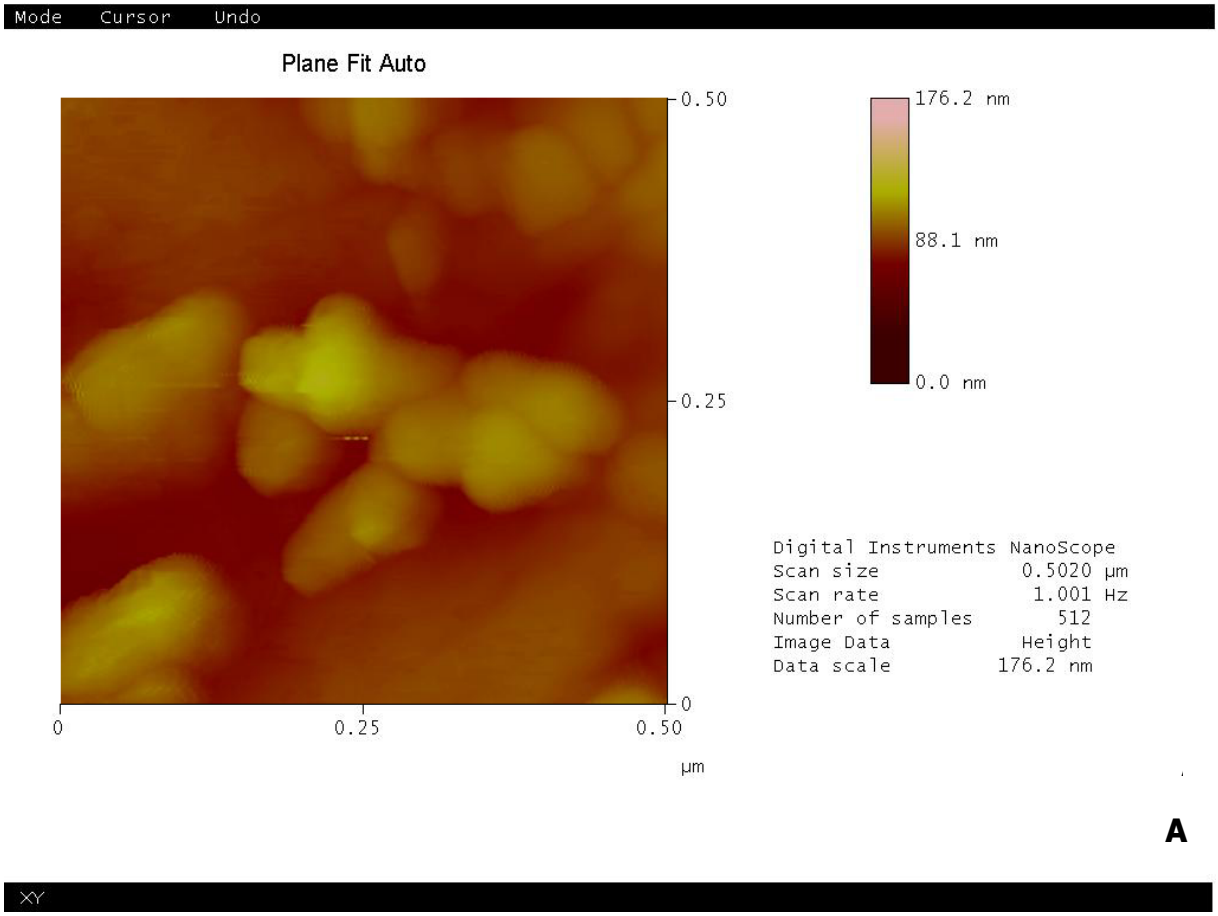

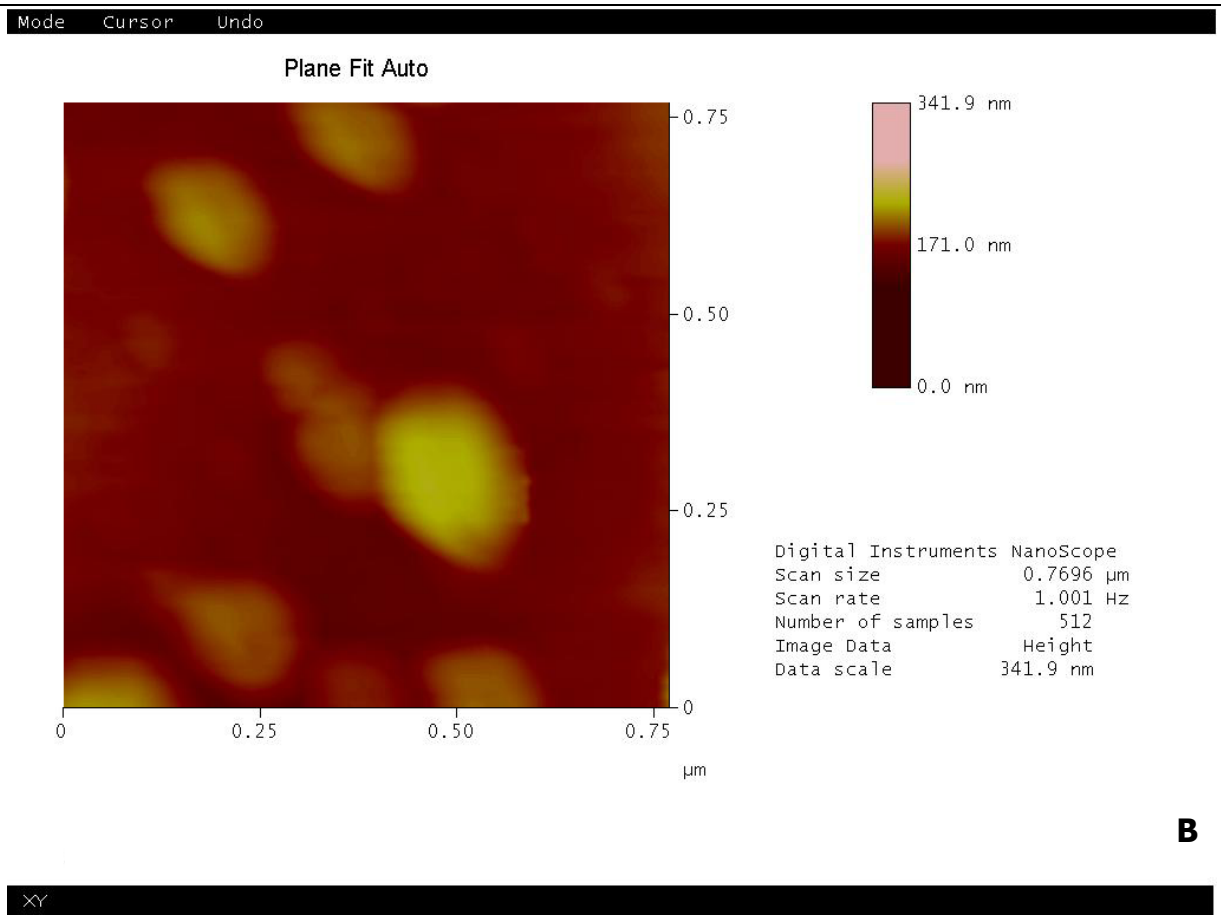
Mode Cursor Undo
Plane Fit Auto
0.75
0.50
0.25
0
0
0.25
0.50
0.75
µm
341.9 nm
171.0 nm
0.0 nm
Digital Instruments NanoScope
Scan size 0.7696 µm
Scan rate 1.001 Hz
Number of samples 512
Image Data Height
Data scale 341.9 nm
B
XY

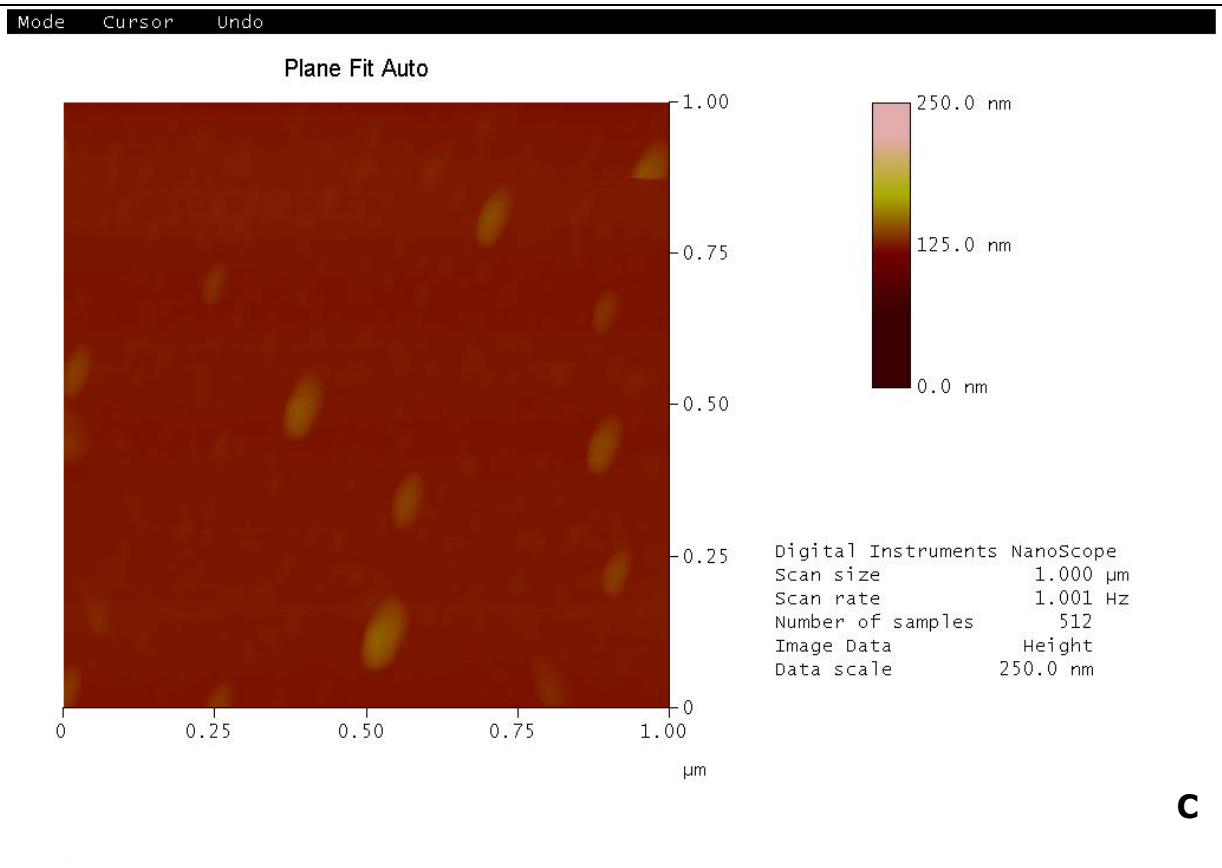
Mode Cursor Undo
Plane Fit Auto
1.00
0.75
0.50
0.25
0
0 0.25 0.50 0.75 1.00
µm
250.0 nm
125.0 nm
0.0 nm
Digital Instruments NanoScope
Scan size 1.000 µm
Scan rate 1.001 Hz
Number of samples 512
Image Data Height
Data scale 250.0 nm
C
XY

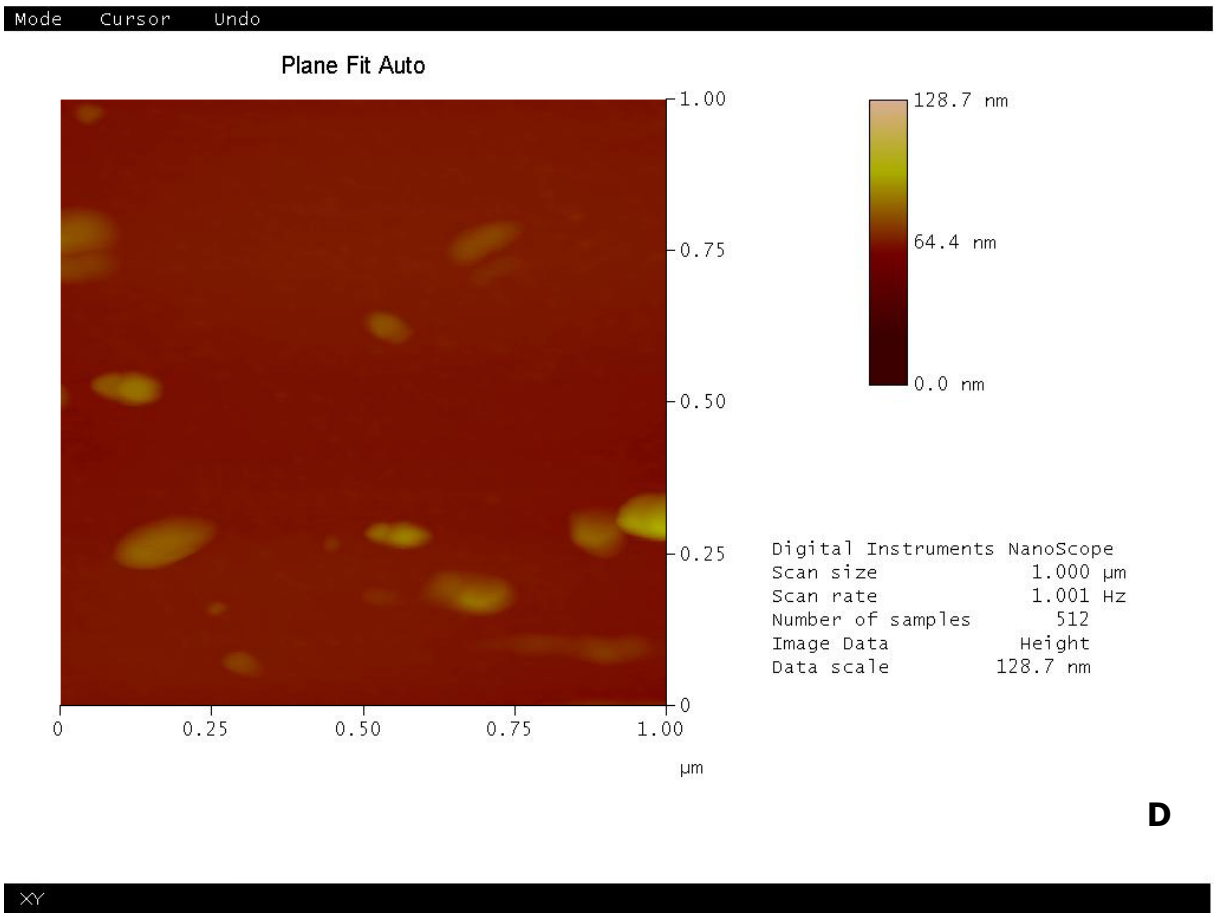
Mode Cursor Undo
Plane Fit Auto
1.00
0.75
0.50
0.25
0
0 0.25 0.50 0.75 1.00
µm
128.7 nm
64.4 nm
0.0 nm
Digital Instruments NanoScope
Scan size 1.000 µm
Scan rate 1.001 Hz
Number of samples 512
Image Data Height
Data scale 128.7 nm
D
XY

Fig. 8: AFM images of the solid residues A: Cd 500 mg/L t = 48h; B: Cu 100 mg/L t = 48h; C: Pb 100 mg/L t = 24h; D: Zn 500 mg/L t = 2h. – Fig. 8: Immagini dei materiali solidi eseguite all'AFM A: Cd 500 mg/L t = 48h; B: Cu 100 mg/L t = 48h; C: Pb 100 mg/L t = 24h; D: Zn 500 mg/L t = 2h.

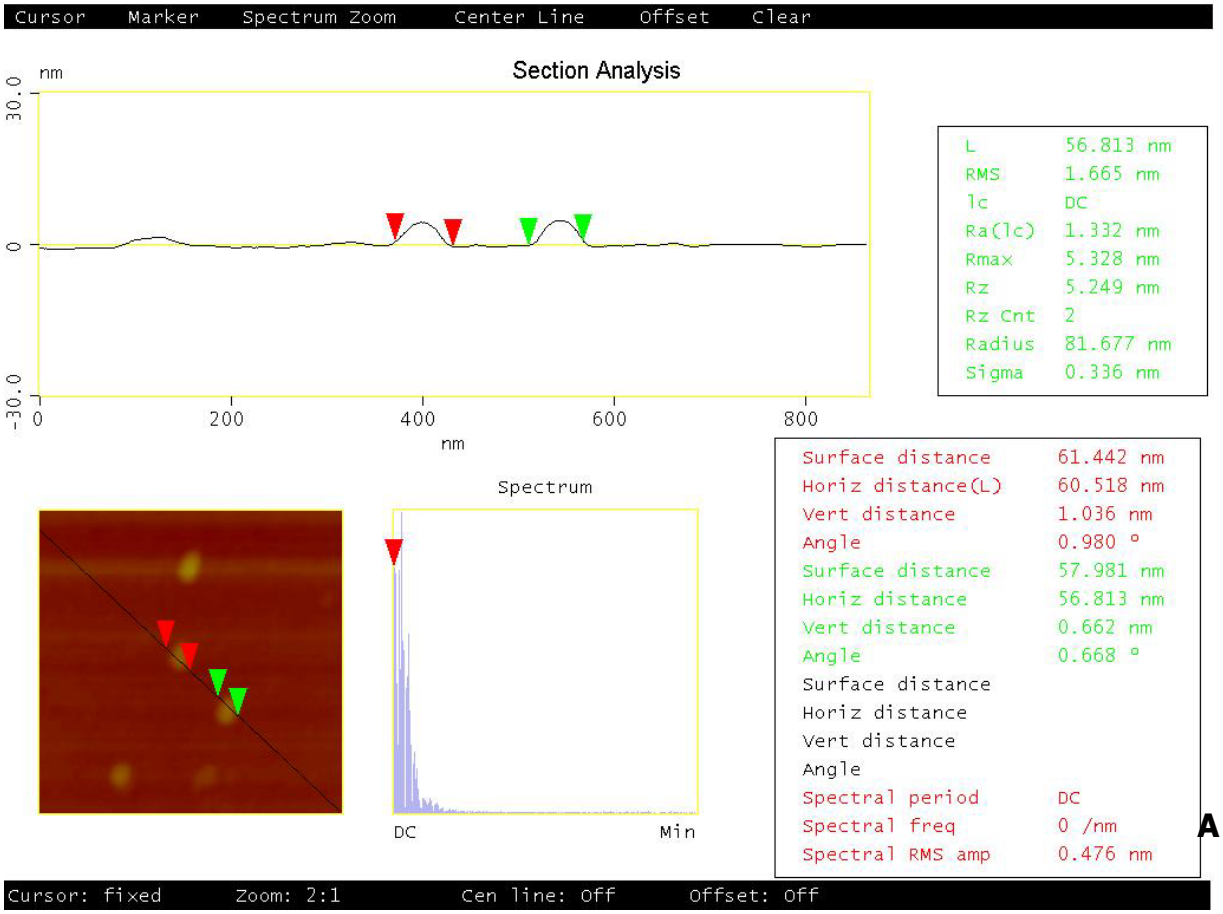

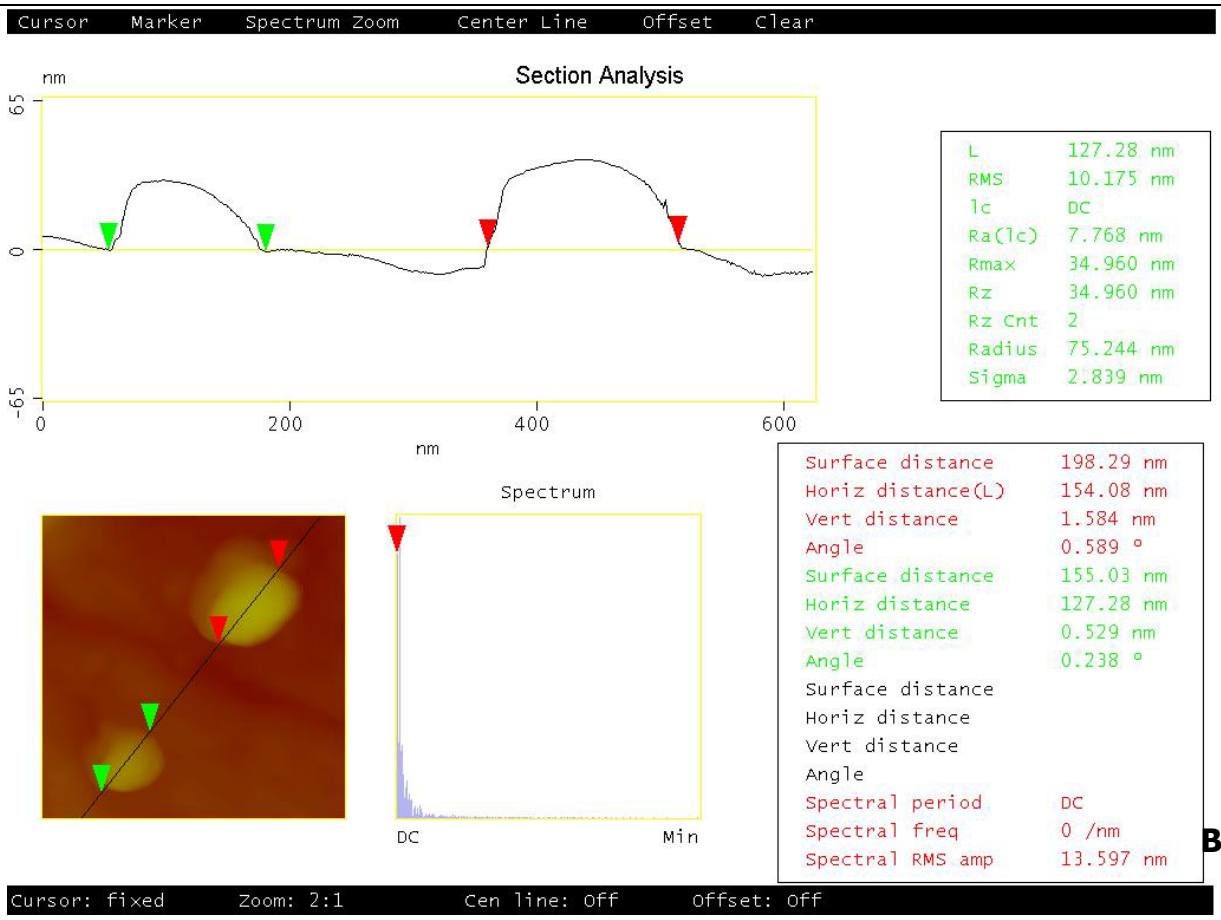
Cursor Marker Spectrum Zoom Center Line Offset Clear
Section Analysis
nm
65
0
-65
0
200
400
600
nm
L 127.28 nm
RMS 10.175 nm
lc DC
Ra(lc) 7.768 nm
Rmax 34.960 nm
Rz 34.960 nm
Rz Cnt 2
Radius 75.244 nm
Sigma 2.839 nm
Spectrum
DC
Min
Surface distance 198.29 nm
Horiz distance(L) 154.08 nm
Vert distance 1.584 nm
Angle 0.589 °
Surface distance 155.03 nm
Horiz distance 127.28 nm
Vert distance 0.529 nm
Angle 0.238 °
Surface distance
Horiz distance
Vert distance
Angle
Spectral period DC
Spectral freq 0 /nm
Spectral RMS amp 13.597 nm
Cursor: fixed Zoom: 2:1 Cen line: Off Offset: Off

B

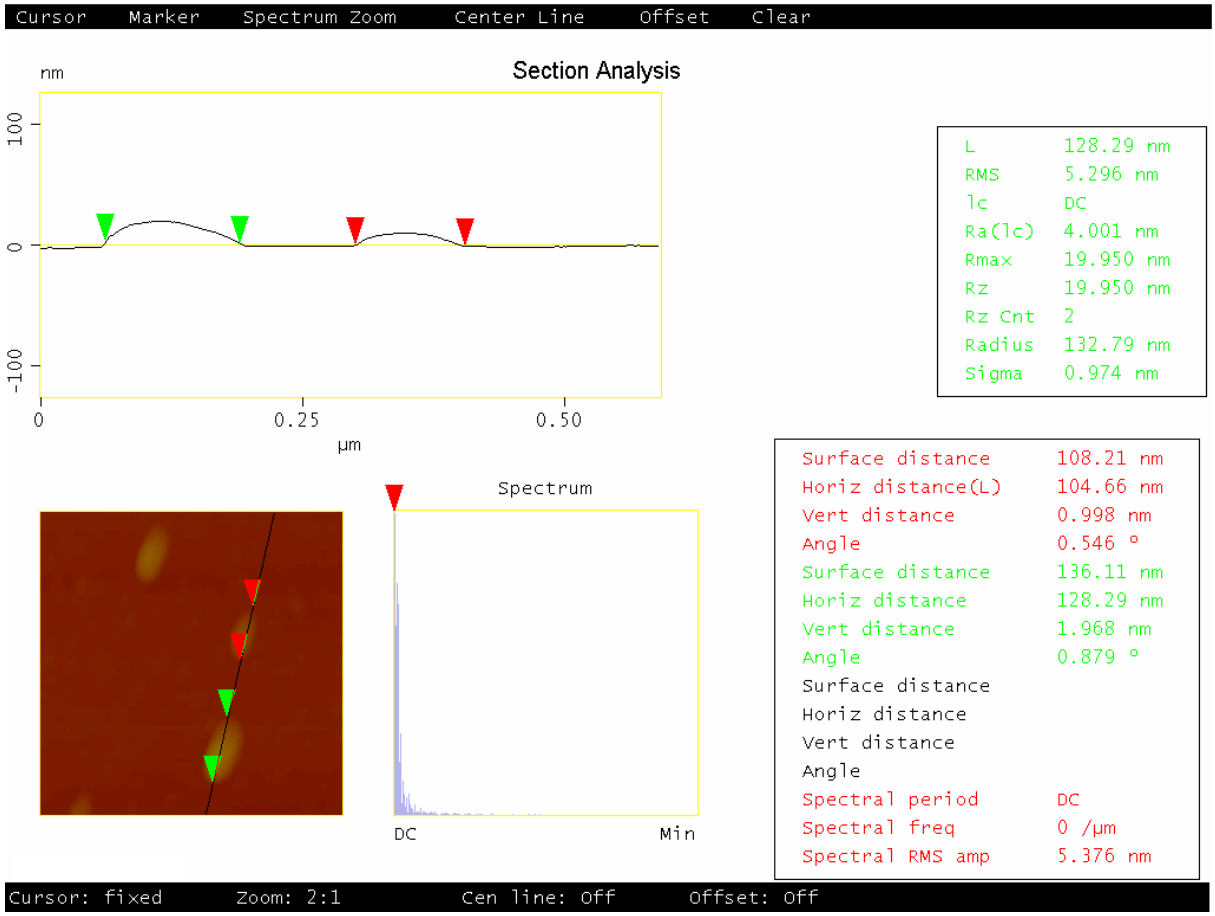
Cursor Marker Spectrum Zoom Center Line Offset Clear
Section Analysis
nm
100
0
-100
0
0.25
0.50
µm
L 128.29 nm
RMS 5.296 nm
lc DC
Ra(lc) 4.001 nm
Rmax 19.950 nm
Rz 19.950 nm
Rz Cnt 2
Radius 132.79 nm
Sigma 0.974 nm
Spectrum
DC
Min
Surface distance 108.21 nm
Horiz distance(L) 104.66 nm
Vert distance 0.998 nm
Angle 0.546 °
Surface distance 136.11 nm
Horiz distance 128.29 nm
Vert distance 1.968 nm
Angle 0.879 °
Surface distance
Horiz distance
Vert distance
Angle
Spectral period DC
Spectral freq 0 /µm
Spectral RMS amp 5.376 nm
Cursor: fixed Zoom: 2:1 Cen line: Off Offset: Off

C

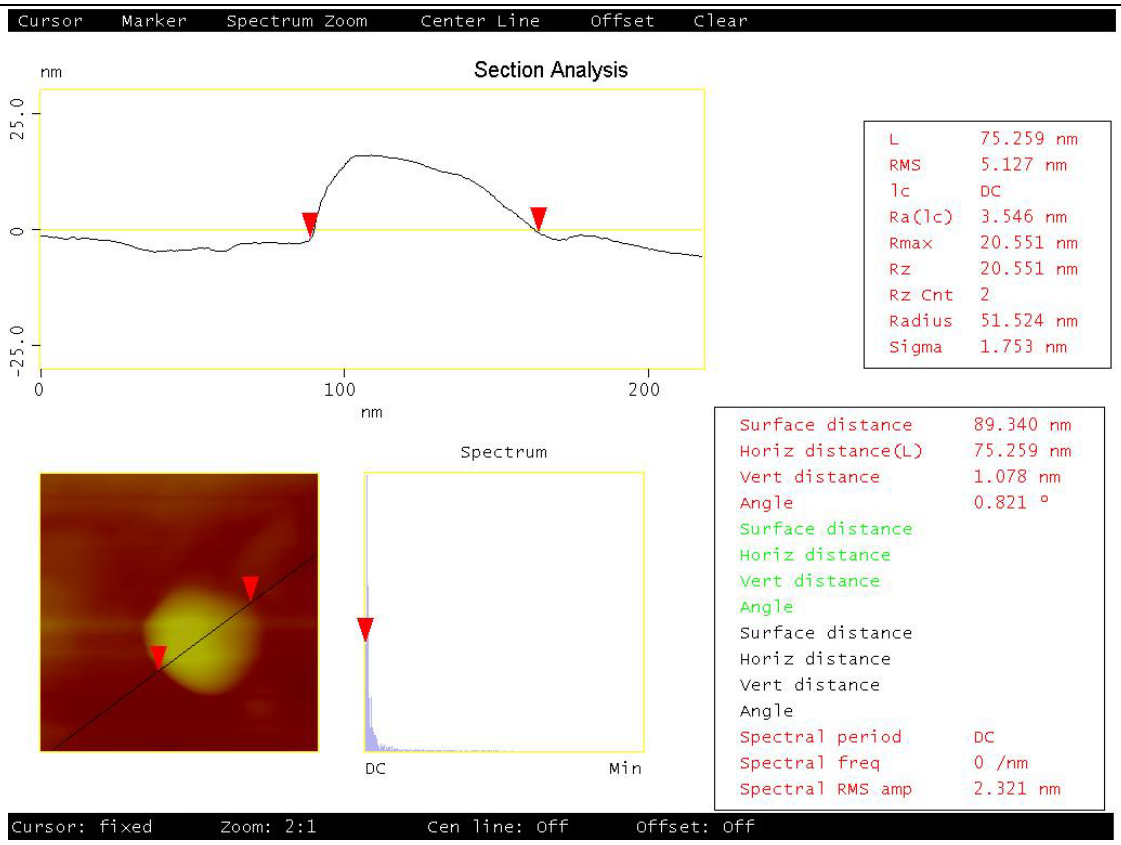

Fig. 9: AFM images of the solid residues showing the average size of the particles. A: Cd 500 mg/L t =4h; B: Cu 500 mg/L t = 2h; C: Pb 500 mg/L t = 2h; D: Zn 500 mg/L t = 48h. – Fig. 9: Immagini AFMdei materiali solidi mostranti le dimensioni medie dei granuli di HA. A: Cd 500 mg/L t =4h; B: Cu 500 mg/L t = 2h; C: Zn 500 mg/L t = 48h.

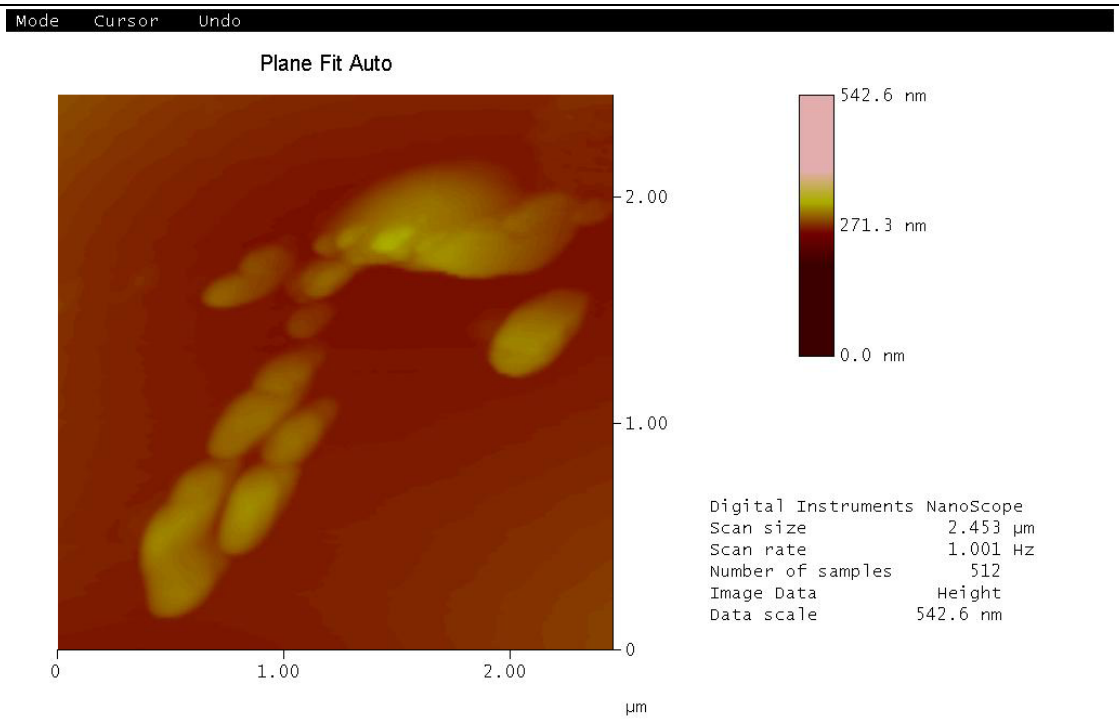
Mode Cursor Undo
Plane Fit Auto
542.6 nm
271.3 nm
0.0 nm
2.00
1.00
0
0
1.00
2.00
µm
Digital Instruments NanoScope
Scan size 2.453 µm
Scan rate 1.001 Hz
Number of samples 512
Image Data Height
Data scale 542.6 nm

A

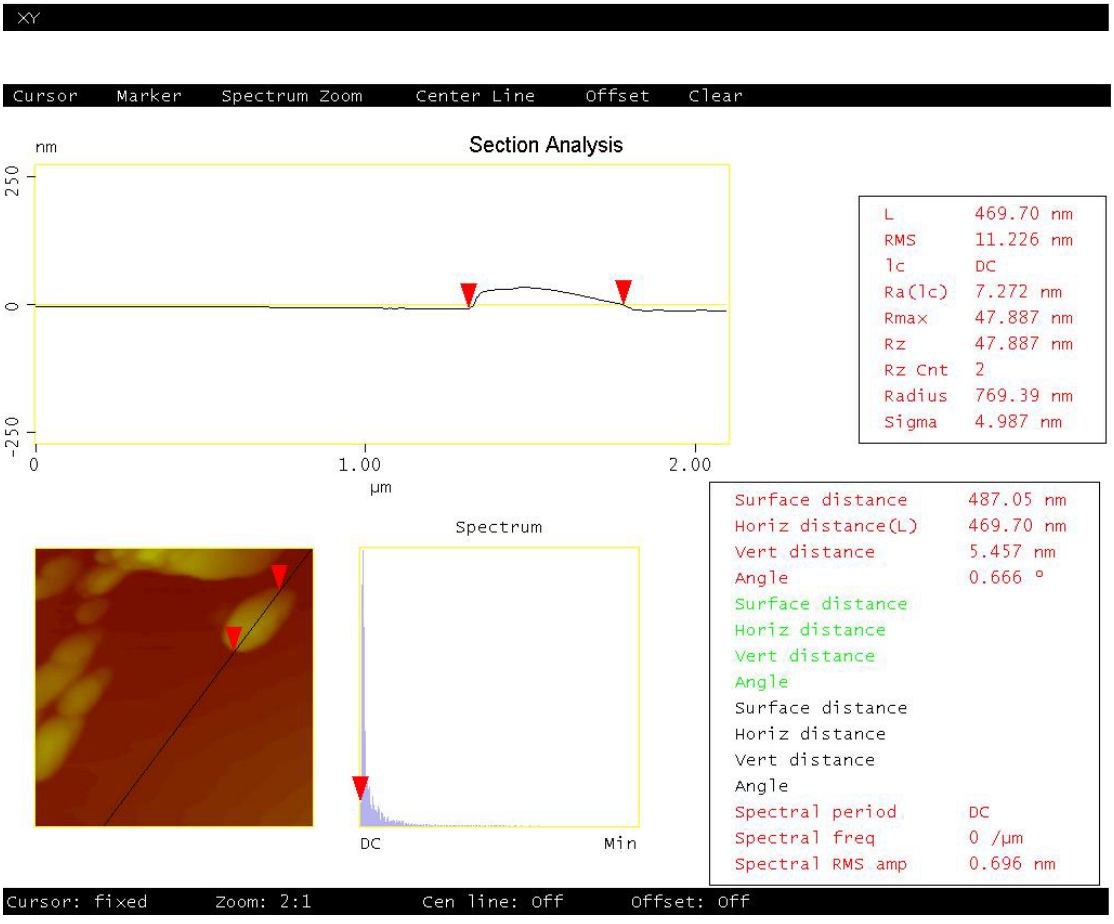
XY
Cursor Marker Spectrum Zoom Center Line Offset Clear
Section Analysis
nm
250
0
-250
0
1.00
2.00
µm
L 469.70 nm
RMS 11.226 nm
lc DC
Ra(lc) 7.272 nm
Rmax 47.887 nm
Rz 47.887 nm
Rz Cnt 2
Radius 769.39 nm
Sigma 4.987 nm
Spectrum
DC
Min
Surface distance 487.05 nm
Horiz distance(L) 469.70 nm
Vert distance 5.457 nm
Angle 0.666 °
Surface distance
Horiz distance
Vert distance
Angle
Surface distance
Horiz distance
Vert distance
Angle
Spectral period DC
Spectral freq 0 /µm
Spectral RMS amp 0.696 nm
Cursor: fixed Zoom: 2:1 Cen line: Off Offset: Off

B

Fig. 10: AFM image of a blank (t = 24h HA = 0.2 g). - Fig. 10: Immagine AFM del blank (t = 24h HA = 0.2 g).

5.1.5 ICP-AES analyses

The proportions of heavy metal blocked per unit mass of HA are listed in Table 1, whereas the immobilization efficiency is reported in Table 2 and shown in Figs. 11-13.

As already said, the experiments were carried out with two different initial mass of HA to choose the suitable amount of HA to obtain the maximum metal immobilization.

The best immobilization is usually achieved after 24h of reaction, but mainly the immobilization depends on the initial metal ion concentration. However, in all cases, aqueous heavy metals concentrations were reduced below the intervention criteria for waters (Tab. 2).

Cd, Cu, Pb and Zn = 10 mg/L; HA = 0.1 g.				
	Cd	*Cu*	*Pb*	*Zn*
2h	9.73	9.94	9.83	9.89
4h	9.87	9.91	9.67	9.89
24h	9.89	9.89	9.92	9.95
48h	9.78	9.97	9.74	9.96

Cd, Cu, Pb and Zn = 10 mg/L; HA = 0.2 g.				
	Cd	*Cu*	*Pb*	*Zn*
2h	9.94	9.89	9.83	9.88
4h	9.95	9.95	9.92	9.89
24h	9.98	9.86	9.91	9.77
48h	9.84	9.94	9.82	9.97

Cd, Cu, Pb and Zn= 100 mg/L; HA = 0.1 g.				
	Cd	*Cu*	*Pb*	*Zn*
2h	88.82	95.53	93.95	96.38
4h	94.23	93.65	99.78	95.80
24h	91.44	92.35	97.98	95.35
48h	91.93	95.57	99.68	96.09

Cd, Cu, Pb and Zn = 100 mg/L; HA = 0.2 g.				
	Cd	*Cu*	*Pb*	*Zn*
2h	94.31	97.29	99.88	96.74
4h	96.26	94.86	99.89	96.80
24h	93.65	98.50	99.78	97.32
48h	95.39	97.07	99.84	97.29

Cd, Cu, Pb and Zn = 500 mg/L; HA = 0.1 g.				
	Cd	*Cu*	*Pb*	*Zn*
2h	457.28	465.15	480.14	499.85
4h	473.17	481.32	458.15	499.91
24h	485.35	484.78	496.63	499.93
48h	473.88	483.55	488.21	499.97

Cd, Cu, Pb and Zn = 500 mg/L; HA = 0.2 g.				
	Cd	*Cu*	*Pb*	*Zn*
2h	473.96	483.12	469.49	499.98
4h	472.52	482.51	499.89	499.97
24h	482.79	486.46	497.24	499.97
48h	472.06	482.32	484.31	499.99

Table 1: Proportions of blocked heavy metals per unit mass of HA (mg/g) for the two initial mass of HA. – Tabella 1: Entità dell'immobilizzazione dei metalli per unità di massa di HA (mg/g) per le due quantità di HA.

Cd, Cu, Pb and Zn = 10 mg/L; HA = 0.1 g.				
	Cd	*Cu*	*Pb*	*Zn*
2h	97.28	99.40	98.29	88.69
4h	98.72	99.13	96.72	89.02
24h	98.92	98.93	99.23	94.55
48h	97.75	99.68	97.41	96.13

Cd, Cu, Pb and Zn = 10 mg/L; HA = 0.2 g.				
	Cd	*Cu*	*Pb*	*Zn*
2h	99.40	98.87	98.28	88.17
4h	99.52	99.47	99.17	88.83
24h	99.76	98.64	99.06	77.02
48h	98.41	99.35	98.20	96.93

Cd, Cu, Pb and Zn= 100 mg/L; HA = 0.1 g.				
	Cd	*Cu*	*Pb*	*Zn*
2h	88.82	95.53	93.95	63.79
4h	94.23	93.65	99.78	58.03
24h	91.44	92.35	97.98	53.46
48h	91.93	95.57	99.68	60.86

Cd, Cu, Pb and Zn = 100 mg/L; HA = 0.2 g.				
	Cd	*Cu*	*Pb*	*Zn*
2h	94.31	97.29	99.88	67.43
4h	96.26	94.86	99.89	67.99
24h	93.65	98.50	99.78	73.25
48h	95.39	97.07	99.84	72.91

Cd, Cu, Pb and Zn = 500 mg/L; HA = 0.1 g.				
	Cd	*Cu*	*Pb*	*Zn*
2h	91.46	93.03	96.03	99.69
4h	94.63	96.26	91.63	99.82
24h	97.07	96.96	99.33	99.85
48h	94.78	96.71	97.64	99.93

Cd, Cu, Pb and Zn = 500 mg/L; HA = 0.2 g.				
	Cd	*Cu*	*Pb*	*Zn*
2h	94.79	96.62	93.90	99.95
4h	94.50	96.50	99.98	99.94
24h	96.56	97.29	99.45	99.95
48h	94.41	96.46	96.86	99.99

Table 2: In the table the values of the immobilization (%) are listed for each monometal system vs. HA. – Tabella 2: Nella tabella sono elencati i valori dell'immobilizzazione (%) in soluzione a metallo singolo vs. HA.

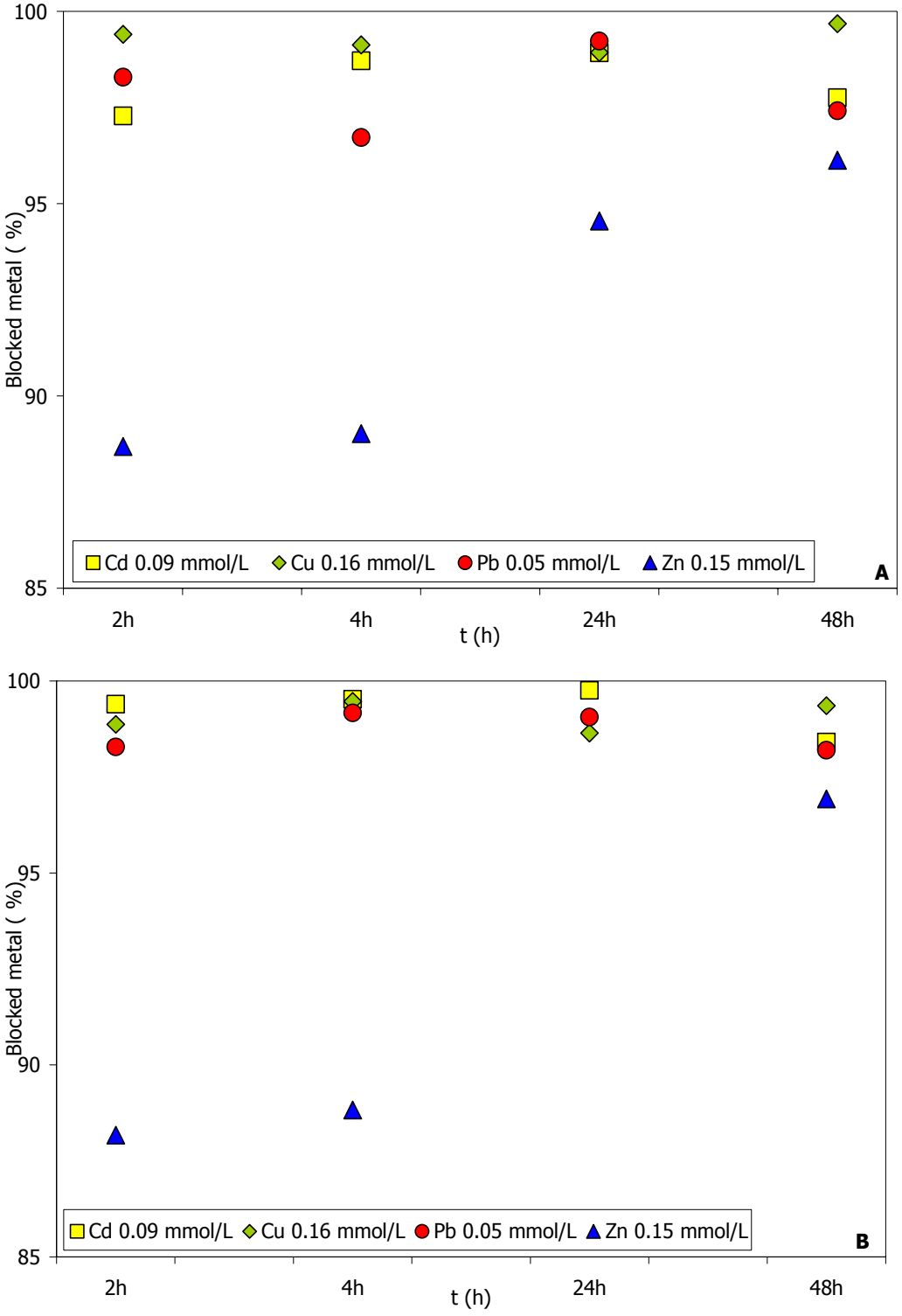

Fig. 11: Variation of the amount of blocked metal with time for the two initial mass of HA (A = 0.1 g and B = 0.2 g). – Fig. 11: Variazione delle percentuali di metalli immobilizzati in funzione del tempo di interazione per le due quantità iniziali di HA (A = 0.1 g and B = 0.2 g).

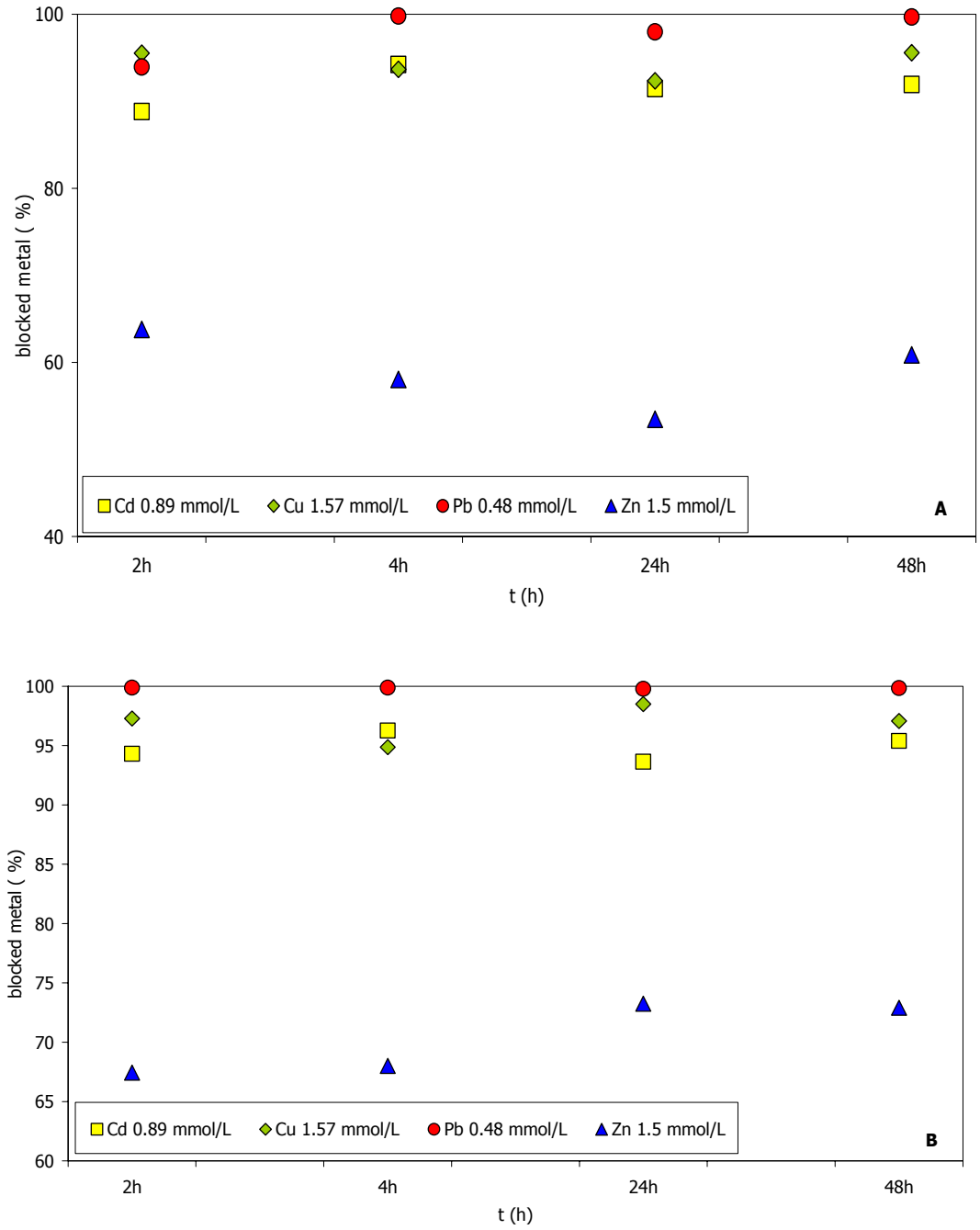

Fig. 12: Variation of the amount of blocked metal with time for the two initial mass of HA (A = 0.1 g and B = 0.2 g). – Fig. 12: Variazione delle percentuali di metalli immobilizzati in funzione del tempo di interazione per le due quantità iniziali di HA (A = 0.1 g and B = 0.2 g).

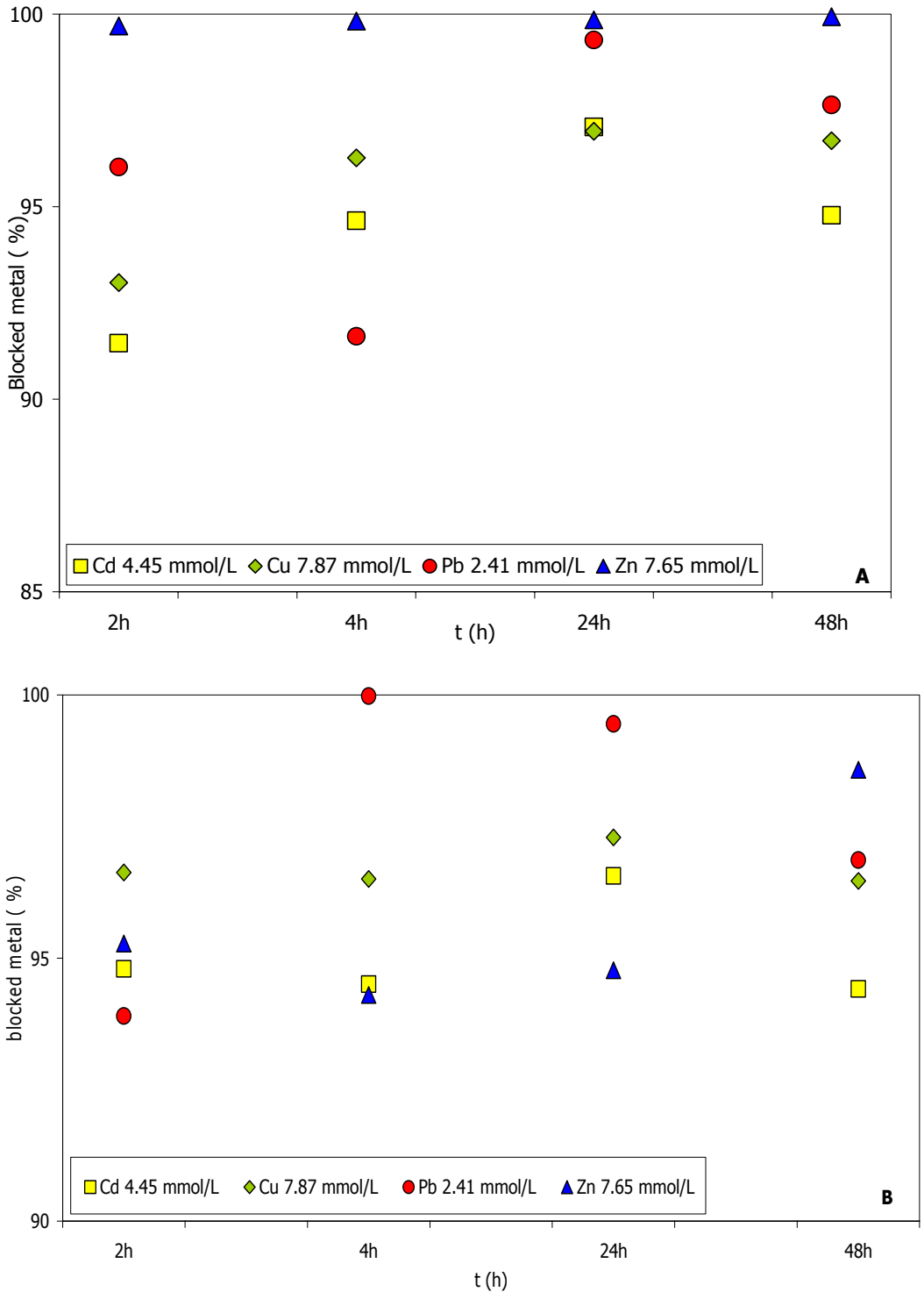

Fig. 13: Variation of the amount of blocked metal with time for the two initial mass of HA (A = 0.1 g and B = 0.2 g). – Fig. 13: Variazione delle percentuali di metalli immobilizzati in funzione del tempo di interazione per le due quantità iniziali di HA (A = 0.1 g and B = 0.2 g).

Cd immobilization ranges from 9.98 to 482.79 mg/g. For both amounts of HA, 0.1 or 0.2 g, values of blocked metal are high so that the immobilization is always good. The

suitable immobilization time seems to be 4h for the lower initial metal concentration and running up to 4.45 mmol/L (500 mg/L) the best time for immobilization is 24h. On the contrary, at 48h the percentage of immobilization decreases from about 96% to 94% probably it is due to the release of the immobilized ions.

Cu immobilization runs from 9.95 to 486.46 mg/g. The average of the immobilization is higher if it is used 0.2 g than 0.1 g of HA, the efficiency values bare 96% respect to 98%. Generally, the maximum immobilization is achieved after 24h. However, increasing the metal concentration to 7.87 mmol/L (500 mg/L) the efficiency of the immobilization decreases to values about 96%, notwithstanding always good.

Lead is always well immobilized with an amount of blocked metal ranging from a minum of 9.92 mg/g to a maximum of 497.99 mg/g. When lead concentration is about 2.41 mmol/L (500 mg/L) the maximum immobilization is achieved at 24h but there are some differences if the initial mass of HA is 0.1 or 0.2 g. For a mass of HA of about 0.1 g the amounts of blocked Pb at 4h and 48h are lower than those obtained at 2h and 24h. On the contrary, if the amount of HA is 0.2 g the minum immobilization is at 48h.

The process which involves lead immobilization is the dissolution of HA and precipitation of hydroxypyromorphite (HP) with a fast reaction, about 2h *(95)*.

The amount of blocked zinc ranges from 9.77 to 497.92 mg/g. The immobilization seems to depend on the initial Zn concentration and not the amount of HA. In fact, looking at the case of Zn = 1.5 mmol/L (100 mg/L), in both cases the percentage of blocked zinc is similar, about the 60-70% and it doesn't depend on the contact time. Looking at the concentration of 7.65 mmol/L (500 mg/L), it appears that HA can better immobilize higher concentration than a minor amount of zinc *(95)*.

Monometal sorption isotherms for Cd, Cu and Zn (Fig. 14 A, B, C, D, E, F, G, and H) suggest they belong to type L subtype 2 according to the classification of Giles et al. *(62)* and this shape means that theoretical monolayer has been completed. The isotherms present an initial linear part which is short and a sharp knee, suggesting a phenomenon of adsorption and surface precipitation, instead Pb isotherm shows also a straight line (H type) for t = 4h, which means the solute has such high affinity that in dilute solutions it is completely adsorbed, or at least there is no measurable amount remaining in solution. The initial part of the isotherm is therefore vertical and it suggests a precipitation mechanism *(49)*. The shapes of the sorption isotherms obtained for the two different initial mass of

HA are similar and show the same L2 type for Cd, Cu and Zn. On the contrary, for Pb at 4h with 0.2 g HA the isotherm was a vertical line.

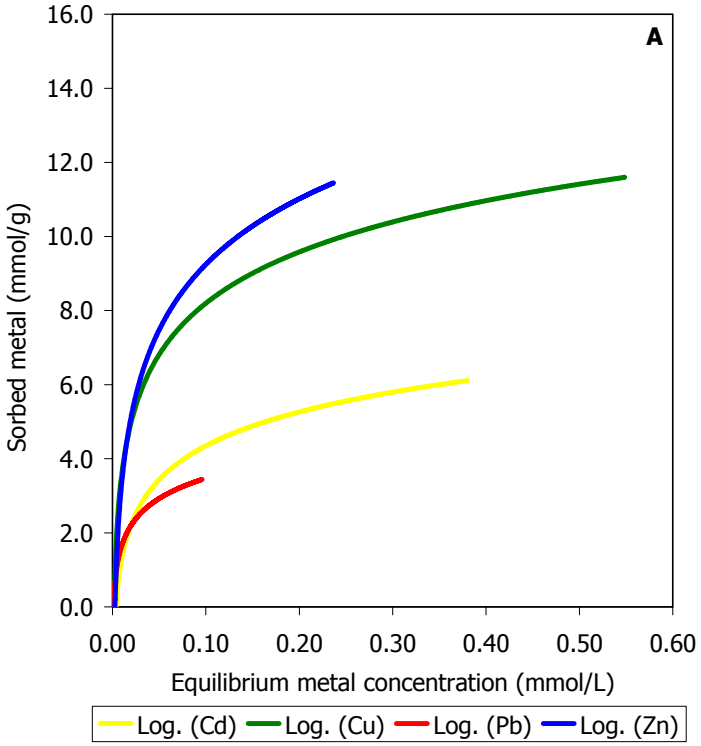

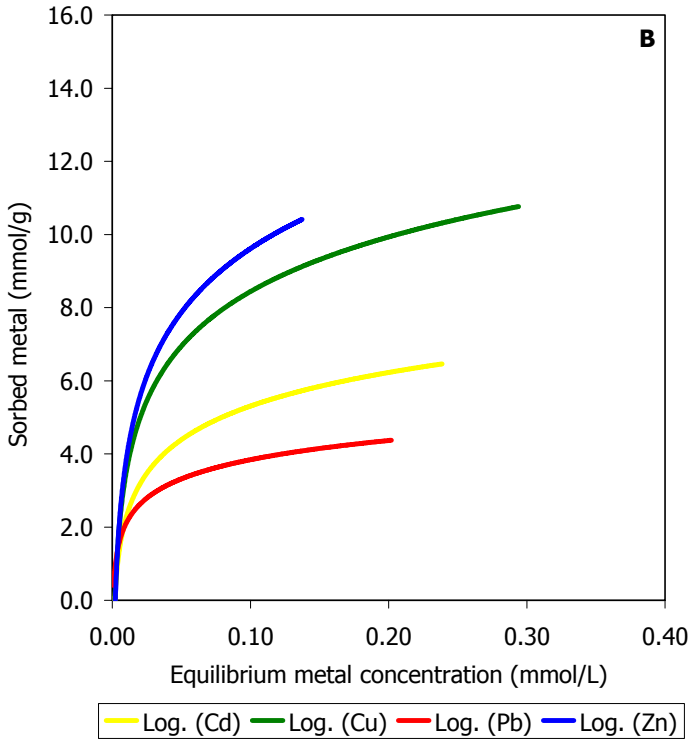

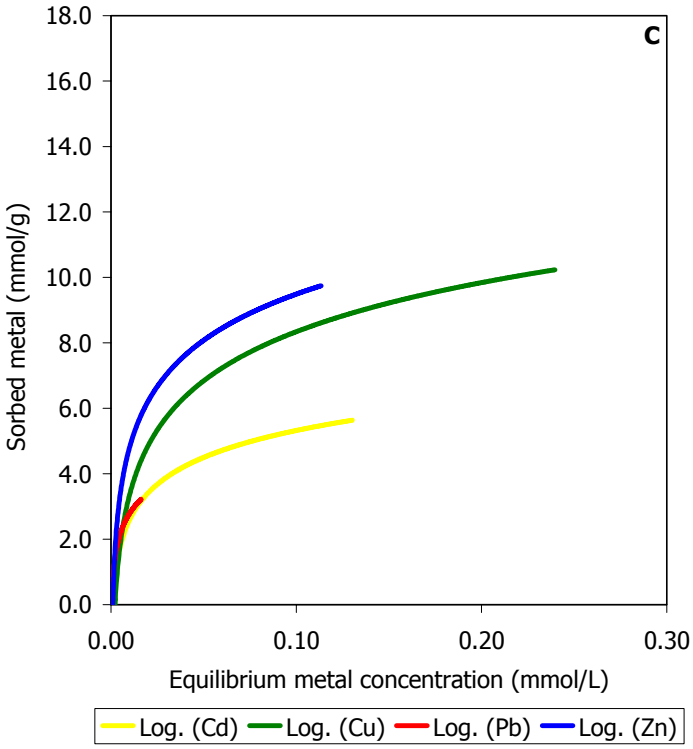
C
18.0
16.0
14.0
12.0
10.0
8.0
6.0
4.0
2.0
0.0
Sorbed metal (mmol/g)
0.00
0.10
0.20
0.30
Equilibrium metal concentration (mmol/L)
Log. (Cd)
Log. (Cu)
Log. (Pb)
Log. (Zn)

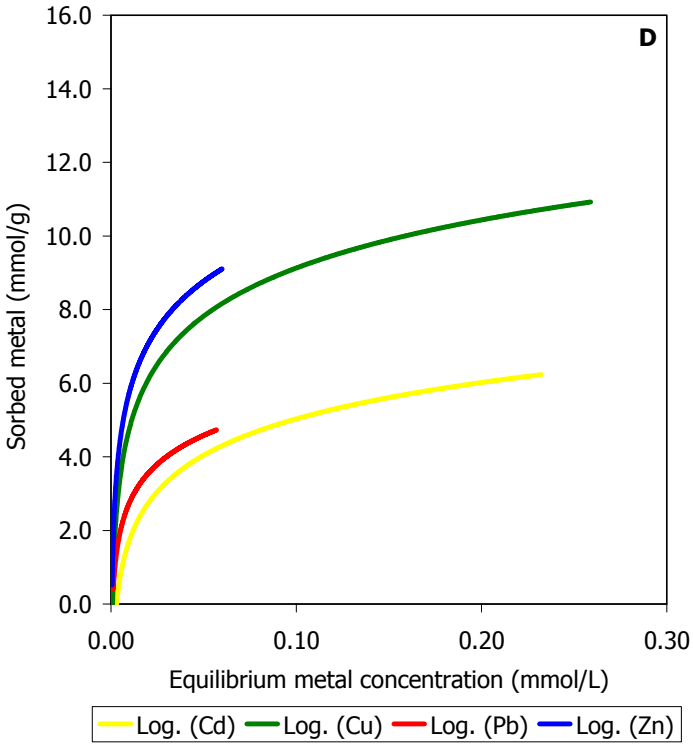
D
16.0
14.0
12.0
10.0
8.0
6.0
4.0
2.0
0.0
Sorbed metal (mmol/g)
0.00
0.10
0.20
0.30
Equilibrium metal concentration (mmol/L)
Log. (Cd)
Log. (Cu)
Log. (Pb)
Log. (Zn)

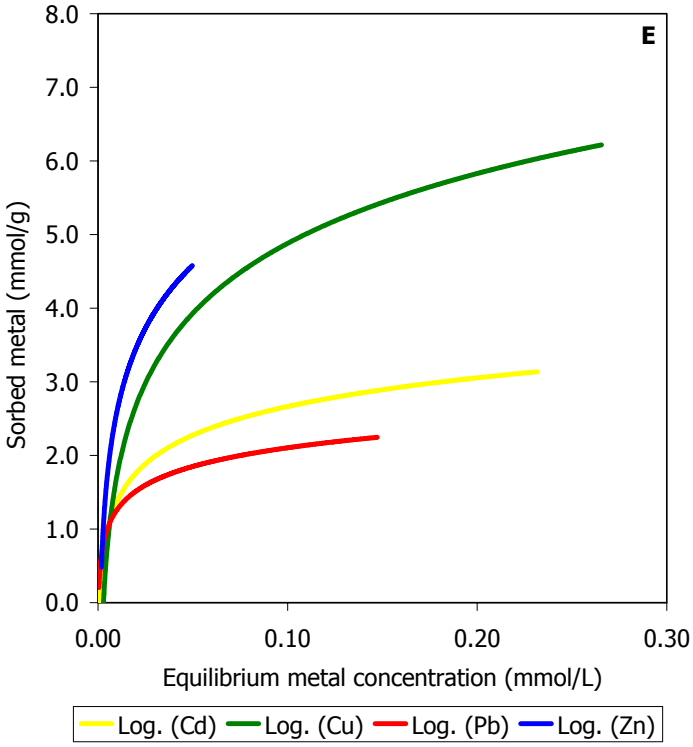
E
8.0
7.0
6.0
5.0
4.0
3.0
2.0
1.0
0.0
Sorbed metal (mmol/g)
0.00
0.10
0.20
0.30
Equilibrium metal concentration (mmol/L)
Log. (Cd)
Log. (Cu)
Log. (Pb)
Log. (Zn)

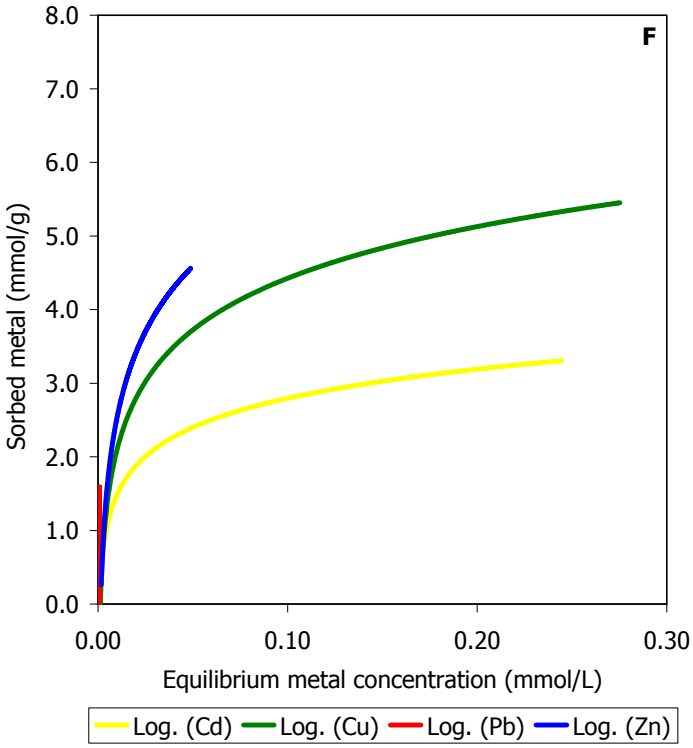
F
8.0
7.0
6.0
5.0
4.0
3.0
2.0
1.0
0.0
Sorbed metal (mmol/g)
0.00
0.10
0.20
0.30
Equilibrium metal concentration (mmol/L)
Log. (Cd)
Log. (Cu)
Log. (Pb)
Log. (Zn)

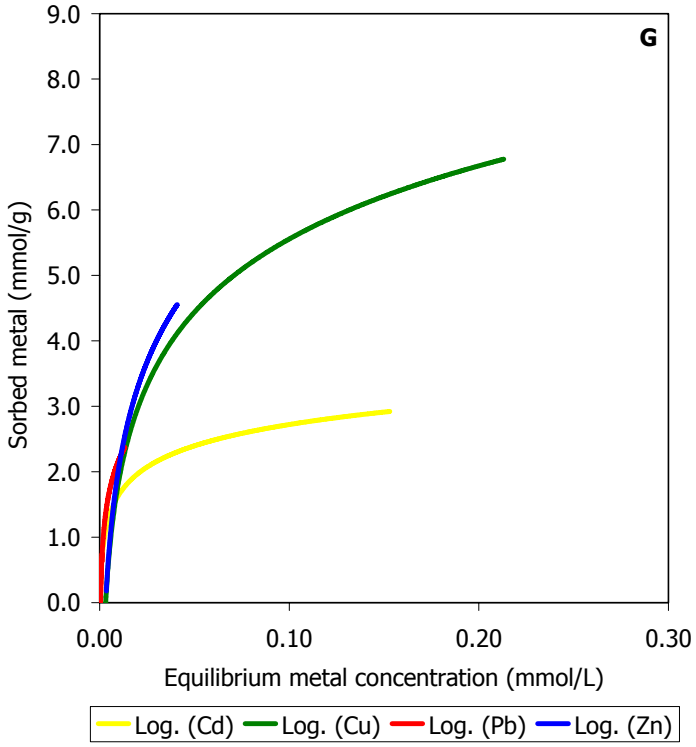

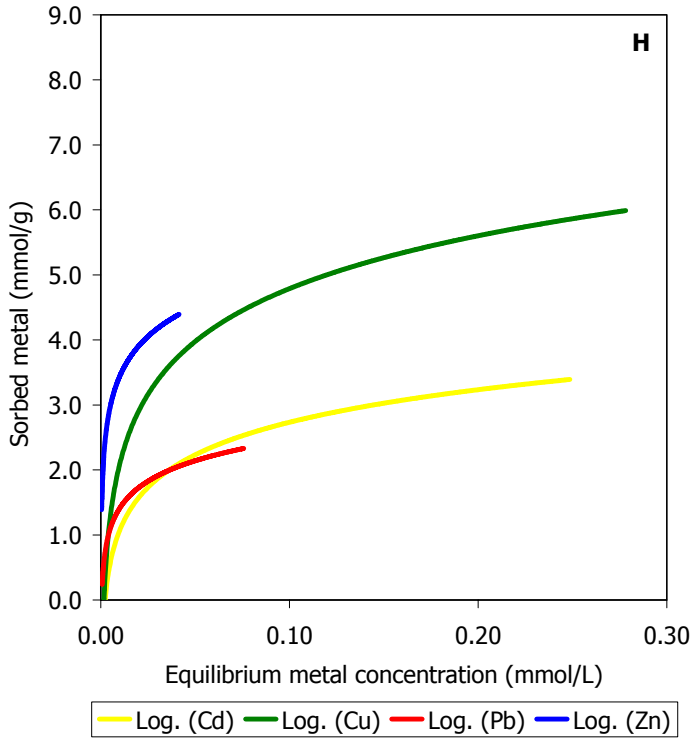

Fig. 14: Sorption isotherm for the monometal system for the four times (2h, 4h, 24h and 48h) and vs. 0.1 g and 0.2 g HA. Relation between the metal sorbed (mmol/g) and the metal concentration at the equilibrium (mmol/L). A: 2h and 0.1 g HA; B: 4h and 0.1 g HA; C: 24h and 0.1 g HA; D: 48h and 0.1 g HA; E: 2h and 0.2 g HA; F: 4h and 0.2 g HA; G: 24h and 0.2g HA; H: 48h and 0.2g HA. – Fig. 14: Isoterme di

assorbimento per il sistema metallo-singolo per i quattro diversi tempi (2h, 4h, 24h e 48h) e vs. 0.1 g e 0.2 g di HA. Relazione tra il metallo assorbito (mmol/g) e la concentrazione del metallo all'equilibrio (mmol/L). A: 2h e 0.1 g HA; B: 4h e 0.1 g HA; C: 24h e 0.1 g HA; D: 48h e 0.1 g HA; E: 2h e 0.2 g HA; F: 4h e 0.2 g HA; G: 24h e 0.2g HA; H: 48h e 0.2g HA.

Estimating which sorption mechanisms can be the most suitable the molar ratio Q_S was determined, that is the ratio of the cations bound by HA to the Ca cations released from HA. When $Q_S = 1$ the amounts of the bound and released cations are equal indicating the ion exchange between HA and the solution. Q_S values > 1 indicates that a quantity of bound ions is more than the released ones, suggesting non stoichiometric sorption (surface – complexation or filling the cationic vacancies in HA crystal lattice) dominates. When $Q_s < 1$ dissolution of HA and precipitation of new phosphate mineral having a lower amount of cations compared to phosphate molar ratio occurs *(121)*.

Q_s values for each heavy metal mainly show two cases, $Q_s< 1$ and $Q_s>1$, in the first case the most probable mechanism is the precipitation of a new phases, probably an amorphous phase and in the second one the adsorption. The only exception is Pb, whose Q_S values are always < 1, suggesting the precipitation of a phosphate mineral. Nevertheless, XRD analyses did not detect any new crystal phase. Generally, increasing the metal concentration from 100 mg/L to 500 mg/L Q_S values change from < 1 to >. Only for Zn t the concentration of 10 mg/L $Q_S = 1$, meaning the most suitable mechanism is the ion exchange. Increasing the metal concentration, some of the Q_S values for Cu and Zn increase to values > 2 (Table 3).

Cd, Cu, Pb and Zn = 10 mg/L; HA = 0.1 g.					Cd, Cu, Pb and Zn = 10 mg/L; HA = 0.2 g.			
Cd	Cu	Pb	Zn		Cd	Cu	Pb	Zn
0.790	0.621	0.968	1.664	*2h*	0.713	0.593	0.739	1.077
0.696	0.620	0.971	1.662	*4h*	0.675	0.579	1.064	1.104
0.649	0.631	0.868	1.257	*24h*	0.667	0.512	0.695	0.820
0.657	0.584	1.041	0.941	*48h*	0.568	0.583	0.762	0.792
Cd, Cu, Pb and Zn= 100 mg/L; HA = 0.1 g.					Cd, Cu, Pb and Zn = 100 mg/L; HA = 0.2 g.			
Cd	Cu	Pb	Zn		Cd	Cu	Pb	Zn
3.568	2.728	3.258	5.072	*2h*	1.985	1.595	2.183	4.482
3.632	2.771	1.853	4.868	*4h*	1.952	1.552	1.669	4.402
3.058	2.272	2.457	4.629	*24h*	1.635	1.428	1.954	4.168
2.835	2.330	3.136	4.455	*48h*	1.575	1.344	2.652	3.850
Cd, Cu, Pb and Zn = 500 mg/L; HA = 0.1 g.					Cd, Cu, Pb and Zn = 500 mg/L; HA = 0.2 g.			
Cd	Cu	Pb	Zn		Cd	Cu	Pb	Zn
18.922	13.412	21.178	18.307	*2h*	9.944	8.139	20.708	19.819
18.322	28.167	21.282	17.042	*4h*	9.562	7.388	10.064	10.025
43.755	11.721	13.483	16.958	*24h*	8.471	6.365	7.855	8.254
14.900	11.265	14.682	14.860	*48h*	7.668	6.187	7.681	8.732

Table 3: Q_S values for the single-metal sistem vs. HA. - Tabella 3: Valori di Qs per il sistema a metallo singolo vs. HA.

During the heavy metal retention by HA, Ca at the equilibrium increased slightly with the increasing of heavy metals disappearance and also with the increasing of the initial heavy metal concentration (Fig. 15, 16, 17, 18). In particular, Ca contents increase as a function of the HA amount and contact time.

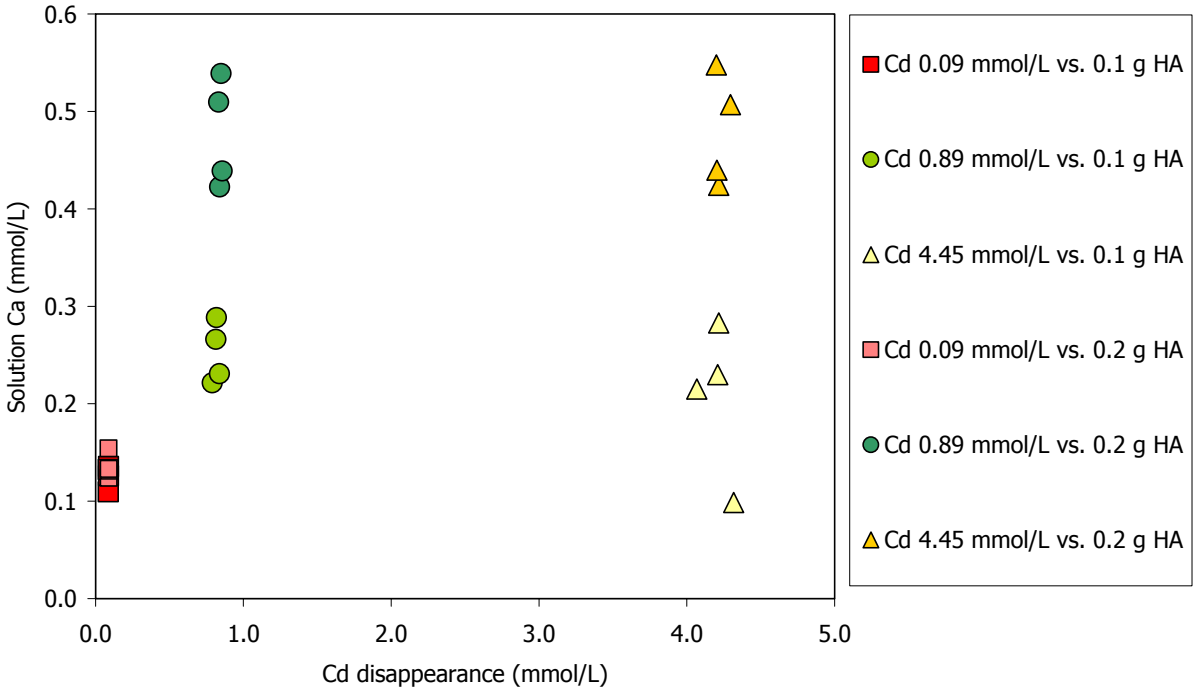

Fig. 15: Relation between Ca (mmol/g) and the amount of Cd (mmol/g) sorbed on HA surface in the solution. Cd initial concentration is from 0.09 mmol/L to 4.45 mmol/L and the HA one is 0.1 and 0.2 g. – Fig. 15: Relazione tra il Ca (mmol/g) e il Cd (mmol/g) assorbito sulla superficie dell'HA in soluzione. La concentrazione iniziale del Cd varia da 0.09 mmol/L a 4.45 mmol/L e quella dell'HA è 0.1 e 0.2 g.

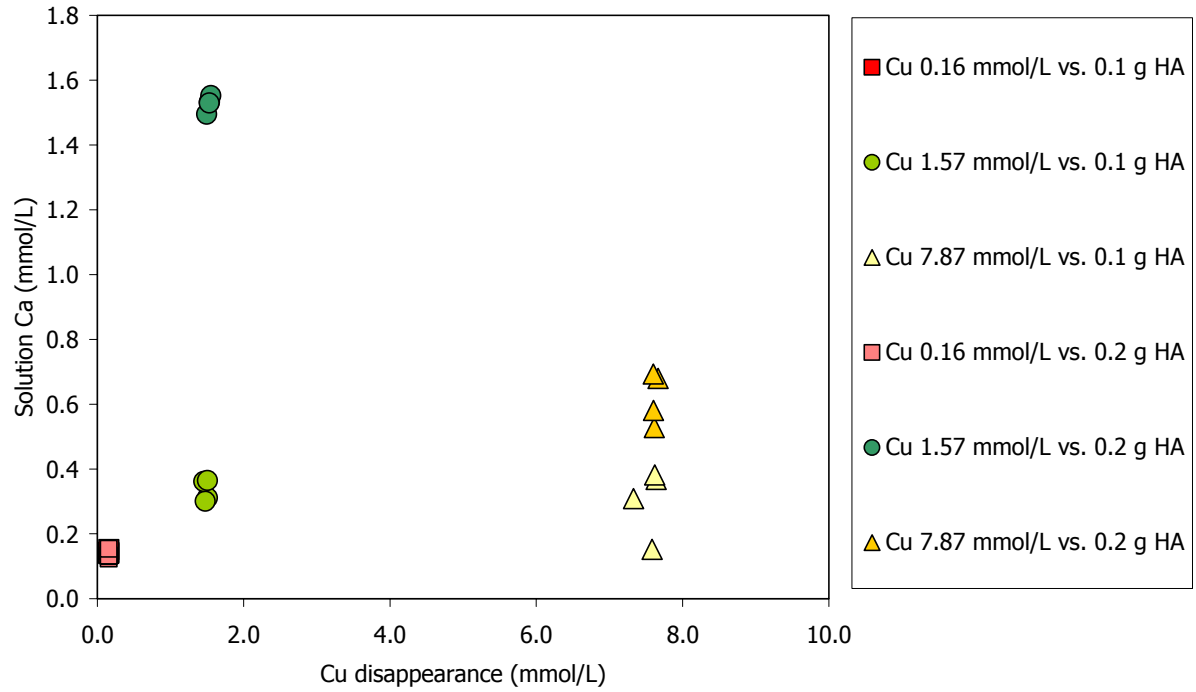

Fig. 16: Relation between Ca (mmol/g) and the amount of Cu (mmol/g) sorbed on HA surface in the solution. Cu initial concentration is from 0.16 mmol/L to 7.87 mmol/L and HA one is 0.1 and 0.2 g. – Fig. 16:

Relazione tra il Ca (mmol/g) e il Cu (mmol/g) assorbito sulla superficie dell'HA in soluzione. La concentrazione iniziale del Cu varia da 0.16 mmol/L a 7.87 mmol/L e quella dell'HA è 0.1 e 0.2 g.

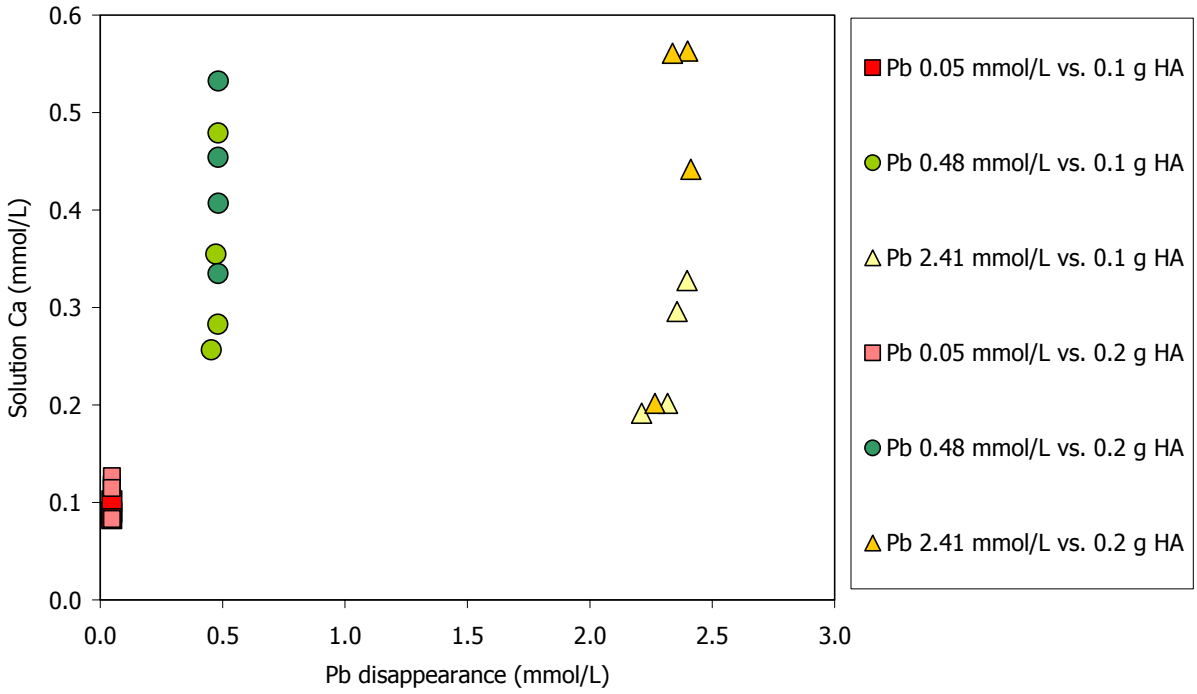

Fig. 17: Relation between Ca (mmol/g) and the amount of Pb (mmol/g) sorbed on HA surface in the solution. Pb initial concentration is from 0.05 mmol/L to 2.41 mmol/L and HA one is 0.1 and 0.2 g. – Fig. 17: Relazione tra il Ca (mmol/g) e il Pb (mmol/g) assorbito sulla superficie dell'Ha in soluzione. La concentrazione iniziale del Pb varia da 0.05 mmol/L a 2.41 mmol/L e quella dell'HA è 0.1 e 0.2 g.

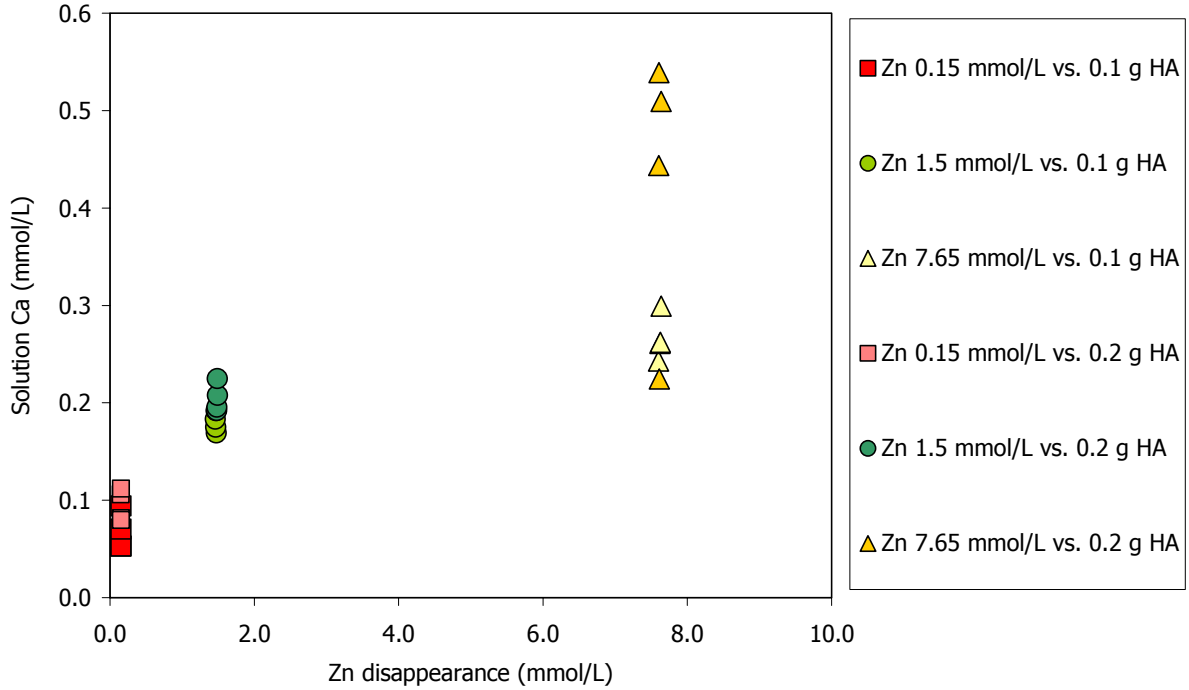

Fig. 18: Relation between Ca (mmol/g) and the amount of Zn (mmol/g) sorbed on HA surface in the

solution. Zn initial concentration is from 0.15 mmol/L to 7.67 mmol/L and HA one is 0.1 and 0.2 g. – Fig. 18: Relazione tra il Ca (mmol/g) e il Zn (mmol/g) assorbito sulla superfiicie dell'Ha in soluzione. La concentrazione iniziale dello Zn varia da 0.15 mmol/L a 7.67 mmol/L e quella dell'HA è 0.1 e 0.2 g.

The amount of P in the solution is very low (Fig. 19, 20, 21, 22) and a direct relationship between P and heavy metal concentrations does not appear. Moreover, from experimental data, the concentration of solution P does not depend on the amount of HA.

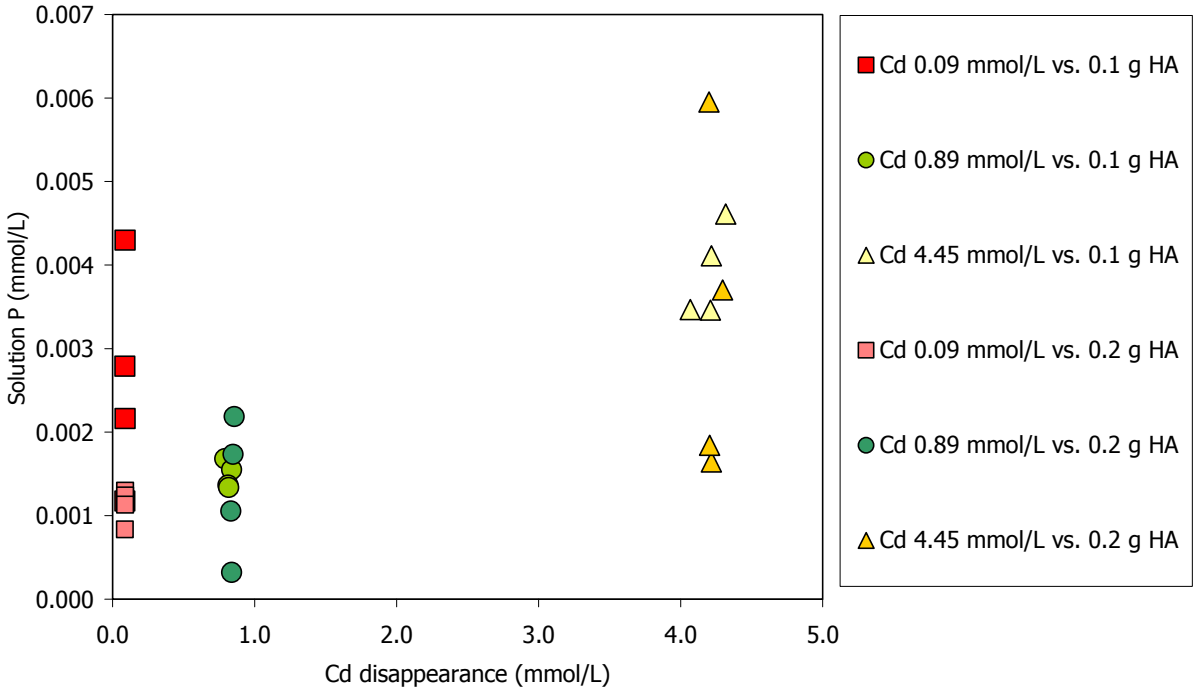

Fig. 19: Relation between P (mmol/g) and the amount of Cd (mmol/g) sorbed on HA surface in the solution. Cd initial concentration is from 0.09 mmol/L to 4.45 mmol/L and HA one is 0.1 and 0.2 g. – Fig 19: Relazione tra P (mmol/g) e il quantitativo di Cd (mmol/g) assorbito sulla superficie HA in soluzione. La concentrazione iniziale del Cd varia tra 0.09 mmol/L a 4.45 mmol/L e quella dell'HA varia tra 0.1 e 0.2 g.

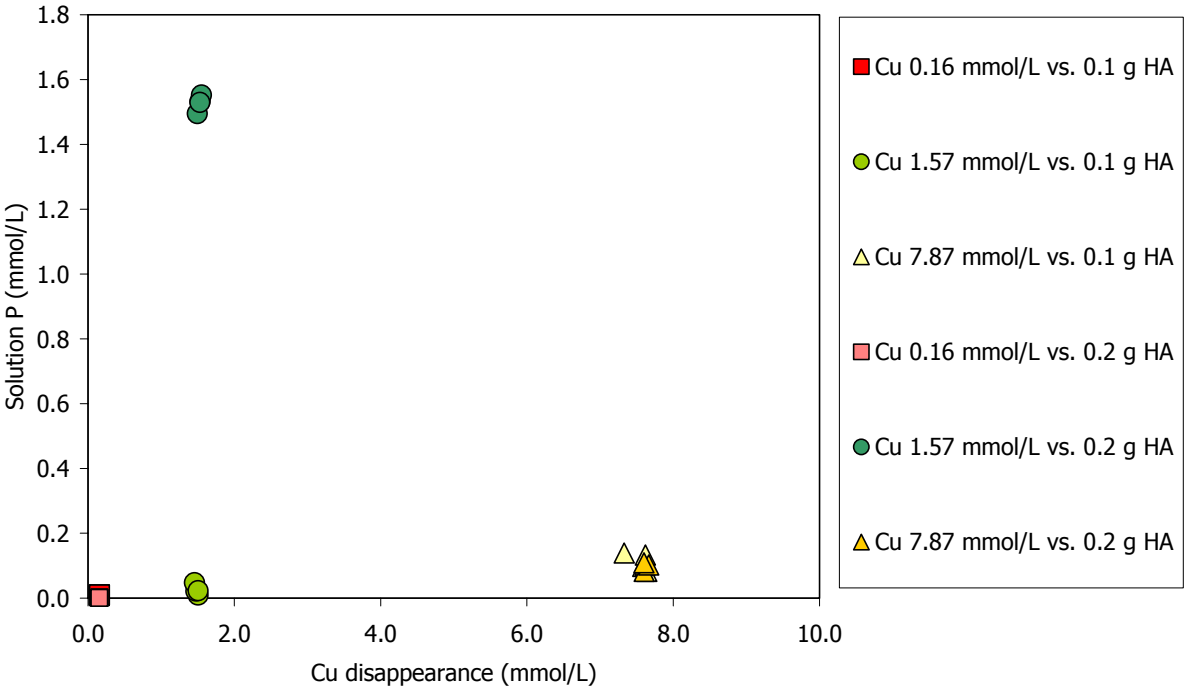

Fig. 20: Relation between P (mmol/g) and the amount of Cu (mmol/g) sorbed on HA surface in the solution. Cu initial concentration is from 0.16 mmol/L to 7.87 mmol/L and HA one is 0.1 and 0.2 g. – Fig. 20: Relazione tra P (mmol/g) e il quantitativo di Cu (mmol/g) assorbito sulla superficie HA in soluzione. La concentrazione iniziale del Cu varia tra 0.16 mmol/L a 7.87 mmol/L e quella dell'HA varia tra 0.1 e 0.2 g.

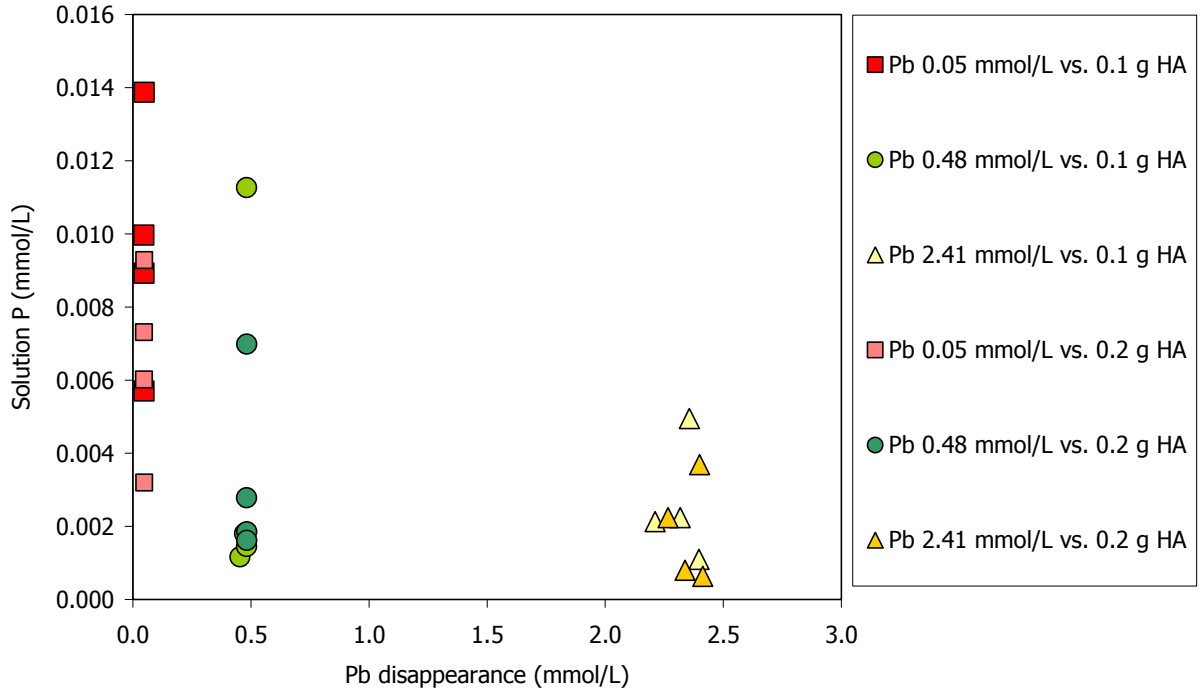

Fig. 21: Relation between P (mmol/g) and the amount of Pb (mmol/g) sorbed on HA surface in the solution. Pb initial concentration is from 0.05 mmol/L to 2.41 mmol/L and HA one is 0.1 and 0.2 g. – Fig. 21:

Relazione tra P (mmol/g) e il quantitativo di Pb (mmol/g) assorbito sulla superficie HA in soluzione. La concentrazione iniziale del Pb varia tra 0.05 mmol/L a 2.41 mmol/L e quella dell'HA varia tra 0.1 e 0.2 g.

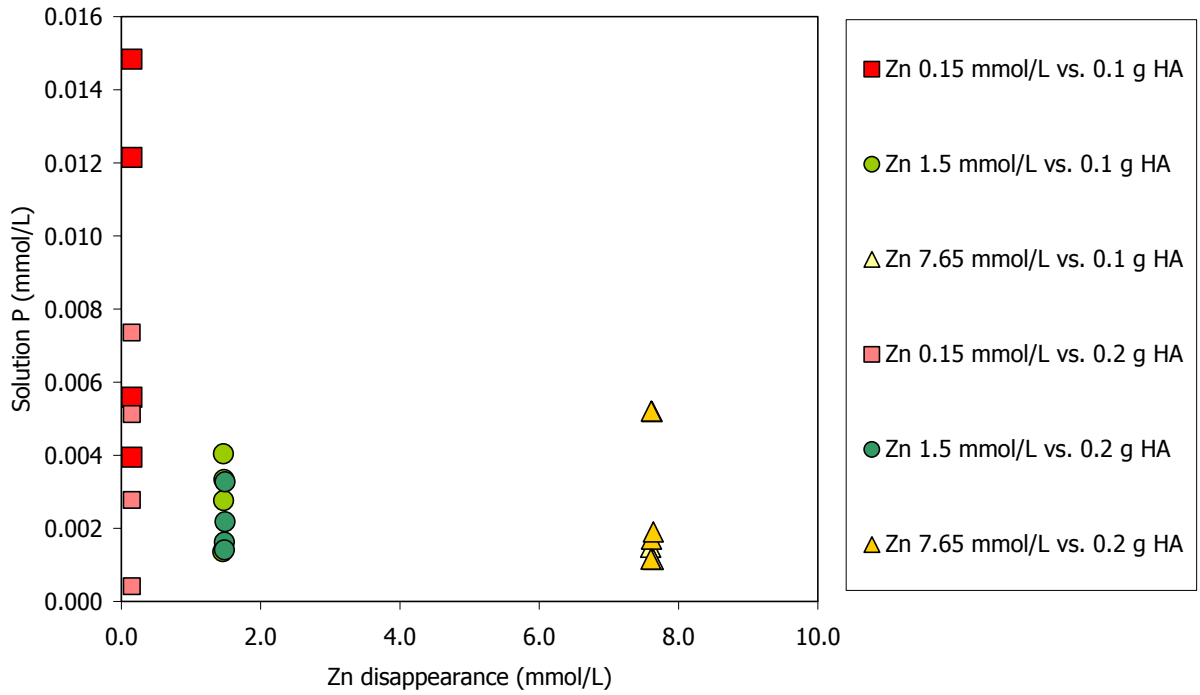

Fig. 22: Relation between P (mmol/g) and the amount of Zn (mmol/g) sorbed on HA surface in the solution. Zn initial concentration is from 0.15 mmol/L to 7.67 mmol/L and HA one is 0.1 and 0.2 g. – Fig 22: Relazione tra P (mmol/g) e il quantitativo di Zn (mmol/g) assorbito sulla superficie HA in soluzione. La concentrazione iniziale dello Zn varia tra 0.15 mmol/L a 7.67 mmol/L e quella dell'HA varia tra 0.1 e 0.2 g.

5.2 SINGLE-METAL SYSTEM SORBED ON FLUORAPATITE (FAP)

5.2.1 SEM analyses

SEM micrographs of the FAP, before (Fig. 5A see in materials) and after the sorption experiments, do not reveal any kind of differences. The original FAP shows an irregular flake shape; furthermore no different shaped precipitates were visible on FAP surface (Fig. 1 A, B, C and D). However, EDS analyses detected the presence of the heavy metals on the FAP surface, as already said for the single-metal vs. HA (Fig. 2 A, B, C and D).

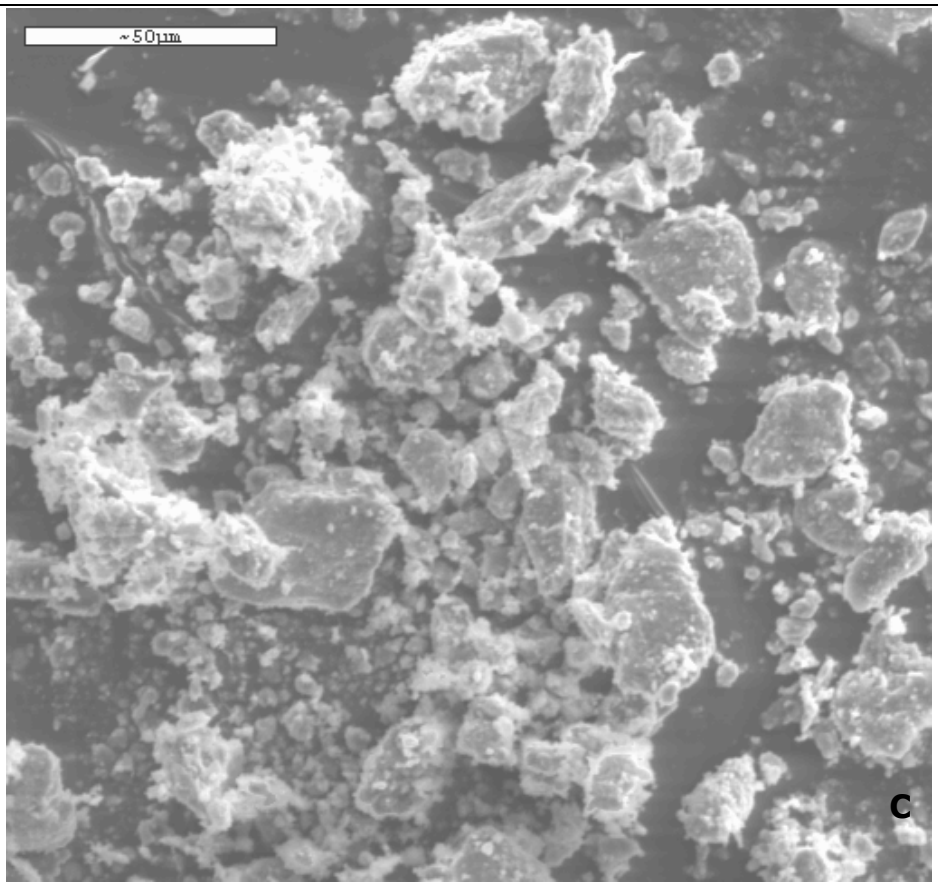
~50µm
C

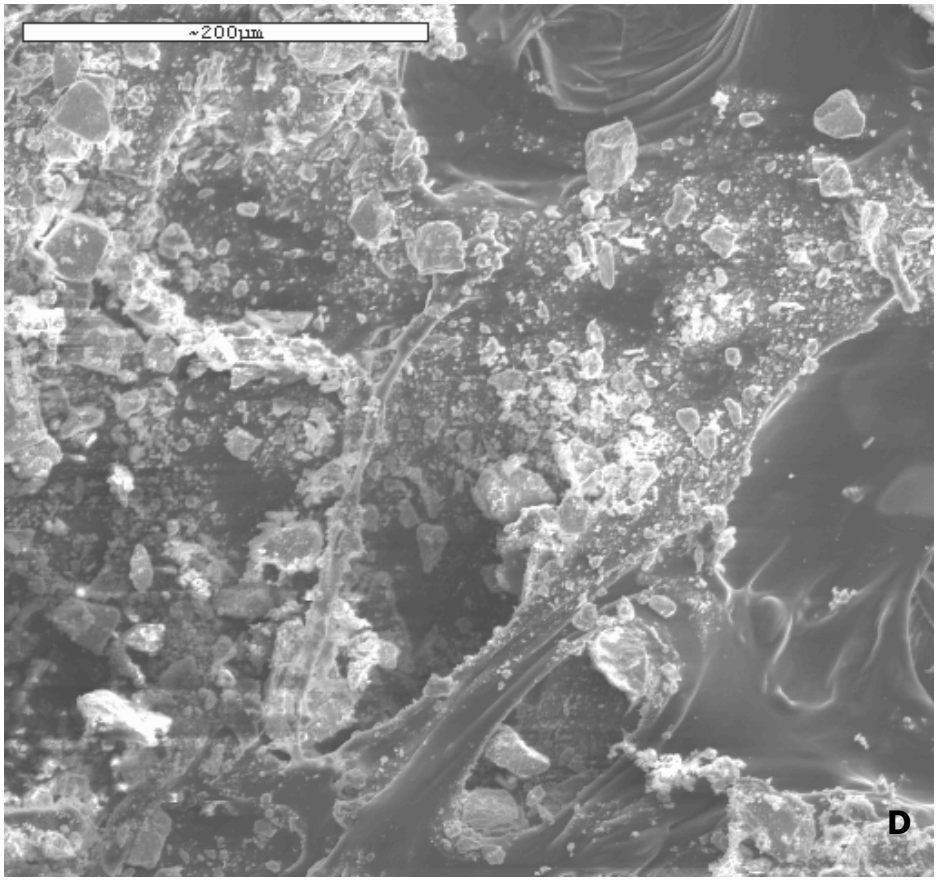
~200µm
D

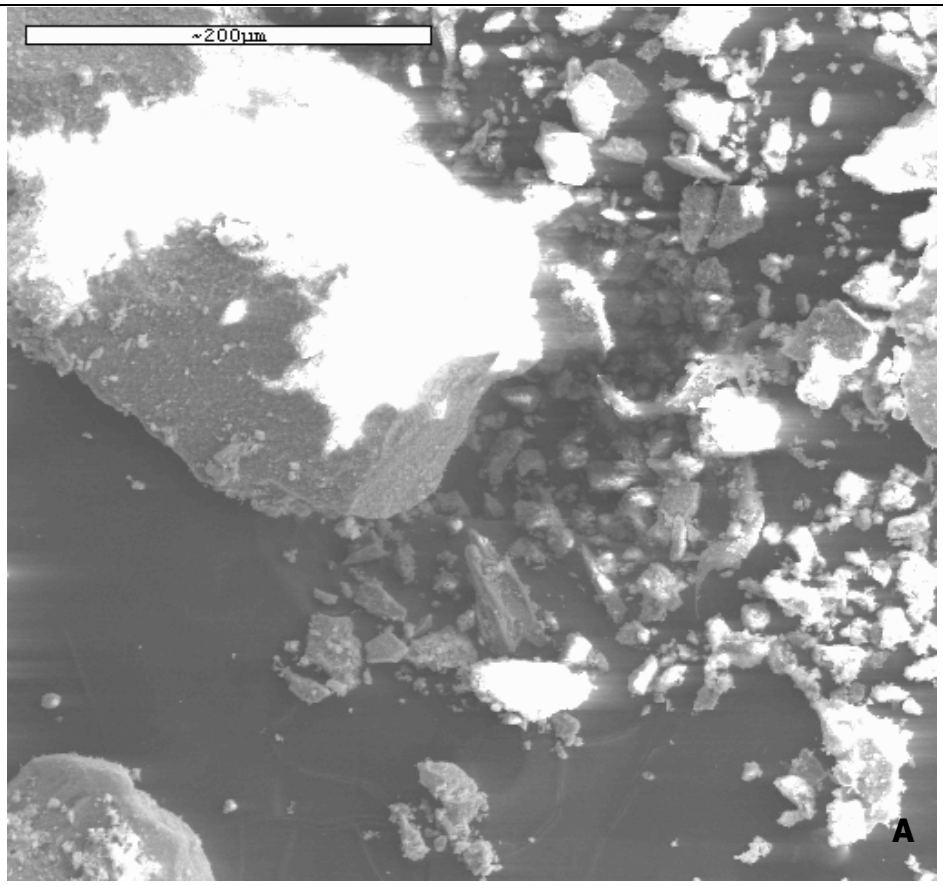
~200µm
A

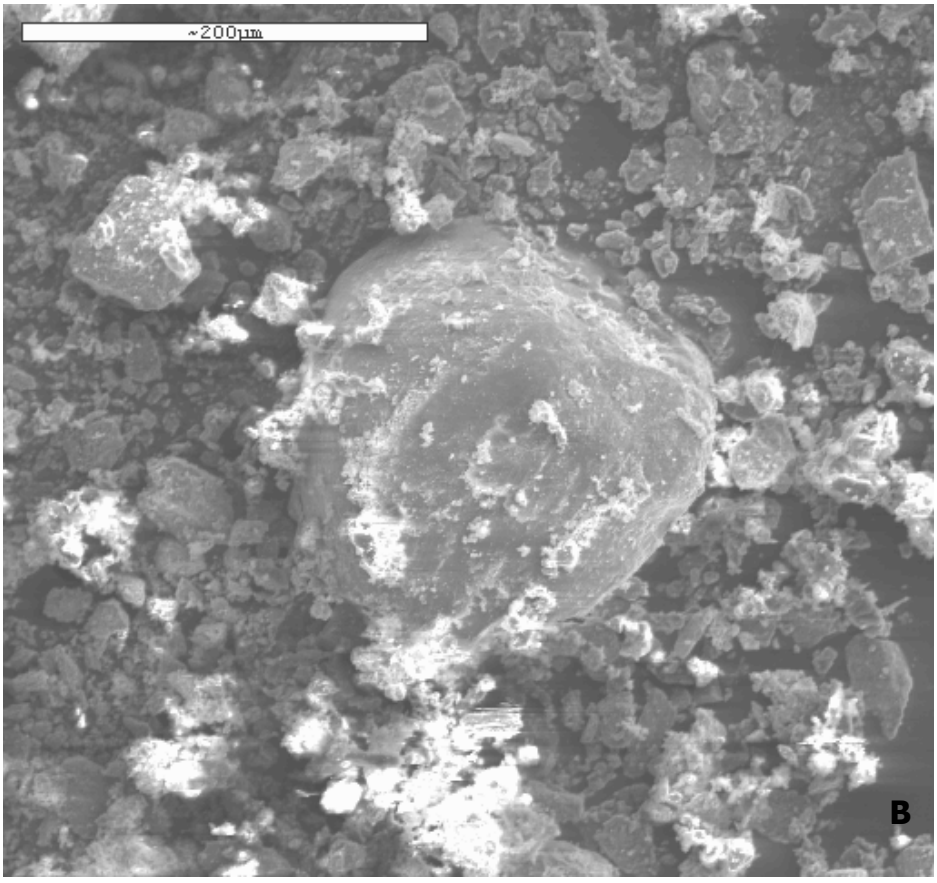
~200µm
B

Fig. 1 SEM micrographs of FAP particles after the sorption experiments: A = Cd 0.09 mmol/L t = 24h; B = Cu 1.57 mmol/L t = 24h; C = Pb 0.48 mmol/L t = 4h; D = Zn 0.15 mmol/L t = 4h. - Fig. 27 Immagini al SEM di particelle di FAP estratte dagli esperimenti di sorption: A = Cd 0.89 mmol/L t = 24h; B = Cu 1.57 mmol/L t = 24h; C = Pb 0.48 mmol/L t = 4h; D = Zn 0.15 mmol/L t = 4h.

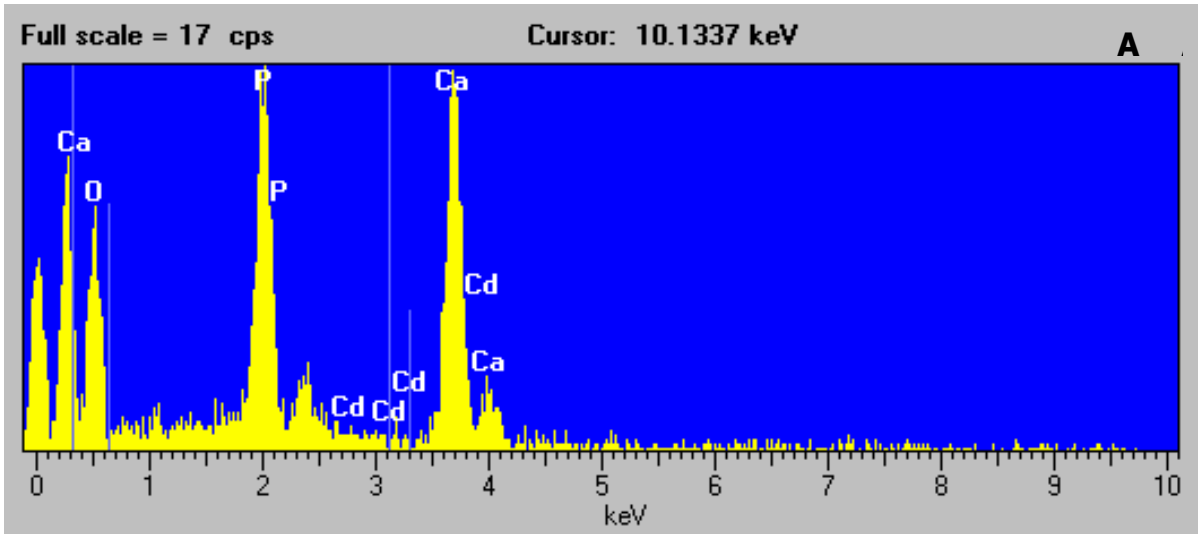

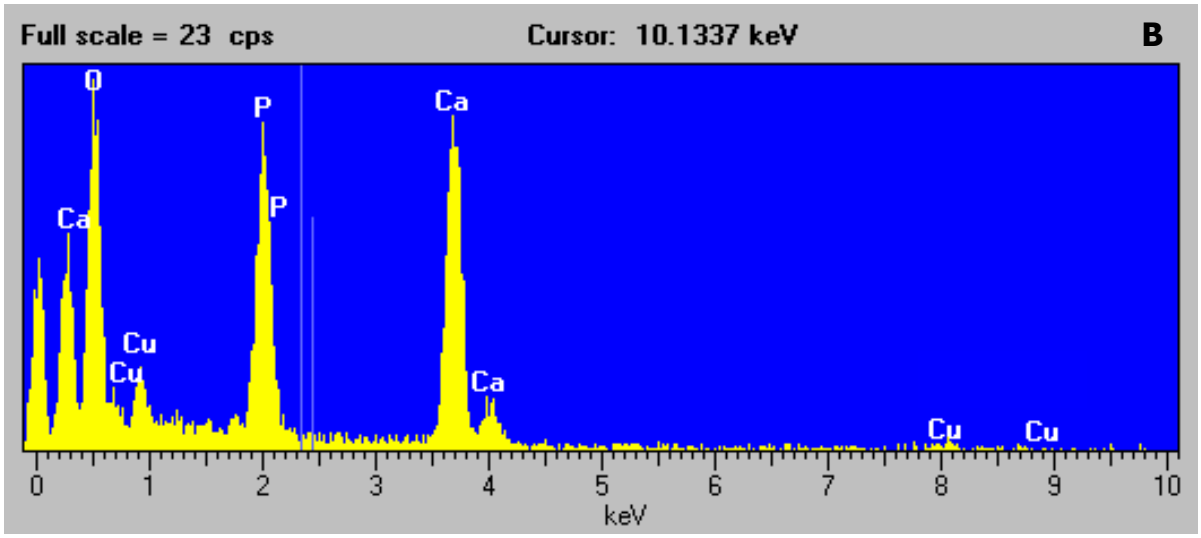

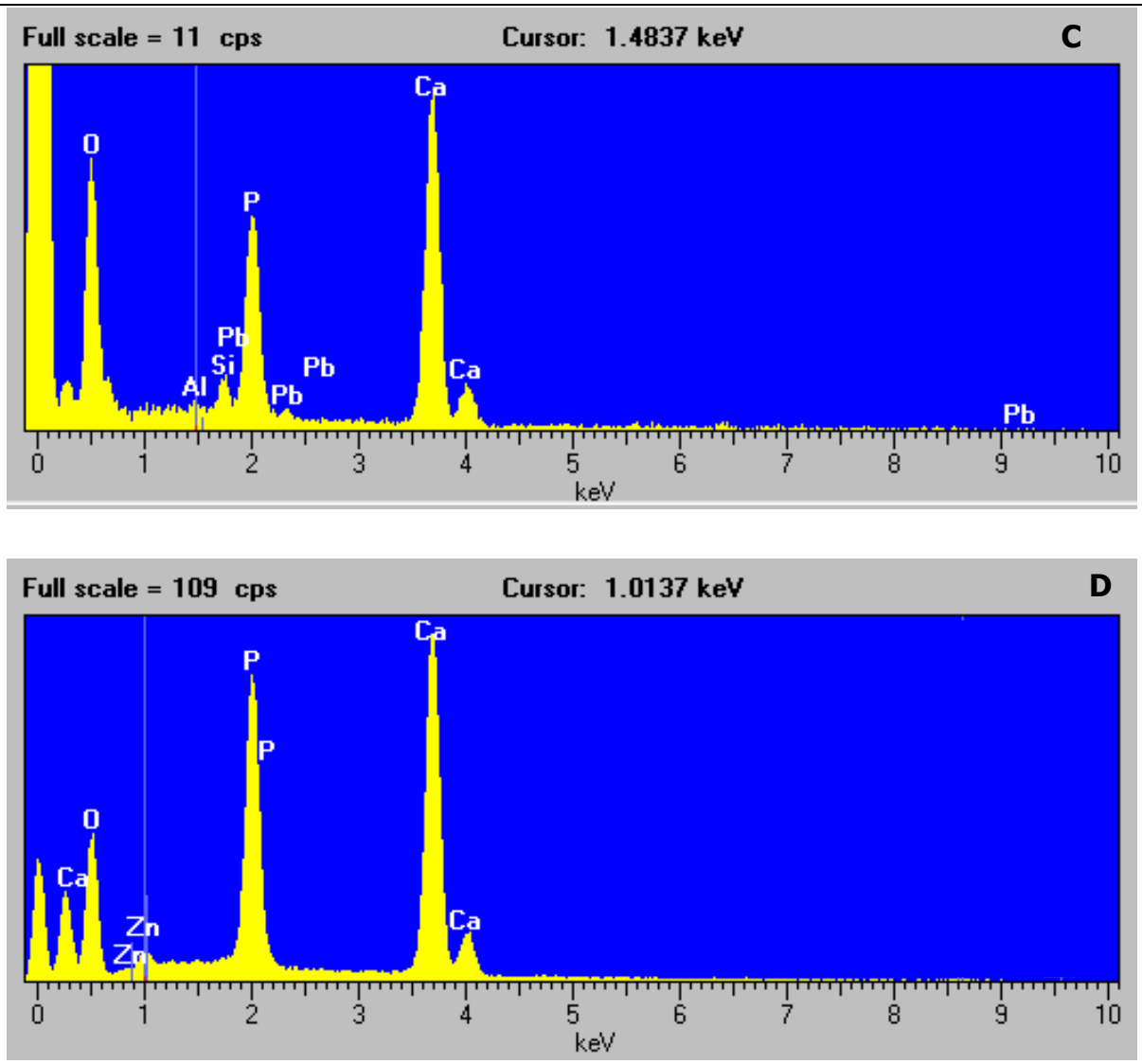

Fig. 2 EDS spectra of the previous SEM micrographs. – Fig. 2 Spettri EDS delle precedenti immagini al SEM.

5.2.2 AFM analyses

The analyzed FAP samples are generally interacted with solutions containing 100 and 500 mg/L for the four interaction times (2, 4, 24 and 48h). They always show a spherical shape (Fig. 3 A, B, C, and D) with an average diameter (horizontal distance) (Fig. 4 A, B, C and D) of about 100-200 nm. Particles don't show any different features from the original FAP (Fig. 6A see in materials) and nor among each single-metal system.

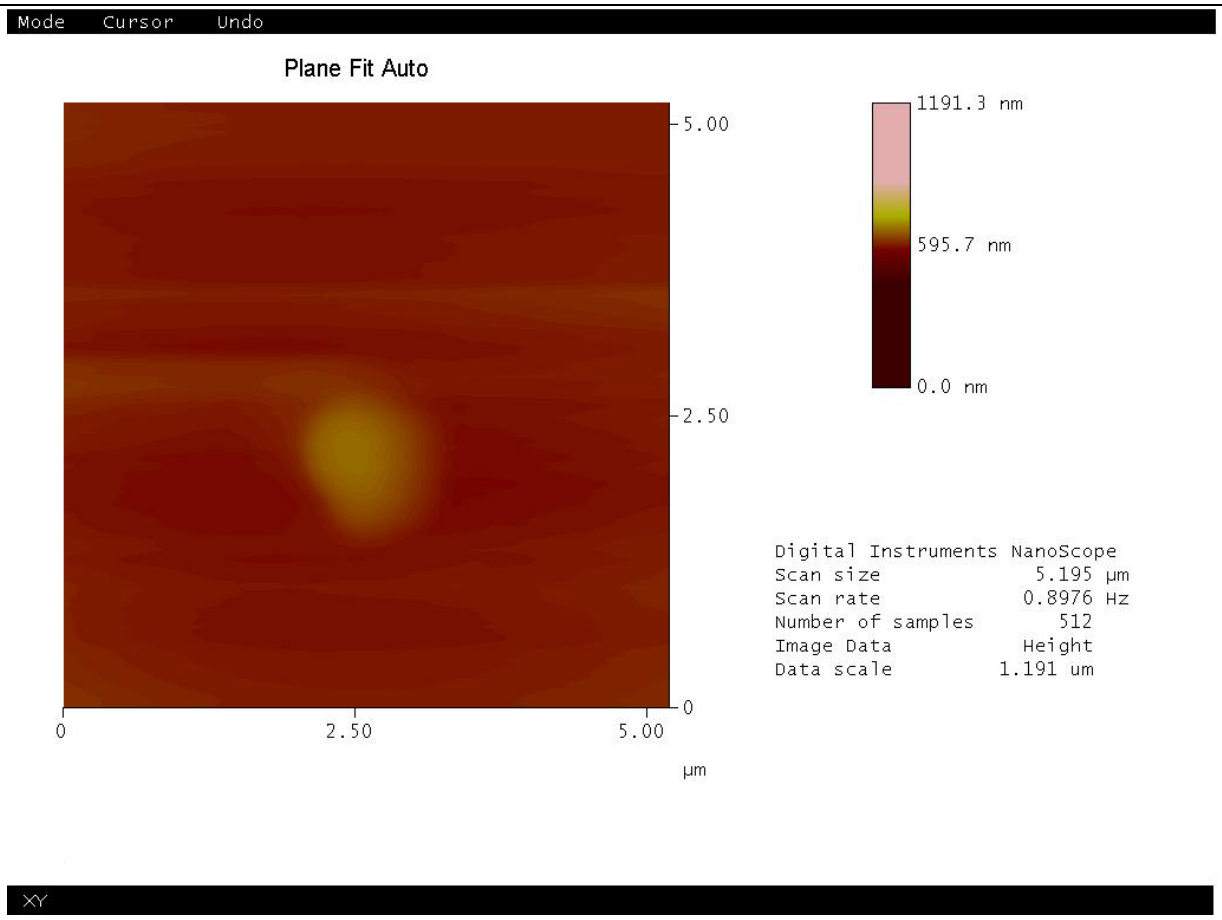
Mode Cursor Undo
Plane Fit Auto
5.00
2.50
0
0
2.50
5.00
µm
1191.3 nm
595.7 nm
0.0 nm
Digital Instruments NanoScope
Scan size 5.195 µm
Scan rate 0.8976 Hz
Number of samples 512
Image Data Height
Data scale 1.191 um
XY

A

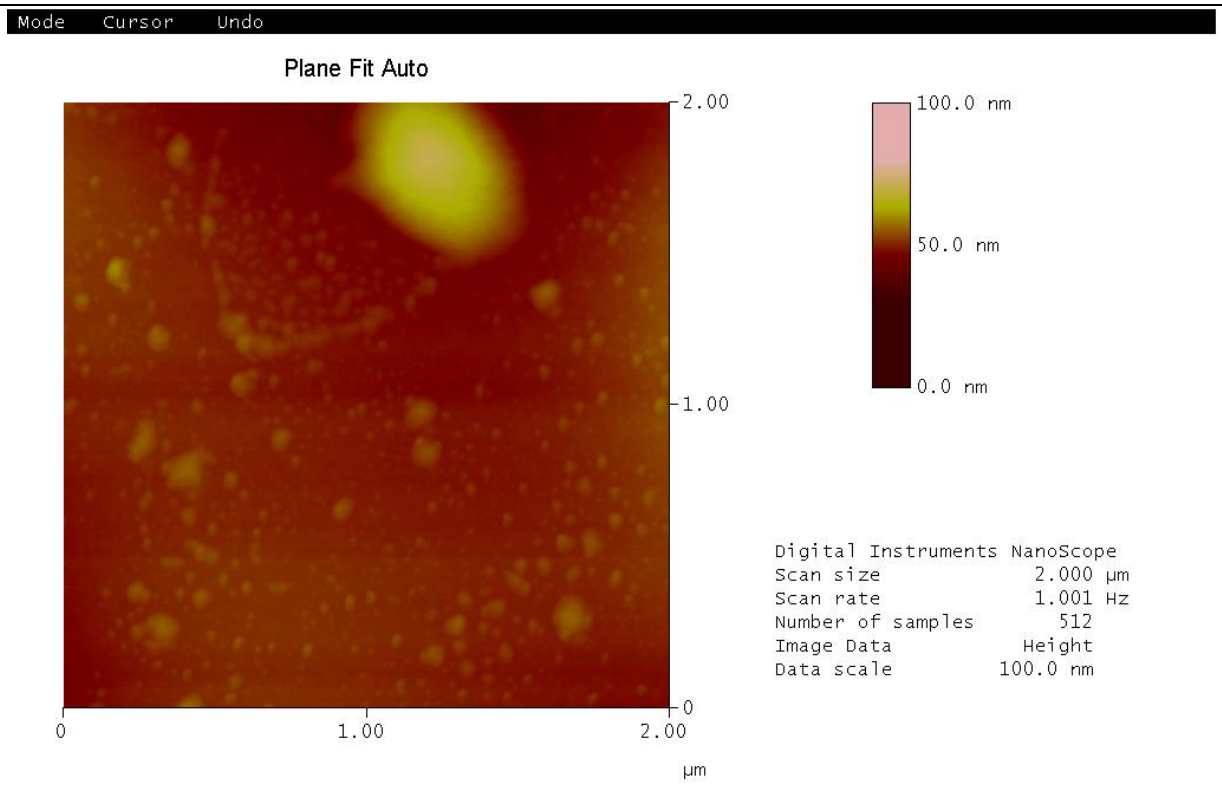
Mode Cursor Undo
Plane Fit Auto
2.00
1.00
0
0
1.00
2.00
µm
100.0 nm
50.0 nm
0.0 nm
Digital Instruments NanoScope
Scan size 2.000 µm
Scan rate 1.001 Hz
Number of samples 512
Image Data Height
Data scale 100.0 nm
XY

B

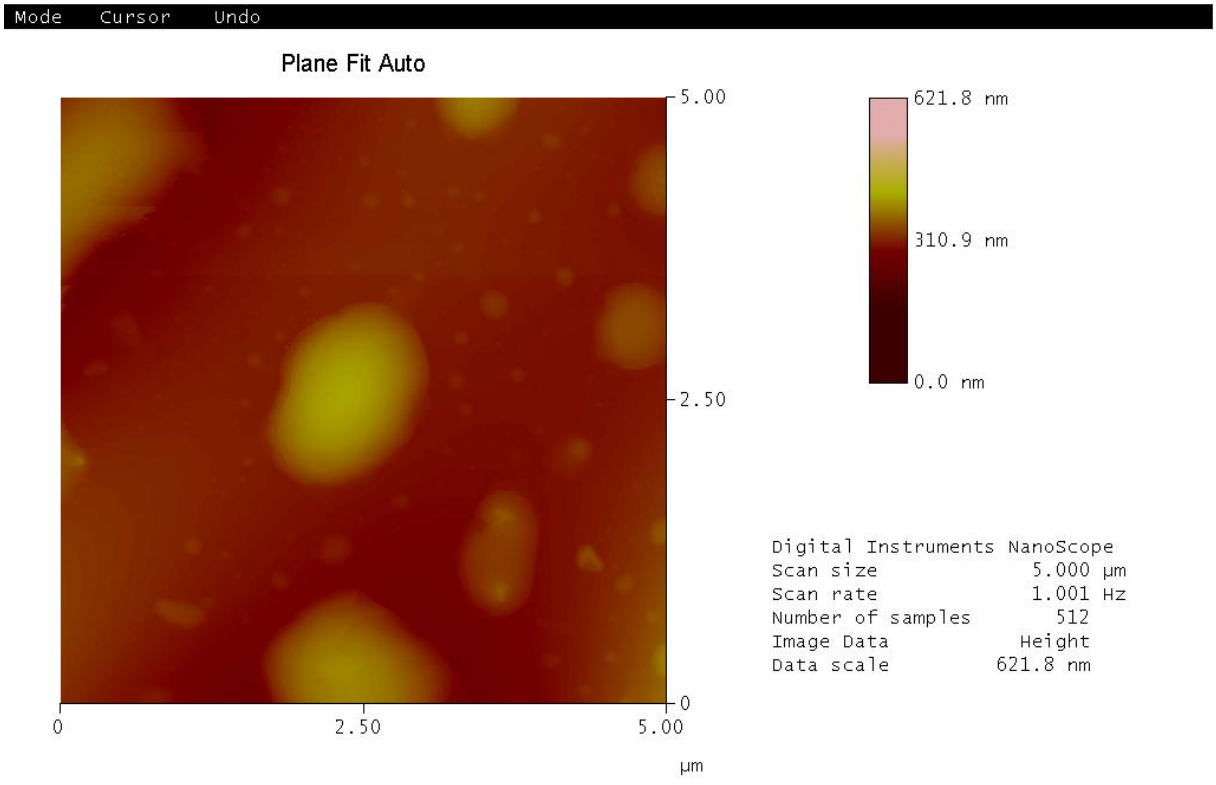
Mode Cursor Undo
Plane Fit Auto
5.00
2.50
0
0
2.50
5.00
µm
621.8 nm
310.9 nm
0.0 nm
Digital Instruments NanoScope
Scan size 5.000 µm
Scan rate 1.001 Hz
Number of samples 512
Image Data Height
Data scale 621.8 nm
XY

C

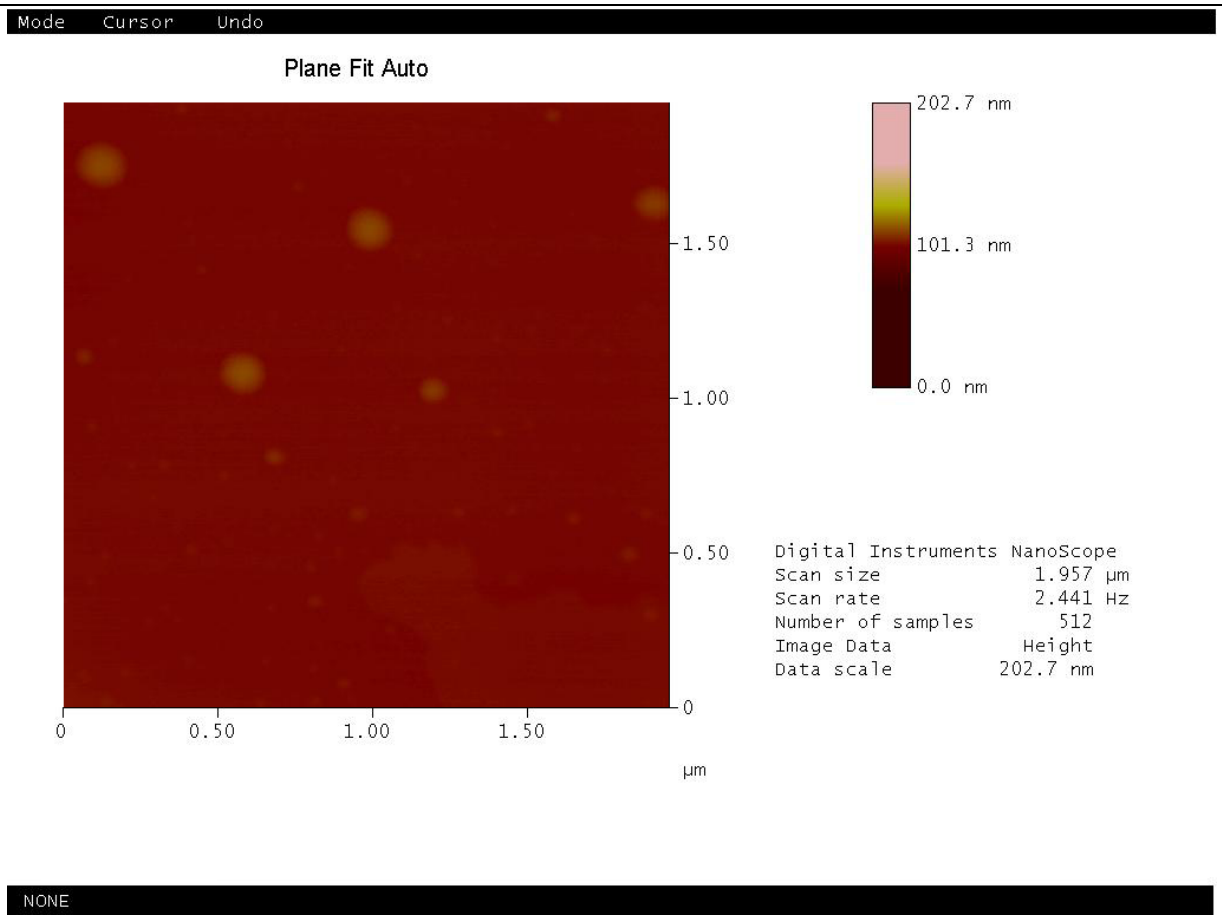

Fig. 3 AFM images of solid residues. A: Cd 4.45 mmol/L t = 2h; B: Cu 1.57 mmol/L t = 2h; C: Pb 0.48 mmol/L t = 48h; D: Zn 7.65 mmol/L t = 48h. – Fig. 3 AFM immagini. A: Cd 4.45 mmol/L t = 2h; B: Cu 1.57 mmol/L t = 2h; C: Pb 0.48 mmol/L t = 48h; D: Zn 7.65 mmol/L t = 48h.

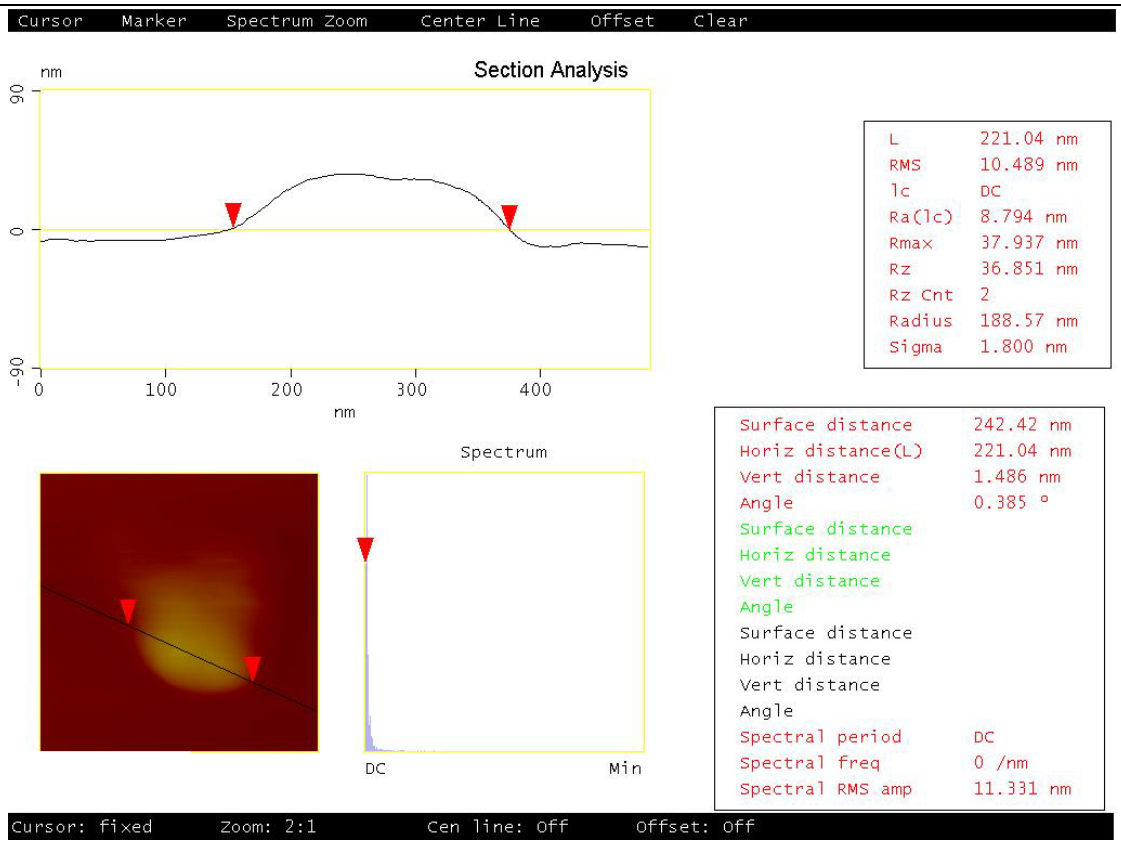
Cursor Marker Spectrum Zoom Center Line Offset Clear
Section Analysis
nm
90
0
-90
0
100
200
300
400
nm
L 221.04 nm
RMS 10.489 nm
lc DC
Ra(lc) 8.794 nm
Rmax 37.937 nm
Rz 36.851 nm
Rz Cnt 2
Radius 188.57 nm
Sigma 1.800 nm
Spectrum
DC
Min
Surface distance 242.42 nm
Horiz distance(L) 221.04 nm
Vert distance 1.486 nm
Angle 0.385 °
Surface distance
Horiz distance
Vert distance
Angle
Surface distance
Horiz distance
Vert distance
Angle
Spectral period DC
Spectral freq 0 /nm
Spectral RMS amp 11.331 nm
Cursor: fixed Zoom: 2:1 Cen line: Off Offset: Off

A

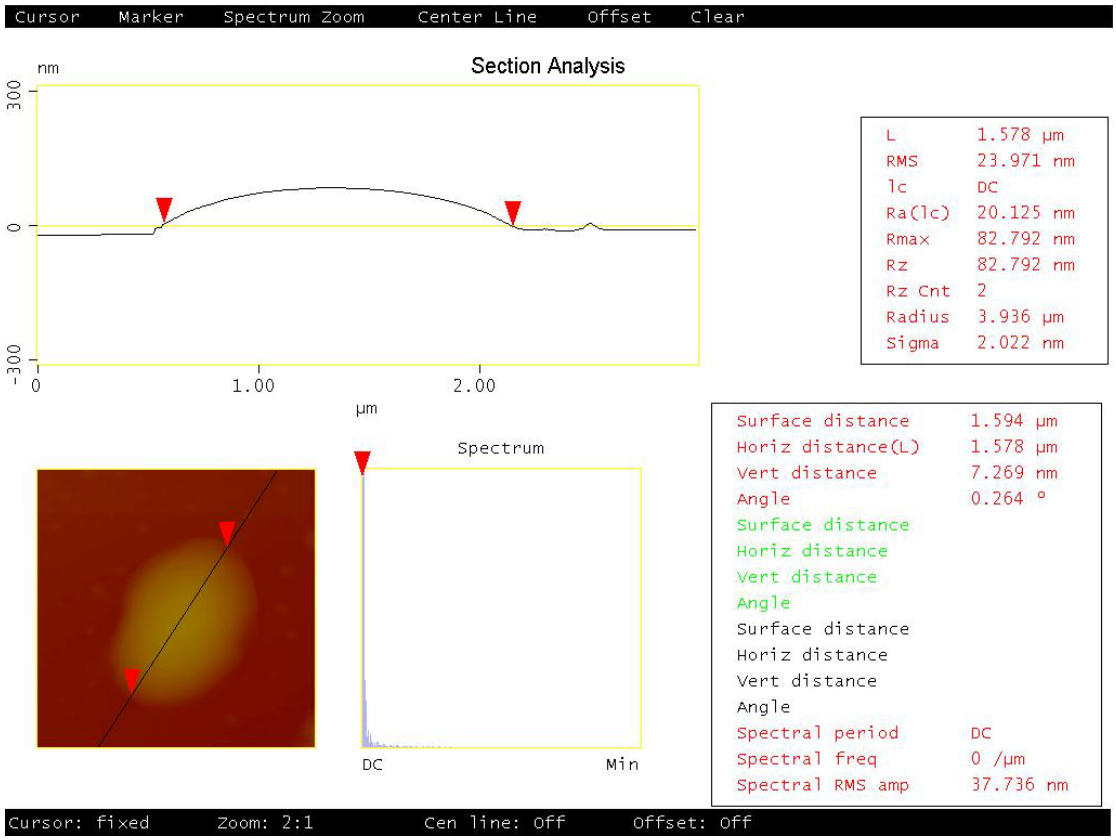
Cursor Marker Spectrum Zoom Center Line Offset Clear
Section Analysis
nm
300
0
-300
0
1.00
2.00
µm
L 1.578 µm
RMS 23.971 nm
lc DC
Ra(lc) 20.125 nm
Rmax 82.792 nm
Rz 82.792 nm
Rz Cnt 2
Radius 3.936 µm
Sigma 2.022 nm
Spectrum
DC
Min
Surface distance 1.594 µm
Horiz distance(L) 1.578 µm
Vert distance 7.269 nm
Angle 0.264 °
Surface distance
Horiz distance
Vert distance
Angle
Surface distance
Horiz distance
Vert distance
Angle
Spectral period DC
Spectral freq 0 /µm
Spectral RMS amp 37.736 nm
Cursor: fixed Zoom: 2:1 Cen line: Off Offset: Off

B

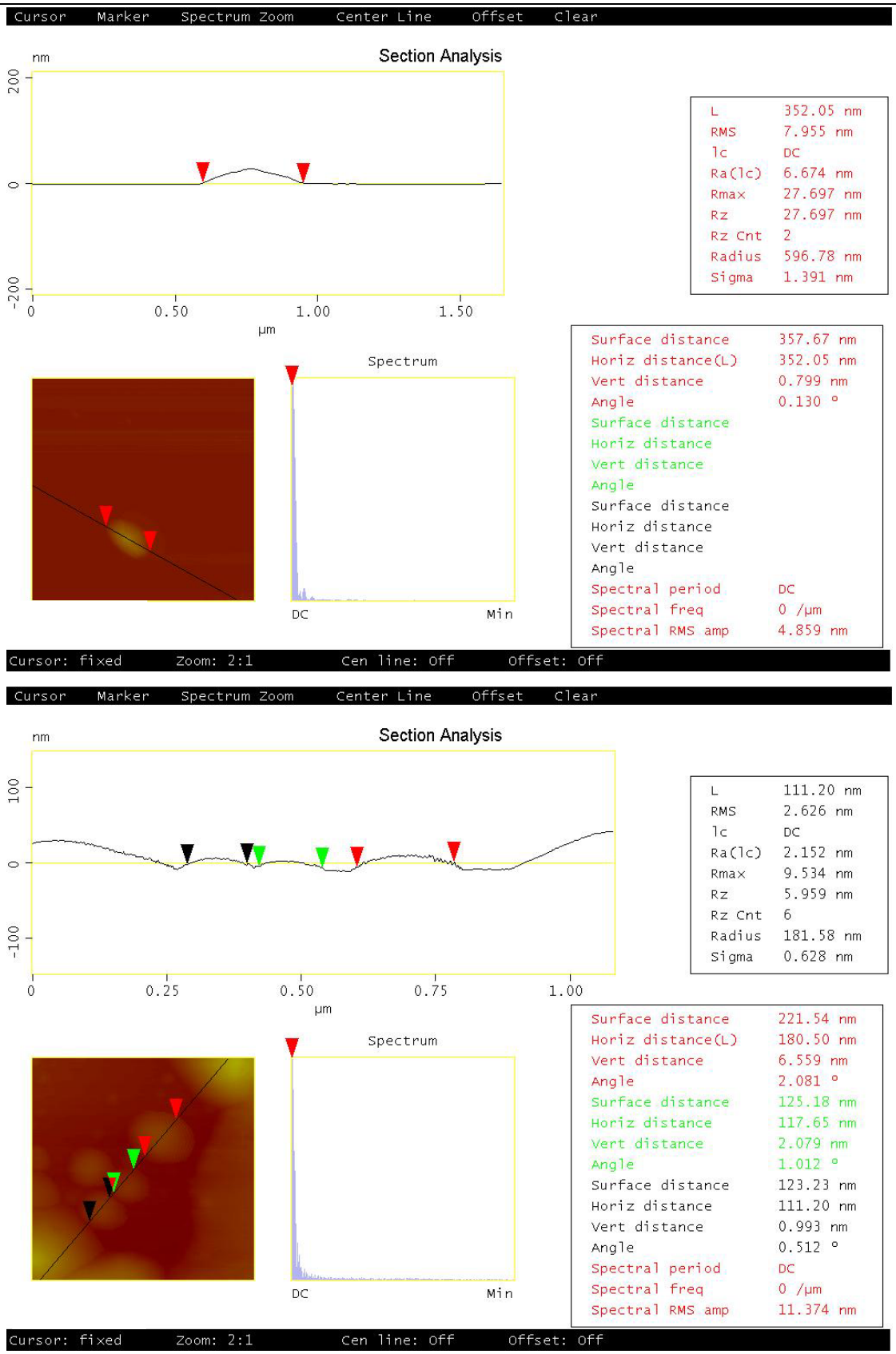

Fig. 4 AFM images of the solid residues showing the average size of the particles. A: Cd 0.89mmol/L t = 2h; B: Cu 7.87 mmol/L t = 48h; C: Pb 0.48 mmol/L t = 48 h. – Fig. 4 Immagini AFM dei materiali solidi

mostranti le dimensioni medie dei granuli. A: Cd 0.89mmol/L t = 2h; B: Cu 7.87 mmol/L t = 48h; C: Pb 0.48 mmol/L t = 48h; D: Zn 7.65 mmol/L t = 48h.

5.2.3 ICP-AES analyses

The proportions of heavy metal blocked per unit mass of FAP and the immobilization efficiency are listed in Table 1 and 2 and shown in Figs. 5-7.

The most higher immobilization is achieved after 48h of reaction, but it seems that the percentage of immobilization depends on the metal in solution. Generally, heavy metals concentrations were reduced with an average of 60%.

Cd, Cu, Pb and Zn = 10 mg/L; FAP = 1 g.				
	Cd	*Cu*	*Pb*	*Zn*
2h	9.54	9.96	9.94	9.17
4h	9.92	9.95	9.90	9.80
24h	9.87	9.96	9.82	9.79
48h	9.99	9.95	9.89	9.87

Cd, Cu, Pb and Zn = 100 mg/L; FAP = 1 g.				
	Cd	*Cu*	*Pb*	*Zn*
2h	10.16	11.36	18.93	10.44
4h	7.28	13.21	19.40	3.71
24h	14.63	19.31	19.97	4.66
48h	17.80	19.89	19.90	5.05

Cd, Cu, Pb and Zn = 500 mg/L; FAP = 1 g.				
	Cd	*Cu*	*Pb*	*Zn*
2h	88.84	40.94	31.73	-17.84
4h	51.98	50.63	40.61	-19.40
24h	51.74	77.89	67.80	-8.25
48h	60.33	91.73	68.06	-8.46

Table 1: Proportions of blocked heavy metals per unit mass of FAP (mg/g) for FAP = 1g. – Tabella 1: Entità dell'immobilizzazione dei metalli per unità di massa di FAP (mg/g), FAP = 1g.

Cd, Cu, Pb and Zn = 10 mg/L; FAP = 1 g.

	Cd	*Cu*	*Pb*	*Zn*
2h	95.45	99.64	99.36	91.68
4h	99.24	99.54	98.96	98.00
24h	98.73	99.55	98.20	97.87
48h	99.88	99.50	98.92	98.71

Cd, Cu, Pb and Zn = 100 mg/L; FAP = 1 g.

	Cd	*Cu*	*Pb*	*Zn*
2h	50.78	56.79	94.64	5.70
4h	36.41	66.06	97.02	18.53
24h	73.13	96.55	99.85	23.28
48h	89.02	99.45	99.51	25.26

Cd, Cu, Pb and Zn = 500 mg/L; FAP = 1 g.

	Cd	*Cu*	*Pb*	*Zn*
2h	88.84	82.23	31.73	-17.84
4h	51.98	89.60	40.61	-19.40
24h	51.74	89.65	67.80	-8.25
48h	60.33	87.93	68.06	-8.46

Table 2: In the table the values of the immobilization (%) are listed for each mono-metal system vs. FAP. – Tabella 2: Nella tabella sono elencati i valori dell'immobilizzazione (%) in soluzione a metallo singolo vs. FAP.

Cd immobilization is from 9.99 to 88.84 mg/g. The more suitable time for the interaction is 48h, except the case of the most high concentration (500 mg/L) where the maximum immobilization is achieved at t =2h, whereas the increasing of the time produces a reduction of the amount of blocked Cd. Increasing the initial metal concentration the immoblilization decreases (Fig. 5, 6, and 7).

Cu immobilization is very good, running from 9.95 mg/g to 91.73 mg/g. In general the maximum immobilization is achieved after 24h. Increasing the initial metal concentration the amount blocked metal decreases but it is still good. Generally the amount of sorbed metal increases with the increasing of the contact time.

Lead is quite well immobilized with an amount of blocked metal per unit mass of HA ranging from a minimum of 9.82 to a maximum of 68.06 mg/g. According to Ma et al. *(94)*, generally, the chemical reaction is very rapid, about less than two hours, but this

reaction seems to depend also on the original concentration of lead and the kind of amendant. Our experimental data further suggest that the initial Pb concentration seems to play a main role in the immobilization as the amount of blocked Pb decreases with increasing initial metal concentration.

For the highest initial Pb concentration (500 mg/L = 2.48 mmol/L) the maximum retention is achieved at 24h and 48h. On the contrary, at the lowest Pb initial concentration (10 mg/L = 0.05 mmol/L) the maximum immobilization is obtained after 2h and increasing the contact time Pb retention slightly decreases.

Zinc retention ranges from -19.40 to 10.44 mg/g of FAP, but in all the experiments at the highest concentration (7.65 mmol/L) the metal immobilization didn't occur and the FAP released some of its original Zn content. At the other two concentrations (0.15 and 1.5 mmol/L) Zn immobilization, generally, increases with the time, but it decreases with the increase of the initial concentration from 0.15 to 1.5 mmol/L.

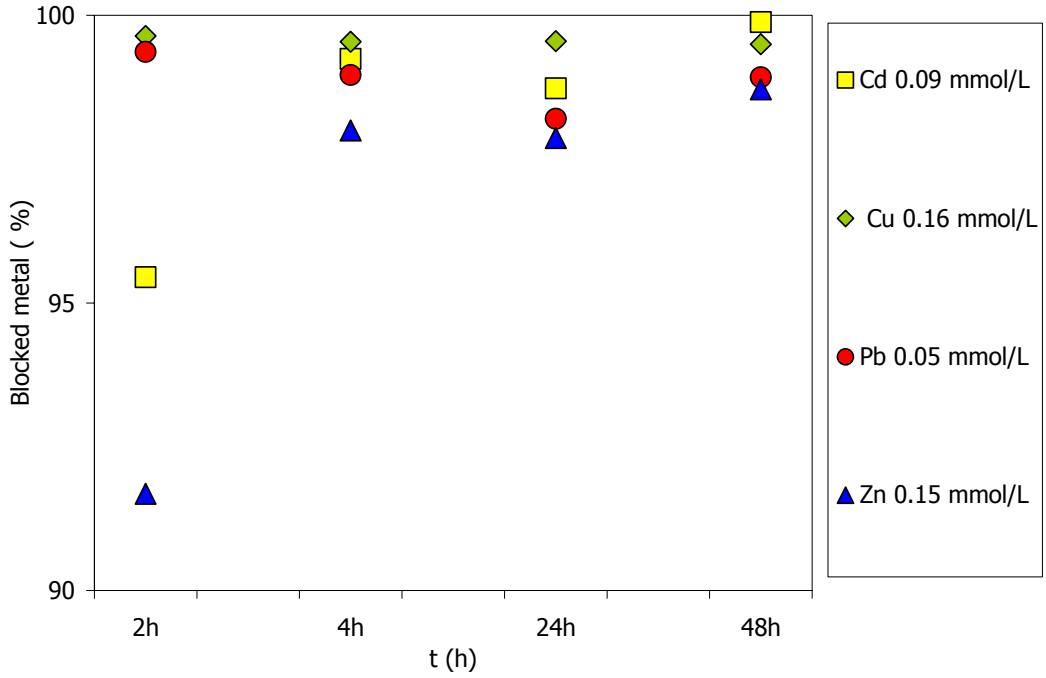

Fig. 5: Variation of the amount of blocked metal with time for FAP = 1 g. - Fig. 5: Variazione delle percentuali di metalli immobilizzati in funzione del tempo di interazione per FAP = 1g.

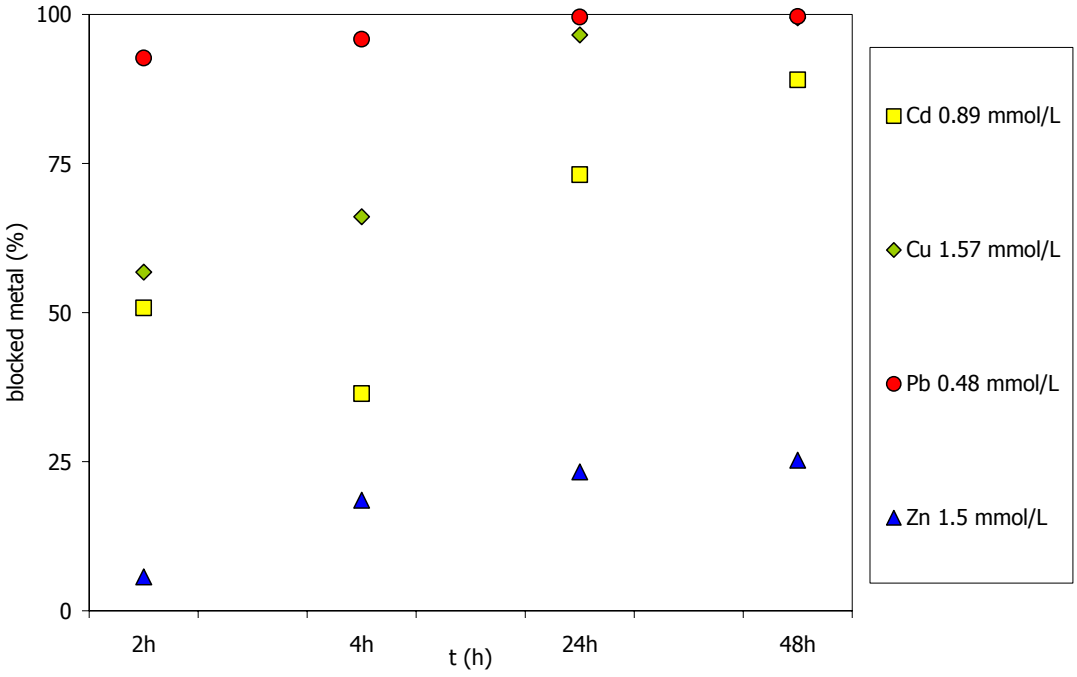

Fig. 6: Variation of the amount of blocked metal with time for FAP = 1 g. - Fig. 6: Variazione delle percentuali di metalli immobilizzati in funzione del tempo di interazione per FAP = 1g.

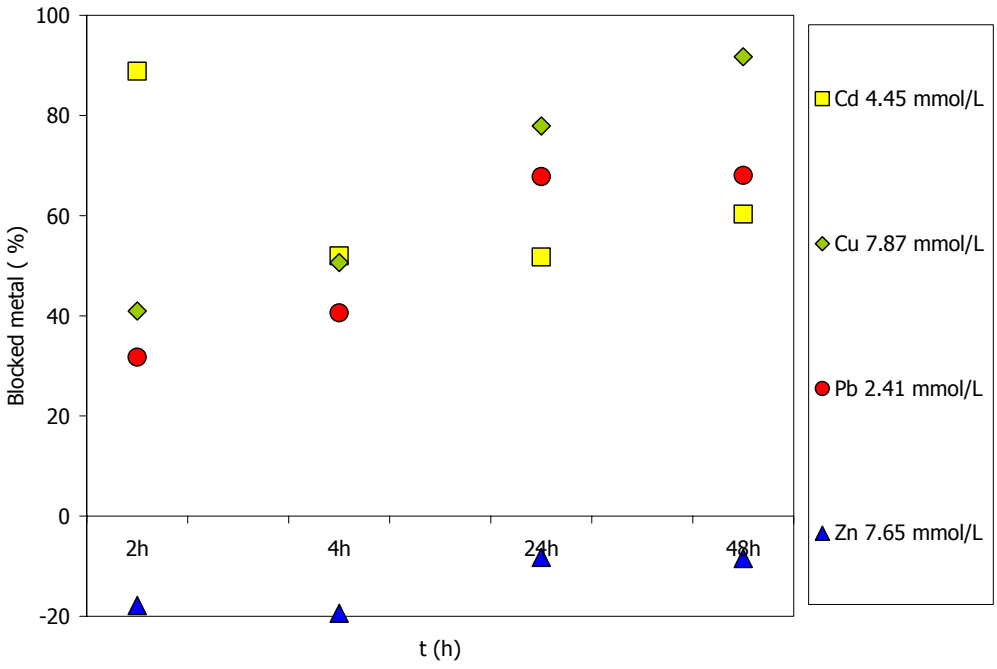

Fig. 7: Variation of the amount of blocked metal with time for FAP = 1 g. - Fig. 7: Variazione delle percentuali di metalli immobilizzati in funzione del tempo di interazione per FAP = 1g.

The molar ratio (Q_S) values for these types of experiment are very particular (Tab. 3) as values are >>1. Generally, for the lower metal concentration (10 mg/L) the Q_S

values are <1 and this suggests a dissolution/precipitation phenomenon. Increasing the concentration at a medium value (100 mg/L) Q_S values are about 5-35, meaning an adsorption mechanism. For high amounts of Cd, Cu and Pb Q_S values are >>1, that is a few moles of Ca are released in the solution compared to the amount of sorbed. But Zn shows a different beaviour, as the Q_S values are < 1. In this last case, we observe that increasing the interaction time, the Q_S values increase suggesting the achievement of equilibrium at time longer than 48h.

Cd, Cu, Pb and Zn = 10 mg/L; FAP = 1 g.				
t	Cd	Cu	Pb	Zn
2h	0.45	0.69	0.16	0.46
4h	0.38	0.60	0.38	0.57
24h	0.25	0.45	0.16	0.57
48h	0.24	0.37	0.16	0.29
Cd, Cu, Pb and Zn = 100 mg/L; FAP = 1 g.				
	Cd	Cu	Pb	Zn
2h	10.40	20.78	12.62	23.51
4h	7.64	21.87	13.80	5.38
24h	8.80	18.66	8.14	5.48
48h	9.02	12.78	35.48	8.78
Cd, Cu, Pb and Zn = 500 mg/L; FAP = 1 g.				
	Cd	Cu	Pb	Zn
2h	213.25	121.47	92.16	-68.65
4h	106.66	131.58	129.09	-42.72
24h	51.74	126.21	118.00	-11.37
48h	56.17	118.83	112.52	-10.59

Tab. 3: List of Q_S values in the single metal system vs. FAP. Tab. 3: Elenco dei valori del Q_S nel sistema a metallo singolo vs. FAP.

The shape of the sorption isotherms (Fig. 8 A, B, C and D), generally, show a short linear part and a knee indicating a phenomenon of adsorption and surface precipitation. Generally, the isotherms present an initial linear part which is shorter and a sharp knee (type L subtype 2 according Giles et al. *(62)*) suggesting phenomena of adsorption and surface precipitation. Zn isotherms shows always negative values because of a reprecipitation phenomenon. Our experimental results suggest that the sorption mechanisms are constants and they are not a function of the interaction time with the FAP, depending mainly on the heavy metal.

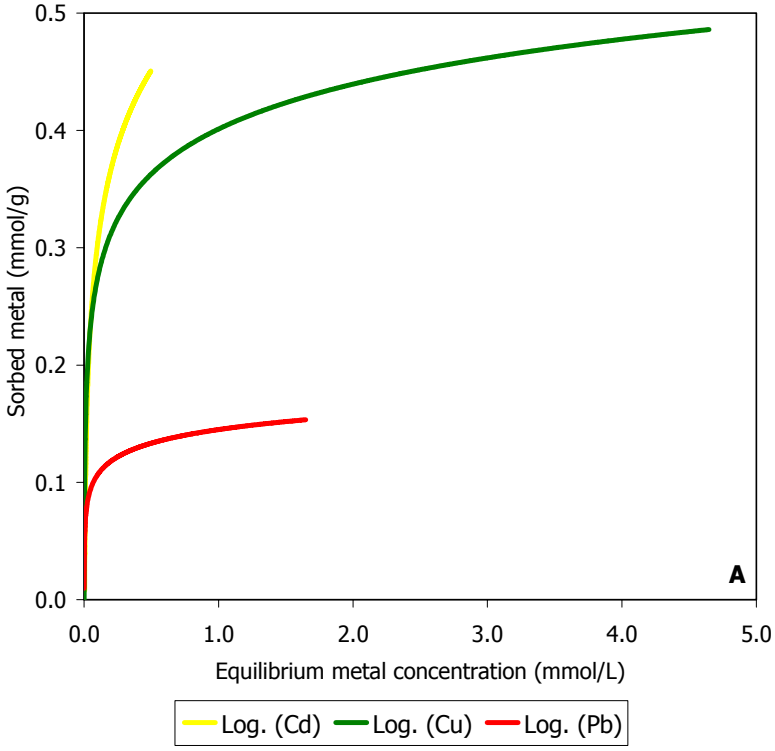
0.5
0.4
0.3
0.2
0.1
0.0
Sorbed metal (mmol/g)
0.0
1.0
2.0
3.0
4.0
5.0
Equilibrium metal concentration (mmol/L)
A
Log. (Cd)
Log. (Cu)
Log. (Pb)

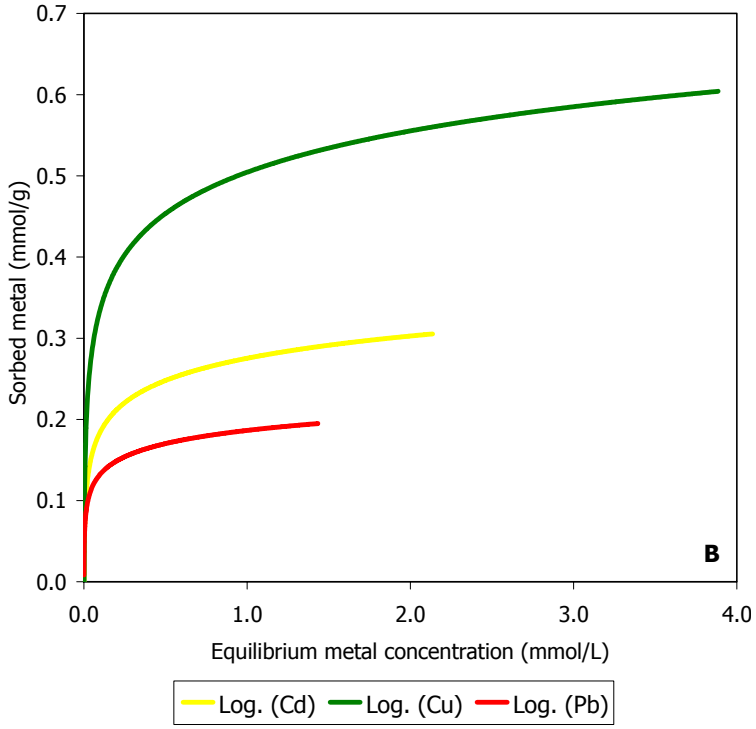
0.7
0.6
0.5
0.4
0.3
0.2
0.1
0.0
Sorbed metal (mmol/g)
0.0
1.0
2.0
3.0
4.0
Equilibrium metal concentration (mmol/L)
B
Log. (Cd)
Log. (Cu)
Log. (Pb)

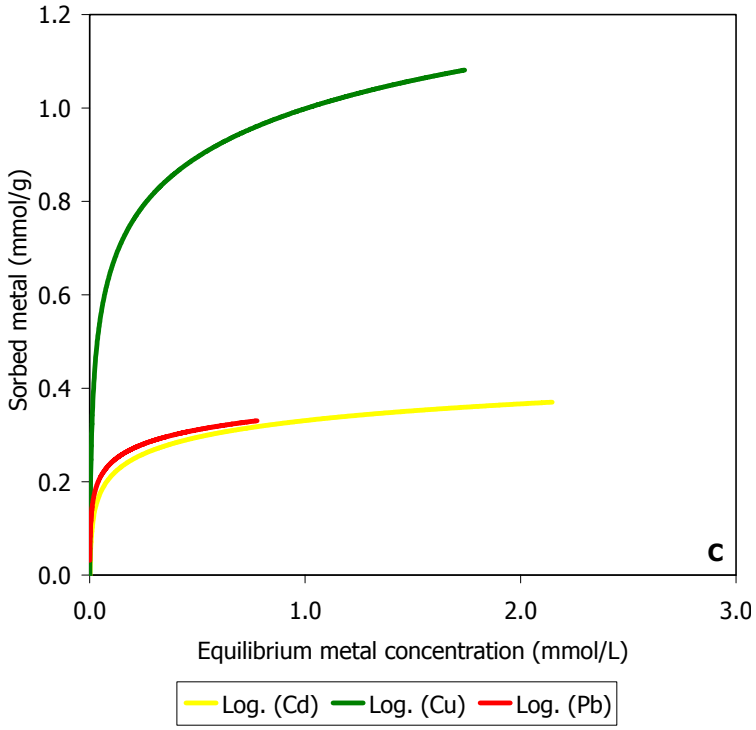

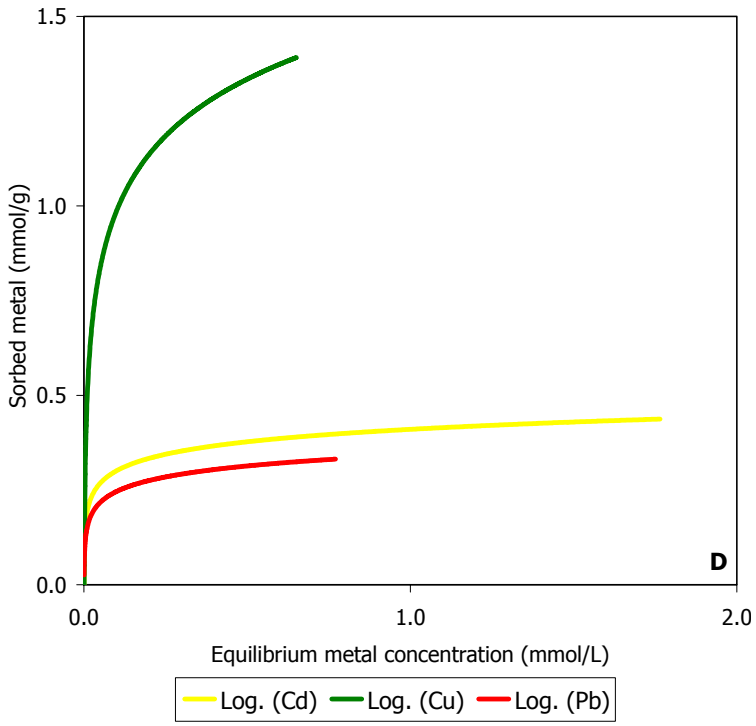

Fig. 8: Sorption isotherm for the monometal system for the four times (2h, 4h, 24h and 48h) and vs. 1g FAP. Relation between the metal sorbed (mmol/g) and the metal concentration at the equilibrium (mmol/L) A: 2h; B: 4h; C: 24h and D: 48h. – Fig. 8: Isoterme di assorbimento per il sistema a metallo singolo per i quattro diversi tempi (2h, 4h, 24h e 48h) e vs. 1h FAP. Relazione tra I lmetallo assorbito (mmol/g) e la concentrazione del metallo all'equilibrio (mmol/L). A: 2H; B: 4h; C: 24h e D: 48h.

Heavy metals retention by FAP produces an increases of Ca concentration in the solution. Generally Ca amount increases with contact time, whereas with the increasing of the initial metal concentration the amount of Ca released decreases. The only exception is lead, Ca concentration is similar for the last two concentration (0.48 mmol/L and 2.41 mmol/L), it is about 0.10-0.30 mmol/g (Fig. 9, 10 and 11).

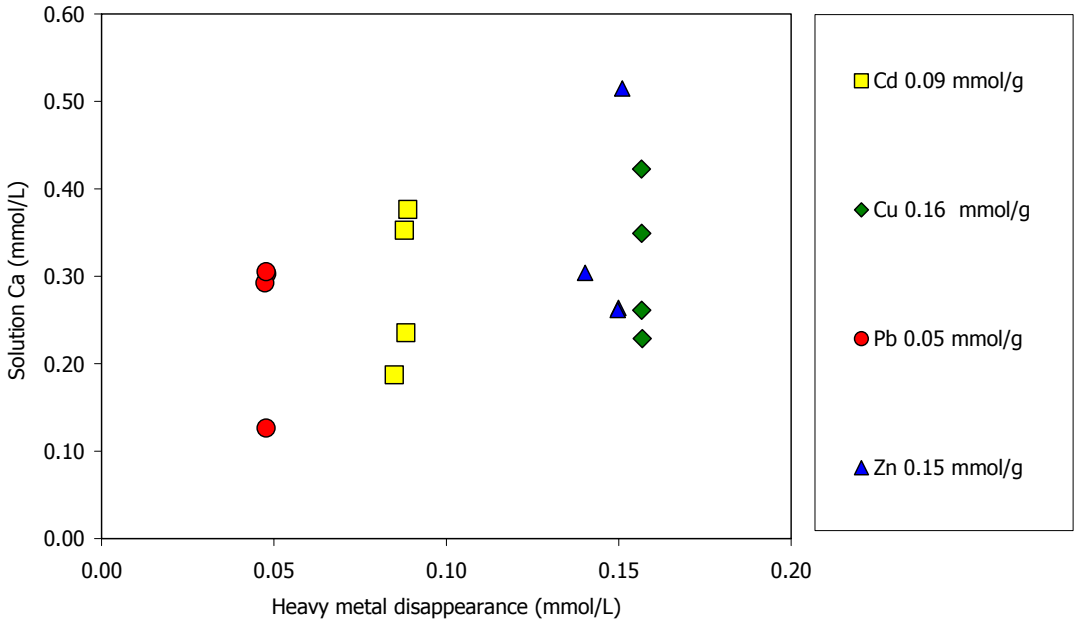

Fig. 9 Relation between Ca (mmol/g) and the amount of heavy metals (mmol/g) sorbed on FAP surface in the solution. – Fig. 9 relazione tra il Ca (mmol/g) e il quantitativo di metalli pesante assorbito sulla superficie della FAP in soluzione.

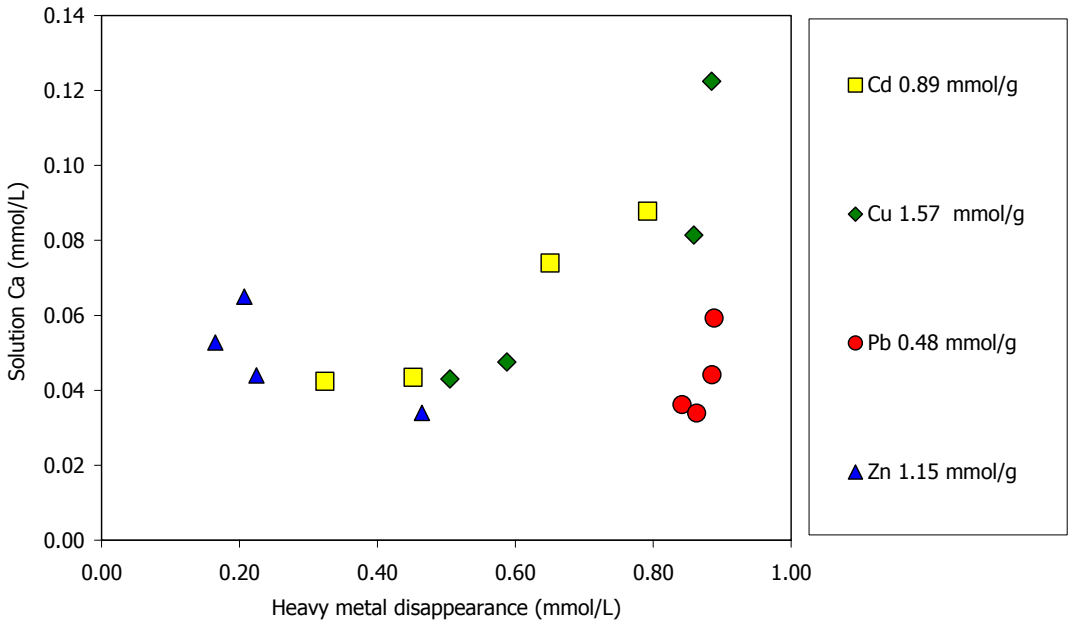

Fig. 10 Relation between Ca (mmol/g) and the amount of heavy metals (mmol/g) sorbed on FAP surface in the solution. – Fig. 10 Relazione tra il Ca (mmol/g) e il quantitativo di metalli pesante assorbito sulla superficie della FAP in soluzione.

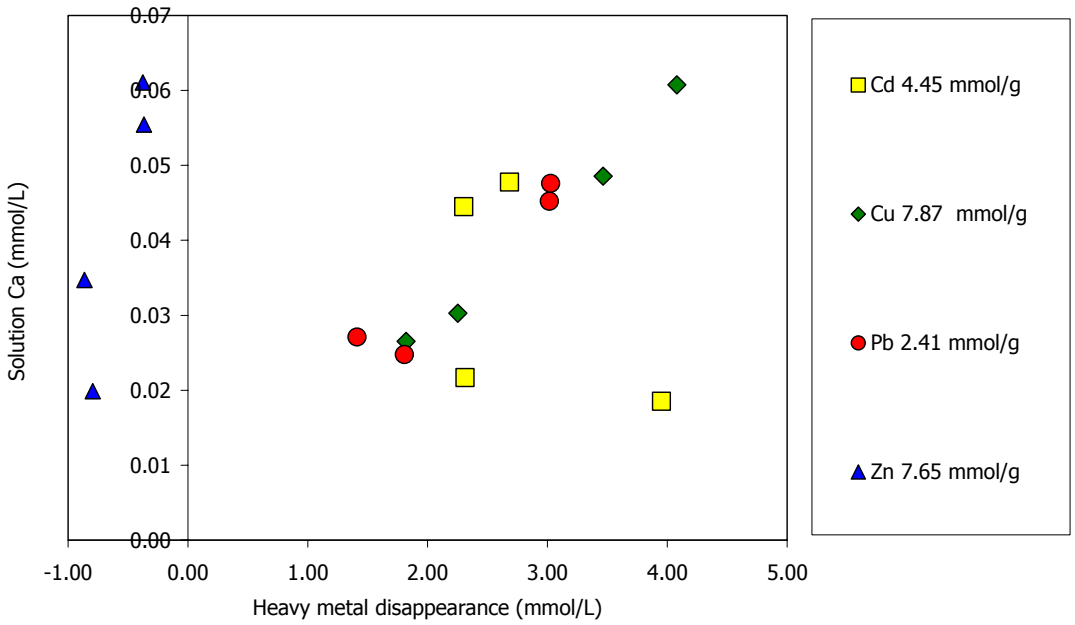

Fig. 11 Relation between Ca (mmol/g) and the amount of heavy metals (mmol/g) sorbed on FAP surface in the solution. - Fig. 11 Relazione tra il Ca (mmol/g) e il quantitativo di metalli pesante assorbito sulla superficie della FAP in soluzione.

The P concentration in solution is very low and it seems not to depend on the contact time or on the initial concentration of each heavy metal. The P concentration is always the same for the three different concentrations of the four heavy metals, about 0.05-0.10 mmol/g suggesting a non-stoichiometric dissolution of FAP (Fig. 12, 13 and 14).

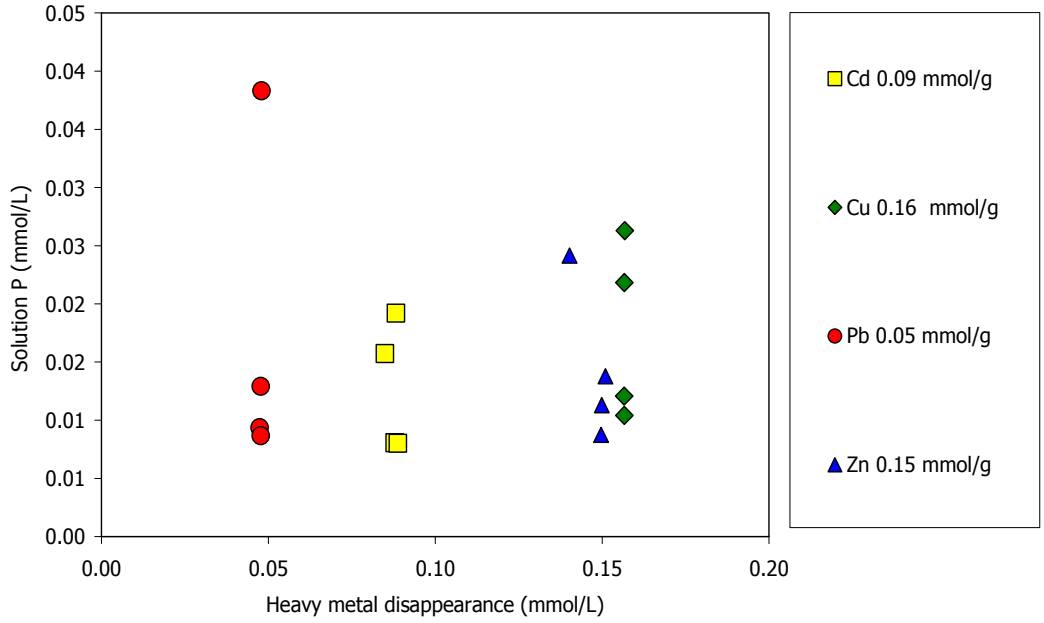

Fig. 12 Relation between P (mmol/g) and the amount of heavy metals (mmol/g) sorbed on FAP surface in the solution. - Fig. 12 Relazione tra il P (mmol/g) e il quantitativo di metallo pesante (mmol/g) assorbito sulla superficie della FAP in soluzione.

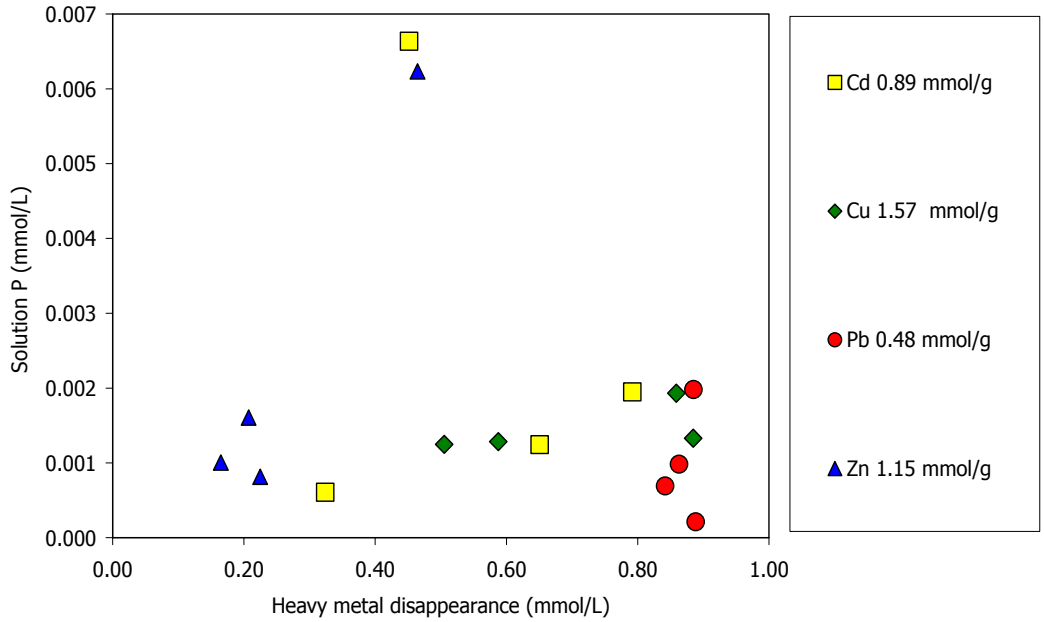

Fig. 13 Relation between P (mmol/g) and the amount of heavy metals (mmol/g) sorbed on FAP surface in the solution. - Fig. 13 Relazione tra il P (mmol/g) e il quantitativo di metallo pesante (mmol/g) assorbito sulla superficie della FAP in soluzione.

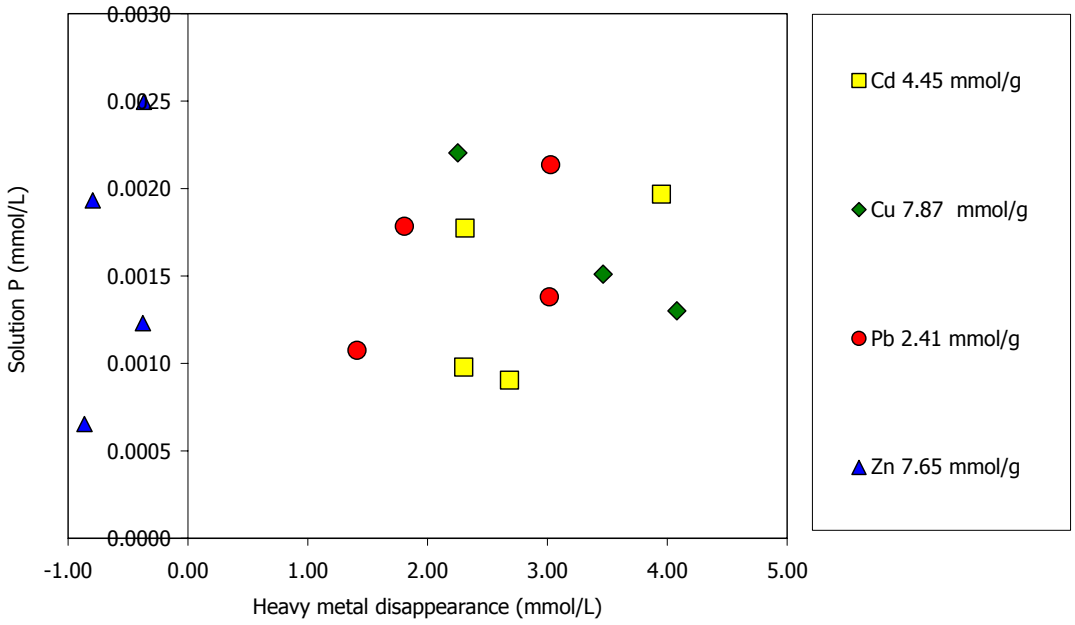

Fig. 14 Relation between P (mmol/g) and the amount of heavy metals (mmol/g) sorbed on FAP surface in the solution. - Fig. 14 Relazione tra il P (mmol/g) e il quantitativo di metallo pesante (mmol/g) assorbito sulla superficie della FAP in soluzione.

6 RESULTS MULTI-METAL SYSTEM

6.1 MULTI-METAL SYSTEM SORBED ON SYNTHETIC HYDROXYAPATITE (HA)

6.1.1 XRD analyses

On random samples of solid residues, were carried out some XRD analyses which don't show any mineral peak but those of the original HA. The solid samples are almost similar to the original HA and XRD patterns of different samples are well overlapped (Fig. 1). Generally, HA peak intensity is bigger than that of the solid materials, allowing to infer that solid residues have low crystallinity than the original HA.

Lattice parameters were calculated to determine if new phosphate phases precipitated during the experiments. The lattice values close to the ones of HA confirm that no any new crystalline phase is precipitated with an amount higher than 1% (during the sorption experiments) (Fig. 2).

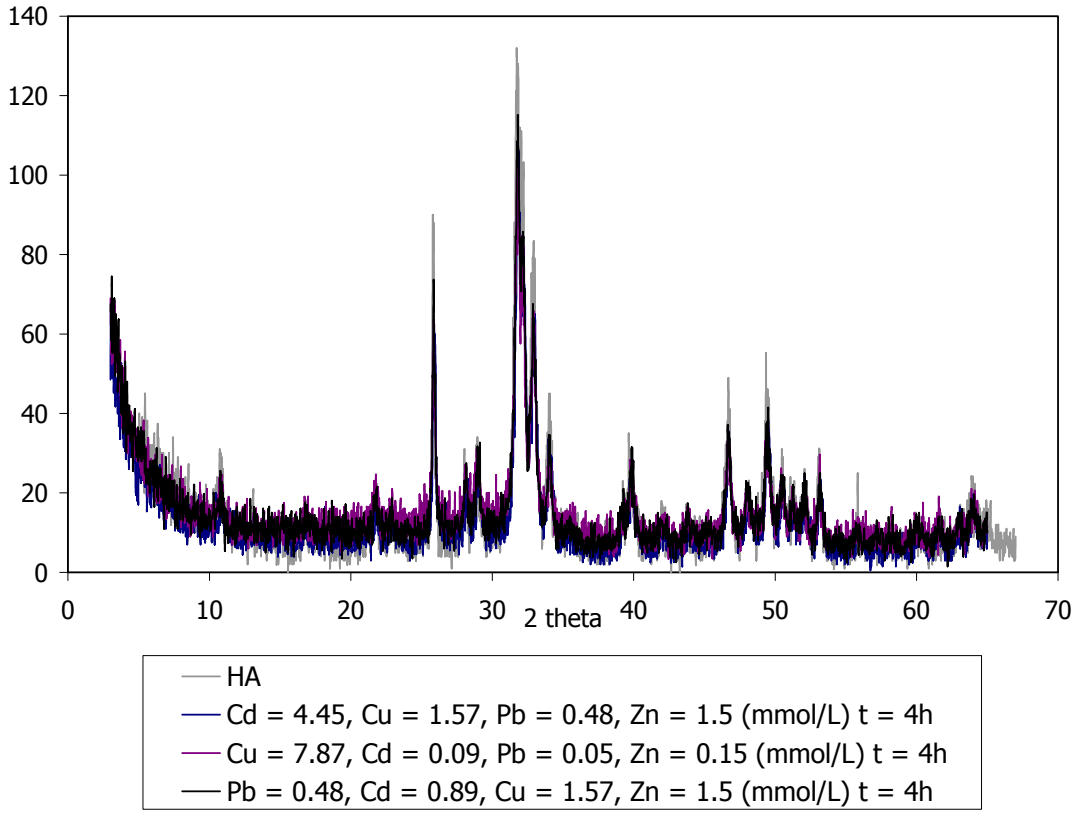

Fig. 1: Examples of XRD patterns of the solid materials from multi – metal system and starting HA showing a good overlapping. – Fig. 1: Esempi di diffrattogrammi dei materiali solidi degli esperimenti del sistema multi–metal. É evidente la sovrapposizione completa con il tracciato ottenuto per la HA.

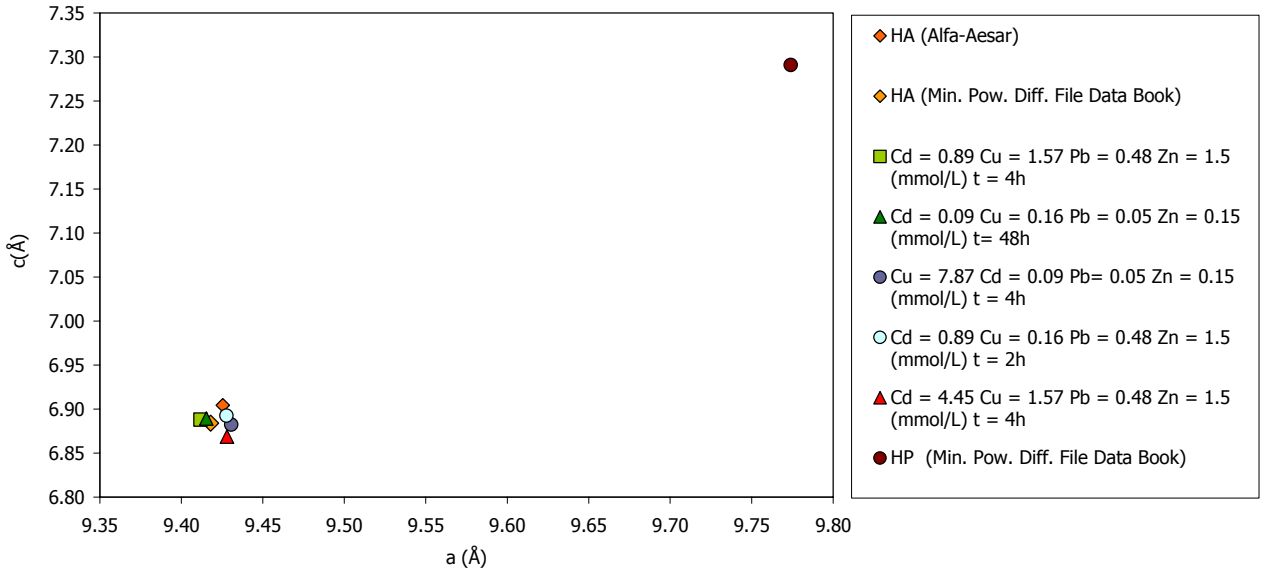

Fig. 2: Lattice parameters for some solid materials from multi-metal systems. – Fig. 2: Parametri di cella per alcuni materiali solidi del sistema multi-metal.

6.1.2 SEM analyses

As in the single-metal system, SEM micrographs of the solid materials don't show any kind of morphological differences or orientation in the particles in comparison with the HA (Fig. 3 A, B, C and D). On the contrary, EDS confirms the presence of the heavy metals on HA surface (Fig. 4 A, B, C, and D). EDS peaks let say the sorbed heavy metal are in different concentration, although this is a qualitative measure. The reason for this might be SEM was unable to achieve high enough resolution to detect the shape

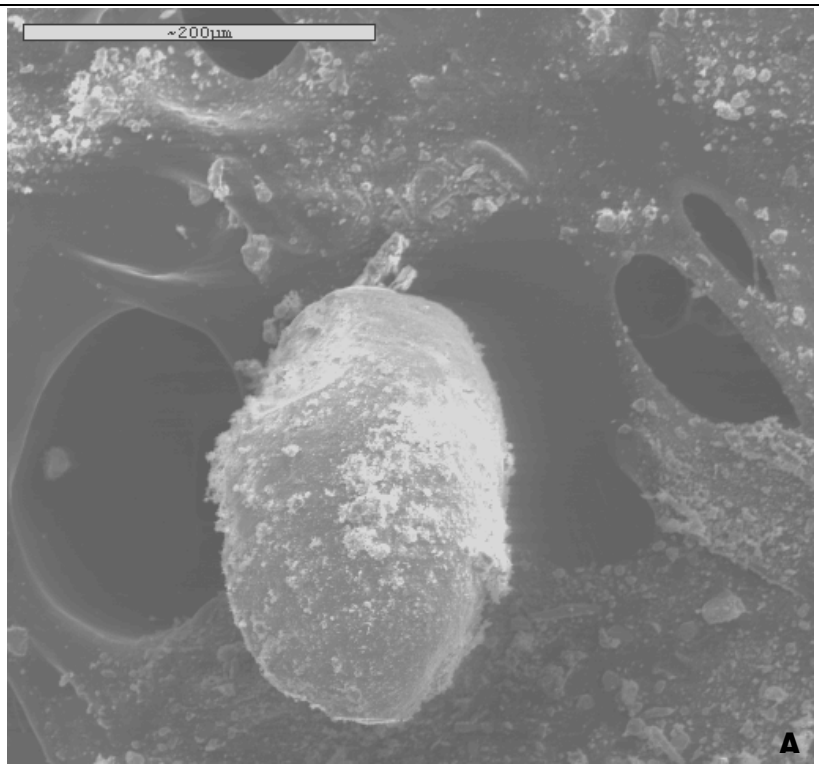
~200µm
A

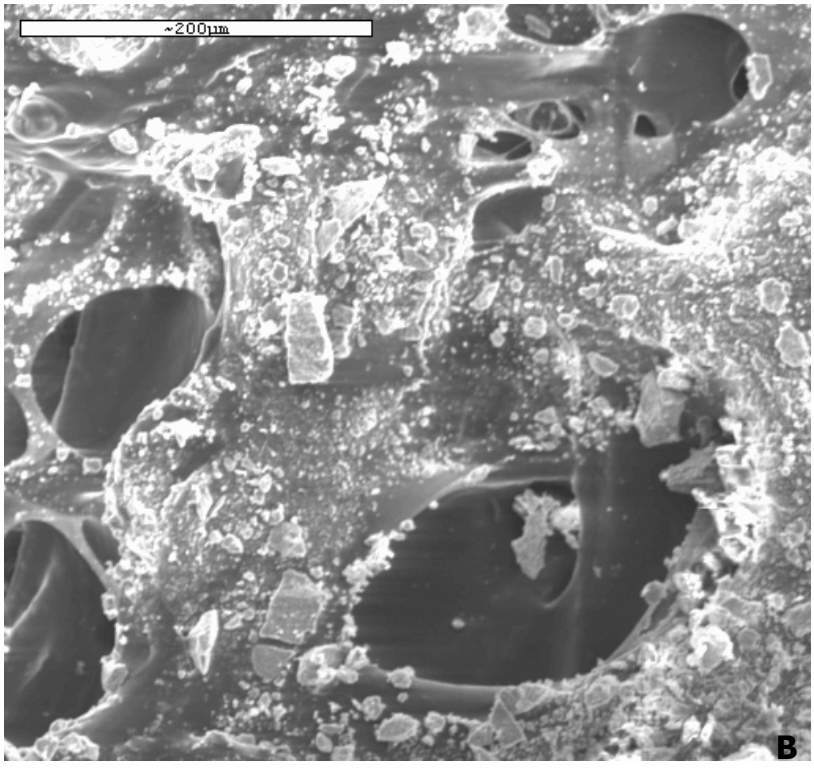
~200µm
B

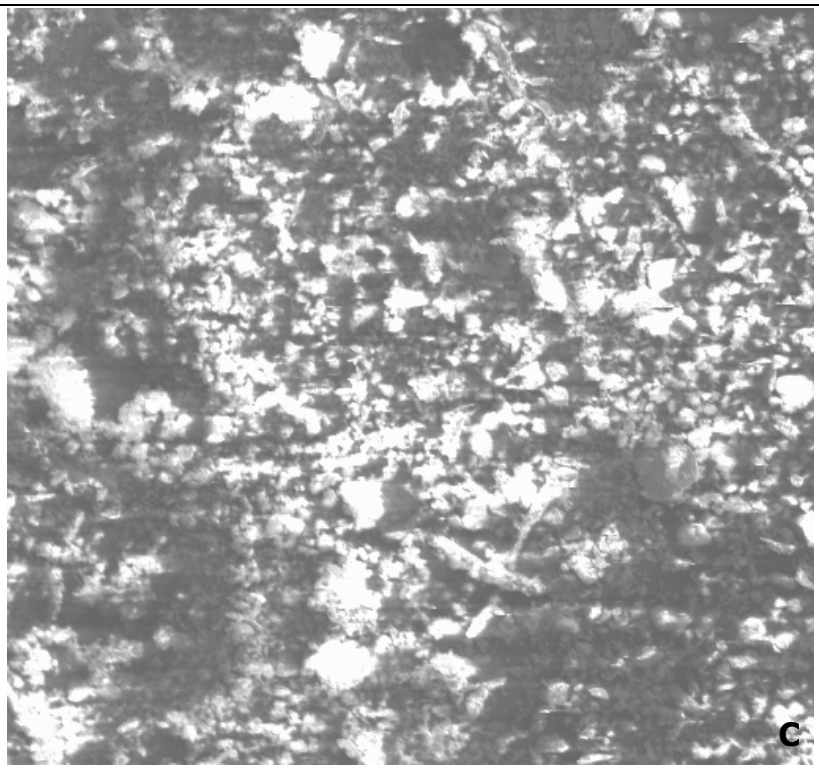

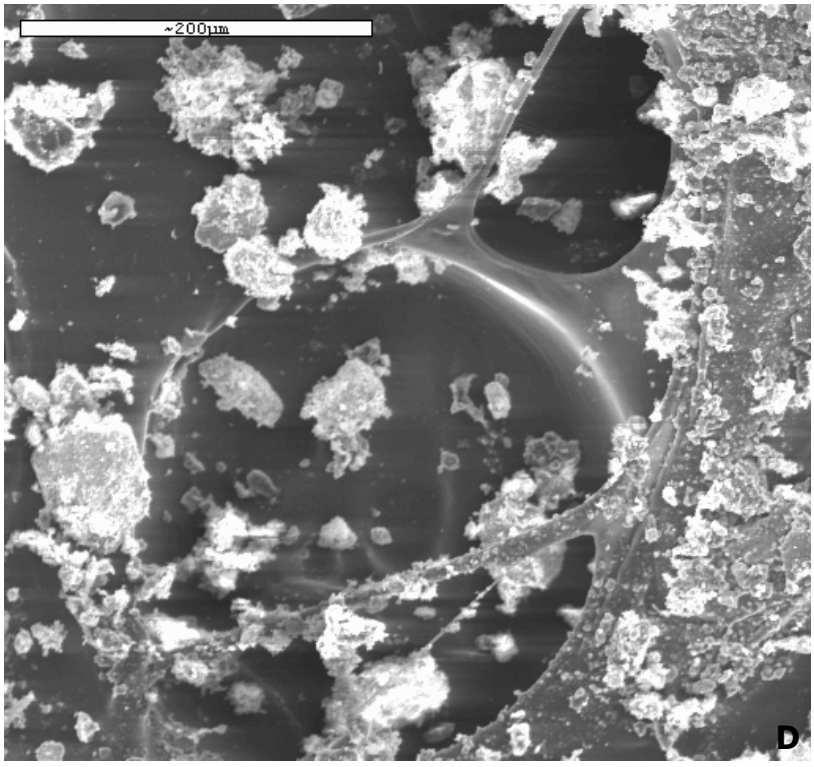

Fig. 3: Examples of SEM micrographs of solid residues. A: Cd = 10 mg/L, Cu, Pb and Zn = 500 mg/L t = 48h; B: Cu = 500 mg/L, Cd, Pb and Zn = 10 mg/L t = 4h; C: Pb, Cd, Cu and Zn = 100 mg/L t = 24h; D: Zn = 100 mg/L, Cd, Cu and Pb = 500 mg/L t = 4h. – Fig. 3: Esempio delle foto al SEM per il sistema multi-metal. A: Cd = 10 mg/L, Cu, Pb and Zn = 500 mg/L t = 48h; B: Cu = 500 mg/L, Cd, Pb and Zn = 10 mg/L t = 4h; C: Pb, Cd, Cu and Zn = 100 mg/L t = 24h; D: Zn = 100 mg/L, Cd, Cu and Pb = 500 mg/L t = 4h.

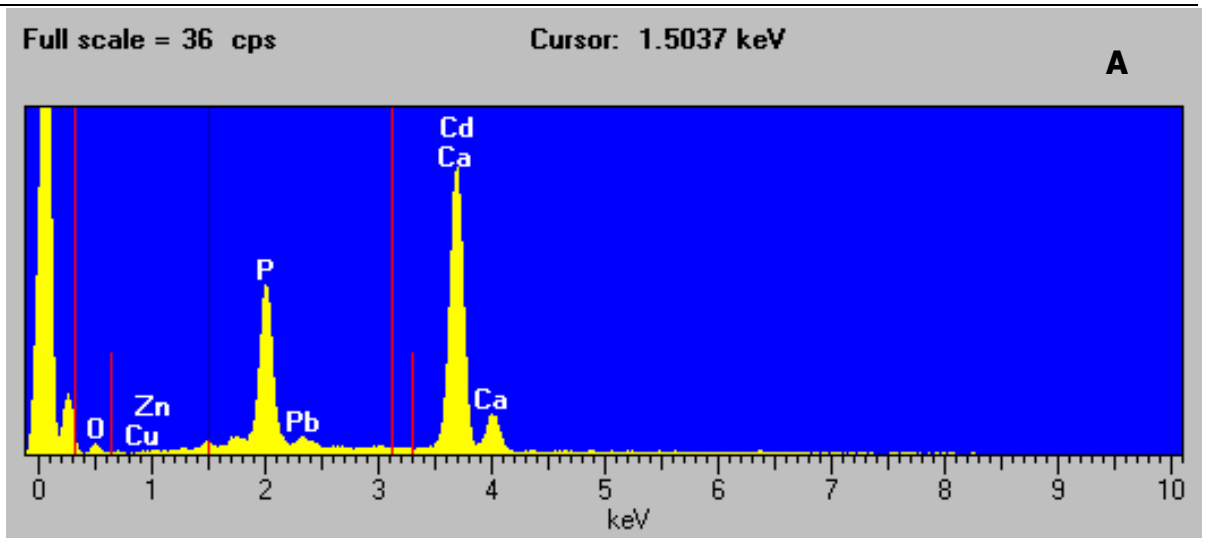
Full scale = 36 cps
Cursor: 1.5037 keV
A
Cd
Ca
P
O
Zn
Cu
Pb
Ca
0 1 2 3 4 5 6 7 8 9 10
keV

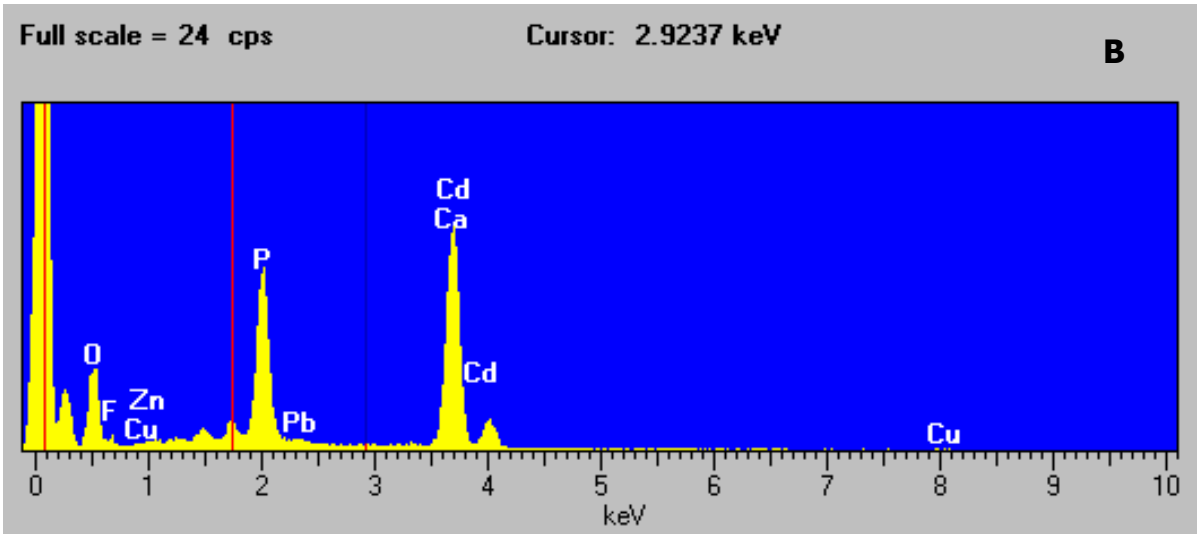
Full scale = 24 cps
Cursor: 2.9237 keV
B
Cd
Ca
P
O
F
Zn
Cu
Pb
Cd
Cu
0 1 2 3 4 5 6 7 8 9 10
keV

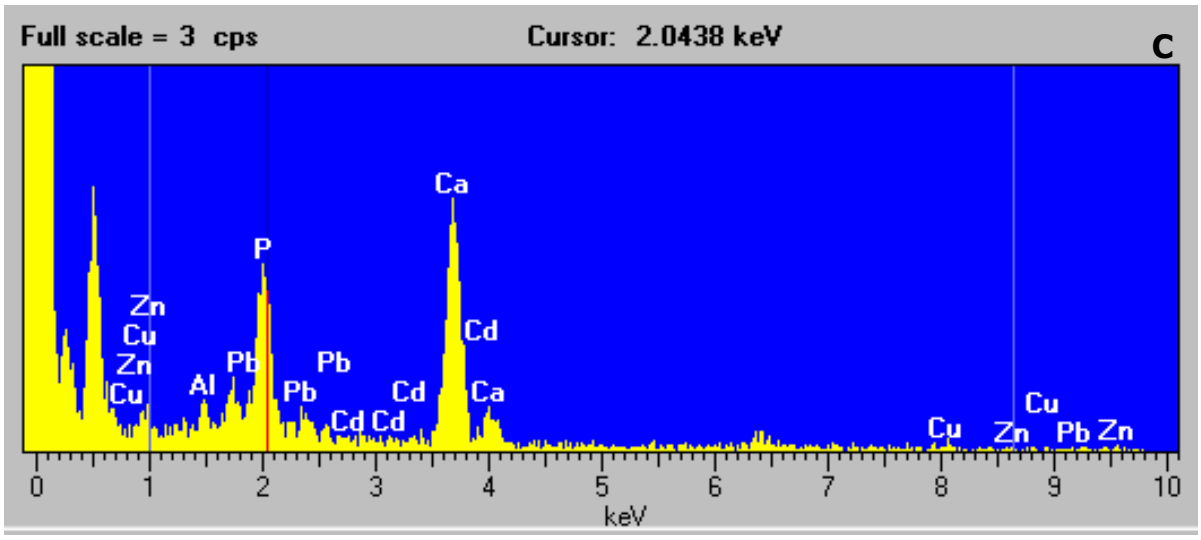
Full scale = 3 cps
Cursor: 2.0438 keV
C
Ca
P
Zn
Cu
Zn
Cu
Al
Pb
Pb
Pb
Cd
Cd
Cd
Ca
Cu
Cu
Zn
Pb
Zn
0 1 2 3 4 5 6 7 8 9 10
keV

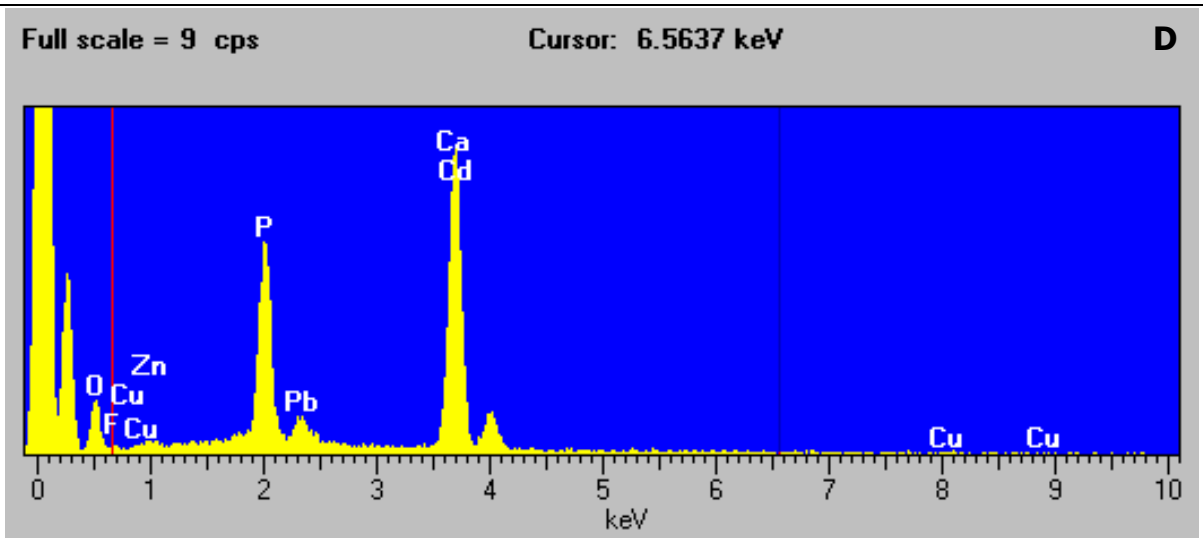

Fig. 4: EDS spectra of the SEM micrographs in Fig. 3. - Fig. 4:Spettri EDS delle immagini al SEM di Fig. 3.

6.1.3 AFM analyses

Assuming that any kind of sorption mechanisms have taken place at a scale invisible to the previous techniques, the solid materials were analyzed through AFM (Atomic Force Microscope).

The analyzed samples are generally of the higher amount for all the four interaction times. Each sample shows spherical particles (Fig. 5 A, B, C and D) with an average diameter of about of about 80 - 200 nm (Fig. 6 A, B, C and D). The AFM images show no different features from the original HA (Fig. 4b in materials), neither from blank samples (Fig. 9 A and B in single-metal system) and nor from each multi-metal system.

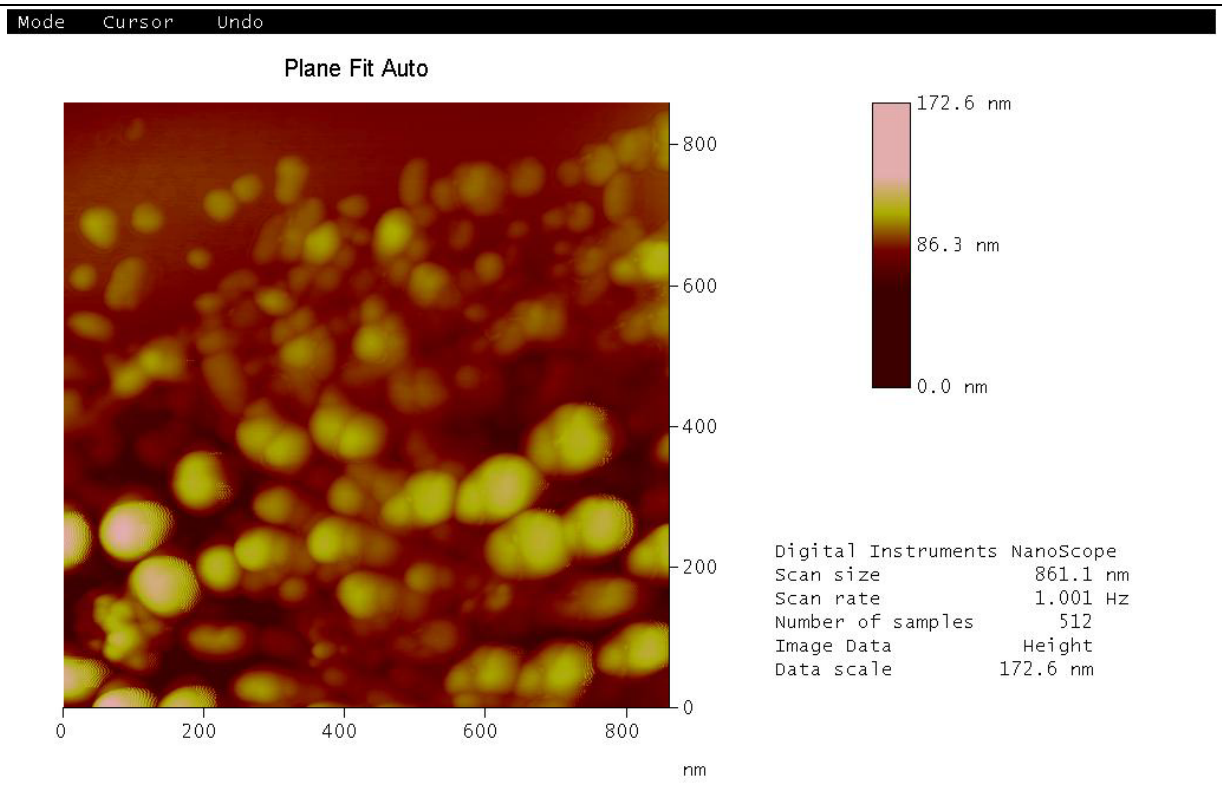
Mode Cursor Undo
Plane Fit Auto
800
600
400
200
0
0
200
400
600
800
nm
172.6 nm
86.3 nm
0.0 nm
Digital Instruments NanoScope
Scan size 861.1 nm
Scan rate 1.001 Hz
Number of samples 512
Image Data Height
Data scale 172.6 nm
XY

A

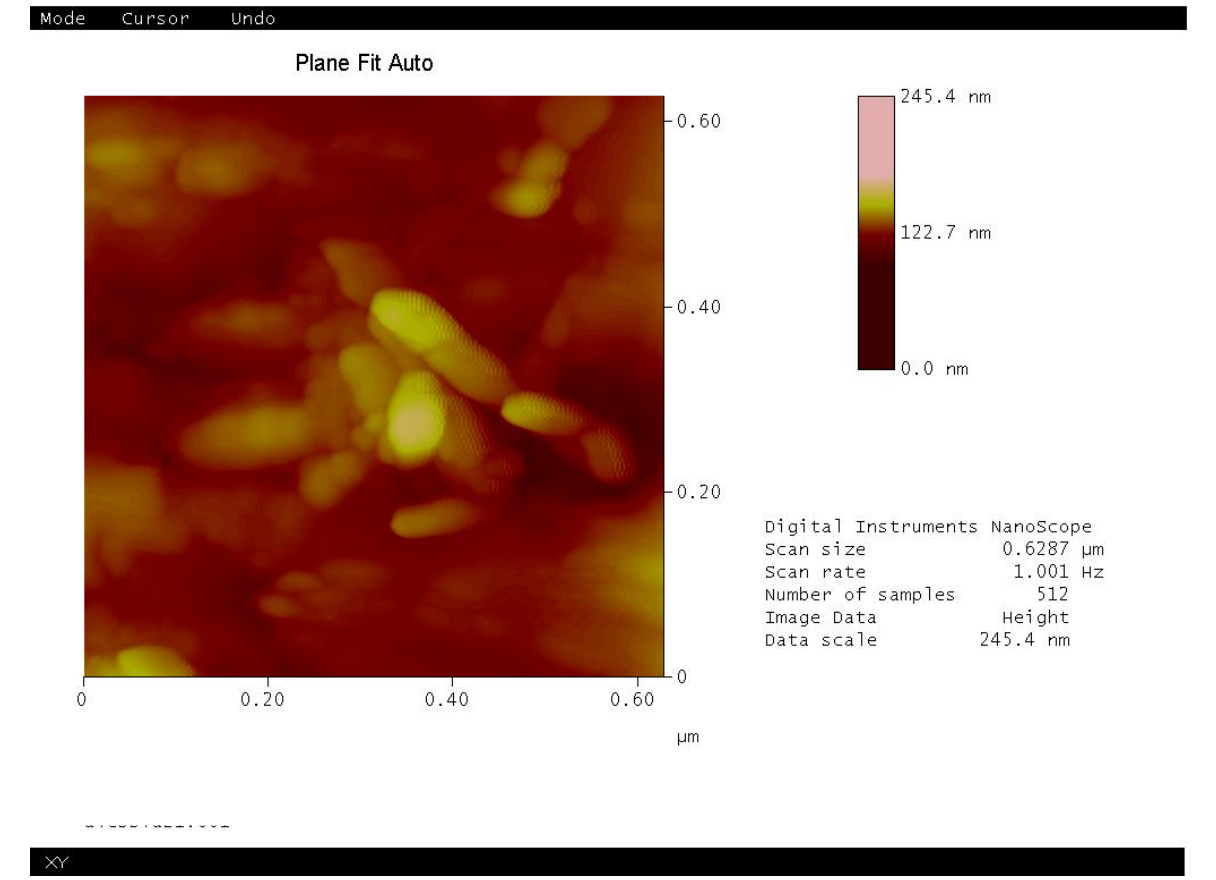
Mode Cursor Undo
Plane Fit Auto
0.60
0.40
0.20
0
0
0.20
0.40
0.60
µm
245.4 nm
122.7 nm
0.0 nm
Digital Instruments NanoScope
Scan size 0.6287 µm
Scan rate 1.001 Hz
Number of samples 512
Image Data Height
Data scale 245.4 nm
XY

B

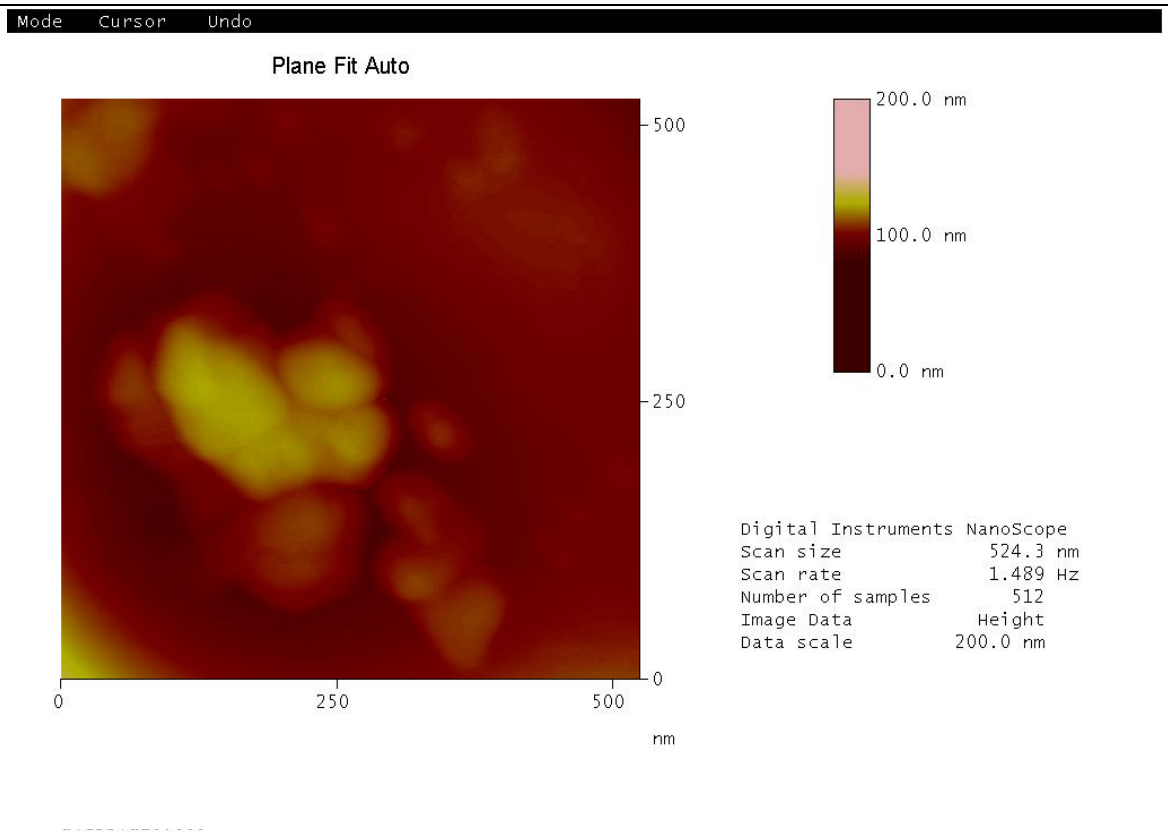
Mode Cursor Undo
Plane Fit Auto
500
250
0
0
250
500
nm
200.0 nm
100.0 nm
0.0 nm
Digital Instruments NanoScope
Scan size 524.3 nm
Scan rate 1.489 Hz
Number of samples 512
Image Data Height
Data scale 200.0 nm

C

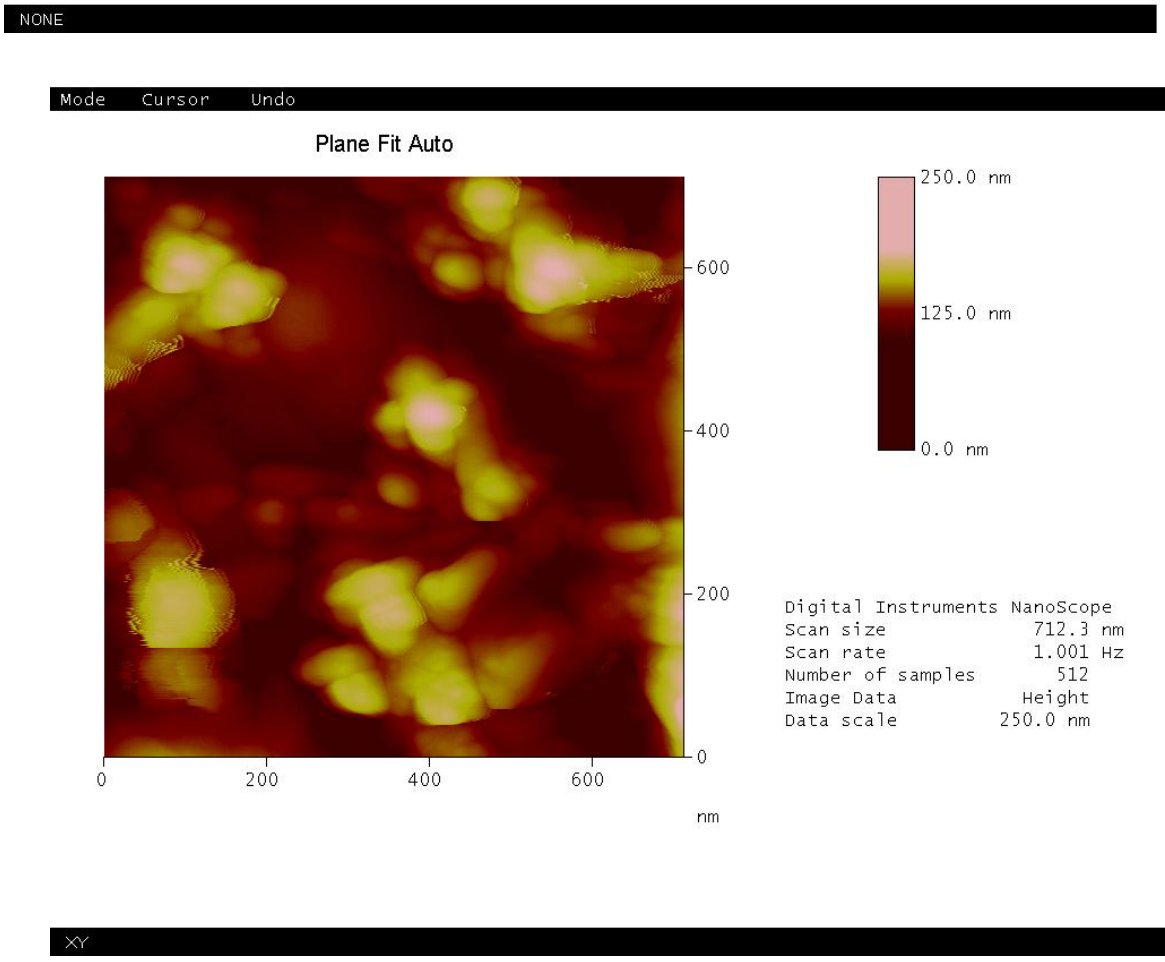
NONE
Mode Cursor Undo
Plane Fit Auto
600
400
200
0
0
200
400
600
nm
250.0 nm
125.0 nm
0.0 nm
Digital Instruments NanoScope
Scan size 712.3 nm
Scan rate 1.001 Hz
Number of samples 512
Image Data Height
Data scale 250.0 nm

D

XY

Fig. 5: AFM images of the solid material after the interaction with HA. A: Cd = 100 mgl/L, Cu, Pb and Zn = 500 mg/L, t = 2h; B: Cu = 100 mg/L, Cd, Pb and Zn = 500 mg/L, t = 2h; C: Cd, Cu, Pb and Zn = 10 mg/L, t = 24h; D: Zn = 100 mg/L, Cd, Cu and Pb = 500 mg/L t= 48h. – Fig. 5 Immagini AFM dei materiali solidi dopo l'interazione con l'HA. A: Cd = 100 mgl/L, Cu, Pb and Zn = 500 mg/L, t = 2h; B: Cu = 100 mg/L, Cd, Pb and Zn = 500 mg/L, t = 2h; C: Cd, Cu, Pb and Zn = 10 mg/L, t = 24h; D: Zn = 100 mg/L, Cd, Cu and Pb = 500 mg/L t= 48h.

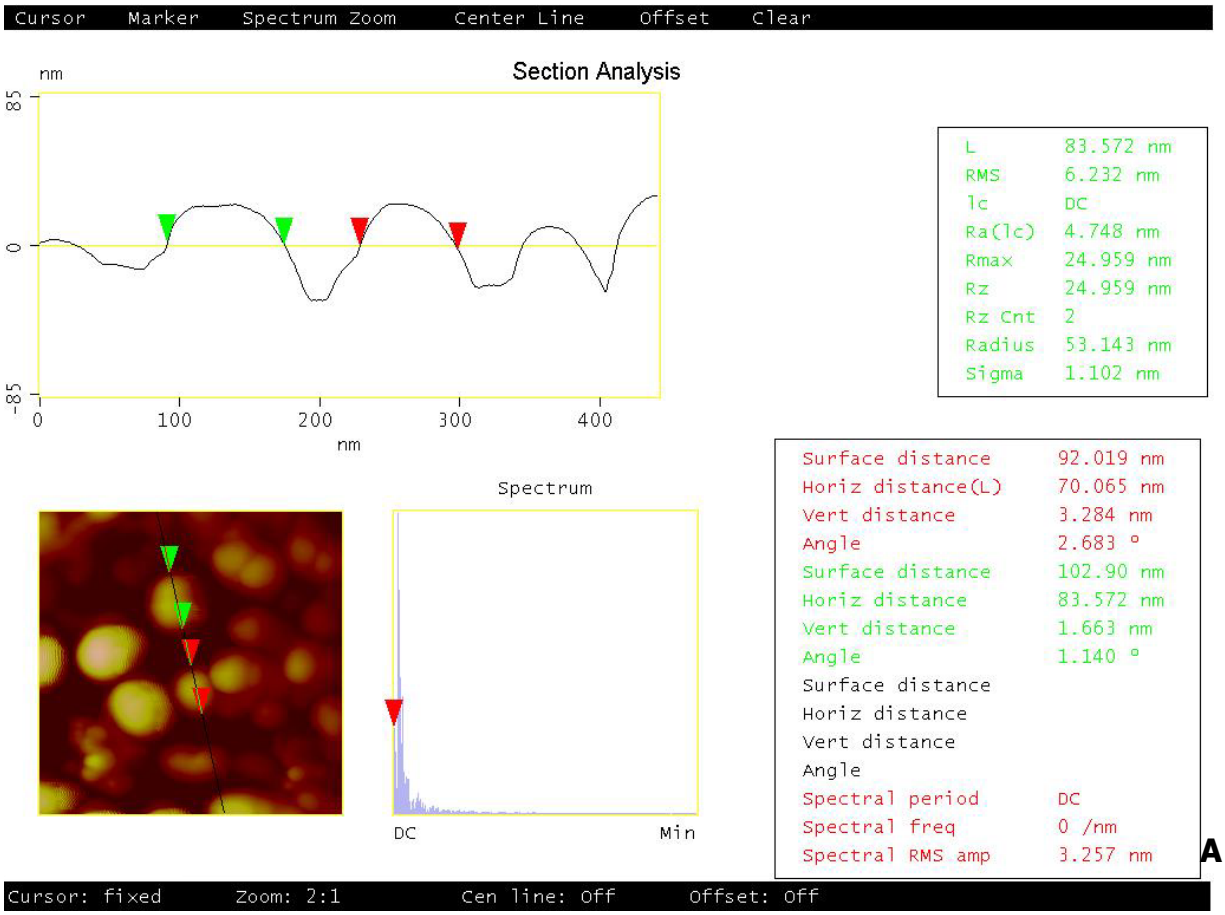

A

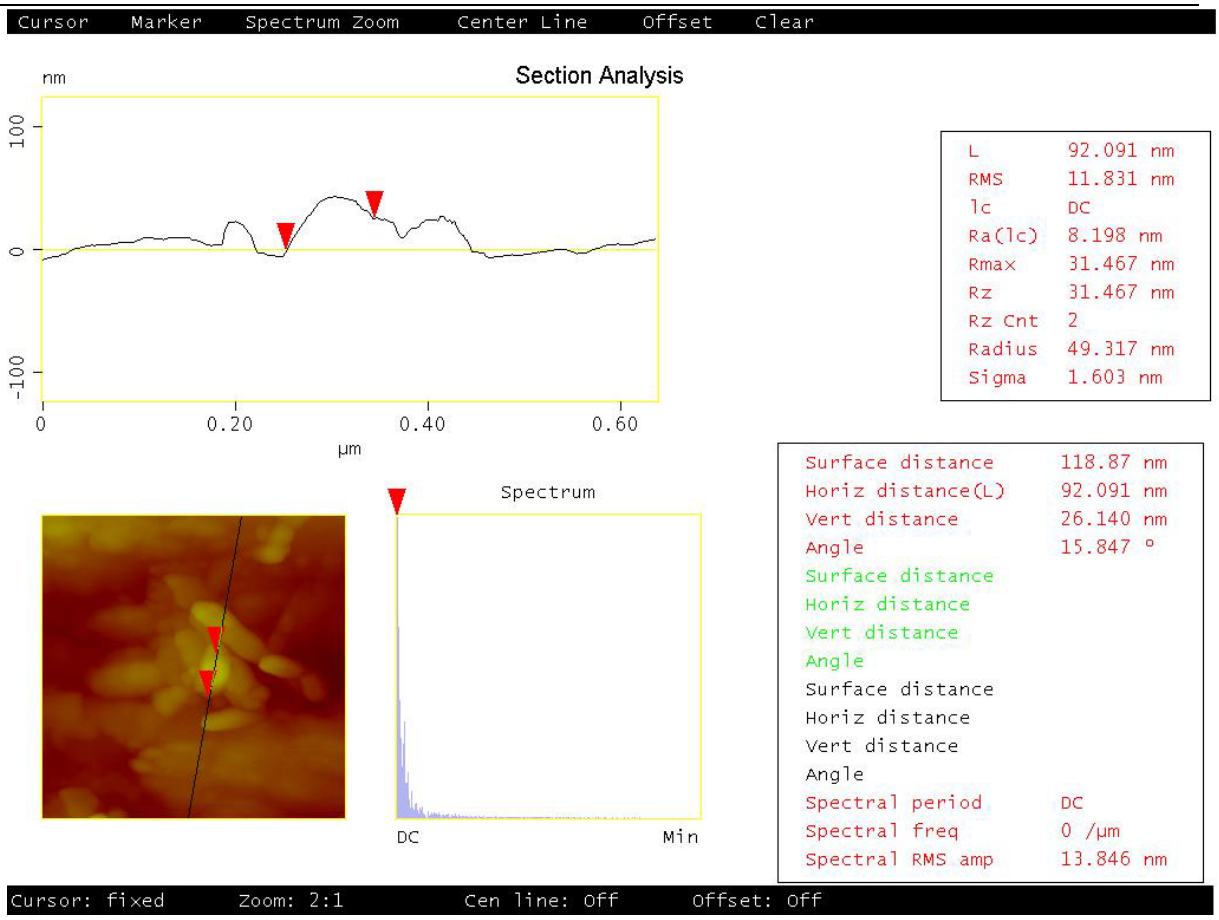
Cursor Marker Spectrum Zoom Center Line Offset Clear
Section Analysis
nm
100
0
-100
0
0.20
0.40
0.60
µm
L 92.091 nm
RMS 11.831 nm
lc DC
Ra(lc) 8.198 nm
Rmax 31.467 nm
Rz 31.467 nm
Rz Cnt 2
Radius 49.317 nm
Sigma 1.603 nm
Spectrum
DC
Min
Surface distance 118.87 nm
Horiz distance(L) 92.091 nm
Vert distance 26.140 nm
Angle 15.847 °
Surface distance
Horiz distance
Vert distance
Angle
Surface distance
Horiz distance
Vert distance
Angle
Spectral period DC
Spectral freq 0 /µm
Spectral RMS amp 13.846 nm
Cursor: fixed Zoom: 2:1 Cen line: Off Offset: Off

B

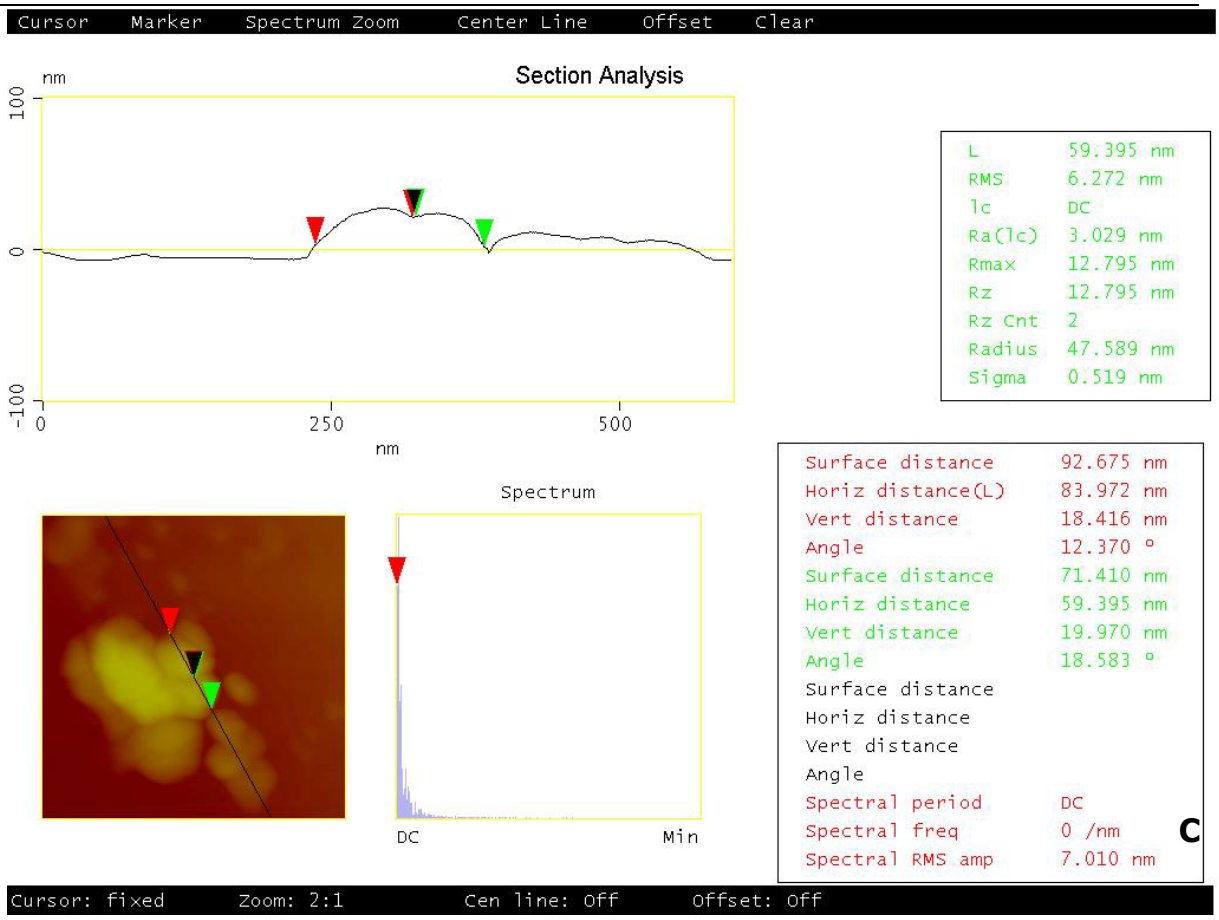
Cursor Marker Spectrum Zoom Center Line Offset Clear
Section Analysis
nm
100
0
-100
0
250
500
nm
L 59.395 nm
RMS 6.272 nm
lc DC
Ra(lc) 3.029 nm
Rmax 12.795 nm
Rz 12.795 nm
Rz Cnt 2
Radius 47.589 nm
Sigma 0.519 nm
Spectrum
DC
Min
Surface distance 92.675 nm
Horiz distance(L) 83.972 nm
Vert distance 18.416 nm
Angle 12.370 °
Surface distance 71.410 nm
Horiz distance 59.395 nm
Vert distance 19.970 nm
Angle 18.583 °
Surface distance
Horiz distance
Vert distance
Angle
Spectral period DC
Spectral freq 0 /nm
Spectral RMS amp 7.010 nm
C
Cursor: fixed Zoom: 2:1 Cen line: Off Offset: Off

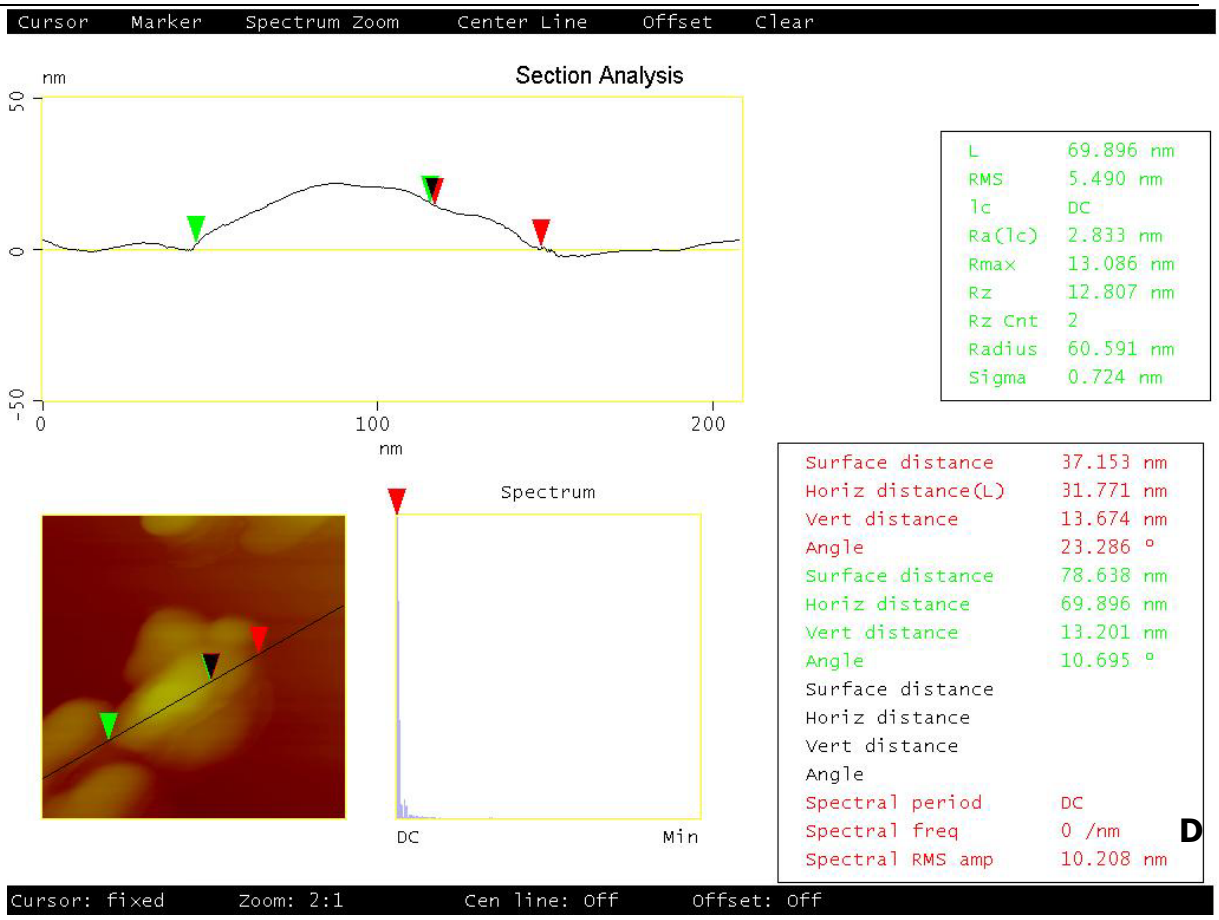

Fig. 6: AFM images showing the dimension of the particles of Fig. 5. – Fig. 6 Immagini AFM che mostrano le dimensioni delle particelle di Fig. 5.6.1.4

6.1.4 ICP-AES analyses

As in single-metal systems also in multi-metal, after the interaction with HA heavy metal concentrations are reduced under the values of the Italian law (D.L 477/91).The immobilization seems to achieve its maximum after contact time of 24h and 48h,

The proportions of blocked heavy metals per unit mass of HA with constant Cd concentration are listed in Table 2, whereas the immobilization efficiency is shown in Fig. 7. Each heavy metal is well immobilized and the initial concentration seems to influence the immobilization, on the other hand time seems to play an important role, generally t = 24 is the suitable time for the highest immobilization. From the experimental data, the proportion of the heavy metal immobilized mass varies in the order Pb > Zn > Cu > Cd and it seems the internal competition doesn't influence this system.

pH has been measured before and after the interaction. The average pH values ranges from 4 to 6 with an increase of the final values of 0.5 units with respect to the initial values.

Cd = 10 mg/L	Cu = 100 mg/L	Pb = 100 mg/L	Zn = 100 mg/L
8.718	93.354	96.134	88.087
8.965	93.249	95.936	87.475
9.066	98.297	99.652	87.948
9.023	93.559	96.276	87.369
Cd = 10 mg/L	Cu = 500 mg/L	Pb = 500 mg/L	Zn = 500 mg/L
9.155	478.617	474.467	468.141
9.344	483.092	482.323	471.378
9.353	483.842	485.437	471.282
9.354	485.810	487.079	470.763
Cd = 100 mg/L	Cu = 10 mg/L	Pb = 10 mg/L	Zn = 10 mg/L
91.149	9.497	9.650	8.328
90.269	9.421	9.721	8.585
92.225	9.904	9.875	9.280
91.725	9.857	9.896	8.888
Cd = 100 mg/L	Cu = 500 mg/L	Pb = 500 mg/L	Zn = 500 mg/L
94.827	481.468	478.599	469.275
95.195	480.886	479.206	470.425
95.520	483.380	484.017	473.182
19.279	316.383	239.920	497.235
Cd = 500 mg/L	Cu = 10 mg/L	Pb = 10 mg/L	Zn = 10 mg/L
477.704	9.579	9.732	9.015
476.849	9.667	9.674	9.374
476.696	9.932	9.971	9.453
477.939	9.860	9.953	9.467
Cd = 500 mg/L	Cu = 100 mg/L	Pb = 100 mg/L	Zn = 100 mg/L
475.766	97.024	98.294	94.286
475.495	98.327	99.301	99.649
475.928	97.057	97.782	94.273
475.707	98.567	99.186	94.231

Table 2: Proportions of blocked heavy metals per unit mass of HA (mg/g) for the multi-metal system when Cd is constant. – Tabella 2: Entità dell'immobilizzazione dei metalli per unità di massa di HA (mg/g) per il sistema multi-metal con concentrazione del Cd costante.

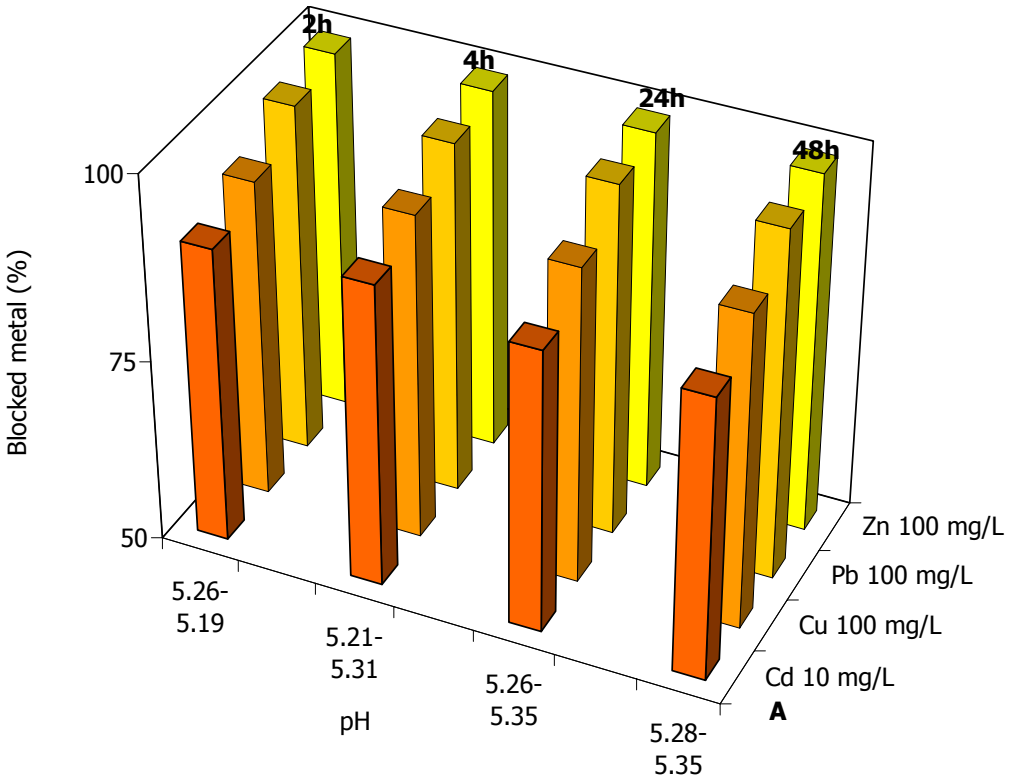
2h
4h
24h
48h
100
75
50
Blocked metal (%)
5.26-
5.19
5.21-
5.31
5.26-
5.35
5.28-
5.35
pH
Zn 100 mg/L
Pb 100 mg/L
Cu 100 mg/L
Cd 10 mg/L
A

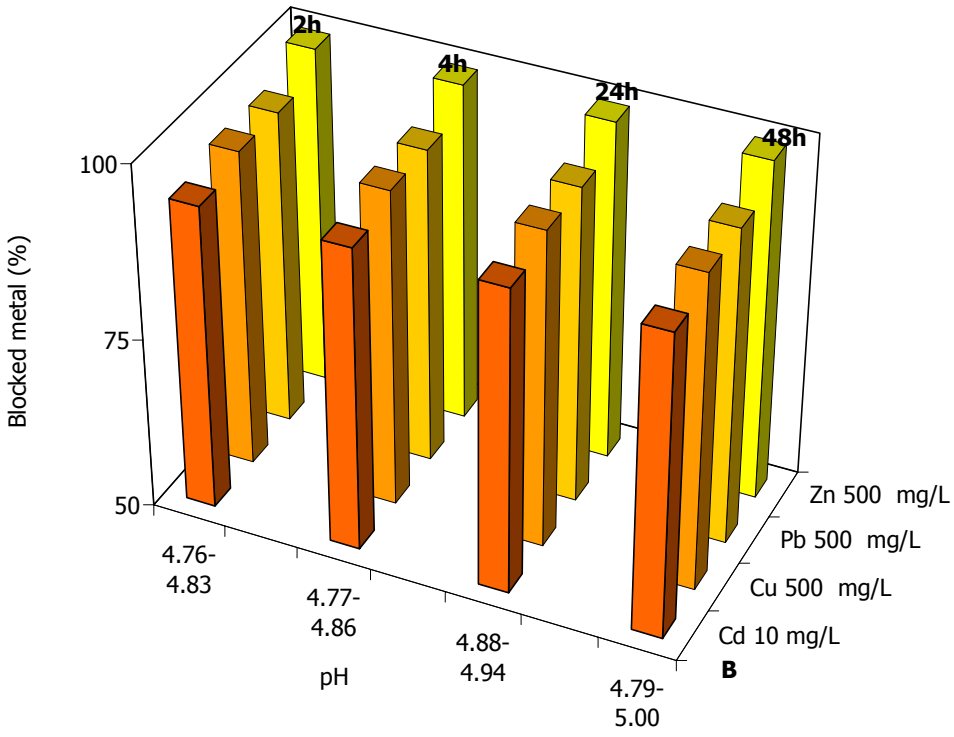
2h
4h
24h
48h
100
75
50
Blocked metal (%)
4.76-
4.83
4.77-
4.86
4.88-
4.94
4.79-
5.00
pH
Zn 500 mg/L
Pb 500 mg/L
Cu 500 mg/L
Cd 10 mg/L
B

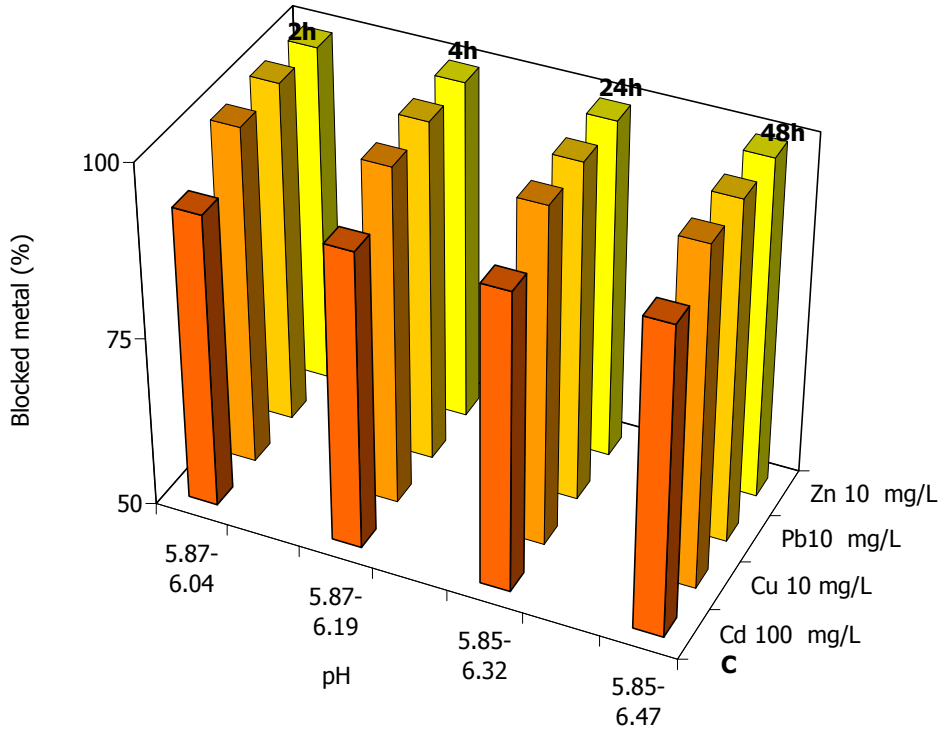
2h
4h
24h
48h
100
75
50
Blocked metal (%)
5.87-
6.04
5.87-
6.19
5.85-
6.32
5.85-
6.47
pH
Zn 10 mg/L
Pb10 mg/L
Cu 10 mg/L
Cd 100 mg/L
C

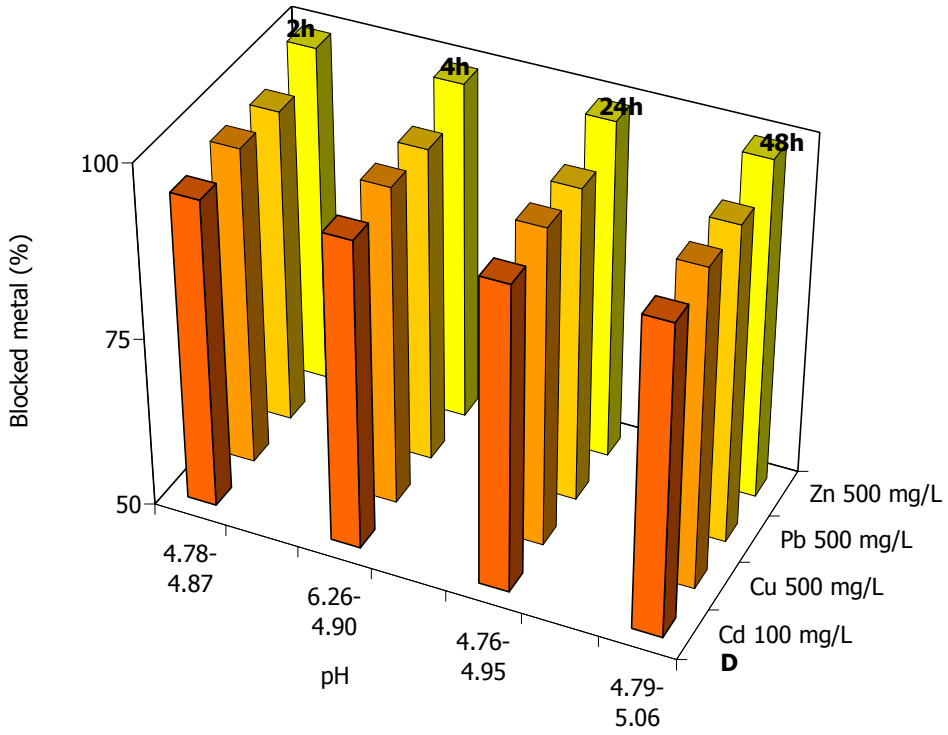
2h
4h
24h
48h
100
75
50
Blocked metal (%)
4.78-
4.87
6.26-
4.90
4.76-
4.95
4.79-
5.06
pH
Zn 500 mg/L
Pb 500 mg/L
Cu 500 mg/L
Cd 100 mg/L
D

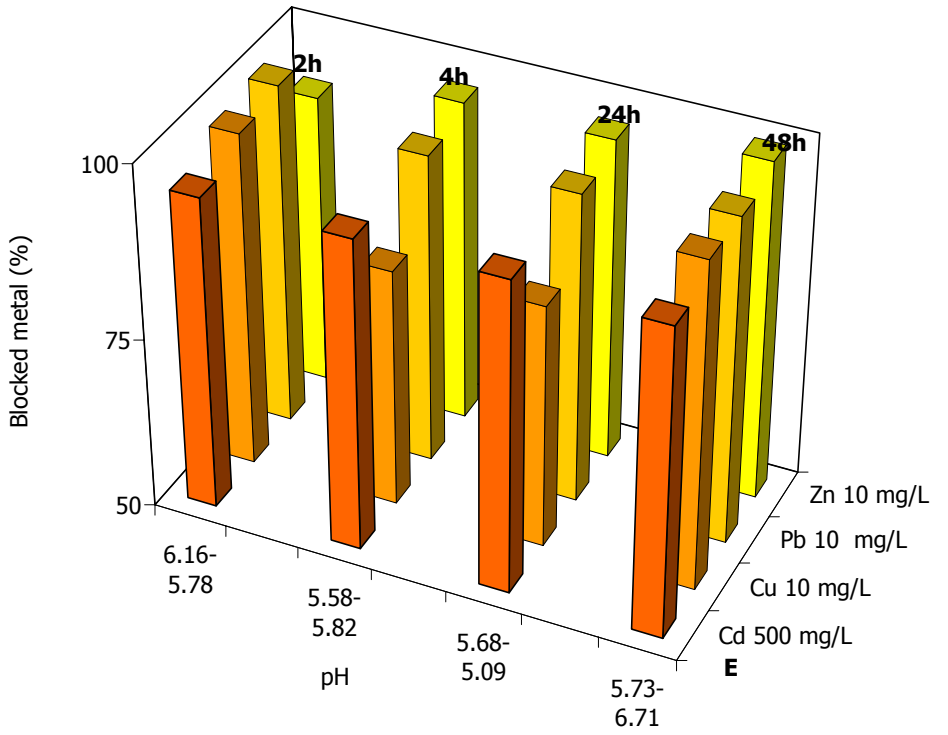

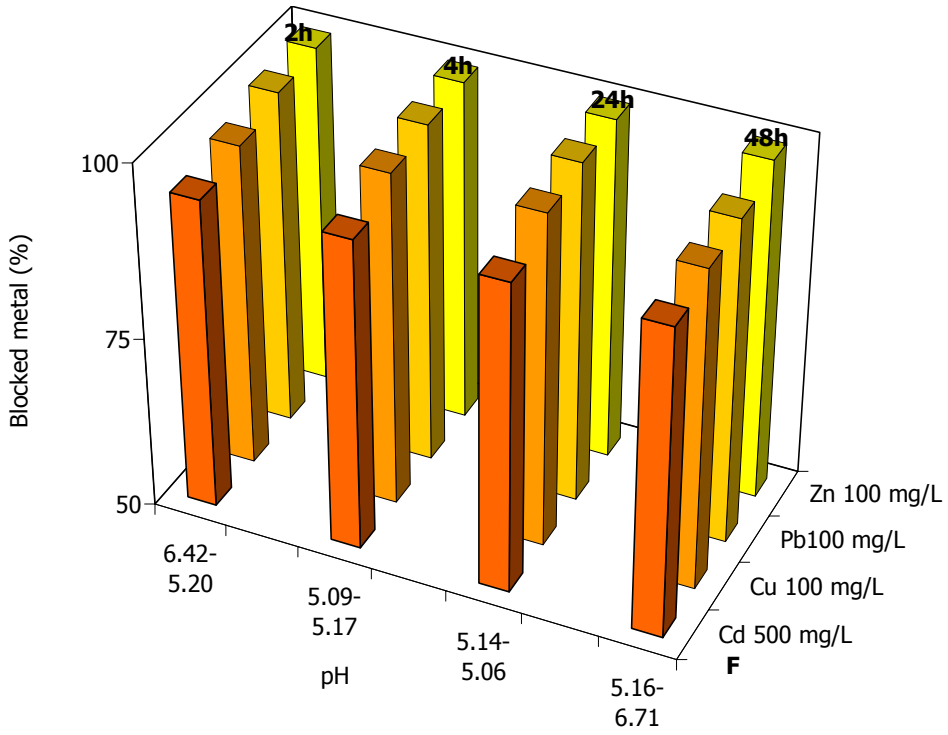

Fig. 7: Variation of the amount of blocked metal with time for the mass of HA (0.2 g) in the multi-metal system where Cd is constant. Initial and final pH values are reported. – Fig. 7: Variazione delle percentuali dei metalli immobilizzati in funzione del tempo di interazione per la quantità di HA (0.2 g) nel sistema multi-metal in cui Cd è l'elemento costante. Sono riportati i valori iniziali e finali del pH.

The molar ratio (Q_S) (Table 3) values are always < 1 suggesting the precipitation of a new phosphate phase, except for Cu at 100 mg/L and 500 mg/L at low Cd concentration, Q_S values are > 1 and = 1. Respectively, the former values suggest an adsorption mechanism and the latter an ion exchange mechanism.

Cd = 10 mg/L	Cu = 100 mg/L	Pb = 100 mg/L	Zn = 100 mg/L
0.03	3.23	0.35	0.43
0.03	3.71	0.41	0.51
0.03	3.11	0.28	0.46
0.03	3.27	0.33	0.48
Cd = 10 mg/L	Cu = 500 mg/L	Pb = 500 mg/L	Zn = 500 mg/L
0.02	1.39	0.45	0.20
0.02	1.23	0.39	0.18
0.02	1.13	0.34	0.16
0.02	1.11	0.34	0.16
Cd = 100 mg/L	Cu = 10 mg/L	Pb = 10 mg/L	Zn = 10 mg/L
0.18	0.003	0.0002	0.002
0.10	0.002	0.0003	0.001
0.14	0.003	0.0007	0.002
0.06	0.001	0.0001	0.001
Cd = 100 mg/L	Cu = 500 mg/L	Pb = 500 mg/L	Zn = 500 mg/L
0.14	0.90	0.31	0.14
0.18	1.17	0.41	0.18
0.12	0.71	0.25	0.11
0.03	0.17	0.06	0.03
Cd = 500 mg/L	Cu = 10 mg/L	Pb = 10 mg/L	Zn = 10 mg/L
0.03	0.0003	0.00002	0.0015
0.75	0.09	0.01	0.02
0.67	0.08	0.01	0.02
0.60	0.01	0.00	0.00
Cd = 500 mg/L	Cu = 100 mg/L	Pb = 100 mg/L	Zn = 100 mg/L
0.86	0.20	0.03	0.03
0.47	0.06	0.01	0.01
0.58	0.07	0.01	0.01
0.58	0.14	0.03	0.02

Table 3: Q_S values for the multi - metal systems when Cd has a constant concentration. Tabella 3: Valori di Q_S per i sistemi multi-metal nei quali la concentrazione di Cd è stata mantenuta costante.

Sorption isotherms (Fig. 8 A, B, C and D) are H type for t = 2h, meaning a precipitation mechanism, likely a non crystalline phases, as XRD and AFM analyses did not detect any new crystalline phase. For the other three times the isotherms are always the type L and subtype 2. The shapes of the isotherms point as sorption mechanism the adsorption and surface precipitation.

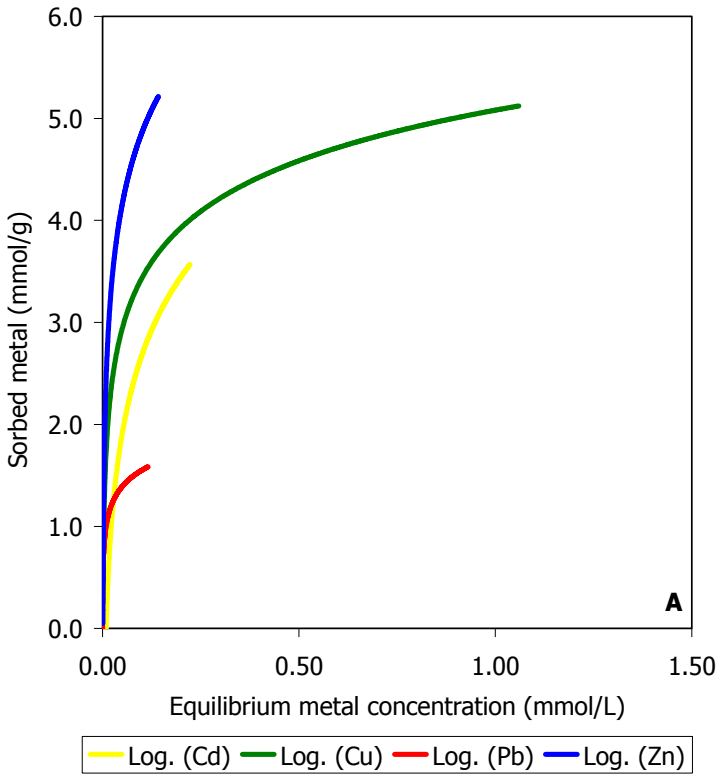
6.0
5.0
4.0
3.0
2.0
1.0
0.0
Sorbed metal (mmol/g)
0.00
0.50
1.00
1.50
Equilibrium metal concentration (mmol/L)
A
Log. (Cd)
Log. (Cu)
Log. (Pb)
Log. (Zn)

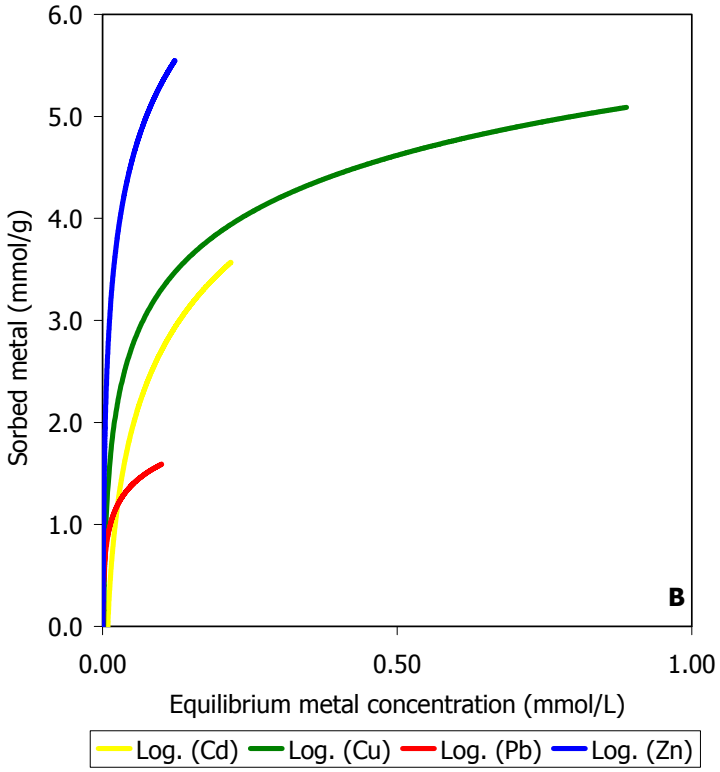
6.0
5.0
4.0
3.0
2.0
1.0
0.0
Sorbed metal (mmol/g)
0.00
0.50
1.00
Equilibrium metal concentration (mmol/L)
B
Log. (Cd)
Log. (Cu)
Log. (Pb)
Log. (Zn)

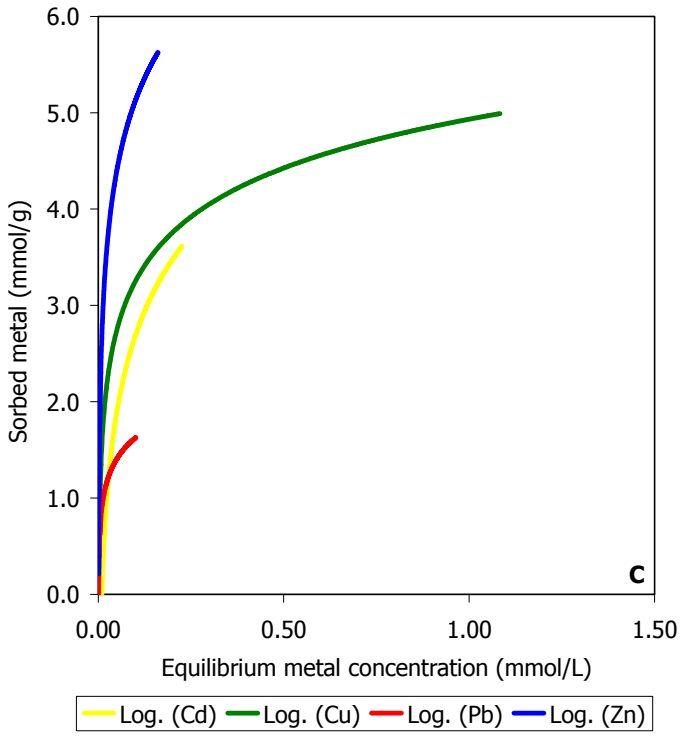

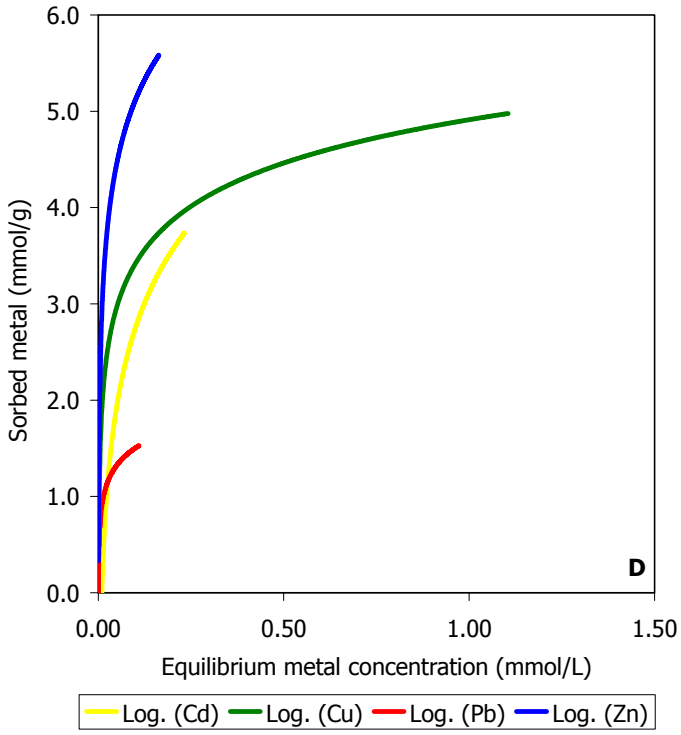

Fig. 8: Sorption isotherms for the multi-metal system where Cd is constant for the four contact times (2h, 4h, 24h and 48h) and vs. 0.2 g HA. Relation between the metal sorbed (mmol/g) and the final concentration (mmol/L) in solution. A: t = 2h; B: t = 4h; C: t = 24h and D: t = 48h. – Fig. 8: Curve isotermiche per il sistema multi-metal in cui Cd è costante per i quattro tempi di contatto (2h, 4h, 24h and

48h) e vs. 0.2 g di HA. Relazione tra il metallo assorbito (mmol/g) e la concentrazione finale (mmol/L) in soluzione. A: t = 2h; B: t = 4h; C: t = 24h and D: t = 48h.

At the equilibrium Ca concentration is not proportional to the amount of the sorbed heavy metal (Fig. 9 A, B, C, D, E and F), the average Ca is about 0.3-0.4 mmol/L and the four metals show a concentration about 0 – 8 mmol/g, this behaviour suggests a non stoichiometric dissolution so that the most probable sorption mechanism is the adsorption.

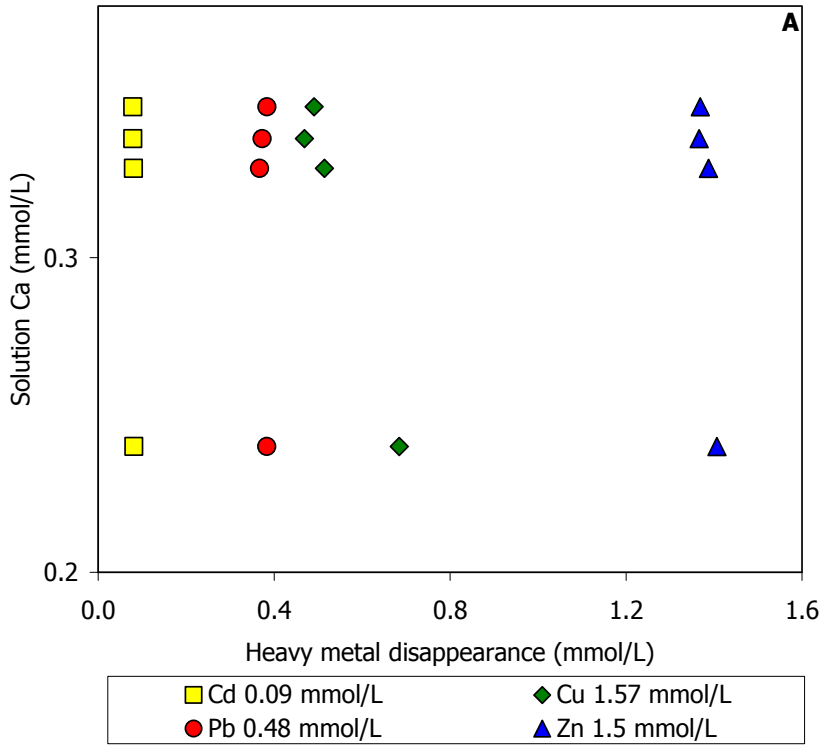

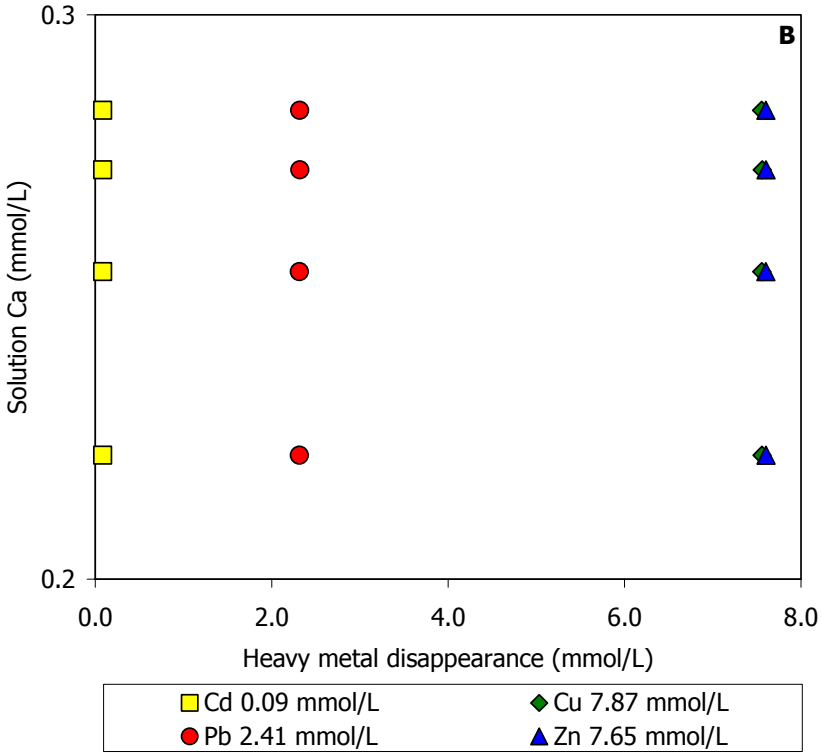
B
0.3
0.2
Solution Ca (mmol/L)
0.0
2.0
4.0
6.0
8.0
Heavy metal disappearance (mmol/L)
Cd 0.09 mmol/L
Cu 7.87 mmol/L
Pb 2.41 mmol/L
Zn 7.65 mmol/L

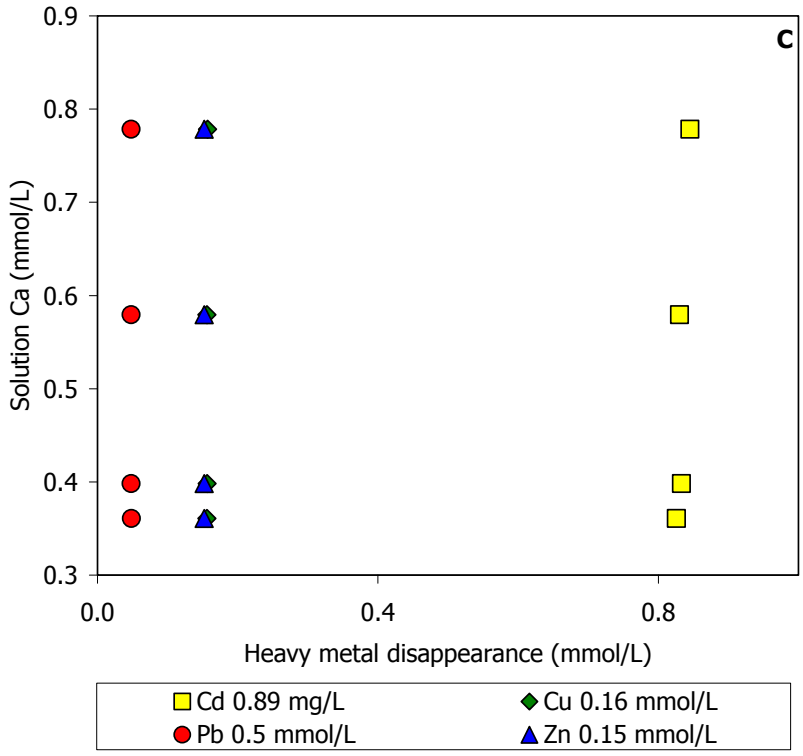
C
0.9
0.8
0.7
0.6
0.5
0.4
0.3
Solution Ca (mmol/L)
0.0
0.4
0.8
Heavy metal disappearance (mmol/L)
Cd 0.89 mg/L
Cu 0.16 mmol/L
Pb 0.5 mmol/L
Zn 0.15 mmol/L

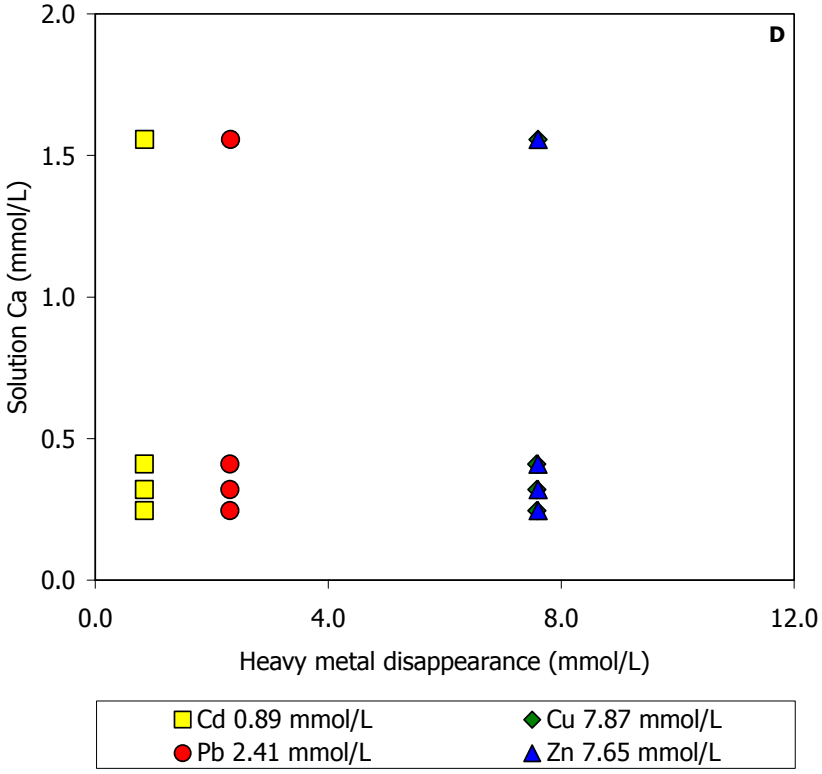
D
2.0
1.5
1.0
0.5
0.0
Solution Ca (mmol/L)
0.0
4.0
8.0
12.0
Heavy metal disappearance (mmol/L)
Cd 0.89 mmol/L
Cu 7.87 mmol/L
Pb 2.41 mmol/L
Zn 7.65 mmol/L

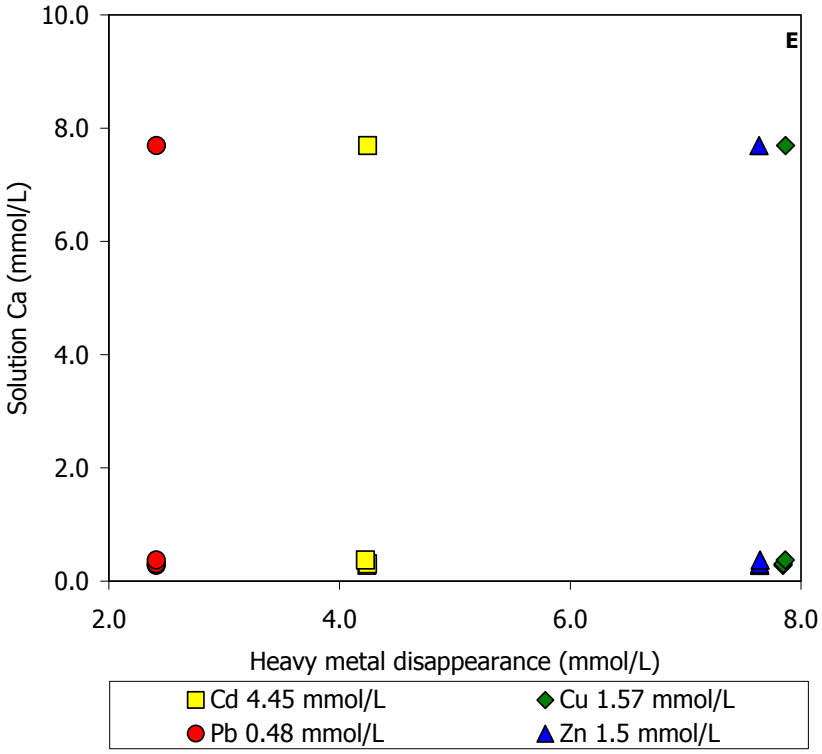
E
10.0
8.0
6.0
4.0
2.0
0.0
Solution Ca (mmol/L)
2.0
4.0
6.0
8.0
Heavy metal disappearance (mmol/L)
Cd 4.45 mmol/L
Cu 1.57 mmol/L
Pb 0.48 mmol/L
Zn 1.5 mmol/L

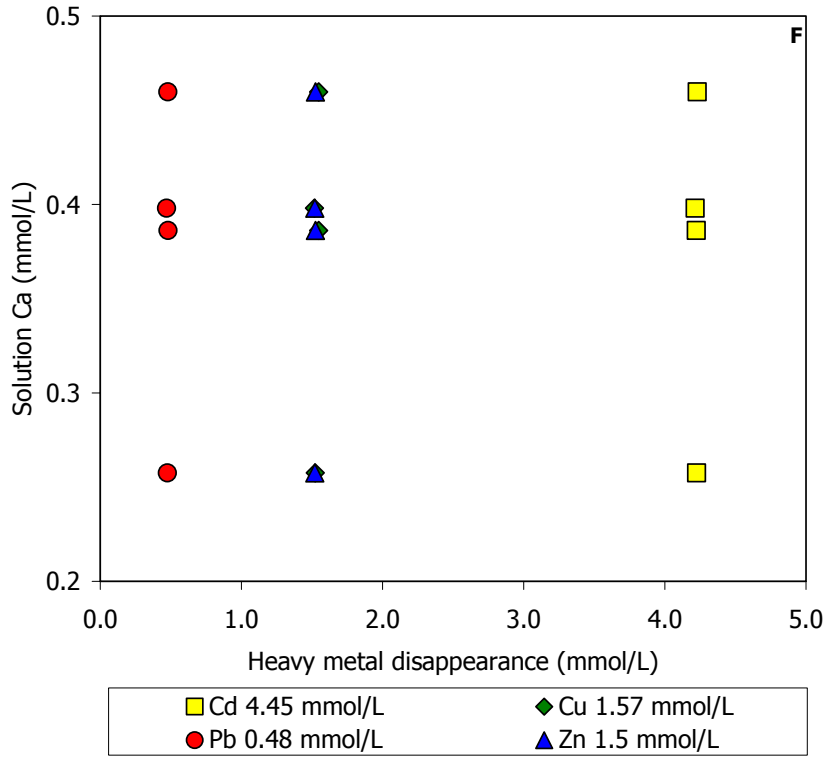

Fig. 9: Relation between Ca in solution (mmol/L) and the amount of heavy metals disappeared (mmol/L) sorbed on HA surface at the equilibrium in a multi-metal system when Cd is constant. Each initial concentration of the multi-metal system is written in the legend. - Fig. 9: Relazione tra il quantitativo di Ca in soluzione (mmol/L) e di ciascun metallo pesante adsorbito (mmol/L) nel sistema multi-metal quando Cd è costante. La concentrazione iniziale di ogni elemento del sistema multi-metal è in leggenda.

The P amount is very low (Fig. 10 A, B, C, D, E and F), about 0 – 0.4 mmol/L, whereas the sorbed heavy metals show a concentration from 0 to 8 mmol/L, pointing a non stoichiometric dissolution as for Ca desorption at the equilibrium. The Ca and P non stoichiometric dissolution suggests as sorption mechanism the adsorption.

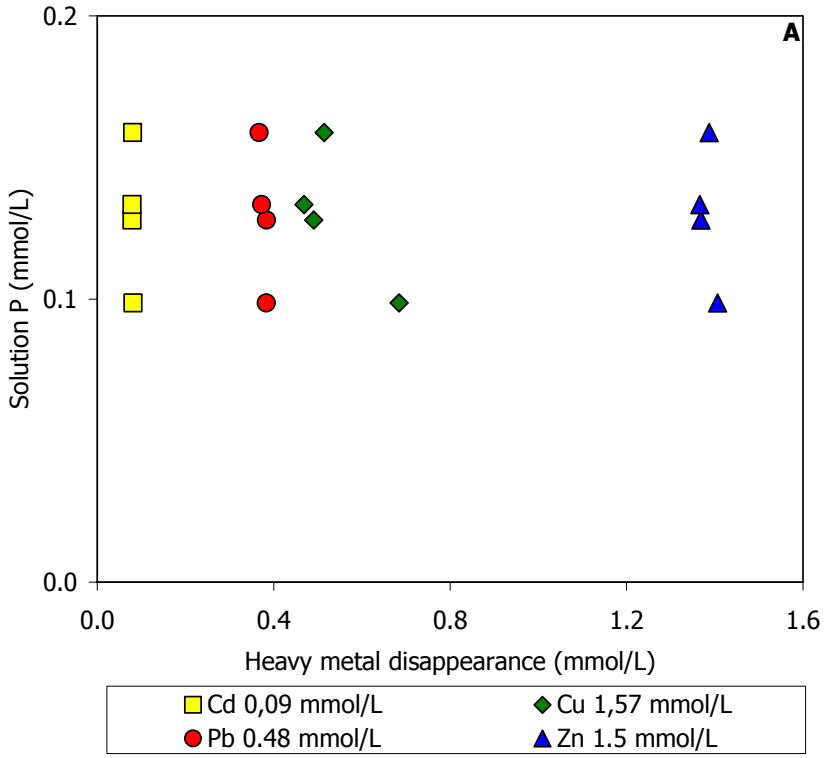
A
0.2
0.1
0.0
Solution P (mmol/L)
0.0
0.4
0.8
1.2
1.6
Heavy metal disappearance (mmol/L)
Cd 0,09 mmol/L
Cu 1,57 mmol/L
Pb 0.48 mmol/L
Zn 1.5 mmol/L

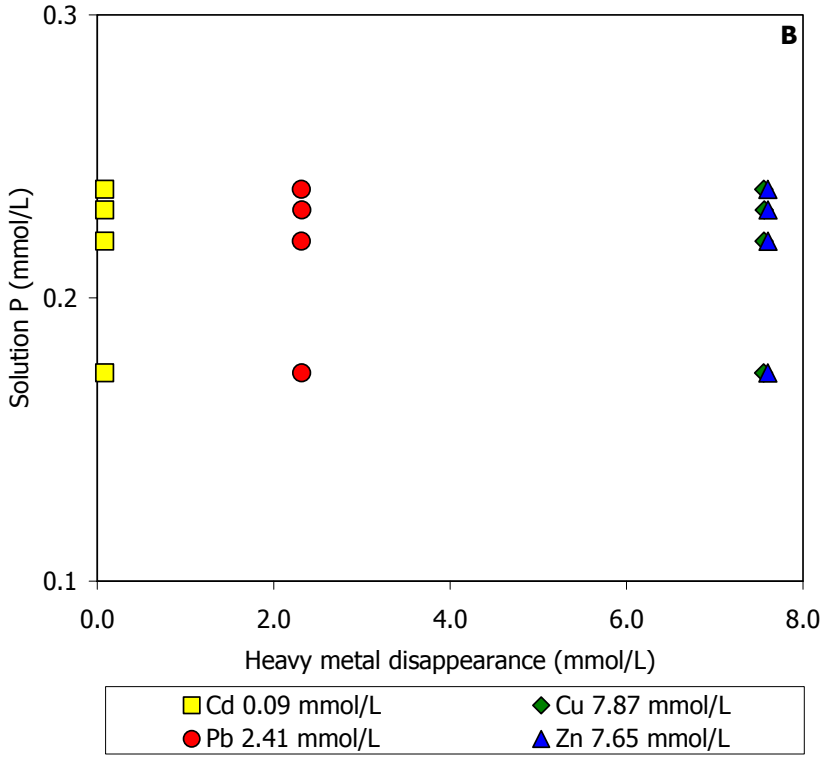
B
0.3
0.2
0.1
Solution P (mmol/L)
0.0
2.0
4.0
6.0
8.0
Heavy metal disappearance (mmol/L)
Cd 0.09 mmol/L
Cu 7.87 mmol/L
Pb 2.41 mmol/L
Zn 7.65 mmol/L

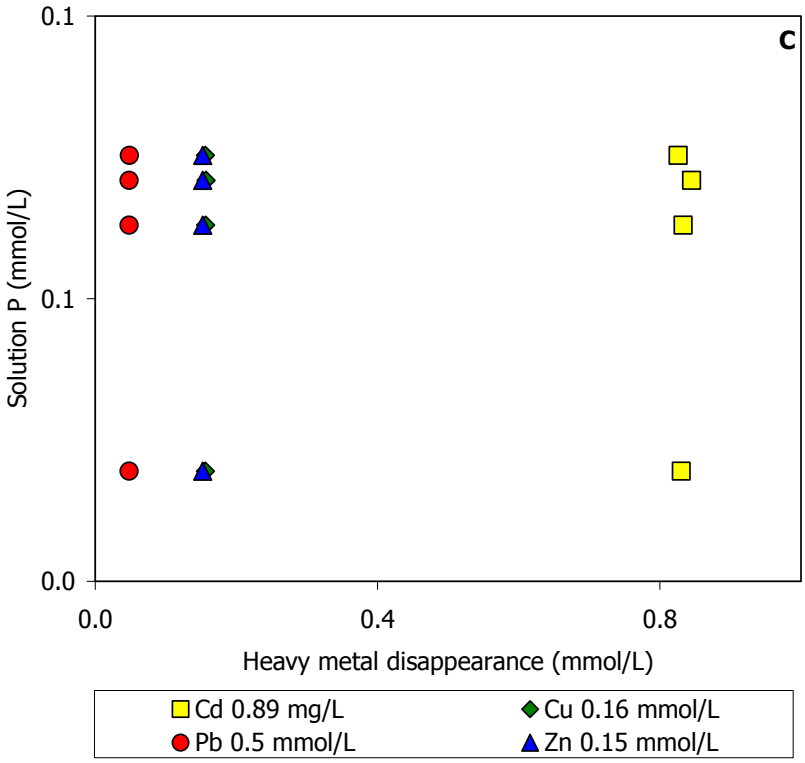
C
0.1
0.1
0.0
Solution P (mmol/L)
0.0
0.4
0.8
Heavy metal disappearance (mmol/L)
Cd 0.89 mg/L
Cu 0.16 mmol/L
Pb 0.5 mmol/L
Zn 0.15 mmol/L

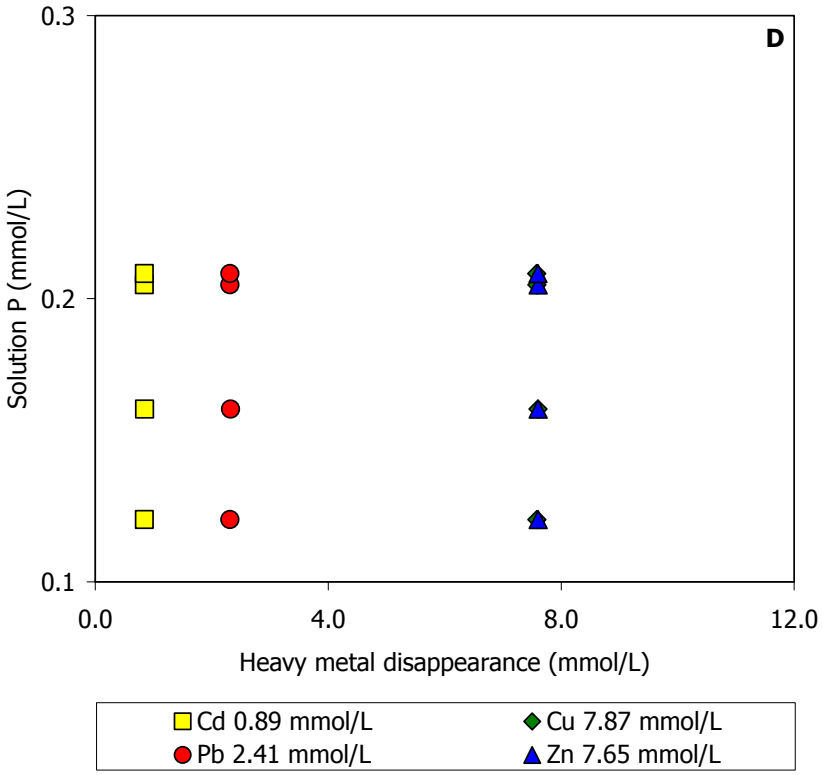
D
0.3
0.2
0.1
Solution P (mmol/L)
0.0
4.0
8.0
12.0
Heavy metal disappearance (mmol/L)
Cd 0.89 mmol/L
Cu 7.87 mmol/L
Pb 2.41 mmol/L
Zn 7.65 mmol/L

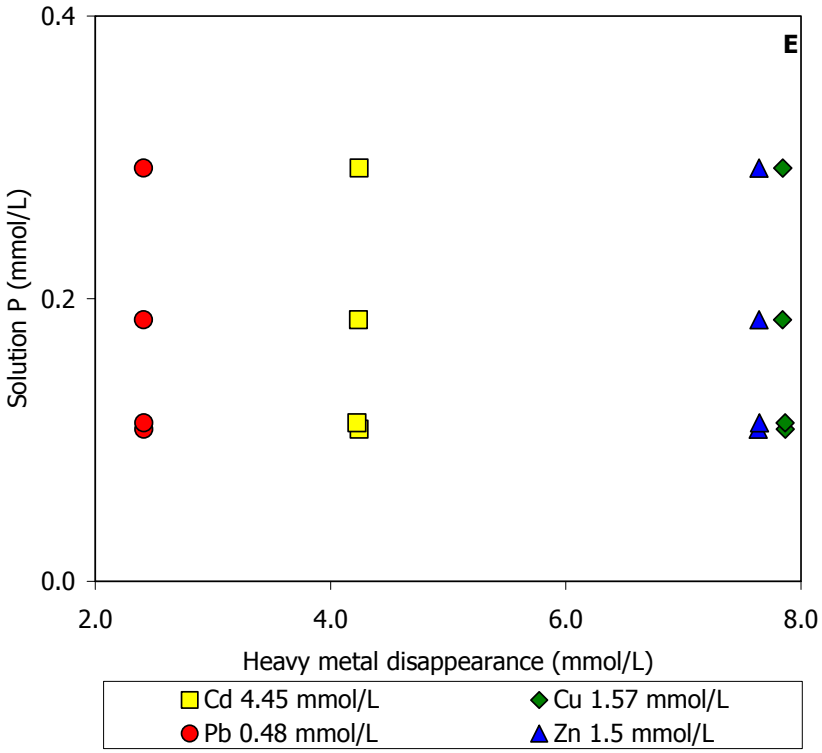

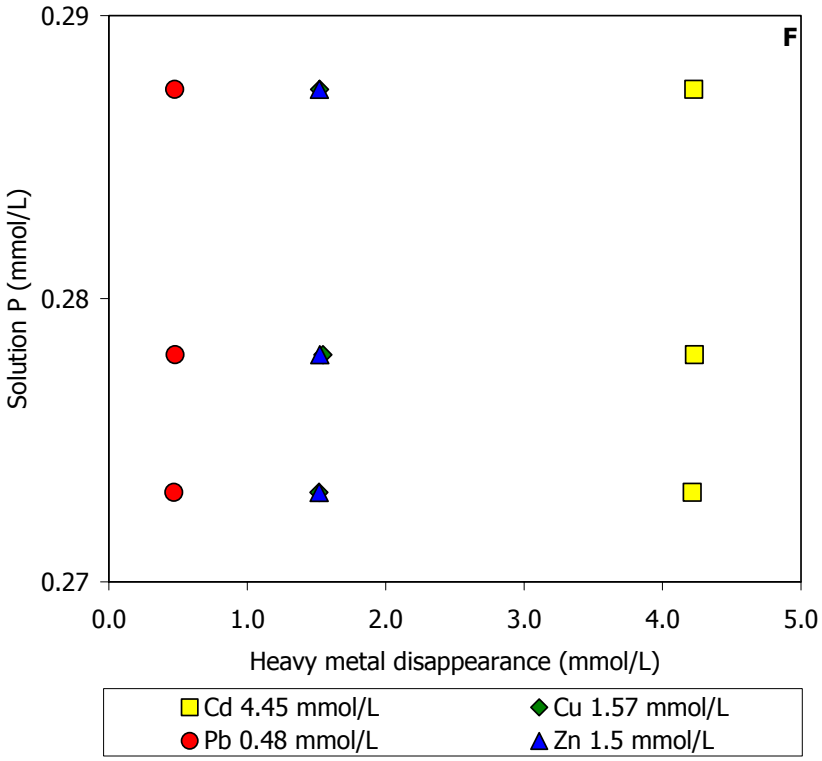

Fig. 10: Relation between P in solution (mmol/L) and the amount of disappeared heavy metals (mmol/L) sorbed on HA surface at the equilibrium in a multi-metal system when Cd is constant. Each initial concentration of the multi-metal system is written in the legend. - Fig. 10: Relazione tra il quantitativo di P in

soluzione (mmol/L) e di ciascun metallo pesante adsorbito (mmol/L) nel sistema multi-metal quando Cd è costante. La concentrazione iniziale di ogni elemento del sistema multi-metal è in leggenda.

In the multi-metal system with Cu constant the efficiency of HA in immobilizing the heavy metals in the system is listed in Table 4, all the four heavy metal are well blocked from the HA not depending on the original concentration or time (Fig. 11 A, B, C, D, E, and F). The only exception is, when Cu concentration is about 500 mg/L and the concentration of the other three metals is 10 mg/L, Cd and Pb are less immobilized in particular at 4h and 48h.

pH values are almost constant, few cases show an increase or decrease of few units. The proportions of the sorbed metal mass follow the same order as the previous system (Pb > Zn > Cu > Cd).

Cd = 100 mg/L	Cu = 10 mg/L	Pb = 100 mg/L	Zn = 100 mg/L
90.038	9.459	96.524	98.864
90.580	9.537	97.020	98.924
90.502	9.671	98.932	98.886
90.018	9.607	98.853	98.836
Cd = 500 mg/L	Cu = 10 mg/L	Pb = 500 mg/L	Zn = 500 mg/L
474.405	9.671	481.834	497.044
474.739	9.681	482.522	497.069
476.147	9.711	485.562	497.249
474.632	9.694	483.981	497.038
Cd = 10 mg/L	Cu = 100 mg/L	Pb = 10 mg/L	Zn = 10 mg/L
9.380	5.984	9.963	9.872
9.352	5.994	9.891	9.839
9.430	6.382	10.001	9.860
9.721	6.603	9.876	9.874
Cd = 500 mg/L	Cu = 100 mg/L	Pb = 500 mg/L	Zn = 500 mg/L
474.741	96.627	481.510	497.070
475.595	96.748	485.941	496.952
477.209	96.962	483.756	497.293
475.347	96.754	483.089	497.059
Cd = 10 mg/L	Cu = 500 mg/L	Pb = 10 mg/L	Zn = 10 mg/L
9.530	484.101	499.962	499.440
5.493	484.394	498.479	499.463
9.567	484.924	500.004	499.399
5.091	482.962	498.349	499.397
Cd = 100 mg/L	Cu = 500 mg/L	Pb = 100 mg/L	Zn = 100 mg/L
99.484	482.804	99.880	99.450
99.558	485.609	99.981	99.491
95.093	483.151	98.672	99.437
95.093	483.250	98.528	99.444

Table 4: Proportions of blocked heavy metals per unit mass of HA (mg/g) for the multi-metal system when Cu is constant. – Tabella 24: Entità dell'immobilizzazione dei metalli per unità di massa di HA (mg/g) per il sistema multi-metal con concentrazione del Cu costante.

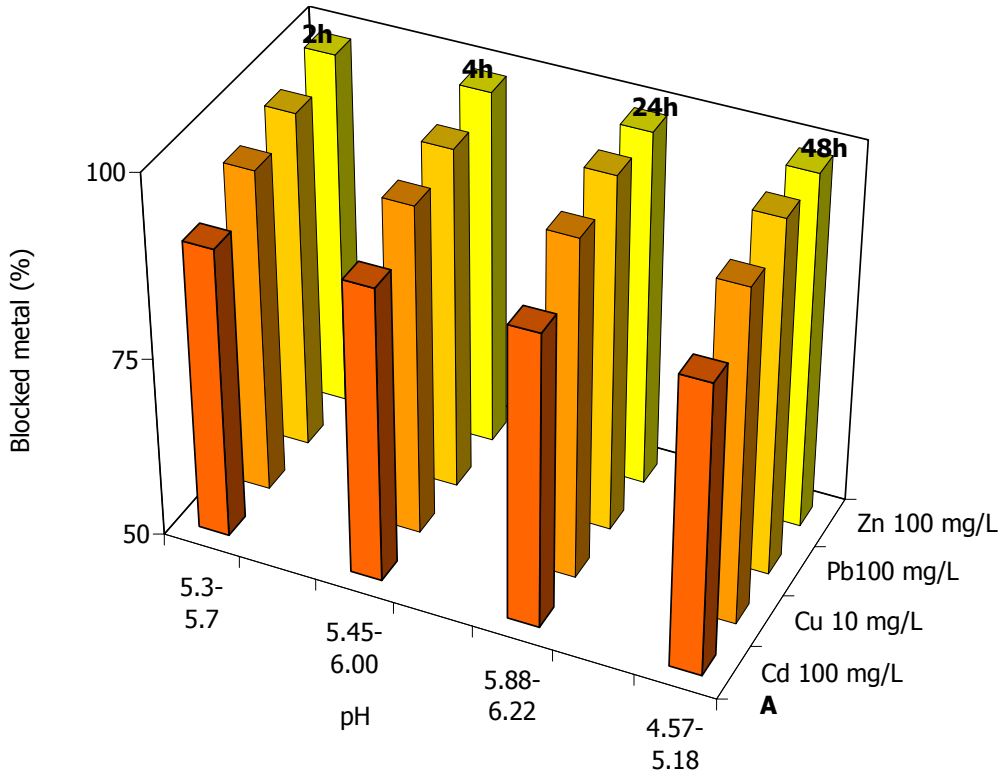
2h
4h
24h
48h
100
75
50
Blocked metal (%)
5.3-
5.7
5.45-
6.00
5.88-
6.22
4.57-
5.18
pH
Zn 100 mg/L
Pb100 mg/L
Cu 10 mg/L
Cd 100 mg/L
A

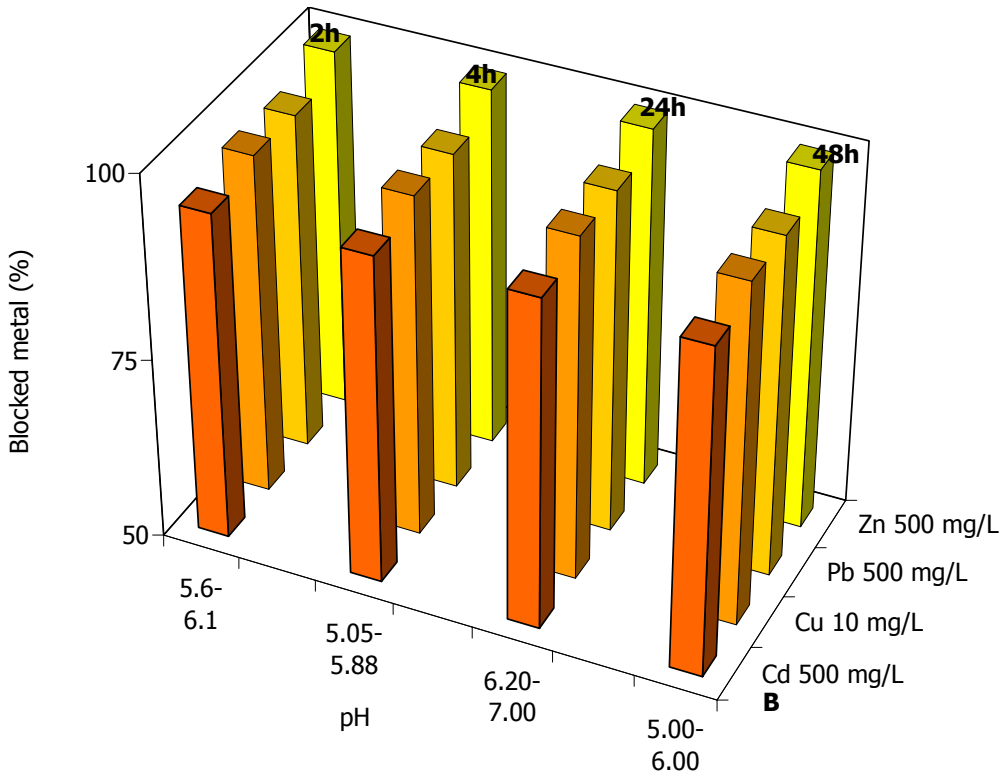
2h
4h
24h
48h
100
75
50
Blocked metal (%)
5.6-
6.1
5.05-
5.88
6.20-
7.00
5.00-
6.00
pH
Zn 500 mg/L
Pb 500 mg/L
Cu 10 mg/L
Cd 500 mg/L
B

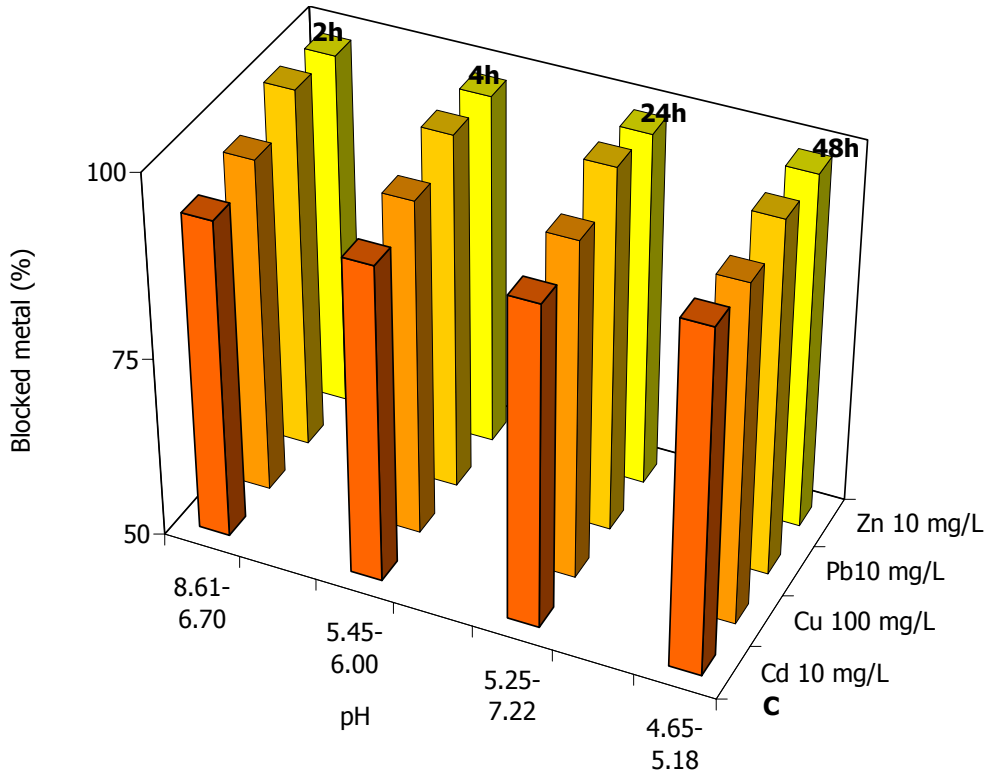
2h
4h
24h
48h
100
75
50
Blocked metal (%)
8.61-
6.70
5.45-
6.00
5.25-
7.22
4.65-
5.18
pH
Zn 10 mg/L
Pb10 mg/L
Cu 100 mg/L
Cd 10 mg/L
C

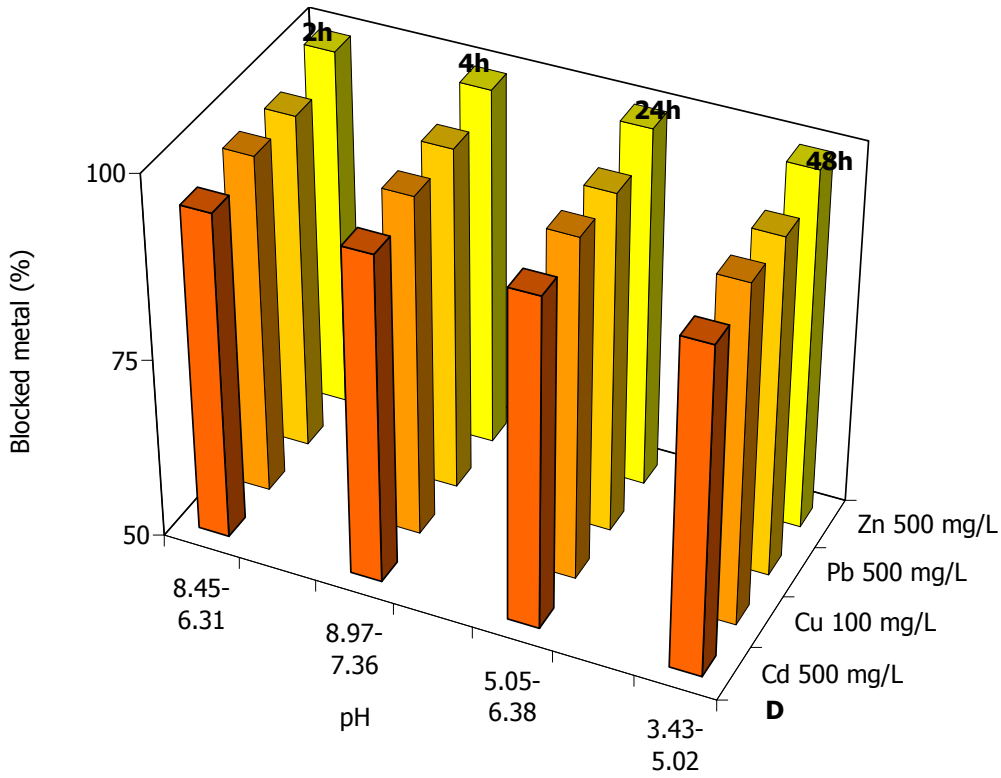
2h
4h
24h
48h
100
75
50
Blocked metal (%)
8.45-
6.31
8.97-
7.36
5.05-
6.38
3.43-
5.02
pH
Zn 500 mg/L
Pb 500 mg/L
Cu 100 mg/L
Cd 500 mg/L
D

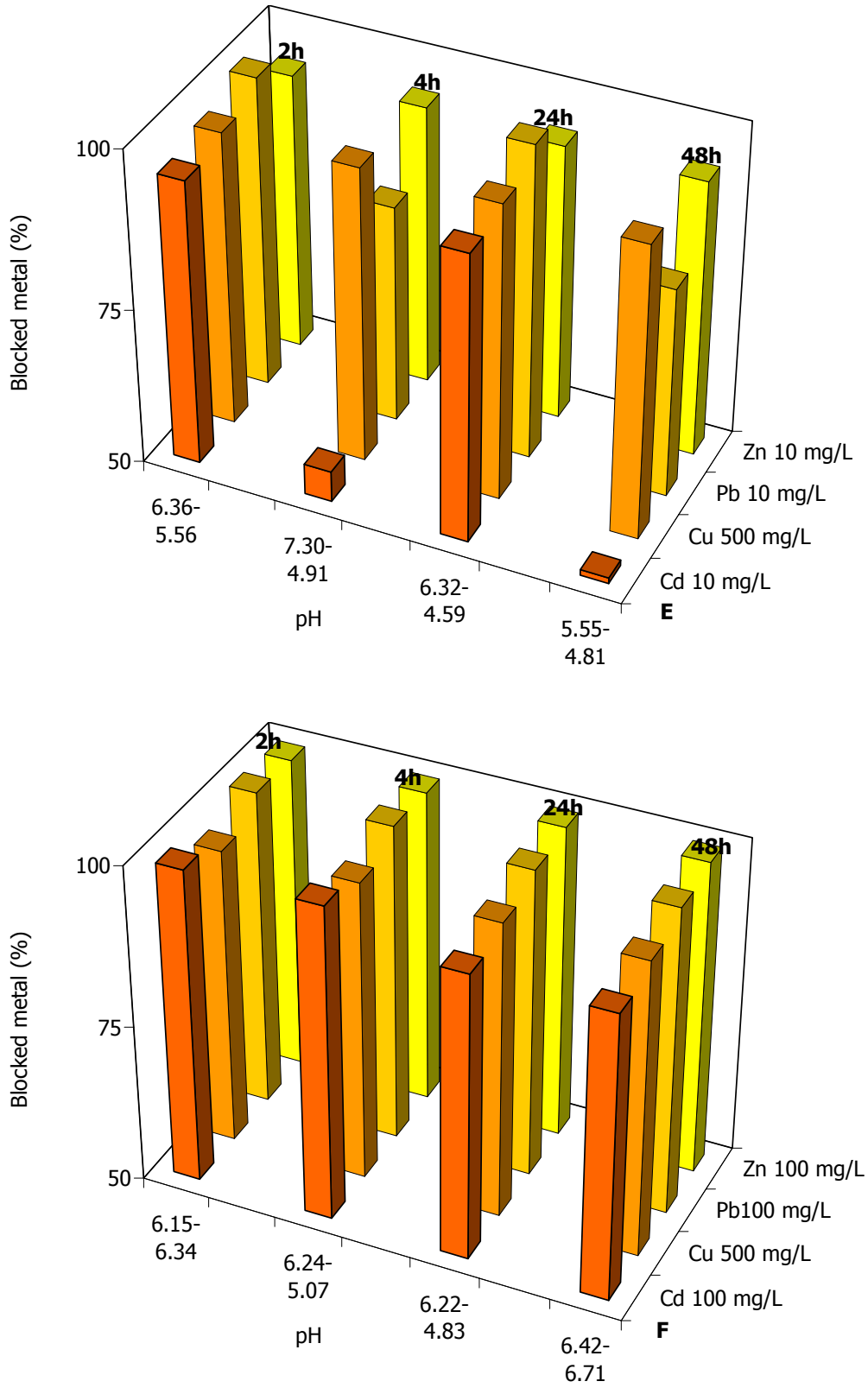

Fig. 11: Variation of the amount of blocked metal with time for the mass of HA (0.2 g) in the multi-metal system where Cu is constant. Initial and final pH values are reported. – Fig. 11: Variazione delle percentuali dei metalli immobilizzati in funzione del tempo di interazione per la quantità di HA (0.2 g) nel sistema multi-metal in cui Cu è l'elemento costante. Sono riportati i valori iniziali e finali del pH.

The molar ratio (Q_S) (Table 5) is always < 1 meaning an amorphous precipitation. On the contrary, the sorption isotherms (Fig. 12 A, B, C and D) show a different behavior according to the metals and the time. Zn shows always an isotherm of H type confirming the amorphous precipitation, Pb and Cd have a L2 isotherm suggesting an adsorption mechanism and a surface precipitation process. Cu shows for t = 2h a vertical isotherm (H type) and then it passes to a L2 type, probably time is the key factor.

Cd = 100 mg/L	Cu = 10 mg/L	Pb = 100 mg/L	Zn = 100 mg/L
0.233	0.022	0.044	0.046
0.673	0.058	0.115	0.132
0.212	0.013	0.013	0.043
0.215	0.015	0.013	0.043
Cd = 500 mg/L	Cu = 10 mg/L	Pb = 500 mg/L	Zn = 500 mg/L
0.044	0.001	0.017	0.009
0.716	0.016	0.269	0.143
0.384	0.008	0.126	0.076
0.483	0.010	0.165	0.097
Cd = 10 mg/L	Cu = 100 mg/L	Pb = 10 mg/L	Zn = 10 mg/L
0.006	0.068	0.0002	0.002
0.001	0.016	0.0001	0.001
0.002	0.024	-0.000002	0.001
0.000	0.008	0.0001	0.000
Cd = 500 mg/L	Cu = 100 mg/L	Pb = 500 mg/L	Zn = 500 mg/L
0.054	0.013	0.022	0.011
0.036	0.009	0.011	0.008
0.106	0.025	0.041	0.022
0.043	0.010	0.016	0.009
Cd = 10 mg/L	Cu = 500 mg/L	Pb = 10 mg/L	Zn = 10 mg/L
0.003	0.159	0.000	0.005
0.010	0.062	0.002	0.002
0.001	0.060	0.000	0.002
0.008	0.050	0.001	0.002
Cd = 100 mg/L	Cu = 500 mg/L	Pb = 100 mg/L	Zn = 100 mg/L
0.008	0.450	0.001	0.014
0.005	0.273	0.000	0.009
0.104	0.632	0.015	0.021
0.067	0.403	0.011	0.013

Table 5: Q_S values for the multi - metal systems when Cu has a constant concentration. Tabella 5: Valori di Q_S per i sistemi multi-metal nei quali la concentrazione di Cu è stata mantenuta costante.

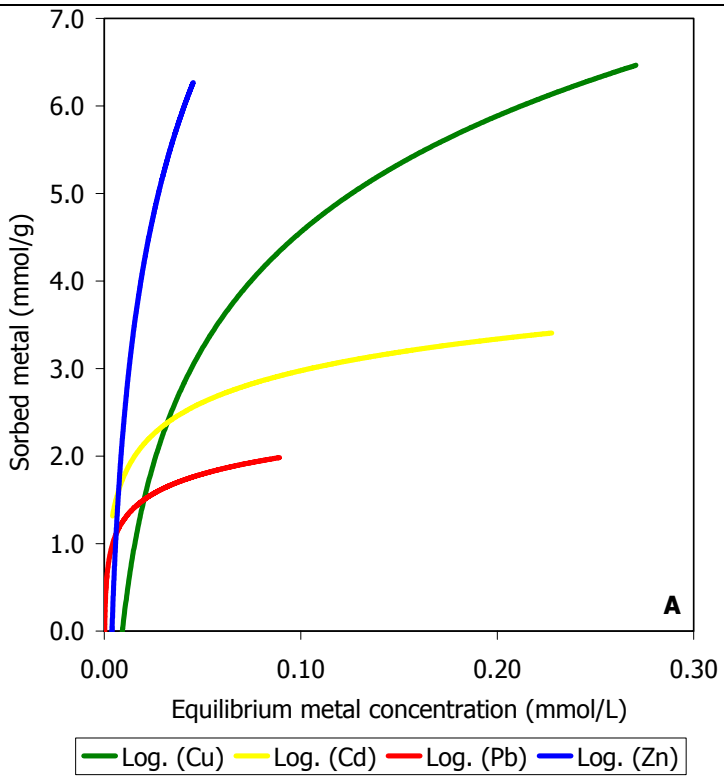
7.0
6.0
5.0
4.0
3.0
2.0
1.0
0.0
Sorbed metal (mmol/g)
0.00
0.10
0.20
0.30
Equilibrium metal concentration (mmol/L)
A
Log. (Cu)
Log. (Cd)
Log. (Pb)
Log. (Zn)

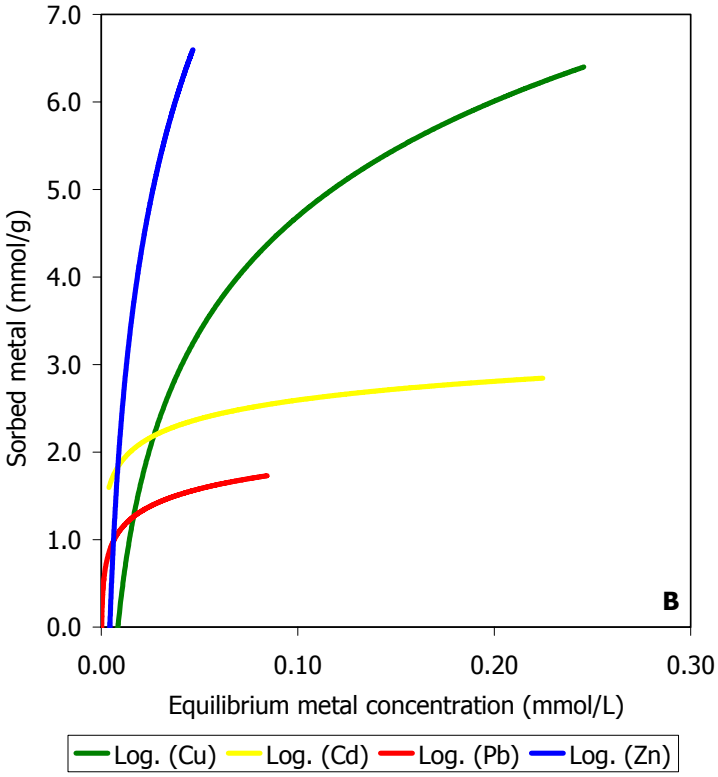
7.0
6.0
5.0
4.0
3.0
2.0
1.0
0.0
Sorbed metal (mmol/g)
0.00
0.10
0.20
0.30
Equilibrium metal concentration (mmol/L)
B
Log. (Cu)
Log. (Cd)
Log. (Pb)
Log. (Zn)

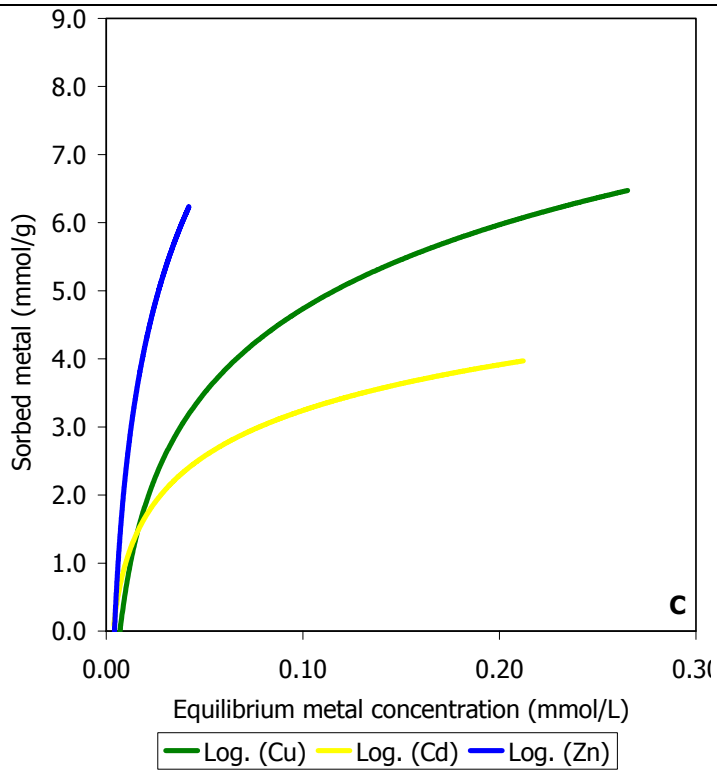

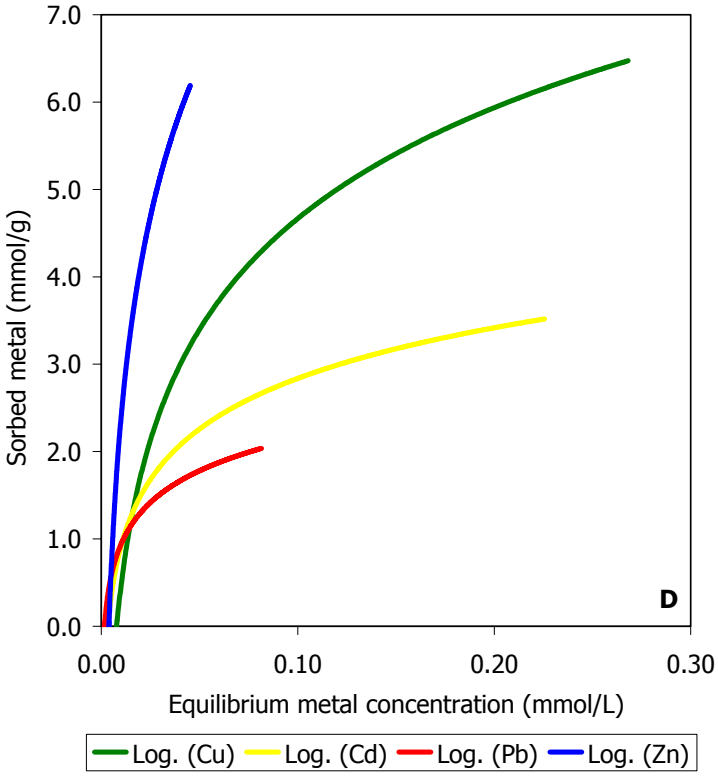

Fig. 12: Sorption isotherms for the multi-metal system where Cu is constant for the four contact times (2h, 4h, 24h and 48h) and vs. 0.2 g HA. Relation between the metal sorbed (mmol/g) and the final concentration (mmol/L) in solution. A: t = 2h; B: t = 4h; C: t = 24h and D: t = 48h. – Fig. 12: Curve isotermiche per il sistema multi-metal in cui Cu è costante per i quattro tempi di contatto (2h, 4h, 24h and

48h) e vs. 0.2 g di HA. Relazione tra il metallo assorbito (mmol/g) e la concentrazione finale (mmol/L) in soluzione. A: t = 2h; B: t = 4h; C: t = 24h and D: t = 48h.

The desorbed Ca amount is almost proportional to the amount of sorbed metal at the equilibrium with an average values from 0 to 6 mmol/L (Fig. 13 A, B, C, D, E and F), allowing to infer a stoichiometric dissolution and probably the precipitation mechanism as the sorption process. This is supported by the low amount of P in the solution at the equilibrium (Fig. 14 A, B, C, D and F) with values ranging from 0 to 0.3 mmol/L and the amount of sorbed metals is about 0 – 6 mmol/L. The low values of P in solution let to think that the element it is used for the precipitation of a new phosphate phase.

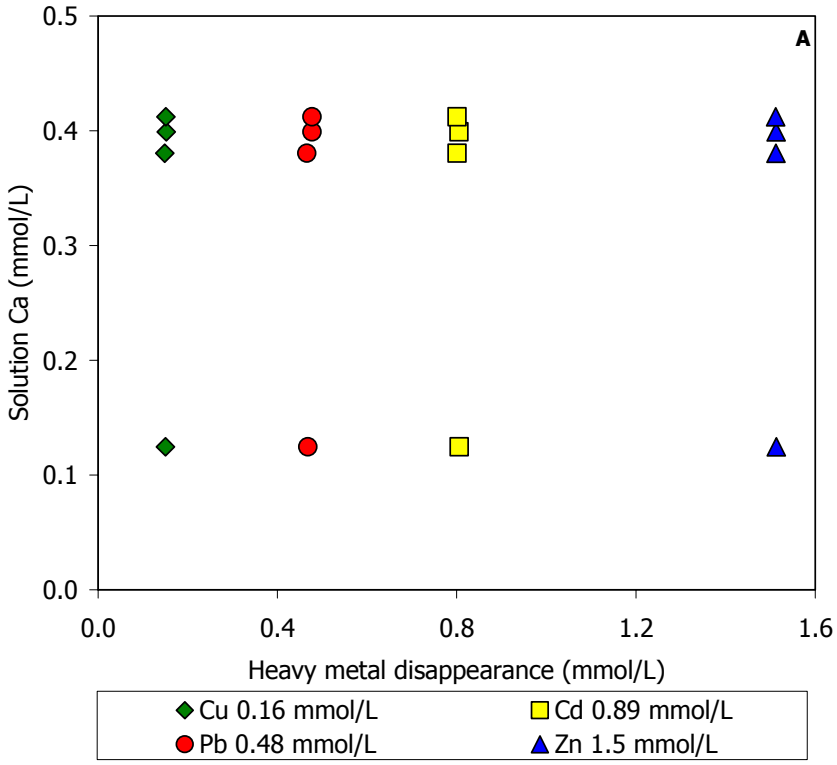

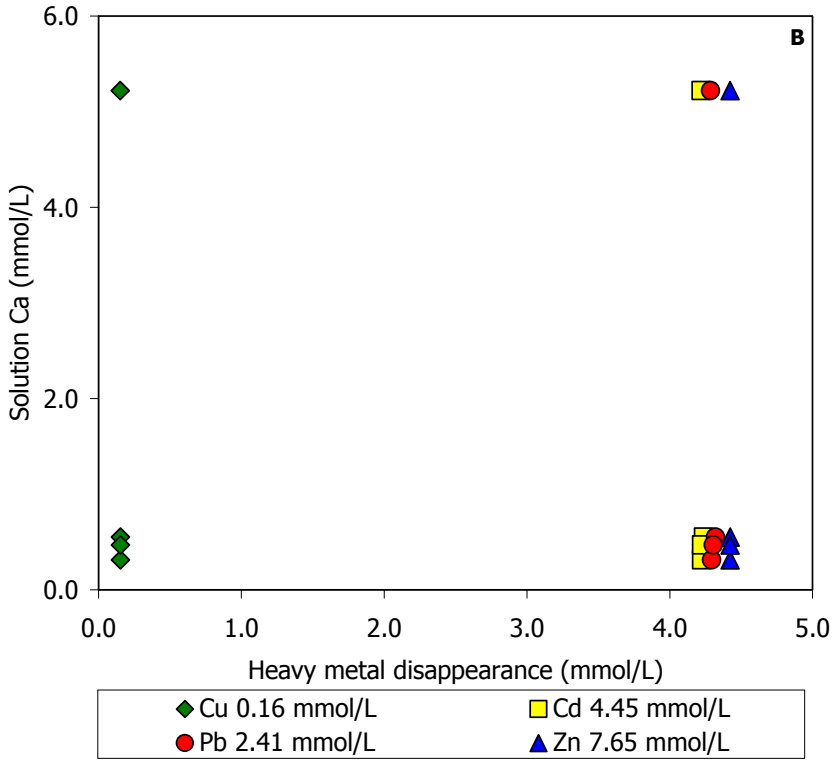
B
6.0
4.0
2.0
0.0
Solution Ca (mmol/L)
0.0
1.0
2.0
3.0
4.0
5.0
Heavy metal disappearance (mmol/L)
Cu 0.16 mmol/L
Cd 4.45 mmol/L
Pb 2.41 mmol/L
Zn 7.65 mmol/L

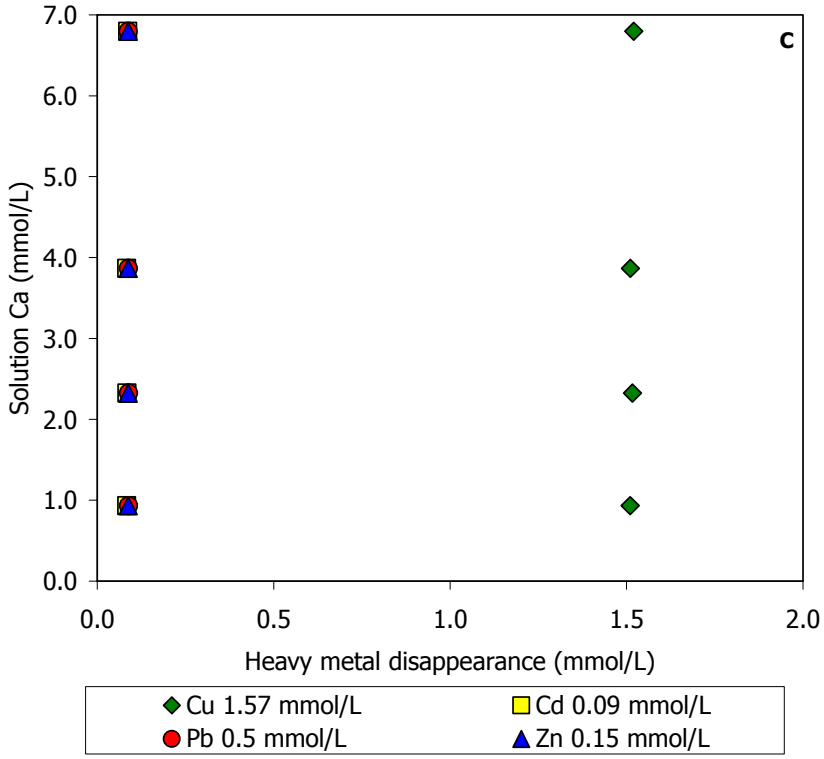
C
7.0
6.0
5.0
4.0
3.0
2.0
1.0
0.0
Solution Ca (mmol/L)
0.0
0.5
1.0
1.5
2.0
Heavy metal disappearance (mmol/L)
Cu 1.57 mmol/L
Cd 0.09 mmol/L
Pb 0.5 mmol/L
Zn 0.15 mmol/L

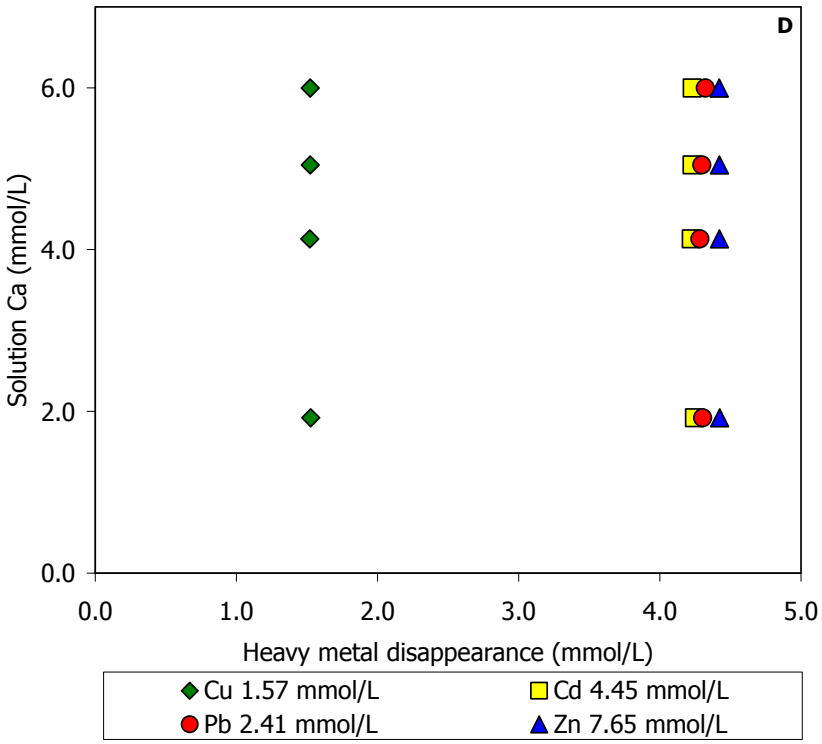
D
6.0
4.0
2.0
0.0
Solution Ca (mmol/L)
0.0
1.0
2.0
3.0
4.0
5.0
Heavy metal disappearance (mmol/L)
Cu 1.57 mmol/L
Cd 4.45 mmol/L
Pb 2.41 mmol/L
Zn 7.65 mmol/L

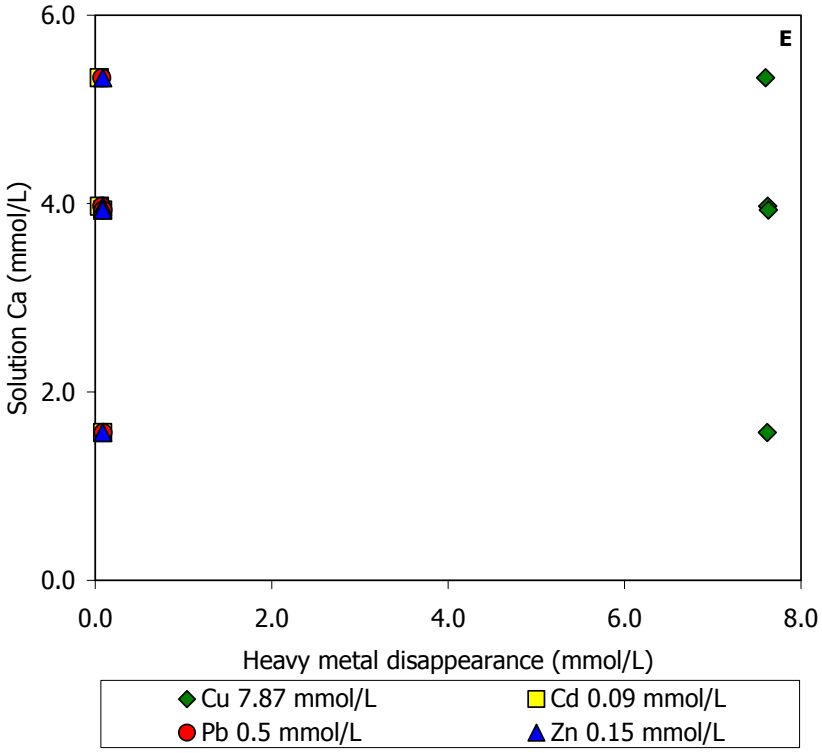
E
6.0
4.0
2.0
0.0
Solution Ca (mmol/L)
0.0
2.0
4.0
6.0
8.0
Heavy metal disappearance (mmol/L)
Cu 7.87 mmol/L
Cd 0.09 mmol/L
Pb 0.5 mmol/L
Zn 0.15 mmol/L

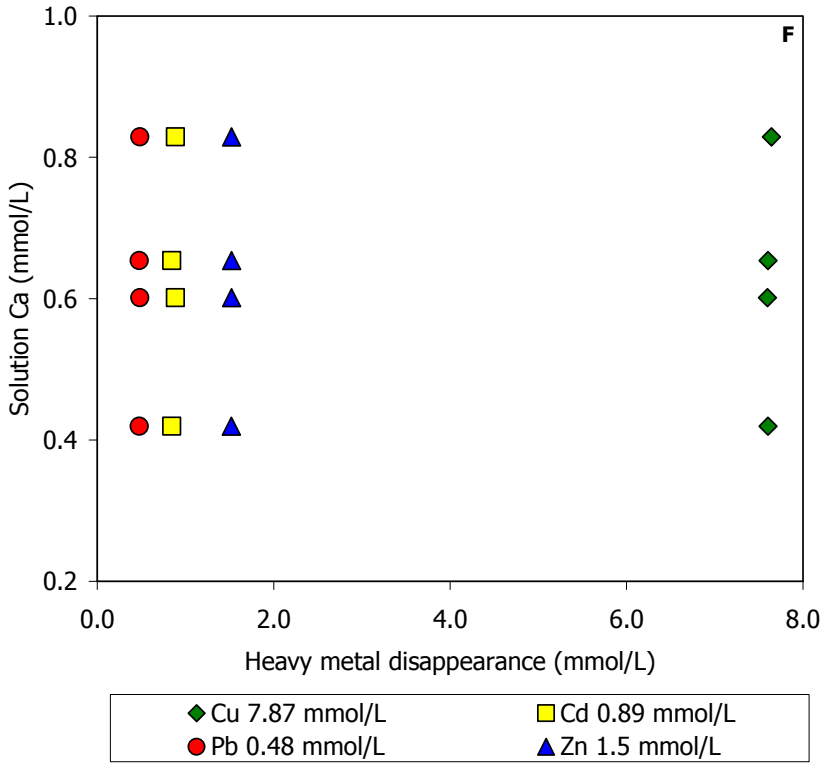

Fig. 13: Relation between Ca in solution (mmol/L) and the amount of heavy metals disappeared (mmol/L) sorbed on HA surface at the equilibrium in a multi-metal system when Cu is constant. Each initial concentration of the multi-metal system is written in the legend. - Fig. 13: Relazione tra il quantitativo di Ca in soluzione (mmol/L) e di ciascun metallo pesante adsorbito (mmol/L) nel sistema multi-metal quando Cu è costante. La concentrazione iniziale di ogni elemento del sistema multi-metal è in leggenda.

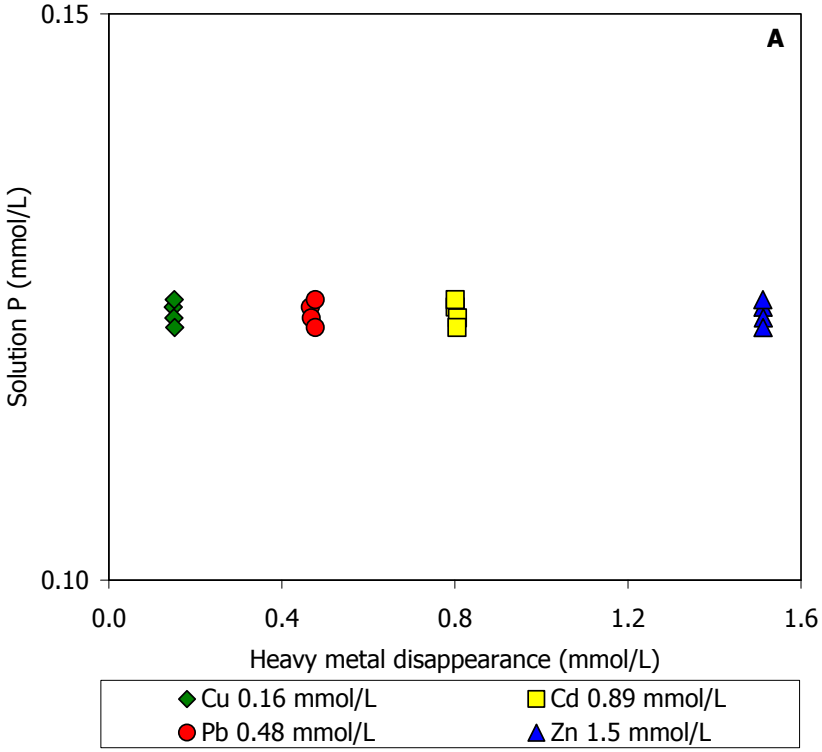
A
0.15
0.10
Solution P (mmol/L)
0.0
0.4
0.8
1.2
1.6
Heavy metal disappearance (mmol/L)
Cu 0.16 mmol/L
Cd 0.89 mmol/L
Pb 0.48 mmol/L
Zn 1.5 mmol/L

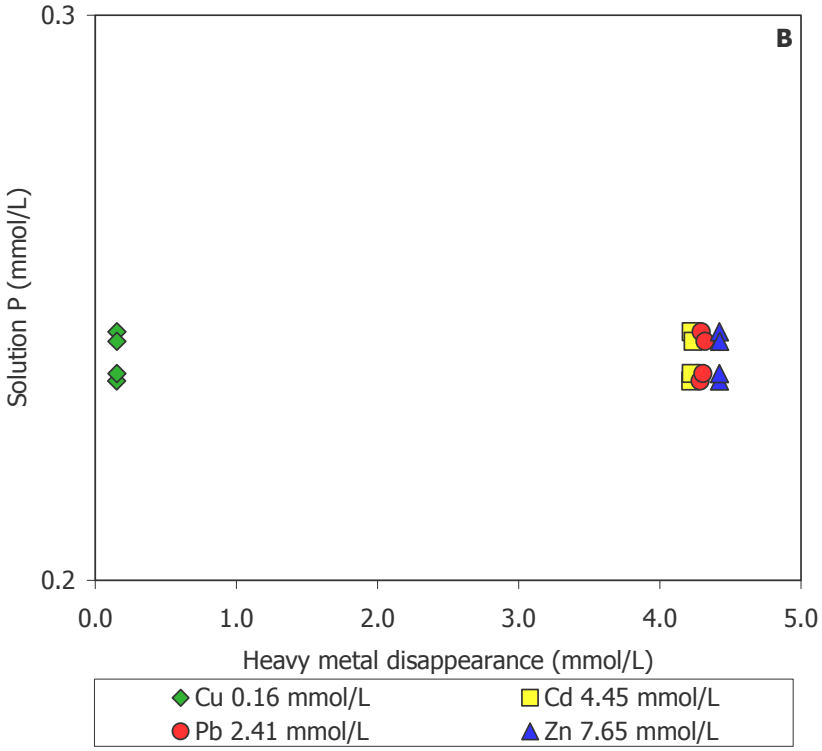
B
0.3
0.2
Solution P (mmol/L)
0.0
1.0
2.0
3.0
4.0
5.0
Heavy metal disappearance (mmol/L)
Cu 0.16 mmol/L
Cd 4.45 mmol/L
Pb 2.41 mmol/L
Zn 7.65 mmol/L

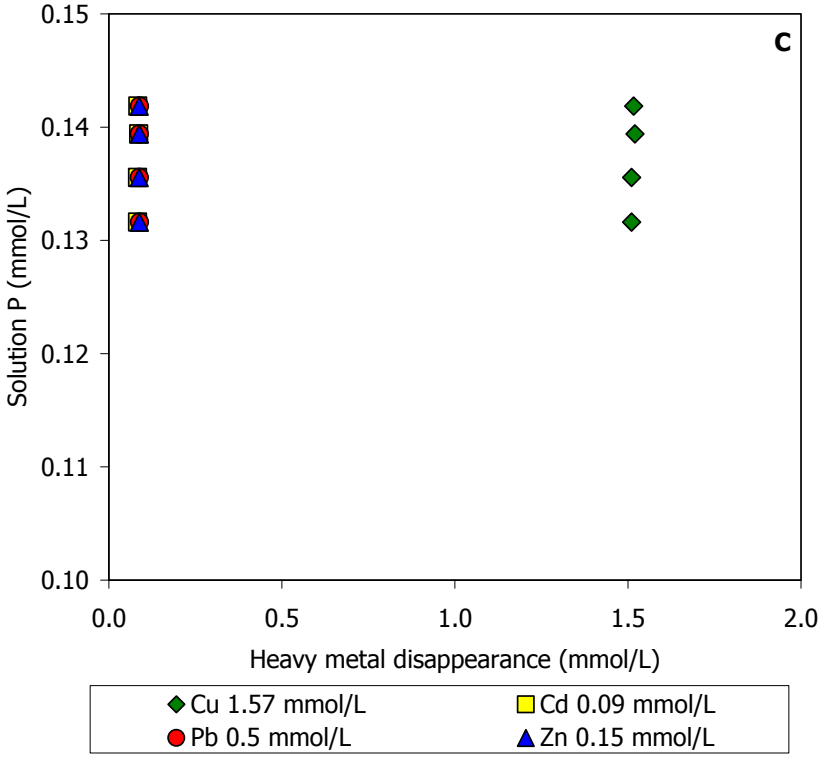
C
0.15
0.14
0.13
0.12
0.11
0.10
Solution P (mmol/L)
0.0
0.5
1.0
1.5
2.0
Heavy metal disappearance (mmol/L)
Cu 1.57 mmol/L
Cd 0.09 mmol/L
Pb 0.5 mmol/L
Zn 0.15 mmol/L

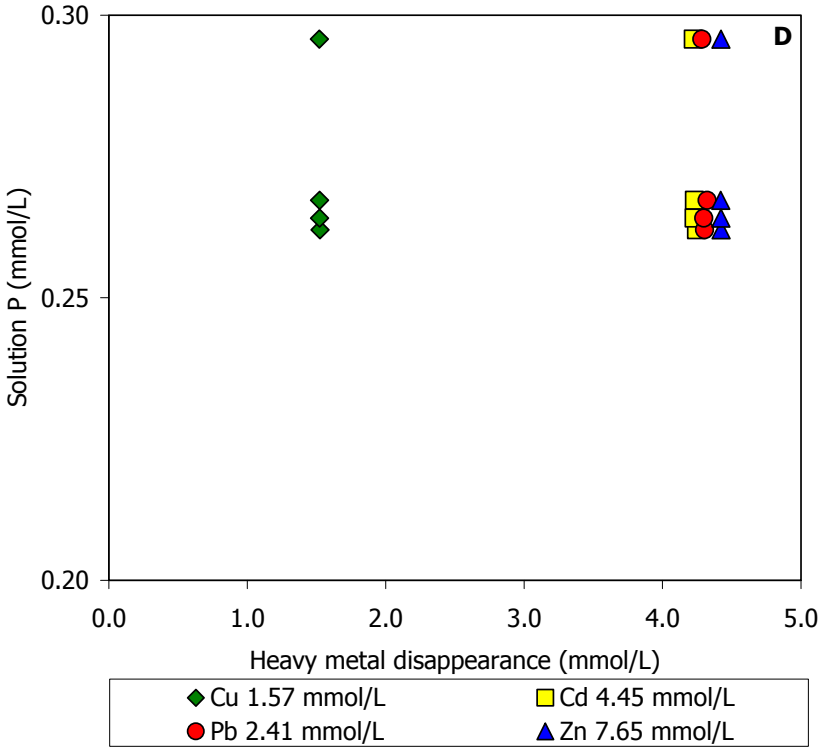
D
0.30
0.25
0.20
Solution P (mmol/L)
0.0
1.0
2.0
3.0
4.0
5.0
Heavy metal disappearance (mmol/L)
Cu 1.57 mmol/L
Cd 4.45 mmol/L
Pb 2.41 mmol/L
Zn 7.65 mmol/L

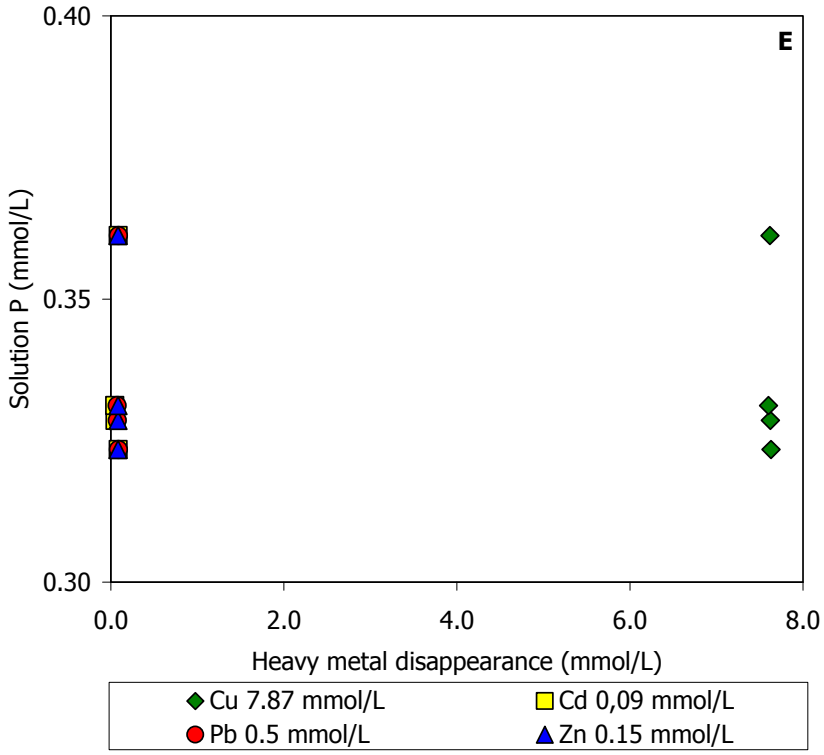

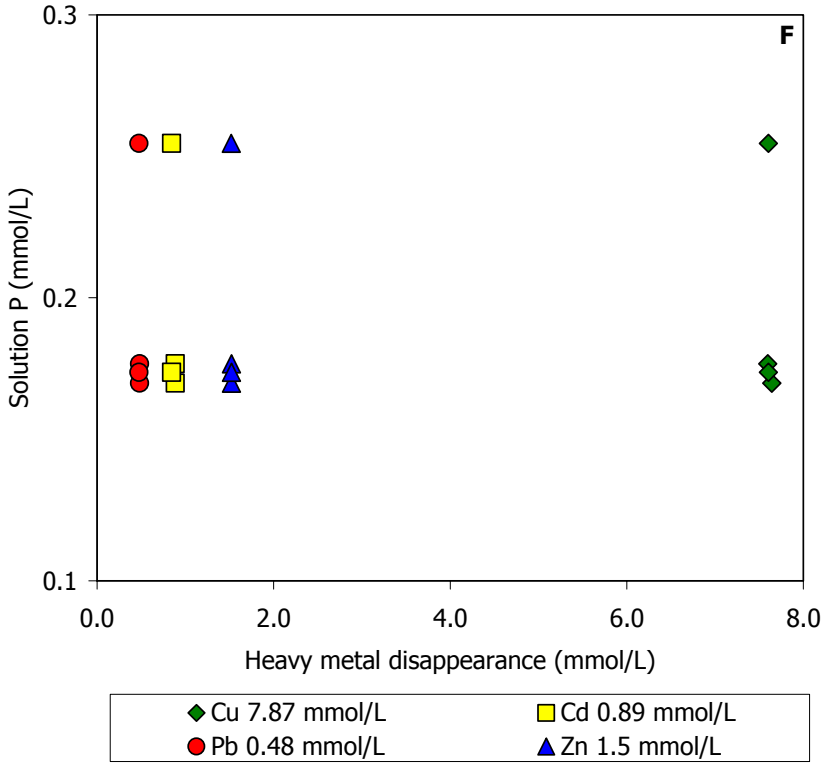

Fig. 14: Relation between P in solution (mmol/L) and the amount of disappeared heavy metals (mmol/L) sorbed on HA surface at the equilibrium in a multi-metal system when Cu is constant. Each initial concentration of the multi-metal system is written in the legend. - Fig. 14: Relazione tra il quantitativo di P in

soluzione (mmol/L) e di ciascun metallo pesante adsorbito (mmol/L) nel sistema multi-metal quando Cu è costante. La concentrazione iniziale di ogni elemento del sistema multi-metal è in leggenda.

The proportions of blocked heavy metals per unit mass of HA with constant Pb, all of the metals are well immobilized (Fig. 15 A, B, C, D, E, F, G, H and I), that is the presence of the other three metals doesn't compromise the immobilization. The immobilization efficiency (Table 6) is very high for each of the heavy metals and it is possible to distinguish two order of immobilization according to the initial metal concentration. The first one is Pb > Zn > Cd > Cu whereas the second one is Zn > Pb > Cu > Cd, the second order being defined when the concentration of the four element is ≥100 mg/L.

Cd = 10 mg/L	Cu = 10 mg/L	Pb = 10 mg/L	Zn = 10 mg/L
9.583	9.977	9.963	9.957
9.662	9.974	9.970	9.949
9.772	9.963	9.987	9.980
9.454	9.978	9.943	9.931
Cd = 100 mg/L	Cu = 100 mg/L	Pb = 10 mg/L	Zn = 100 mg/L
89.348	94.032	9.912	98.952
90.162	94.855	9.939	99.002
90.559	95.193	9.939	99.033
90.434	95.276	9.978	99.033
Cd = 500 mg/L	Cu = 500 mg/L	Pb = 10 mg/L	Zn = 500 mg/L
444.038	461.818	9.937	494.230
444.534	463.268	9.924	494.006
445.289	464.169	9.995	493.837
445.376	463.777	9.953	493.527
Cd = 10 mg/L	Cu = 10 mg/L	Pb = 100 mg/L	Zn = 10 mg/L
9.001	9.680	99.652	9.860
9.029	9.724	99.741	9.877
9.177	9.811	99.702	9.898
9.330	9.875	99.887	9.897
Cd = 100 mg/L	Cu = 100 mg/L	Pb = 100 mg/L	Zn = 100 mg/L
89.154	93.437	96.803	98.852
88.929	93.475	96.748	98.830
89.137	93.669	97.451	98.849
89.209	93.851	97.889	98.833
Cd = 500 mg/L	Cu = 500 mg/L	Pb = 100 mg/L	Zn = 500 mg/L
473.721	481.937	98.165	497.080
473.299	489.063	90.147	496.881
473.187	481.502	98.262	496.990
472.779	481.411	98.274	496.949
Cd = 10 mg/L	Cu = 10 mg/L	Pb = 500 mg/L	Zn = 10 mg/L
9.425	9.626	480.070	9.978
9.462	9.649	481.275	9.976
9.477	9.696	481.311	9.981
9.458	9.673	481.395	9.974
Cd = 100 mg/L	Cu = 100 mg/L	Pb = 500 mg/L	Zn = 100 mg/L
94.721	96.343	479.884	99.447
95.362	96.790	482.560	99.508
94.601	96.218	480.383	99.454
94.586	96.214	480.477	99.442
Cd = 500 mg/L	Cu = 500 mg/L	Pb = 500 mg/L	Zn = 100 mg/L
474.474	481.453	480.577	497.138
473.283	480.564	479.390	496.990
474.163	481.275	480.922	497.080
474.719	481.723	481.434	497.088

Table 6: Efficiency values for the multi - metal system when Pb has a constant concentration.

Tabella 6: Valori dell'efficienza nell'immobilizzare i metalli pesanti per il sistema multi-metal in cui il Pb mantiene costante le concentrazione.

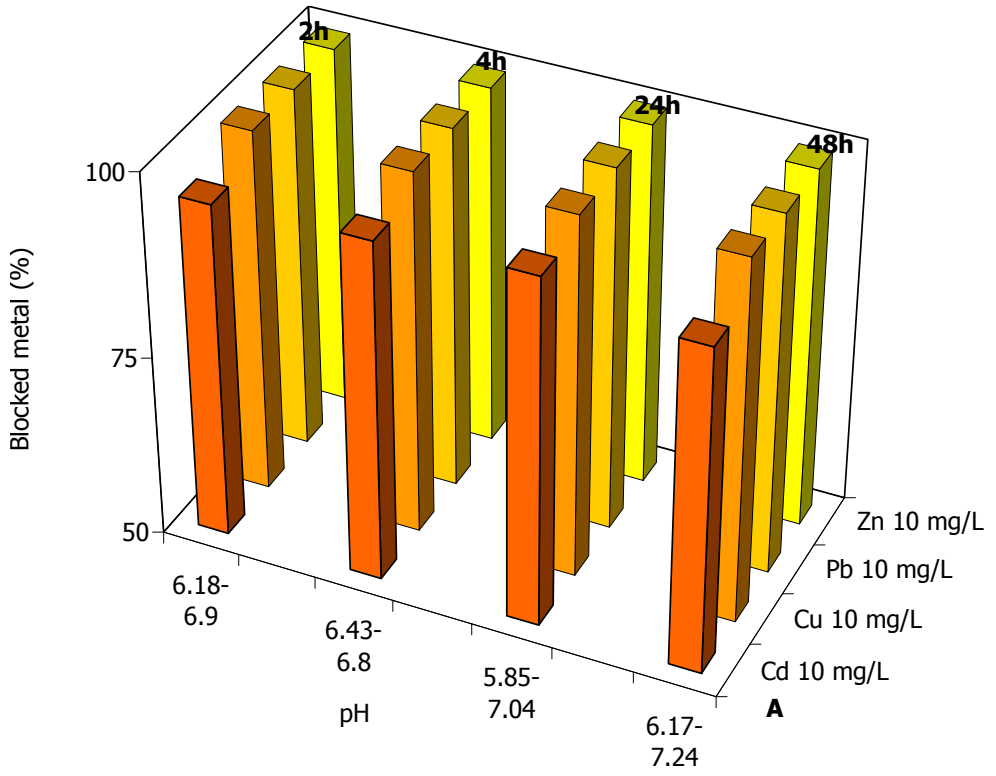
2h
4h
24h
48h
100
75
50
Blocked metal (%)
6.18-
6.9
6.43-
6.8
5.85-
7.04
6.17-
7.24
pH
Zn 10 mg/L
Pb 10 mg/L
Cu 10 mg/L
Cd 10 mg/L
A

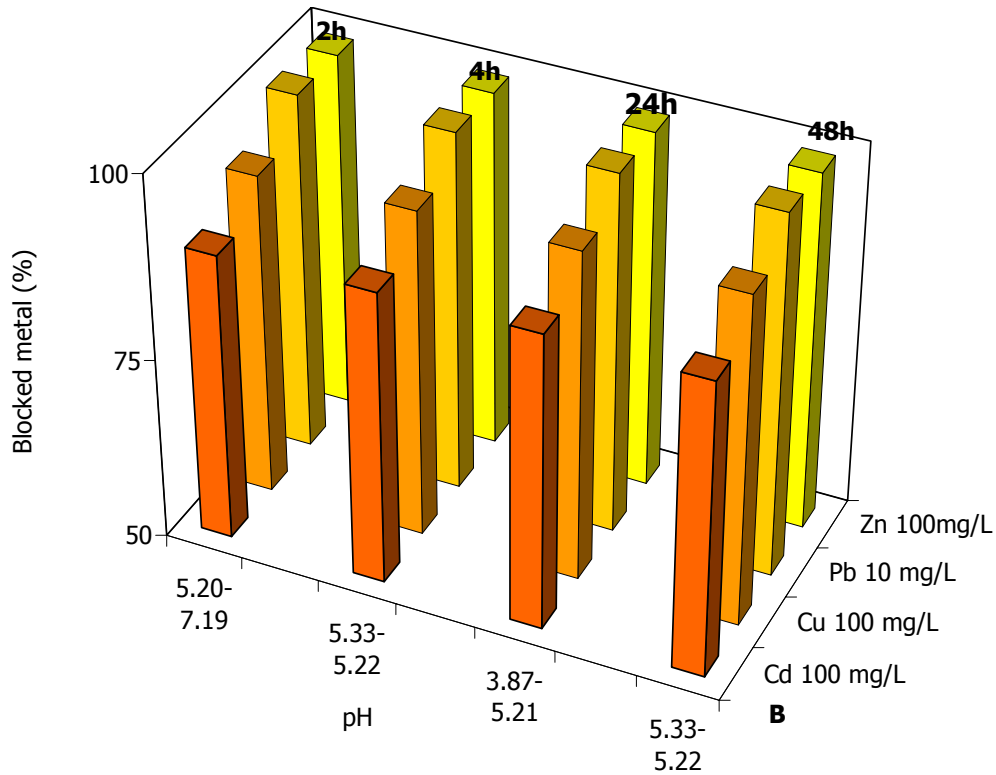
2h
4h
24h
48h
100
75
50
Blocked metal (%)
5.20-
7.19
5.33-
5.22
3.87-
5.21
5.33-
5.22
pH
Zn 100mg/L
Pb 10 mg/L
Cu 100 mg/L
Cd 100 mg/L
B

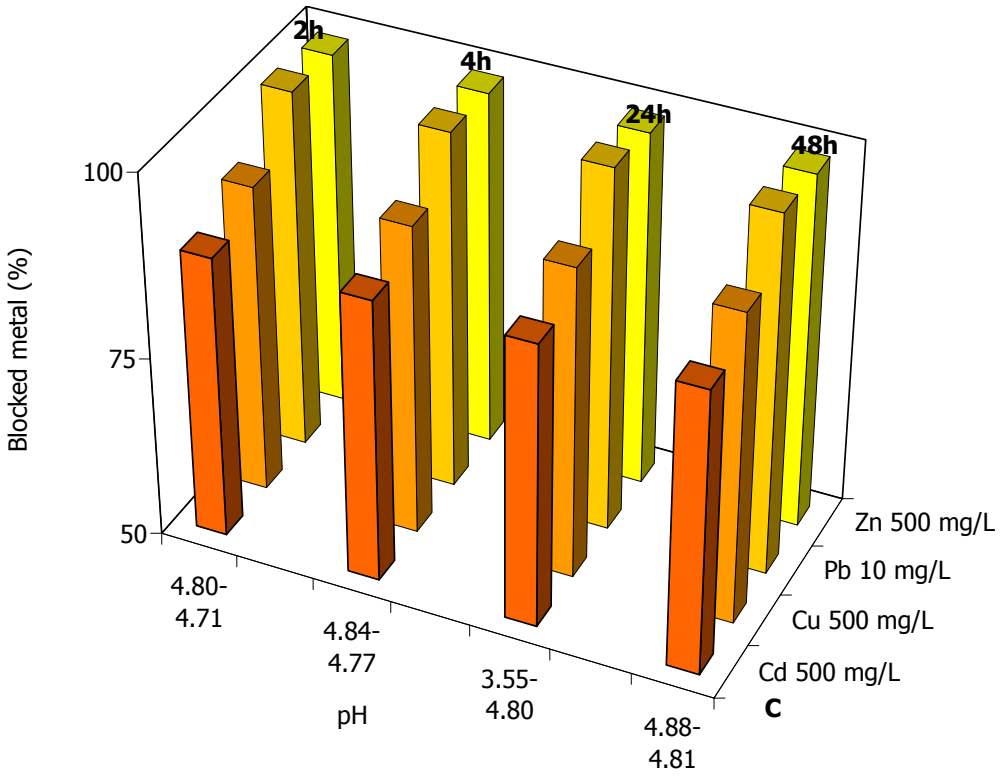
2h
4h
24h
48h
100
75
50
Blocked metal (%)
4.80-
4.71
4.84-
4.77
3.55-
4.80
4.88-
4.81
pH
Zn 500 mg/L
Pb 10 mg/L
Cu 500 mg/L
Cd 500 mg/L
C

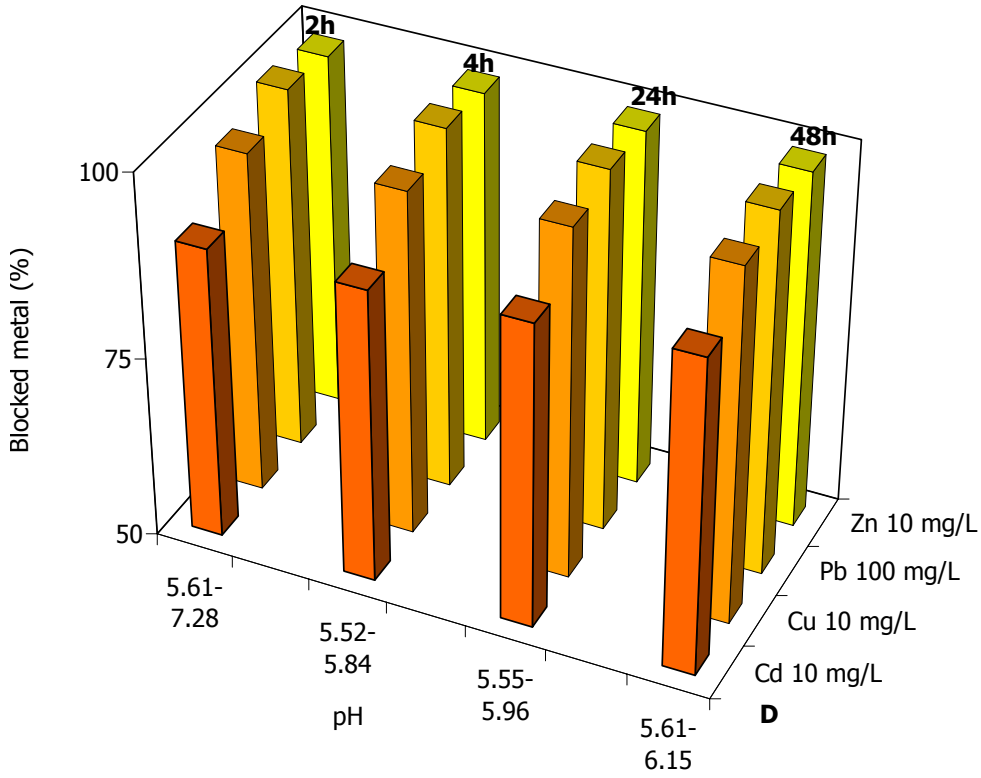
2h
4h
24h
48h
100
75
50
Blocked metal (%)
5.61-
7.28
5.52-
5.84
5.55-
5.96
5.61-
6.15
pH
Zn 10 mg/L
Pb 100 mg/L
Cu 10 mg/L
Cd 10 mg/L
D

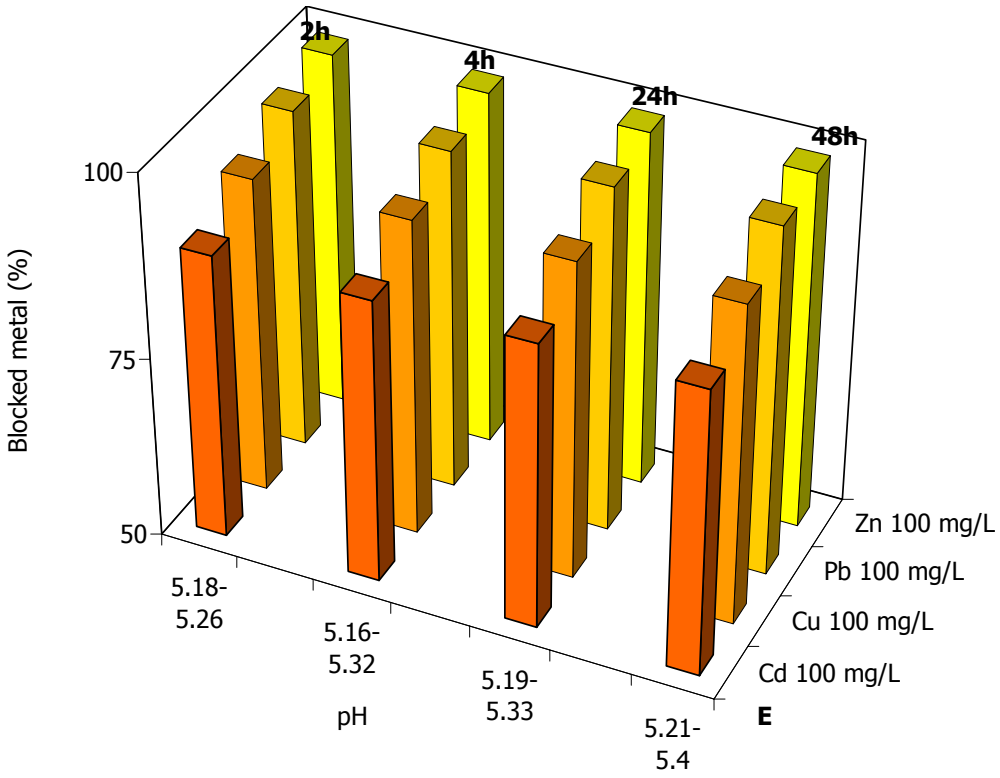
2h
4h
24h
48h
100
75
50
Blocked metal (%)
5.18-
5.26
5.16-
5.32
5.19-
5.33
5.21-
5.4
pH
Zn 100 mg/L
Pb 100 mg/L
Cu 100 mg/L
Cd 100 mg/L
E

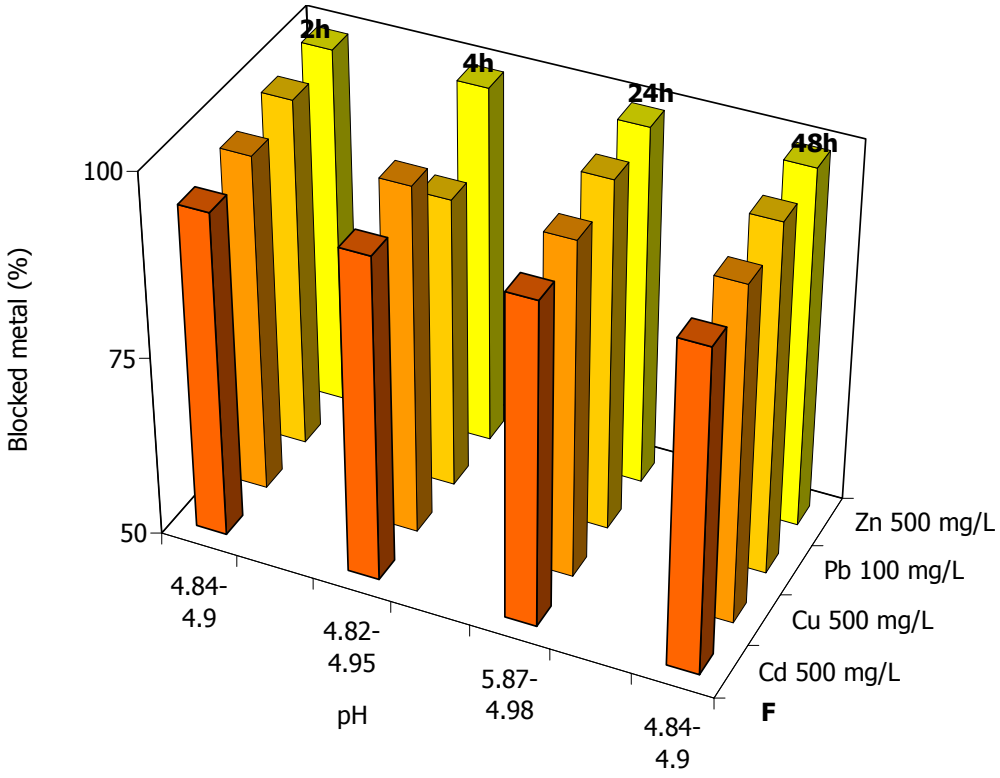
2h
4h
24h
48h
100
75
50
Blocked metal (%)
4.84-
4.9
4.82-
4.95
5.87-
4.98
4.84-
4.9
pH
Zn 500 mg/L
Pb 100 mg/L
Cu 500 mg/L
Cd 500 mg/L
F

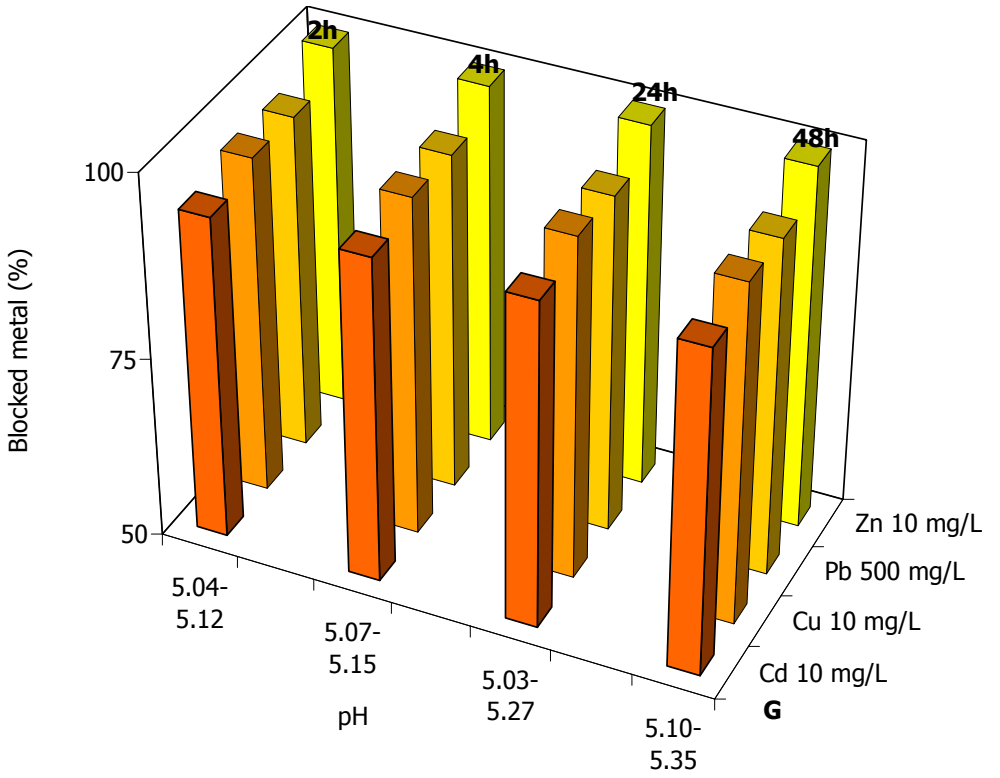
2h
4h
24h
48h
100
75
50
Blocked metal (%)
5.04-
5.12
5.07-
5.15
5.03-
5.27
5.10-
5.35
pH
Zn 10 mg/L
Pb 500 mg/L
Cu 10 mg/L
Cd 10 mg/L
G

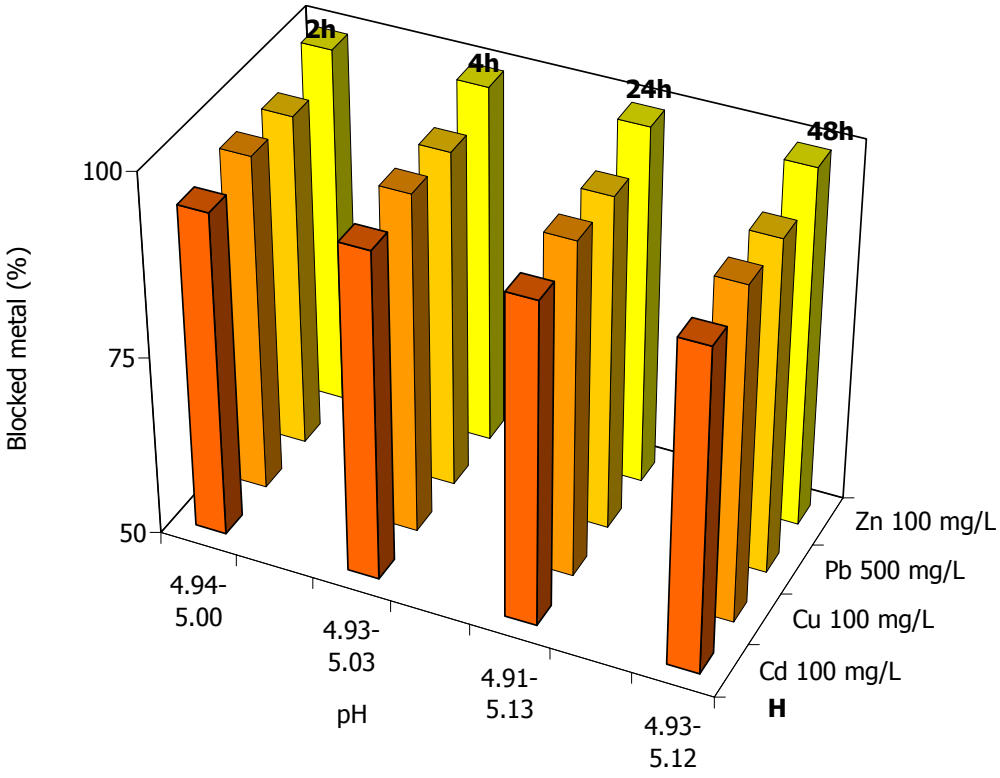
2h
4h
24h
48h
100
75
50
Blocked metal (%)
4.94-
5.00
4.93-
5.03
4.91-
5.13
4.93-
5.12
pH
Zn 100 mg/L
Pb 500 mg/L
Cu 100 mg/L
Cd 100 mg/L
H

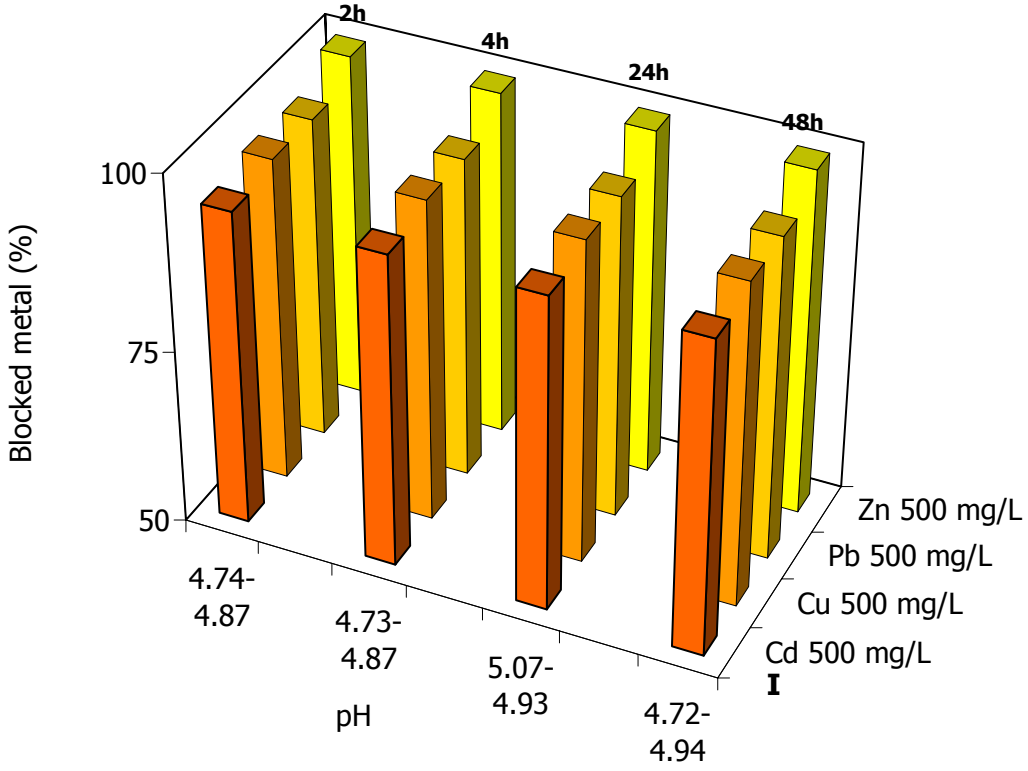

Fig. 15: Variation of the amount of blocked metal with time for the mass of HA (0.2 g) in the multi-metal system where Pb is constant. – Fig. 15: Variazione delle percentuali dei metalli immobilizzati in funzione del tempo di interazione per la quantità di HA (0.2 g) nel sistema multi-metal in cui Pb è l'elemento costante.

The values of the molar ratio (Q_S) (Tab. 7) are always < 1 as in the system where Cu is constant, suggesting as sorption mechanism the precipitation of new phosphates.

The sorption isotherms (Fig. 16 A, B, C and D) are quite different according to the interaction time as for t = 2h Pb, Cu and Zn show a L2 type and Cd a C type (almost horizontal) which means a constant partition of solute between solution and substrate. Increasing the time (t = 4h) only for Pb the curve has the before mentioned shape, whereas Cd, Cu and Zn show a vertical line (H type). Finally, for t = 24 and 48h the sorption isotherm for all of the four metals are H type.

Cd = 10 mg/L	Cu = 10 mg/L	Pb = 10 mg/L	Zn = 10 mg/L
0.01	0.001	0.001	0.003
0.01	0.002	0.001	0.003
0.01	0.002	0.000	0.001
0.04	0.003	0.002	0.008
Cd = 100 mg/L	Cu = 100 mg/L	Pb = 10 mg/L	Zn = 100 mg/L
0.20	0.20	0.001	0.03
0.18	0.17	0.001	0.03
0.15	0.14	0.001	0.03
0.14	0.12	0.000	0.02
Cd = 500 mg/L	Cu = 500 mg/L	Pb = 10 mg/L	Zn = 500 mg/L
0.95	1.14	0.001	0.17
0.97	1.13	0.001	0.18
0.86	1.00	0.00004	0.17
0.95	1.11	0.0004	0.19
Cd = 10 mg/L	Cu = 10 mg/L	Pb = 100 mg/L	Zn = 10 mg/L
0.02	0.01	0.004	0.005
0.02	0.01	0.003	0.004
0.02	0.01	0.003	0.003
0.01	0.00	0.001	0.003
Cd = 100 mg/L	Cu = 100 mg/L	Pb = 100 mg/L	Zn = 100 mg/L
0.26	0.28	0.04	0.05
0.25	0.26	0.04	0.05
0.21	0.22	0.03	0.04
0.20	0.20	0.02	0.04
Cd = 500 mg/L	Cu = 500 mg/L	Pb = 100 mg/L	Zn = 500 mg/L
0.60	0.73	0.02	0.11
1.06	0.77	0.21	0.21
0.50	0.61	0.02	0.10
0.50	0.60	0.02	0.10
Cd = 10 mg/L	Cu = 10 mg/L	Pb = 500 mg/L	Zn = 10 mg/L
0.01	0.02	0.26	0.001
0.01	0.01	0.23	0.001
0.01	0.01	0.19	0.001
0.01	0.01	0.18	0.001
Cd = 100 mg/L	Cu = 100 mg/L	Pb = 500 mg/L	Zn = 100 mg/L
0.24	0.29	0.50	0.04
0.12	0.14	0.24	0.02
0.20	0.25	0.39	0.03
0.10	0.13	0.20	0.02
Cd = 500 mg/L	Cu = 500 mg/L	Pb = 500 mg/L	Zn = 500 mg/L
0.67	0.87	0.28	0.13
0.69	0.89	0.29	0.13
0.54	0.69	0.22	0.10
0.50	0.64	0.20	0.10

Table 7: Q_S values for the multi - metal systems when Pb has a constant concentration. Tabella 7: Valori di Q_S per i sistemi multi-metal nei quali la concentrazione di Pb è stata mantenuta costante.

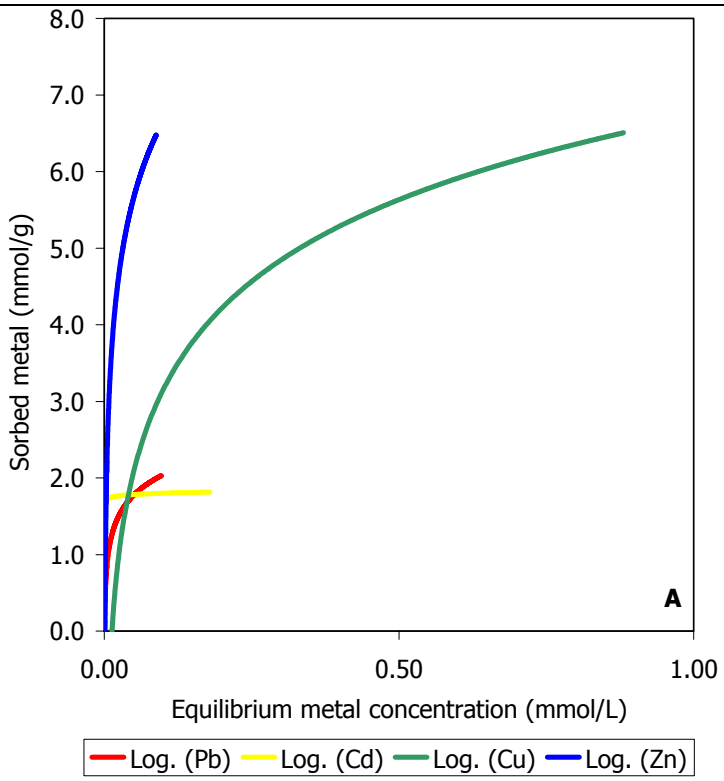
8.0
7.0
6.0
5.0
4.0
3.0
2.0
1.0
0.0
Sorbed metal (mmol/g)
0.00
0.50
1.00
Equilibrium metal concentration (mmol/L)
A
Log. (Pb)
Log. (Cd)
Log. (Cu)
Log. (Zn)

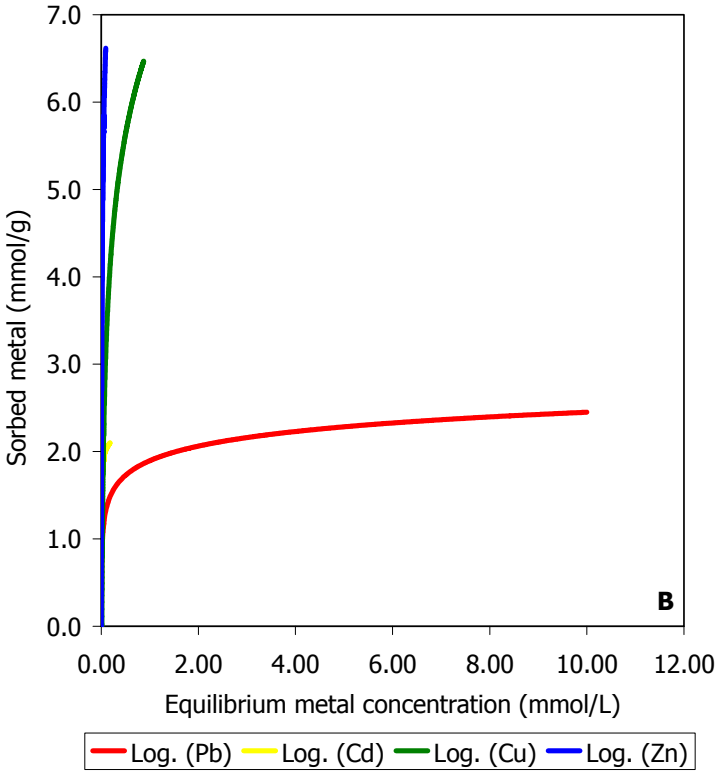
7.0
6.0
5.0
4.0
3.0
2.0
1.0
0.0
Sorbed metal (mmol/g)
0.00
2.00
4.00
6.00
8.00
10.00
12.00
Equilibrium metal concentration (mmol/L)
B
Log. (Pb)
Log. (Cd)
Log. (Cu)
Log. (Zn)

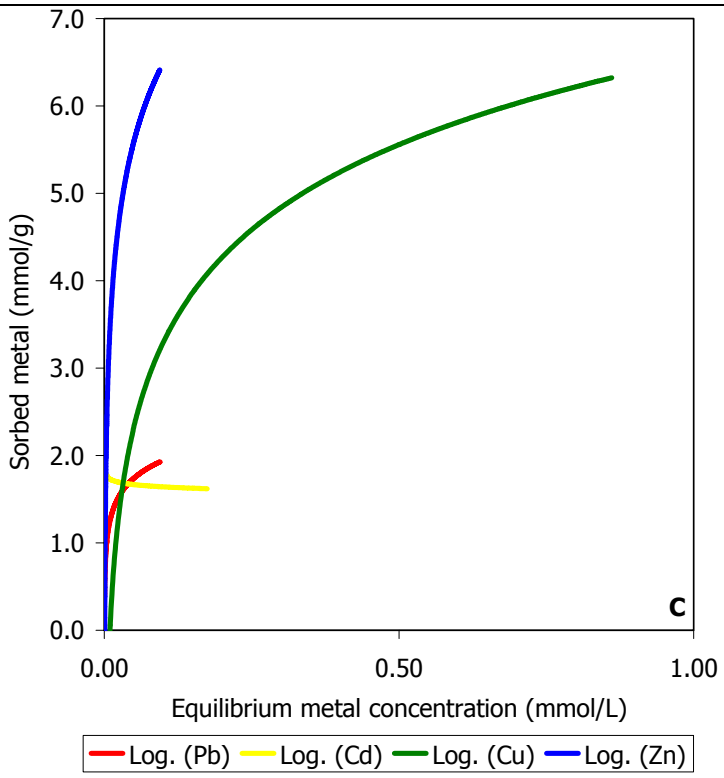

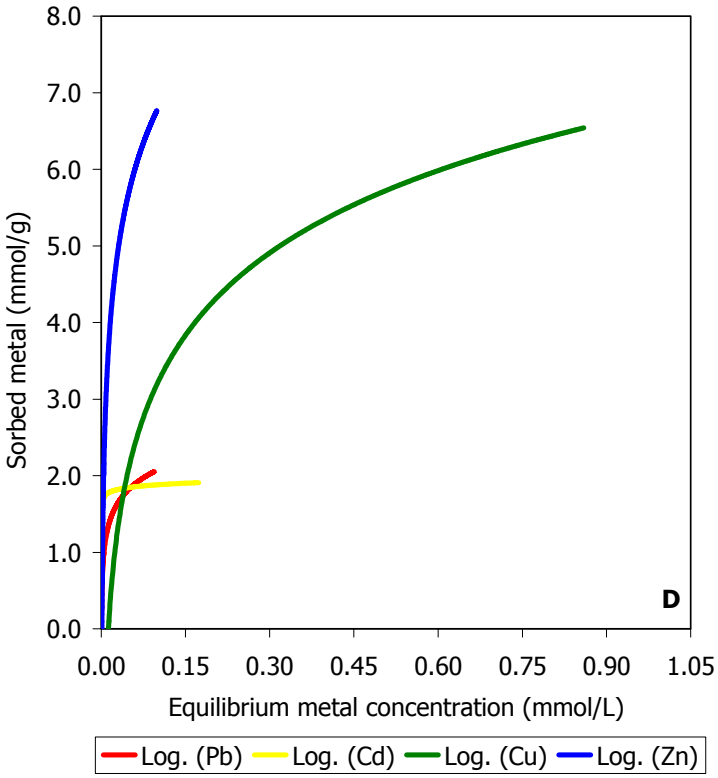

Fig. 16: Sorption isotherms for the multi-metal system where Pb is constant for the four contact times (2h, 4h, 24h and 48h) and vs. 0.2 g HA. Relation between the metal sorbed (mmol/g) and the final concentration (mmol/L) in solution. A: t = 2h; B: t = 4h; C: t = 24h and D: t = 48h. – Fig. 14: Curve isotermiche per il sistema multi-metal in cui Pb è costante per i quattro tempi di contatto (2h, 4h, 24h and

48h) e vs. 0.2 g di HA. Relazione tra il metallo assorbito (mmol/g) e la concentrazione finale (mmol/L) in soluzione. A: t = 2h; B: t = 4h; C: t = 24h and D: t = 48h.

The amount of Ca desorbed at the equilibrium (Fig, 17 A, B, C, D, E, F, G, H and I) (0 – 0.6 mmol/L) is not proportional to the amount of the sorbed metal, suggesting an HA non-stoichiometric dissolution, consequently the possible sorption mechanism is the adsorption and not the precipitation and this is suggested also by P amount (Fig. 18 A, B, C, D, E, F, G, H and I) (0 – 0.1 mmol/L).

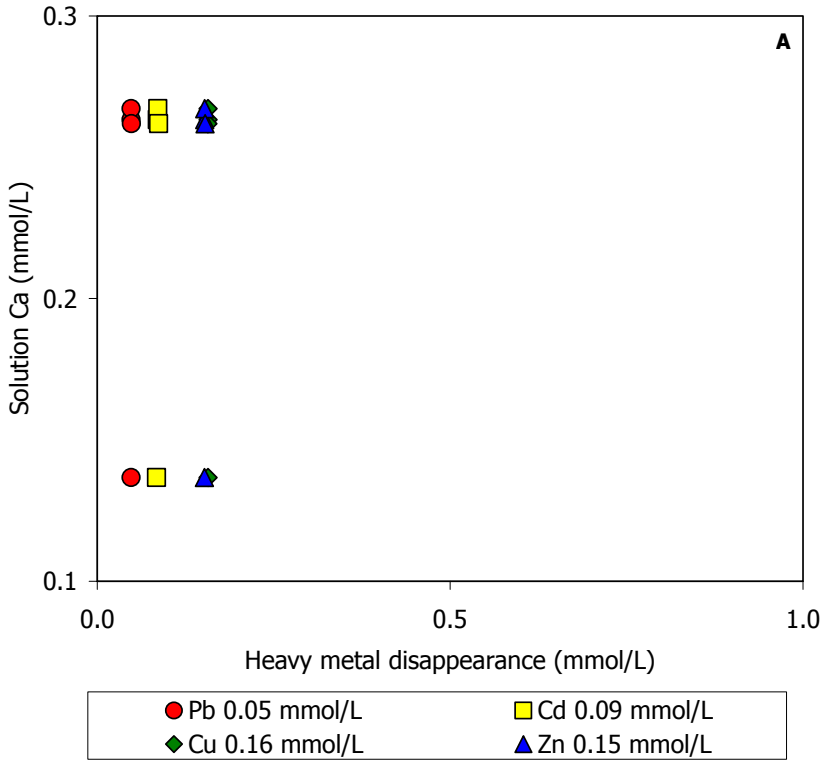

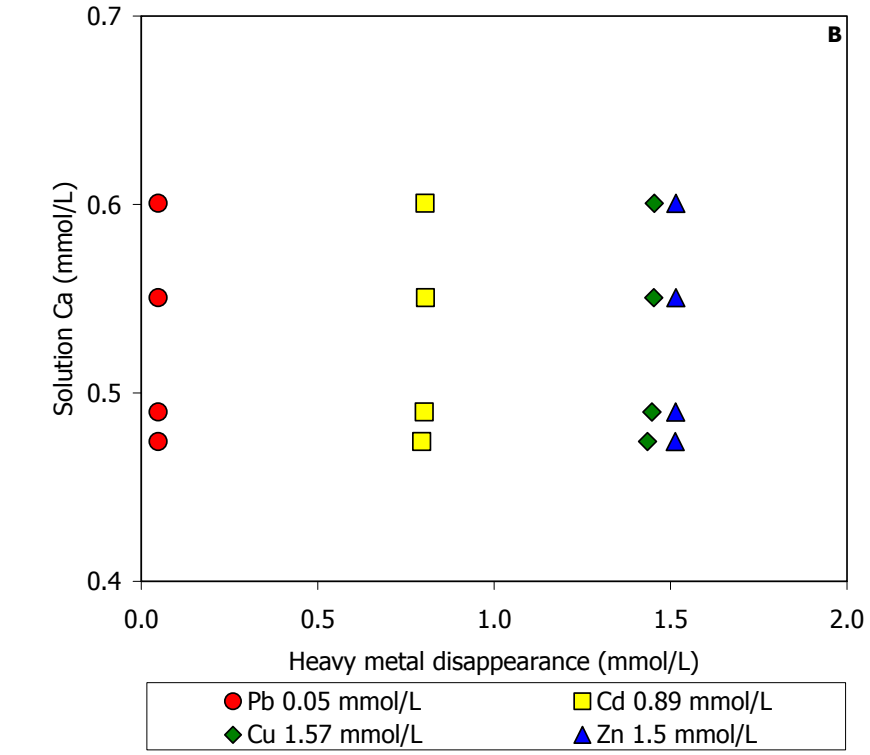
B
0.7
0.6
0.5
0.4
Solution Ca (mmol/L)
0.0
0.5
1.0
1.5
2.0
Heavy metal disappearance (mmol/L)
Pb 0.05 mmol/L
Cd 0.89 mmol/L
Cu 1.57 mmol/L
Zn 1.5 mmol/L

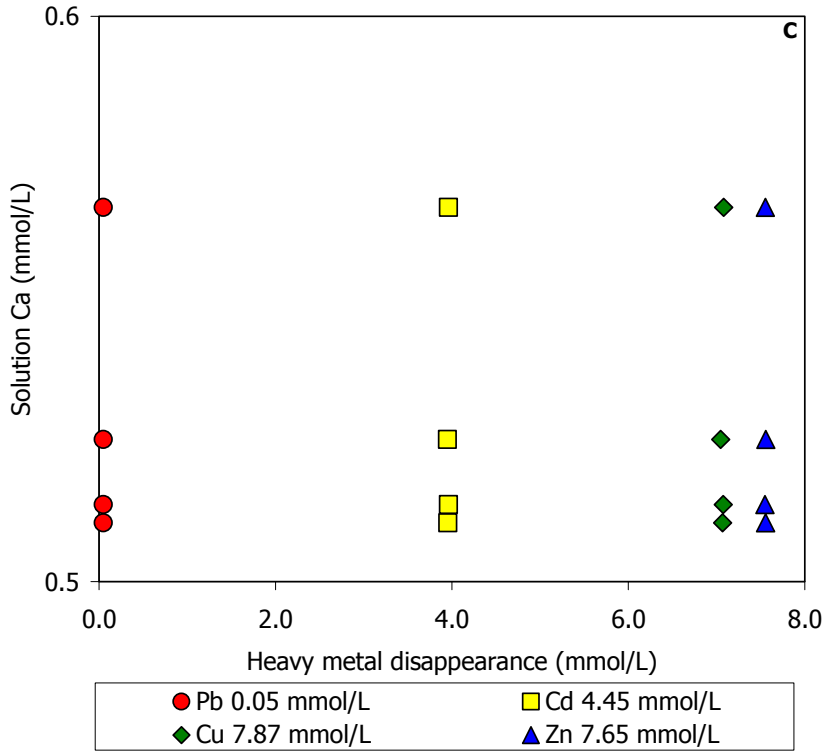
C
0.6
0.5
Solution Ca (mmol/L)
0.0
2.0
4.0
6.0
8.0
Heavy metal disappearance (mmol/L)
Pb 0.05 mmol/L
Cd 4.45 mmol/L
Cu 7.87 mmol/L
Zn 7.65 mmol/L

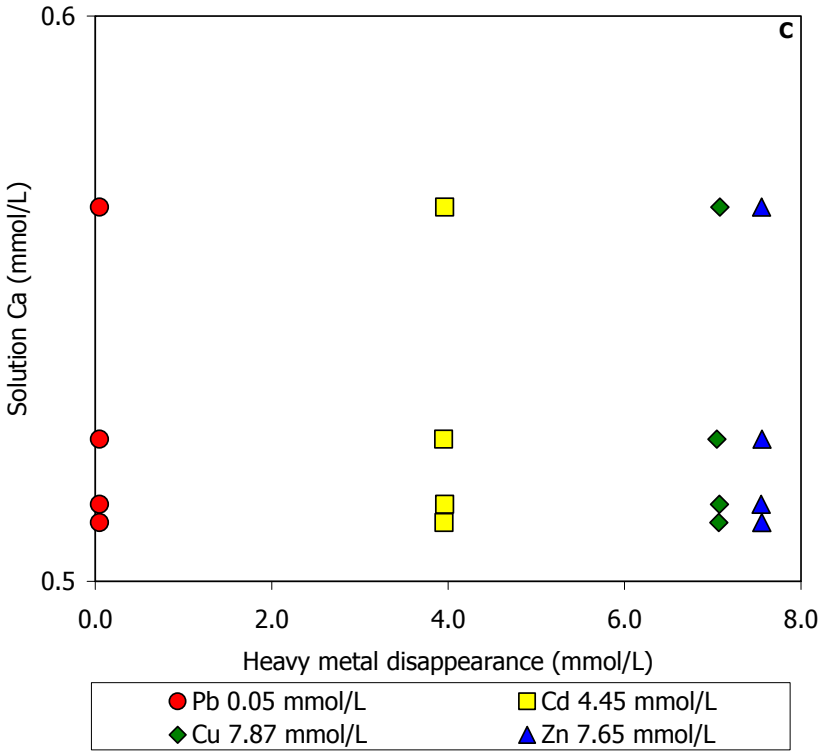
C
0.6
0.5
Solution Ca (mmol/L)
0.0
2.0
4.0
6.0
8.0
Heavy metal disappearance (mmol/L)
Pb 0.05 mmol/L
Cd 4.45 mmol/L
Cu 7.87 mmol/L
Zn 7.65 mmol/L

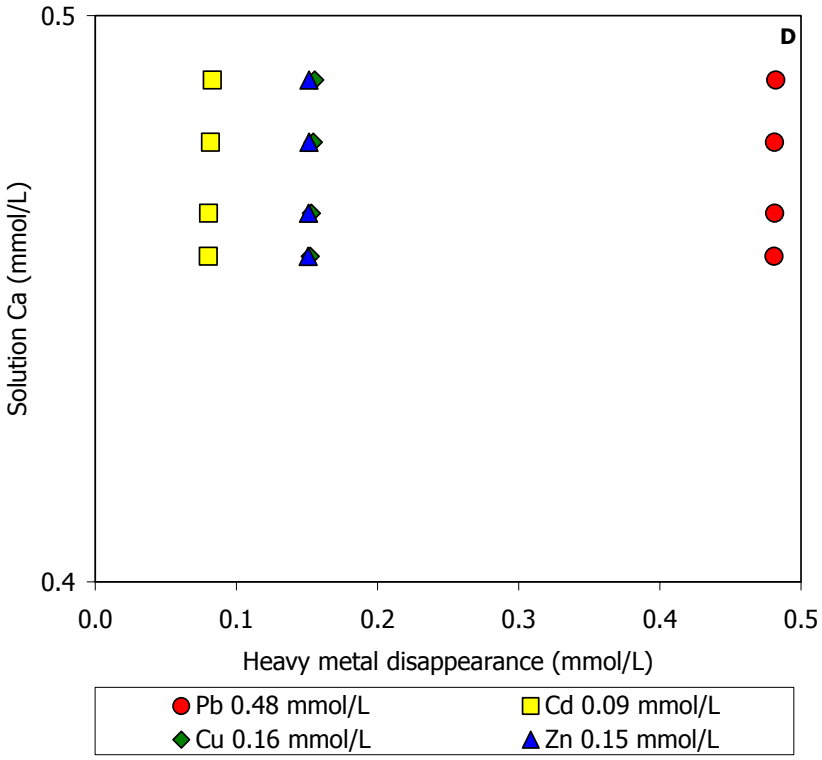
D
0.5
0.4
Solution Ca (mmol/L)
0.0
0.1
0.2
0.3
0.4
0.5
Heavy metal disappearance (mmol/L)
Pb 0.48 mmol/L
Cd 0.09 mmol/L
Cu 0.16 mmol/L
Zn 0.15 mmol/L

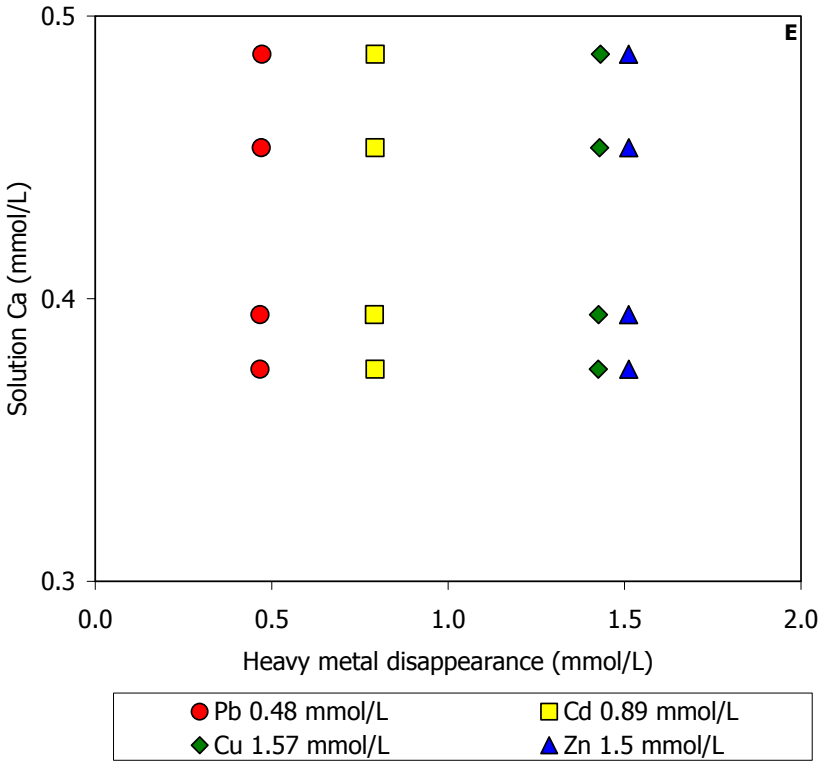
E
0.5
0.4
0.3
Solution Ca (mmol/L)
0.0
0.5
1.0
1.5
2.0
Heavy metal disappearance (mmol/L)
Pb 0.48 mmol/L
Cd 0.89 mmol/L
Cu 1.57 mmol/L
Zn 1.5 mmol/L

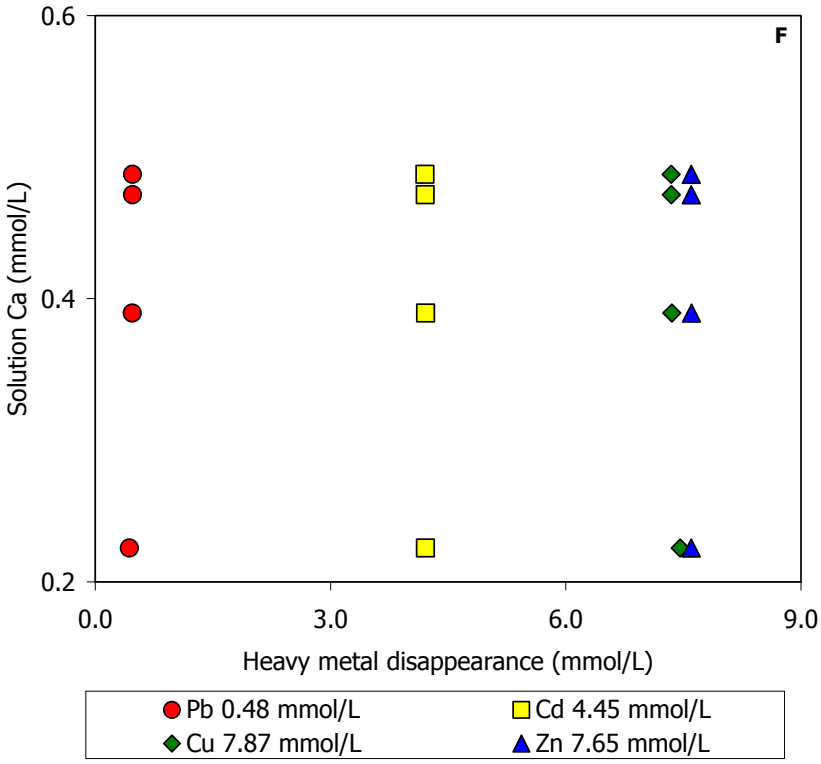
F
0.6
0.4
0.2
Solution Ca (mmol/L)
0.0
3.0
6.0
9.0
Heavy metal disappearance (mmol/L)
Pb 0.48 mmol/L
Cd 4.45 mmol/L
Cu 7.87 mmol/L
Zn 7.65 mmol/L

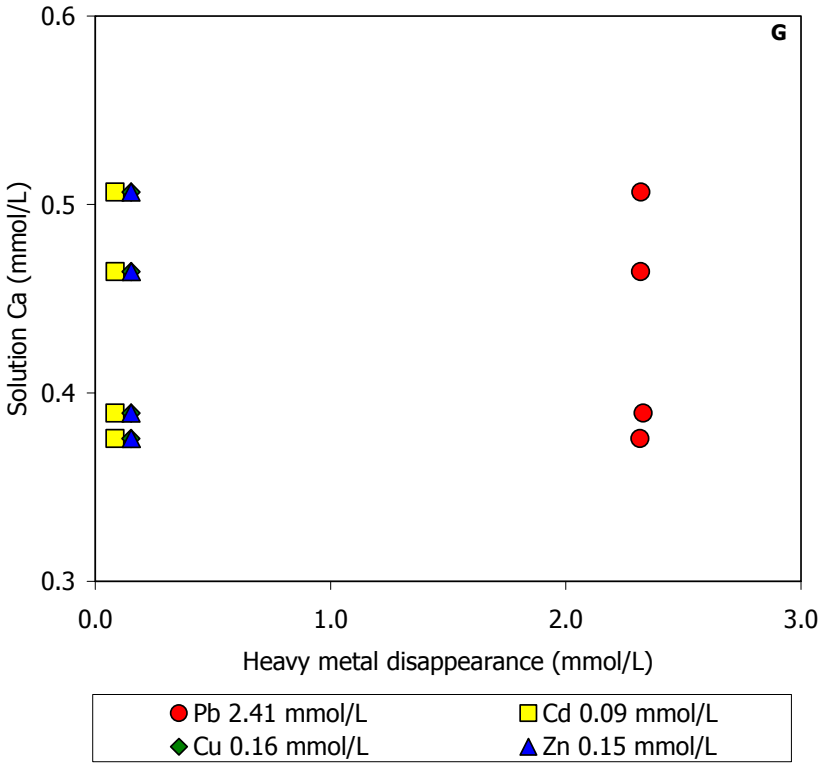
G
0.6
0.5
0.4
0.3
Solution Ca (mmol/L)
0.0
1.0
2.0
3.0
Heavy metal disappearance (mmol/L)
Pb 2.41 mmol/L
Cd 0.09 mmol/L
Cu 0.16 mmol/L
Zn 0.15 mmol/L

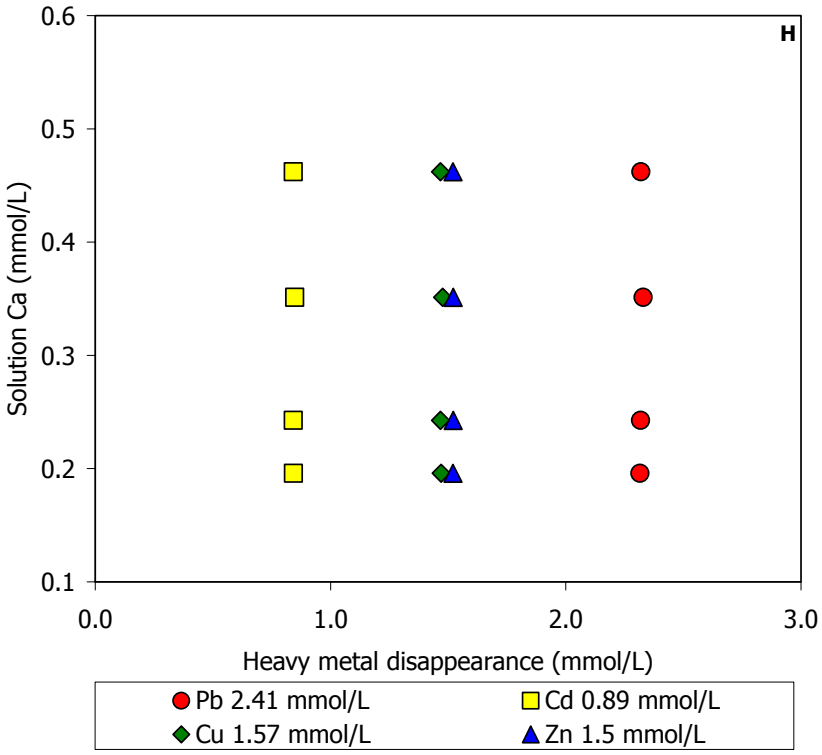
H
0.6
0.5
0.4
0.3
0.2
0.1
Solution Ca (mmol/L)
0.0
1.0
2.0
3.0
Heavy metal disappearance (mmol/L)
Pb 2.41 mmol/L
Cd 0.89 mmol/L
Cu 1.57 mmol/L
Zn 1.5 mmol/L

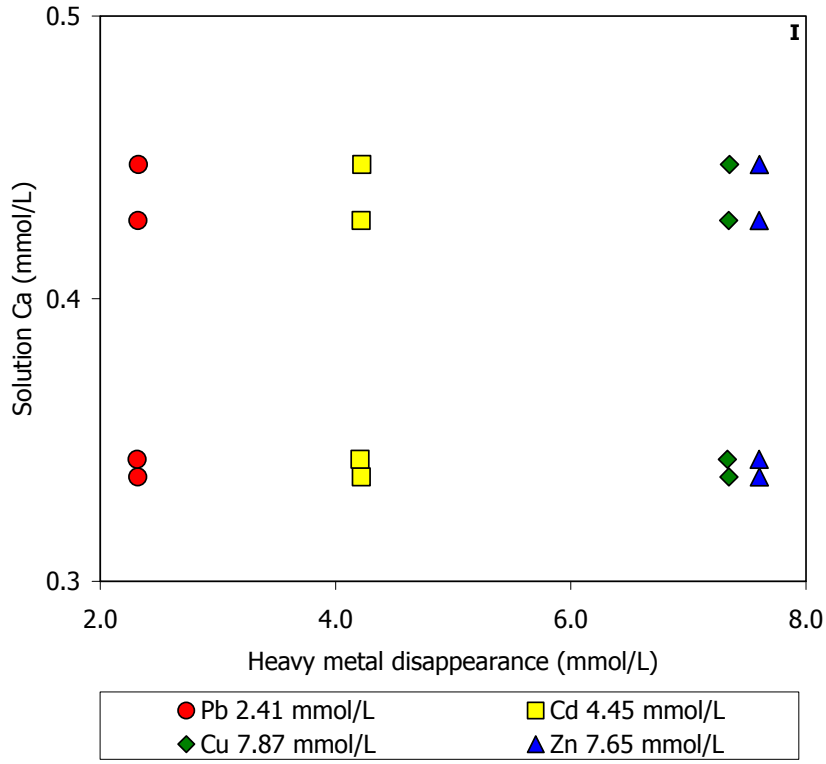

Fig. 17: Relation between Ca in solution (mmol/L) and the amount of heavy metals disappeared (mmol/L) sorbed on HA surface at the equilibrium in a multi-metal system when Pb is constant. Each initial concentration of the multi-metal system is written in the legend. - Fig. 17: Relazione tra il quantitativo di Ca in soluzione (mmol/L) e di ciascun metallo pesante adsorbito (mmol/L) nel sistema multi-metal quando Pb è costante. La concentrazione iniziale di ogni elemento del sistema multi-metal è in leggenda.

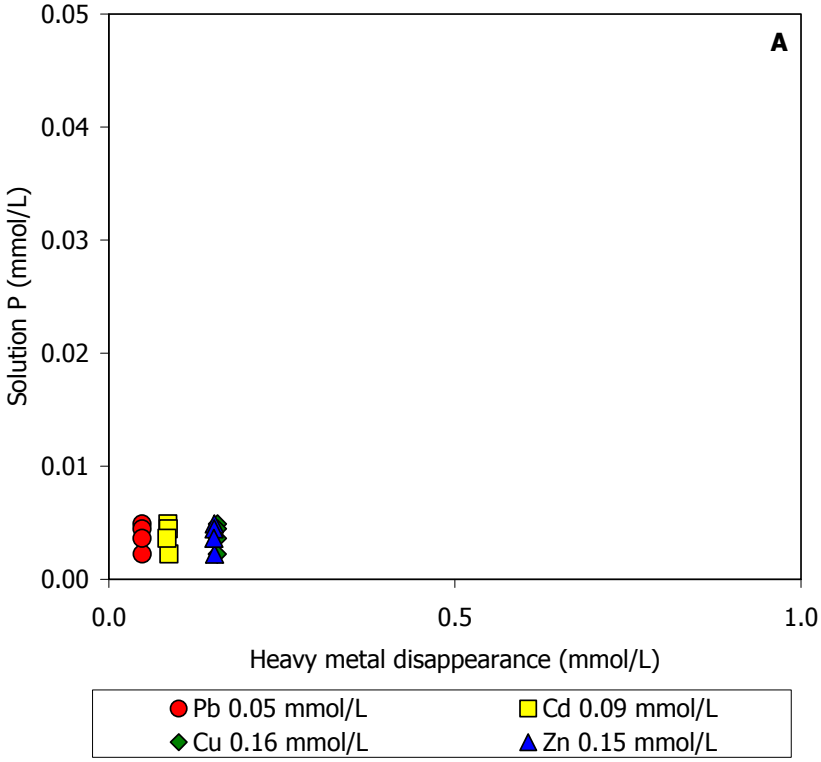
A
0.05
0.04
0.03
0.02
0.01
0.00
Solution P (mmol/L)
0.0
0.5
1.0
Heavy metal disappearance (mmol/L)
Pb 0.05 mmol/L
Cd 0.09 mmol/L
Cu 0.16 mmol/L
Zn 0.15 mmol/L

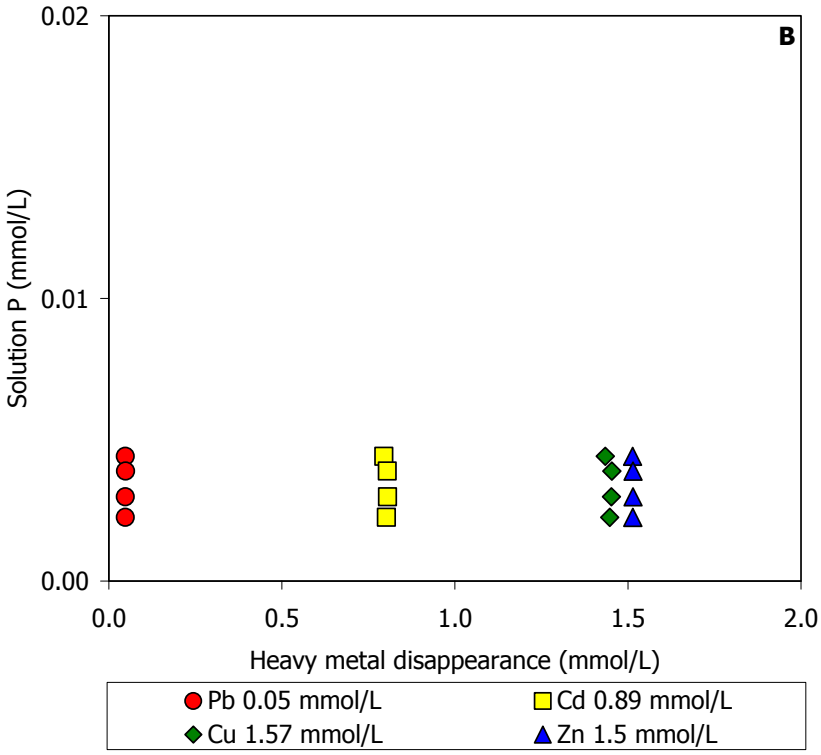
B
0.02
0.01
0.00
Solution P (mmol/L)
0.0
0.5
1.0
1.5
2.0
Heavy metal disappearance (mmol/L)
Pb 0.05 mmol/L
Cd 0.89 mmol/L
Cu 1.57 mmol/L
Zn 1.5 mmol/L

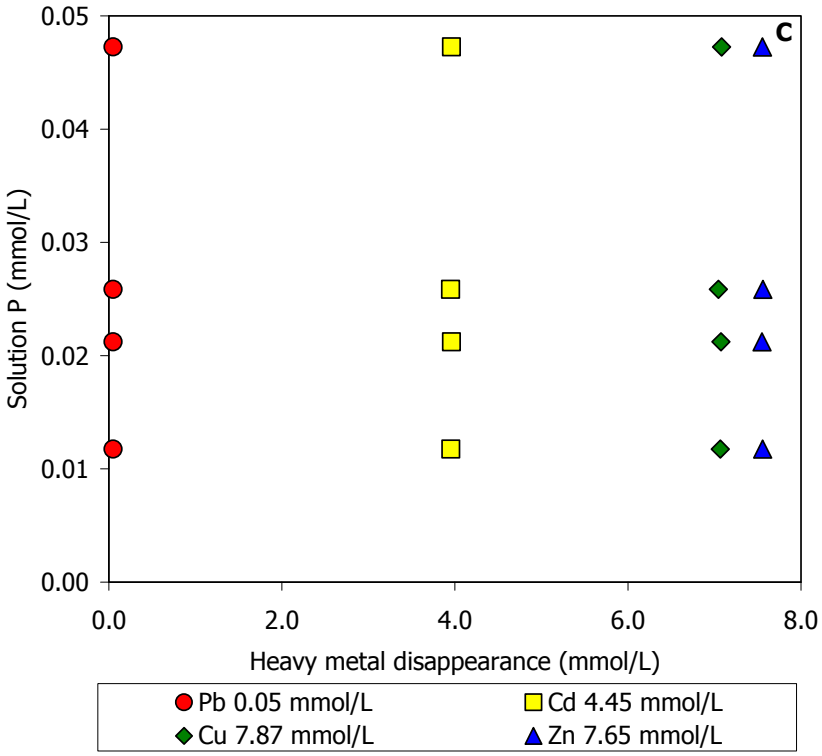
C
0.05
0.04
0.03
0.02
0.01
0.00
Solution P (mmol/L)
0.0
2.0
4.0
6.0
8.0
Heavy metal disappearance (mmol/L)
Pb 0.05 mmol/L
Cd 4.45 mmol/L
Cu 7.87 mmol/L
Zn 7.65 mmol/L

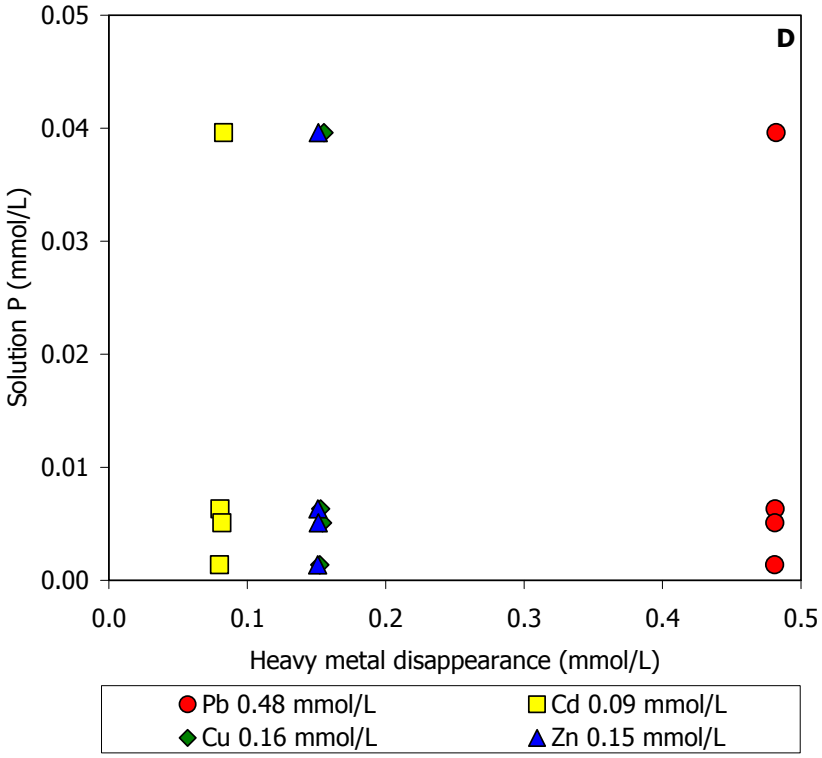
D
0.05
0.04
0.03
0.02
0.01
0.00
Solution P (mmol/L)
0.0
0.1
0.2
0.3
0.4
0.5
Heavy metal disappearance (mmol/L)
Pb 0.48 mmol/L
Cd 0.09 mmol/L
Cu 0.16 mmol/L
Zn 0.15 mmol/L

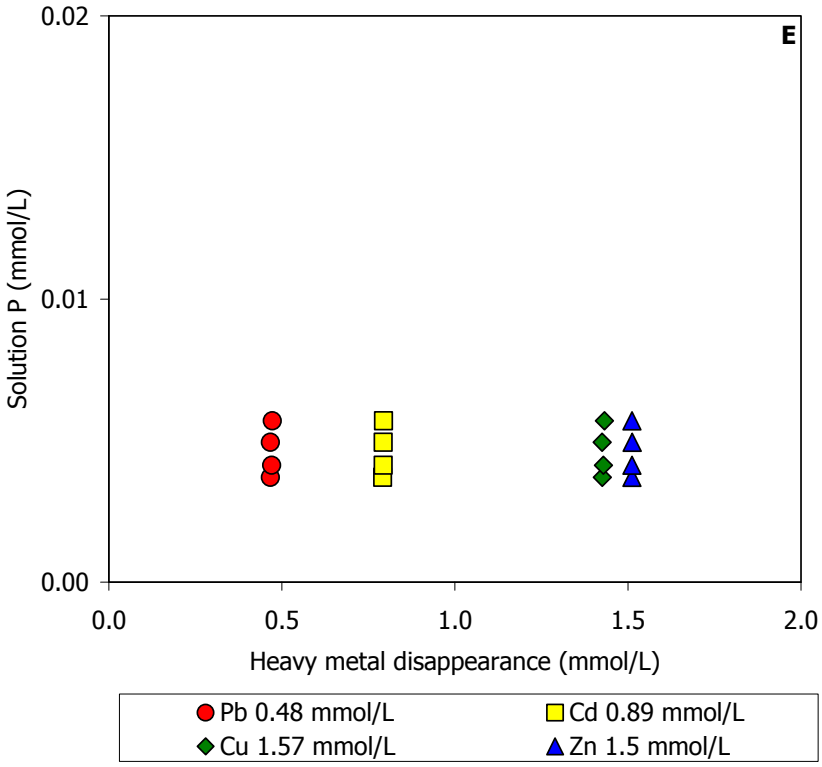
E
0.02
0.01
0.00
Solution P (mmol/L)
0.0
0.5
1.0
1.5
2.0
Heavy metal disappearance (mmol/L)
Pb 0.48 mmol/L
Cd 0.89 mmol/L
Cu 1.57 mmol/L
Zn 1.5 mmol/L

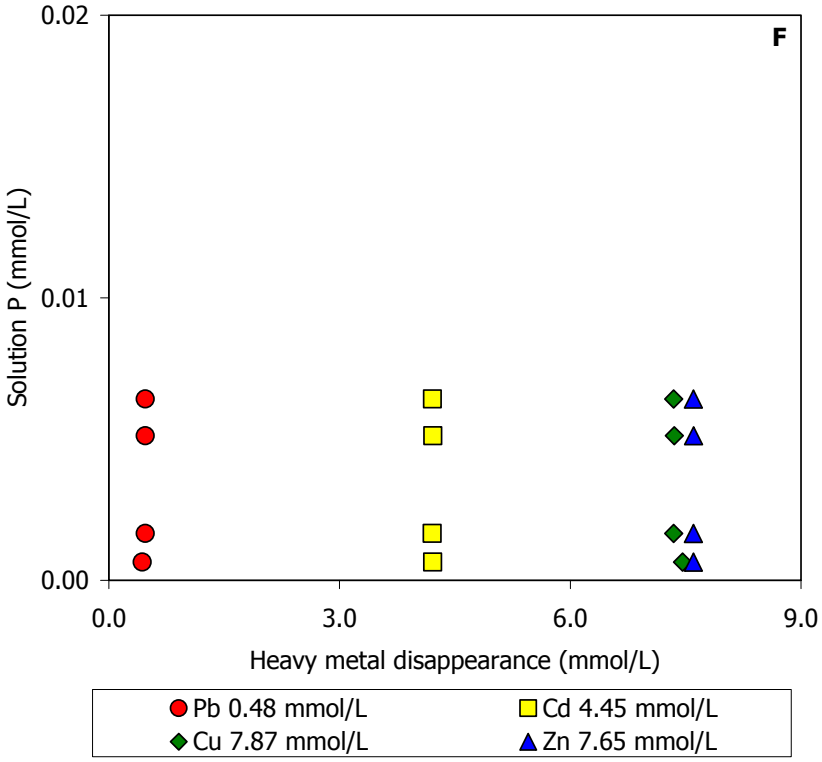
F
0.02
0.01
0.00
Solution P (mmol/L)
0.0
3.0
6.0
9.0
Heavy metal disappearance (mmol/L)
Pb 0.48 mmol/L
Cd 4.45 mmol/L
Cu 7.87 mmol/L
Zn 7.65 mmol/L

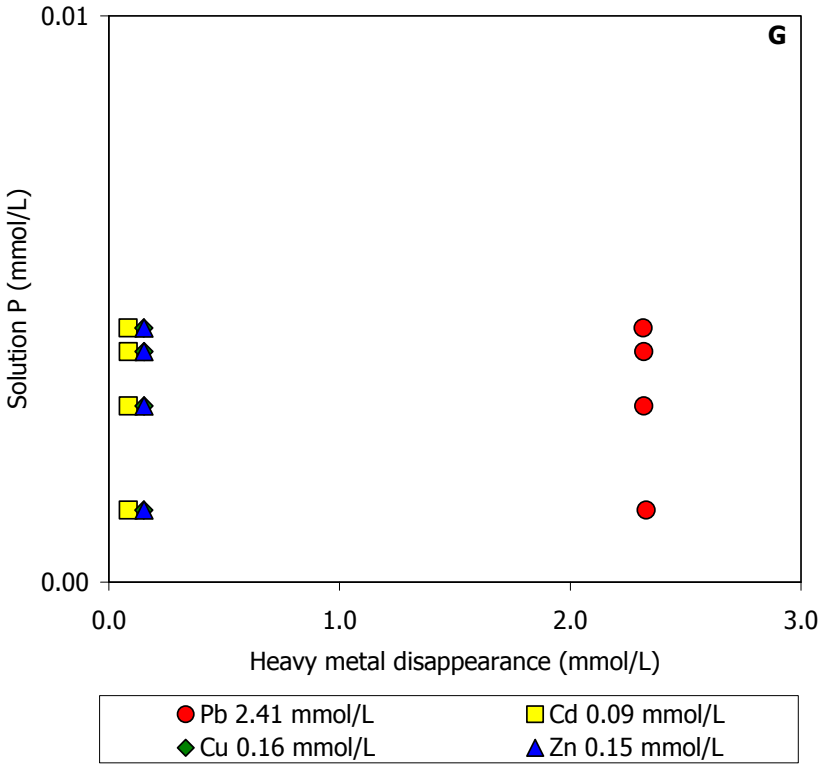
G
0.01
0.00
Solution P (mmol/L)
0.0
1.0
2.0
3.0
Heavy metal disappearance (mmol/L)
Pb 2.41 mmol/L
Cd 0.09 mmol/L
Cu 0.16 mmol/L
Zn 0.15 mmol/L

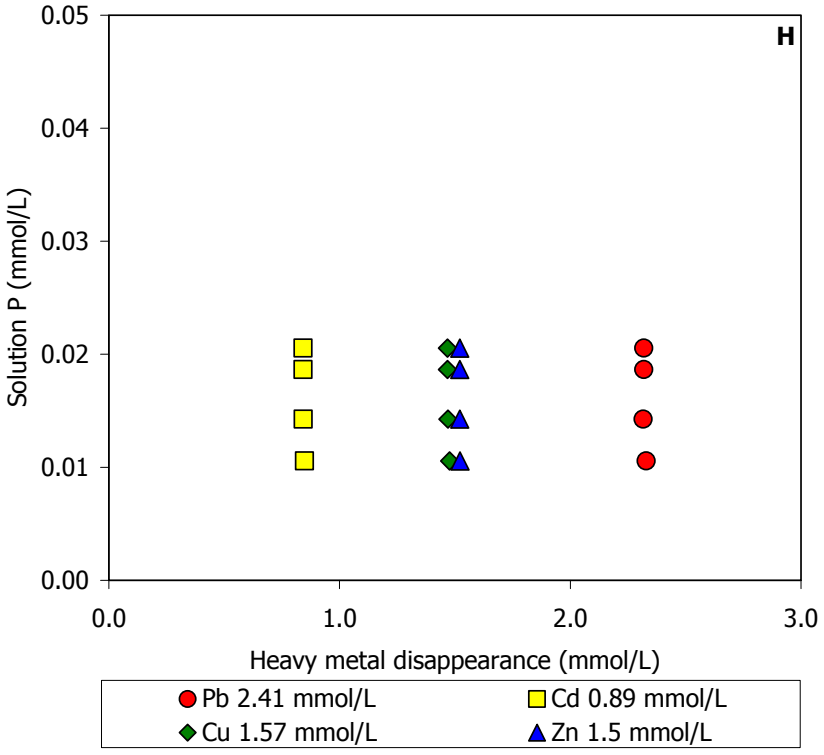
H
0.05
0.04
0.03
0.02
0.01
0.00
Solution P (mmol/L)
0.0
1.0
2.0
3.0
Heavy metal disappearance (mmol/L)
Pb 2.41 mmol/L
Cd 0.89 mmol/L
Cu 1.57 mmol/L
Zn 1.5 mmol/L

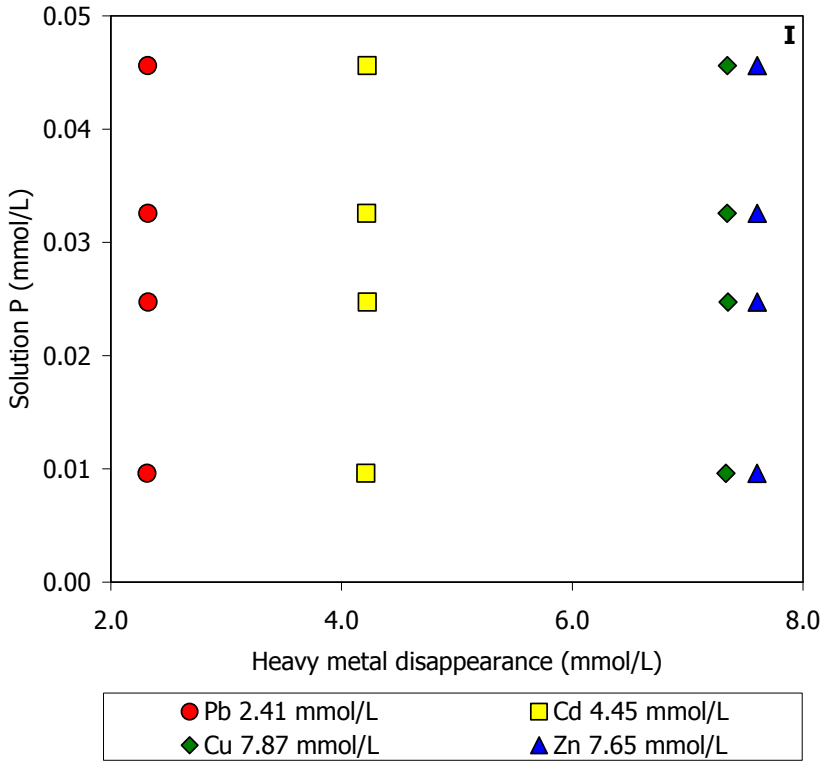

Fig. 18: Relation between P in solution (mmol/L) and the amount of disappeared heavy metals (mmol/L) sorbed on HA surface at the equilibrium in a multi-metal system when Pb is constant. Each initial concentration of the multi-metal system is written in the legend. - Fig. 18: Relazione tra il quantitativo di P in soluzione (mmol/L) e di ciascun metallo pesante adsorbito (mmol/L) nel sistema multi-metal quando Pb è costante. La concentrazione iniziale di ogni elemento del sistema multi-metal è in leggenda.

The immobilization efficiency in the system, where Zn is the constant metal, is comparable to previous three systems (Tab. 8) and the immobilization order is Pb > Zn > Cu > Cd, as in the other systems. Each heavy metal is well immobilized (Fig. 19 A, B, C, D, E and F). The only exception was found for Cu when metals have a concentration of 10 mg/L and Zn a concentration of 500 mg/L. In this case, Cu was blocked for 85% for t = 4h and 24h, whereas the other metals usually show an immobilization efficiency higher than 95%.

Cd = 10 mg/L	Cu = 10 mg/L	Pb = 10 mg/L	Zn = 100 mg/L
99.456	99.634	99.817	9.968
99.472	99.645	99.806	9.969
99.477	99.655	99.847	9.969
99.477	99.634	99.676	9.970
Cd = 500 mg/L	Cu = 500 mg/L	Pb = 500 mg/L	Zn = 100 mg/L
497.296	498.066	497.819	9.970
497.390	498.124	497.881	9.969
497.510	498.215	498.024	9.969
497.136	497.952	497.506	9.967
Cd = 10 mg/L	Cu = 10 mg/L	Pb = 10 mg/L	Zn = 100 mg/L
2.838	9.926	9.985	99.943
3.357	9.913	9.966	99.957
3.650	9.930	9.943	99.939
5.014	9.970	9.979	99.958
Cd = 500 mg/L	Cu = 500 mg/L	Pb = 500 mg/L	Zn = 100 mg/L
497.438	498.089	498.081	99.936
497.400	498.082	498.070	99.934
497.395	498.058	498.073	99.934
497.295	497.973	497.796	99.963
Cd = 10 mg/L	Cu = 10 mg/L	Pb = 10 mg/L	Zn = 500 mg/L
9.973	9.991	9.977	499.781
9.977	9.992	9.983	499.895
9.993	9.999	9.994	499.848
9.973	9.983	9.998	499.911
Cd = 100 mg/L	Cu = 100 mg/L	Pb = 100 mg/L	Zn = 500 mg/L
99.488	99.648	99.855	499.744
99.513	99.667	99.892	499.742
99.524	99.679	99.909	499.744

Table 8: Efficiency values for the multi - metal system when Zn has a constant concentration.

Tabella 8: Valori dell'efficienza nell'immobilizzare i metalli pesanti per il sistema multi-metal in cui lo Zn mantiene costante la concentrazione.

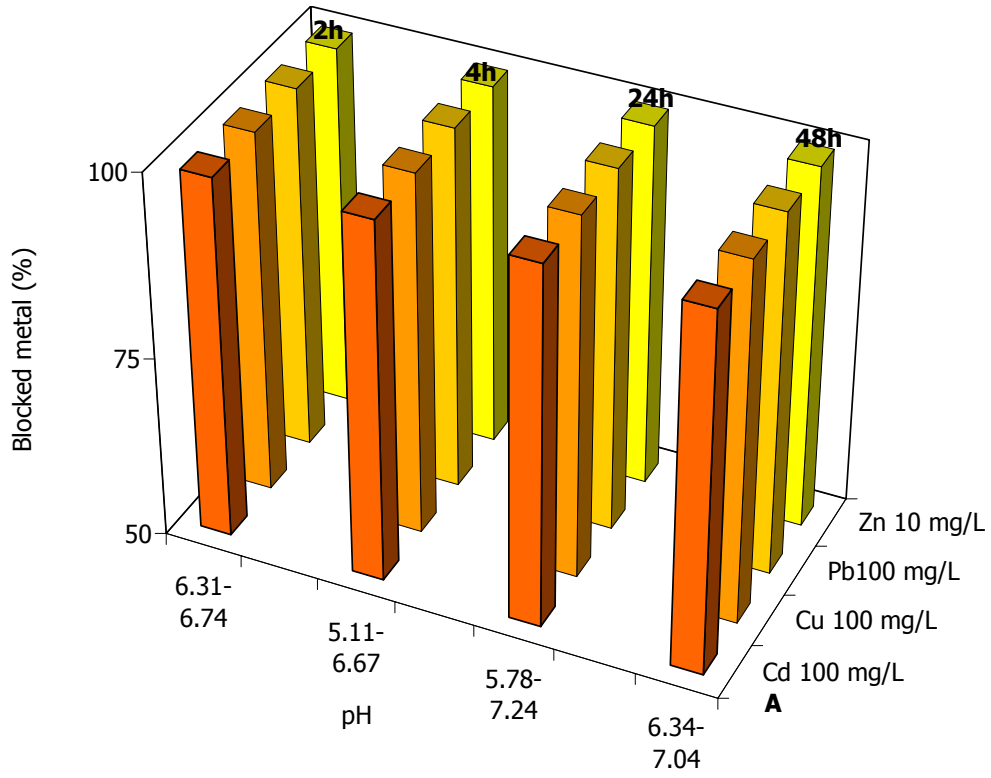
2h
4h
24h
48h
100
75
50
Blocked metal (%)
6.31-
6.74
5.11-
6.67
5.78-
7.24
6.34-
7.04
pH
Zn 10 mg/L
Pb100 mg/L
Cu 100 mg/L
Cd 100 mg/L
A

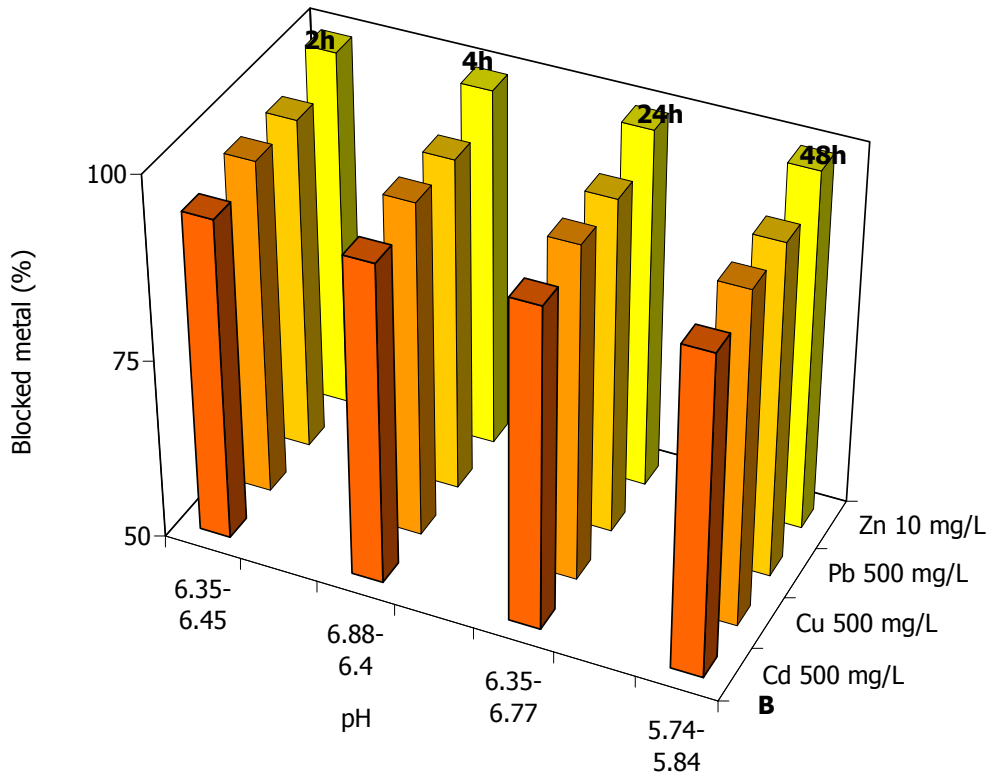
2h
4h
24h
48h
100
75
50
Blocked metal (%)
6.35-
6.45
6.88-
6.4
6.35-
6.77
5.74-
5.84
pH
Zn 10 mg/L
Pb 500 mg/L
Cu 500 mg/L
Cd 500 mg/L
B

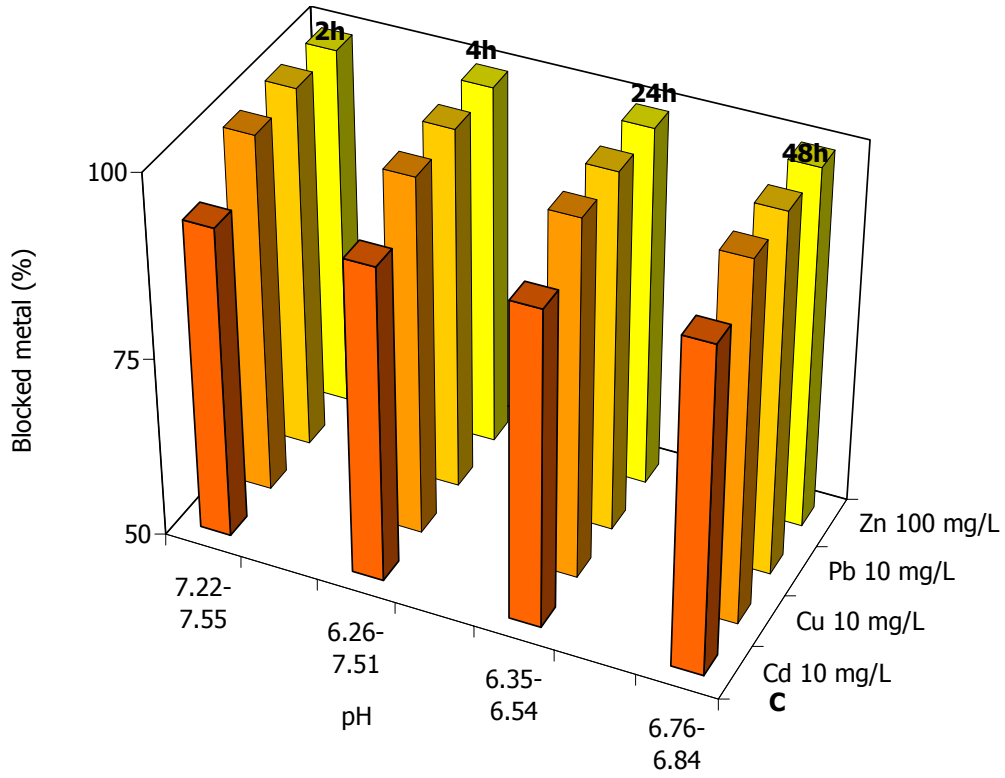
2h
4h
24h
48h
100
75
50
Blocked metal (%)
7.22-
7.55
6.26-
7.51
6.35-
6.54
6.76-
6.84
pH
Zn 100 mg/L
Pb 10 mg/L
Cu 10 mg/L
Cd 10 mg/L
C

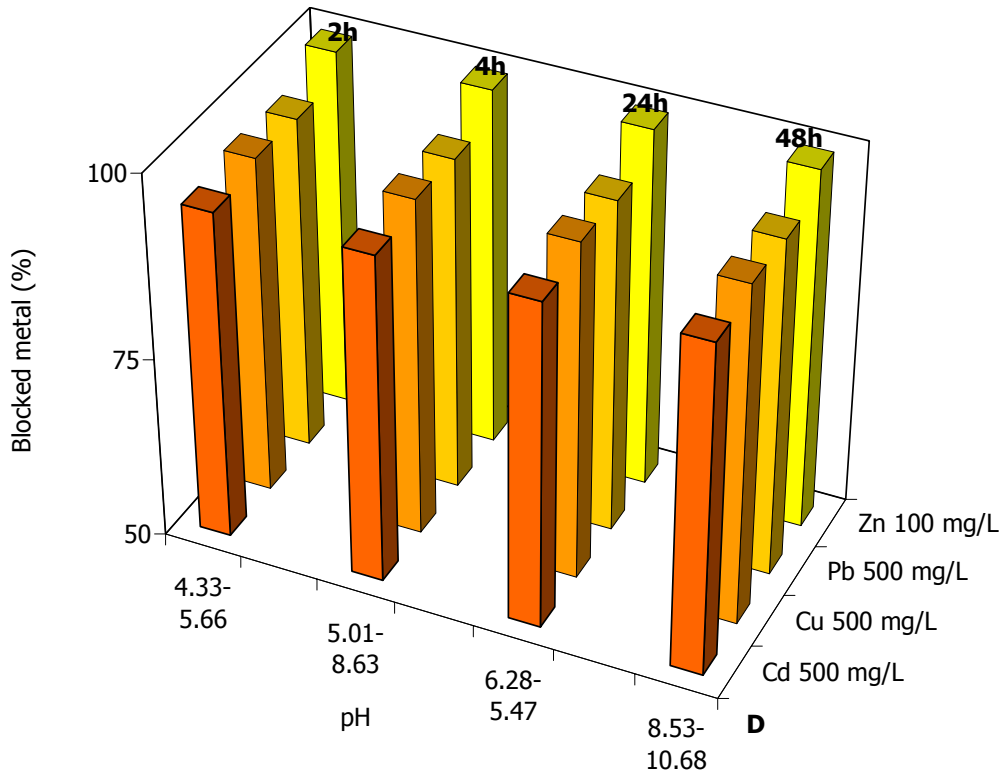
2h
4h
24h
48h
100
75
50
Blocked metal (%)
4.33-
5.66
5.01-
8.63
6.28-
5.47
8.53-
10.68
pH
Zn 100 mg/L
Pb 500 mg/L
Cu 500 mg/L
Cd 500 mg/L
D

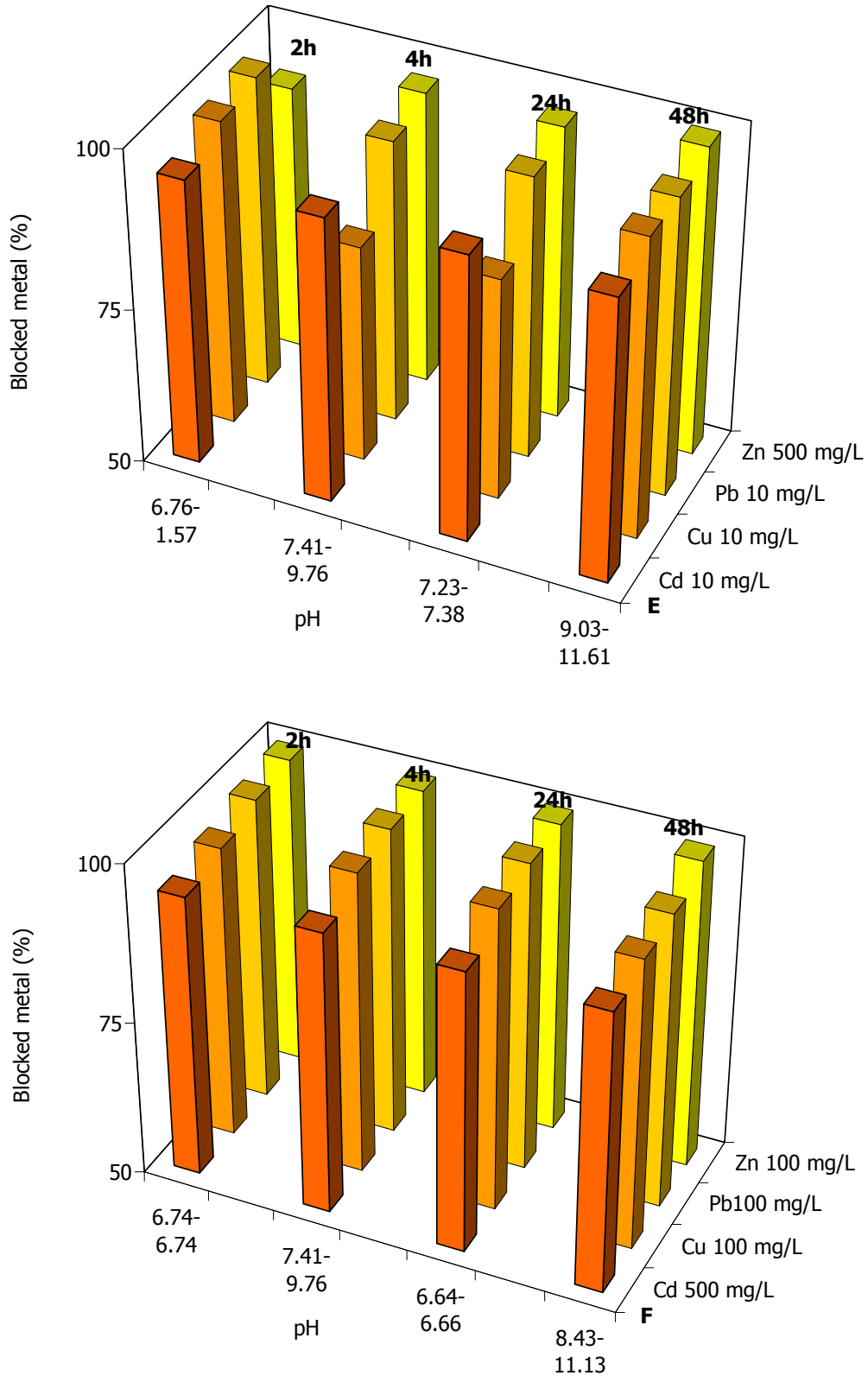

Fig. 19: Variation of the amount of blocked metal with time for the mass of HA (0.2 g) in the multi-metal system where Zn is constant.. – Fig. 19: Variazione delle percentuali dei metalli immobilizzati in funzione del tempo di interazione per la quantità di HA (0.2 g) nel sistema multi-metal in cui Zn è l'elemento costante.

Q_S values are solely < 1 as in the other systems, suggesting the precipitation of new phase of phosphates (Table 9). This mechanism is suggested also by the sorption isotherms (Fig. 20 A, B, C and D) which are always vertical, that is H type. The only exception is Zn for t = 2h which shows an isotherm of L2 type meaning an adsorption mechanism.

Cd = 100 mg/L	Cu = 100 mg/L	Pb = 100 mg/L	Zn = 10 mg/L
0.0159	0.0190	0.0029	0.0016
0.0159	0.0189	0.0032	0.0016
0.0137	0.0160	0.0022	0.0014
0.0132	0.0163	0.0044	0.0013
Cd = 500 mg/L	Cu = 500 mg/L	Pb =500 mg/L	Zn = 10 mg/L
0.0903	0.1143	0.0395	0.0018
0.0873	0.1110	0.0385	0.0018
0.0755	0.0958	0.0325	0.0016
0.0723	0.0915	0.0342	0.0014
Cd = 10 mg/L	Cu = 10 mg/L	Pb = 10 mg/L	Zn = 100 mg/L
0.0252	0.0005	0.0000	0.0003
0.0193	0.0004	0.0001	0.0002
0.0184	0.0004	0.0001	0.0003
0.0136	0.0001	0.0000	0.0002
Cd = 500 mg/L	Cu = 500 mg/L	Pb =500 mg/L	Zn = 100 mg/L
0.0038	0.0050	0.0015	0.0002
0.0036	0.0047	0.0014	0.0002
0.0031	0.0041	0.0013	0.0001
0.0031	0.0042	0.0014	0.0001
Cd = 10 mg/L	Cu = 10 mg/L	Pb = 10 mg/L	Zn = 500 mg/L
0.00005	0.00003	0.00002	0.0006
0.00003	0.00002	0.00001	0.0003
0.00001	0.000002	0.000004	0.0003
0.00004	0.00004	0.000002	0.0002
Cd = 100 mg/L	Cu = 100 mg/L	Pb = 100 mg/L	Zn = 500 mg/L
0.0150	0.0182	0.0023	0.0129
0.0119	0.0144	0.0014	0.0108
0.0105	0.0125	0.0011	0.0097
0.0111	0.0140	0.0032	0.0102

Table 9: Q_S values for the multi - metal systems when Zn has a constant concentration. Tabella 9: Valori di Q_S per i sistemi multi-metal nei quali la concentrazione di Zn è stata mantenuta costante.

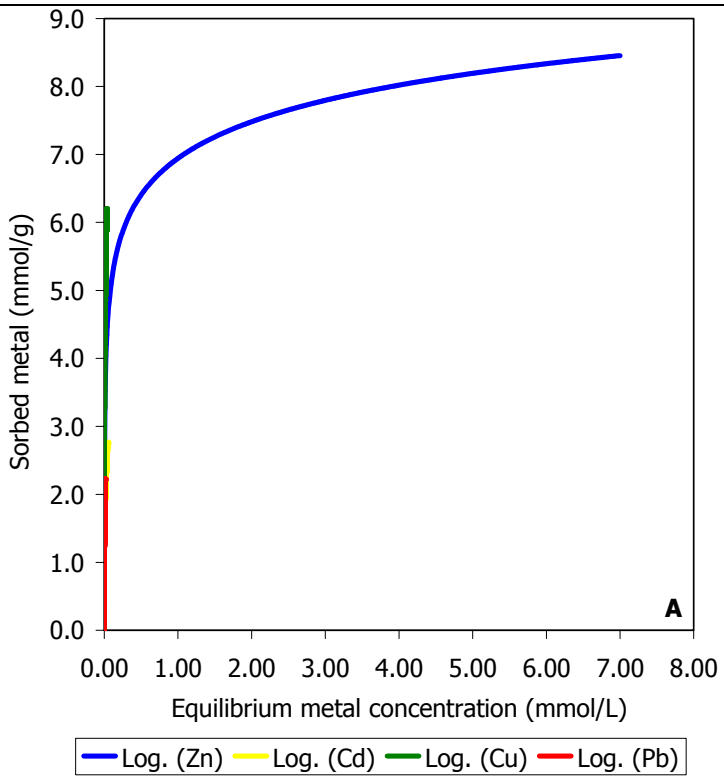
9.0
8.0
7.0
6.0
5.0
4.0
3.0
2.0
1.0
0.0
Sorbed metal (mmol/g)
A
0.00
1.00
2.00
3.00
4.00
5.00
6.00
7.00
8.00
Equilibrium metal concentration (mmol/L)
Log. (Zn)
Log. (Cd)
Log. (Cu)
Log. (Pb)

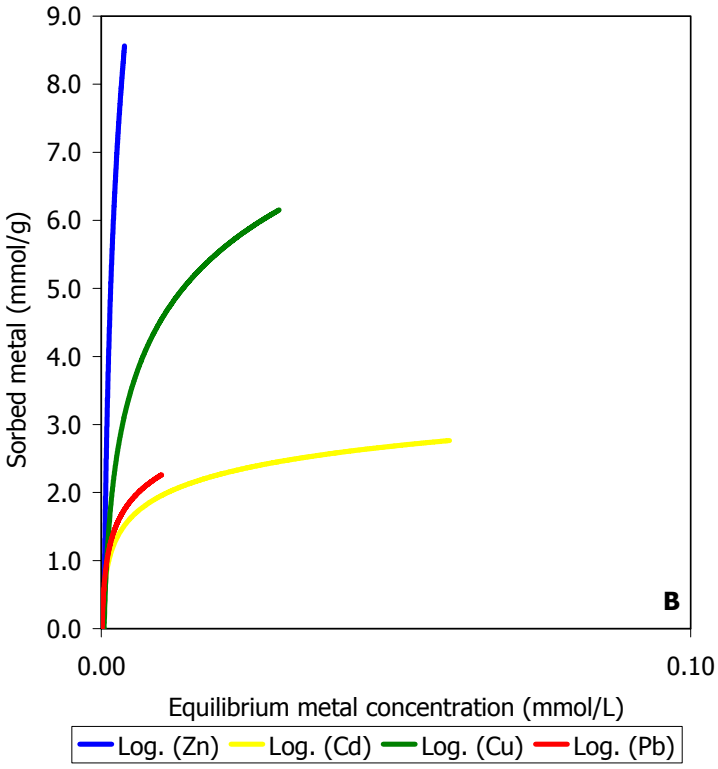
9.0
8.0
7.0
6.0
5.0
4.0
3.0
2.0
1.0
0.0
Sorbed metal (mmol/g)
B
0.00
0.10
Equilibrium metal concentration (mmol/L)
Log. (Zn)
Log. (Cd)
Log. (Cu)
Log. (Pb)

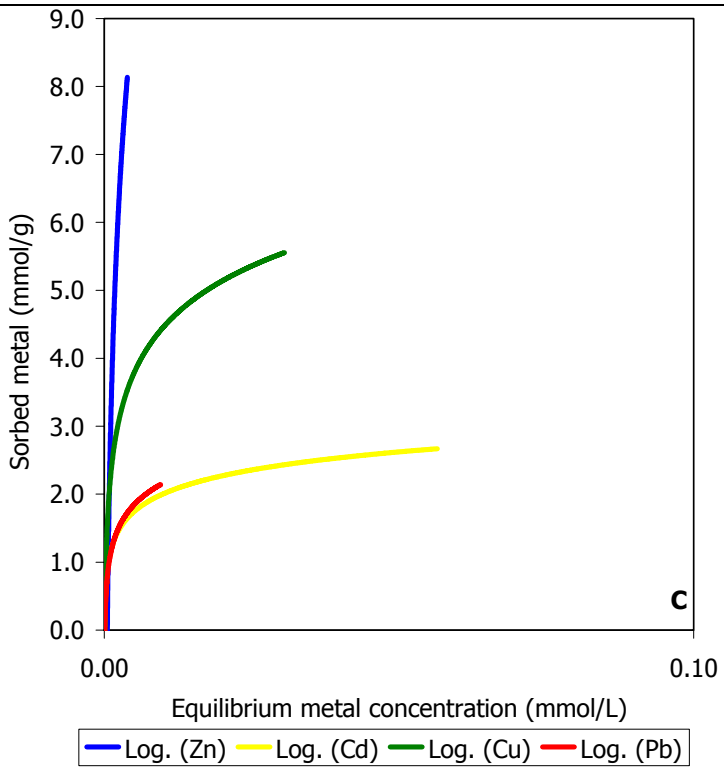

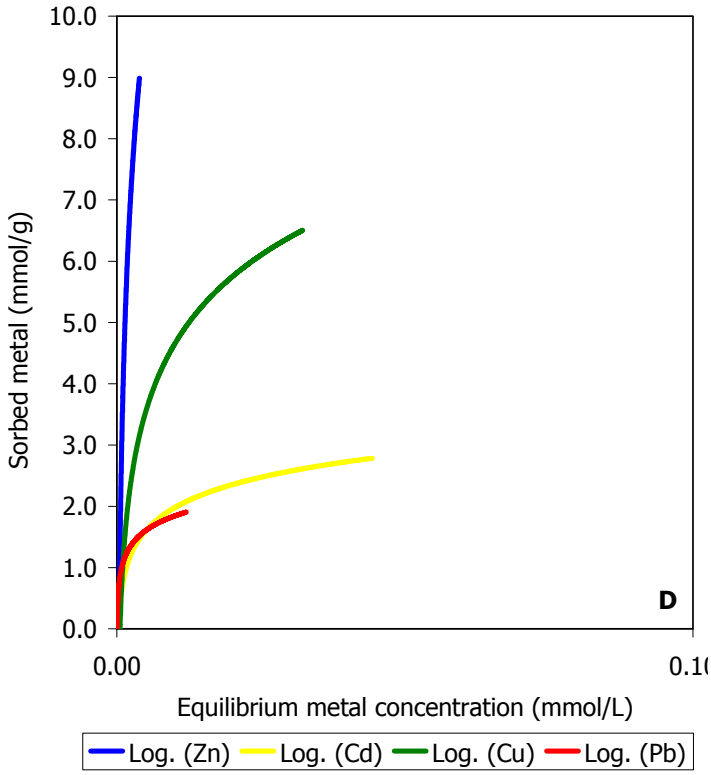

Fig. 20: Sorption isotherms for the multi-metal system where Zn is constant for the four contact times (2h, 4h, 24h and 48h) and vs. 0.2 g HA. Relation between the metal sorbed (mmol/g) and the final concentration (mmol/L) in solution. A: t = 2h; B: t = 4h; C: t = 24h and D: t = 48h. – Fig. 20: Curve isotermiche per il sistema multi-metal in cui Zn è costante per i quattro tempi di contatto (2h, 4h, 24h and

48h) e vs. 0.2 g di HA. Relazione tra il metallo assorbito (mmol/g) e la concentrazione finale (mmol/L) in soluzione. A: t = 2h; B: t = 4h; C: t = 24h and D: t = 48h.

The amount of desorbed Ca shows two behaviors (Fig. 21 A, B, C, D, E and F), the first one indicates a non stoichiometric dissolution and the second one a stoichiometric dissolution, so that sorption mechanism are the adsorption and the precipitation. The amount of P desorbed further support these behaviors (Fig. 22).

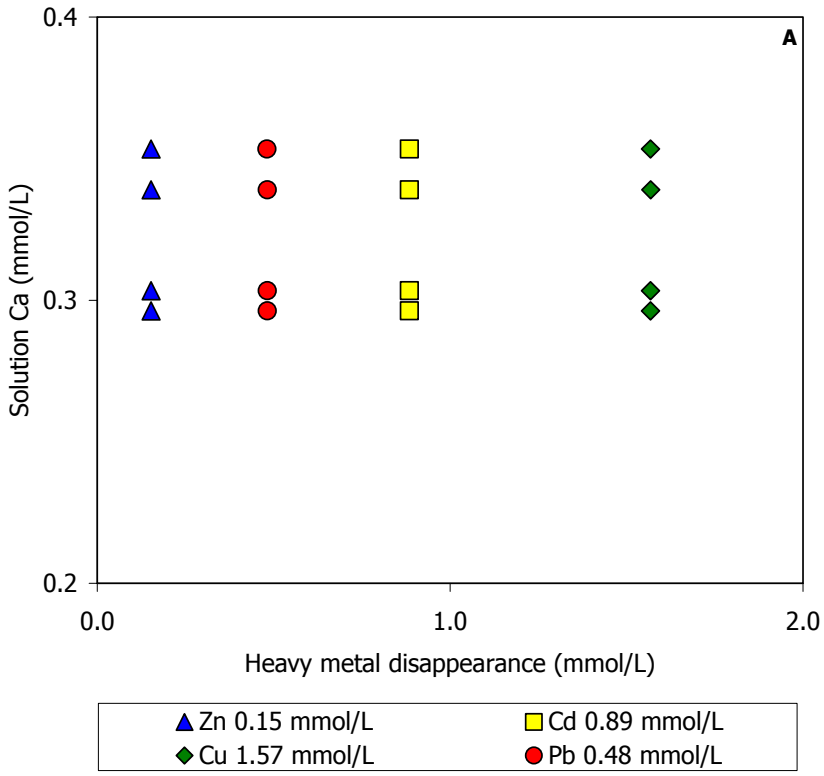

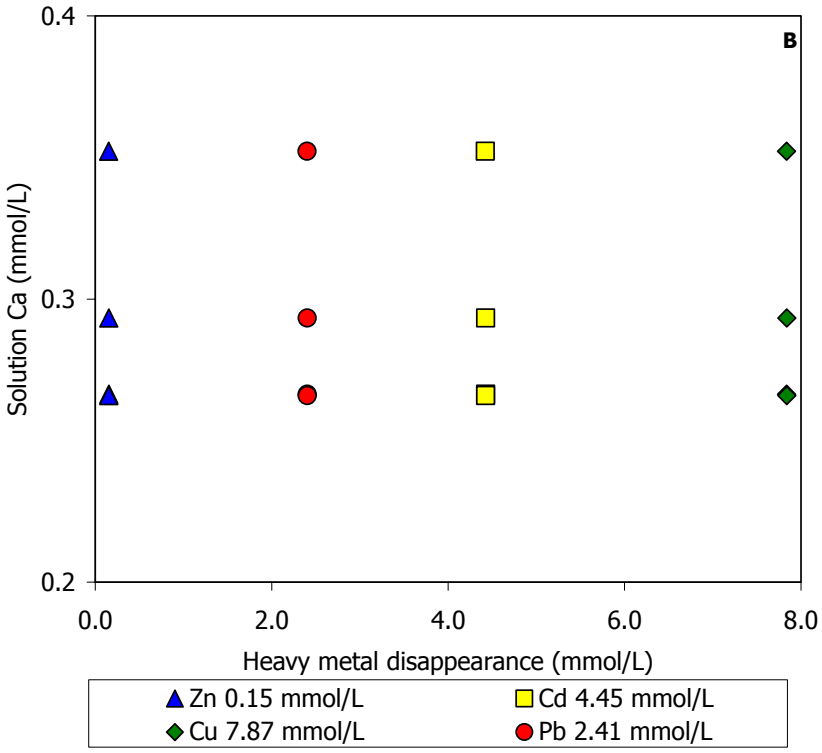
B
0.4
0.3
0.2
Solution Ca (mmol/L)
0.0
2.0
4.0
6.0
8.0
Heavy metal disappearance (mmol/L)
Zn 0.15 mmol/L
Cd 4.45 mmol/L
Cu 7.87 mmol/L
Pb 2.41 mmol/L

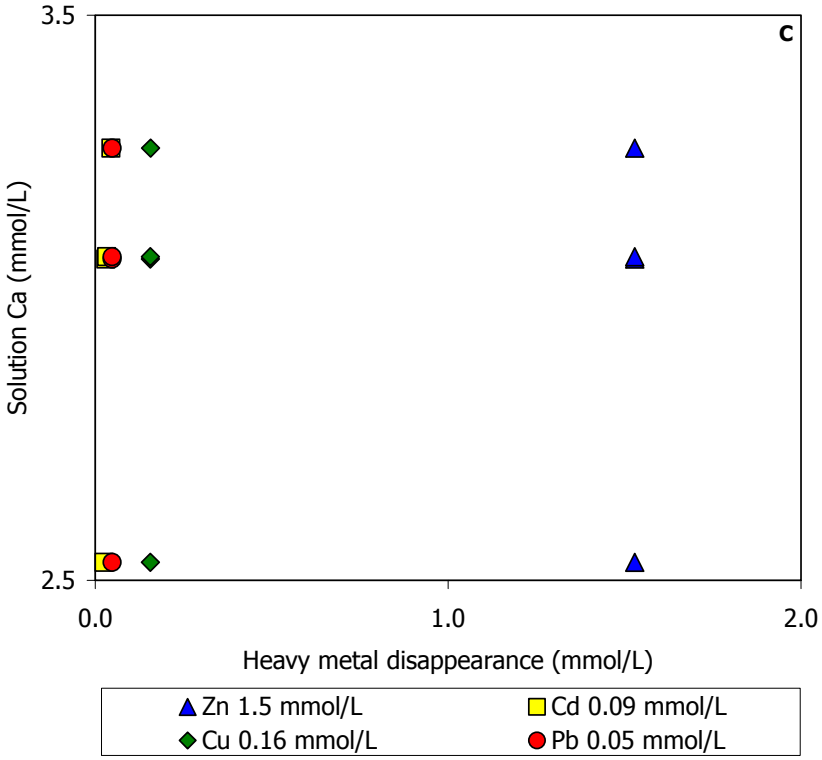
C
3.5
2.5
Solution Ca (mmol/L)
0.0
1.0
2.0
Heavy metal disappearance (mmol/L)
Zn 1.5 mmol/L
Cd 0.09 mmol/L
Cu 0.16 mmol/L
Pb 0.05 mmol/L

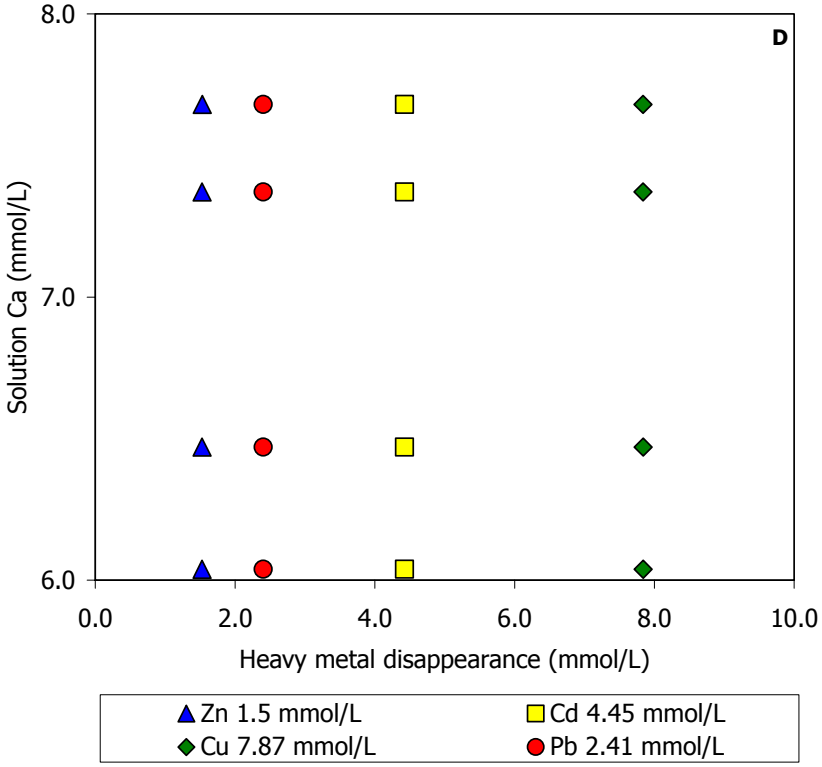
D
8.0
7.0
6.0
Solution Ca (mmol/L)
0.0
2.0
4.0
6.0
8.0
10.0
Heavy metal disappearance (mmol/L)
Zn 1.5 mmol/L
Cd 4.45 mmol/L
Cu 7.87 mmol/L
Pb 2.41 mmol/L

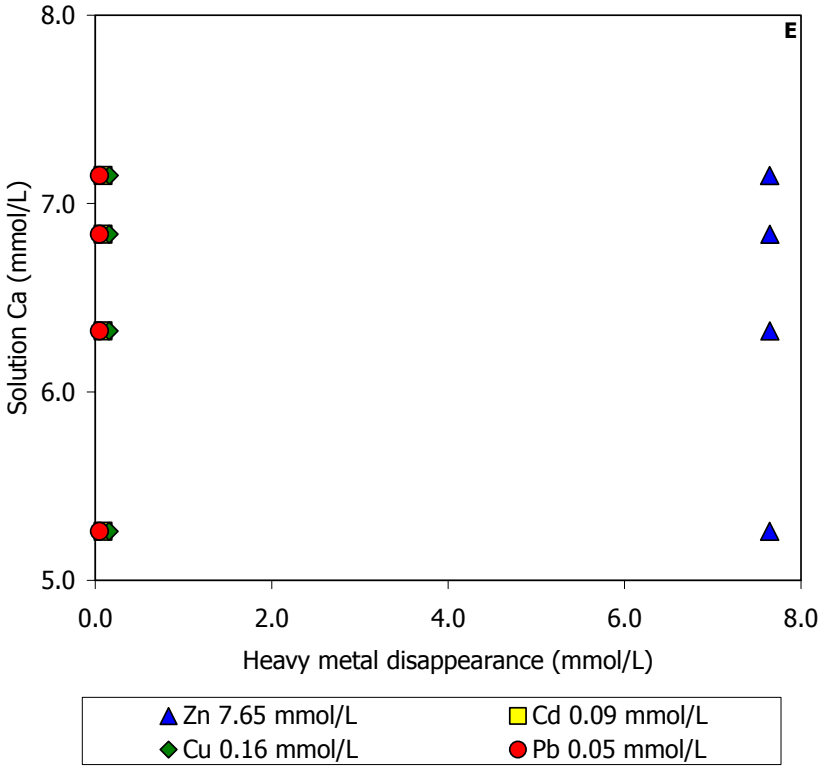
E
8.0
7.0
6.0
5.0
Solution Ca (mmol/L)
0.0
2.0
4.0
6.0
8.0
Heavy metal disappearance (mmol/L)
Zn 7.65 mmol/L
Cd 0.09 mmol/L
Cu 0.16 mmol/L
Pb 0.05 mmol/L

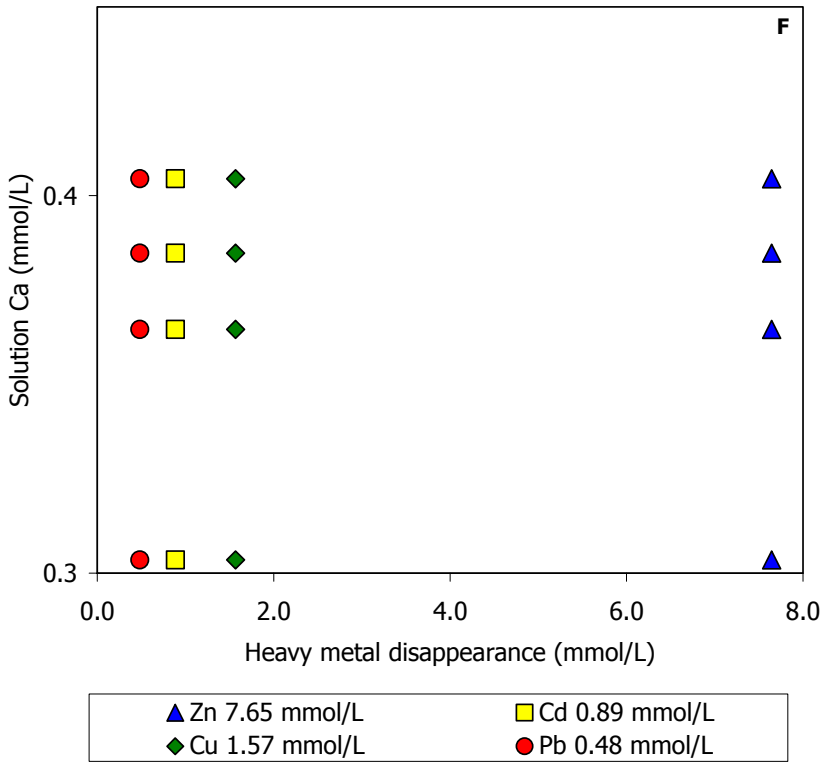

Fig. 21: Relation between Ca in solution (mmol/L) and the amount of heavy metals disappeared (mmol/L) sorbed on HA surface at the equilibrium in a multi-metal system when Zn is constant. Each initial concentration of the multi-metal system is written in the legend. - Fig. 21: Relazione tra il quantitative di Ca in soluzione (mmol/L) e di ciascun metallo pesante adsorbito (mmol/L) nel sistema multi-metal quando Zn è costante. La concentrazione iniziale di ogni elemento del sistema multi-metal è in leggenda.

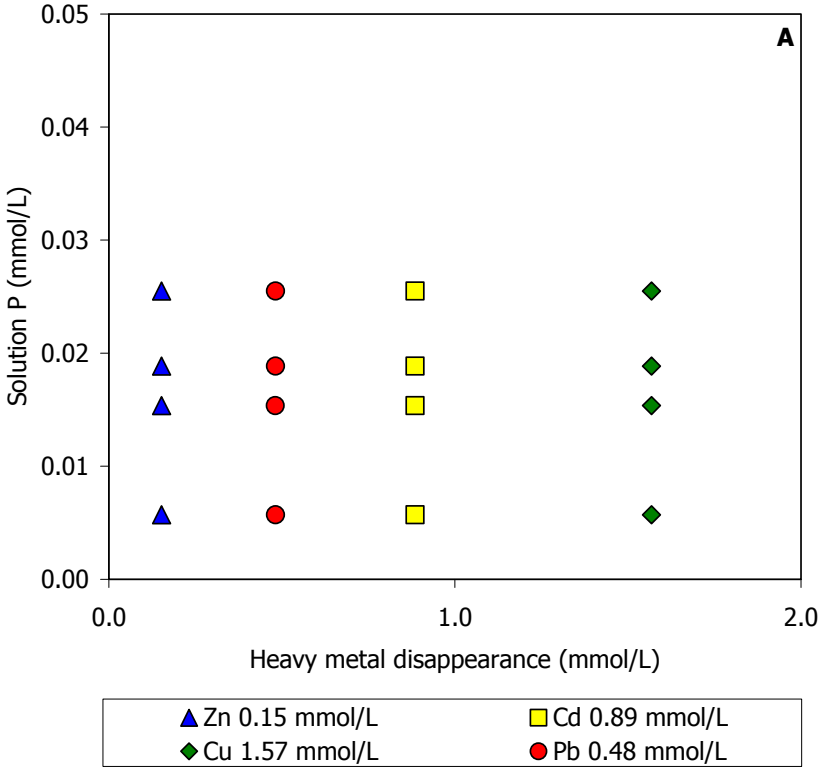
A
0.05
0.04
0.03
0.02
0.01
0.00
Solution P (mmol/L)
0.0
1.0
2.0
Heavy metal disappearance (mmol/L)
Zn 0.15 mmol/L
Cd 0.89 mmol/L
Cu 1.57 mmol/L
Pb 0.48 mmol/L

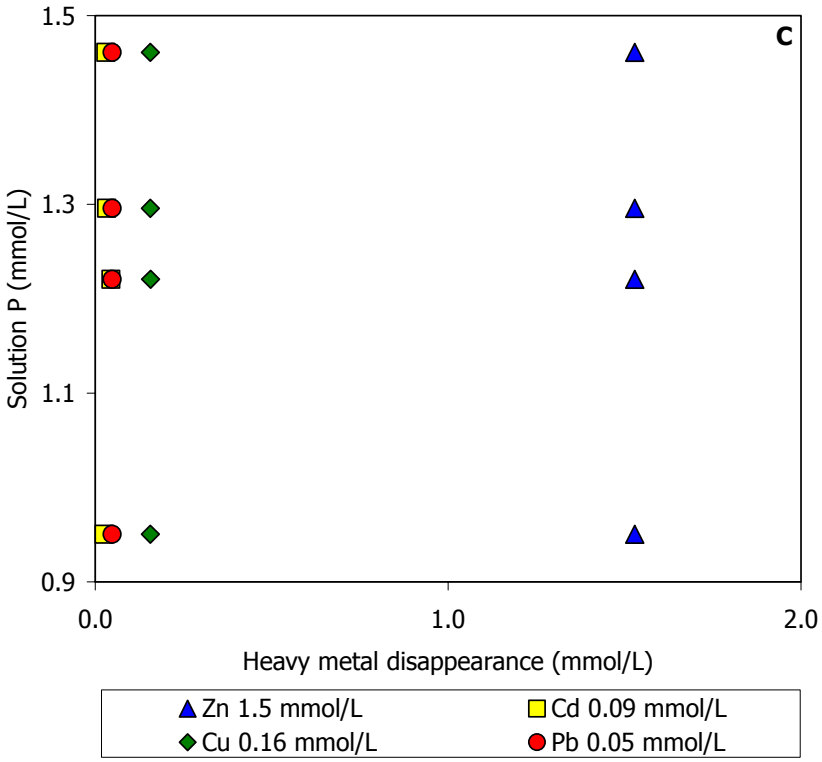
C
1.5
1.3
1.1
0.9
Solution P (mmol/L)
0.0
1.0
2.0
Heavy metal disappearance (mmol/L)
Zn 1.5 mmol/L
Cd 0.09 mmol/L
Cu 0.16 mmol/L
Pb 0.05 mmol/L

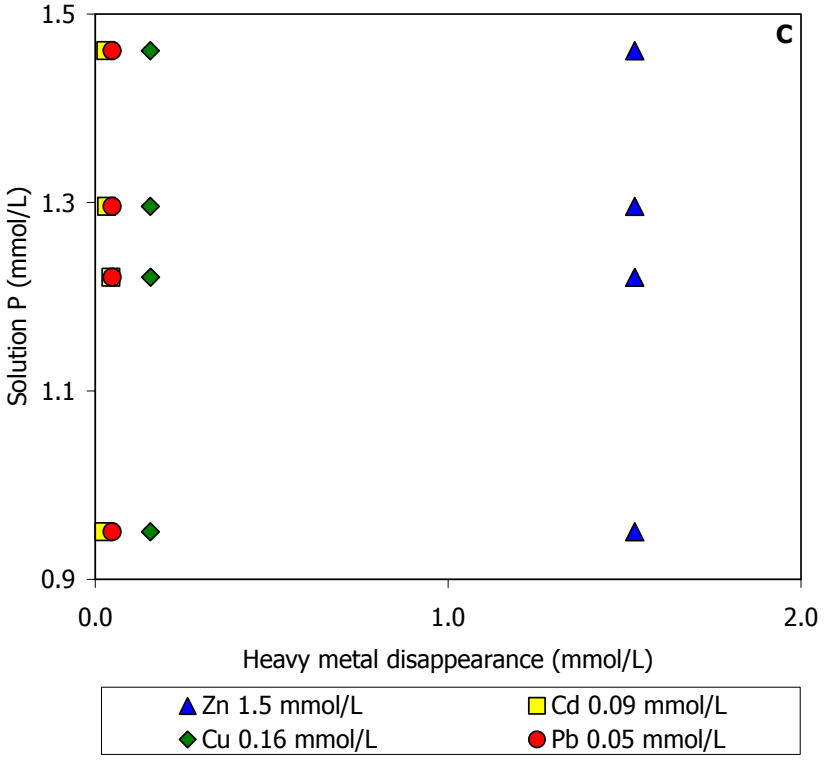
C
1.5
1.3
1.1
0.9
Solution P (mmol/L)
0.0
1.0
2.0
Heavy metal disappearance (mmol/L)
Zn 1.5 mmol/L
Cd 0.09 mmol/L
Cu 0.16 mmol/L
Pb 0.05 mmol/L

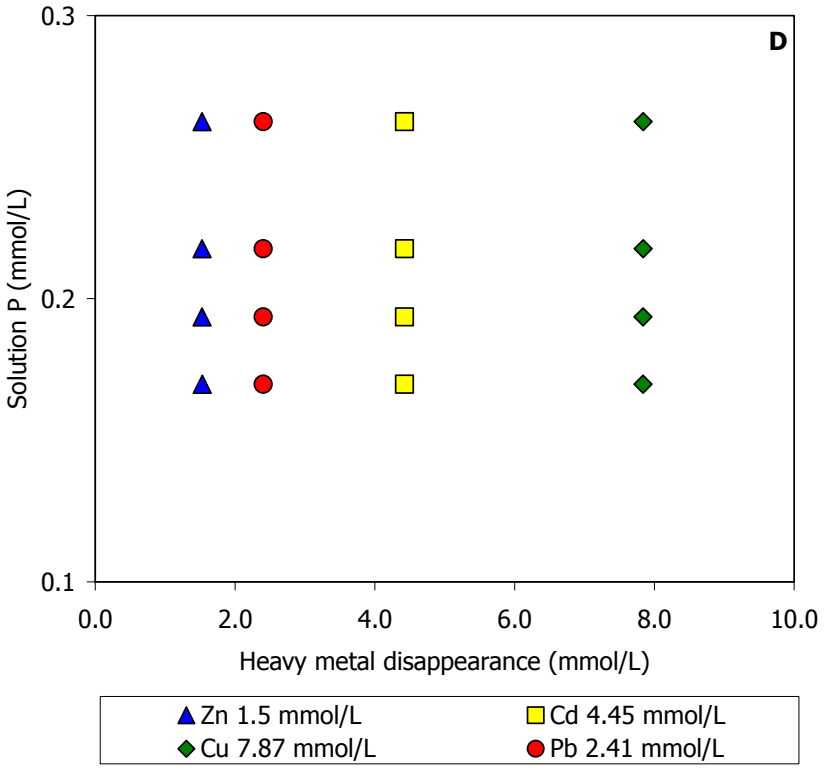
D
0.3
0.2
0.1
Solution P (mmol/L)
0.0
2.0
4.0
6.0
8.0
10.0
Heavy metal disappearance (mmol/L)
Zn 1.5 mmol/L
Cd 4.45 mmol/L
Cu 7.87 mmol/L
Pb 2.41 mmol/L

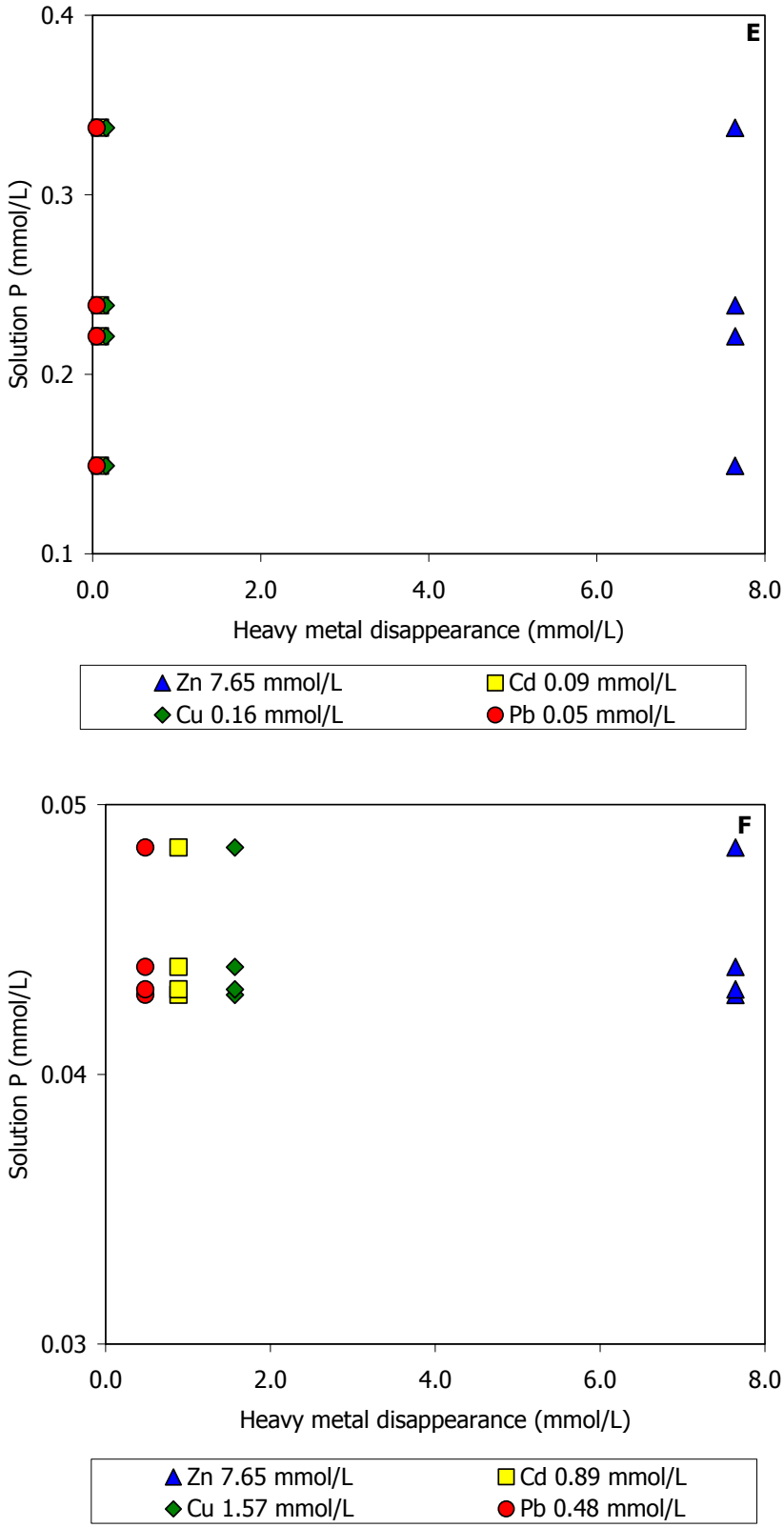

Fig. 22: Relation between P in solution (mmol/L) and the amount of disappeared heavy metals (mmol/L) sorbed on HA surface at the equilibrium in a multi-metal system when Zn is constant. Each initial concentration of the multi-metal system is written in the legend. - Fig. 22: Relazione tra il quantitativo di P in

soluzione (mmol/L) e di ciascun metallo pesante adsorbito (mmol/L) nel sistema multi-metal quando Zn è costante. La concentrazione iniziale di ogni elemento del sistema multi-metal è in leggenda.

6.2 MULTI-METAL SYSTEM SORBED ON FLUOROAPATITE FROM FLORIDA (FAP)

6.2.1 SEM analyses

The SEM micrographs on these solid materials obtained show some difference compared to the HA ones as the morphology of the grain is not usually spherical. On the contrary, the particles have often sharp corners (Fig. 1 A, B, C and D) and they don't show any kind of difference from the original one (Fig. 5 in Materials) or any type of orientation. EDS confirms the presence of the heavy metals on FAP surface (Fig. 2 A, B, C, and D).

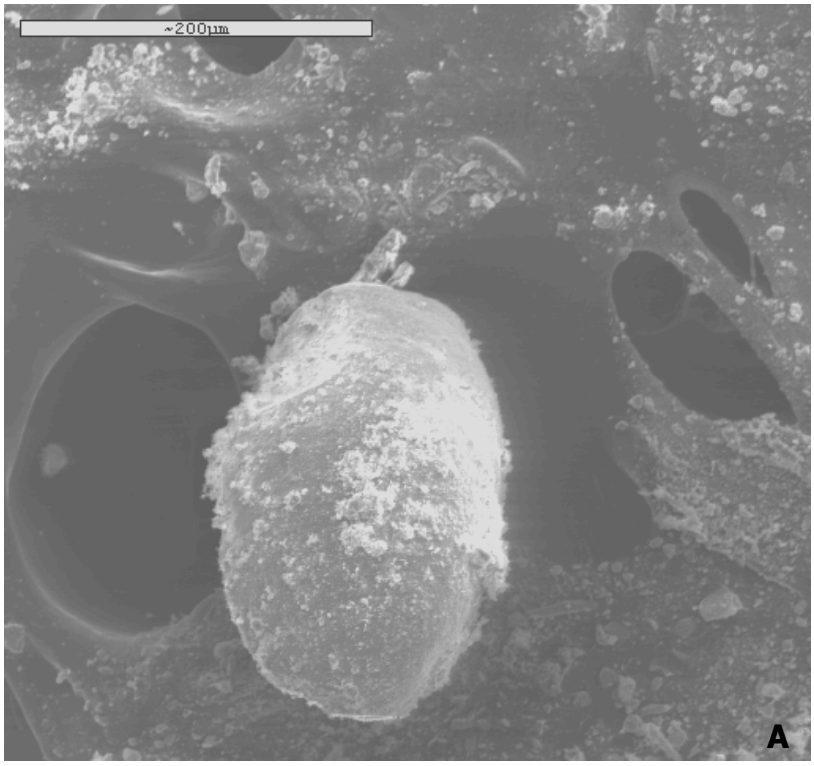

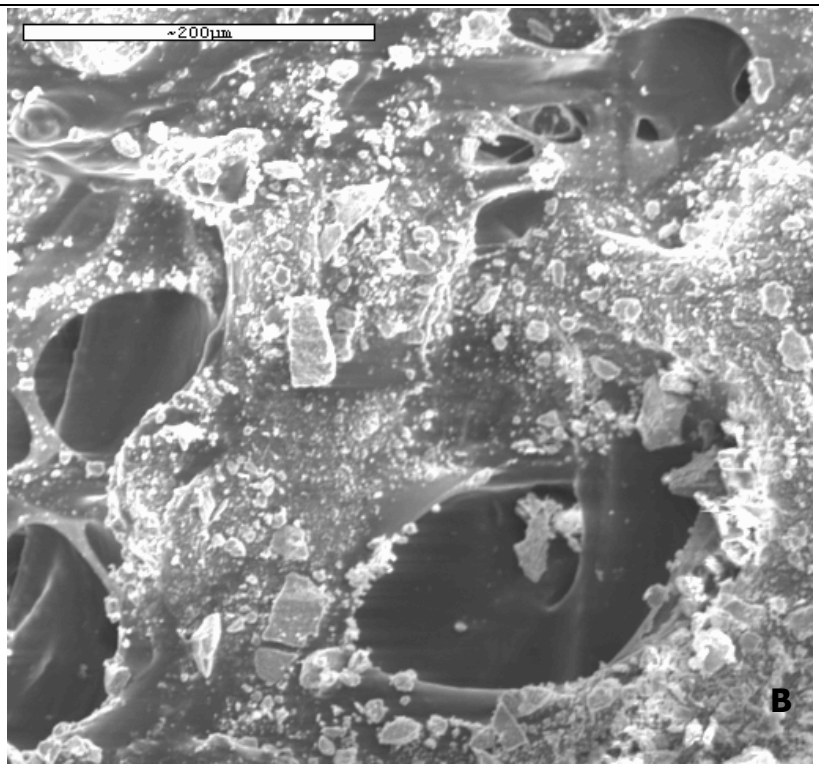
~200µm
B

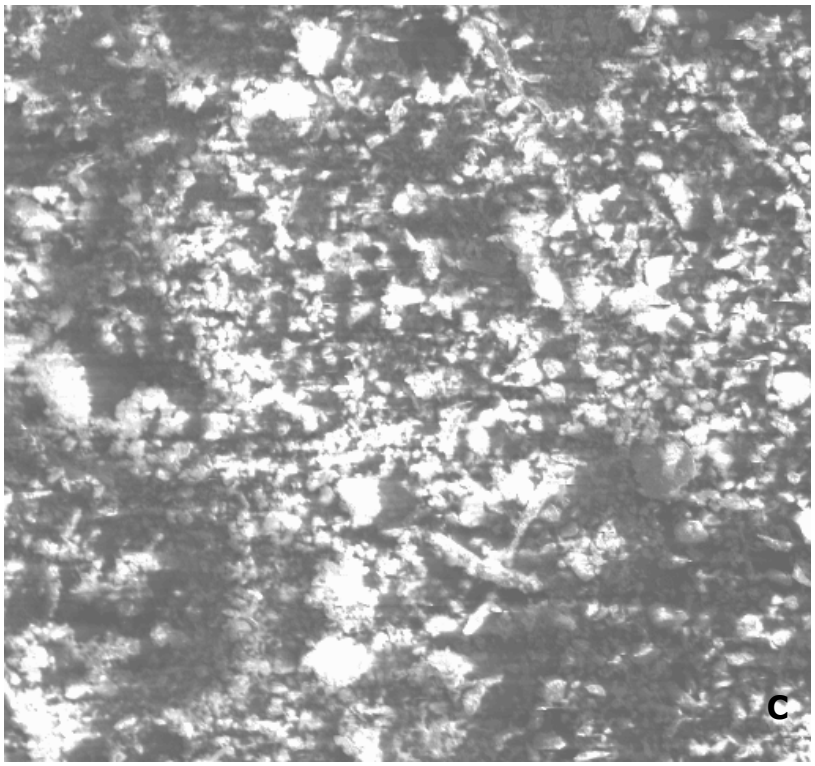
C

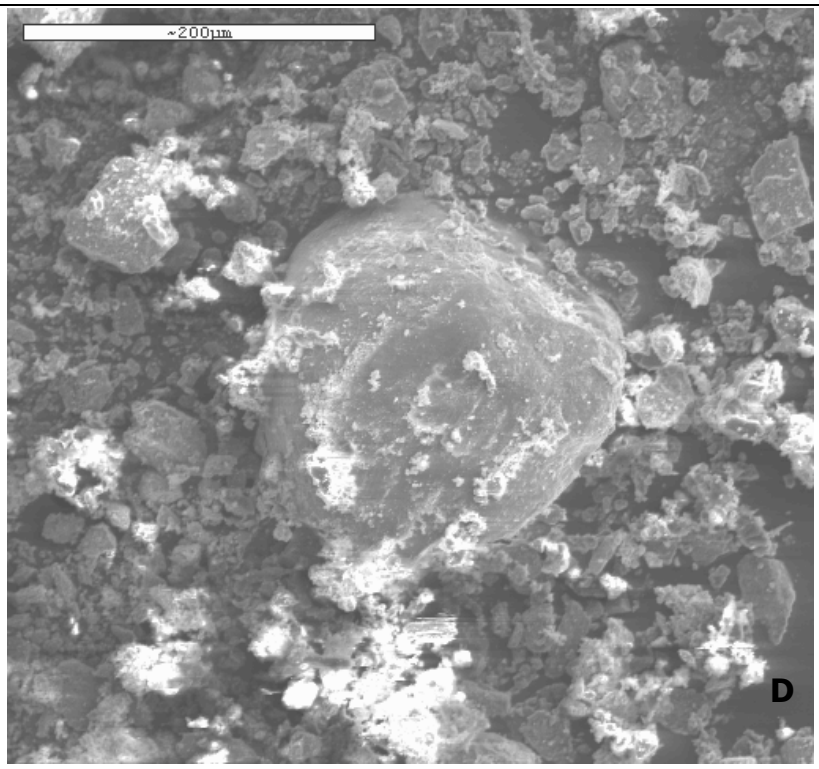

Fig. 1: Examples of SEM micrographs of solid residues. A: Cd = 10 mg/L, Cu, Pb and Zn = 500 mg/L t = 48h; B: Cu = 500 mg/L Cd, Pb and Zn = 10 mg/L t = 4h; C: Pb, Cd, Cu and Zn = 100 mg/L t = 24h; D: Zn = 100 mg/L, Cd, Cu and Pb = 500 mg/L t = 4h. – Fig. 1: Foto al SEM del sistema multi-metal. A: Cd = 10 mg/L, Cu, Pb and Zn = 500 mg/L t = 48h; B: Cu = 500 mg/L Cd, Pb and Zn = 10 mg/L t = 4h; C: Pb, Cd, Cu and Zn = 100 mg/L t = 24h; D: Zn = 100 mg/L, Cd, Cu and Pb = 500 mg/L t = 4h.

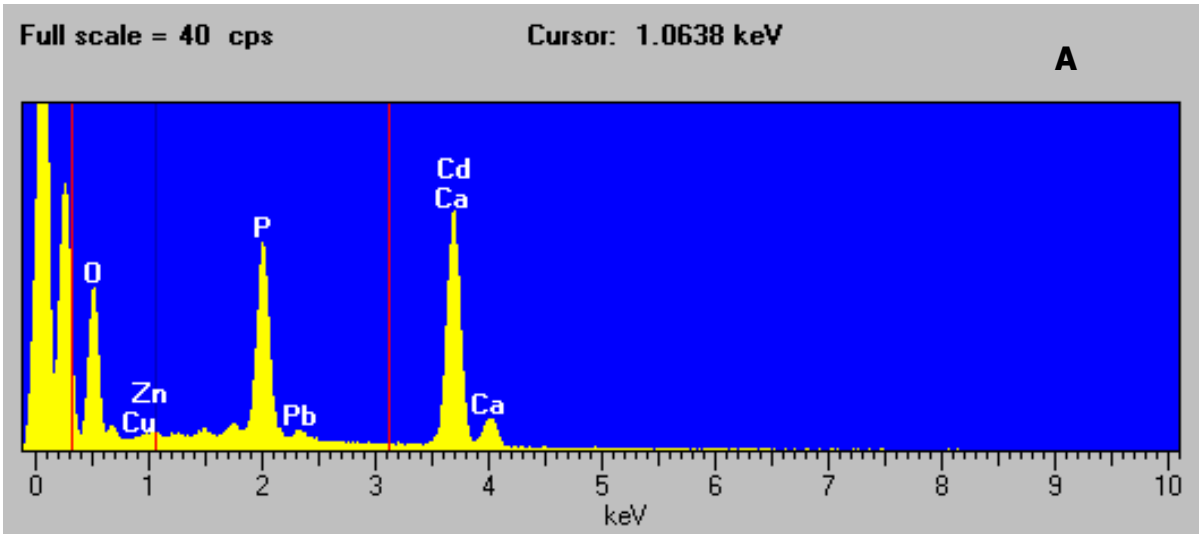

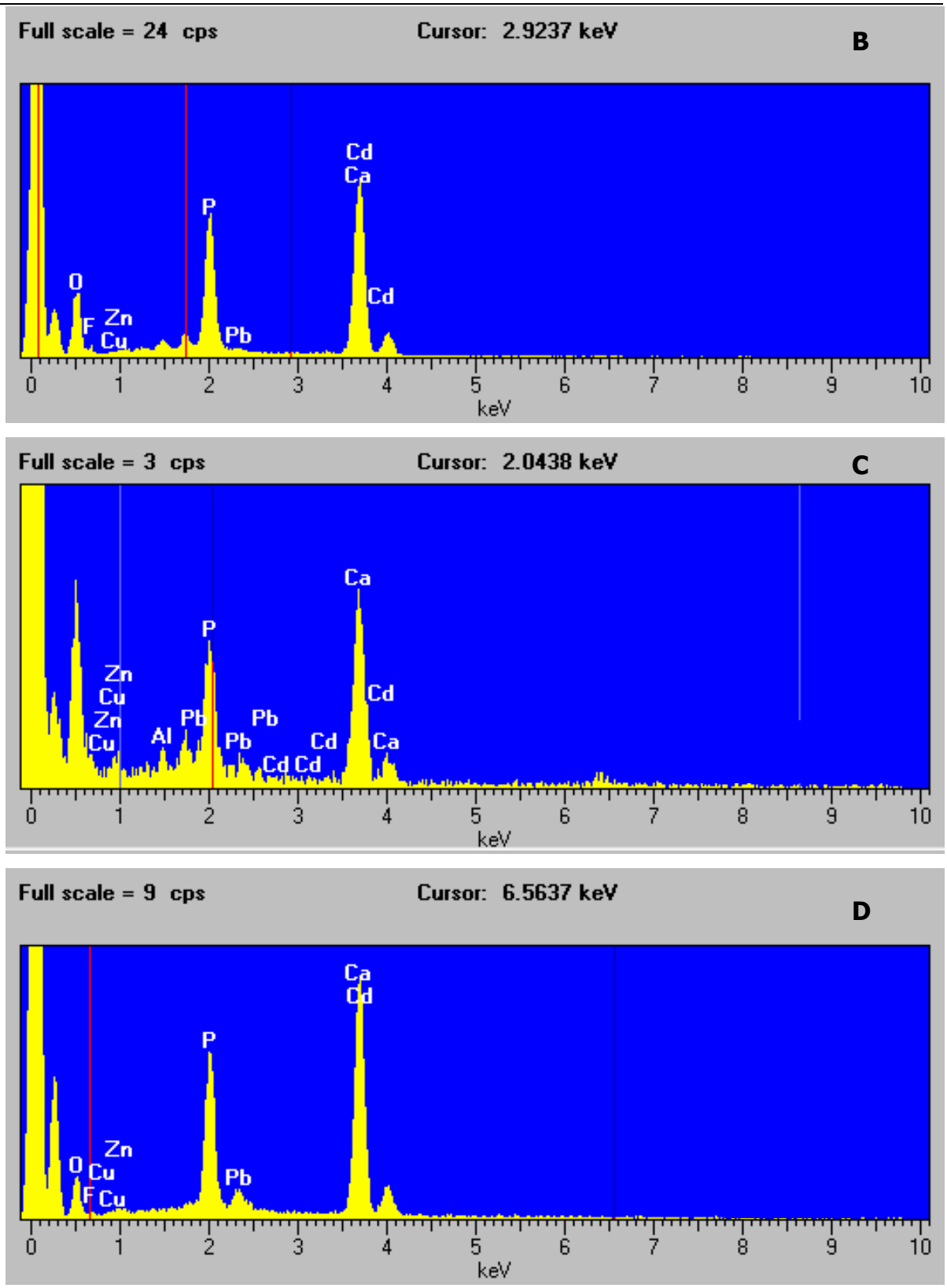

Fig. 2: EDS spectra of the previous SEM micrographs. – Fig. 2: Spettri ESD delle precedenti foto al SEM.

6.2.2 AFM analyses

Random samples were analyzed through AFM. Assuming that any kind of sorption mechanisms have taken place at a invisible scale to the previous technique.

The AFM images show a different morphology compared to the SEM micrographs, as the particles are spherical and don't show sharp edges (Fig. 3 A, B, C, D), being the shape similar to that HA particles' shape. The dimension of the particles (Fig. 4 A, B, C and D) ranging between 100-200 nm for Cd and Pb multi-metal system, whereas for Cu and Zn systems the particles ranges between a dimension of 1-2 μm.

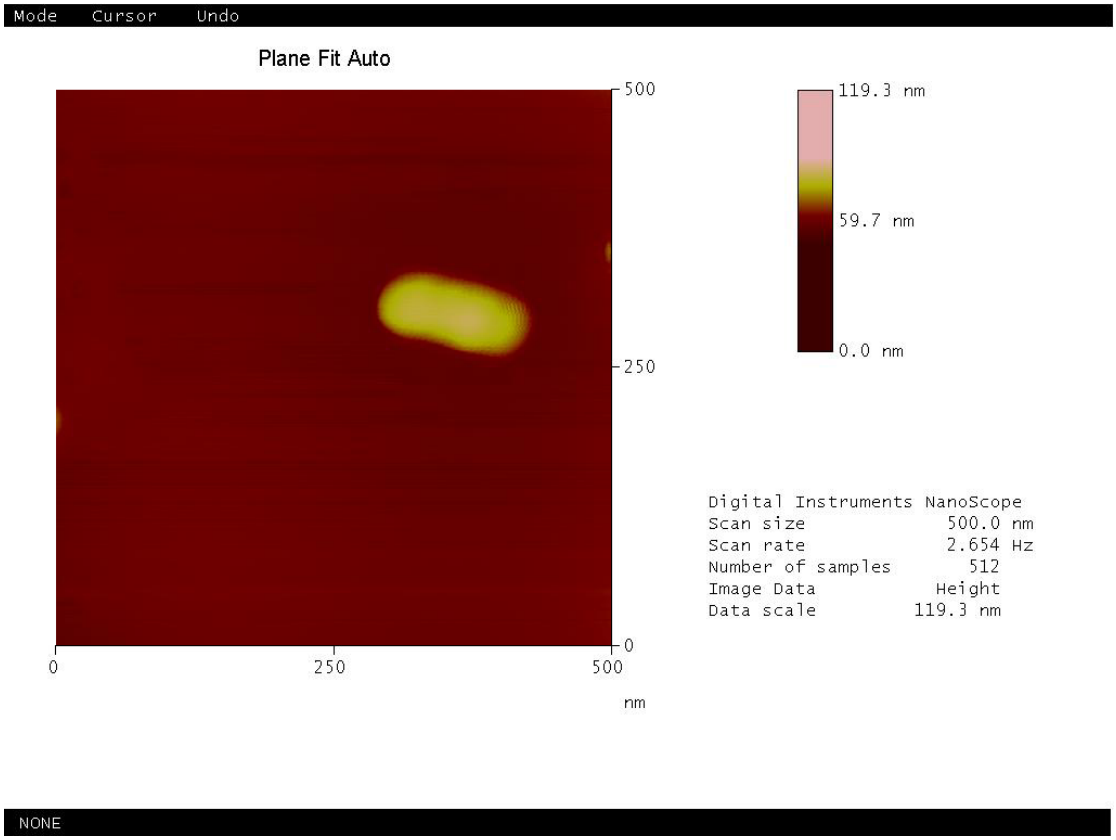

A

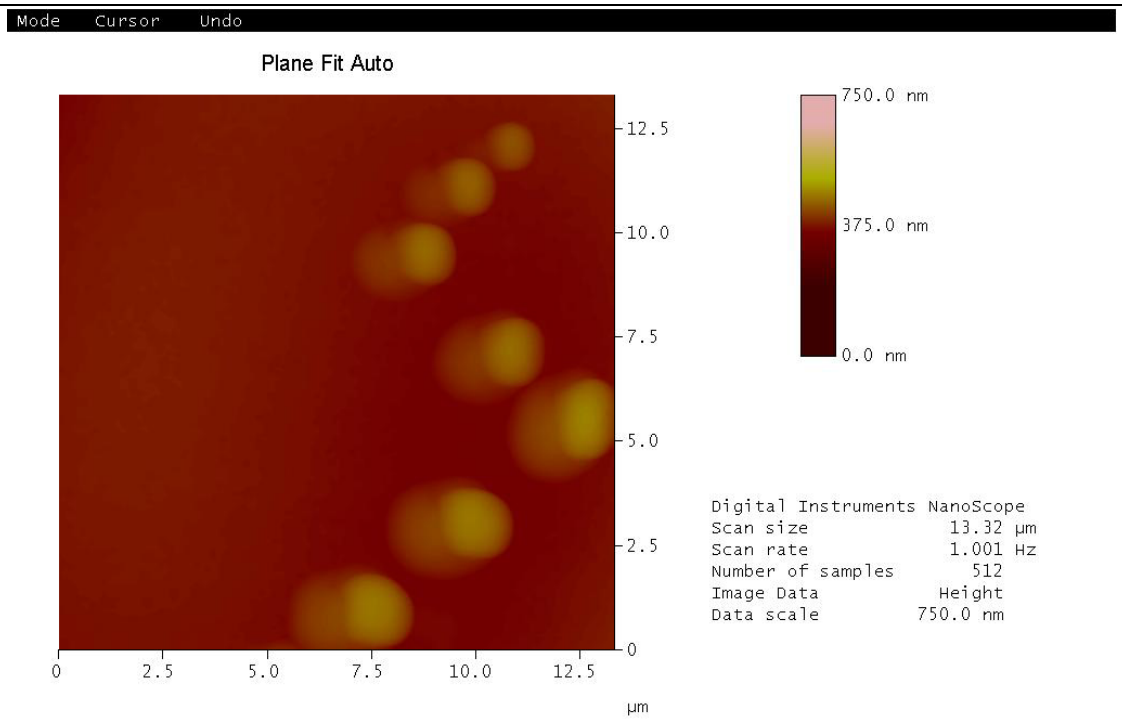
Mode Cursor Undo
Plane Fit Auto
750.0 nm
375.0 nm
0.0 nm
12.5
10.0
7.5
5.0
2.5
0
0 2.5 5.0 7.5 10.0 12.5
µm
Digital Instruments NanoScope
Scan size 13.32 µm
Scan rate 1.001 Hz
Number of samples 512
Image Data Height
Data scale 750.0 nm

B

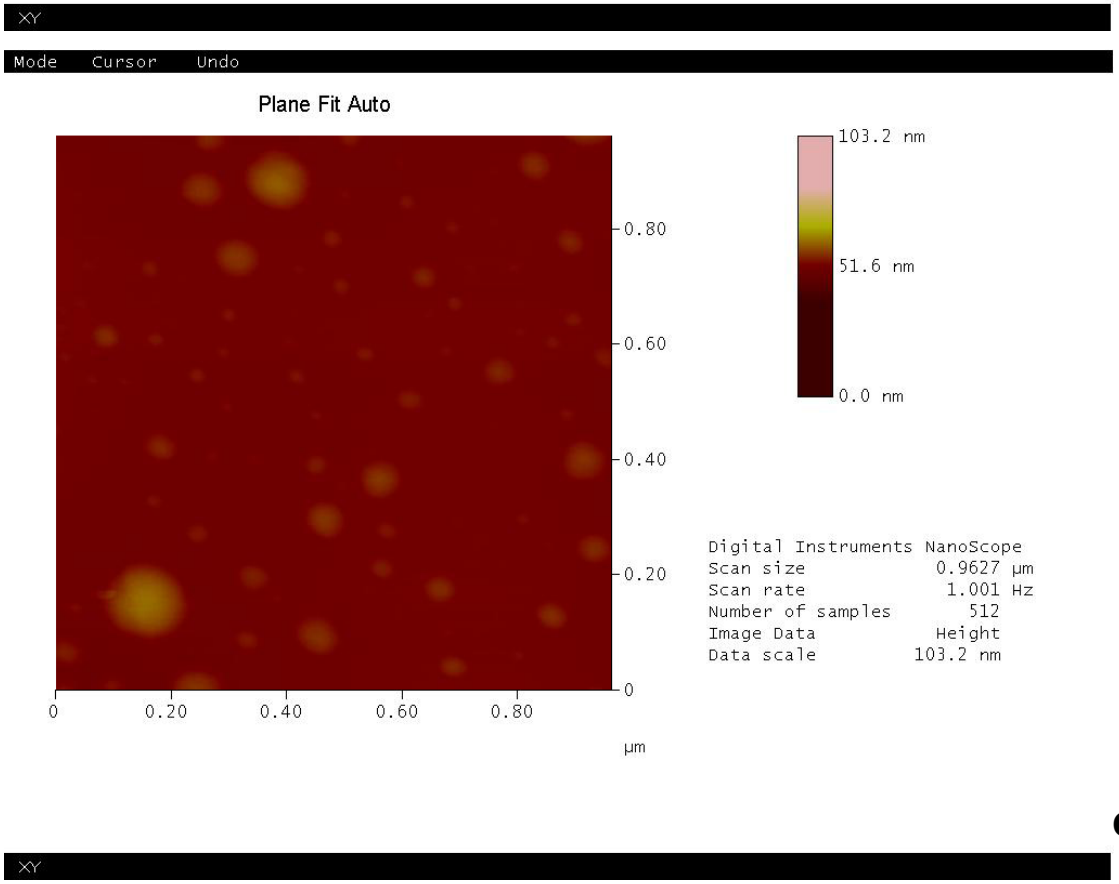
XY
Mode Cursor Undo
Plane Fit Auto
103.2 nm
51.6 nm
0.0 nm
0.80
0.60
0.40
0.20
0
0 0.20 0.40 0.60 0.80
µm
Digital Instruments NanoScope
Scan size 0.9627 µm
Scan rate 1.001 Hz
Number of samples 512
Image Data Height
Data scale 103.2 nm

C

XY

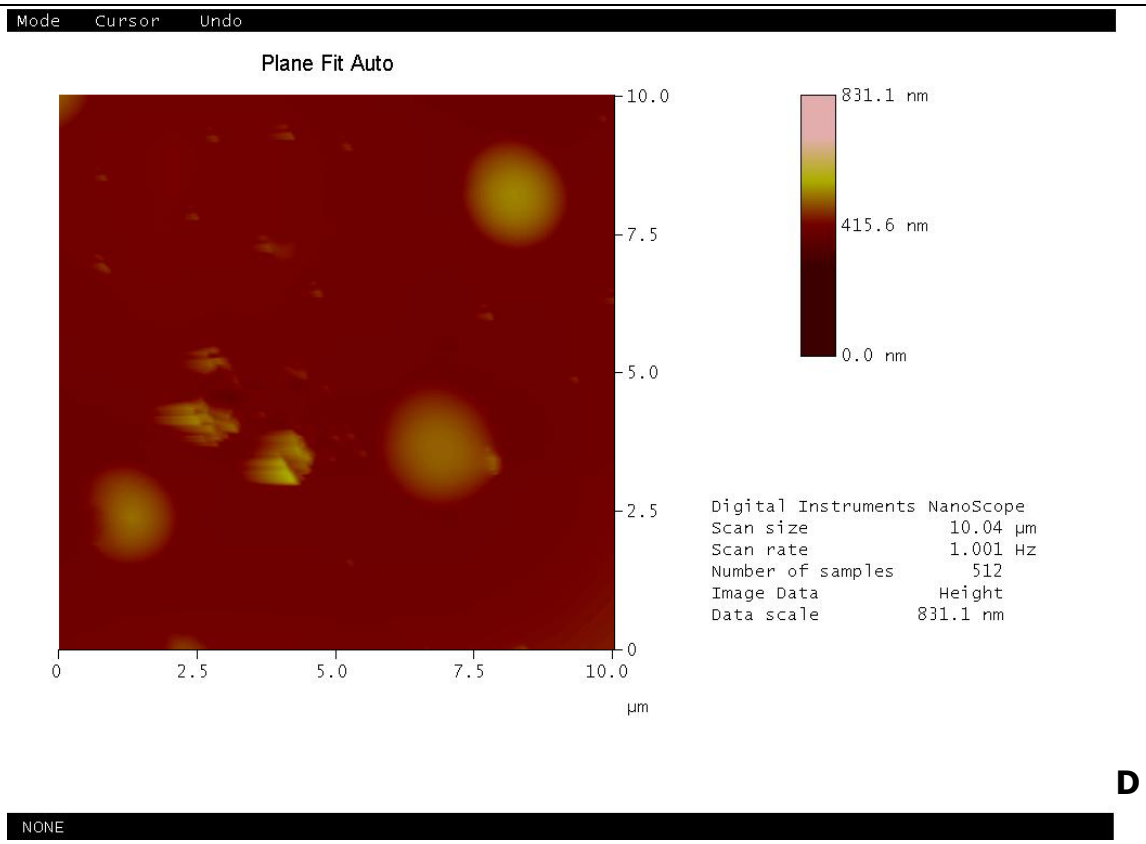

Fig. 3: AFM images of multi-metal system vs. FAP. A: Cd = 100 mg/L, Cu, Pb and Zn = 500 mg/L t = 2h; B: Cu = 100 mg/L, Cd, Pb and Zn = 500 mg/L t = 24h, C: Pb = 500 mg/L, Cd, Cu and Zn = 100 mg/L t = 2h; D: Zn = 500 mg/L, Cd, Cu and Pb = 100 mg/L t = 24h. – Fig. 3: Immagini all'AFM del sistema multi-metal vs. FAP. A: Cd = 100 mg/L, Cu, Pb and Zn = 500 mg/L t = 2h; B: Cu = 100 mg/L, Cd, Pb and Zn = 500 mg/L t = 24h, C: Pb = 500 mg/L, Cd, Cu and Zn = 100 mg/L t = 2h; D: Zn = 500 mg/L, Cd, Cu and Pb = 100 mg/L t = 24h.

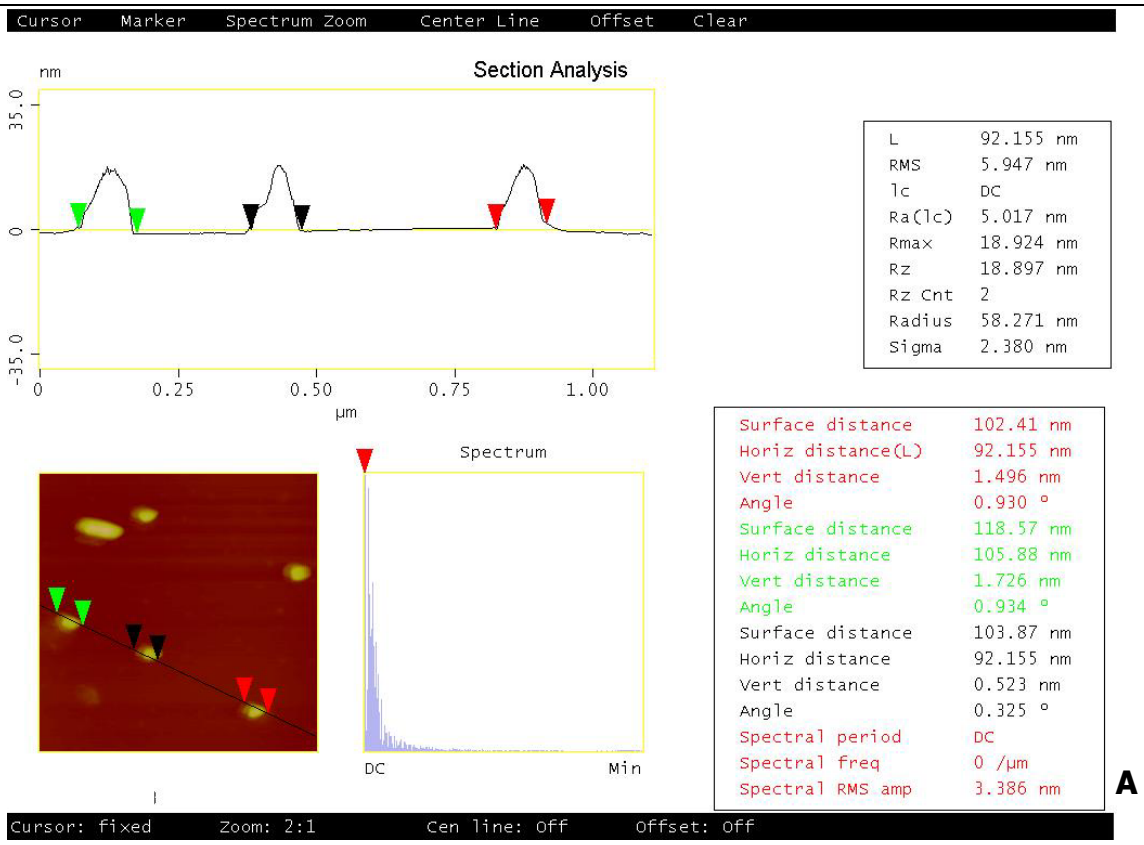
Cursor Marker Spectrum Zoom Center Line Offset Clear
Section Analysis
nm
35.0
0
-35.0
0
0.25
0.50
0.75
1.00
µm
L 92.155 nm
RMS 5.947 nm
lc DC
Ra(lc) 5.017 nm
Rmax 18.924 nm
Rz 18.897 nm
Rz Cnt 2
Radius 58.271 nm
Sigma 2.380 nm
Spectrum
DC
Min
Surface distance 102.41 nm
Horiz distance(L) 92.155 nm
Vert distance 1.496 nm
Angle 0.930 °
Surface distance 118.57 nm
Horiz distance 105.88 nm
Vert distance 1.726 nm
Angle 0.934 °
Surface distance 103.87 nm
Horiz distance 92.155 nm
Vert distance 0.523 nm
Angle 0.325 °
Spectral period DC
Spectral freq 0 /µm
Spectral RMS amp 3.386 nm
Cursor: fixed Zoom: 2:1 Cen line: Off Offset: Off

A

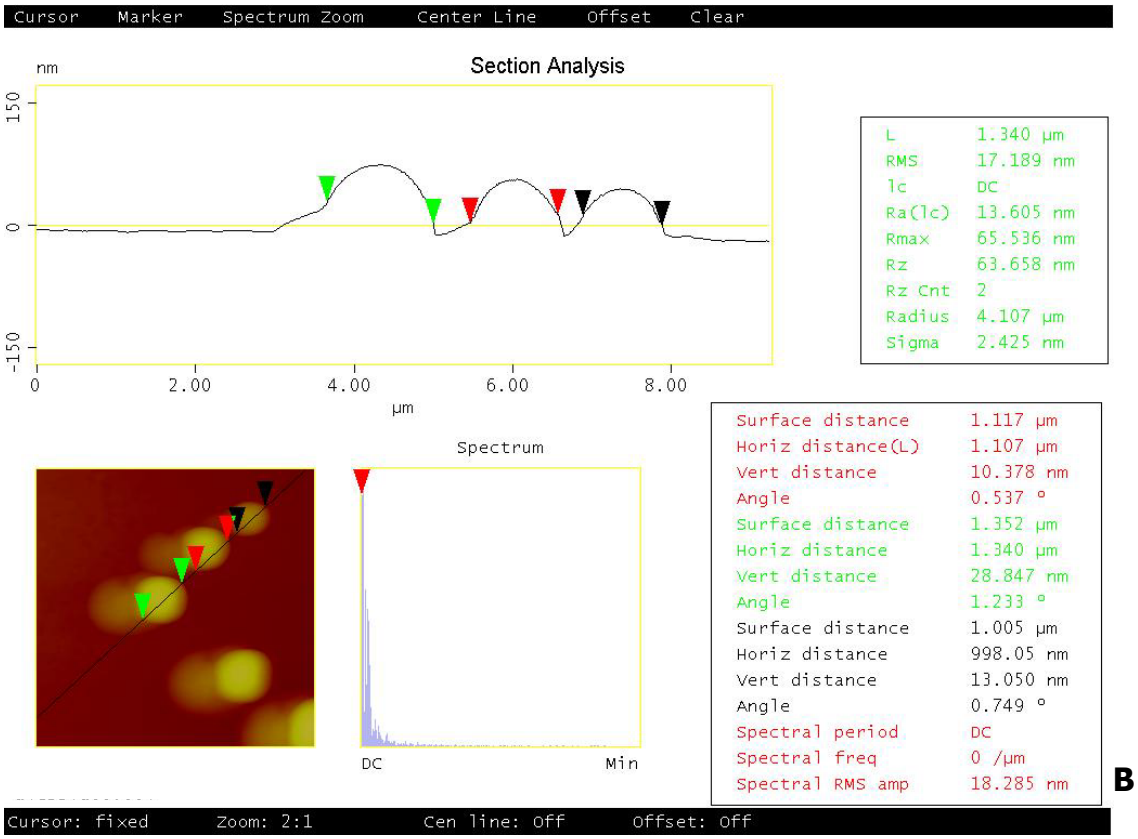
Cursor Marker Spectrum Zoom Center Line Offset Clear
Section Analysis
nm
150
0
-150
0
2.00
4.00
6.00
8.00
µm
L 1.340 µm
RMS 17.189 nm
lc DC
Ra(lc) 13.605 nm
Rmax 65.536 nm
Rz 63.658 nm
Rz Cnt 2
Radius 4.107 µm
Sigma 2.425 nm
Spectrum
DC
Min
Surface distance 1.117 µm
Horiz distance(L) 1.107 µm
Vert distance 10.378 nm
Angle 0.537 °
Surface distance 1.352 µm
Horiz distance 1.340 µm
Vert distance 28.847 nm
Angle 1.233 °
Surface distance 1.005 µm
Horiz distance 998.05 nm
Vert distance 13.050 nm
Angle 0.749 °
Spectral period DC
Spectral freq 0 /µm
Spectral RMS amp 18.285 nm
Cursor: fixed Zoom: 2:1 Cen line: Off Offset: Off

B

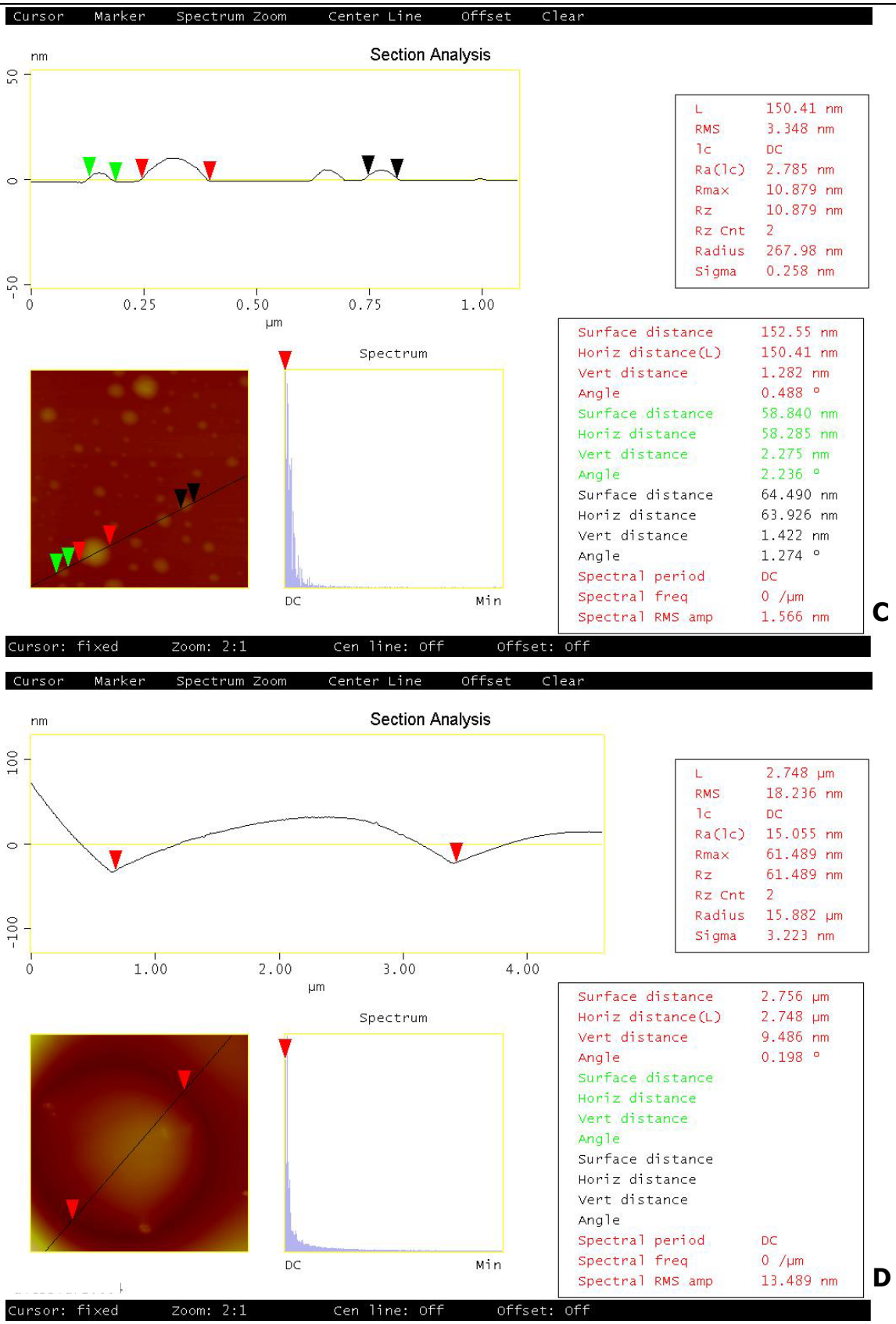

Fig. 4: AFM images showing the dimension of the particles of Fig. 3 – Fig. 4: Immagini all'AFM mostrante le dimensioni delle particelle di Fig. 3.

6.2.3 ICP-AES analyses

In the system where the initial Cd concentration (Fig. 5 A, B, C, D, E and F) is constant, FAP efficiency of the immobilization experiments are listed in Table 1 and the best immobilization is usually achieved after 24 hours at interaction, even though in some case there are some exception depending on the concentration of the heavy metals. Compared to the immobilization rate obtained with the HA, the values are slightly lower. Generally, Zn is less immobilized than the other three heavy metals. The immobilization seems to depend on the concentration of each metals. However it is difficult to determine only one order of the immobilization of the metals. We could suggest the following: Pb > Cu > Cd > Zn as the more common, but there are other orders depending on the initial concentration of each metals. pH values usually increase and/or decrease of about 0.5 units, and only in few cases the difference between the initial and final value is larger than 0.5 units.

Cd = 10 mg/L	Cu = 100 mg/L	Pb = 100 mg/L	Zn = 100 mg/L
1.744	18.671	19.227	17.617
1.793	18.650	19.187	17.495
1.813	19.659	19.930	17.590
1.805	18.712	19.255	17.474
Cd = 10 mg/L	Cu = 500 mg/L	Pb = 500 mg/L	Zn = 500 mg/L
1.831	95.723	94.893	93.628
1.869	96.618	96.465	94.276
1.871	96.768	97.087	94.256
1.871	97.162	97.416	94.153
Cd = 100 mg/L	Cu = 10 mg/L	Pb = 10 mg/L	Zn = 10 mg/L
18.230	1.899	1.930	1.666
18.054	1.884	1.944	1.717
18.445	1.981	1.975	1.856
18.345	1.971	1.979	1.778
Cd = 100 mg/L	Cu = 500 mg/L	Pb = 500 mg/L	Zn = 500 mg/L
18.965	96.294	95.720	93.855
19.039	96.177	95.841	94.085
19.104	96.676	96.803	94.636
3.856	63.277	47.984	-19.188
Cd = 500 mg/L	Cu = 10 mg/L	Pb = 10 mg/L	Zn = 10 mg/L
95.541	1.916	1.946	1.803
95.370	1.933	1.935	1.875
95.339	1.986	1.994	1.891
95.588	1.972	1.991	1.893
Cd = 500 mg/L	Cu = 100 mg/L	Pb = 100 mg/L	Zn = 100 mg/L
95.153	19.405	19.659	18.857
100.000	20.000	20.000	20.000
95.186	19.411	19.556	18.855
95.141	19.713	19.837	18.846

Table 1: Proportions of blocked heavy metals per unit mass of FAP (mg/g) for the multi-metal system when Cd is constant. – Tabella 1: Entità dell'immobilizzazione dei metalli per unità di massa di FAP (mg/g) per il sistema multi-metal con concentrazione del Cd costante.

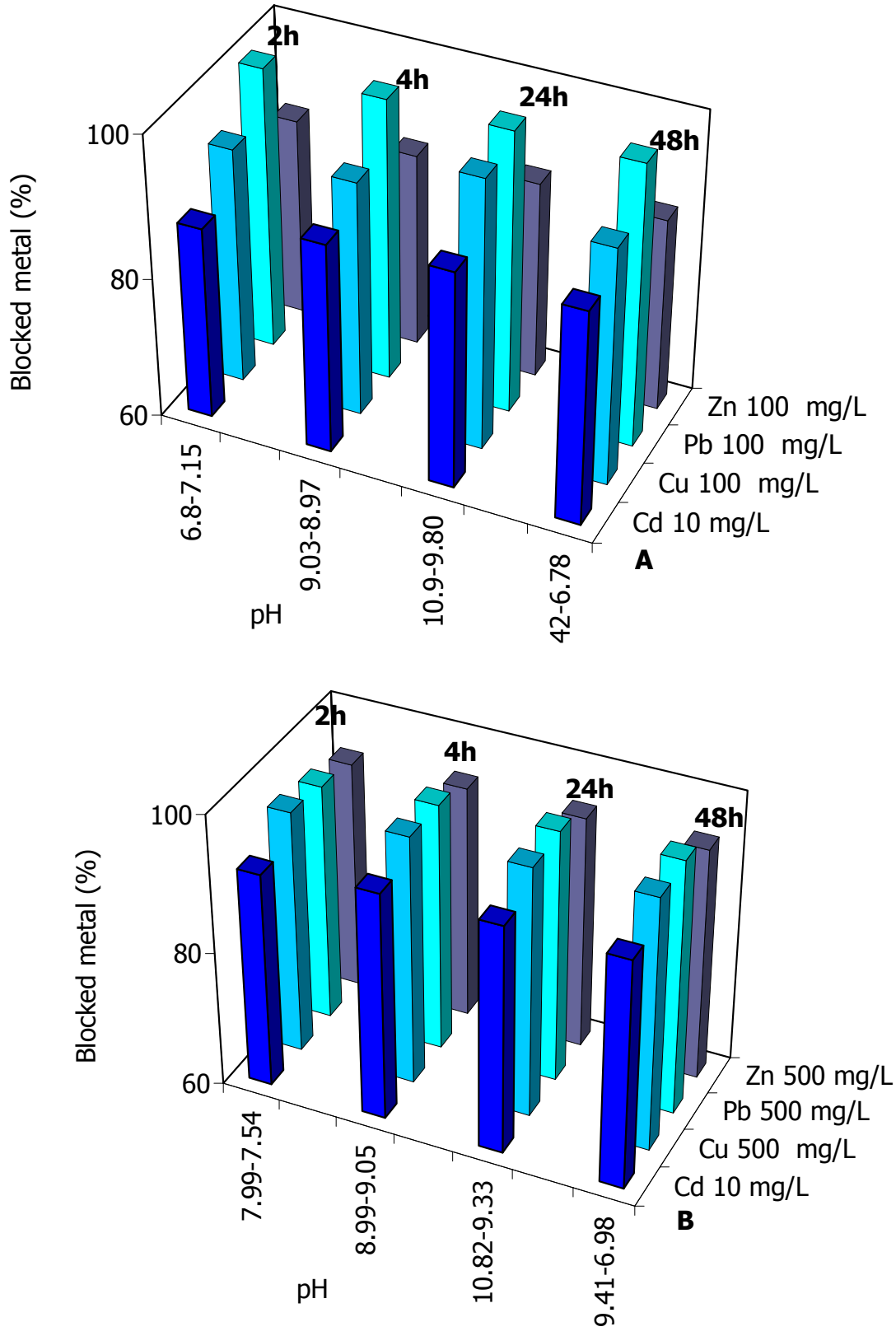

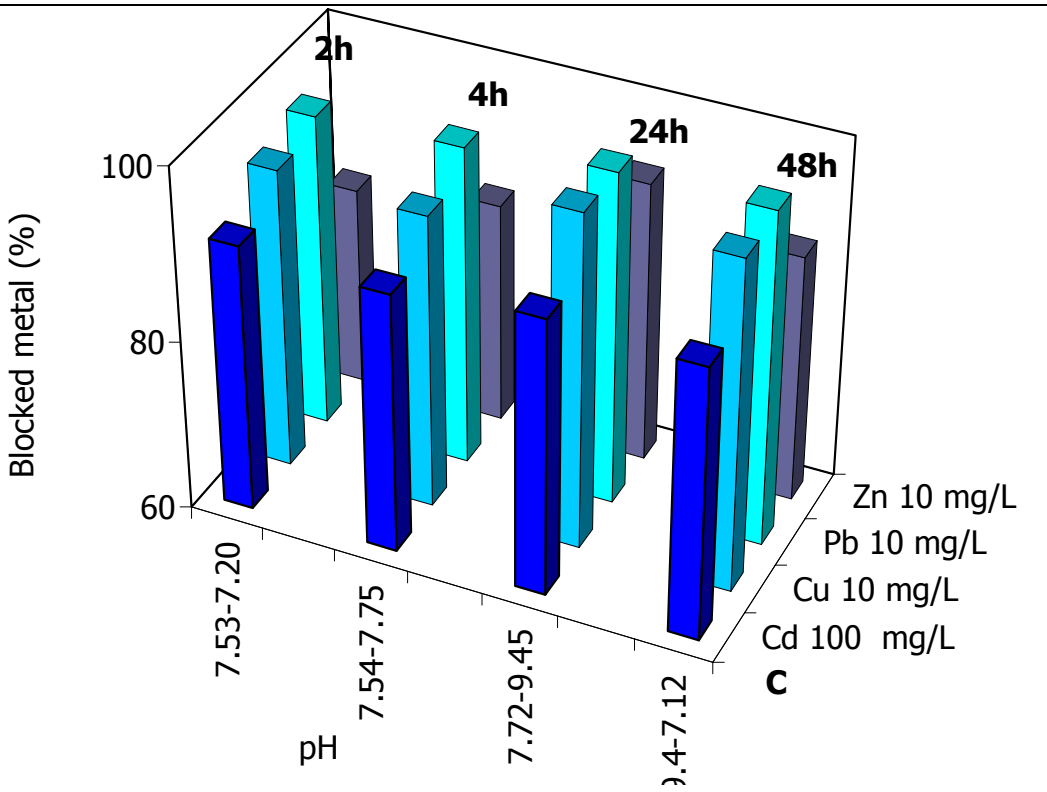
2h
4h
24h
48h
100
80
60
Blocked metal (%)
7.53-7.20
7.54-7.75
7.72-9.45
pH
Zn 10 mg/L
Pb 10 mg/L
Cu 10 mg/L
Cd 100 mg/L
C

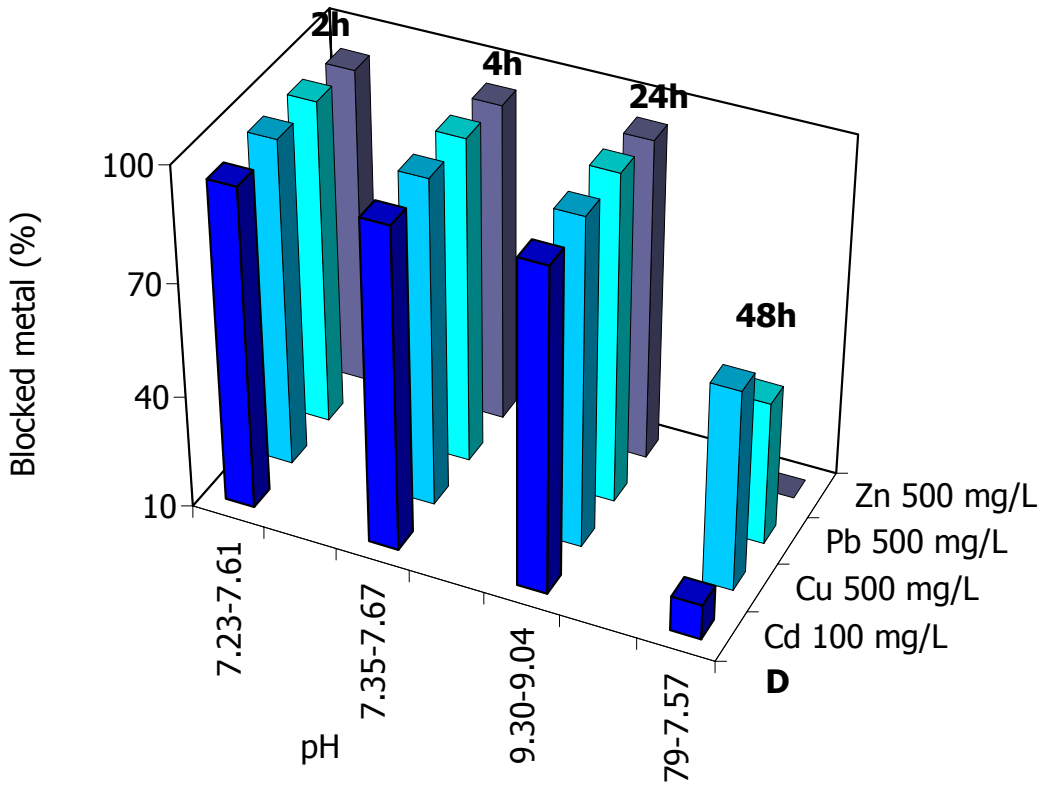
2h
4h
24h
48h
100
70
40
10
Blocked metal (%)
7.23-7.61
7.35-7.67
9.30-9.04
pH
Zn 500 mg/L
Pb 500 mg/L
Cu 500 mg/L
Cd 100 mg/L
D

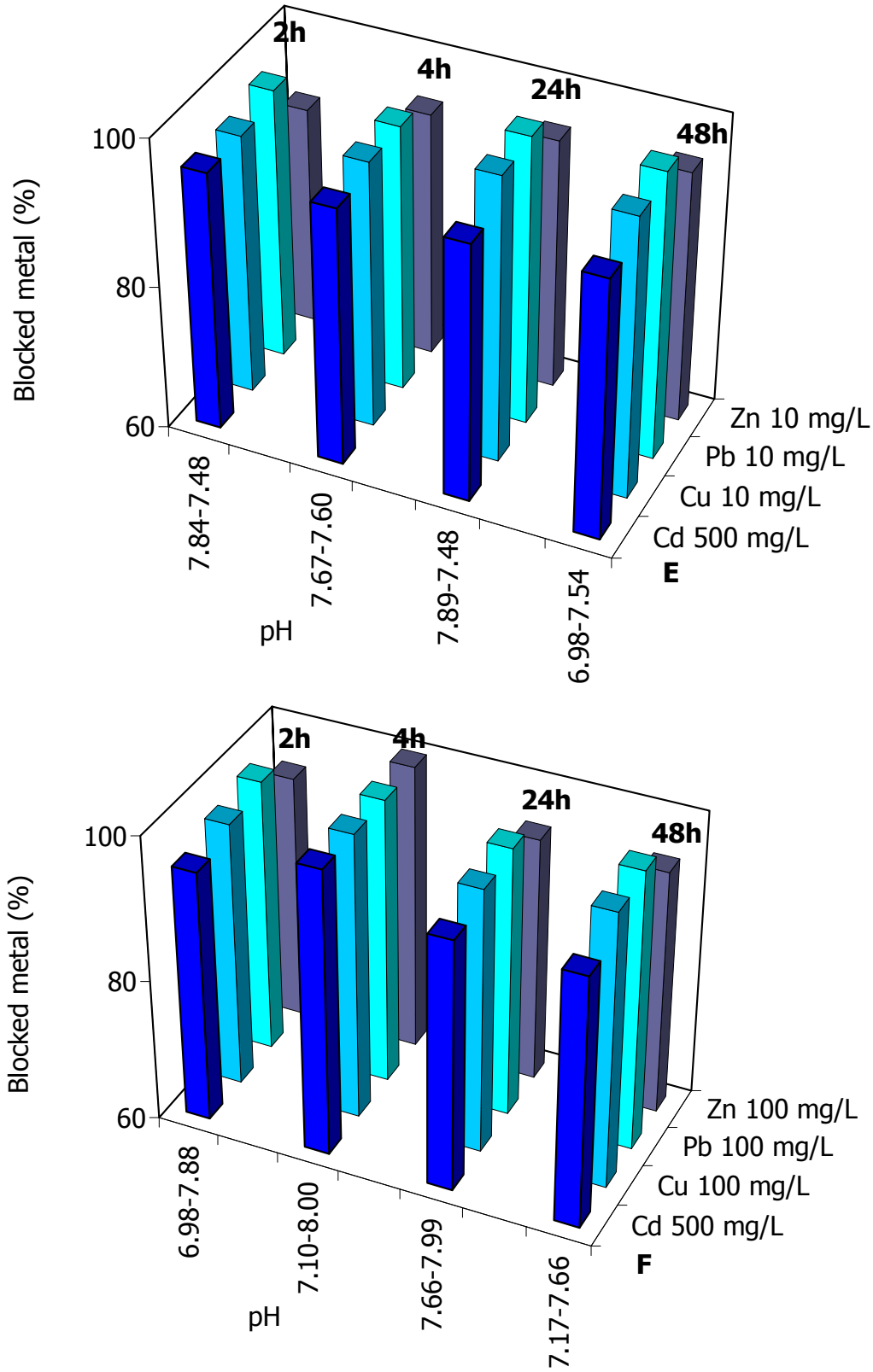

Fig. 5: Variation of the amount of blocked metal with time for the mass of FAP (1 g) in the multi-metal system where Cd is constant. Initial and final pH values are reported. – Fig. 5: Variazione delle percentuali dei metalli immobilizzati in funzione del tempo di interazione per la quantità di FAP (1 g) nel sistema multi-metal in cui Cd è l'elemento costante. Sono riportati i valori iniziali e finali del pH.

The molar ratio Q_S for Cd (Tab. 2) is < 1 for the lower initial concentration (10 mg/L), suggesting a non-crystalline precipitation of a mineral phase; the precipitation is suggested for Pb initial concentration of 100 mg/L, whereas the other metals at 100 mg/L and 500 mg/L show a Q_S >> 1 allowing to infer an adsorption mechanism. Increasing Cd concentration (100 mg/L) Q_S > 1, whereas the molar ratio of the other heavy metals is Q_S < 1 (10 mg/L) and Q_S > 1 (500 mg/L). When Cd concentration is 500 mg/L Q_S is >> 1 and for the other metals is < 1. Thus, the results suggest only two type of sorption processes: the precipitation of a non-crystalline phase and the surface complexation.

Cd = 10 mg/L	Cu = 100 mg/L	Pb = 100 mg/L	Zn = 100 mg/L
0.31	2.87	0.51	5.00
0.21	2.41	0.44	4.34
0.08	0.26	0.02	1.78
0.14	1.61	0.29	3.07
Cd = 10 mg/L	Cu = 500 mg/L	Pb = 500 mg/L	Zn = 500 mg/L
0.41	18.37	6.73	26.60
0.24	10.97	3.52	18.05
0.22	9.67	2.67	16.70
0.15	6.01	1.68	12.04
Cd = 100 mg/L	Cu = 10 mg/L	Pb = 10 mg/L	Zn = 10 mg/L
1.69	0.17	0.04	0.55
3.31	0.35	0.05	0.83
0.71	0.02	0.01	0.11
1.28	0.04	0.01	0.30
Cd = 100 mg/L	Cu = 500 mg/L	Pb = 500 mg/L	Zn = 500 mg/L
1.92	12.15	4.30	19.58
1.91	13.45	4.49	20.22
1.15	7.53	2.22	11.80
0.68	2.74	1.19	8.64
Cd = 500 mg/L	Cu = 10 mg/L	Pb = 10 mg/L	Zn = 10 mg/L
11.83	0.40	0.08	0.90
11.87	0.30	0.09	0.55
6.17	0.03	0.00	0.25
15.71	0.18	0.02	0.65
Cd = 500 mg/L	Cu = 100 mg/L	Pb = 100 mg/L	Zn = 100 mg/L
7.65	1.66	0.29	3.10
0.00	0.00	0.00	0.00
16.67	3.60	0.83	6.82
5.25	0.55	0.10	2.47

Table 2: Q_S values for the multi - metal systems when Cd has a constant concentration. Tabella 2: Valori di Q_S per i sistemi multi-metal nei quali la concentrazione di Cd è stata mantenuta costante.

The sorption isotherms (Fig. 6 A, B, C and D) can be classified of L type and subtype 2 showing a linear part followed by a knee. This shape suggests as sorption

mechanism the surface precipitation and the adsorption, confirming what, has been suggested by the Q_S values. When t = 4h exceptions are the Pb and Zn curves. Zn shows a H type (almost vertical line), that is a curve obtained for the partition of a solute among immiscible solvents, and it could be defined as a "adsorption without solvents" (Giles et al. *(62)*). Pb shows a vertical line defined from Giles et al. *(62)* as a H line; therefore solute has such high affinity that in dilute solutions it is completely adsorbed. For Cd at this contact time is not possible to determine the isotherm because some values are negative. For t = 48h, Cd, Cu and Pb have L2 type isotherm, whereas Zn shows a particular curve, C (horizontal) which means a constant partition of solute between solution and substrate, right up to the maximum possible adsorption, where an abrupt change to a horizontal plateau occurs.

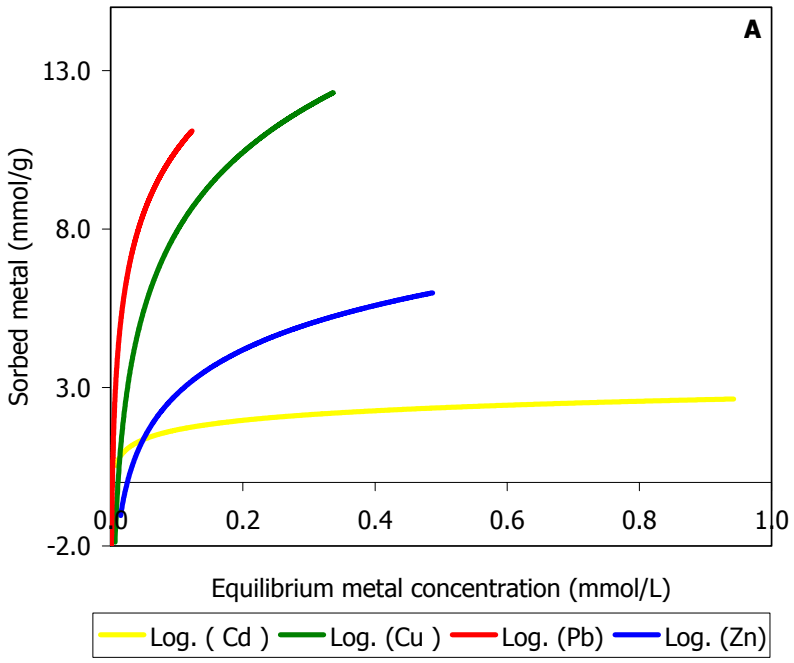

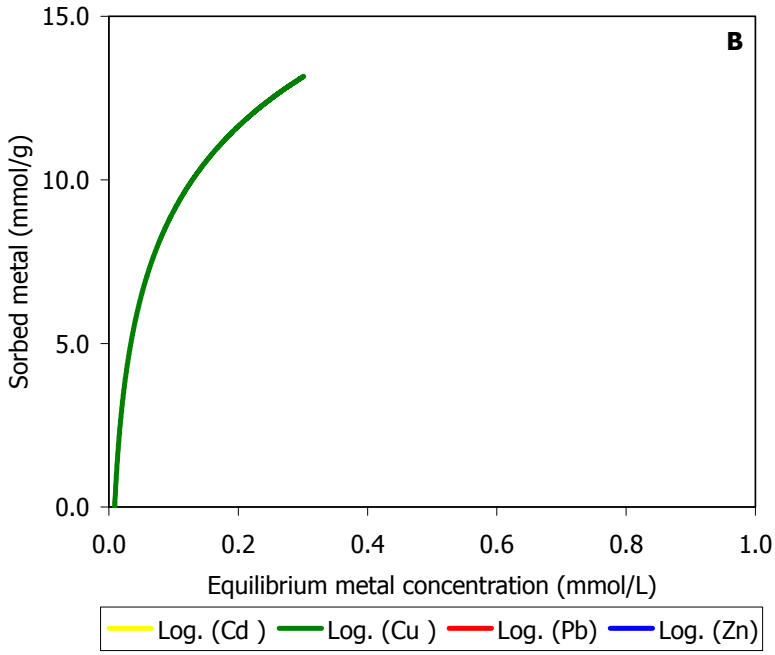
B
15.0
10.0
5.0
0.0
Sorbed metal (mmol/g)
0.0
0.2
0.4
0.6
0.8
1.0
Equilibrium metal concentration (mmol/L)
Log. (Cd)
Log. (Cu)
Log. (Pb)
Log. (Zn)

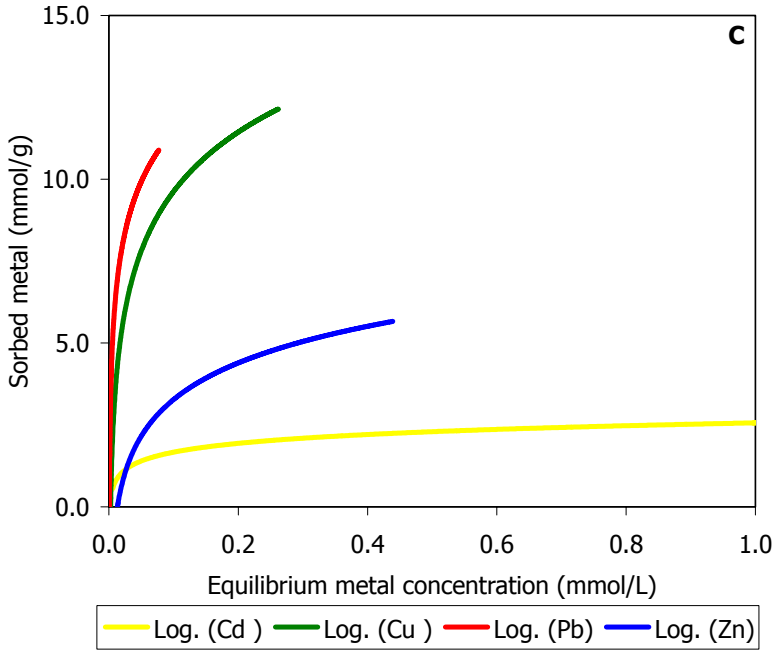
C
15.0
10.0
5.0
0.0
Sorbed metal (mmol/g)
0.0
0.2
0.4
0.6
0.8
1.0
Equilibrium metal concentration (mmol/L)
Log. (Cd)
Log. (Cu)
Log. (Pb)
Log. (Zn)

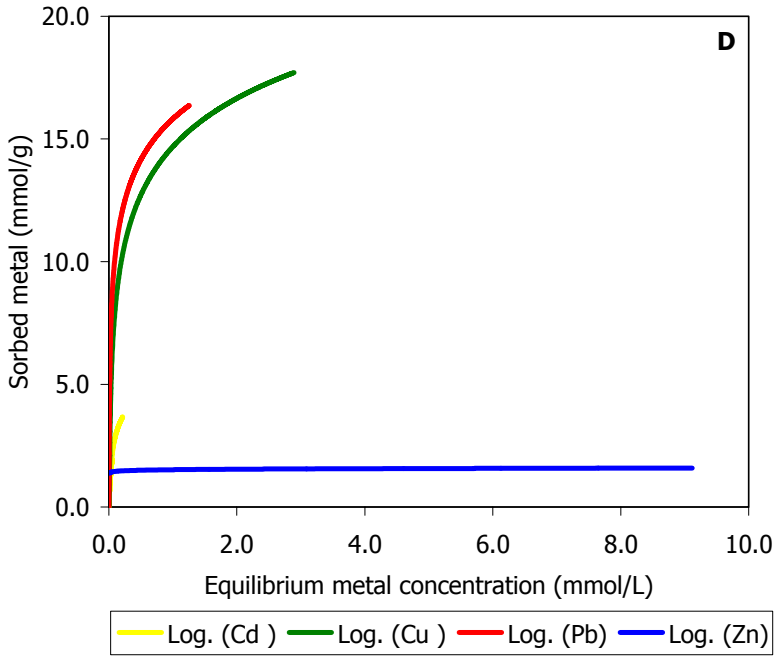

Fig. 6: Sorption isotherms for the multi-metal system where Cd is constant for the four contact times (2h, 4h, 24h and 48h) and vs. 1 g FAP. Relation between the metal sorbed (mmol/g) and the final concentration (mmol/L) in solution. A: t = 2h; B: t = 4h; C: t = 24h and D: t = 48h. – Fig. 6: Curve isotermiche per il sistema multi-metal in cui Cd è costante per i quattro tempi di contatto (2h, 4h, 24h and 48h) e vs. 1 g di FAP. Relazione tra il metallo assorbito (mmol/g) e la concentrazione finale (mmol/L) in soluzione. A: t = 2h; B: t = 4h; C: t = 24h and D: t = 48h.

The amount of Ca and P in the solution at the equilibrium are not proportional to the amount of the sorbed heavy metals, not depending on the initial concentration or interaction time. The amount of Ca ranges between values <b.d.l. and 1.2 mmol/g, the most common value about 0.05 mmol/g (Fig. 7 A, B, C, D, E and F), whereas P concentration ranges from < b.d.l. to 0.03 mmol/g (Fig. 8 A, B, C, D, E and F). In both cases this suggests a non stoichiometric dissolution of FAP.

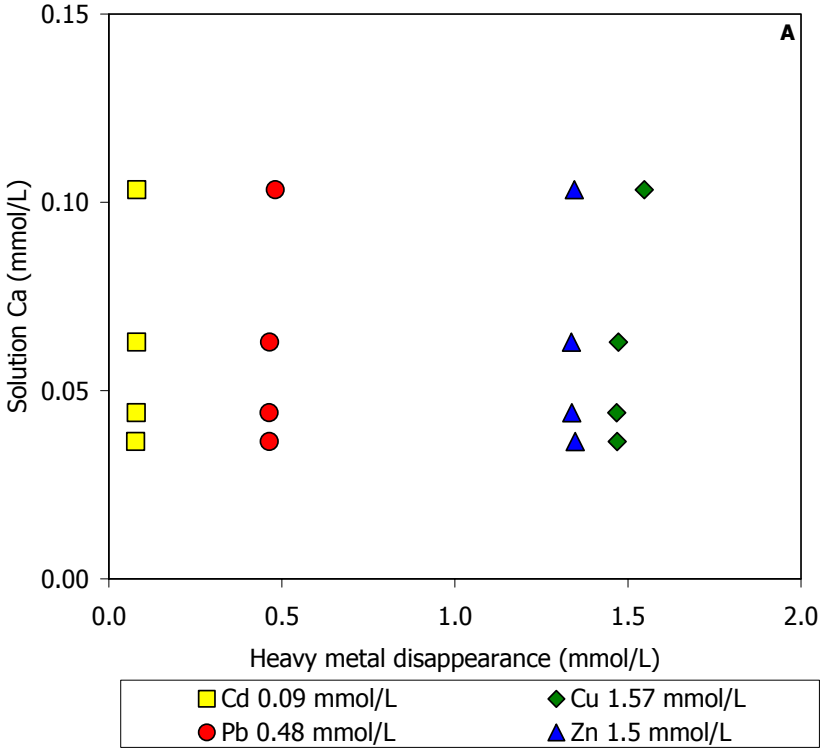
A
0.15
0.10
0.05
0.00
Solution Ca (mmol/L)
0.0
0.5
1.0
1.5
2.0
Heavy metal disappearance (mmol/L)
Cd 0.09 mmol/L
Cu 1.57 mmol/L
Pb 0.48 mmol/L
Zn 1.5 mmol/L

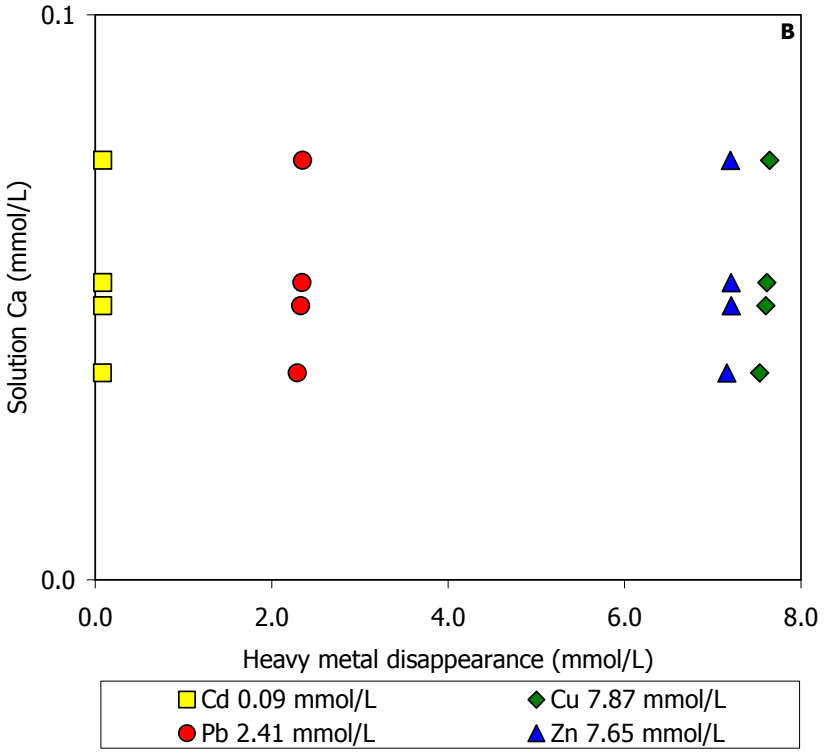
B
0.1
0.0
Solution Ca (mmol/L)
0.0
2.0
4.0
6.0
8.0
Heavy metal disappearance (mmol/L)
Cd 0.09 mmol/L
Cu 7.87 mmol/L
Pb 2.41 mmol/L
Zn 7.65 mmol/L

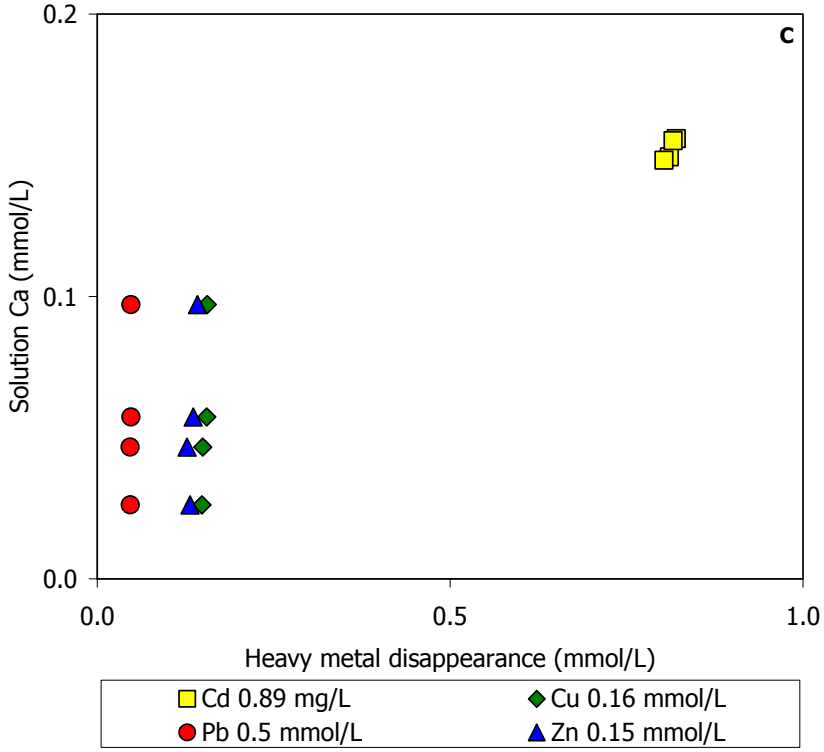
C
0.2
0.1
0.0
Solution Ca (mmol/L)
0.0
0.5
1.0
Heavy metal disappearance (mmol/L)
Cd 0.89 mg/L
Cu 0.16 mmol/L
Pb 0.5 mmol/L
Zn 0.15 mmol/L

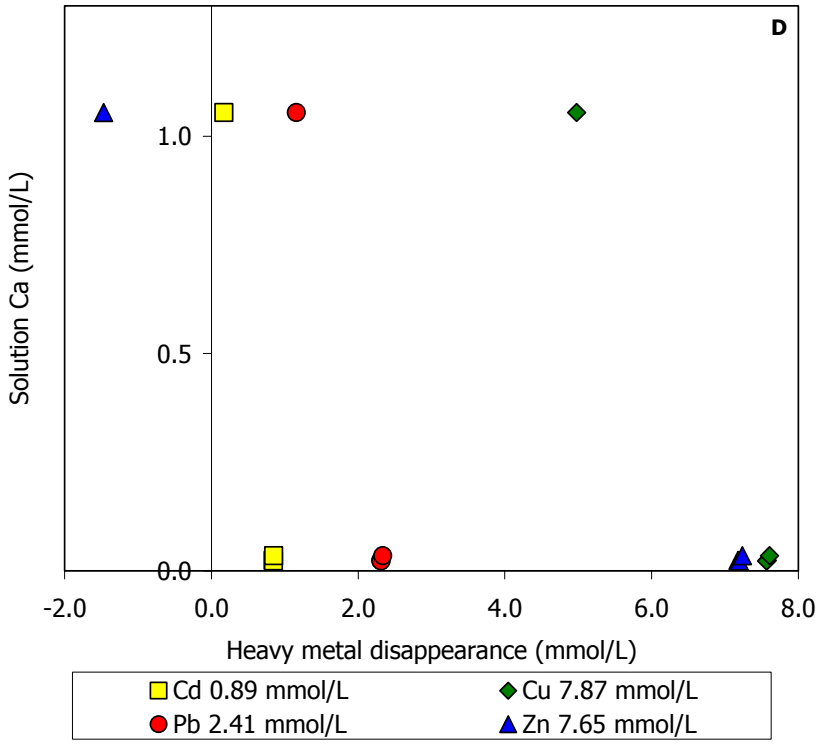
D
1.0
0.5
0.0
Solution Ca (mmol/L)
-2.0
0.0
2.0
4.0
6.0
8.0
Heavy metal disappearance (mmol/L)
Cd 0.89 mmol/L
Cu 7.87 mmol/L
Pb 2.41 mmol/L
Zn 7.65 mmol/L

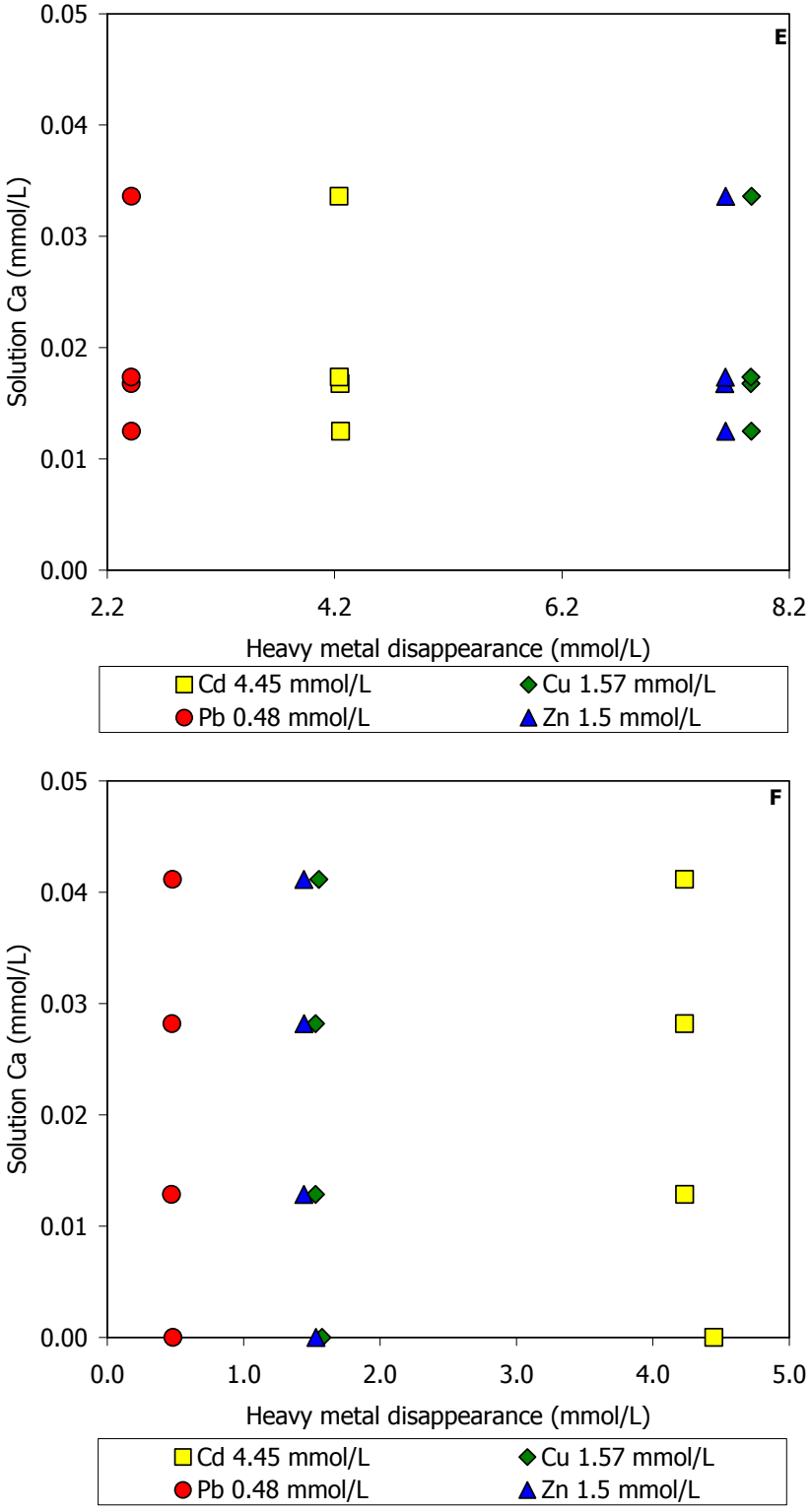

Fig. 7: Relation between Ca in solution (mmol/L) and the amount of heavy metals disappeared (mmol/L) sorbed on FAP surface at the equilibrium in a multi-metal system when Cd is constant. Each initial concentration of the multi-metal system is written in the legend. - Fig. 7: Relazione tra il quantitativo di Ca in soluzione (mmol/L) e di ciascun metallo pesante adsorbito (mmol/L) nel sistema multi-metal quando Cd è costante. La concentrazione iniziale di ogni elemento del sistema multi-metal è in leggenda.

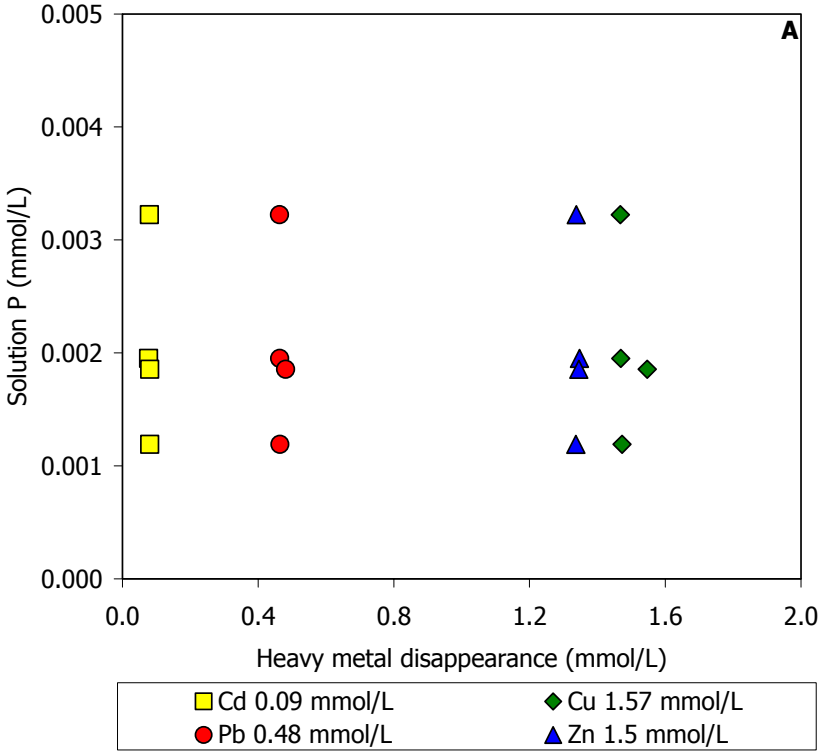
A
0.005
0.004
0.003
0.002
0.001
0.000
Solution P (mmol/L)
0.0
0.4
0.8
1.2
1.6
2.0
Heavy metal disappearance (mmol/L)
Cd 0.09 mmol/L
Cu 1.57 mmol/L
Pb 0.48 mmol/L
Zn 1.5 mmol/L

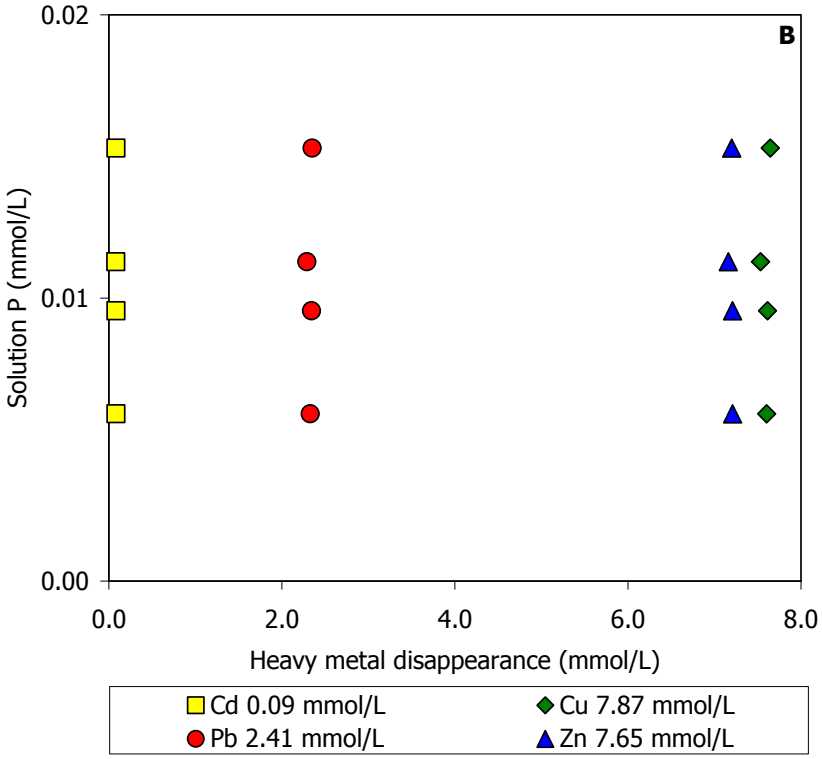
B
0.02
0.01
0.00
Solution P (mmol/L)
0.0
2.0
4.0
6.0
8.0
Heavy metal disappearance (mmol/L)
Cd 0.09 mmol/L
Cu 7.87 mmol/L
Pb 2.41 mmol/L
Zn 7.65 mmol/L

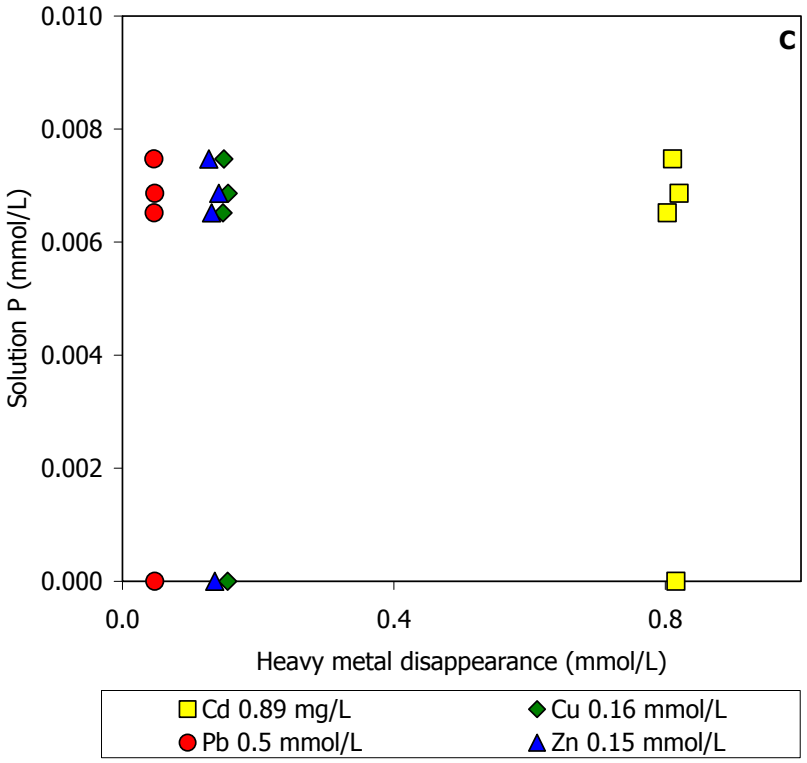
C
0.010
0.008
0.006
0.004
0.002
0.000
Solution P (mmol/L)
0.0
0.4
0.8
Heavy metal disappearance (mmol/L)
Cd 0.89 mg/L
Cu 0.16 mmol/L
Pb 0.5 mmol/L
Zn 0.15 mmol/L

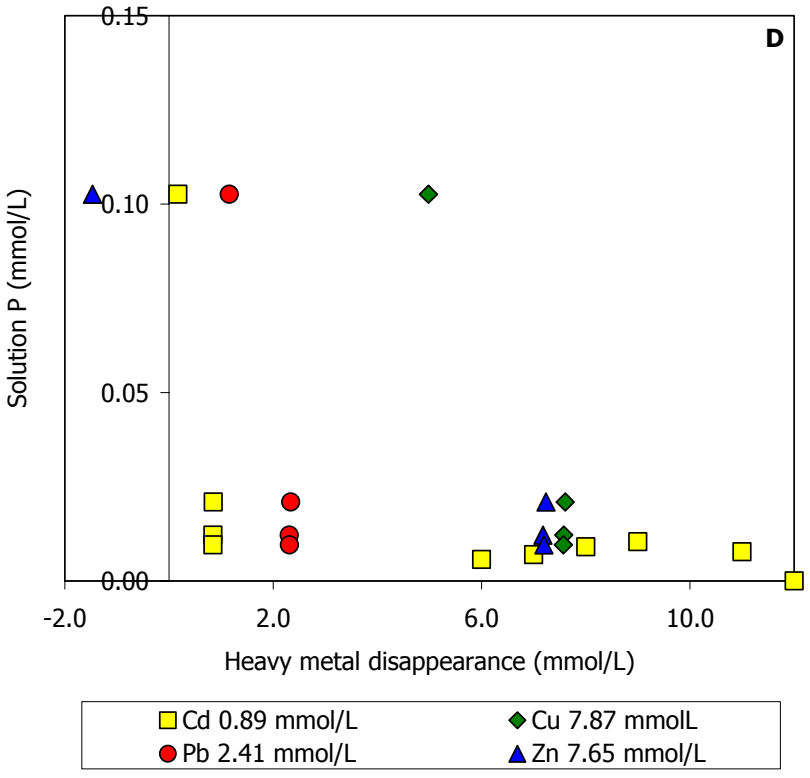
D
0.15
0.10
0.05
0.00
Solution P (mmol/L)
-2.0
2.0
6.0
10.0
Heavy metal disappearance (mmol/L)
Cd 0.89 mmol/L
Cu 7.87 mmolL
Pb 2.41 mmol/L
Zn 7.65 mmol/L

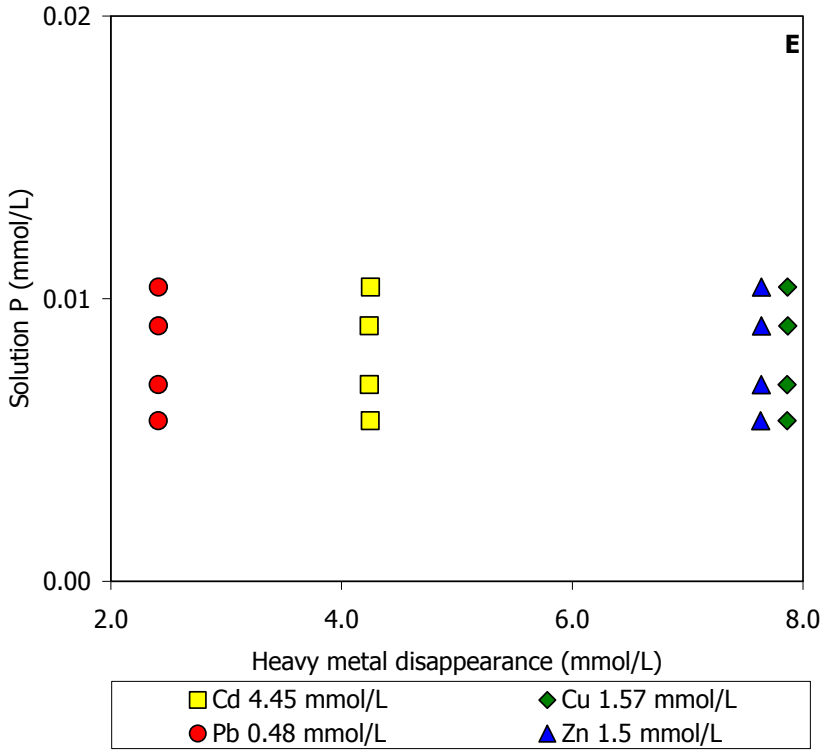

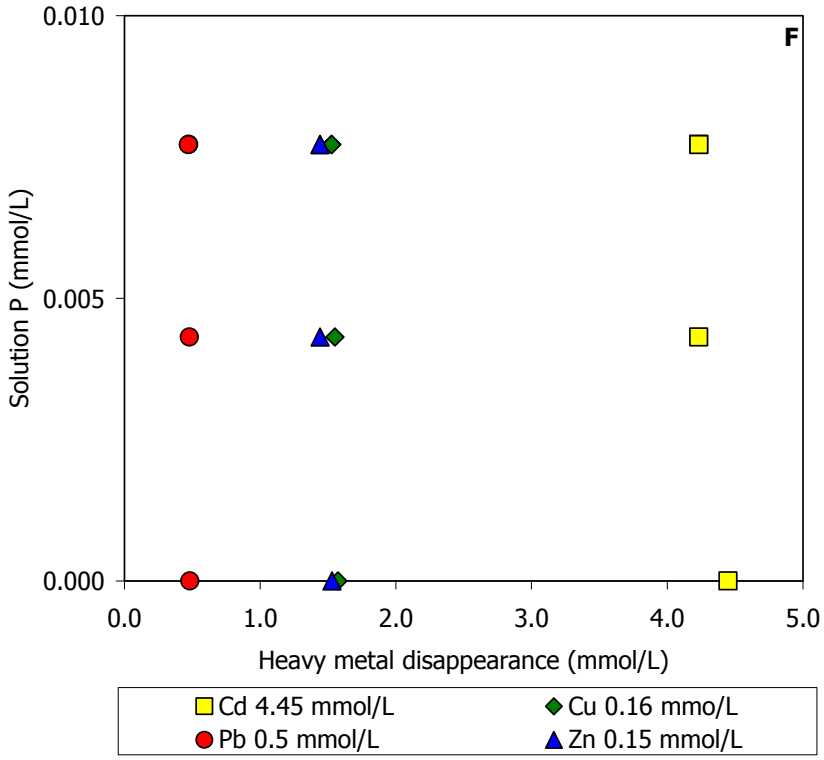

Fig. 8: Relation between P in solution (mmol/L) and the amount of disappeared heavy metals (mmol/L) sorbed on FAP surface at the equilibrium in a multi-metal system when Cd is constant. Each initial concentration of the multi-metal system is written in the legend. - Fig. 8: Relazione tra il quantitativo di P in

soluzione (mmol/L) e di ciascun metallo pesante adsorbito (mmol/L) nel sistema multi-metal quando Cd è costante. La concentrazione iniziale di ogni elemento del sistema multi-metal è in leggenda.

In the Cu system (Tab. 3 and Fig. 9 A, B, C, D, E and F) the time of the best immobilization is 24h. The order of immobilization is Pb > Cu > Cd > Zn, as observed for the previous system. In this system pH decreases of about 0.3-0.5 units after the immobilization.

Cd = 100 mg/L	Cu = 10 mg/L	Pb = 100 mg/L	Zn = 100 mg/L
17.743	-12.674	19.267	16.828
18.017	1.837	18.965	17.532
18.293	1.983	19.965	17.939
18.210	1.894	19.407	17.745
Cd = 500 mg/L	Cu = 10 mg/L	Pb = 500 mg/L	Zn = 500 mg/L
-0.307	19.829	0.766	-0.798
1.683	19.036	1.926	1.543
1.779	19.846	1.976	1.655
1.762	19.526	1.965	1.626
Cd = 10 mg/L	Cu = 100 mg/L	Pb = 10 mg/L	Zn = 10 mg/L
94.651	19.904	98.109	64.684
94.977	19.224	96.766	93.772
94.984	19.273	96.267	93.938
95.165	19.646	96.686	94.326
Cd = 500 mg/L	Cu = 100 mg/L	Pb = 500 mg/L	Zn = 500 mg/L
474.741	96.627	481.510	497.070
475.595	96.748	485.941	496.952
477.209	96.962	483.756	497.293
475.347	96.754	483.089	497.059
Cd = 10 mg/L	Cu = 500 mg/L	Pb = 10 mg/L	Zn = 10 mg/L
1.783	96.699	1.908	1.760
1.864	96.840	1.959	1.855
1.873	96.673	1.955	1.867
1.880	98.900	1.977	1.870
Cd = 100 mg/L	Cu = 500 mg/L	Pb = 100 mg/L	Zn = 100 mg/L
19.127	97.294	19.657	18.882
18.820	99.121	19.383	19.825
9.020	34.646	15.934	7.069
18.853	95.434	19.546	18.529

Table 3: Proportions of blocked heavy metals per unit mass of FAP (mg/g) for the multi-metal system when Cu is constant. – Tabella 3: Entità dell'immobilizzazione dei metalli per unità di massa di FAP (mg/g) per il sistema multi-metal con concentrazione del Cu costante.

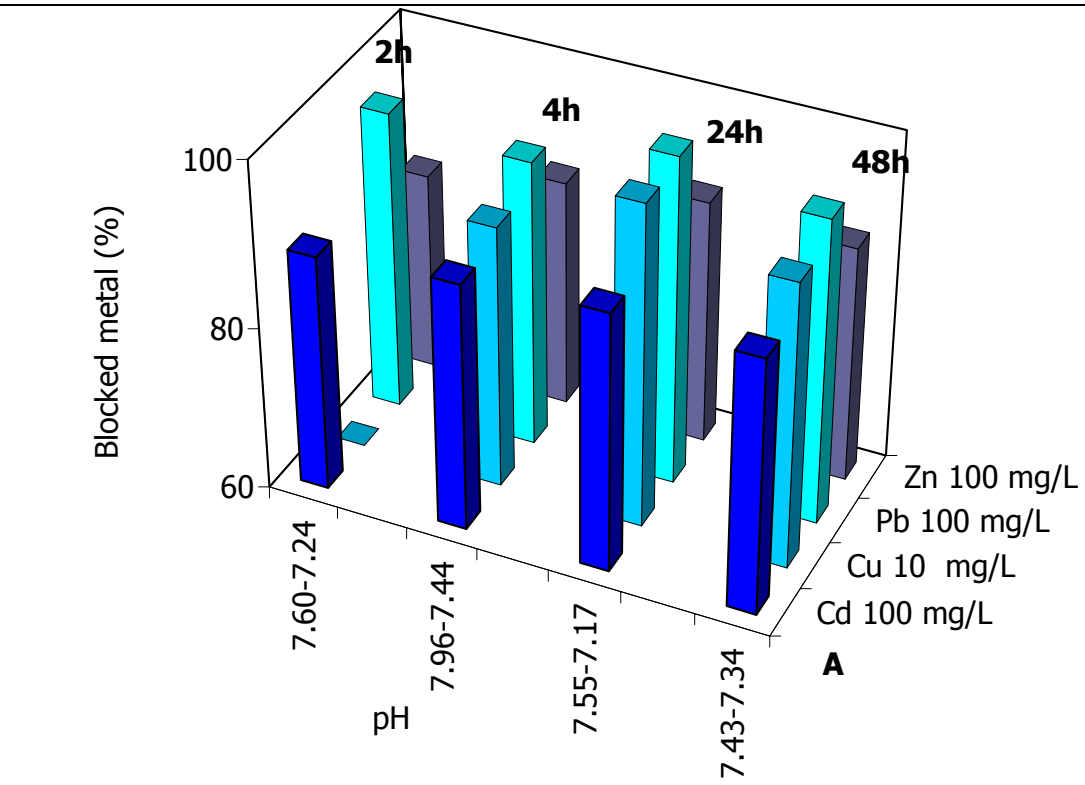
2h
4h
24h
48h
100
80
60
Blocked metal (%)
7.60-7.24
7.96-7.44
7.55-7.17
7.43-7.34
pH
Zn 100 mg/L
Pb 100 mg/L
Cu 10 mg/L
Cd 100 mg/L
A

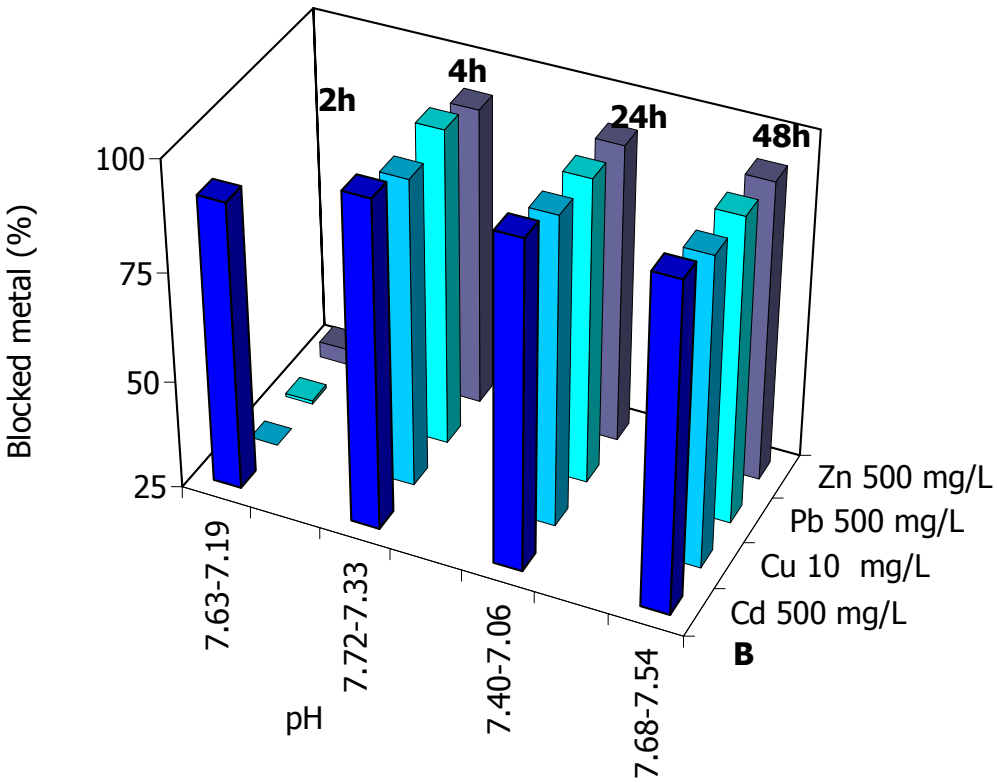
2h
4h
24h
48h
100
75
50
25
Blocked metal (%)
7.63-7.19
7.72-7.33
7.40-7.06
7.68-7.54
pH
Zn 500 mg/L
Pb 500 mg/L
Cu 10 mg/L
Cd 500 mg/L
B

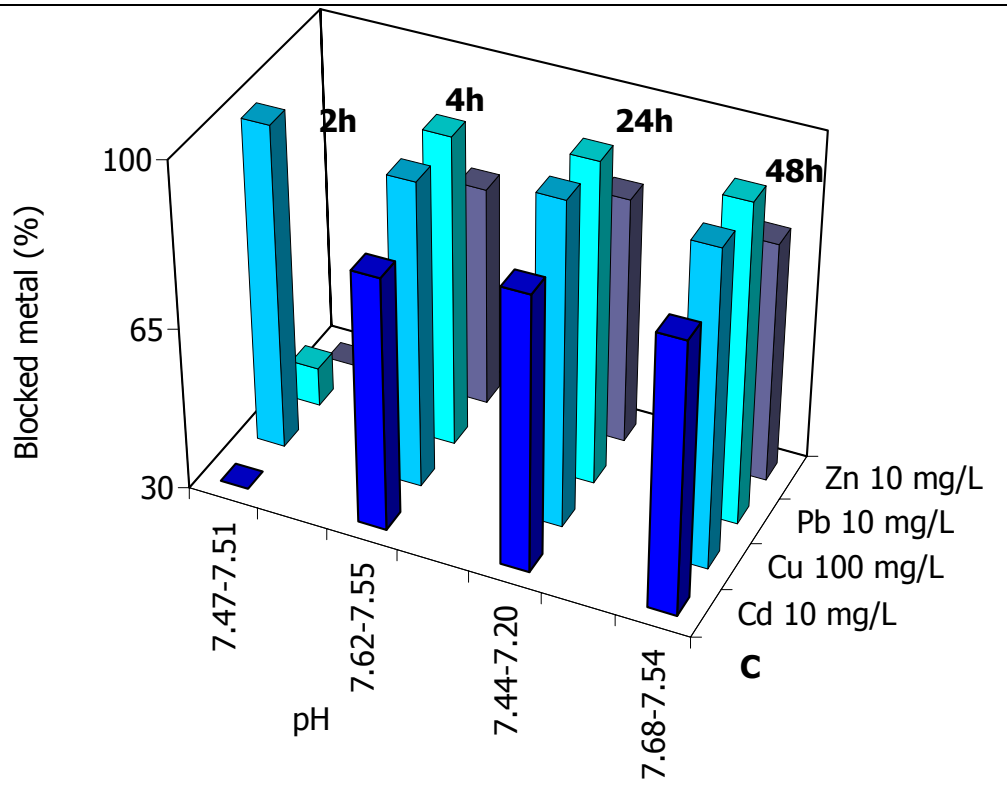
Blocked metal (%)
100
65
30
2h
4h
24h
48h
7.47-7.51
7.62-7.55
7.44-7.20
7.68-7.54
pH
Zn 10 mg/L
Pb 10 mg/L
Cu 100 mg/L
Cd 10 mg/L
C

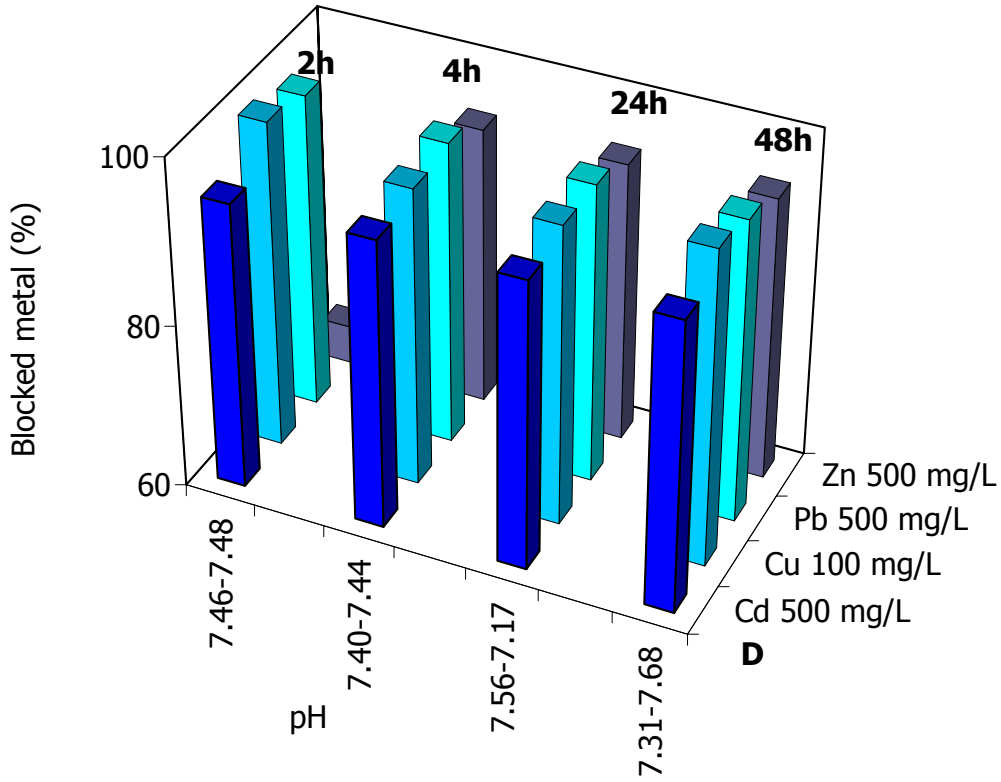
Blocked metal (%)
100
80
60
2h
4h
24h
48h
7.46-7.48
7.40-7.44
7.56-7.17
7.31-7.68
pH
Zn 500 mg/L
Pb 500 mg/L
Cu 100 mg/L
Cd 500 mg/L
D

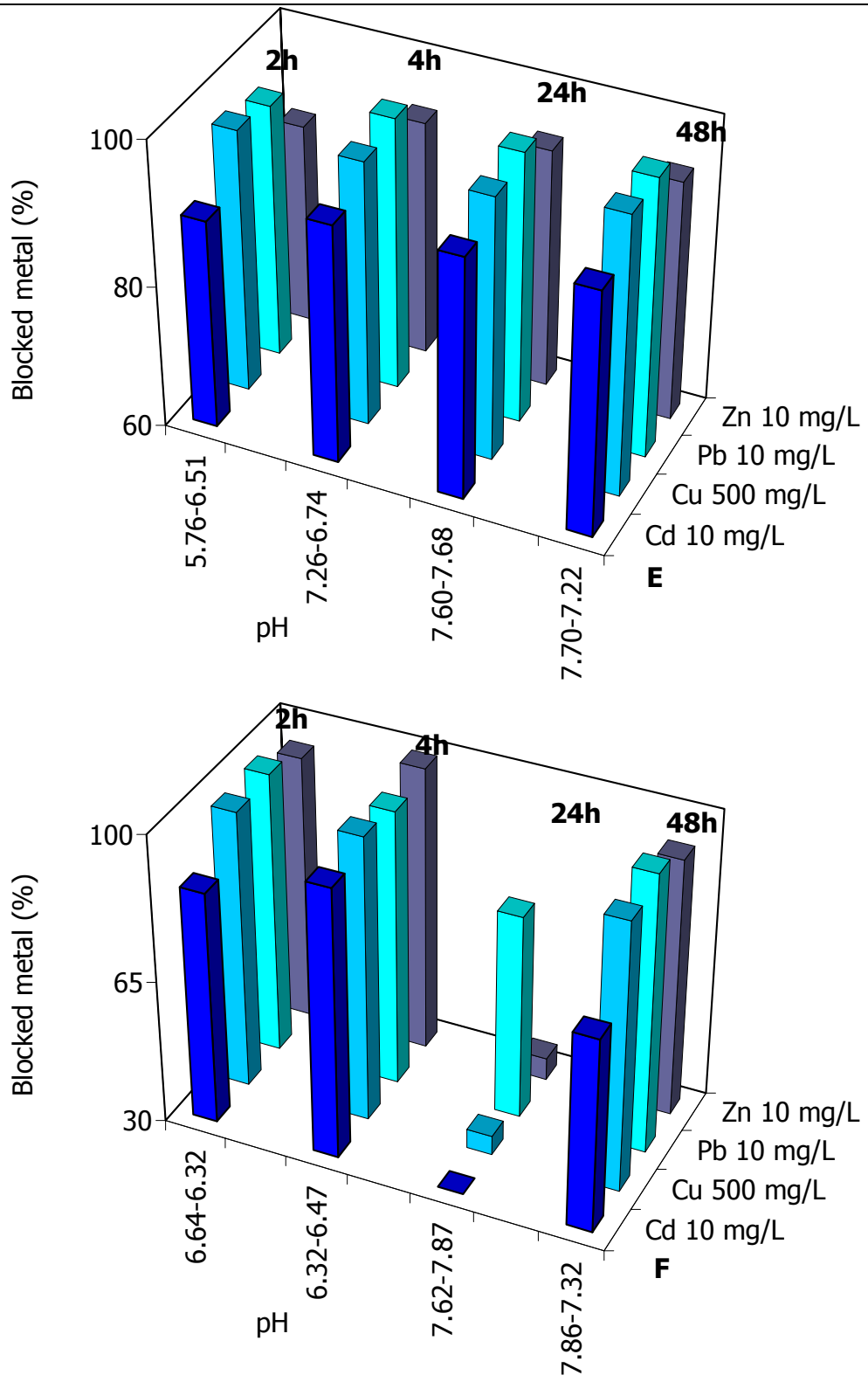

Fig. 9: Variation of the amount of blocked metal with time for the mass of FAP (1 g) in the multi-metal system where Cu is constant. Initial and final pH values are reported. – Fig. 11: Variazione delle percentuali dei metalli immobilizzati in funzione del tempo di interazione per la quantità di FAP (1 g) nel sistema multi-metal in cui Cu è l'elemento costante. Sono riportati i valori iniziali e finali del pH.

For the lower Cu concentration (10 mg/L) (Tab. 4) Q_S values are generally < 1 and >1 only at t = 2h; Cd and Pb show Q_S < 1 and Zn has Q_S > 1 when the concentration is 100 mg/L. Increasing Cd, Pb and Zn concentrations (500 mg/L) Q_S values become>> 1. When Cu concentration is 100 mg/L, Qs < 1 for the low concentration of the other heavy metals; Cd Q_S increases to a value > 1 for heavy metals concentration of 500 mg/L and for Cd, Pb and Zn Q_S >> 1. Finally, for Cu concentration at 500 mg/L Q_S >> 1, Cd, Pb and Zn show a Q_S < 1 for low concentration, and increasing their concentration, Cd and Zn Q_S pass to a value >> 1, instead Pb shows the same Q_S values as before. So that, as in the previous system, the two probable mechanisms are a non-crystalline precipitation and superficial complexation.

Cd = 100 mg/L	Cu = 10 mg/L	Pb = 100 mg/L	Zn = 100 mg/L
0.56	6.45	0.10	1.35
2.16	0.31	0.61	4.61
0.84	0.02	0.01	1.74
1.55	0.16	0.28	3.37
Cd = 500 mg/L	Cu = 10 mg/L	Pb = 500 mg/L	Zn = 500 mg/L
5.79	1.53	3.79	11.53
8.40	0.26	2.28	18.09
7.43	0.21	3.91	15.81
5.79	0.17	3.02	12.24
Cd = 10 mg/L	Cu = 100 mg/L	Pb = 10 mg/L	Zn = 10 mg/L
2.33	0.30	0.67	4.85
0.33	1.77	0.04	0.82
0.10	0.12	0.01	0.27
0.11	0.40	0.01	0.31
Cd = 500 mg/L	Cu = 100 mg/L	Pb = 500 mg/L	Zn = 500 mg/L
10.99	0.35	2.11	124.71
10.47	2.86	3.66	22.32
7.40	1.90	2.99	15.39
4.39	0.57	1.63	8.85
Cd = 10 mg/L	Cu = 500 mg/L	Pb = 10 mg/L	Zn = 10 mg/L
0.51	13.62	0.12	0.96
0.38	15.77	0.06	0.70
0.24	11.17	0.05	0.44
0.09	1.48	0.01	0.17
Cd = 100 mg/L	Cu = 500 mg/L	Pb = 100 mg/L	Zn = 100 mg/L
2.42	13.27	0.52	5.33
0.00	0.00	0.76	0.68
1.74	18.30	0.35	3.52
1.24	8.71	0.27	2.73

Table 4: Q_S values for the multi - metal systems when Cu has a constant concentration. Tabella 4: Valori di Q_S per i sistemi multi-metal nei quali la concentrazione di Cu è stata mantenuta costante.

The sorption isotherms (Fig. 10 A, B, C and D) for this system at t = 2 and 48h present always the same shape of the L type and subtype 2, supporting the sorption processes suggested by the molar ratio results. The only exception is the absence of the Cu isotherm for t = 2h because of negative values. When t = 4 and 24h, Cd and Pb show an H type isotherm, whereas Cu and Zn show the L2 curve. Therefore, it seems the concentration of the heavy metals and interaction time are the key factor for the isotherm curves.

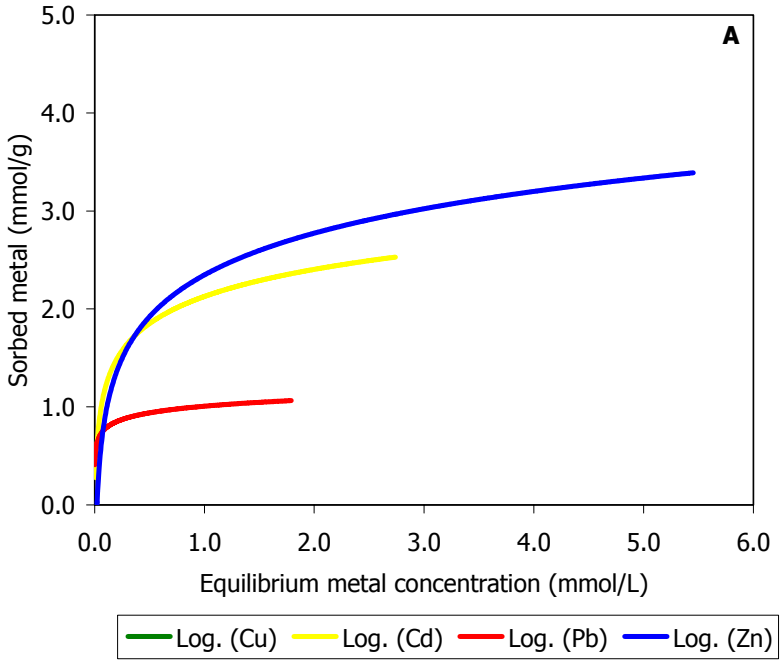

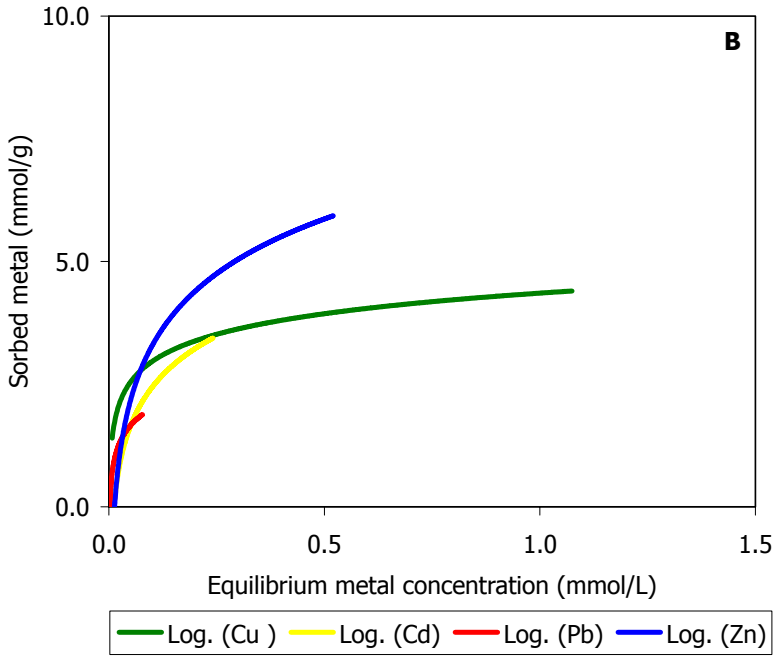

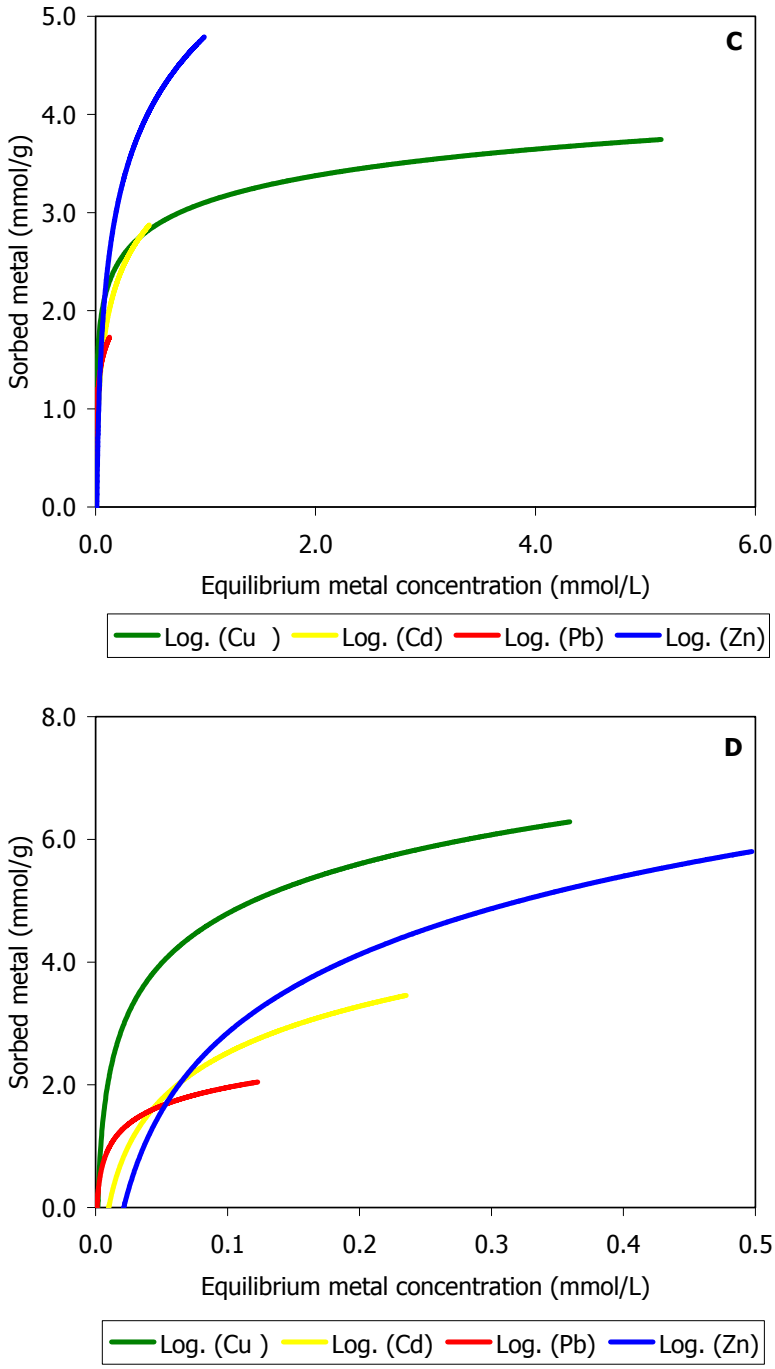

Fig. 10: Sorption isotherms for the multi-metal system where Cu is constant for the four contact times (2h, 4h, 24h and 48h) and vs. 1 g FAP. Relation between the metal sorbed (mmol/g) and the final concentration (mmol/L) in solution. A: t = 2h; B: t = 4h; C: t = 24h and D: t = 48h. – Fig. 10: Curve isotermiche per il sistema multi-metal in cui Cu è costante per i quattro tempi di contatto (2h, 4h, 24h and 48h) e vs. 1 g di FAP. Relazione tra il metallo assorbito (mmol/g) e la concentrazione finale (mmol/L) in soluzione. A: t = 2h; B: t = 4h; C: t = 24h and D: t = 48h.

The amounts of Ca and P in solutions at the equilibrium are low (Fig. 11 A, B, C, D, E and F; 12 A, B, C, D, E and F), indicating also for this system a non stoichiometric dissolution of FAP. The concentration of both element are almost similar to those of Cd system; Ca ranges from 0.015 to 0.5 mmol/g and P from b.d.l. to 0.3 mmol/g. The non stoichiometric dissolution of FAP allows to infer an adsorption phenomenon and the non-crystalline precipitation of a phases.

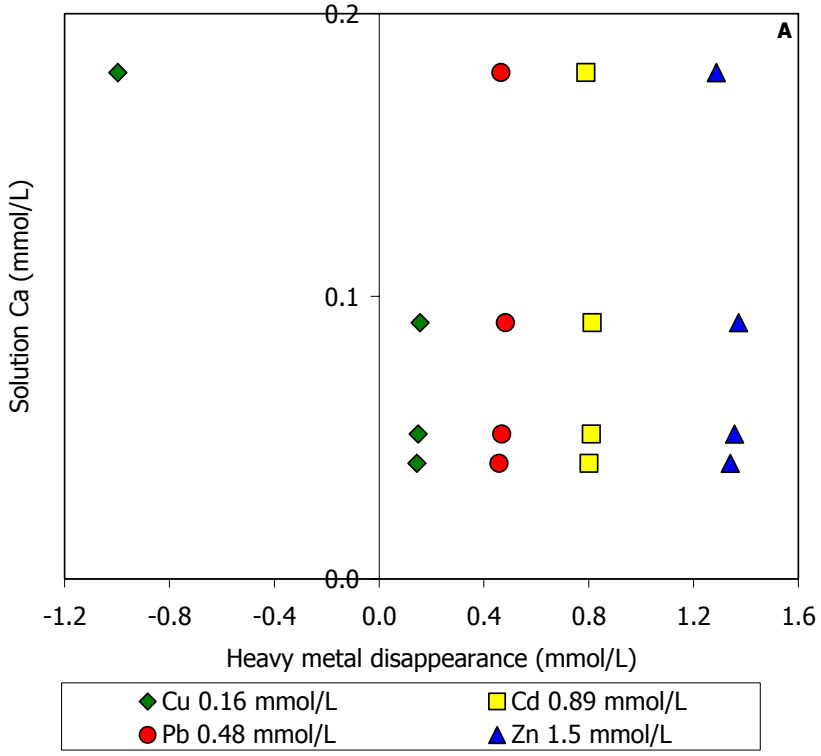

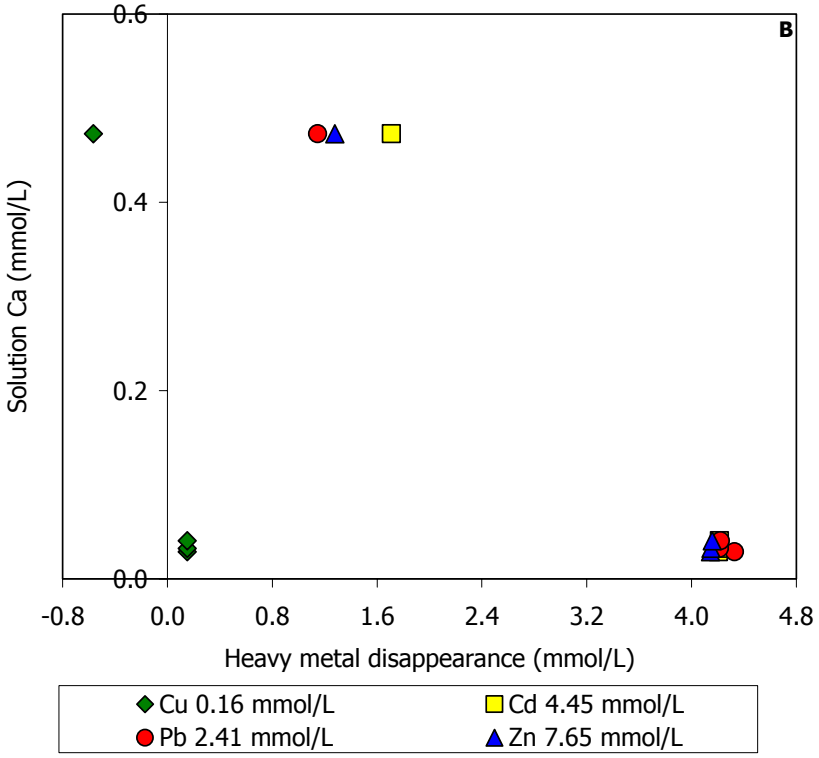
B
0.6
0.4
0.2
0.0
Solution Ca (mmol/L)
-0.8
0.0
0.8
1.6
2.4
3.2
4.0
4.8
Heavy metal disappearance (mmol/L)
Cu 0.16 mmol/L
Cd 4.45 mmol/L
Pb 2.41 mmol/L
Zn 7.65 mmol/L

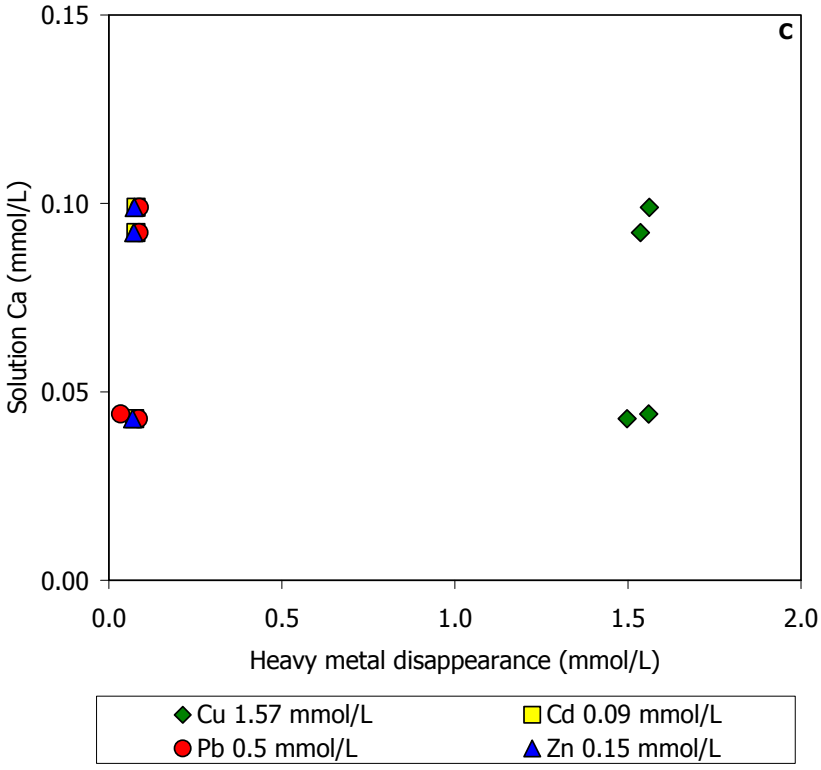
C
0.15
0.10
0.05
0.00
Solution Ca (mmol/L)
0.0
0.5
1.0
1.5
2.0
Heavy metal disappearance (mmol/L)
Cu 1.57 mmol/L
Cd 0.09 mmol/L
Pb 0.5 mmol/L
Zn 0.15 mmol/L

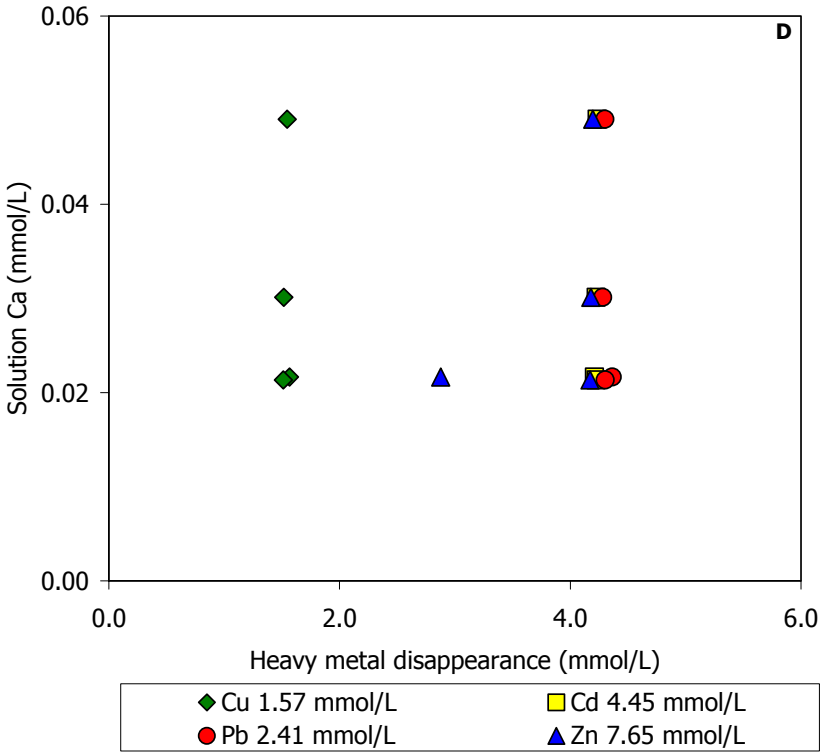
D
0.06
0.04
0.02
0.00
Solution Ca (mmol/L)
0.0
2.0
4.0
6.0
Heavy metal disappearance (mmol/L)
Cu 1.57 mmol/L
Cd 4.45 mmol/L
Pb 2.41 mmol/L
Zn 7.65 mmol/L

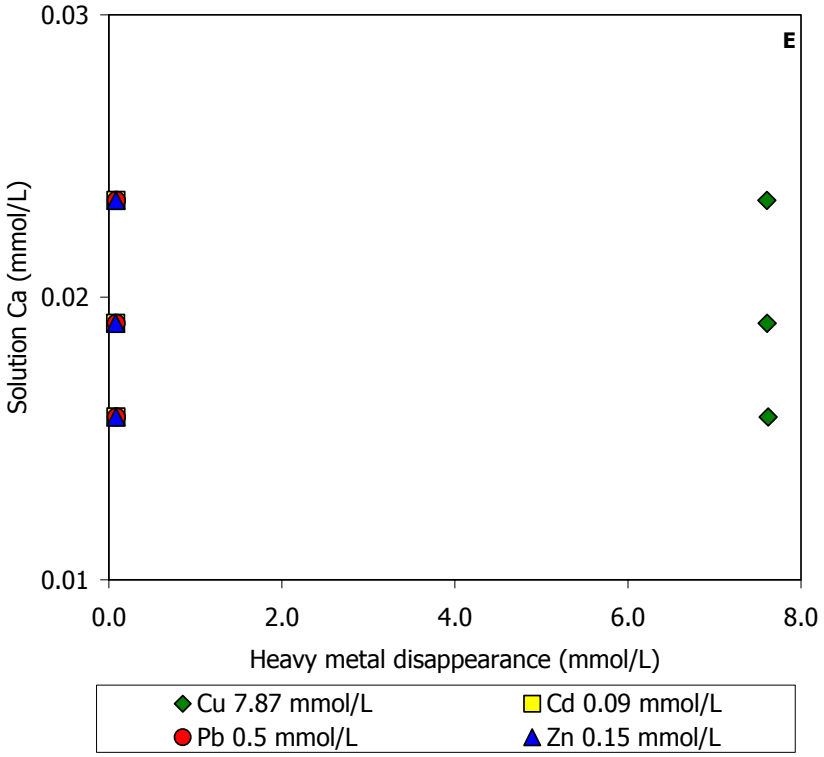
E
0.03
0.02
0.01
Solution Ca (mmol/L)
0.0
2.0
4.0
6.0
8.0
Heavy metal disappearance (mmol/L)
Cu 7.87 mmol/L
Cd 0.09 mmol/L
Pb 0.5 mmol/L
Zn 0.15 mmol/L

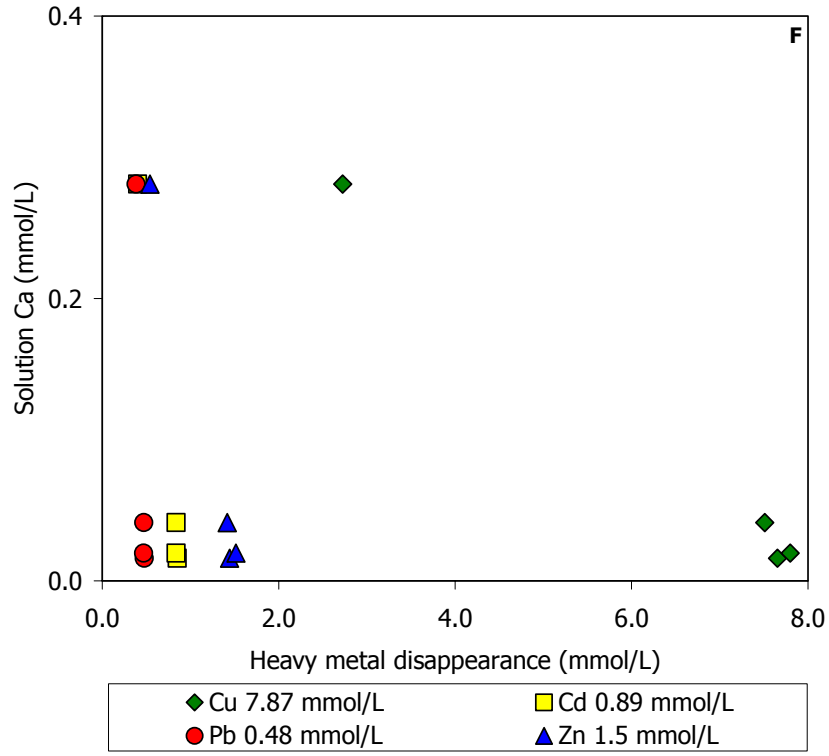

Fig.11: Relation between Ca in solution (mmol/L) and the amount of heavy metals disappeared (mmol/L) sorbed on FAP surface at the equilibrium in a multi-metal system when Cu is constant. Each initial concentration of the multi-metal system is written in the legend. - Fig. 11: Relazione tra il quantitativo di Ca in soluzione (mmol/L) e di ciascun metallo pesante adsorbito (mmol/L) nel sistema multi-metal quando Cu è costante. La concentrazione iniziale di ogni elemento del sistema multi-metal è in leggenda.

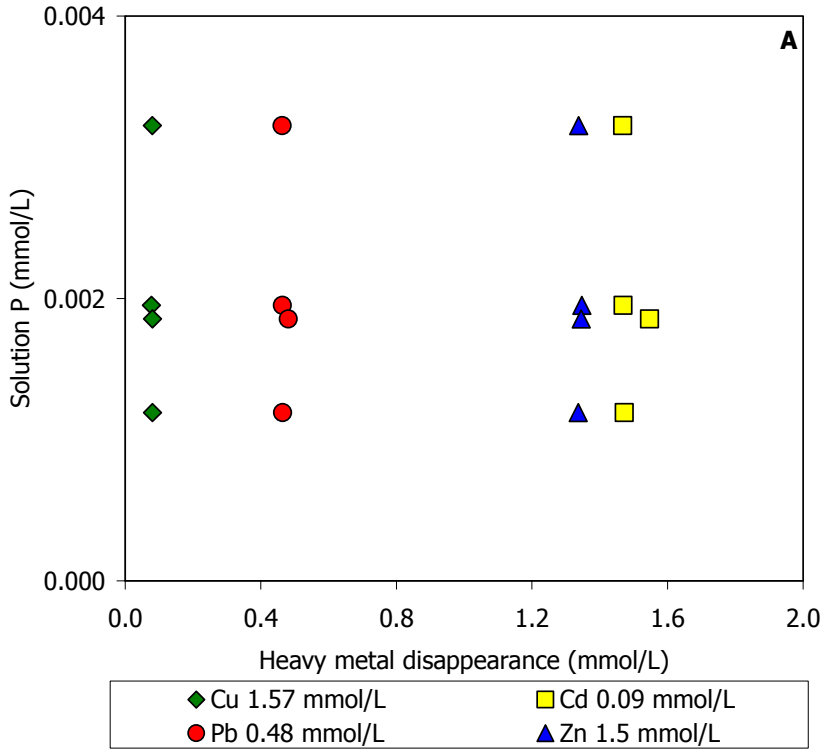
A
0.004
0.002
0.000
Solution P (mmol/L)
0.0
0.4
0.8
1.2
1.6
2.0
Heavy metal disappearance (mmol/L)
Cu 1.57 mmol/L
Cd 0.09 mmol/L
Pb 0.48 mmol/L
Zn 1.5 mmol/L

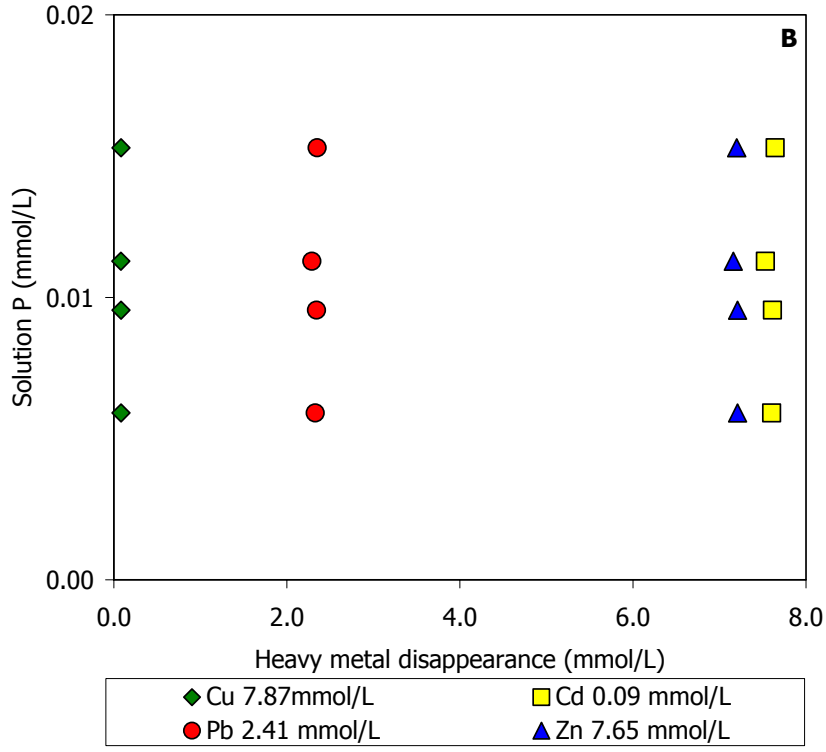
B
0.02
0.01
0.00
Solution P (mmol/L)
0.0
2.0
4.0
6.0
8.0
Heavy metal disappearance (mmol/L)
Cu 7.87mmol/L
Cd 0.09 mmol/L
Pb 2.41 mmol/L
Zn 7.65 mmol/L

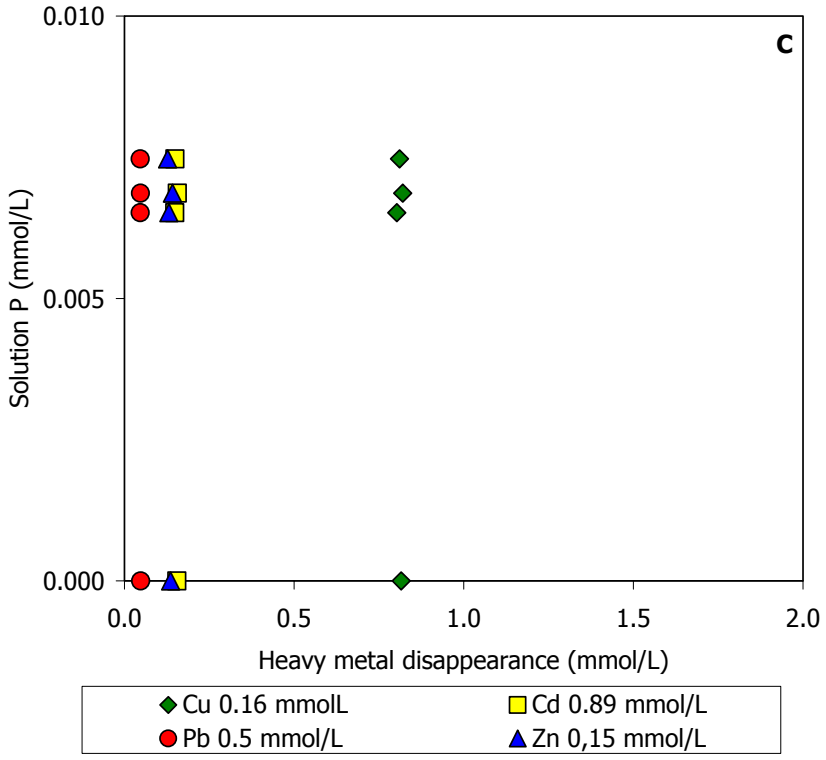
C
0.010
0.005
0.000
Solution P (mmol/L)
0.0
0.5
1.0
1.5
2.0
Heavy metal disappearance (mmol/L)
Cu 0.16 mmolL
Cd 0.89 mmol/L
Pb 0.5 mmol/L
Zn 0,15 mmol/L

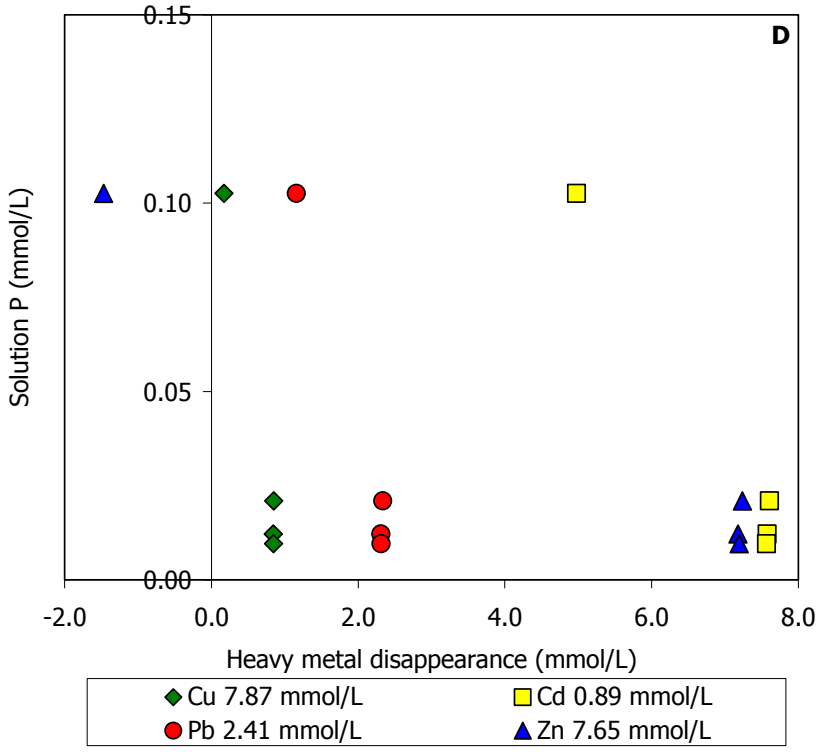
D
0.15
0.10
0.05
0.00
Solution P (mmol/L)
-2.0
0.0
2.0
4.0
6.0
8.0
Heavy metal disappearance (mmol/L)
Cu 7.87 mmol/L
Cd 0.89 mmol/L
Pb 2.41 mmol/L
Zn 7.65 mmol/L

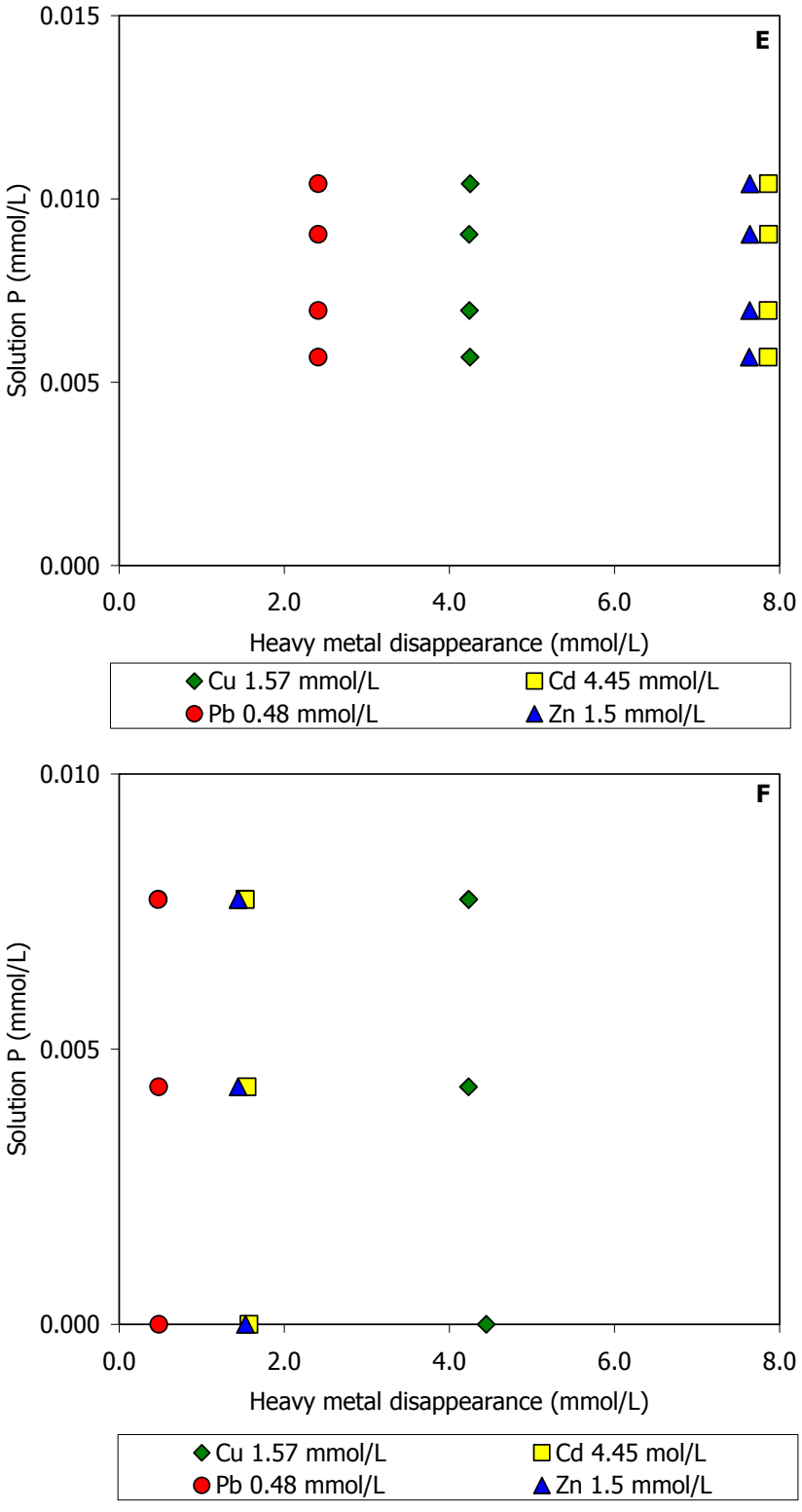

Fig.12: Relation between P in solution (mmol/L) and the amount of disappeared heavy metals (mmol/L) sorbed on FAP surface at the equilibrium in a multi-metal system when Cu is constant. Each initial concentration of the multi-metal system is written in the legend. - Fig. 12: Relazione tra il quantitativo di P in soluzione (mmol/L) e di ciascun metallo pesante adsorbito (mmol/L) nel sistema multi-metal quando Cu è costante. La concentrazione iniziale di ogni elemento del sistema multi-metal è in leggenda.

In the Pb system (Tab. 5 and Fig. 13 A, B, C, D, E, F, G, H and I) the best immobilization time is 48h and the order is Pb > Cu > Cd > Zn. However, Cd and Zn are often not immobilized, showing negative values. pH generally raises of about 0.5-1 units after the experimentation time.

Cd = 10 mg/L	Cu = 10 mg/L	Pb = 10 mg/L	Zn = 10 mg/L
1.322	1.901	1.932	0.823
1.520	1.917	1.976	1.115
1.903	1.989	1.978	1.887
1.915	1.985	1.983	1.931
Cd = 100 mg/L	Cu = 100 mg/L	Pb = 10 mg/L	Zn = 100 mg/L
-1.670	8.329	1.963	-7.001
-2.142	9.364	1.952	-8.147
1.845	14.508	1.852	-3.053
13.891	13.891	1.908	-3.431
Cd = 500 mg/L	Cu = 500 mg/L	Pb = 10 mg/L	Zn = 500 mg/L
4.898	34.827	1.828	57.786
-0.972	30.929	1.703	55.252
-3.654	45.831	1.815	53.835
-10.823	61.042	1.906	50.987
Cd = 10 mg/L	Cu = 10 mg/L	Pb = 100 mg/L	Zn = 10 mg/L
0.138	0.808	12.762	-0.158
-0.659	0.816	14.831	-1.122
-0.377	1.199	18.023	-1.129
-0.188	1.342	18.610	-0.614
Cd = 100 mg/L	Cu = 100 mg/L	Pb = 100 mg/L	Zn = 100 mg/L
-1.190	5.937	5.197	-2.986
7.864	6.345	4.006	-6.558
-4.022	9.055	10.707	-9.368
19.825	19.992	19.886	19.393
Cd = 500 mg/L	Cu = 500 mg/L	Pb = 100 mg/L	Zn = 500 mg/L
98.043	99.951	19.966	99.416
-26.021	25.799	19.145	-23.784
-12.932	36.597	19.343	-24.448
43.090	98.609	19.940	82.427
Cd = 10 mg/L	Cu = 10 mg/L	Pb = 500 mg/L	Zn = 10 mg/L
-0.121	0.529	22.606	-0.041
-1.228	0.350	26.980	-1.713
-0.534	0.483	28.295	-0.483
-0.328	0.544	45.756	-0.265
Cd = 100 mg/L	Cu = 100 mg/L	Pb = 500 mg/L	Zn = 100 mg/L
17.541	18.534	37.904	17.628
3.927	6.876	33.023	-1.220
3.110	6.524	36.385	-2.551
0.165	8.277	36.934	-5.369
Cd = 500 mg/L	Cu = 500 mg/L	Pb = 500 mg/L	Zn = 100 mg/L
2.057	28.452	23.515	-15.900
4.563	36.697	25.561	-13.468
2.434	25.674	27.961	-18.078
2.616	27.372	28.404	-26.949

Table 5: Efficiency values for the multi - metal system when Pb has a constant concentration.

Tabella 5: Valori dell'efficienza nell'immobilizzare i metalli pesanti per il sistema multi-metal in cui il Pb mantiene costante le concentrazione.

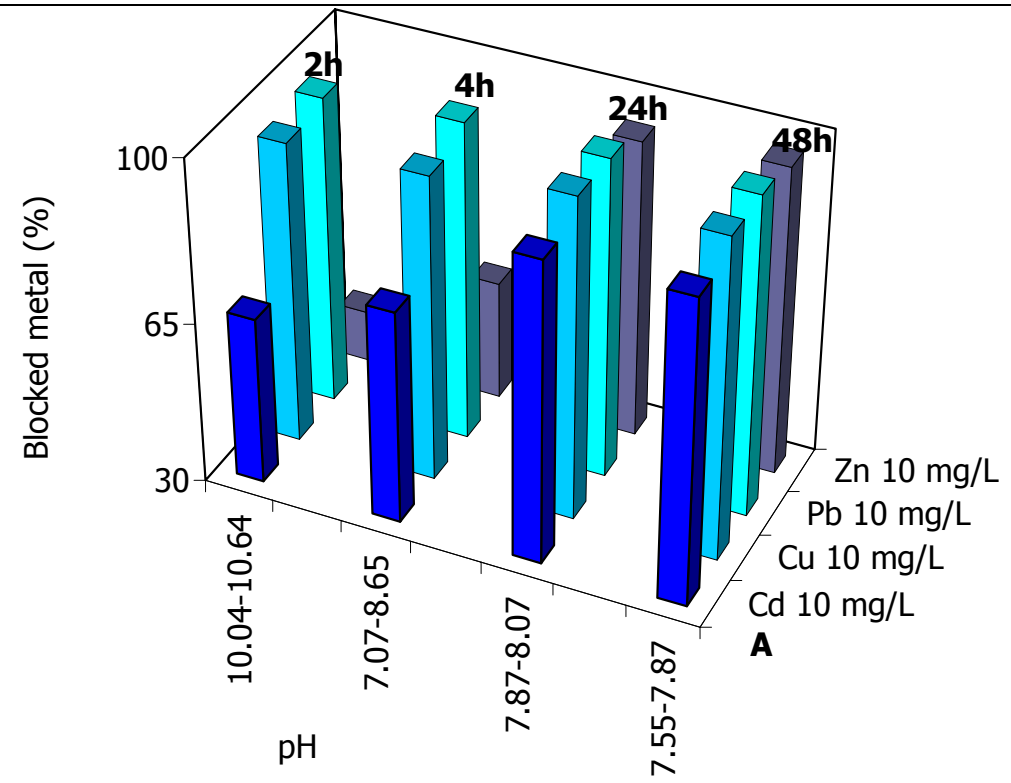
2h
4h
24h
48h
100
65
30
Blocked metal (%)
10.04-10.64
7.07-8.65
7.87-8.07
7.55-7.87
pH
Zn 10 mg/L
Pb 10 mg/L
Cu 10 mg/L
Cd 10 mg/L
A

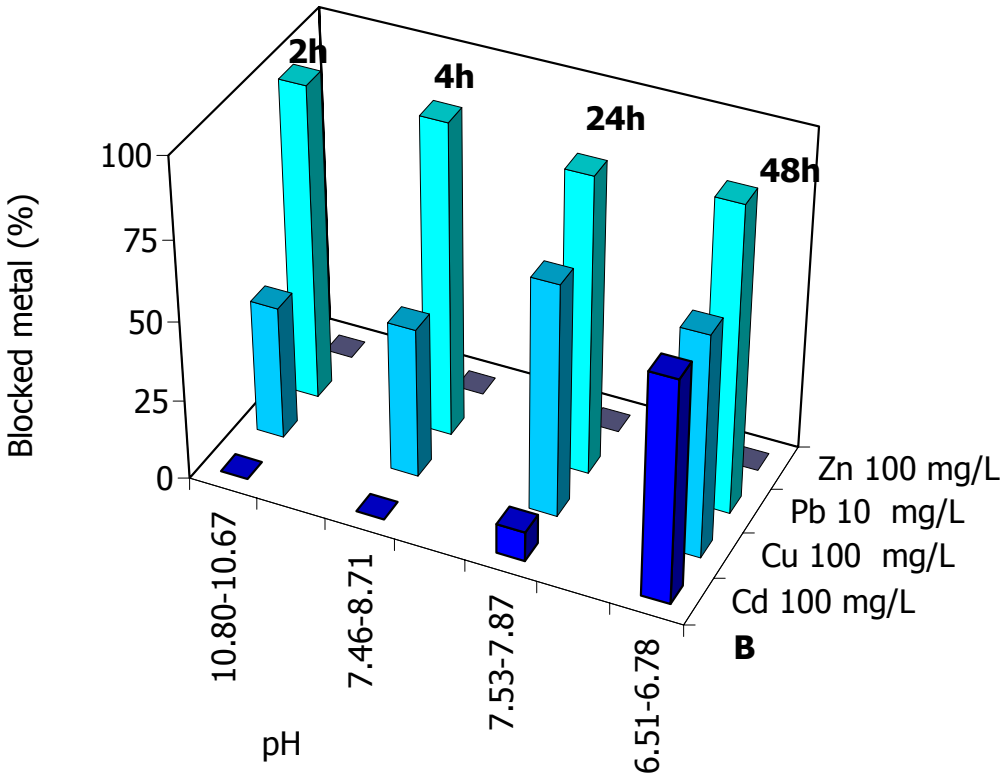
2h
4h
24h
48h
100
75
50
25
0
Blocked metal (%)
10.80-10.67
7.46-8.71
7.53-7.87
6.51-6.78
pH
Zn 100 mg/L
Pb 10 mg/L
Cu 100 mg/L
Cd 100 mg/L
B

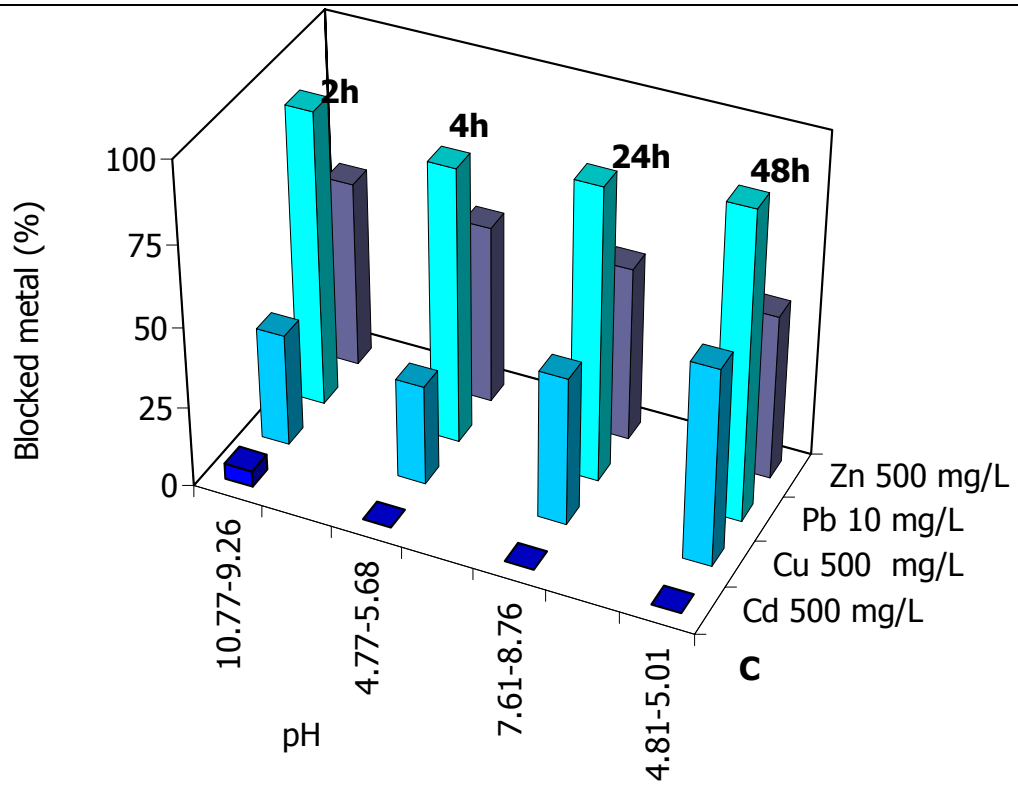
Blocked metal (%)
100
75
50
25
0
2h
4h
24h
48h
10.77-9.26
4.77-5.68
7.61-8.76
4.81-5.01
pH
Zn 500 mg/L
Pb 10 mg/L
Cu 500 mg/L
Cd 500 mg/L
C

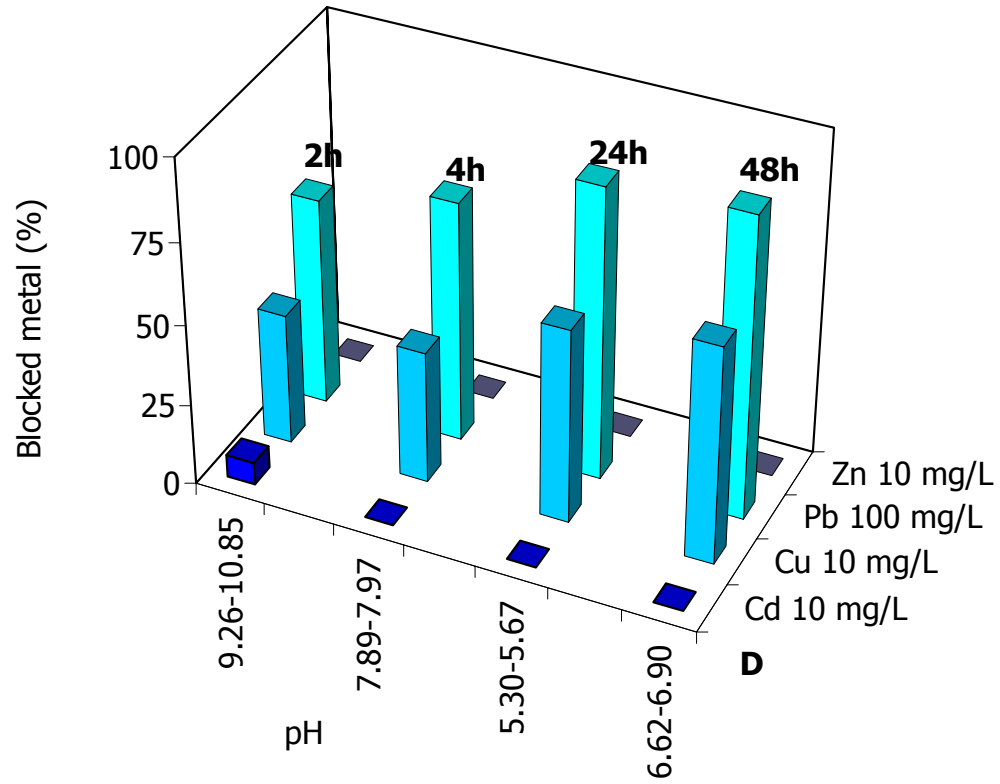
Blocked metal (%)
100
75
50
25
0
2h
4h
24h
48h
9.26-10.85
7.89-7.97
5.30-5.67
6.62-6.90
pH
Zn 10 mg/L
Pb 100 mg/L
Cu 10 mg/L
Cd 10 mg/L
D

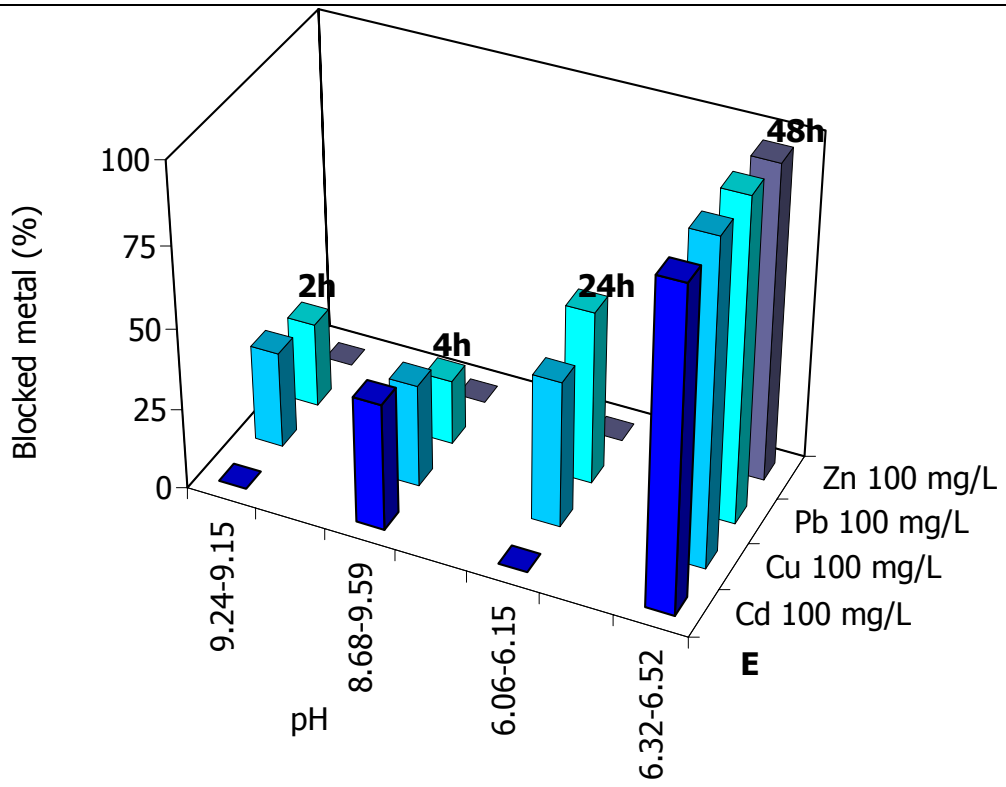
Blocked metal (%)
100
75
50
25
0
2h
4h
24h
48h
9.24-9.15
8.68-9.59
6.06-6.15
6.32-6.52
pH
Zn 100 mg/L
Pb 100 mg/L
Cu 100 mg/L
Cd 100 mg/L
E

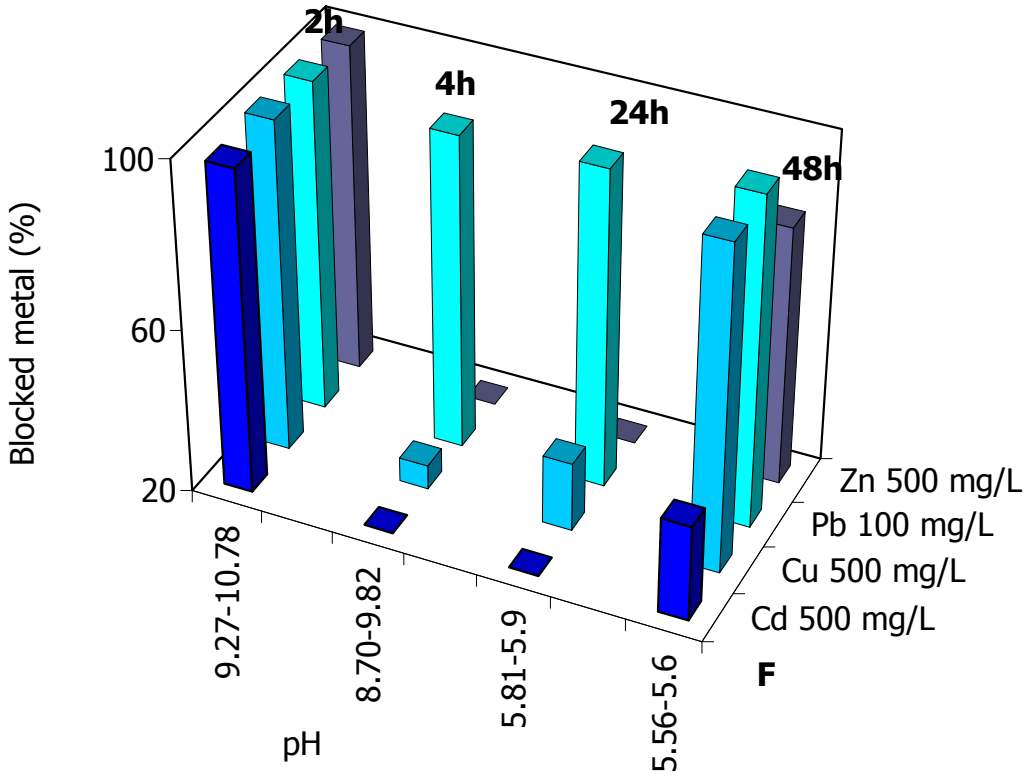
Blocked metal (%)
100
60
20
2h
4h
24h
48h
9.27-10.78
8.70-9.82
5.81-5.9
5.56-5.6
pH
Zn 500 mg/L
Pb 100 mg/L
Cu 500 mg/L
Cd 500 mg/L
F

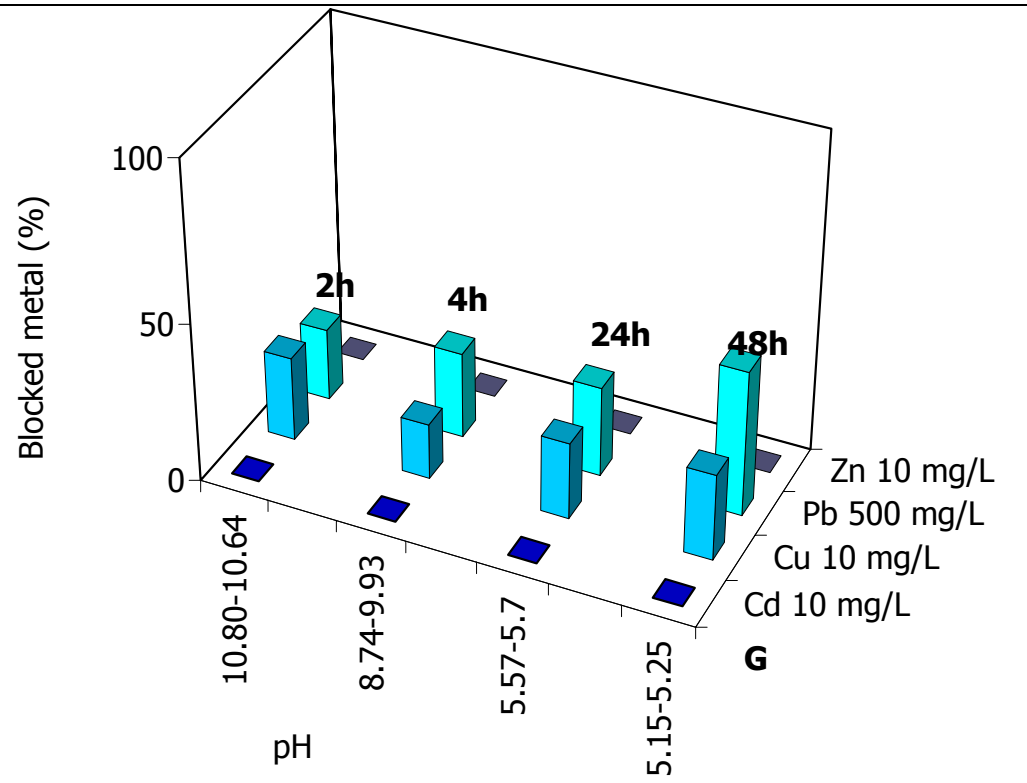
Blocked metal (%)
100
50
0
2h
4h
24h
48h
10.80-10.64
8.74-9.93
5.57-5.7
5.15-5.25
pH
Zn 10 mg/L
Pb 500 mg/L
Cu 10 mg/L
Cd 10 mg/L
G

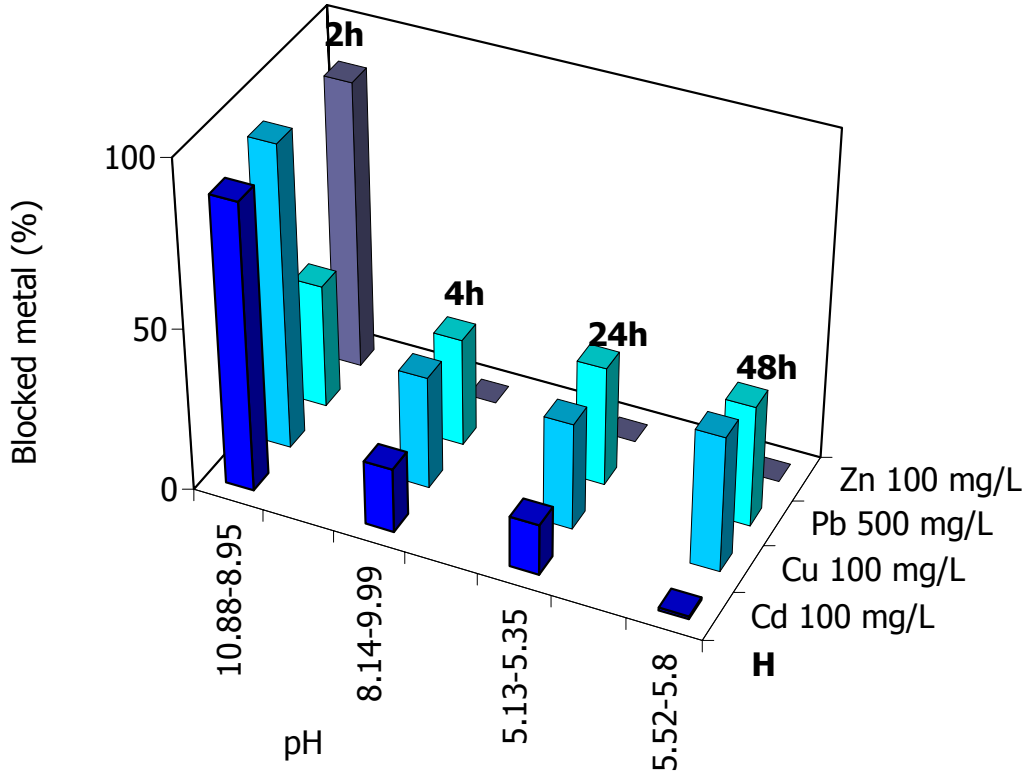
Blocked metal (%)
100
50
0
2h
4h
24h
48h
10.88-8.95
8.14-9.99
5.13-5.35
5.52-5.8
pH
Zn 100 mg/L
Pb 500 mg/L
Cu 100 mg/L
Cd 100 mg/L
H

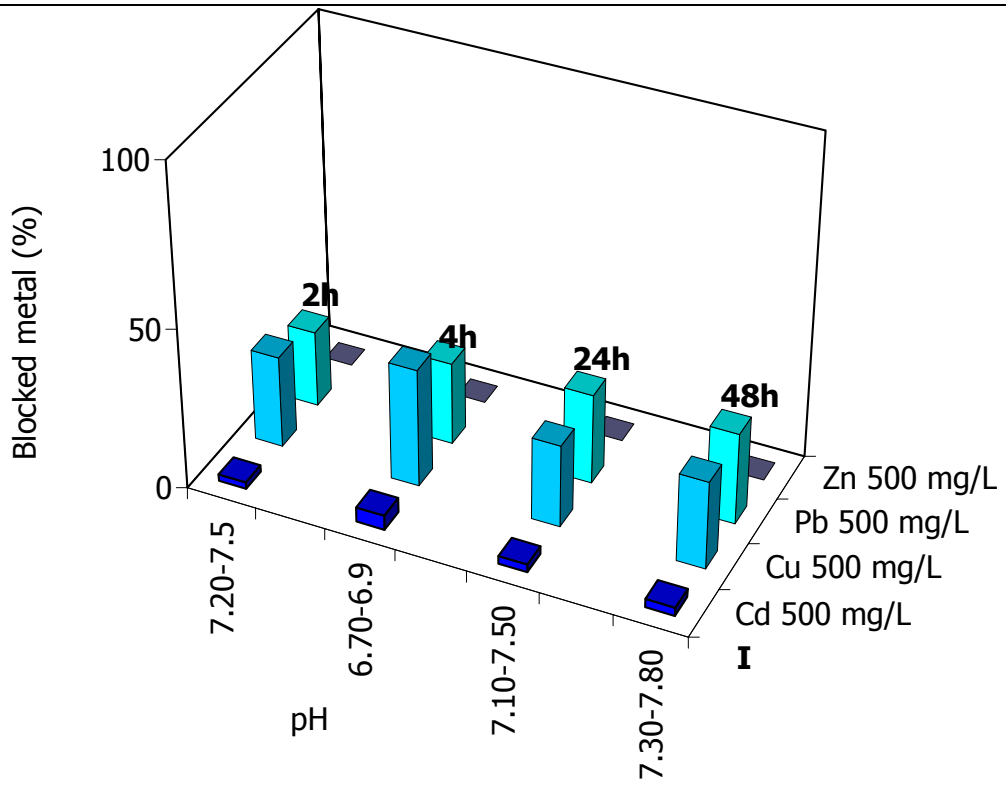

Fig. 13: Variation of the amount of blocked metal with time for the mass of FAP (1 g) in the multi-metal system where Pb is constant. – Fig. 13: Variazione delle percentuali dei metalli immobilizzati in funzione del tempo di interazione per la quantità di FAP (1 g) nel sistema multi-metal in cui Pb è l'elemento costante.

The molar ratio Q_S for this system (Tab. 6) is < 1 for low concentration (10 mg/L) of all the four heavy metals. Increasing the concentration of Cd, Cu and Zn (100 mg/L and 500 mg/L) $Q_S >> 1$ and Pb shows a $Q_S < 1$. When Pb concentration is 100 mg/L its $Q_S < 1$; whether the heavy metal concentration is 100 mg/L, Pb molar ratio is $Q_S > 1$ for t = 2h and 4h and $Q_S < 1$ for t = 24h and 48h. Cd and Cu have $Q_S >> 1$ for t = 2h, $Q_S > 1$ for t = 4h and 24h and $Q_S < 1$ for t = 48h; whereas Zn has a $Q_S >> 1$ for t = 2h, 4h and 24h and $Q_S < 1$ for t = 48h. For a concentration of 500 mg/L, Pb has a $Q_S >> 1$, whereas Cd, Cu and Zn, for low concentration, have a $Q_S < 1$ and raising their concentration also Q_S raises to values > 1. Finally, when all the four heavy metals have the highest concentration $Q_S >> 1$. In this system the molar ratio values seem to depend on the time and the initial concentration of the metals, but the suitable mechanisms are always the same as the previous systems, non-crystalline precipitation of a phase and surface complexation.

Cd = 10 mg/L	Cu = 10 mg/L	Pb = 10 mg/L	Zn = 10 mg/L
0.08	0.02	0.00	0.25
0.04	0.01	0.00	0.11
0.01	0.00	0.00	0.02
0.01	0.00	0.00	0.01
Cd = 100 mg/L	Cu = 100 mg/L	Pb = 10 mg/L	Zn = 100 mg/L
2.25	2.14	0.00	4.82
1.42	1.21	0.00	3.10
0.84	0.45	0.00	1.82
0.37	0.66	0.00	2.44
Cd = 500 mg/L	Cu = 500 mg/L	Pb = 10 mg/L	Zn = 500 mg/L
12.46	15.11	0.01	9.51
11.13	13.47	0.02	8.48
8.22	7.60	0.01	6.29
6.32	3.93	0.00	4.80
Cd = 10 mg/L	Cu = 10 mg/L	Pb = 100 mg/L	Zn = 10 mg/L
0.41	0.46	0.86	0.81
0.33	0.26	0.35	0.67
0.22	0.13	0.10	0.50
0.22	0.12	0.08	0.46
Cd = 100 mg/L	Cu = 100 mg/L	Pb = 100 mg/L	Zn = 100 mg/L
4.51	5.30	1.71	8.42
1.87	3.72	1.34	7.03
1.80	1.45	0.38	3.79
0.01	0.00	0.00	0.06
Cd = 500 mg/L	Cu = 500 mg/L	Pb = 100 mg/L	Zn = 500 mg/L
0.04	0.00	0.00	0.02
0.00	0.00	0.05	21.94
8.48	8.42	0.03	16.07
2.52	0.11	0.00	1.34
Cd = 10 mg/L	Cu = 10 mg/L	Pb = 500 mg/L	Zn = 10 mg/L
0.28	0.35	5.60	0.47
0.33	0.30	4.07	0.66
0.24	0.25	3.69	0.41
0.17	0.19	2.18	0.29
Cd = 100 mg/L	Cu = 100 mg/L	Pb = 500 mg/L	Zn = 100 mg/L
0.18	0.19	2.53	0.31
1.24	1.79	2.80	2.81
0.90	1.27	1.84	2.07
1.22	1.27	2.10	2.68
Cd = 500 mg/L	Cu = 500 mg/L	Pb = 500 mg/L	Zn = 500 mg/L
9.40	12.14	3.98	19.12
8.57	10.05	3.63	17.51
6.48	8.73	2.59	13.47
5.50	7.26	2.20	12.34

Table 6: Q_S values for the multi - metal systems when Pb has a constant concentration. Tabella 6: Valori di Q_S per i sistemi multi-metal nei quali la concentrazione di Pb è stata mantenuta costante.

Generally, the sorption isotherms of this system are type H and subtype 2 (Fig. 14 A, B, C and D). Unfortunately, for Cd and Zn due to desorption phenomenon the isotherms have not meaning.

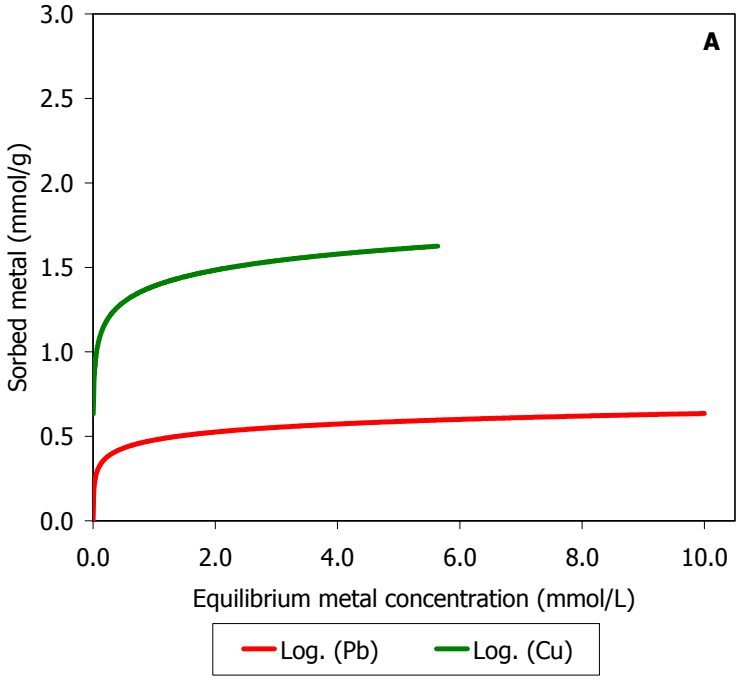

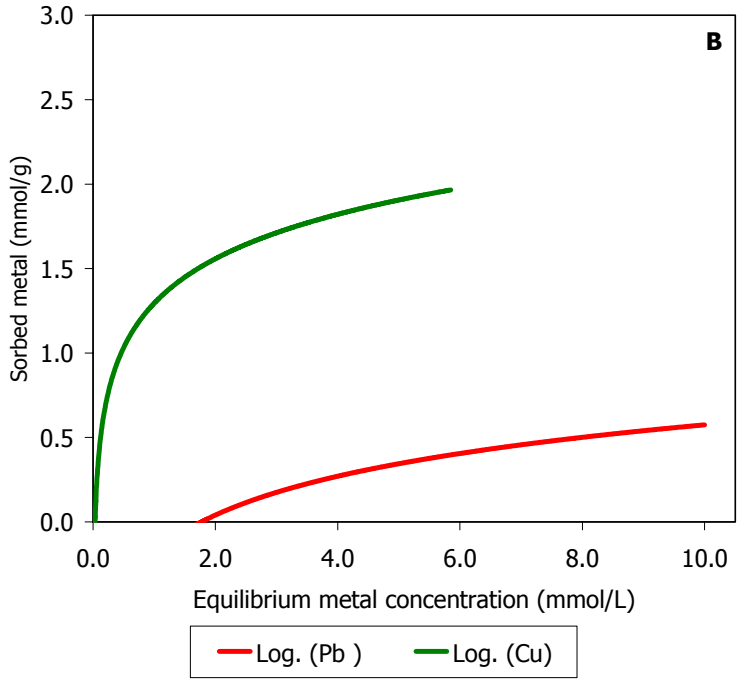

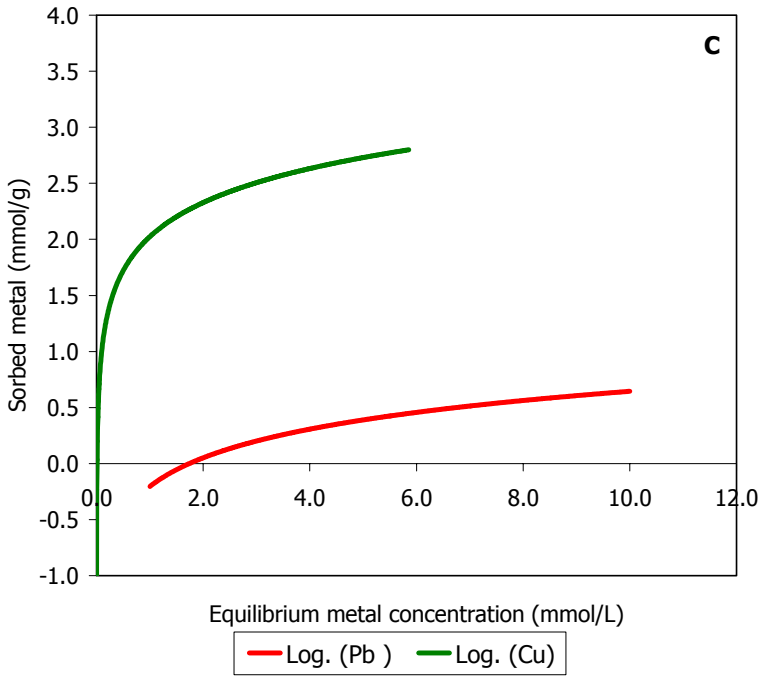

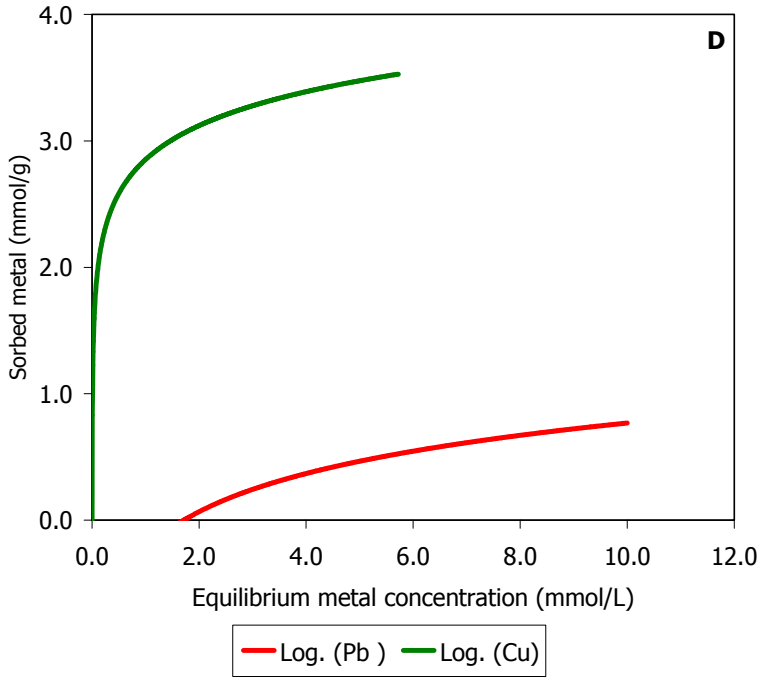

Fig. 14: Sorption isotherms for the multi-metal system where Pb is constant for the four contact times (2h, 4h, 24h and 48h) and vs. 1 g FAP. Relation between the metal sorbed (mmol/g) and the final concentration (mmol/L) in solution. A: t = 2h; B: t = 4h; C: t = 24h and D: t = 48h. – Fig. 14: Curve isotermiche per il sistema multi-metal in cui Pb è costante per i quattro tempi di contatto (2h, 4h, 24h and 48h) e vs. 1 g di FAP. Relazione tra il metallo assorbito (mmol/g) e la concentrazione finale (mmol/L) in soluzione. A: t = 2h; B: t = 4h; C: t = 24h e D: t = 48h.

The concentration of Ca is larger than those detected in the two previous systems (Fig. 15 A, B, C, D, E, F, G, H and I); it usually runs from < b.d.l. to 2 mmol/g and the amount of the four heavy metals in solution at the equilibrium is influenced from the initial concentration and not the interaction time. The average amount of P is about 0.1 mmol/g (Fig. 16 A, B, C, D, E, F, G, H and I), suggesting a non stoichiometric dissolution too. Probably, the sorption processes are different for the four heavy metals, making to infer for Pb a non-crystalline precipitation. On the other hand, in case of the other three heavy metals the coprecipitation process could be more probable, thus their concentration is always more than that of Pb and sometimes they are not immobilized.

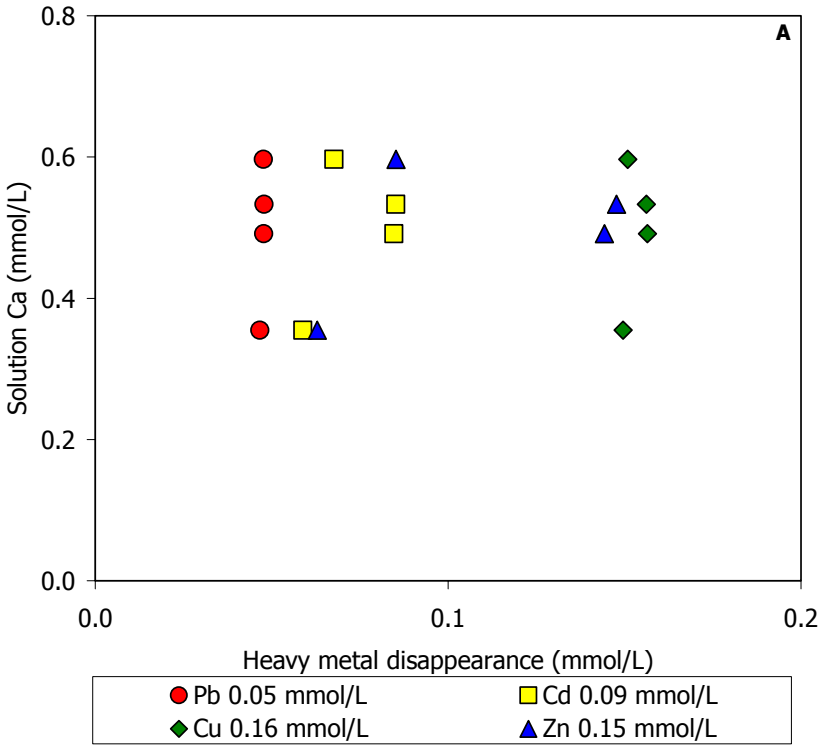

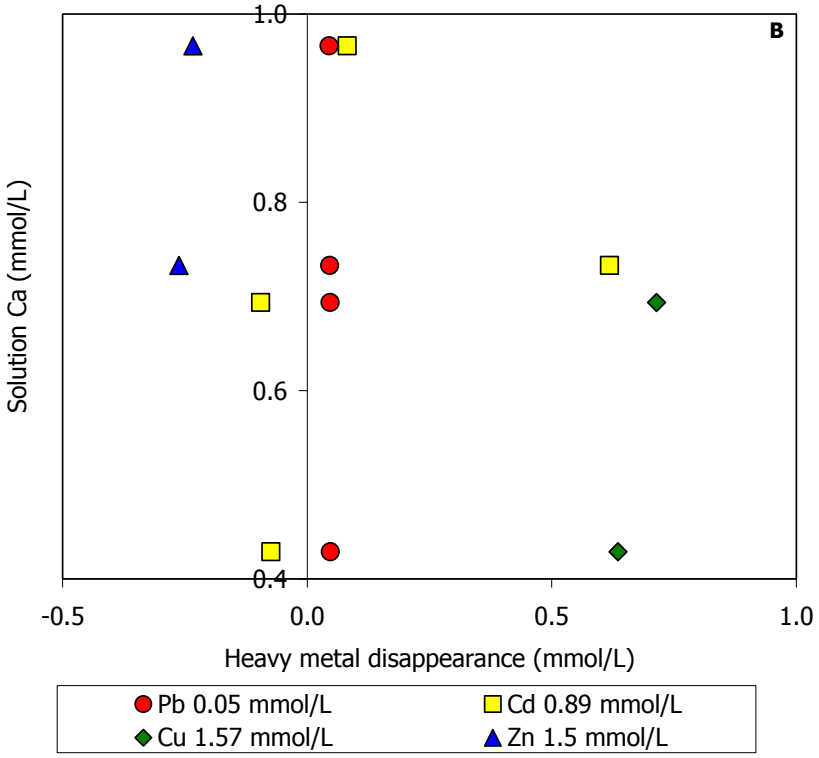
B
1.0
0.8
0.6
0.4
Solution Ca (mmol/L)
-0.5
0.0
0.5
1.0
Heavy metal disappearance (mmol/L)
Pb 0.05 mmol/L
Cd 0.89 mmol/L
Cu 1.57 mmol/L
Zn 1.5 mmol/L

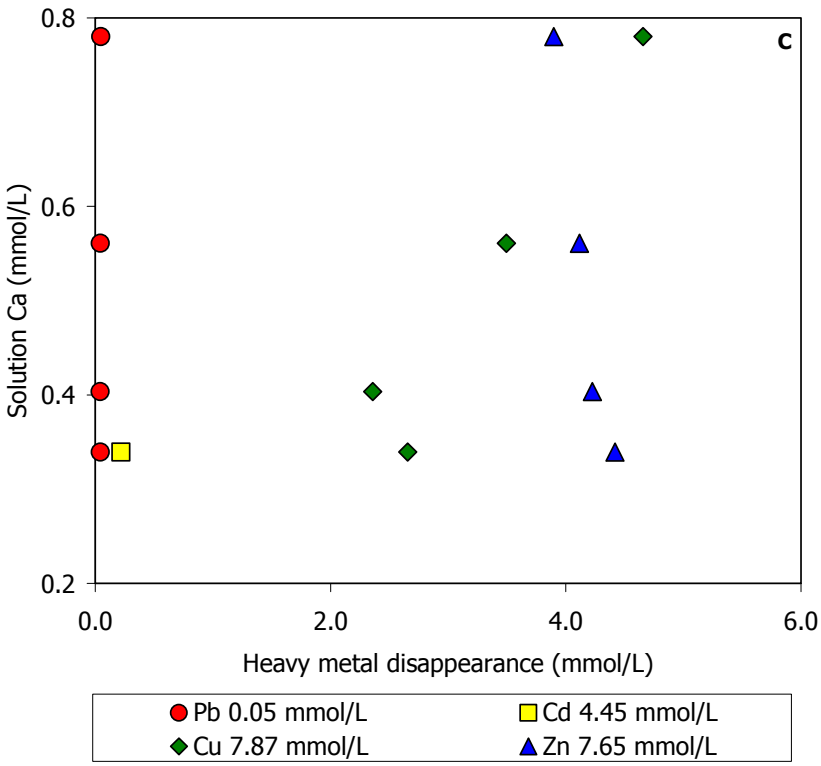
C
0.8
0.6
0.4
0.2
Solution Ca (mmol/L)
0.0
2.0
4.0
6.0
Heavy metal disappearance (mmol/L)
Pb 0.05 mmol/L
Cd 4.45 mmol/L
Cu 7.87 mmol/L
Zn 7.65 mmol/L

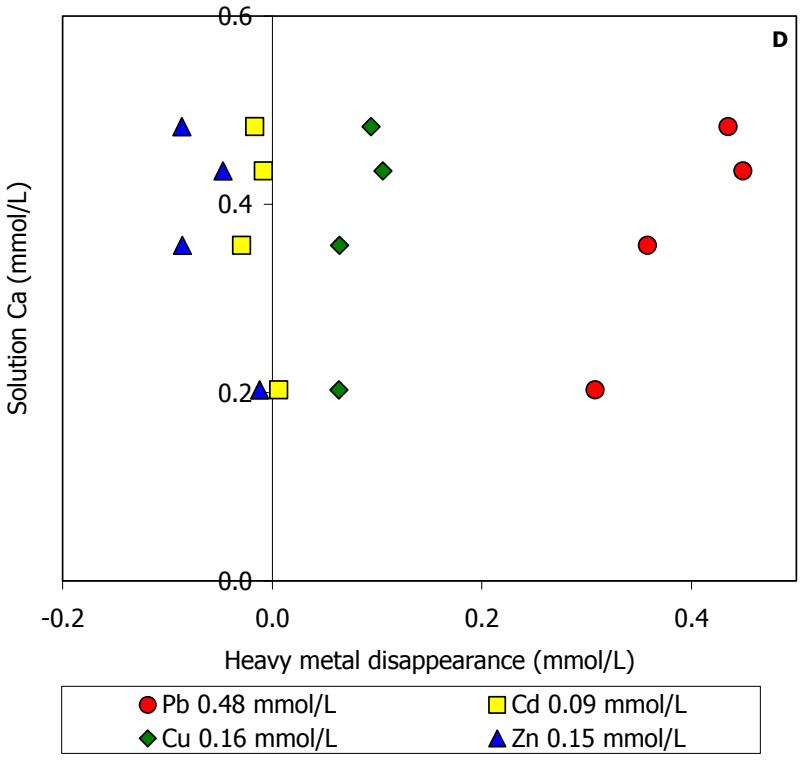
D
0.6
0.4
0.2
0.0
-0.2
0.0
0.2
0.4
Solution Ca (mmol/L)
Heavy metal disappearance (mmol/L)
Pb 0.48 mmol/L
Cd 0.09 mmol/L
Cu 0.16 mmol/L
Zn 0.15 mmol/L

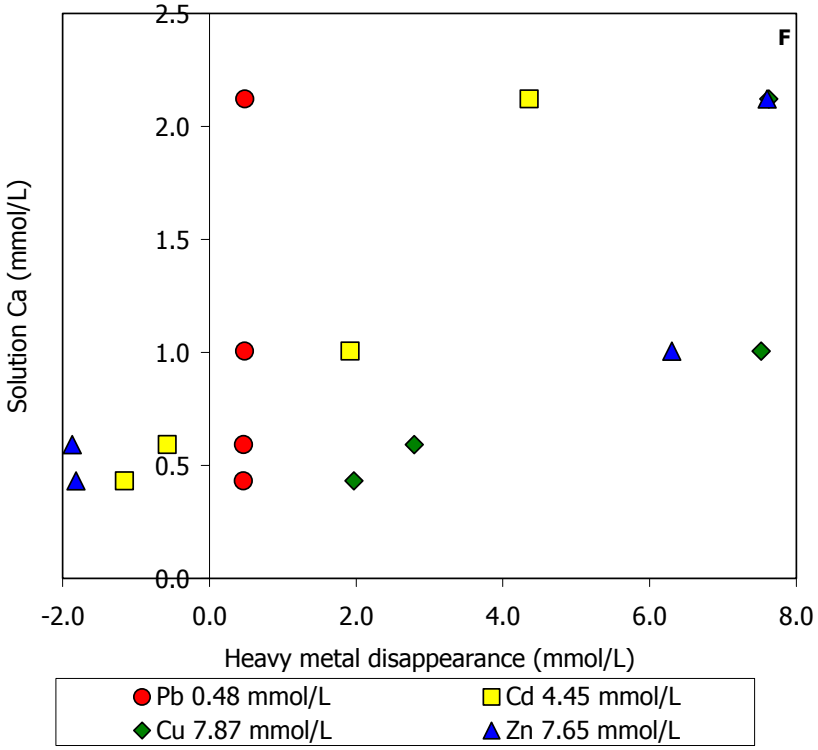
F
2.5
2.0
1.5
1.0
0.5
0.0
-2.0
0.0
2.0
4.0
6.0
8.0
Solution Ca (mmol/L)
Heavy metal disappearance (mmol/L)
Pb 0.48 mmol/L
Cd 4.45 mmol/L
Cu 7.87 mmol/L
Zn 7.65 mmol/L

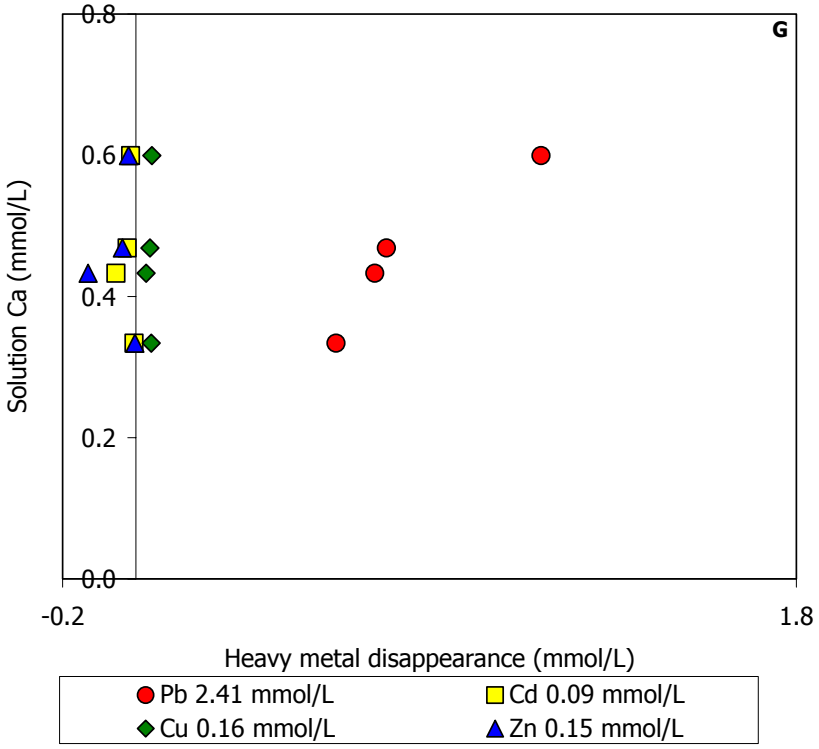
G
0.8
0.6
0.4
0.2
0.0
-0.2
1.8
Solution Ca (mmol/L)
Heavy metal disappearance (mmol/L)
Pb 2.41 mmol/L
Cd 0.09 mmol/L
Cu 0.16 mmol/L
Zn 0.15 mmol/L

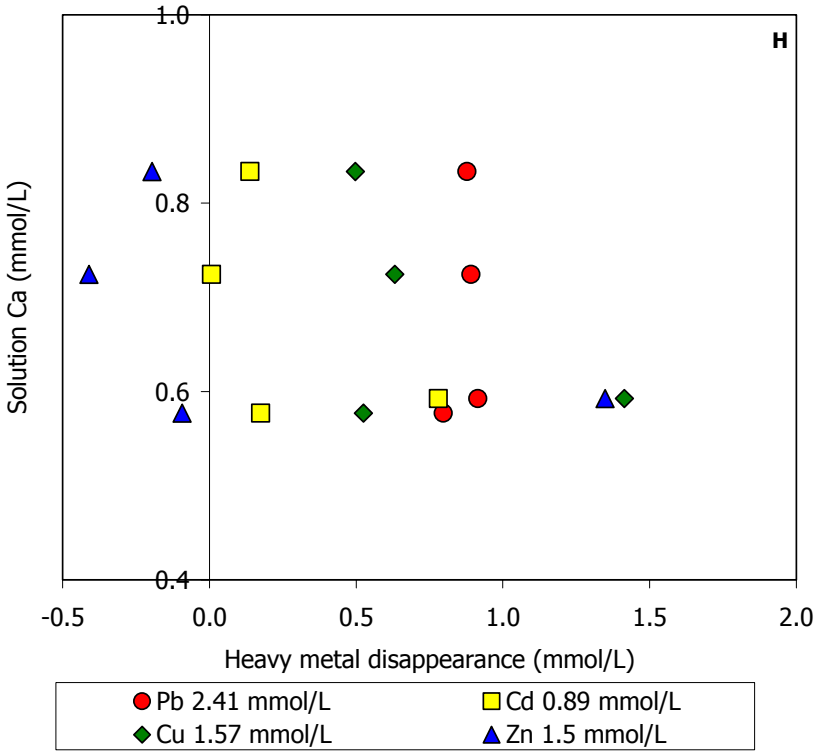
H
1.0
0.8
0.6
0.4
-0.5
0.0
0.5
1.0
1.5
2.0
Solution Ca (mmol/L)
Heavy metal disappearance (mmol/L)
Pb 2.41 mmol/L
Cd 0.89 mmol/L
Cu 1.57 mmol/L
Zn 1.5 mmol/L

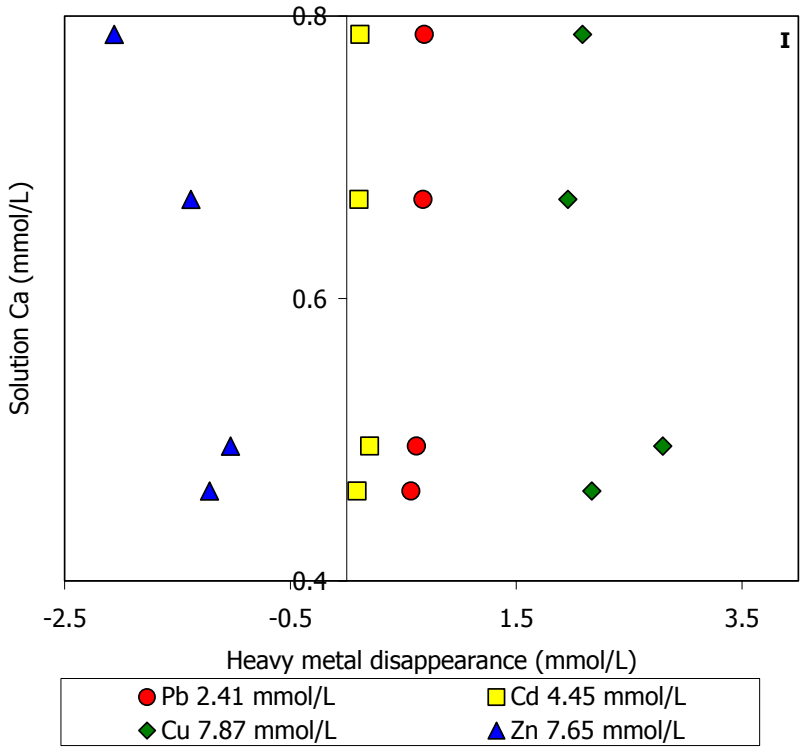

Fig. 15: Relation between Ca in solution (mmol/L) and the amount of heavy metals disappeared (mmol/L) sorbed on FAP surface at the equilibrium in a multi-metal system when Pb is constant. Each initial concentration of the multi-metal system is written in the legend. - Fig. 15: Relazione tra il quantitativo di Ca in soluzione (mmol/L) e di ciascun metallo pesante adsorbito (mmol/L) nel sistema multi-metal quando Pb è costante. La concentrazione iniziale di ogni elemento del sistema multi-metal è in leggenda.

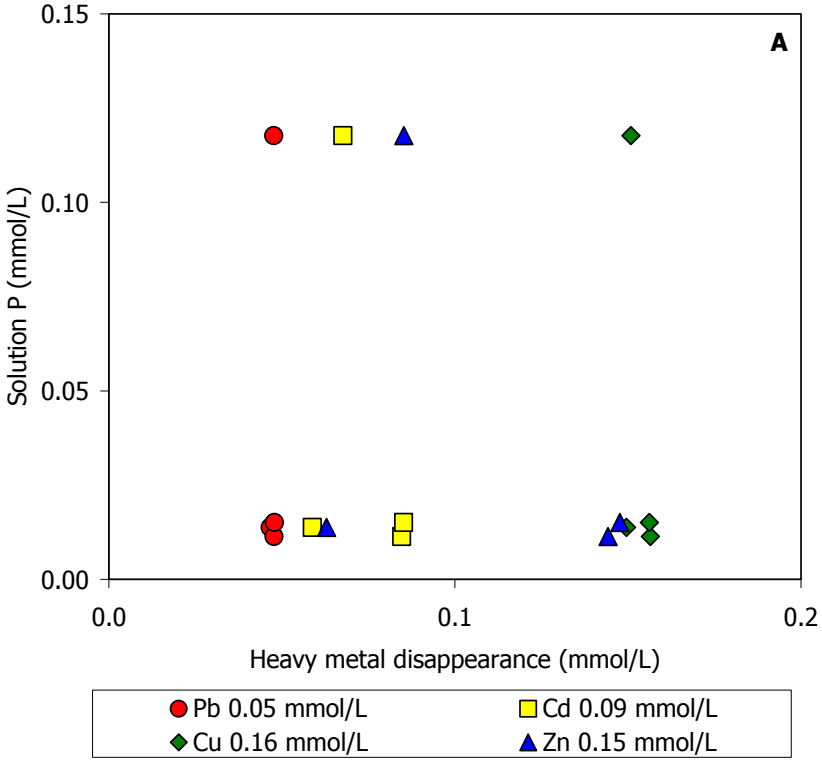
A
0.15
0.10
0.05
0.00
Solution P (mmol/L)
0.0
0.1
0.2
Heavy metal disappearance (mmol/L)
Pb 0.05 mmol/L
Cd 0.09 mmol/L
Cu 0.16 mmol/L
Zn 0.15 mmol/L

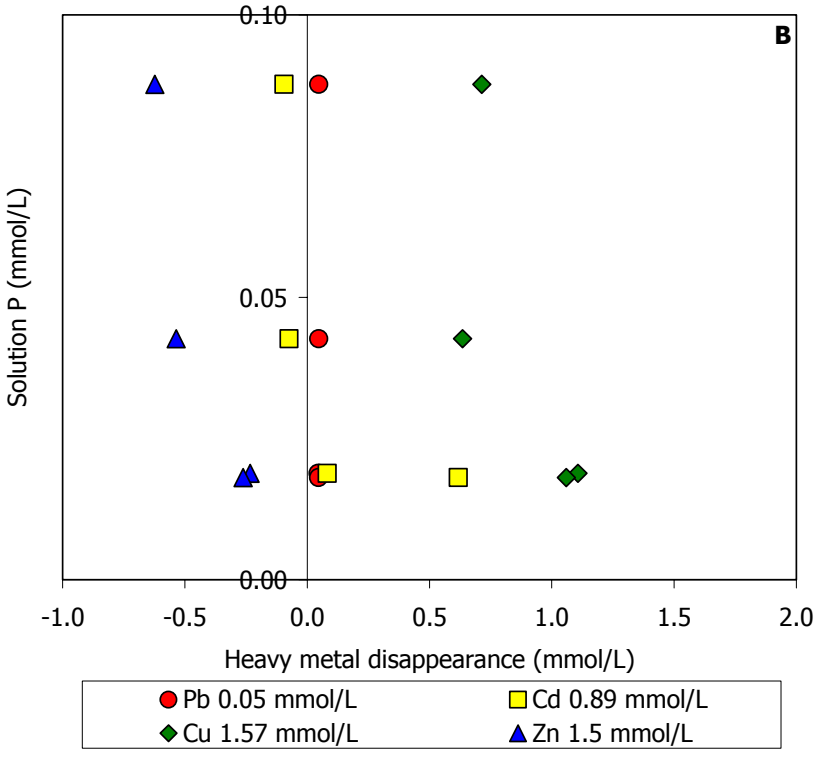
B
0.10
0.05
0.00
Solution P (mmol/L)
-1.0
-0.5
0.0
0.5
1.0
1.5
2.0
Heavy metal disappearance (mmol/L)
Pb 0.05 mmol/L
Cd 0.89 mmol/L
Cu 1.57 mmol/L
Zn 1.5 mmol/L

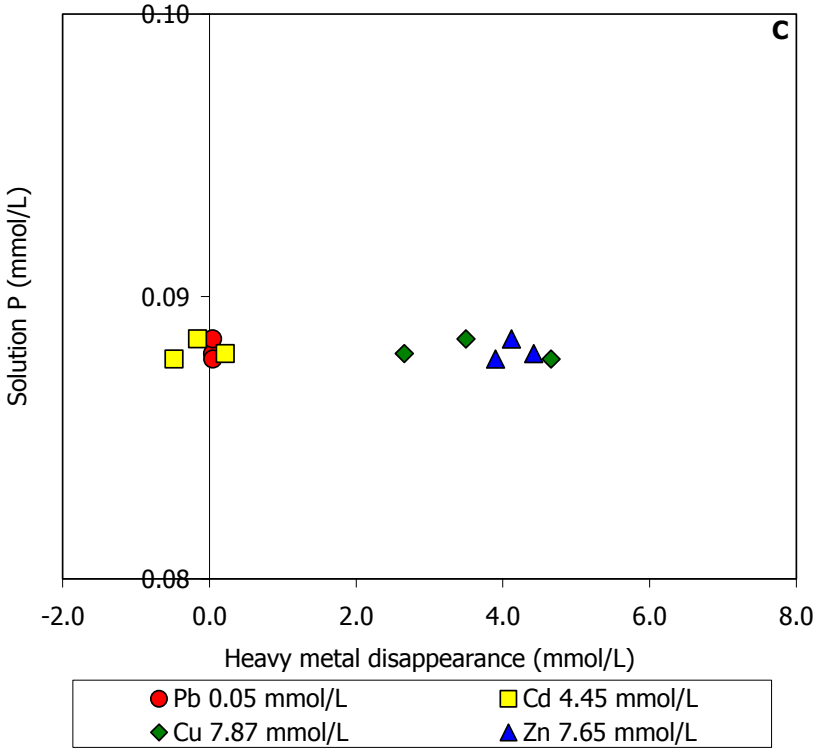
C
0.10
0.09
0.08
Solution P (mmol/L)
-2.0
0.0
2.0
4.0
6.0
8.0
Heavy metal disappearance (mmol/L)
Pb 0.05 mmol/L
Cd 4.45 mmol/L
Cu 7.87 mmol/L
Zn 7.65 mmol/L

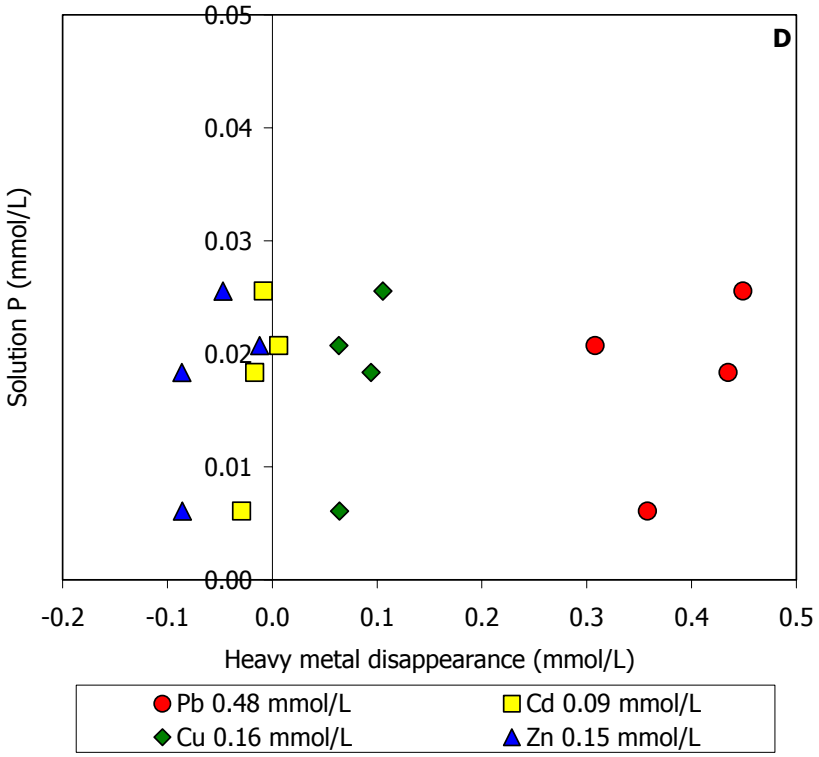
D
0.05
0.04
0.03
0.02
0.01
0.00
Solution P (mmol/L)
-0.2
-0.1
0.0
0.1
0.2
0.3
0.4
0.5
Heavy metal disappearance (mmol/L)
Pb 0.48 mmol/L
Cd 0.09 mmol/L
Cu 0.16 mmol/L
Zn 0.15 mmol/L

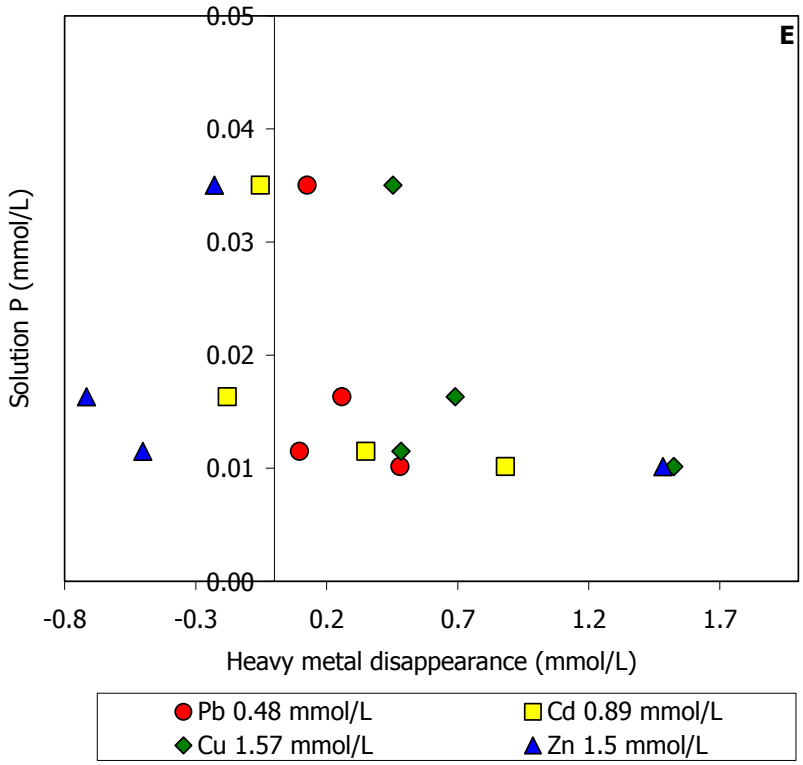
E
0.05
0.04
0.03
0.02
0.01
0.00
Solution P (mmol/L)
-0.8
-0.3
0.2
0.7
1.2
1.7
Heavy metal disappearance (mmol/L)
Pb 0.48 mmol/L
Cd 0.89 mmol/L
Cu 1.57 mmol/L
Zn 1.5 mmol/L

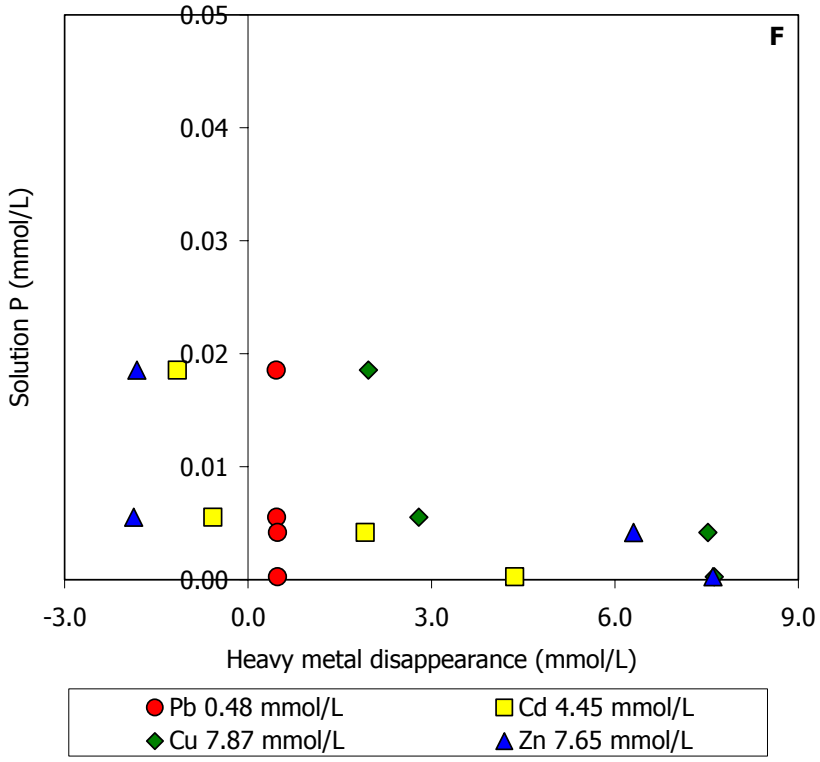
F
0.05
0.04
0.03
0.02
0.01
0.00
Solution P (mmol/L)
-3.0
0.0
3.0
6.0
9.0
Heavy metal disappearance (mmol/L)
Pb 0.48 mmol/L
Cd 4.45 mmol/L
Cu 7.87 mmol/L
Zn 7.65 mmol/L

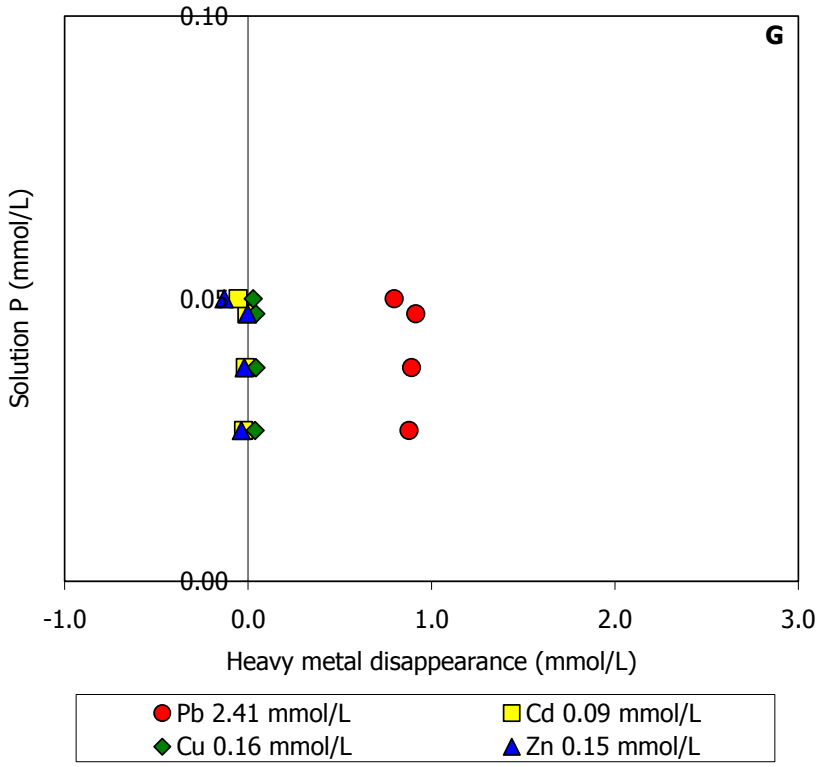
G
0.10
0.05
0.00
Solution P (mmol/L)
-1.0
0.0
1.0
2.0
3.0
Heavy metal disappearance (mmol/L)
Pb 2.41 mmol/L
Cd 0.09 mmol/L
Cu 0.16 mmol/L
Zn 0.15 mmol/L

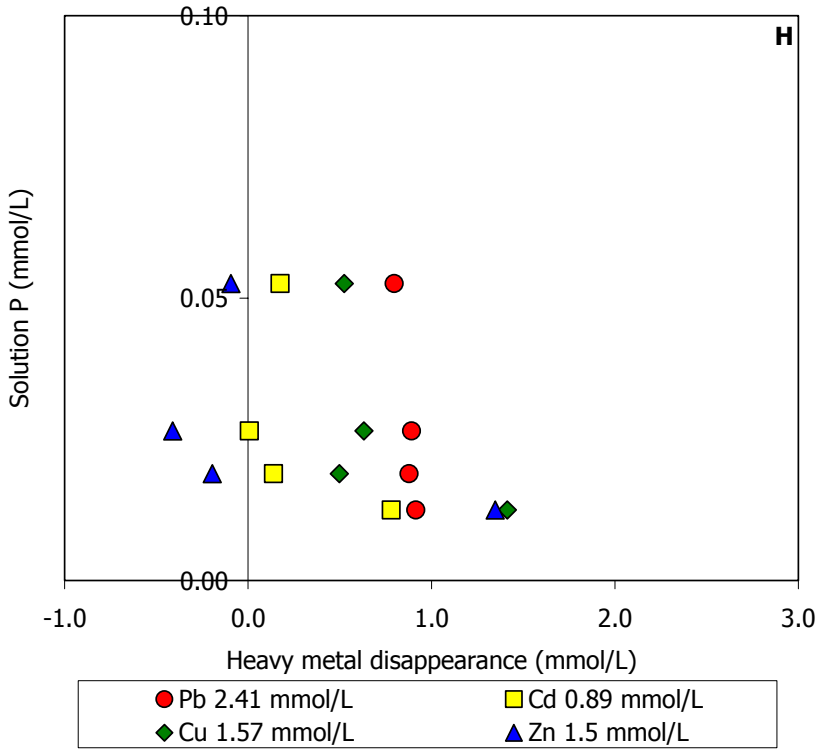
H
0.10
0.05
0.00
Solution P (mmol/L)
-1.0
0.0
1.0
2.0
3.0
Heavy metal disappearance (mmol/L)
Pb 2.41 mmol/L
Cd 0.89 mmol/L
Cu 1.57 mmol/L
Zn 1.5 mmol/L

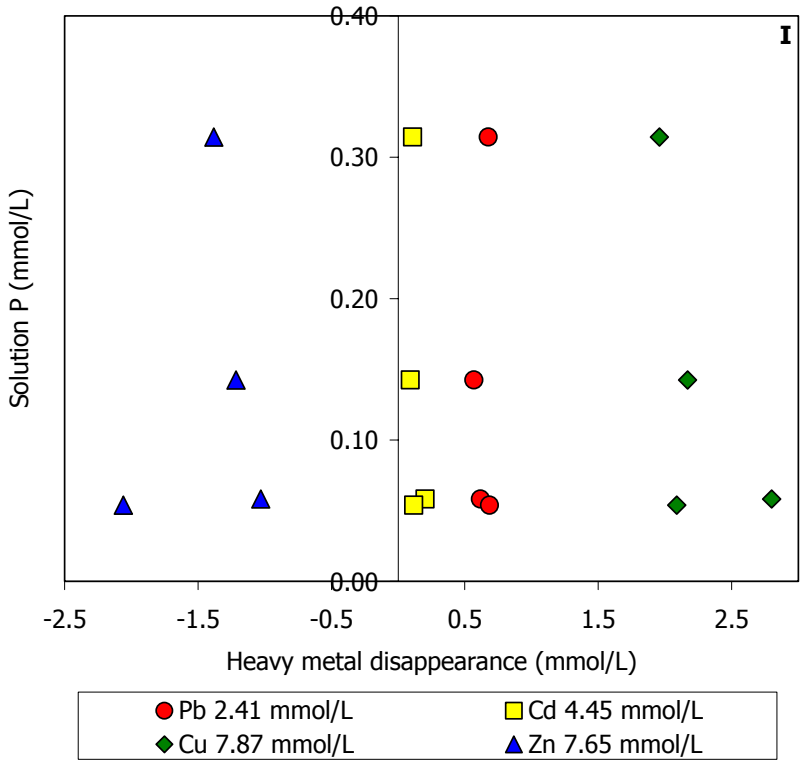

Fig. 16: Relation between P in solution (mmol/L) and the amount of disappeared heavy metals (mmol/L) sorbed on FAP surface at the equilibrium in a multi-metal system when Pb is constant. Each initial concentration of the multi-metal system is written in the legend. - Fig. 16: Relazione tra il quantitativo di P in soluzione (mmol/L) e di ciascun metallo pesante adsorbito (mmol/L) nel sistema multi-metal quando Pb è costante. La concentrazione iniziale di ogni elemento del sistema multi-metal è in leggenda.

In the system where Zn is constant, the time of best immobilization ranges between 24h and 48h (Tab. 7 and Fig. 17 A, B, C, D, E and F). In this system Zn is generally never immobilized due to desorption phenomenon and in some case Cd, Cu and Pb show the same phenomenon. The probable orders of immobilization are Pb > Cu > Cd > Zn and also Cu > Pb > Cd > Zn; probably these two different orders depend on the competition among the heavy metals and subsequently from their initial concentration. As in the previous systems, pH shows increase and decrease of 0.5 units.

Cd = 10 mg/L	Cu = 10 mg/L	Pb = 10 mg/L	Zn = 100 mg/L
-0.026	-14.215	7.712	-12.166
-1.433	-50.706	-14.617	-23.039
1.006	-0.838	19.740	-0.655
2.132	1.562	19.937	0.489
Cd = 500 mg/L	Cu = 500 mg/L	Pb = 500 mg/L	Zn = 100 mg/L
-24.285	8.067	-36.747	-0.522
26.695	42.997	61.267	-0.812
23.833	33.531	57.279	-0.850
5.794	20.982	29.232	0.489
Cd = 10 mg/L	Cu = 10 mg/L	Pb = 10 mg/L	Zn = 100 mg/L
-0.869	0.500	0.558	-1.496
0.528	1.636	1.464	0.447
0.340	1.499	1.570	-2.059
0.547	1.760	1.662	-0.793
Cd = 500 mg/L	Cu = 500 mg/L	Pb = 500 mg/L	Zn = 100 mg/L
14.882	24.986	45.176	-4.436
12.971	25.399	26.265	-4.082
13.166	20.127	9.557	-3.771
18.465	28.292	62.723	-2.667
Cd = 10 mg/L	Cu = 10 mg/L	Pb = 10 mg/L	Zn = 500 mg/L
-1.258	-0.547	-0.226	-9.042
0.082	1.259	0.342	-10.564
0.301	1.634	1.446	-9.514
0.395	1.592	0.573	-7.398
Cd = 100 mg/L	Cu = 100 mg/L	Pb = 100 mg/L	Zn = 500 mg/L
1.075	5.710	5.719	-13.282
1.039	7.471	7.338	-16.330
0.953	15.585	14.764	-15.289
1.419	15.317	15.994	-13.739

Table 7: Efficiency values for the multi - metal system when Zn has a constant concentration.

Tabella 7: Valori dell'efficienza nell'immobilizzare i metalli pesanti per il sistema multi-metal in cui lo Zn mantiene costante la concentrazione.

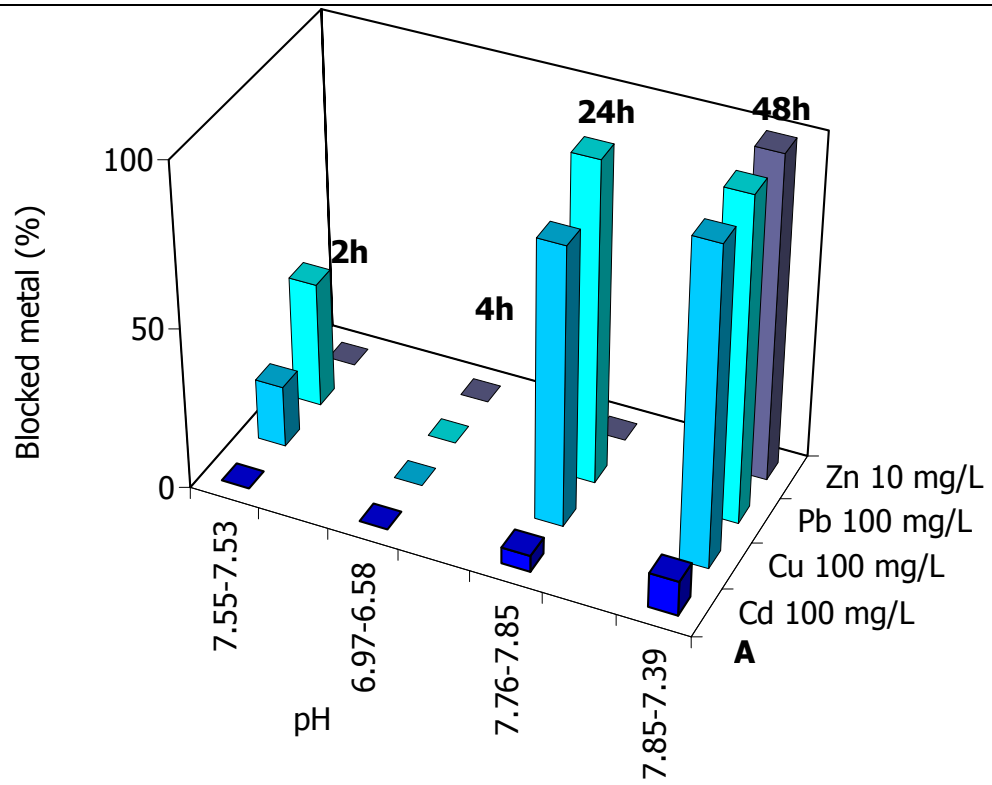
Blocked metal (%)
100
50
0
2h
4h
24h
48h
7.55-7.53
6.97-6.58
7.76-7.85
7.85-7.39
pH
Zn 10 mg/L
Pb 100 mg/L
Cu 100 mg/L
Cd 100 mg/L
A

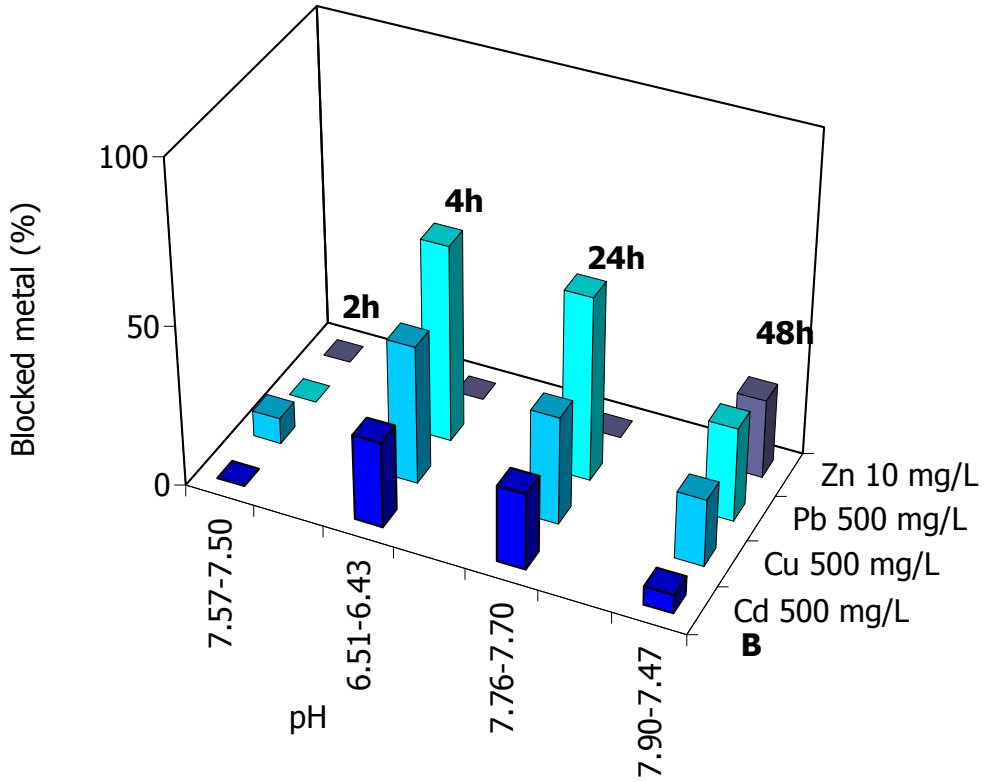
Blocked metal (%)
100
50
0
2h
4h
24h
48h
7.57-7.50
6.51-6.43
7.76-7.70
7.90-7.47
pH
Zn 10 mg/L
Pb 500 mg/L
Cu 500 mg/L
Cd 500 mg/L
B

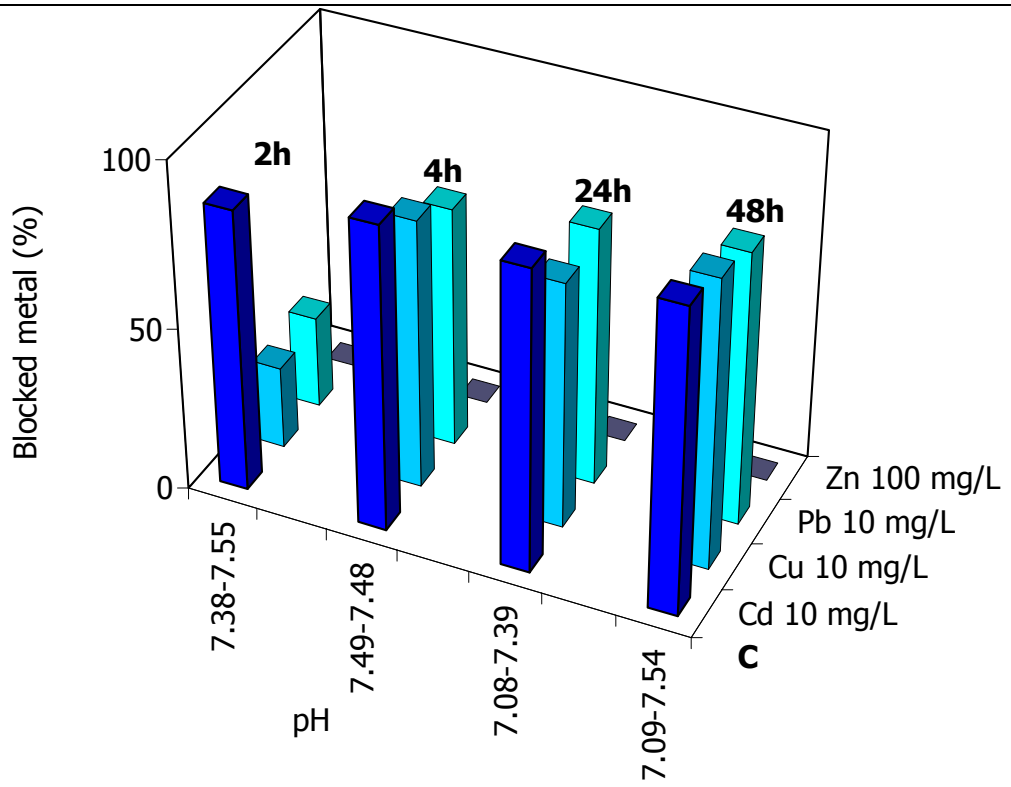
Blocked metal (%)
100
50
0
2h
4h
24h
48h
7.38-7.55
7.49-7.48
7.08-7.39
7.09-7.54
pH
Zn 100 mg/L
Pb 10 mg/L
Cu 10 mg/L
Cd 10 mg/L
C

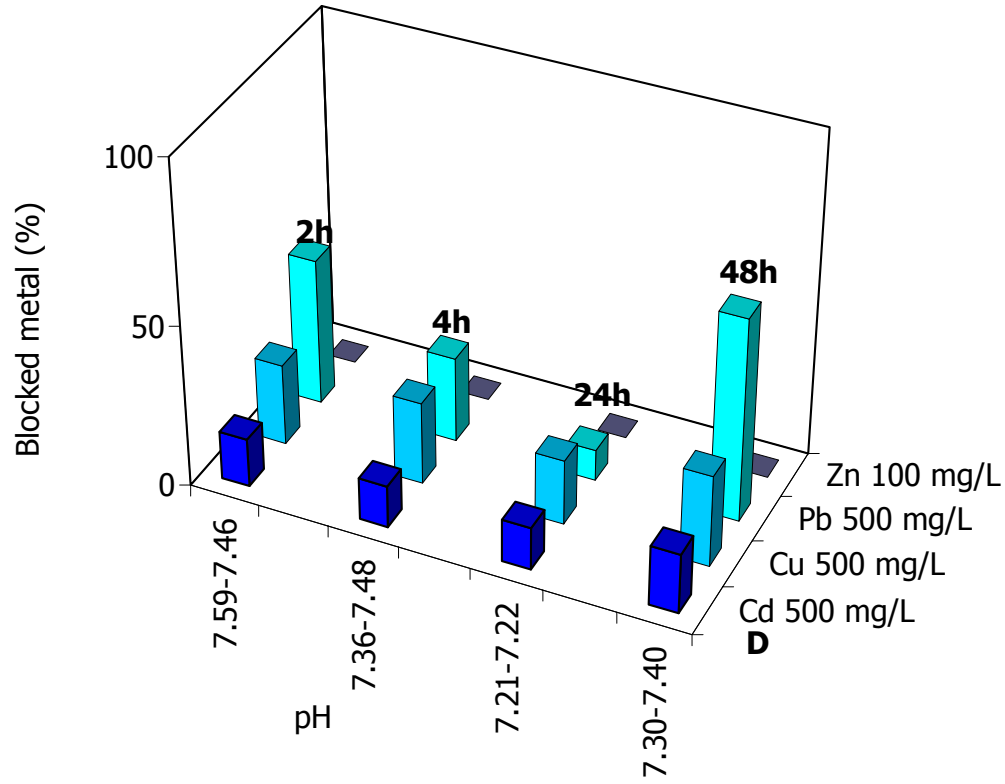
Blocked metal (%)
100
50
0
2h
4h
24h
48h
7.59-7.46
7.36-7.48
7.21-7.22
7.30-7.40
pH
Zn 100 mg/L
Pb 500 mg/L
Cu 500 mg/L
Cd 500 mg/L
D

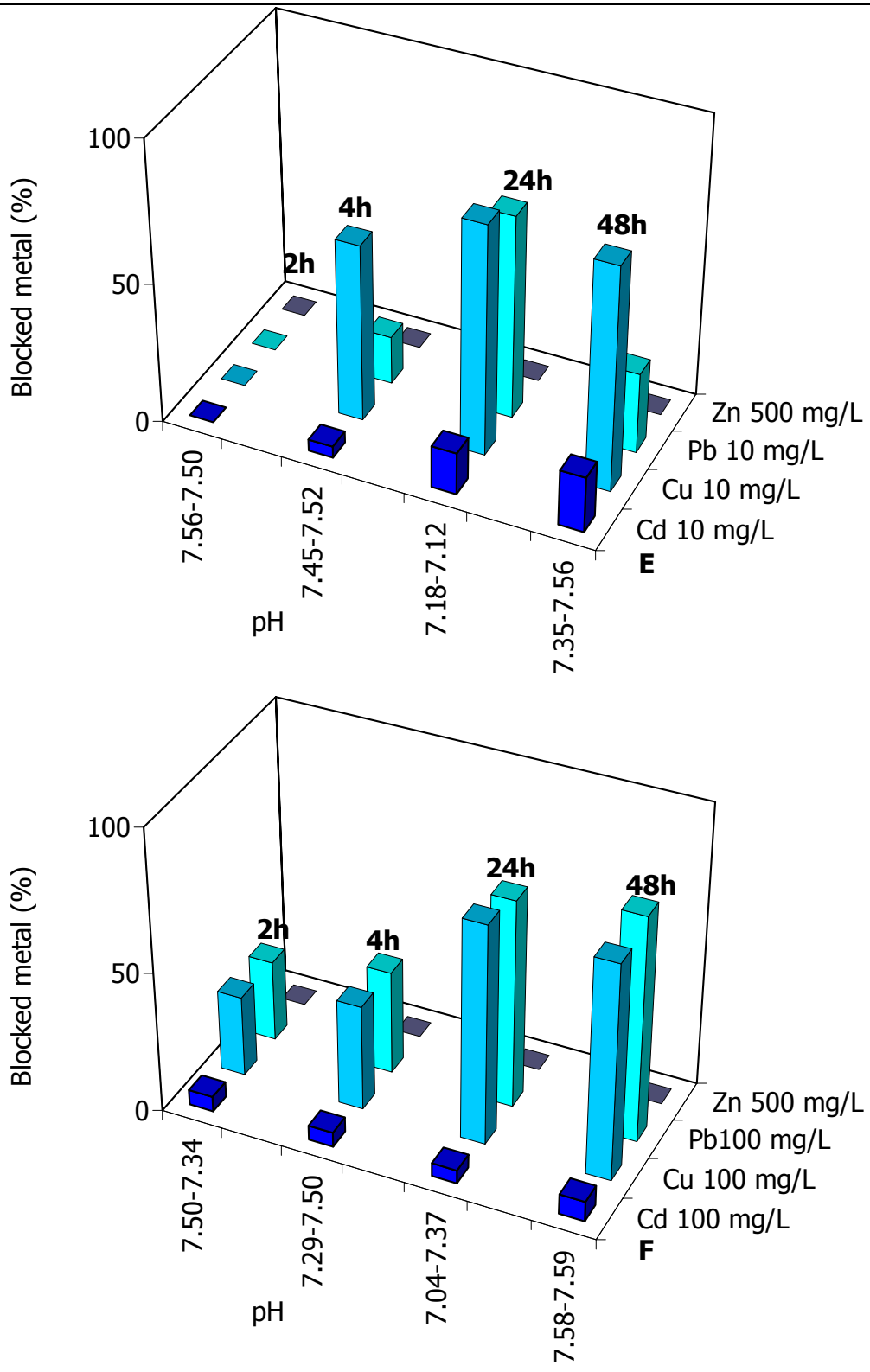

Fig. 17: Variation of the amount of blocked metal with time for the mass of FAP (1 g) in the multi-metal system where Zn is constant.. – Fig. 17: Variazione delle percentuali dei metalli immobilizzati in funzione del tempo di interazione per la quantità di FAP (1 g) nel sistema multi-metal in cui Zn è l'elemento costante.

In this system, generally t = 2h shows Q_S >>1 (Tab. 8); only in one case the molar ratio is < 1 when it has the lower concentration and the other three metals have the highest concentration (500 mg/L). Cd, Cu and Pb, in this case, show Q_S >> 1, whereas when they have the concentration of 100 mg/L, they show Q_S decreasing with the time, from values >> 1 to < 1. For low concentration Cd, Cu and Pb show the opposite behaviour, Qs < 1 which increases with the metal concentration. These results suggest as sorption processes the non-crystalline precipitation and the superficial complexation.

Cd = 100 mg/L	Cu = 100 mg/L	Pb = 100 mg/L	Zn = 10 mg/L
4.22	6.04	1.40	5.13
2.98	12.97	2.61	5.99
0.90	0.24	0.01	0.22
0.67	0.03	0.00	0.10
Cd = 500 mg/L	Cu = 500 mg/L	Pb =500 mg/L	Zn = 10 mg/L
16.97	22.20	10.13	0.59
6.72	9.25	1.93	0.44
6.57	10.14	2.00	0.42
7.09	10.52	2.89	0.20
Cd = 10 mg/L	Cu = 10 mg/L	Pb = 10 mg/L	Zn = 100 mg/L
0.30	0.27	0.08	3.83
0.11	0.05	0.02	2.56
0.21	0.11	0.03	4.72
0.15	0.04	0.02	3.72
Cd = 500 mg/L	Cu = 500 mg/L	Pb =500 mg/L	Zn = 100 mg/L
20.53	32.01	7.18	10.13
7.94	12.03	3.65	3.78
8.16	13.28	4.61	3.84
6.22	9.68	1.54	2.97
Cd = 10 mg/L	Cu = 10 mg/L	Pb = 10 mg/L	Zn = 500 mg/L
0.34	0.46	0.12	19.32
0.23	0.16	0.11	22.78
0.10	0.04	0.02	11.64
0.13	0.06	0.06	15.01
Cd = 100 mg/L	Cu = 100 mg/L	Pb = 100 mg/L	Zn = 500 mg/L
2.60	3.48	1.07	26.80
0.00	0.00	0.75	21.81
1.14	0.47	0.17	11.84
1.33	0.59	0.16	14.04

Table 8: Q_S values for the multi - metal systems when Zn has a constant concentration. Tabella 8: Valori di Q_S per i sistemi multi-metal nei quali la concentrazione di Zn è stata mantenuta costante.

This is a particular system because Zn is never immobilized and in fact its sorption isotherms are always in the negative quadrant, whereas for the other metals, the curve shows always the H shape, indicating the precipitation mechanism.

Sorption isotherms are always vertical for Cd, Cu and Pb (Fig. 18 A, B, C and D), unfortunately for Zn, showing always negative values, are not considered.

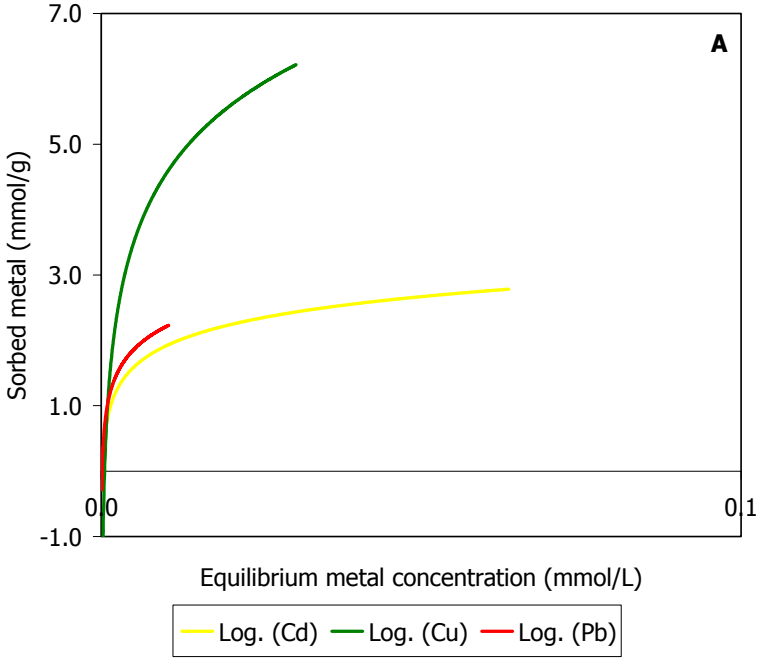

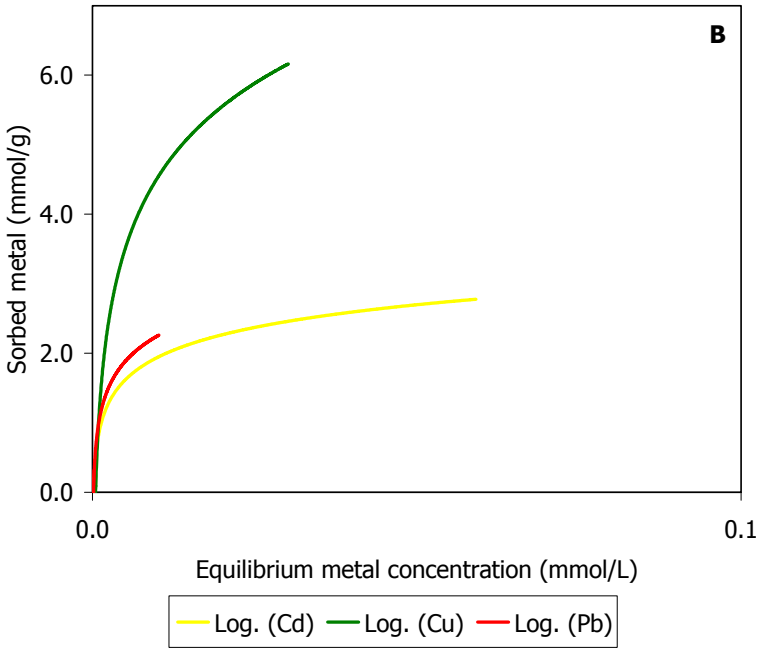

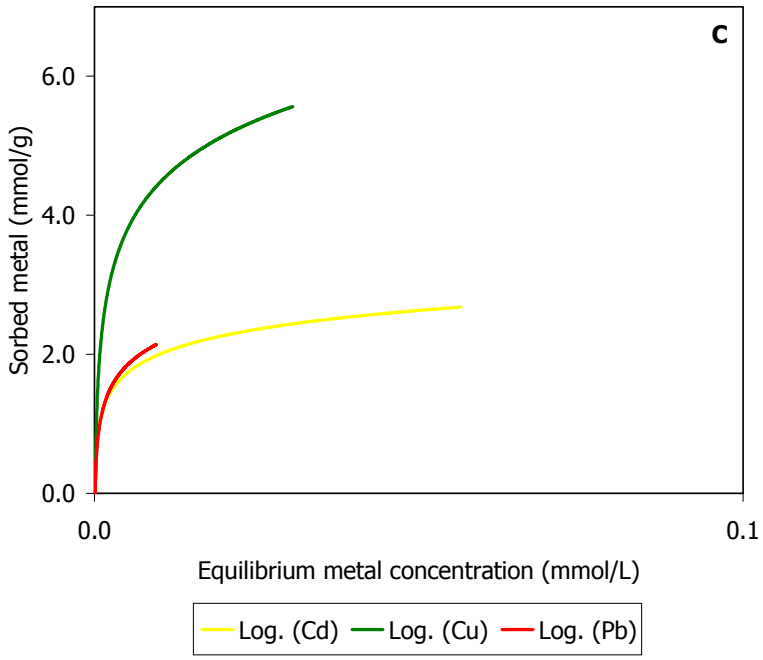

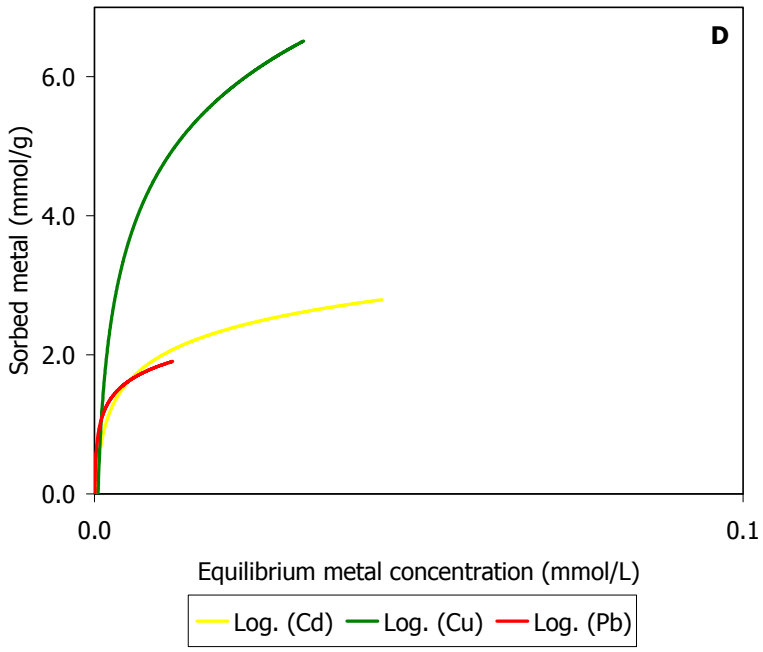

Fig. 18: Sorption isotherms for the multi-metal system where Zn is constant for the four contact times (2h, 4h, 24h and 48h) and vs. 1 g FAP. Relation between the metal sorbed (mmol/g) and the final concentration (mmol/L) in solution. A: t = 2h; B: t = 4h; C: t = 24h and D: t = 48h. – Fig. 18: Curve isotermiche per il sistema multi-metal in cui Zn è costante per i quattro tempi di contatto (2h, 4h, 24h and 48h) e vs. 1 g di FAP. Relazione tra il metallo assorbito (mmol/g) e la concentrazione finale (mmol/L) in soluzione. A: t = 2h; B: t = 4h; C: t = 24h and D: t = 48h.

The amount of Ca in solution at the equilibrium is not proportional to the amount of the heavy metals; suggesting a non stoichiometric dissolution of FAP. In the system where Cd is constant Ca ranges from < b.d.l. to 1 mmol/g, confirming the non stoichiometric dissolution. In case of constant Cu, Ca concentration ranges from < b.d.l. to 7 mmol/g and only in three cases the Ca amount increases independently from the interaction time. In the Pb, system the FAP dissolution (< b.d.l. – 0.7 mmol/g) is non stoichiometric even though the Ca concentration at the equilibrium increases. The low concentration of Ca desorbed allow to infer that, probably, there is the possibility of precipitation and coprecipitation of the heavy metals with HA *(26)* (Fig. 19 A, B, C, D, E and F).

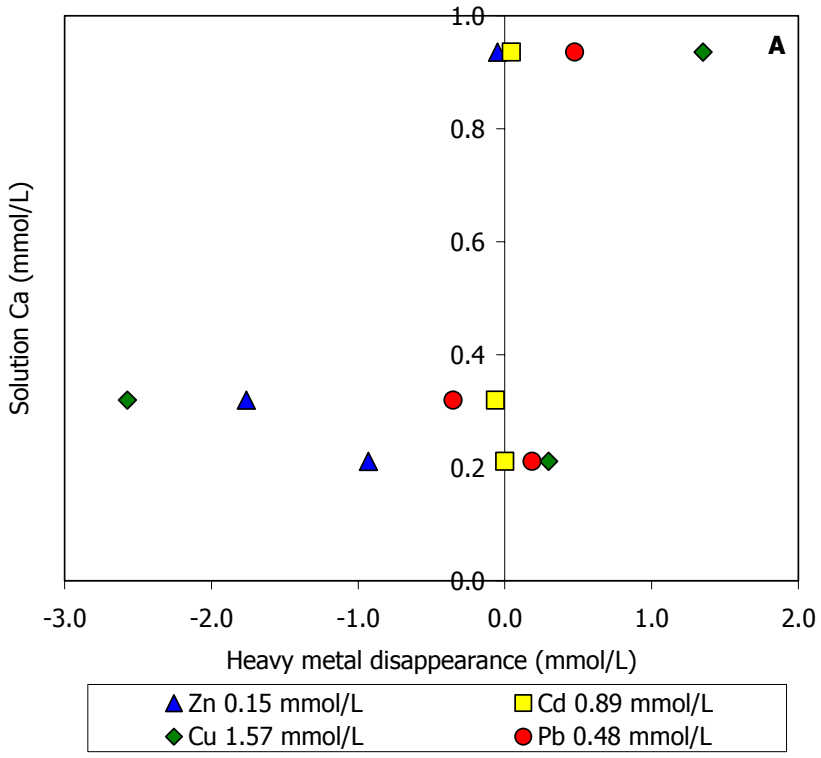

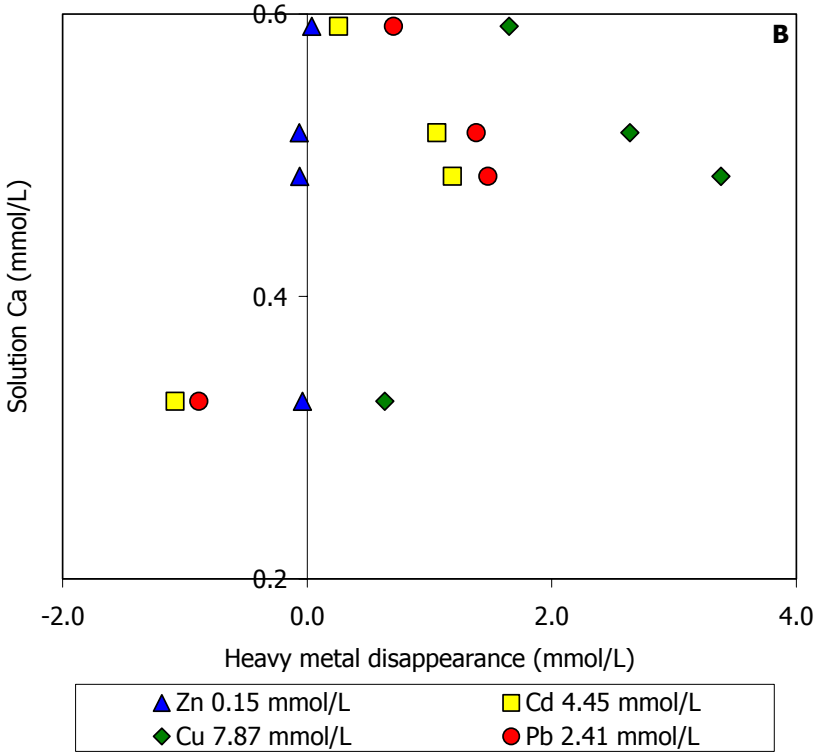
B
0.6
0.4
0.2
Solution Ca (mmol/L)
-2.0
0.0
2.0
4.0
Heavy metal disappearance (mmol/L)
Zn 0.15 mmol/L
Cd 4.45 mmol/L
Cu 7.87 mmol/L
Pb 2.41 mmol/L

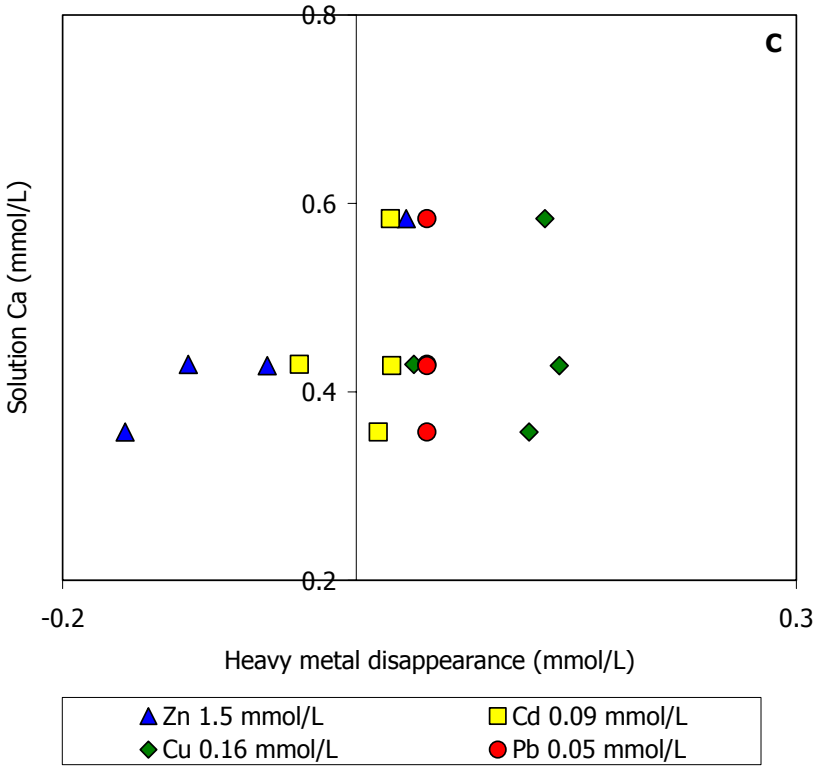
C
0.8
0.6
0.4
0.2
Solution Ca (mmol/L)
-0.2
0.3
Heavy metal disappearance (mmol/L)
Zn 1.5 mmol/L
Cd 0.09 mmol/L
Cu 0.16 mmol/L
Pb 0.05 mmol/L

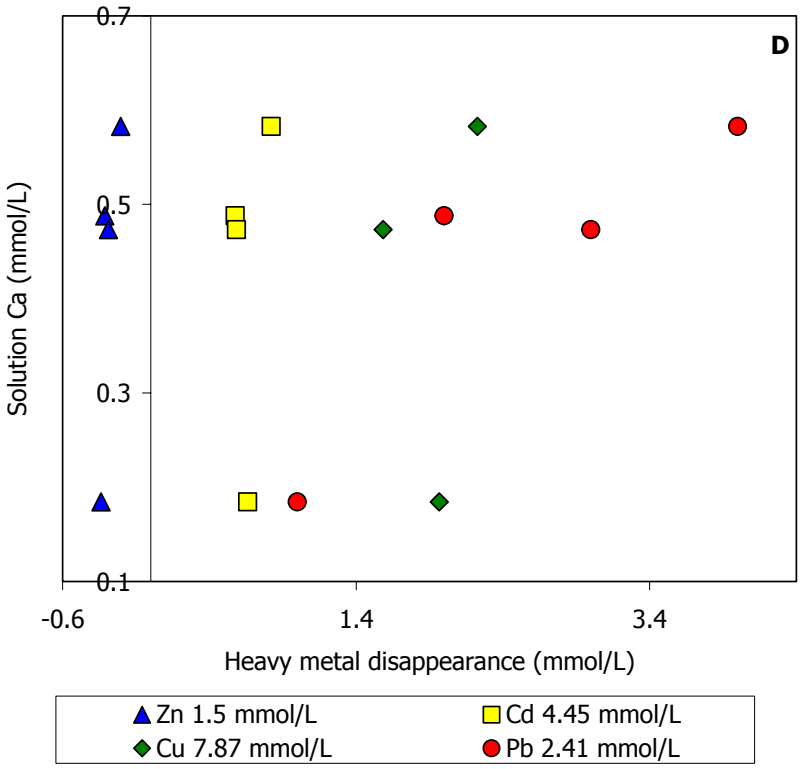
D
0.7
0.5
0.3
0.1
Solution Ca (mmol/L)
-0.6
1.4
3.4
Heavy metal disappearance (mmol/L)
Zn 1.5 mmol/L
Cd 4.45 mmol/L
Cu 7.87 mmol/L
Pb 2.41 mmol/L

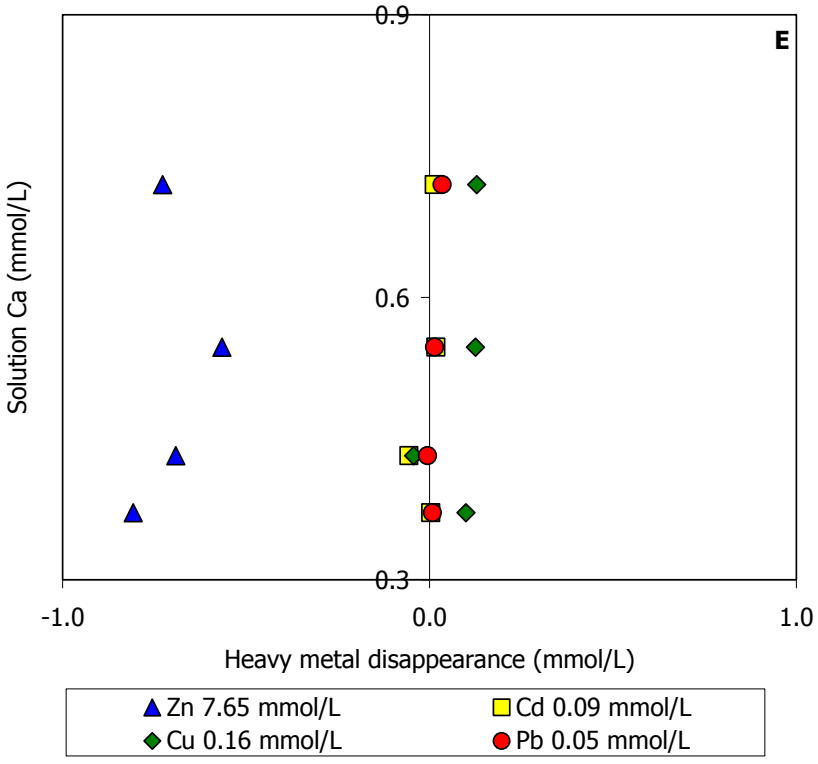
E
0.9
0.6
0.3
Solution Ca (mmol/L)
-1.0
0.0
1.0
Heavy metal disappearance (mmol/L)
Zn 7.65 mmol/L
Cd 0.09 mmol/L
Cu 0.16 mmol/L
Pb 0.05 mmol/L

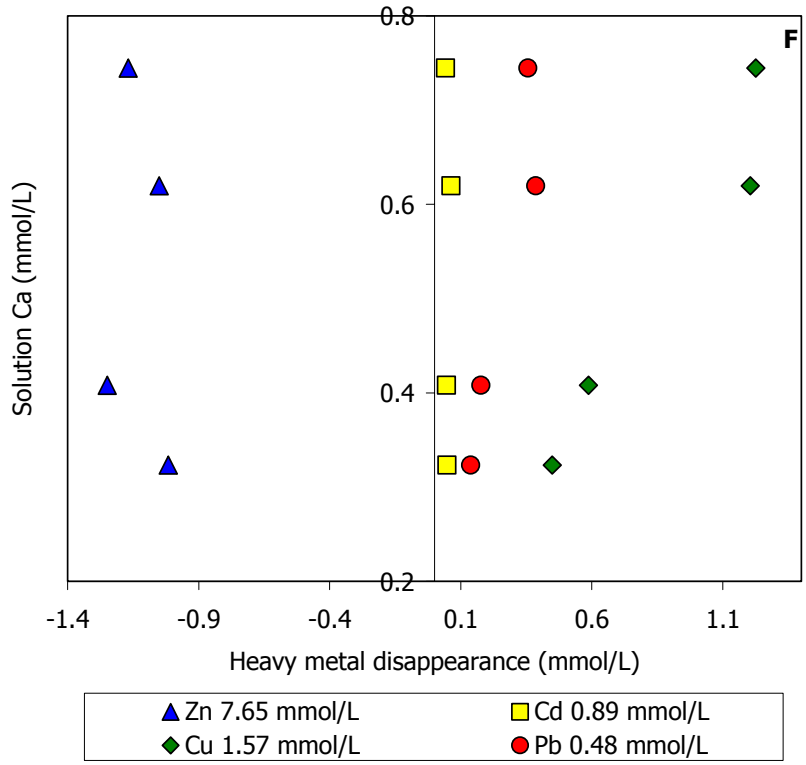

Fig. 19: Relation between Ca in solution (mmol/L) and the amount of heavy metals disappeared (mmol/L) sorbed on FAP surface at the equilibrium in a multi-metal system when Zn is constant. Each initial concentration of the multi-metal system is written in the legend. - Fig. 19: Relazione tra il quantitativo di Ca in soluzione (mmol/L) e di ciascun metallo pesante adsorbito (mmol/L) nel sistema multi-metal quando Zn è costante. La concentrazione iniziale di ogni elemento del sistema multi-metal è in leggenda.

The amount of P in the solution is very low (Fig. 20 A, B, C, D, E and F) and the concentration is not proportional to the amount of the sorbed heavy metals. In both Cd and Cu systems, the amount of P ranges from < b.d.l. to 0.4 mmol/g, in the Pb system the P concentration is lower than these values (< b.d.l. to 0.0 5 mmol/g) and in Zn system the P concentration range is from < b.d.l. to 1.6 mmol/g. The low amount of P at the equilibrium may indicate a precipitation process as sorption mechanism, as P is consumed for the deposition of a new phosphate phase.

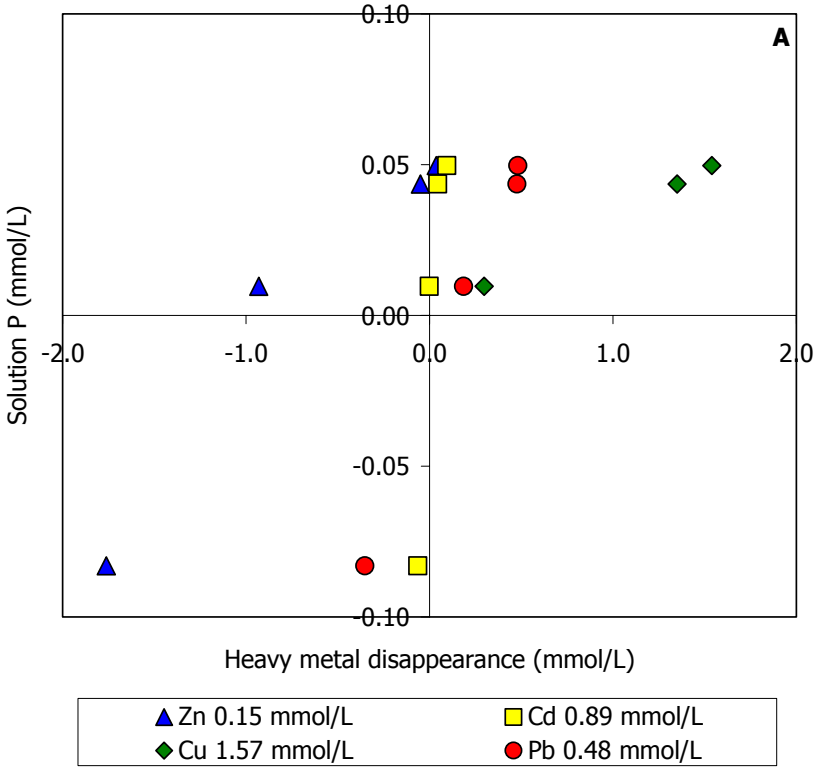
A
0.10
0.05
0.00
-0.05
-0.10
-2.0
-1.0
0.0
1.0
2.0
Solution P (mmol/L)
Heavy metal disappearance (mmol/L)
Zn 0.15 mmol/L
Cd 0.89 mmol/L
Cu 1.57 mmol/L
Pb 0.48 mmol/L

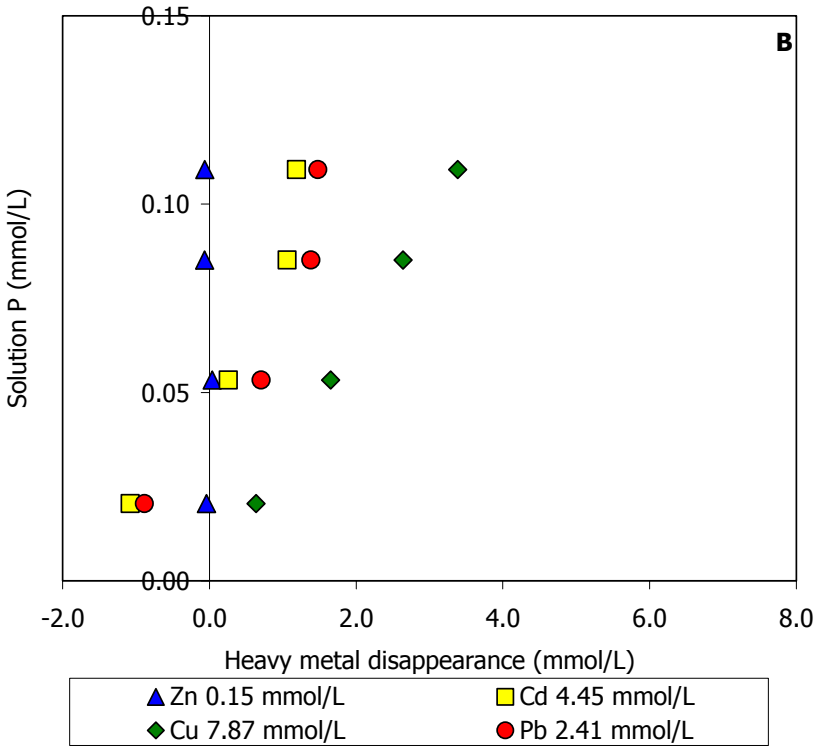
B
0.15
0.10
0.05
0.00
-2.0
0.0
2.0
4.0
6.0
8.0
Solution P (mmol/L)
Heavy metal disappearance (mmol/L)
Zn 0.15 mmol/L
Cd 4.45 mmol/L
Cu 7.87 mmol/L
Pb 2.41 mmol/L

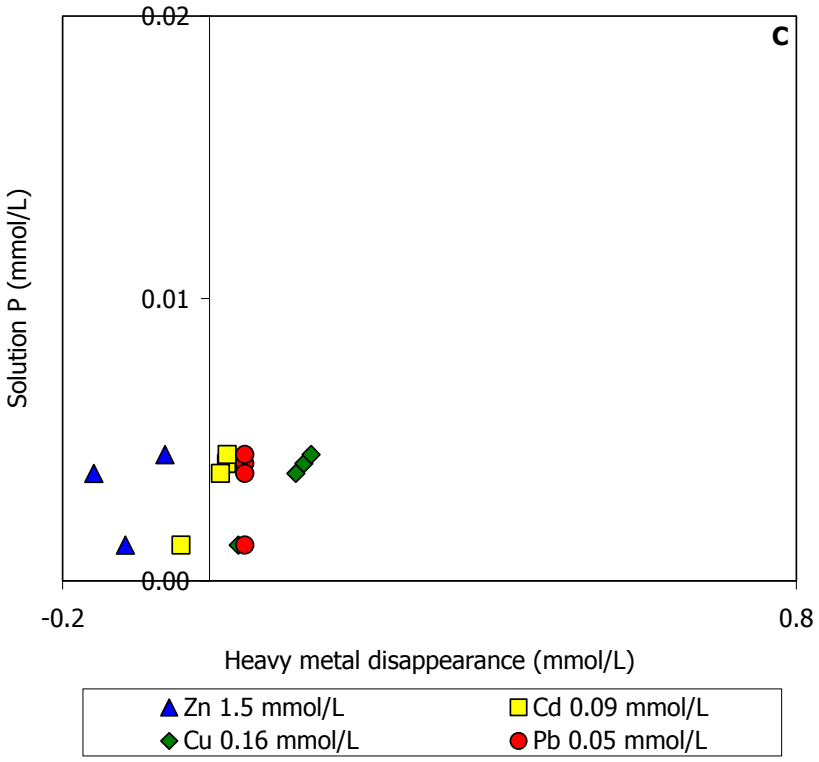
C
0.02
0.01
0.00
Solution P (mmol/L)
-0.2
0.8
Heavy metal disappearance (mmol/L)
Zn 1.5 mmol/L
Cd 0.09 mmol/L
Cu 0.16 mmol/L
Pb 0.05 mmol/L

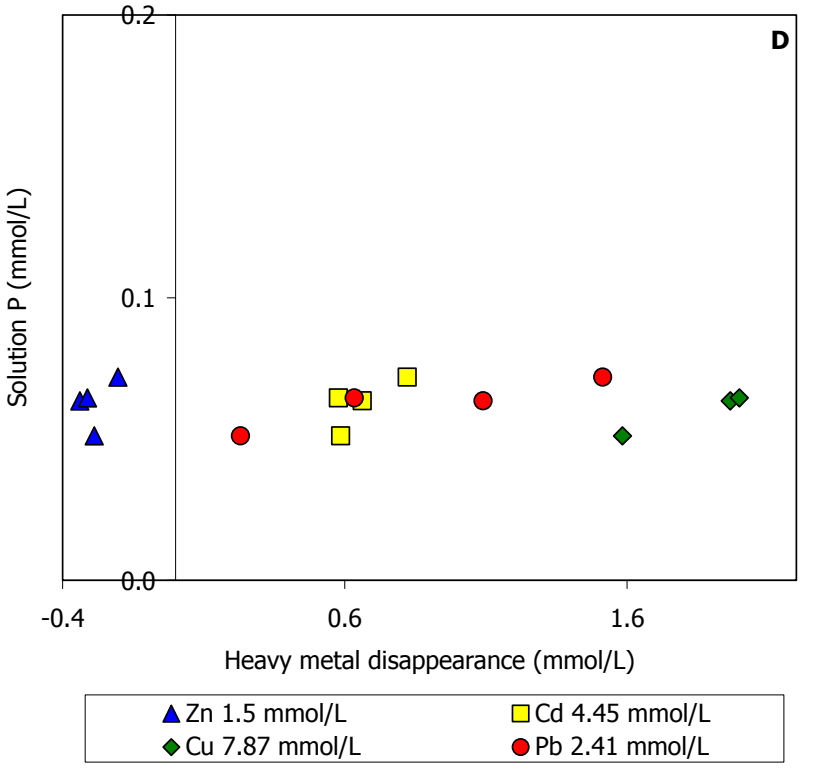
D
0.2
0.1
0.0
Solution P (mmol/L)
-0.4
0.6
1.6
Heavy metal disappearance (mmol/L)
Zn 1.5 mmol/L
Cd 4.45 mmol/L
Cu 7.87 mmol/L
Pb 2.41 mmol/L

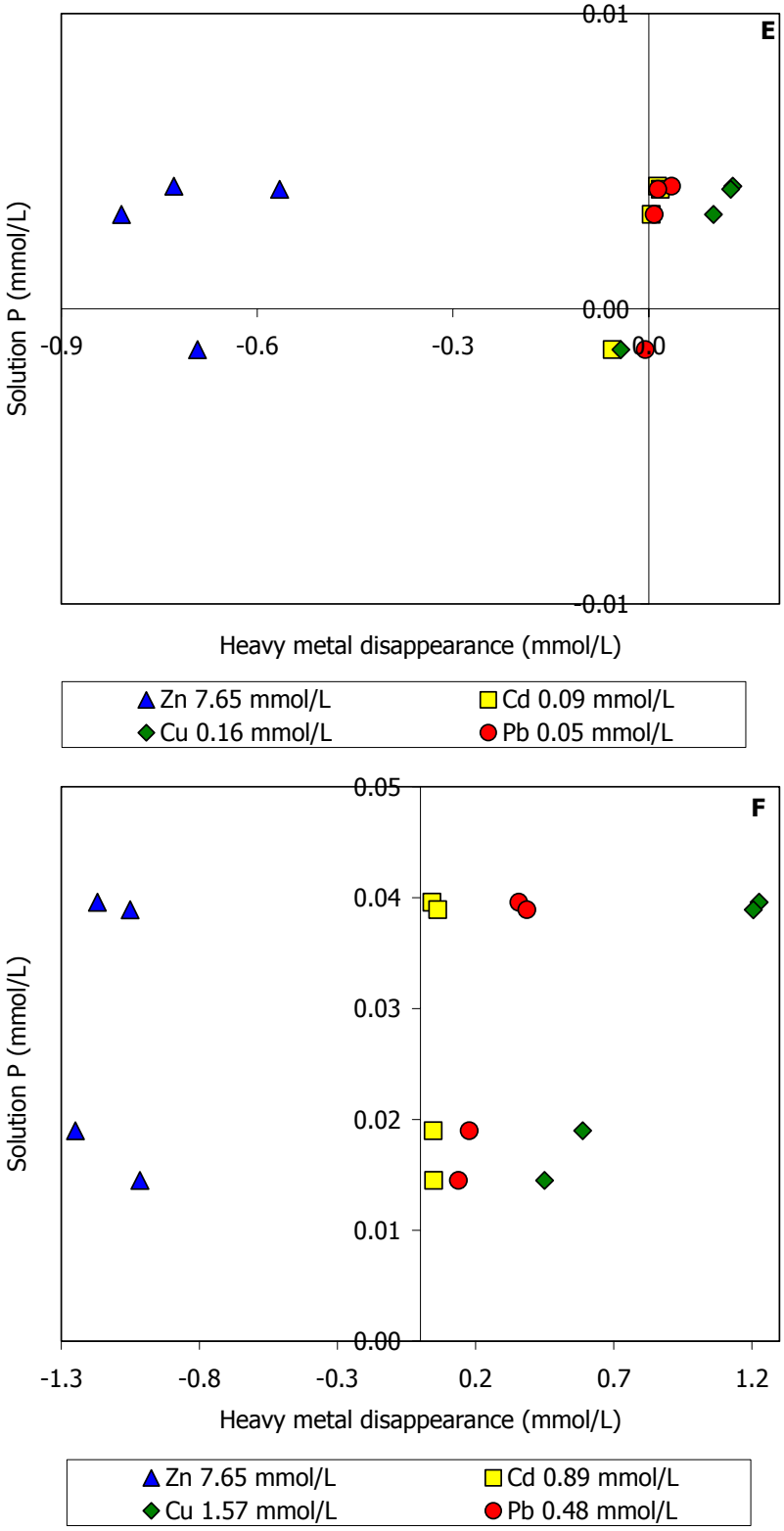

Fig. 20: Relation between P in solution (mmol/L) and the amount of disappeared heavy metals (mmol/L) sorbed on FAP surface at the equilibrium in a multi-metal system when Zn is constant. Each initial concentration of the multi-metal system is written in the legend. - Fig. 20: Relazione tra il quantitativo di P in soluzione (mmol/L) e di ciascun metallo pesante adsorbito (mmol/L) nel sistema multi-metal quando Zn è costante. La concentrazione iniziale di ogni elemento del sistema multi-metal è in leggenda.

6.3 MULTI-METAL SYSTEM SORBED ON FLUOROAPATITE FROM MOROCCO (MAP)

6.3.1 SEM analyses

The SEM micrographs show a semi-round morphology (Fig. 1 A, B, C, and D), as in FAP micrographs, but no differences are visible compared to the original MAP (Fig. 7 in Materials); moreover, no particular orientation are visible. EDS analyses show the presence of the heavy metals on MAP surface (Fig. 2 A, B, C, and D).

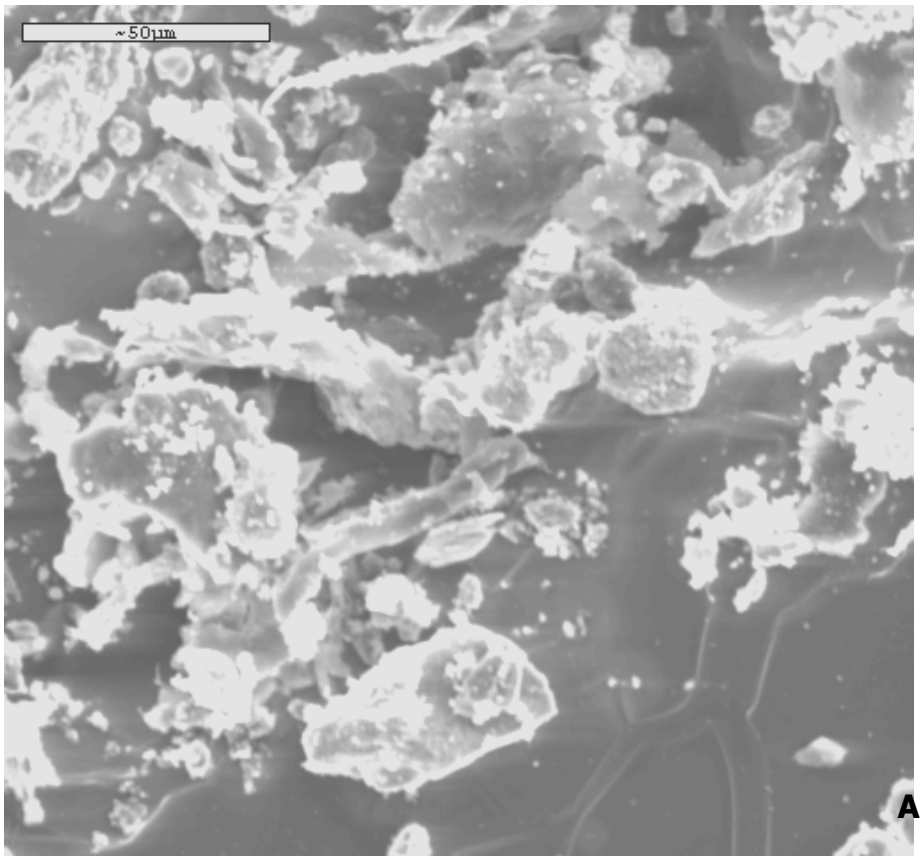

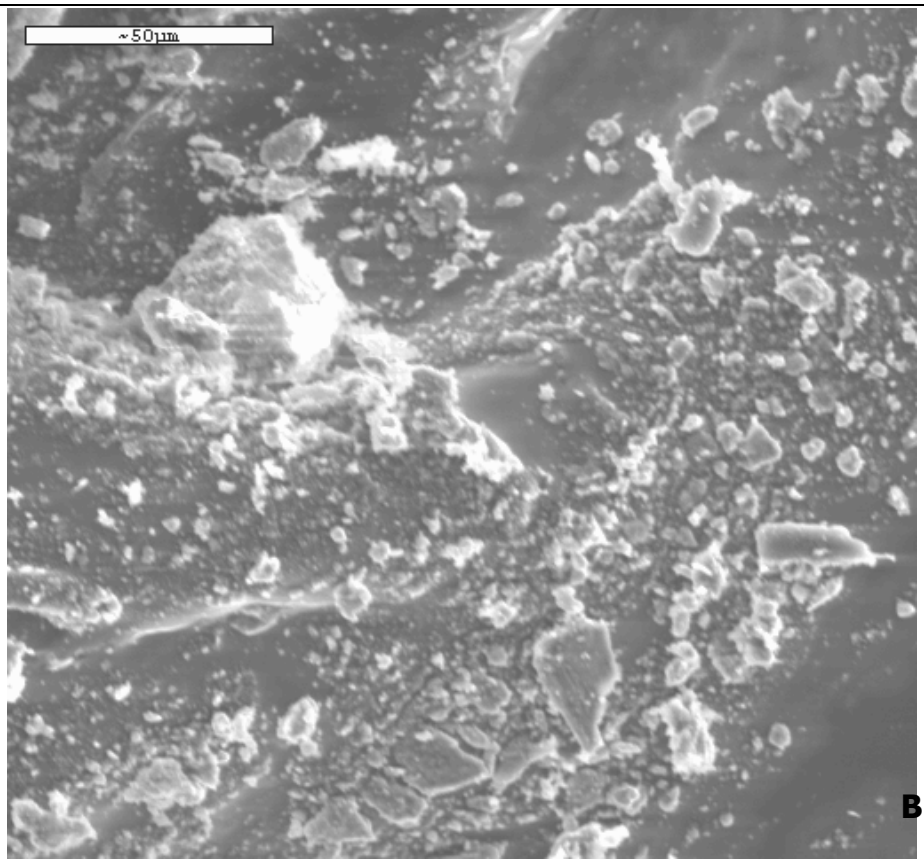
~50µm
B

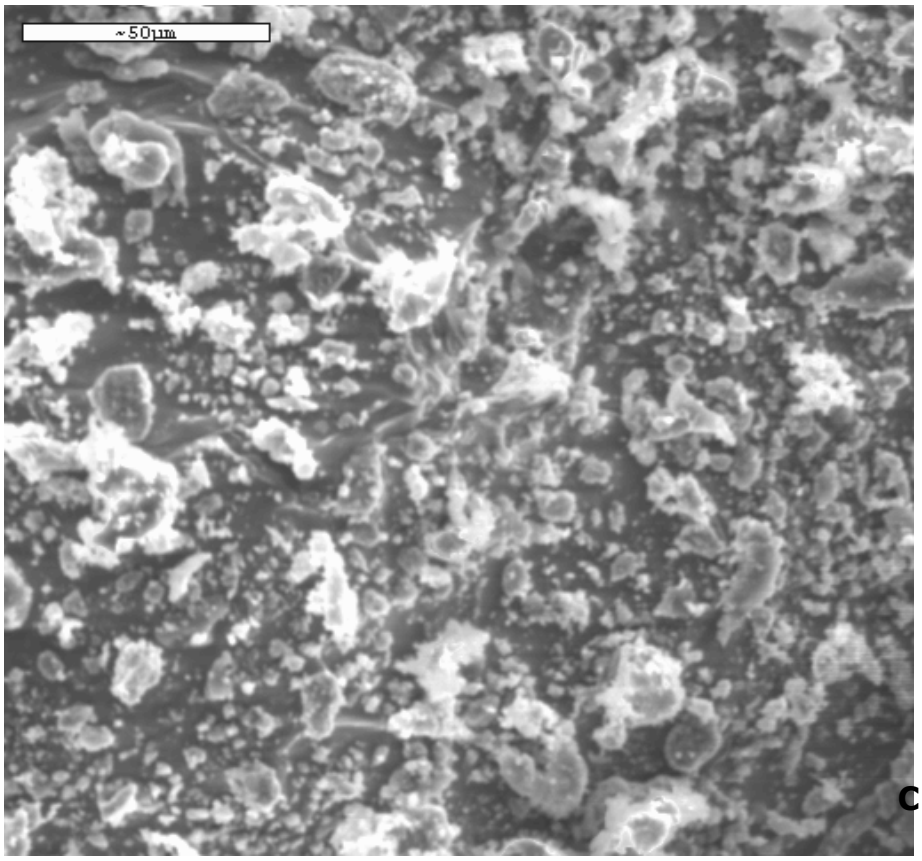
~50µm
C

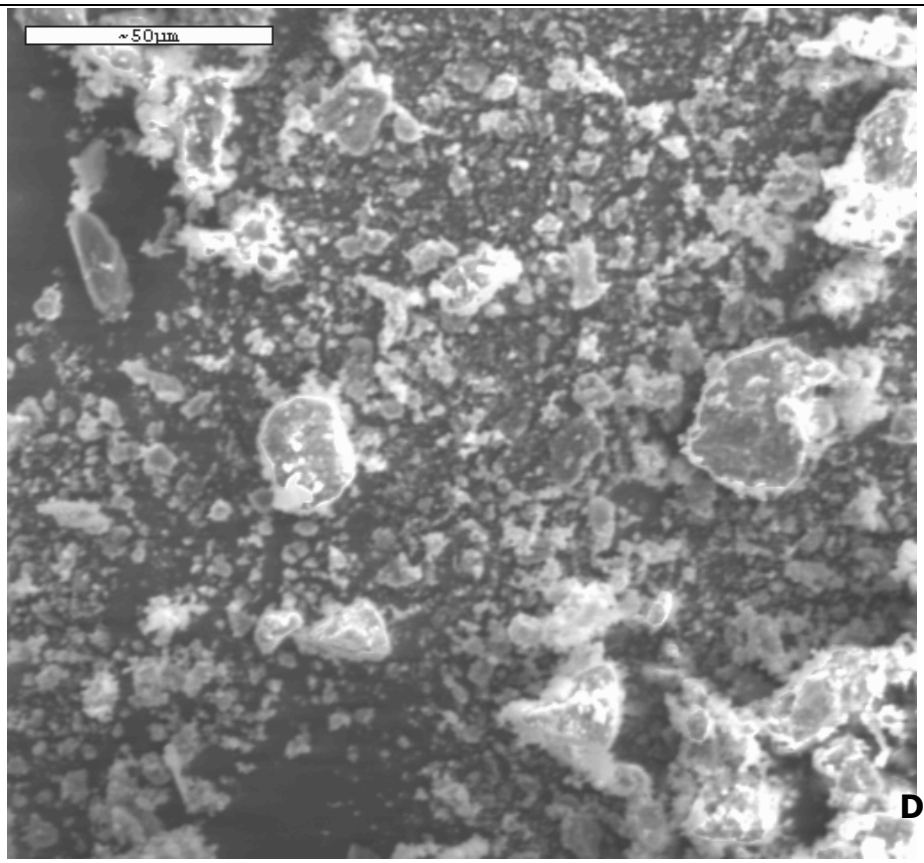

Fig. 1: SEM micrographs of multi-metal system vs. MAP. A: Cd = 100 mg/L, Cu, Pb and Zn = 10 mg/L t = 48h; B: Cu = 500 mg/L Cd, Pb and Zn = 100 mg/L t = 2h; C: Pb = 100 mg/L, Cd, Cu and Zn = 10 mg/L t = 48h; D: Zn = 100 mg/L, Cd, Cu and Pb = 500 mg/L t = 2h. – Fig. 1: Foto al SEM del sistema multi-metal vs. MAP. A: Cd = 100 mg/L, Cu, Pb and Zn = 10 mg/L t = 48h; B: Cu = 500 mg/L Cd, Pb and Zn = 100 mg/L t = 2h; C: Pb = 100 mg/L, Cd, Cu and Zn = 10 mg/L t = 48h; D: Zn = 100 mg/L, Cd, Cu and Pb = 500 mg/L t = 2h.

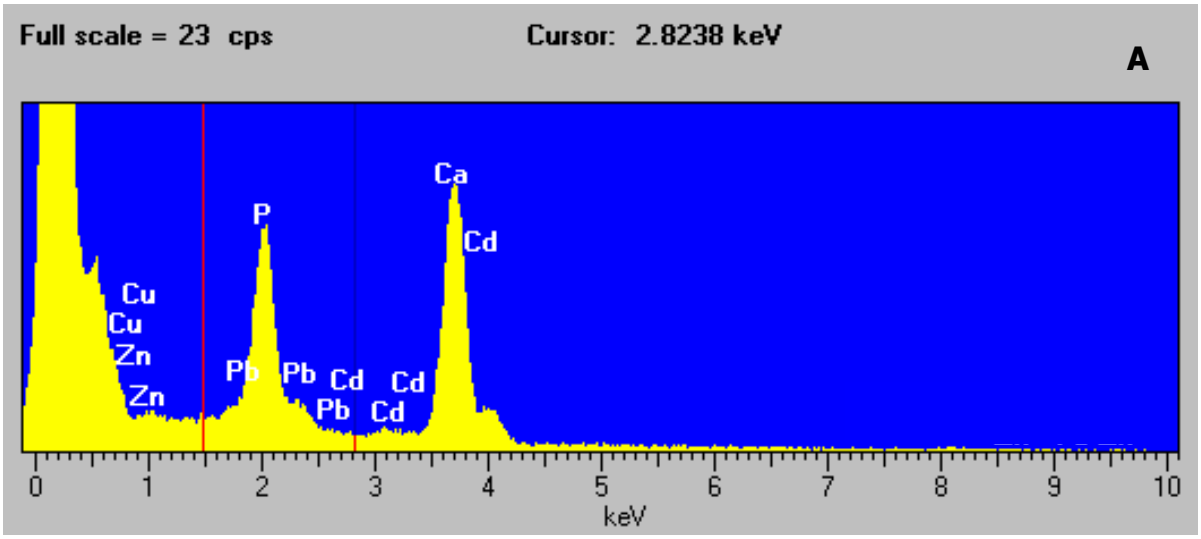

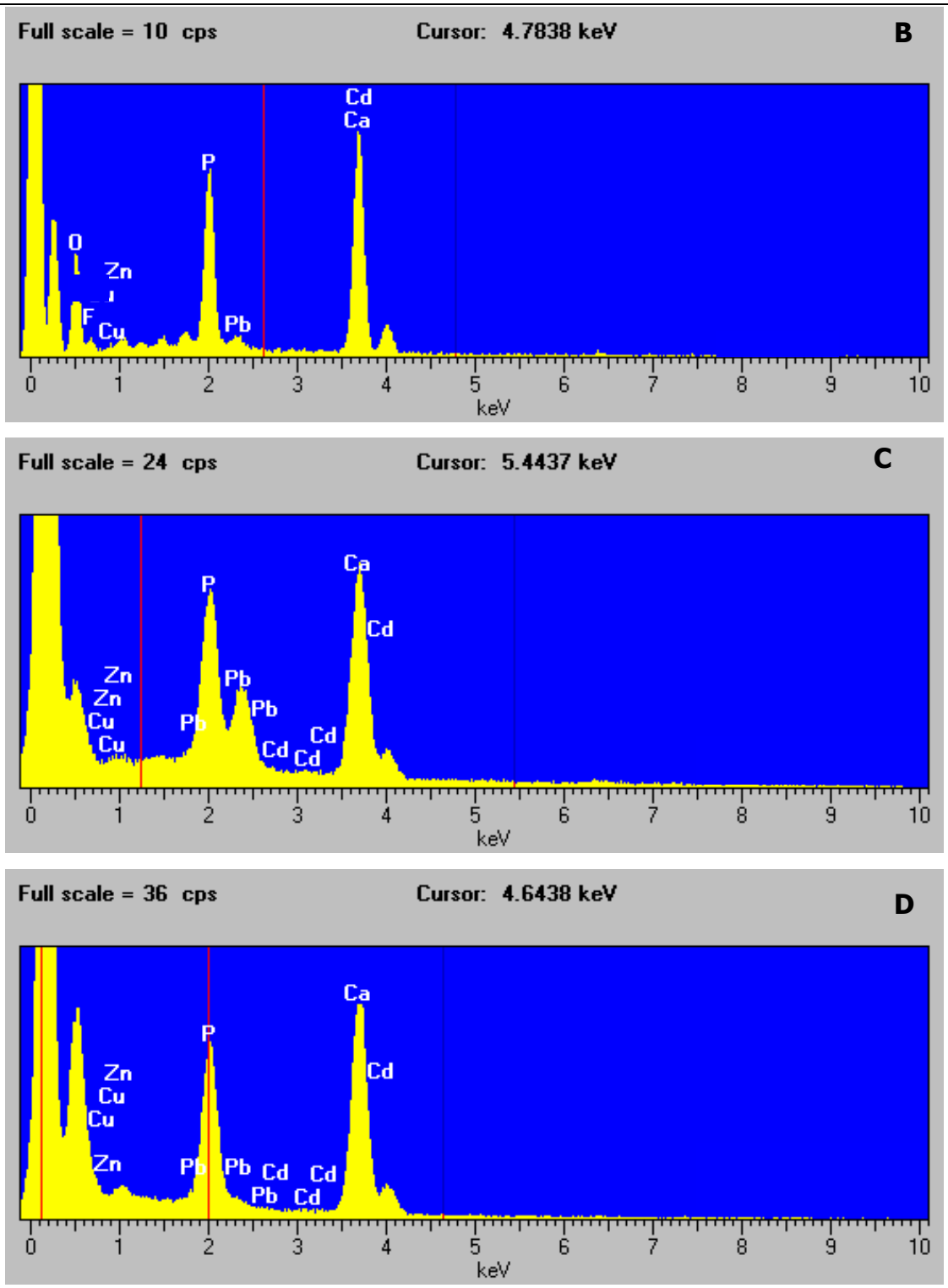

Fig. 2: EDS spectra of the previous SEM micrographs. – Fig. 2: Spettri EDS delle precedenti foto al SEM.

6.3.2 ICP-AES analyses

When Cd concentration is constant in the multi-metal system (Tab. 1 and Fig. 3 A, B, C, D, E and F) the better immobilization is achieved in 2 and 4h, with only one exception (Cd = 100 mg/L; Cu, Pb and Zn = 10 mg/L), probably depending on the heavy metals initial concentration. The percentage immobilization values (Tab. 2) are low compared to the HA values. In the system the order of the immobilization is always different and this can be due to the competitive sorption among the heavy metals and the initial metal concentration.

pH values usually increase of about 0.5 – 1 units after the immobilization and only in few cases the difference between the initial and final value is larger than 0.5 units.

Cd = 10 mg/L	Cu = 100 mg/L	Pb = 100 mg/L	Zn = 100 mg/L
0.622	17.974	24.335	1.798
0.679	21.921	29.085	1.664
-34.420	38.800	37.899	-5.285
-34.174	38.781	37.593	-5.218
Cd = 10 mg/L	Cu = 500 mg/L	Pb = 500 mg/L	Zn = 500 mg/L
0.778	86.217	41.964	45.996
0.805	77.779	52.655	46.857
-161.023	197.697	103.097	-13.259
-42.406	199.135	173.522	154.950
Cd = 100 mg/L	Cu = 10 mg/L	Pb = 10 mg/L	Zn = 10 mg/L
6.782	2.689	3.643	-0.884
12.041	3.661	3.917	-0.045
38.086	3.314	3.934	0.463
37.172	3.649	3.811	0.376
Cd = 100 mg/L	Cu = 500 mg/L	Pb = 500 mg/L	Zn = 500 mg/L
4.743	82.345	43.616	41.450
5.330	80.661	51.747	43.785
-118.374	172.973	66.427	-9.243
-125.980	174.625	50.710	-7.172
Cd = 500 mg/L	Cu = 10 mg/L	Pb = 10 mg/L	Zn = 10 mg/L
35.751	3.154	3.810	-0.149
37.473	3.302	3.875	-0.251
195.506	-122.017	3.321	-1.367
114.990	-68.930	-8.458	-30.605
Cd = 500 mg/L	Cu = 100 mg/L	Pb = 100 mg/L	Zn = 100 mg/L
28.512	17.637	18.911	0.420
30.612	19.287	24.129	0.948
158.525	-89.938	21.770	-6.438
161.360	-48.012	33.249	-2.933

Table 1: Proportions of blocked heavy metals per unit mass of MAP (mg/g) for the multi-metal system when Cd is constant. – Tabella 1: Entità dell'immobilizzazione dei metalli per unità di massa di MAP (mg/g) per il sistema multi-metal con concentrazione del Cd costante.

	% Blocked Metal		
Cd 10 mg/L	Cu 100 mg/L	Pb 100 mg/l	Zn 100 mg/L
15.54	44.94	60.84	4.49
16.97	54.80	72.71	4.16
-860.51	97.00	94.75	-13.21
-854.34	96.95	93.98	-13.05
Cd 10 mg/L	Cu 500 mg/L	Pb 500 mg/L	Zn 500 mg/L
19.45	43.11	20.98	99.38
20.12	38.89	26.33	99.34
-4025.58	98.85	51.55	99.98
-1060.15	99.57	86.76	99.98
Cd 100 mg/L	Cu 10 mg/L	Pb 10 mg/L	Zn 10 mg/L
16.96	67.24	91.08	-22.10
30.10	91.52	97.92	-1.13
95.22	82.85	98.34	11.59
92.93	82.45	99.72	9.39
Cd 100 mg/L	Cu 500 mg/L	Pb 500 mg/L	Zn 500 mg/L
11.86	41.17	21.81	20.73
13.32	40.33	25.87	21.89
-295.93	86.49	33.21	-4.62
-314.95	87.31	25.35	-3.59
Cd 500 mg/L	Cu 10 mg/L	Pb 10 mg/L	Zn 10 mg/L
17.88	78.84	95.24	-3.72
18.74	82.55	96.87	-6.26
97.75	-3050.44	83.01	-34.18
57.49	-1723.25	-211.45	-765.12
Cd 500 mg/L	Cu 100 mg/L	Pb 100 mg/L	Zn 100 mg/L
14.26	44.09	47.28	1.05
15.31	48.22	60.32	2.37
79.26	-224.85	54.43	-16.09
80.68	-120.03	83.12	-7.33

Table 2: Percentage of immobilization for the multi-metal system where Cd is constant. – Tabella 2: Sono riportati i valori della percentuale di immobilizzazione per il sistema multi-metal in cui Cd è costante.

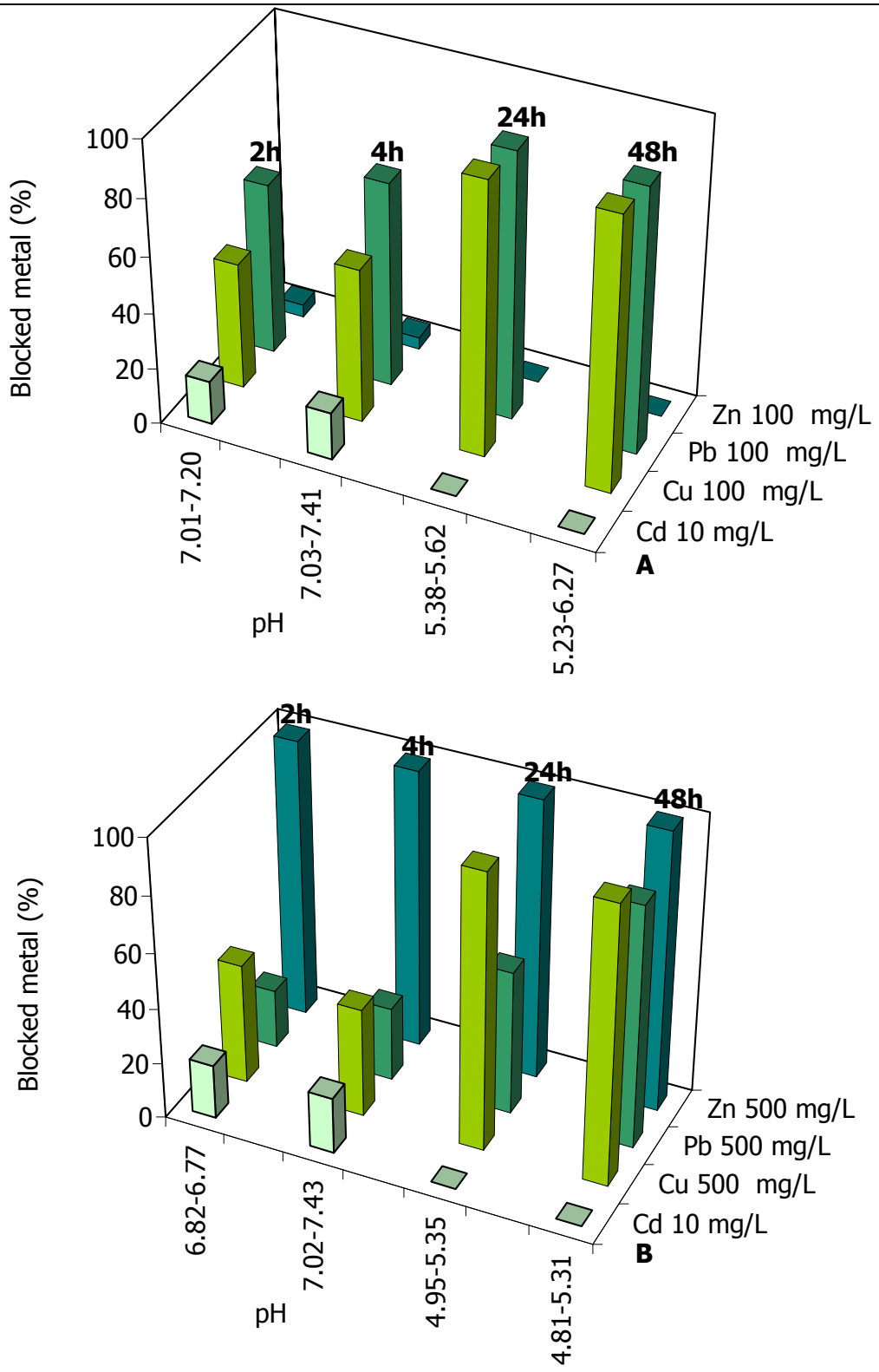
Blocked metal (%)
100
80
60
40
20
0
2h
4h
24h
48h
7.01-7.20
7.03-7.41
5.38-5.62
5.23-6.27
pH
Zn 100 mg/L
Pb 100 mg/L
Cu 100 mg/L
Cd 10 mg/L
A
Blocked metal (%)
100
80
60
40
20
0
2h
4h
24h
48h
6.82-6.77
7.02-7.43
4.95-5.35
4.81-5.31
pH
Zn 500 mg/L
Pb 500 mg/L
Cu 500 mg/L
Cd 10 mg/L
B

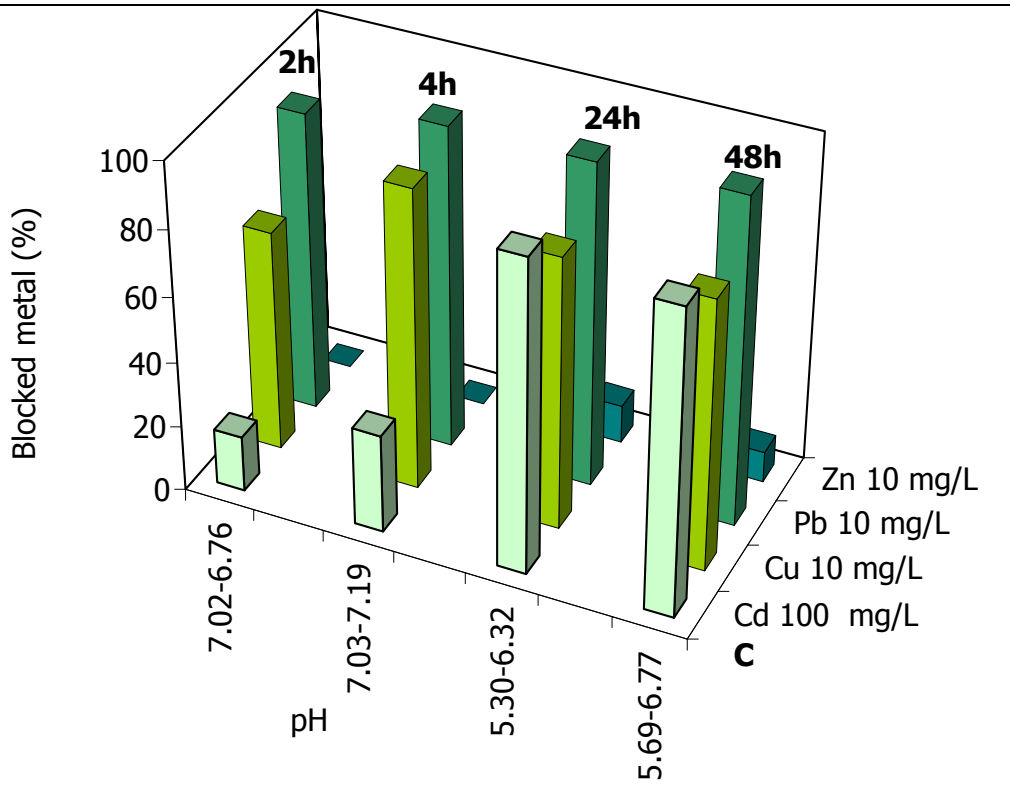
Blocked metal (%)
100
80
60
40
20
0
2h
4h
24h
48h
7.02-6.76
7.03-7.19
5.30-6.32
5.69-6.77
pH
Zn 10 mg/L
Pb 10 mg/L
Cu 10 mg/L
Cd 100 mg/L
C

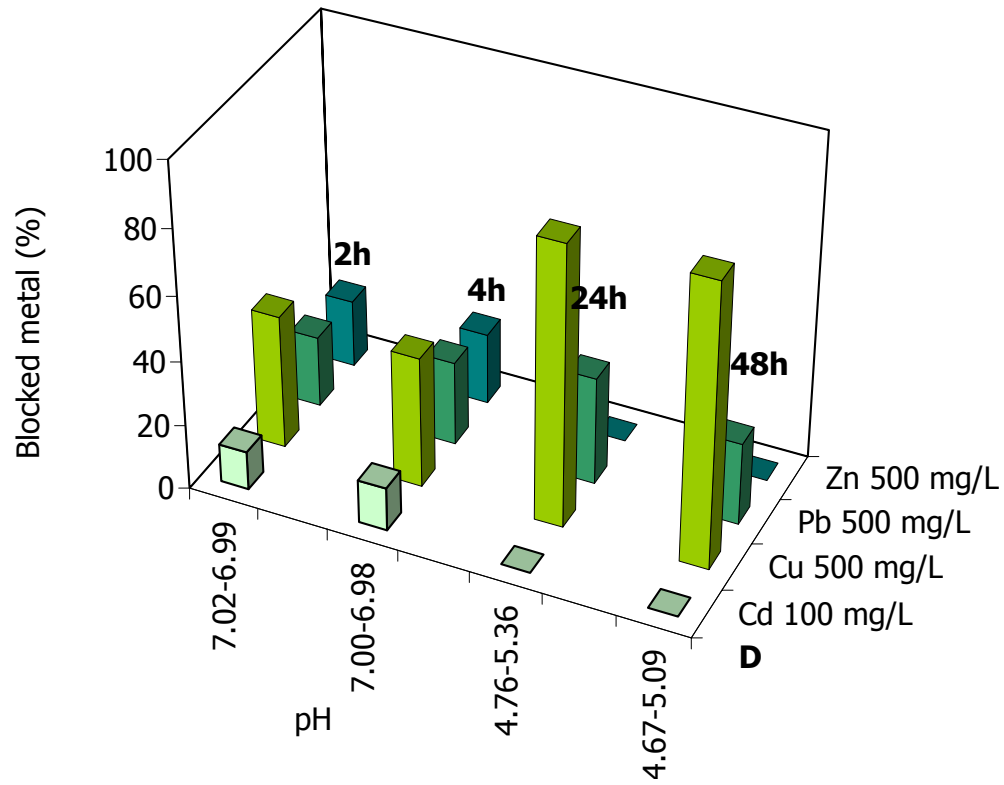
Blocked metal (%)
100
80
60
40
20
0
2h
4h
24h
48h
7.02-6.99
7.00-6.98
4.76-5.36
4.67-5.09
pH
Zn 500 mg/L
Pb 500 mg/L
Cu 500 mg/L
Cd 100 mg/L
D

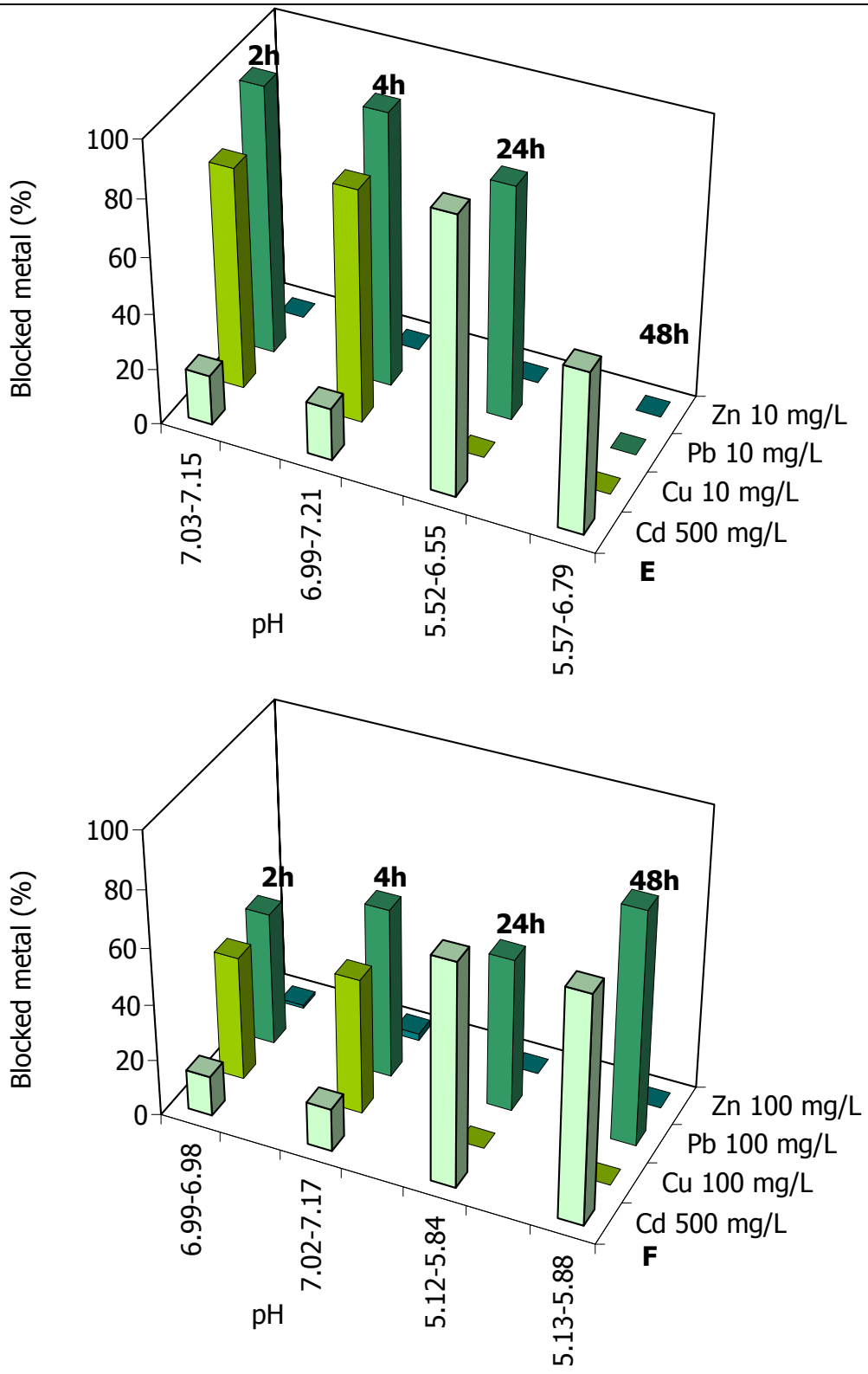

Fig. 3: Variation of the amount of blocked metal with time for the mass of MAP (1 g) in the multi-metal system where Cd is constant. Initial and final pH values are reported. – Fig. 3: Variazione delle percentuali dei metalli immobilizzati in funzione del tempo di interazione per la quantità di MAP (1 g) nel sistema multi-metal in cui Cd è l'elemento costante. Sono riportati i valori iniziali e finali del pH.

The Q_S values (Tab. 3) are really variable and seems on the interaction time and the initial heavy metal concentration. When Cd concentration is 10 mg/L, $Q_S < 1$ only for the interaction time of 2 and 4h, then $Q_S > 1$ and in one case $Q_S >> 1$. In the first case, the values suggest a non-crystalline precipitation and in the second case the adsorption mechanism. Cu shows the opposite behaviour according to the same interaction time. Pb shows $Q_S <1$ for a concentration of 100 mg/L and $Q_S >1$ for a concentration of 500 mg/L. Zn shows always $Q_S>> 1$.

Increasing Cd concentration to 100 mg/L, in the first case Cd shows a behaviour as before, $Q_S <1$ (2 and 4h) and $Q_S >1$ (24 and 48h), and in the second one has a $Q_S >>1$; Q_S seems to be influenced from the initial concentration of the other three heavy metals. Cu, Pb and Zn show a $Q_S < 1$ for a concentration of 10 mg/L and $Q_S >> 1$ for a concentration of 500 mg/L.

When Cd concentration is 500 mg/L, Q_S is always >> 1, Pb shows always $Q_S < 1$, whereas Cu has $Q_S < 1$ for the lower concentration and for time as 2 and 4h, then increasing the interaction time and metal concentration $Q_S > 1$ and for t = 24h $Q_S >>1$. Zn has $Q_S <1$ which increases to $Q_S > 1$ with the initial concentration. For this system the two most probable sorption mechanisms are the non-crystalline precipitation and the adsorption.

Cd = 10 mg/L	Cu = 100 mg/L	Pb = 100 mg/L	Zn = 100 mg/L
0.207	2.389	0.521	4.028
0.150	1.444	0.267	2.975
1.856	0.103	0.055	3.760
1.832	0.103	0.063	3.732
Cd = 10 mg/L	Cu = 500 mg/L	Pb = 500 mg/L	Zn = 500 mg/L
0.213	13.278	5.656	17.467
0.151	10.243	3.787	12.474
8.049	0.199	2.564	17.885
1.777	0.059	0.550	2.966
Cd = 100 mg/L	Cu = 10 mg/L	Pb = 10 mg/L	Zn = 10 mg/L
3.320	0.232	0.019	0.839
1.551	0.033	0.002	0.386
0.045	0.029	0.001	0.143
0.089	0.020	0.003	0.196
Cd = 100 mg/L	Cu = 500 mg/L	Pb = 500 mg/L	Zn = 500 mg/L
1.641	9.684	3.948	12.684
1.522	9.270	3.532	11.794
9.470	2.859	4.333	21.511
7.840	2.120	3.826	16.825
Cd = 500 mg/L	Cu = 10 mg/L	Pb = 10 mg/L	Zn = 10 mg/L
9.157	0.083	0.006	0.398
7.993	0.061	0.003	0.359
0.230	11.433	0.019	0.473
3.690	5.600	0.293	2.582
Cd = 500 mg/L	Cu = 100 mg/L	Pb = 100 mg/L	Zn = 100 mg/L
11.382	2.626	0.759	4.517
9.154	1.980	0.465	3.628
2.037	11.291	0.486	3.922
1.304	5.253	0.124	2.491

Table 3: Q_S values for the multi - metal systems when Cd has a constant concentration. Tabella 3: Valori di Q_S per i sistemi multi-metal nei quali la concentrazione di Cd è stata mantenuta costante Q_S values for the multi - metal system when Cd has a constant concentration.

The sorption isotherms for this systems have been obtained only for Pb and Zn as Cd and Cu show negative values (desorption phenomenon). Pb shows a L2 isotherm and Zn an H type (Fig. 4 A, B, C and C).

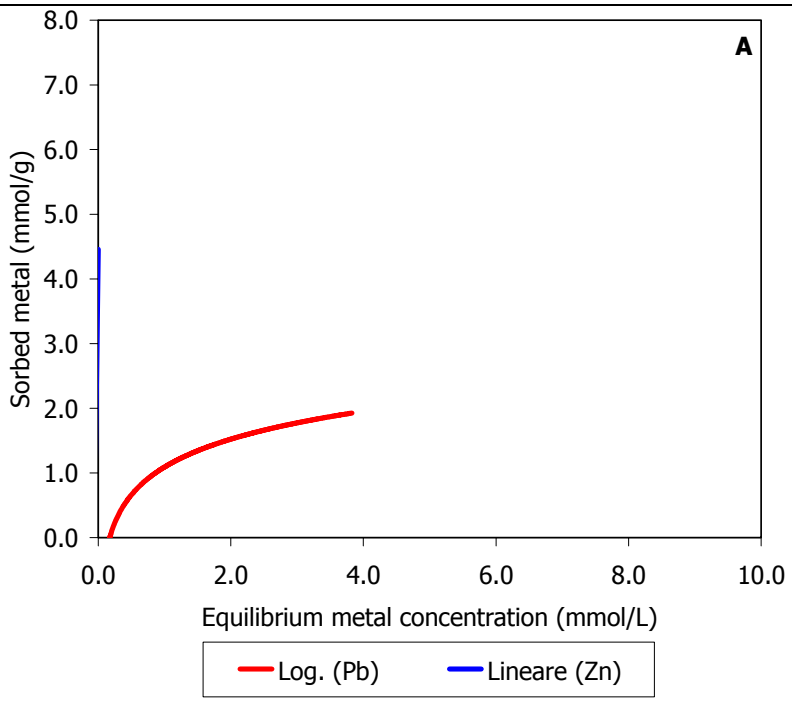
A
8.0
7.0
6.0
5.0
4.0
3.0
2.0
1.0
0.0
Sorbed metal (mmol/g)
0.0
2.0
4.0
6.0
8.0
10.0
Equilibrium metal concentration (mmol/L)
Log. (Pb)
Lineare (Zn)

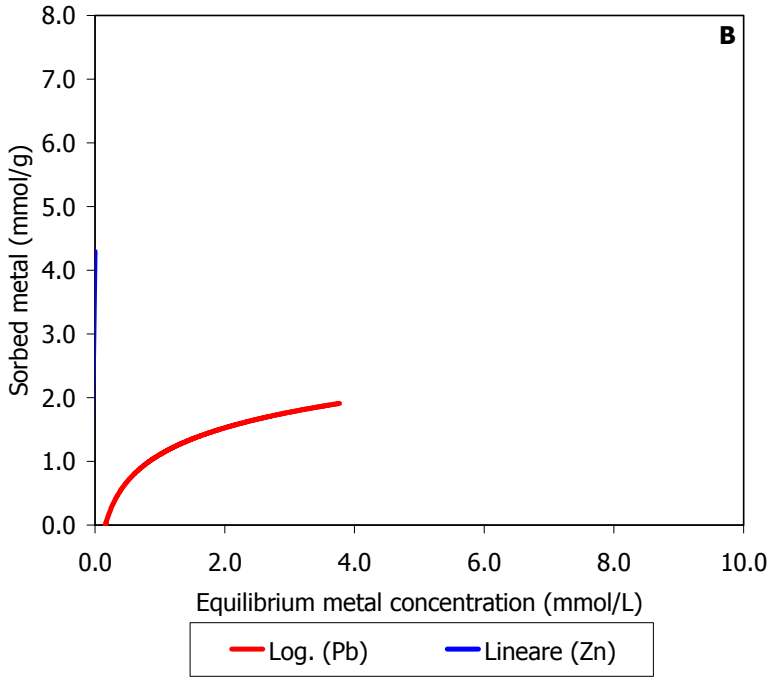
B
8.0
7.0
6.0
5.0
4.0
3.0
2.0
1.0
0.0
Sorbed metal (mmol/g)
0.0
2.0
4.0
6.0
8.0
10.0
Equilibrium metal concentration (mmol/L)
Log. (Pb)
Lineare (Zn)

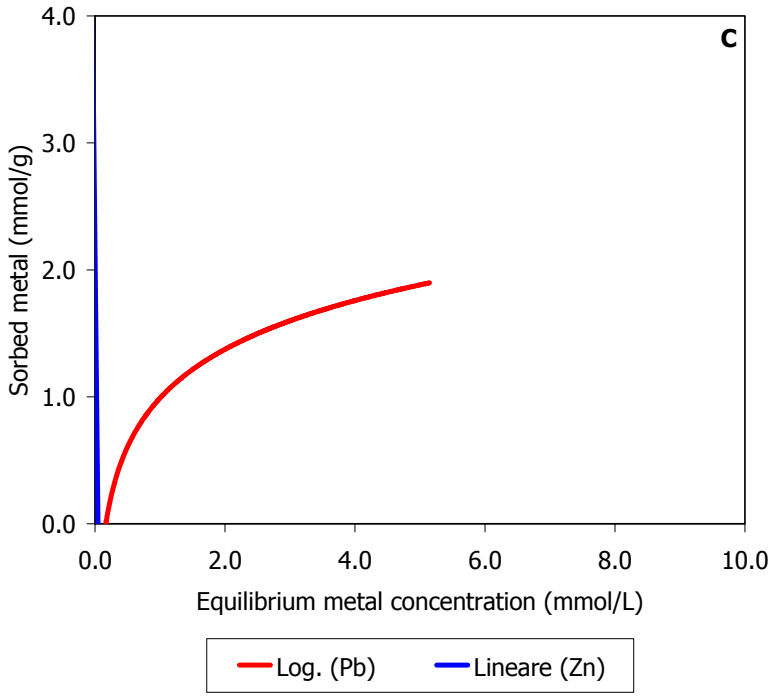

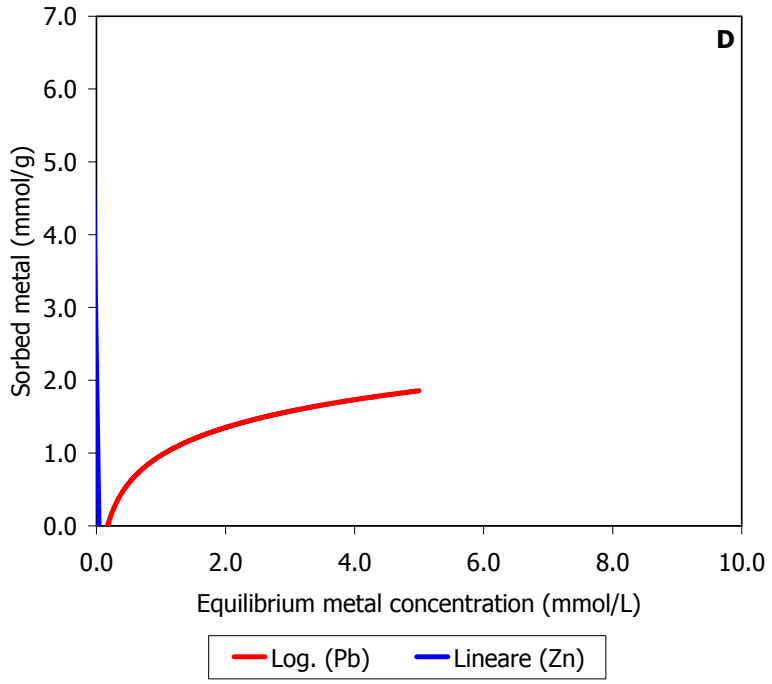

Fig. 4: Sorption isotherms for the multi-metal system where Cd is constant for the four contact times (2h, 4h, 24h and 48h) and vs. 1 g MAP. Relation between the metal sorbed (mmol/g) and the final concentration (mmol/L) in solution. A: t = 2h; B: t = 4h; C: t = 24h and D: t = 48h. – Fig. 4: Curve isotermiche per il sistema multi-metal in cui Cd è costante per i quattro tempi di contatto (2h, 4h, 24h and 48h) e vs. 1 g di MAP. Relazione tra il metallo assorbito (mmol/g) e la concentrazione finale (mmol/L) in soluzione. A: t = 2h; B: t = 4h; C: t = 24h and D: t = 48h.

The amount of Ca in solution (Fig. 5 A, B, C, D, E and F) at the equilibrium is almost proportional to the amount of sorbed heavy metals. Generally, Ca amount ranges from < b.d.l. to 2 mmol/g and Pb and Zn sorbed concentrations is maximum 10 mmol/g.

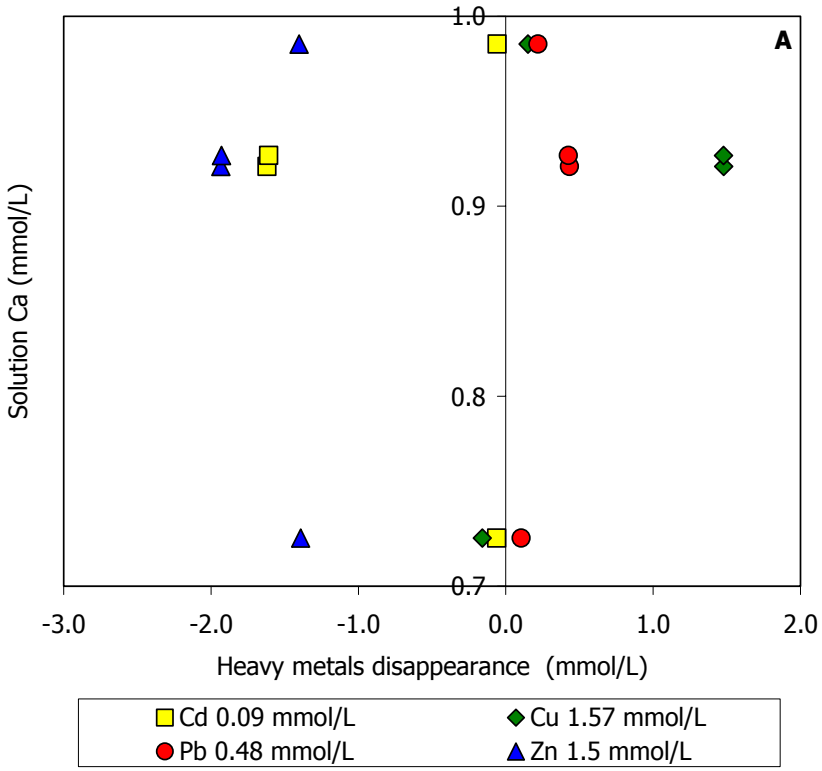

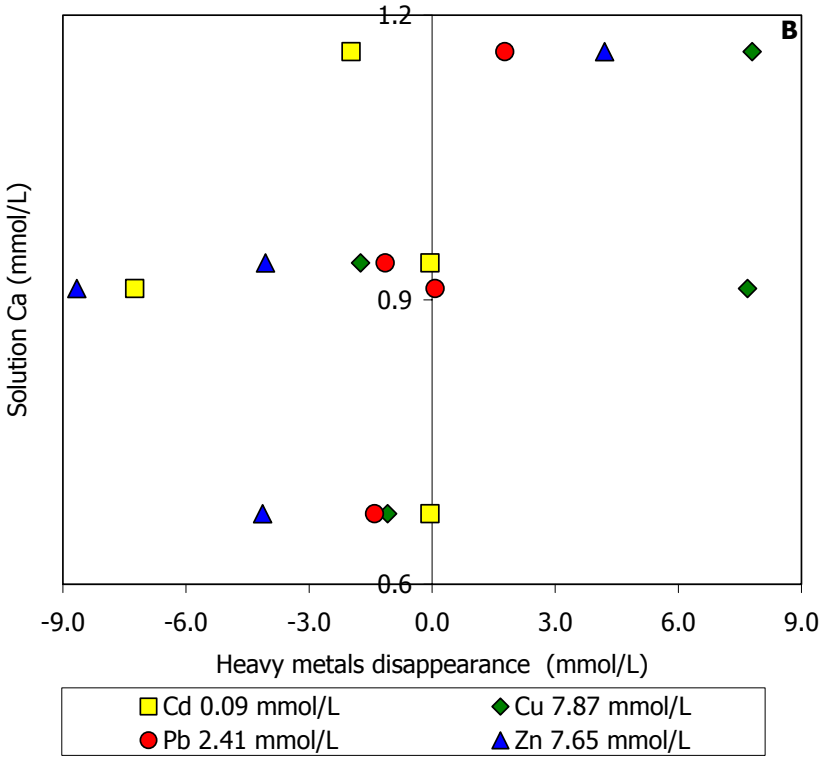

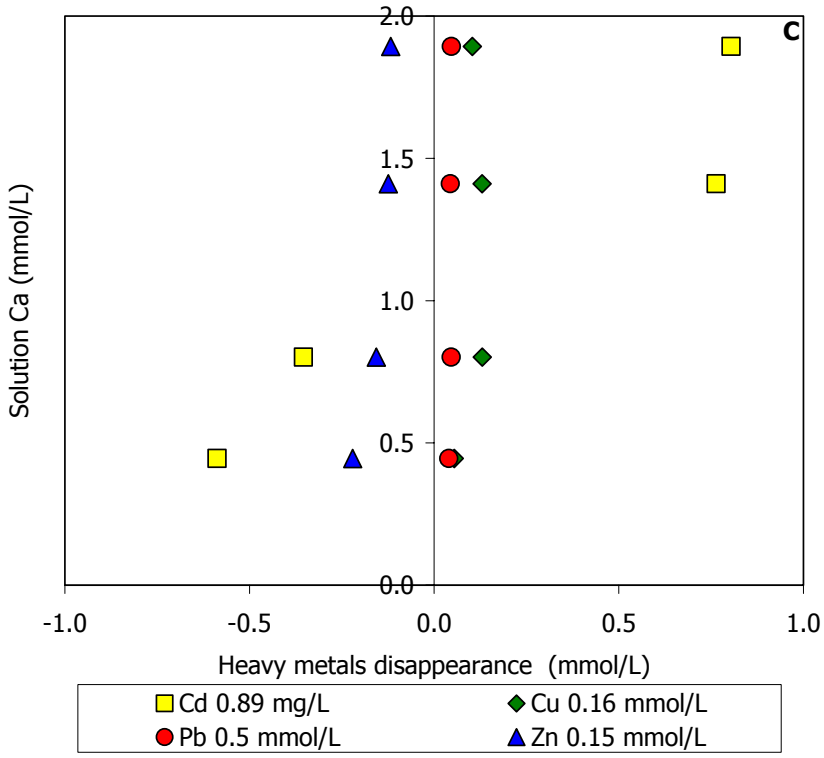
C
2.0
1.5
1.0
0.5
0.0
Solution Ca (mmol/L)
-1.0
-0.5
0.0
0.5
1.0
Heavy metals disappearance (mmol/L)
Cd 0.89 mg/L
Cu 0.16 mmol/L
Pb 0.5 mmol/L
Zn 0.15 mmol/L

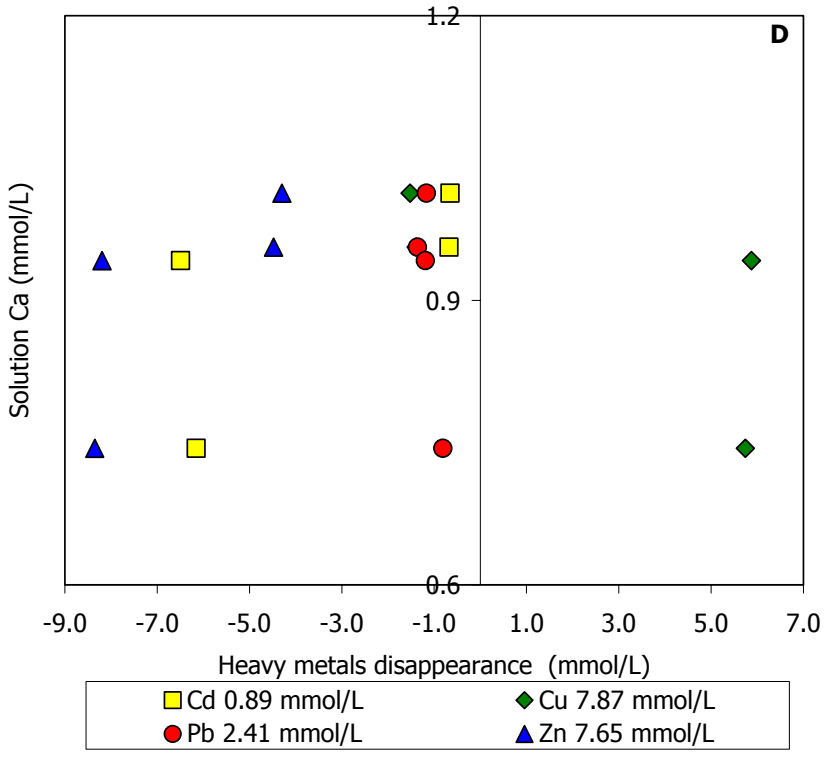
D
1.2
0.9
0.6
Solution Ca (mmol/L)
-9.0
-7.0
-5.0
-3.0
-1.0
1.0
3.0
5.0
7.0
Heavy metals disappearance (mmol/L)
Cd 0.89 mmol/L
Cu 7.87 mmol/L
Pb 2.41 mmol/L
Zn 7.65 mmol/L

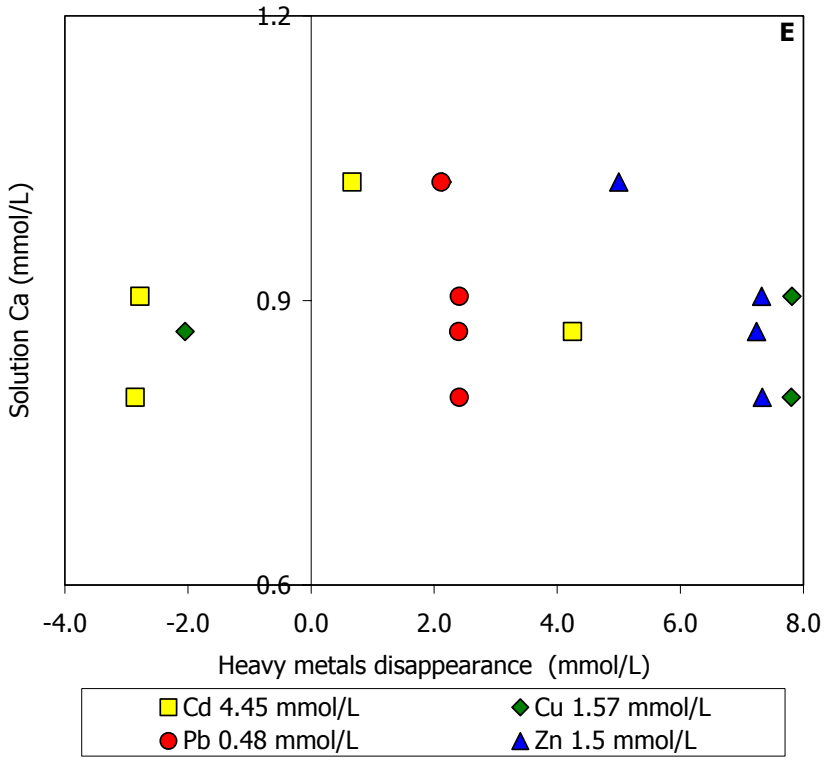

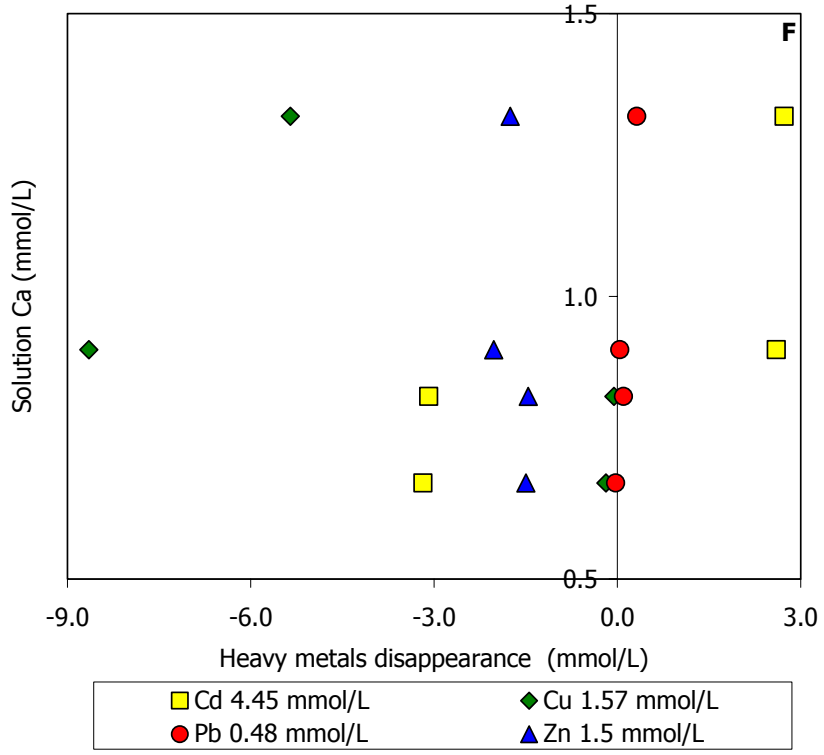

Fig. 5: Relation between Ca in solution (mmol/L) and the amount of heavy metals disappeared (mmol/L) sorbed on MAP surface at the equilibrium in a multi-metal system when Cd is constant. Each initial concentration of the multi-metal system is written in the legend. - Fig. 5: Relazione tra il quantitativo di Ca in

soluzione (mmol/L) e di ciascun metallo pesante adsorbito (mmol/L) nel sistema multi-metal quando Cd è costante. La concentrazione iniziale di ogni elemento del sistema multi-metal è in leggenda.

P concentration at the equilibrium is very low (Fig. 6 A, B, C, D, E and F), the range is about < b.d.l. to 0.6 mmol/g, whereas the amount of sorbed metals is bigger meaning a non-stoichiometric dissolution of MAP and/or P is used for the precipitation of a new phosphatic phase.

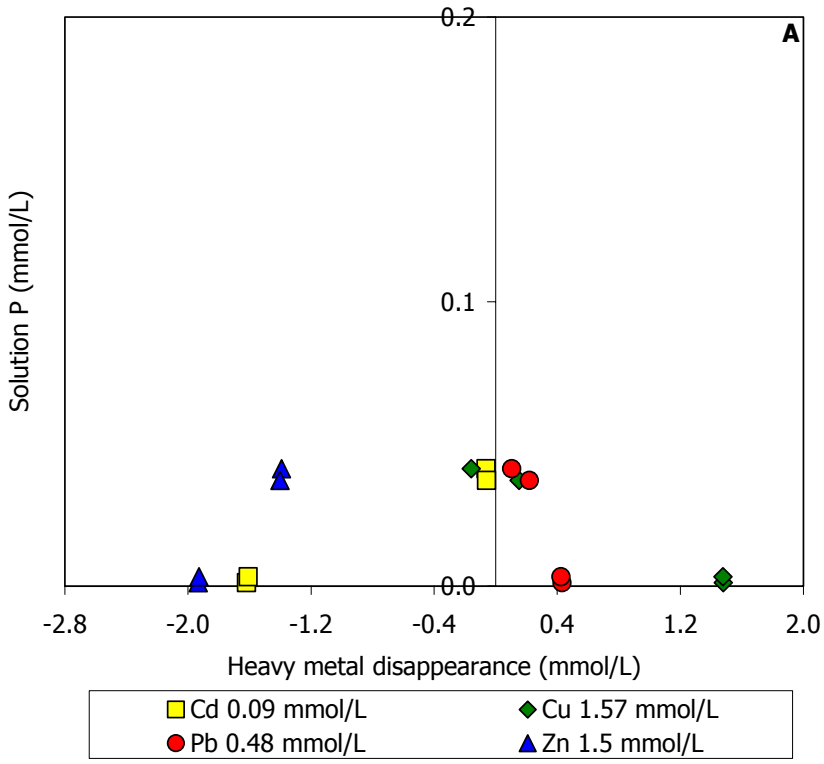

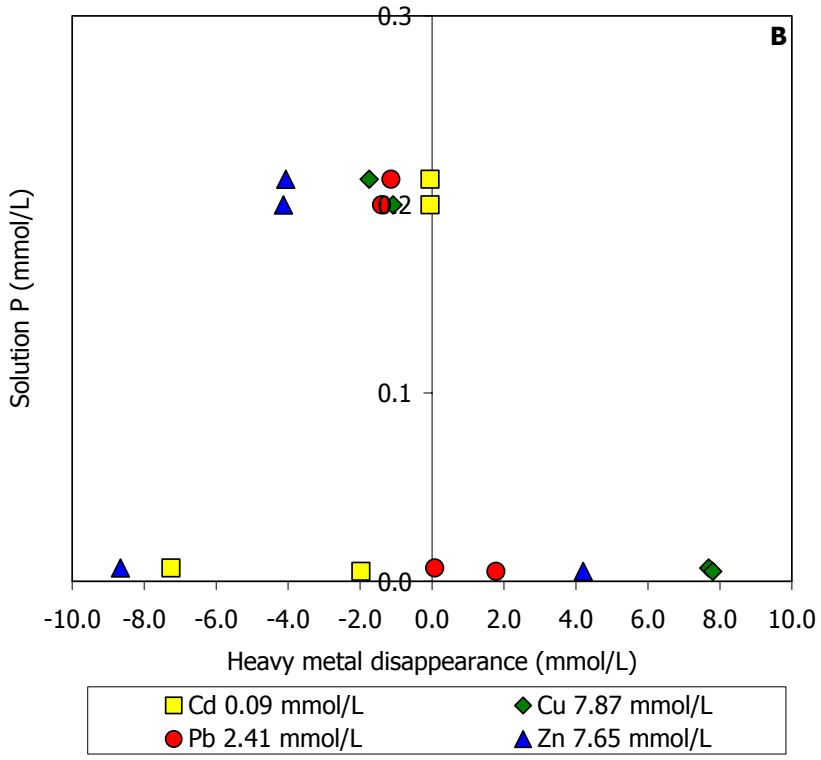
B
0.3
0.2
0.1
0.0
Solution P (mmol/L)
-10.0
-8.0
-6.0
-4.0
-2.0
0.0
2.0
4.0
6.0
8.0
10.0
Heavy metal disappearance (mmol/L)
Cd 0.09 mmol/L
Cu 7.87 mmol/L
Pb 2.41 mmol/L
Zn 7.65 mmol/L

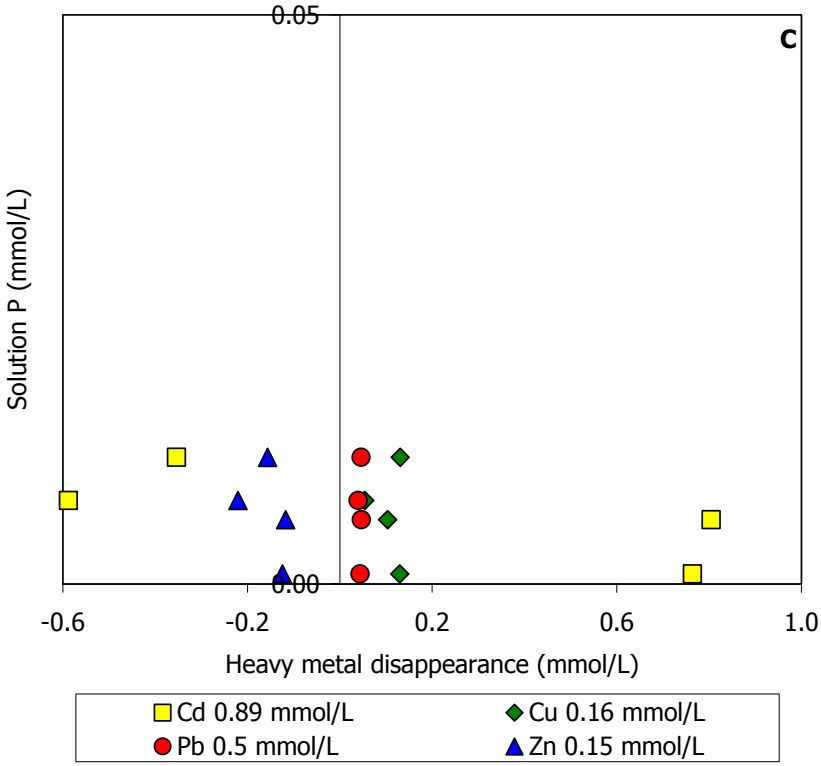
C
0.05
0.00
Solution P (mmol/L)
-0.6
-0.2
0.2
0.6
1.0
Heavy metal disappearance (mmol/L)
Cd 0.89 mmol/L
Cu 0.16 mmol/L
Pb 0.5 mmol/L
Zn 0.15 mmol/L

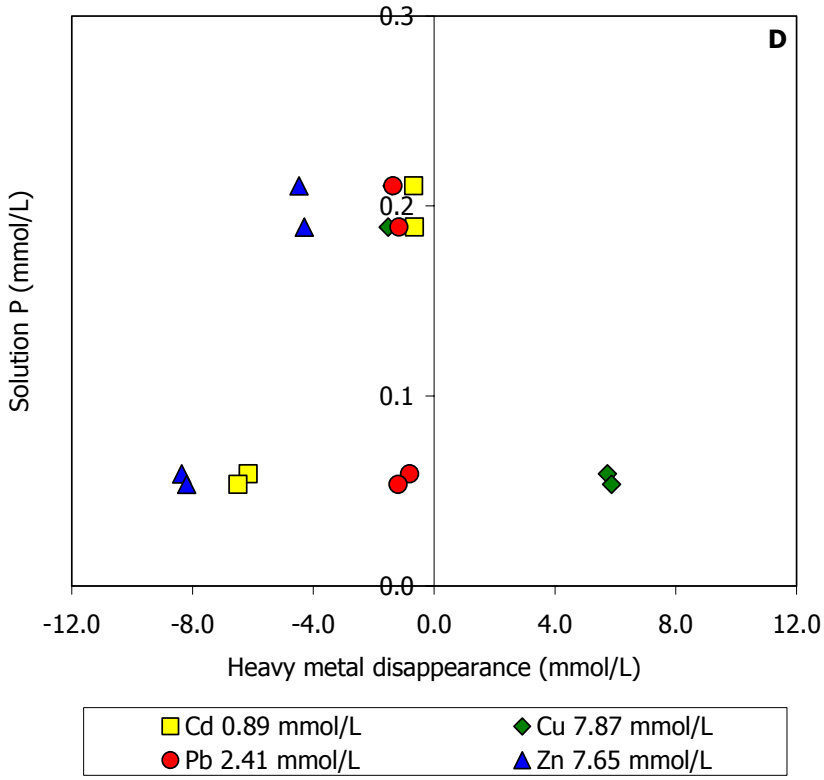
D
0.3
0.2
0.1
0.0
Solution P (mmol/L)
-12.0
-8.0
-4.0
0.0
4.0
8.0
12.0
Heavy metal disappearance (mmol/L)
Cd 0.89 mmol/L
Cu 7.87 mmol/L
Pb 2.41 mmol/L
Zn 7.65 mmol/L

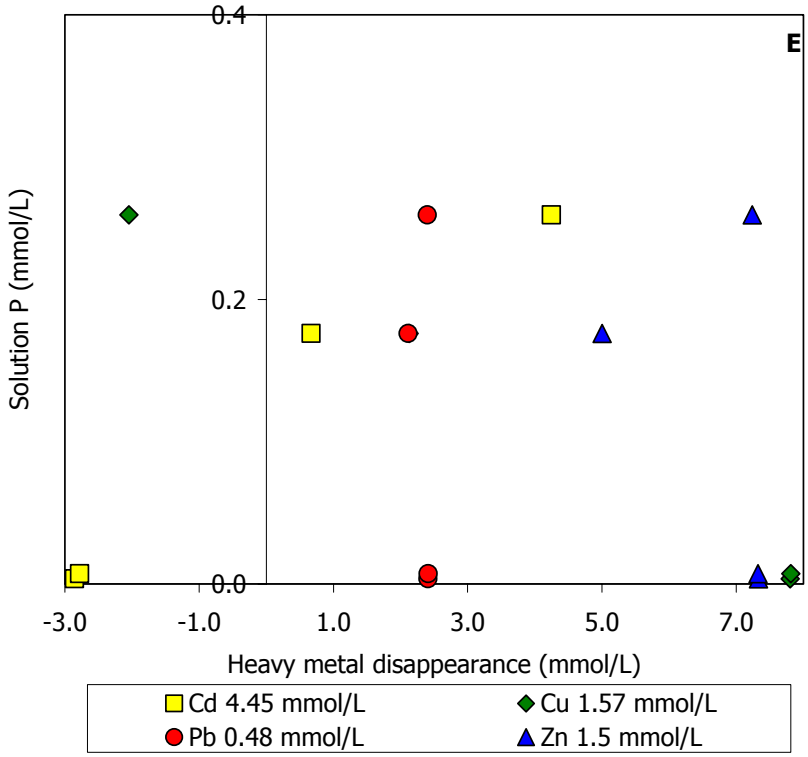
E
0.4
0.2
0.0
Solution P (mmol/L)
-3.0
-1.0
1.0
3.0
5.0
7.0
Heavy metal disappearance (mmol/L)
Cd 4.45 mmol/L
Cu 1.57 mmol/L
Pb 0.48 mmol/L
Zn 1.5 mmol/L

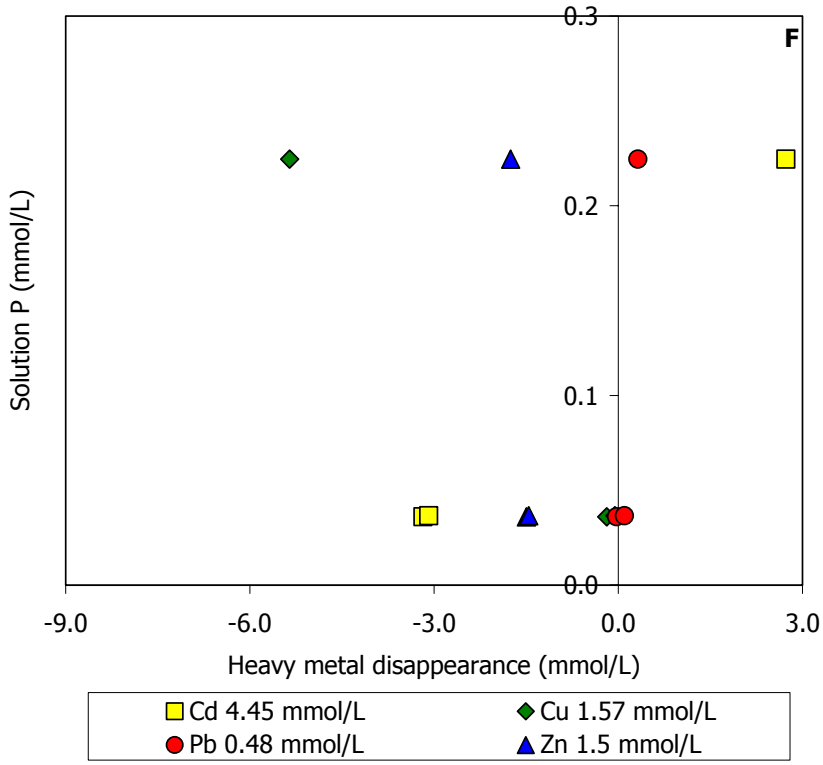

Fig. 6: Relation between P in solution (mmol/L) and the amount of disappeared heavy metals (mmol/L) sorbed on MAP surface at the equilibrium in a multi-metal system when Cd is constant. Each initial concentration of the multi-metal system is written in the legend. - Fig. 6: Relazione tra il quantitativo di P in soluzione (mmol/L) e di ciascun metallo pesante adsorbito (mmol/L) nel sistema multi-metal quando Cd è costante. La concentrazione iniziale di ogni elemento del sistema multi-metal è in leggenda.

In the Cu system (Tab. 4 and Fig. 7 A, B, C, D, E and F) the best time of immobilization is at 48h, although it seems to depend on the heavy metals initial concentration. Sometimes the heavy metals are not immobilized and this might be caused from a desorption phenomenon. For the same reasons is not possible to determine the immobilization order, the most probable order seems to be Pb > Cd > Cu >Zn.

Generally the system shows pH values which decrease for the time of 2 and 4h and increases for the other two times, in both cases the range of the values is about 0.1 – 0.7 units.

Cd = 100 mg/L	Cu = 10 mg/L	Pb = 100 mg/L	Zn = 100 mg/L
3.515	2.190	26.686	-0.656
4.272	2.880	35.438	-0.609
34.277	-7.285	30.059	-8.576
34.984	1.582	38.305	-3.601
Cd = 500 mg/L	Cu = 10 mg/L	Pb = 500 mg/L	Zn = 500 mg/L
61.049	1.881	101.832	46.316
17.687	1.742	31.188	45.870
195.612	-111.862	95.996	-6.409
184.250	-30.695	160.280	153.940
Cd = 10 mg/L	Cu = 100 mg/L	Pb = 10 mg/L	Zn = 10 mg/L
0.006	18.960	0.237	-0.585
0.005	21.872	-0.570	-0.468
-30.622	39.397	3.870	-0.319
-27.546	39.694	3.851	0.151
Cd = 500 mg/L	Cu = 100 mg/L	Pb = 500 mg/L	Zn = 500 mg/L
28.701	-53.767	44.894	44.911
36.561	20.946	69.952	12.337
158.973	-79.570	58.572	-10.613
103.119	-20.942	178.489	155.430
Cd = 10 mg/L	Cu = 500 mg/L	Pb = 10 mg/L	Zn = 10 mg/L
0.088	100.956	2.071	-0.837
0.518	101.625	3.717	-0.398
-185.623	188.834	-0.632	-20.703
-178.284	199.876	3.902	-0.288
Cd = 100 mg/L	Cu = 500 mg/L	Pb = 100 mg/L	Zn = 100 mg/L
5.450	91.096	22.783	-0.569
5.361	95.011	24.134	-0.818
-158.603	176.841	25.728	-4.457
-142.197	188.914	35.403	15.687

Table 4: Proportions of blocked heavy metals per unit mass of MAP (mg/g) for the multi-metal system when Cu is constant. – Tabella 4: Entità dell'immobilizzazione dei metalli per unità di massa di MAP (mg/g) per il sistema multi-metal con concentrazione del Cu costante.

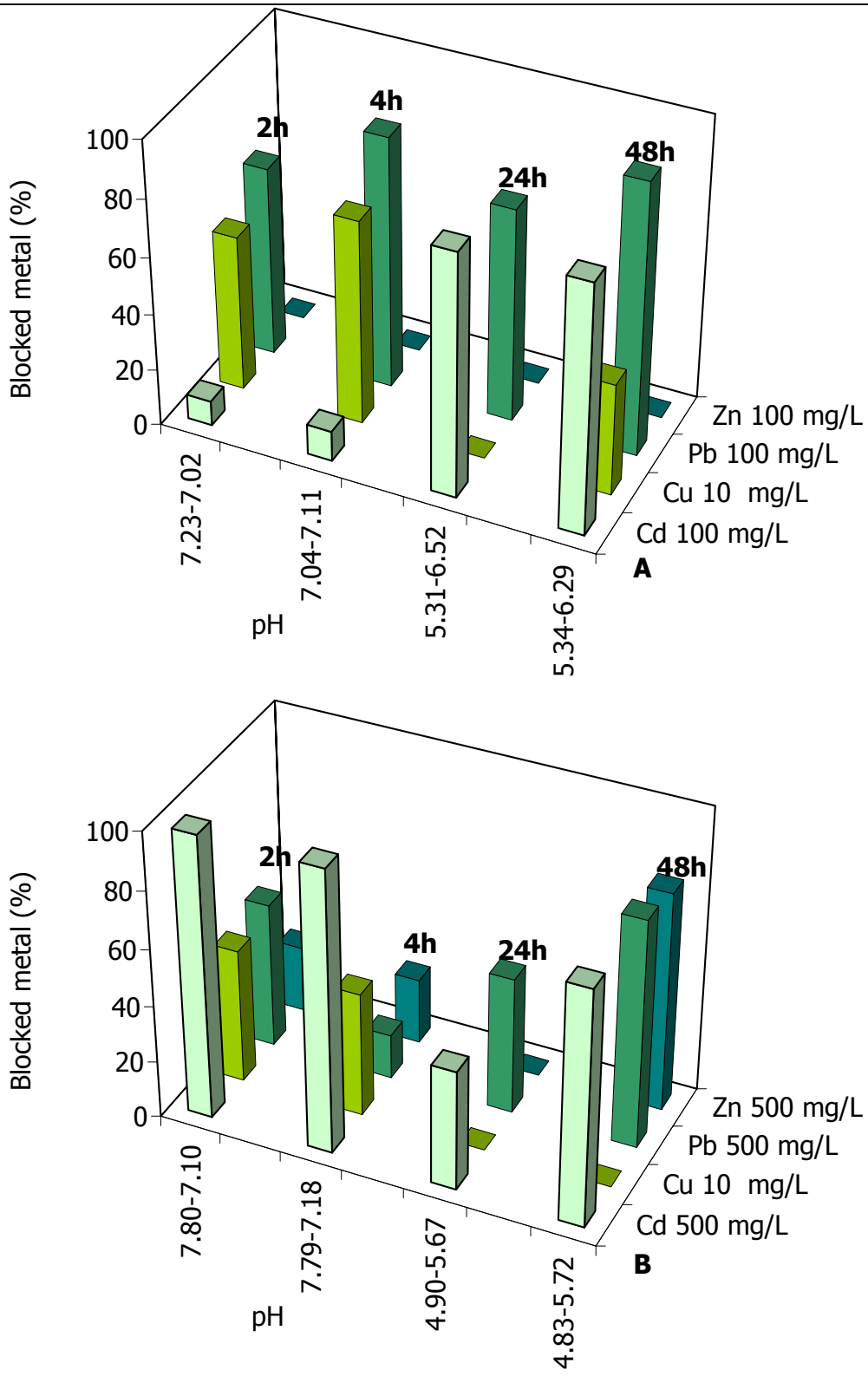
Blocked metal (%)
100
80
60
40
20
0
2h
4h
24h
48h
7.23-7.02
7.04-7.11
5.31-6.52
5.34-6.29
pH
Zn 100 mg/L
Pb 100 mg/L
Cu 10 mg/L
Cd 100 mg/L
A
Blocked metal (%)
100
80
60
40
20
0
2h
4h
24h
48h
7.80-7.10
7.79-7.18
4.90-5.67
4.83-5.72
pH
Zn 500 mg/L
Pb 500 mg/L
Cu 10 mg/L
Cd 500 mg/L
B

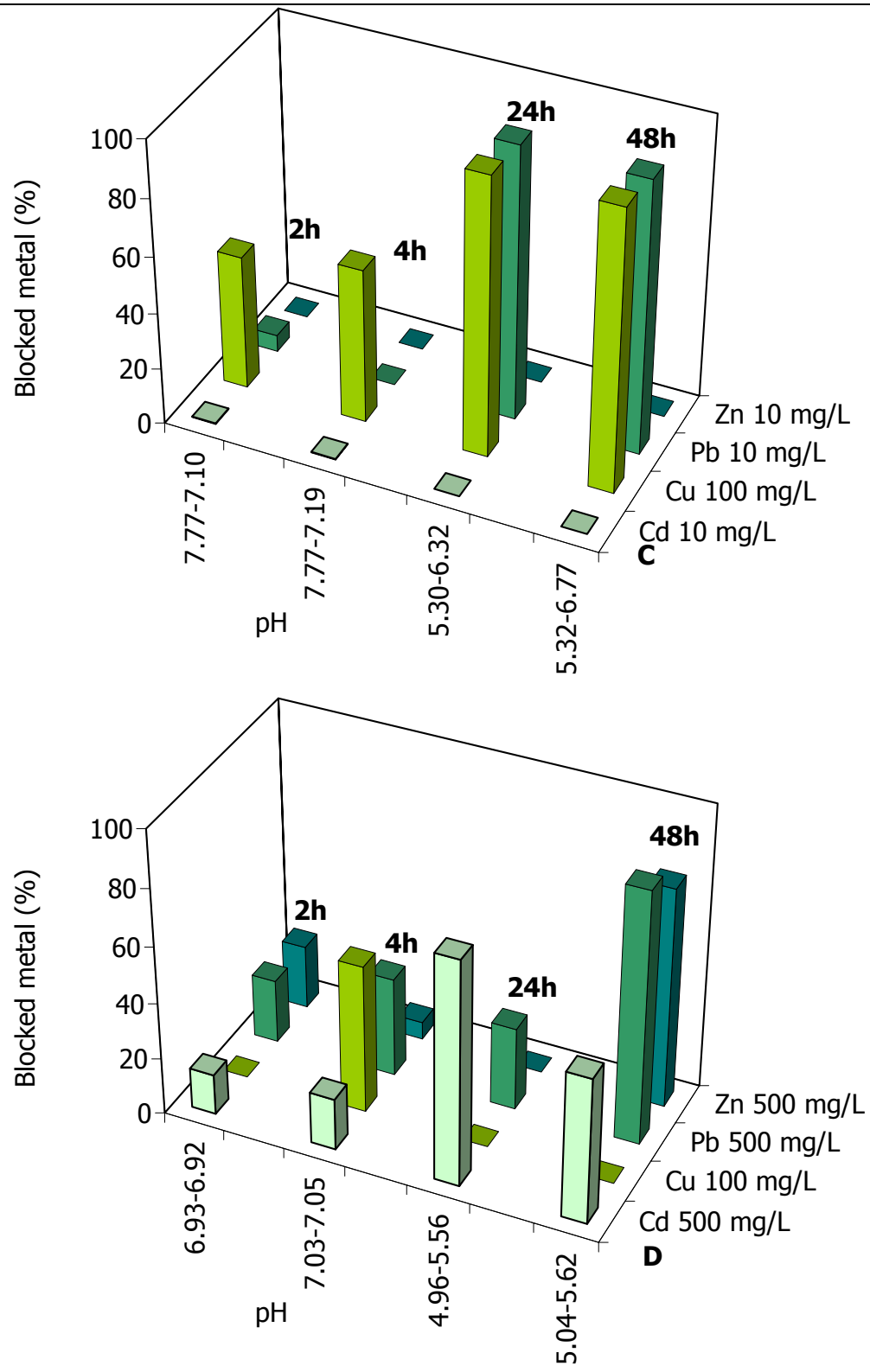
Blocked metal (%)
100
80
60
40
20
0
2h
4h
24h
48h
7.77-7.10
7.77-7.19
5.30-6.32
5.32-6.77
pH
Zn 10 mg/L
Pb 10 mg/L
Cu 100 mg/L
Cd 10 mg/L
C
Blocked metal (%)
100
80
60
40
20
0
2h
4h
24h
48h
6.93-6.92
7.03-7.05
4.96-5.56
5.04-5.62
pH
Zn 500 mg/L
Pb 500 mg/L
Cu 100 mg/L
Cd 500 mg/L
D

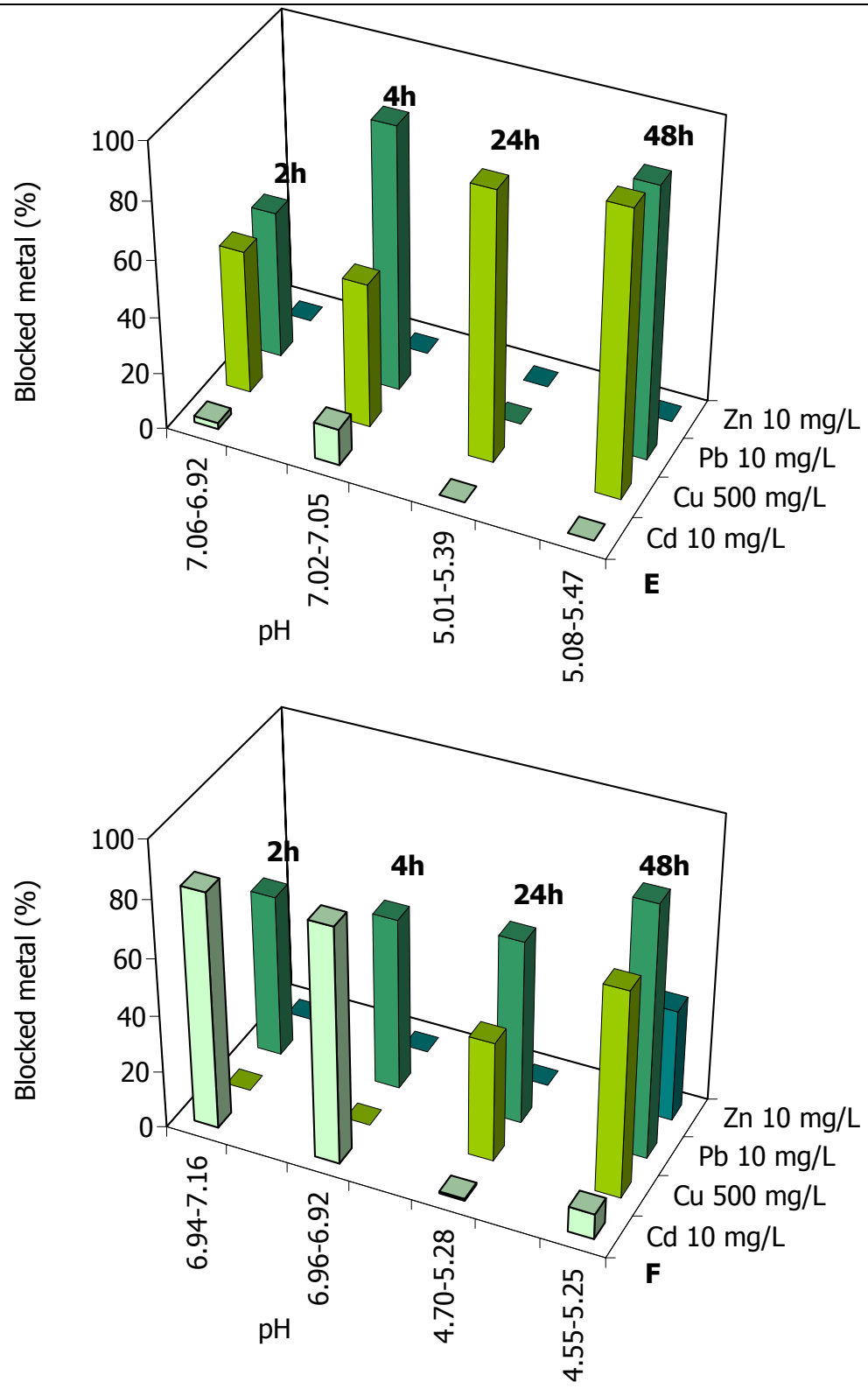

Fig. 7: Variation of the amount of blocked metal with time for the mass of MAP (1 g) in the multi-metal system where Cu is constant. Initial and final pH values are reported. – Fig. 7: Variazione delle percentuali dei metalli immobilizzati in funzione del tempo di interazione per la quantità di MAP (1 g) nel sistema multi-metal in cui Cu è l'elemento costante. Sono riportati i valori iniziali e finali del pH.

The molar ratio Q_S is < 1, > 1 or >>1 (Tab. 5), suggesting two different sorption mechanism, non-crystalline precipitation and adsorption, as in the previous system. Cu at concentration of 10 mg/L shows Q_S < 1, except for t = 24h, with values >1 and >>1. Pb at 100 mg/L has Q_S <1 and increasing the metal concentration Q_S values are>>1. Zn shows always Q_S >>1. Cd has a behaviour depending on the time, for t = 2 and 4h Q_S >> 1 and for t = 24 and 48 Q_S <1.

Increasing Cu concentration at 100 mg/L and the other three metals have a low concentration, it shows Q_S >1 for t = 2 and 4h and Q_S < 1 for t = 24 and 48h; whereas increasing the concentration of the other heavy metals (100 mg/L) Q_S >>1 as Cd, Pb and Zn.

When Cu, has a concentration of 500 mg/L, shows generally Q_S values >>1, instead Pb and Cd have a Q_S <1; Zn shows Q_S <1 for a low concentration and increasing its concentration Q_S has values bigger than one.

Cd = 100 mg/L	Cu = 10 mg/L	Pb = 100 mg/L	Zn = 100 mg/L
2.420	0.212	0.479	4.637
1.609	0.089	0.111	3.144
0.518	1.808	0.488	7.564
0.365	0.312	0.067	5.460
Cd = 500 mg/L	Cu = 10 mg/L	Pb = 500 mg/L	Zn = 500 mg/L
8.941	0.241	3.427	17.004
8.105	0.178	4.072	11.781
0.489	22.830	6.285	39.531
1.198	4.669	1.639	6.024
Cd = 10 mg/L	Cu = 100 mg/L	Pb = 10 mg/L	Zn = 10 mg/L
0.213	1.981	0.109	0.420
0.213	1.706	0.132	0.409
5.191	0.160	0.011	1.113
3.738	0.064	0.010	0.784
Cd = 500 mg/L	Cu = 100 mg/L	Pb = 500 mg/L	Zn = 500 mg/L
10.331	10.004	5.075	16.082
7.696	1.587	3.322	15.193
2.731	14.080	5.108	24.105
6.624	7.371	0.798	5.239
Cd = 10 mg/L	Cu = 500 mg/L	Pb = 10 mg/L	Zn = 10 mg/L
0.309	13.826	0.083	0.656
0.149	7.425	0.007	0.323
17.410	1.814	0.231	3.900
15.616	0.019	0.005	0.632
Cd = 100 mg/L	Cu = 500 mg/L	Pb = 100 mg/L	Zn = 100 mg/L
1.803	10.053	0.487	3.640
1.658	8.890	0.412	3.359
21.738	4.484	0.848	8.366
16.285	1.753	0.223	3.736

Table 5: Q_S values for the multi - metal systems when Cu has a constant concentration. Tabella 5: Valori di Q_S per i sistemi multi-metal nei quali la concentrazione di Cu è stata mantenuta costante.

In this system it was not possible to determine the sorption isotherms (Fig. 8 A) because each metal shows negative values, the only exception are Pb and Zn at 48h with isotherm of L type and 2 subtype.

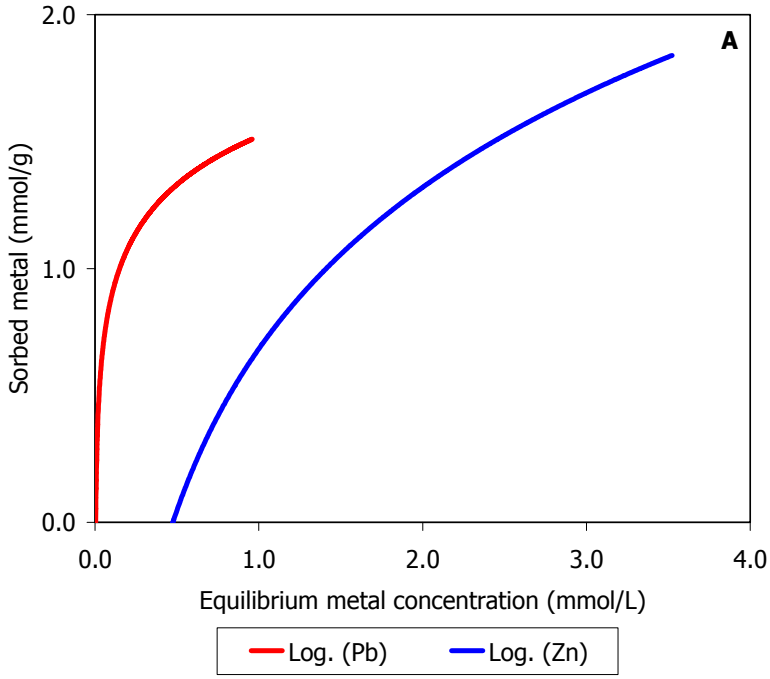

Fig. 8: Sorption isotherms for the multi-metal system where Cu is constant and vs. 1 g MAP. Relation between the metal sorbed (mmol/g) and the final concentration (mmol/L) in solution. A: t = 48h. – Fig. 8: Curve isotermiche per il sistema multi-metal in cui Cu è costante e vs. 1 g di MAP. Relazione tra il metallo assorbito (mmol/g) e la concentrazione finale (mmol/L) in soluzione. A: t = 48h.

Ca concentration at the equilibrium ranges from 0.4 to 1.2 mmol/g (Fig. 9 A, B, C, D, E and F), and i is almost proportional to the sorbed heavy metals concentration. Therefore, it is possible to infer a stoichiometric dissolution of MAP as in the previous system. The desorbed Ca amount is not depending on the interaction time and probably the equilibrium is achieved in a brief time (2h).

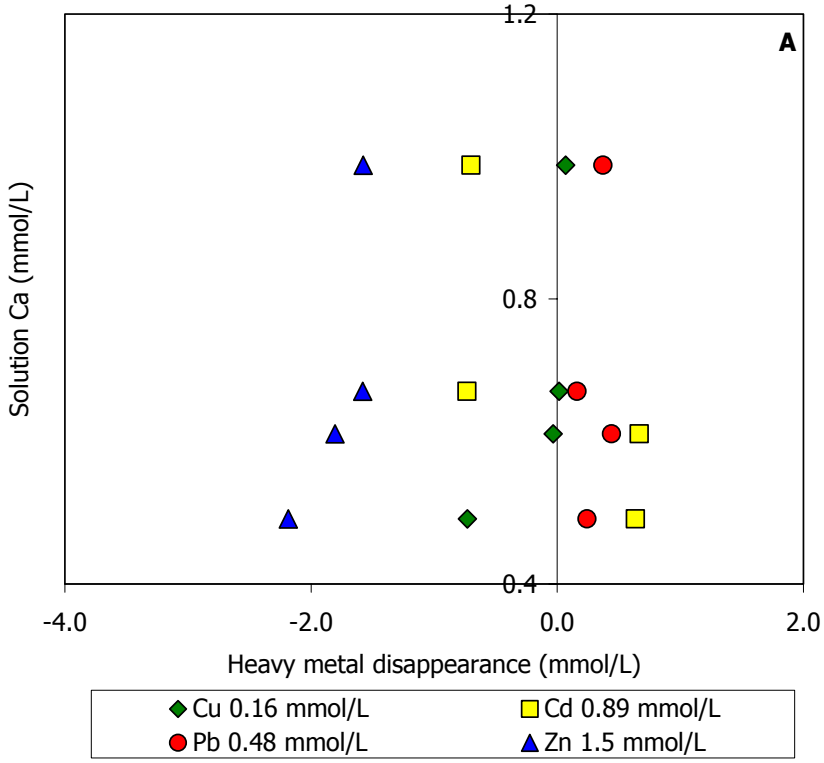
A
1.2
0.8
0.4
Solution Ca (mmol/L)
-4.0
-2.0
0.0
2.0
Heavy metal disappearance (mmol/L)
Cu 0.16 mmol/L
Cd 0.89 mmol/L
Pb 0.48 mmol/L
Zn 1.5 mmol/L

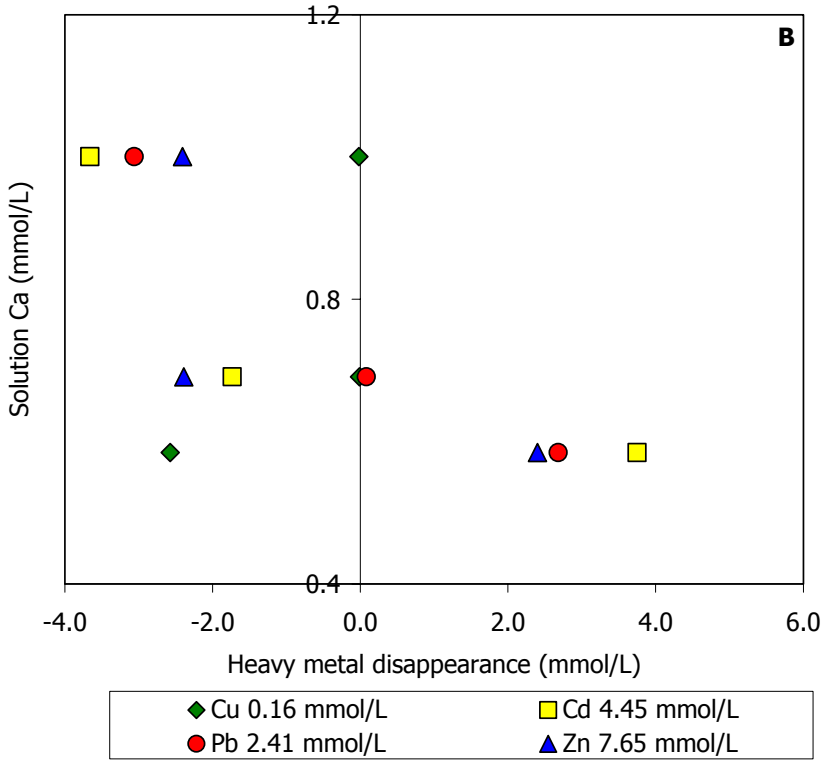
B
1.2
0.8
0.4
Solution Ca (mmol/L)
-4.0
-2.0
0.0
2.0
4.0
6.0
Heavy metal disappearance (mmol/L)
Cu 0.16 mmol/L
Cd 4.45 mmol/L
Pb 2.41 mmol/L
Zn 7.65 mmol/L

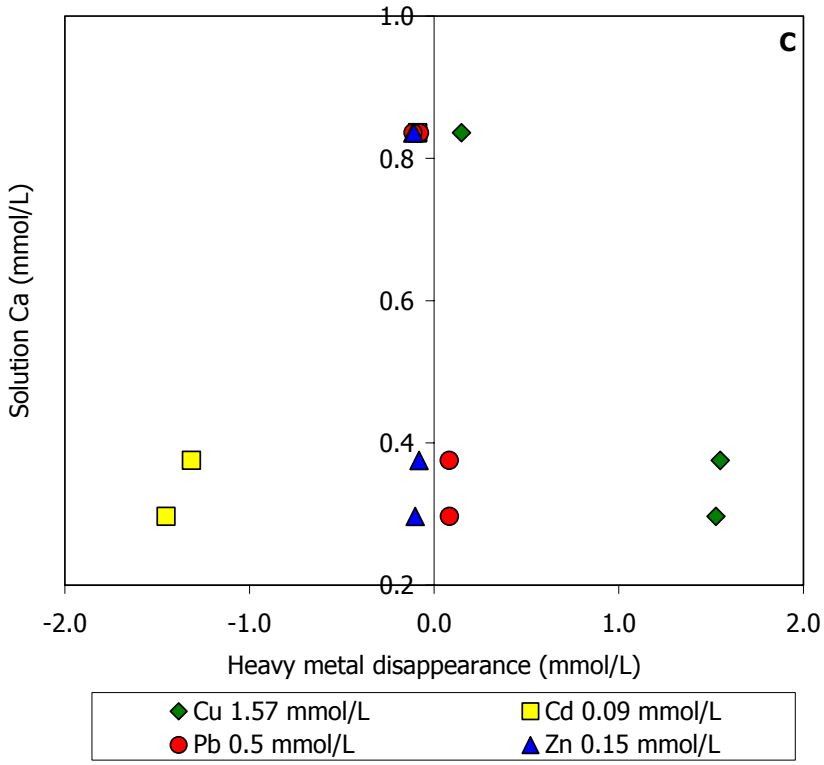
C
1.0
0.8
0.6
0.4
0.2
Solution Ca (mmol/L)
-2.0
-1.0
0.0
1.0
2.0
Heavy metal disappearance (mmol/L)
Cu 1.57 mmol/L
Cd 0.09 mmol/L
Pb 0.5 mmol/L
Zn 0.15 mmol/L

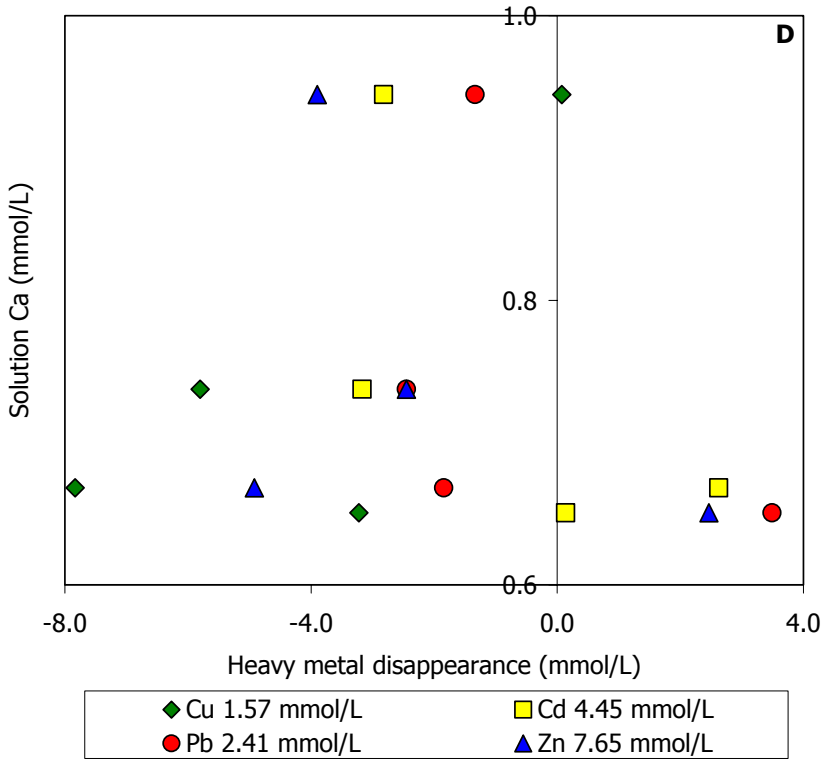
D
1.0
0.8
0.6
Solution Ca (mmol/L)
-8.0
-4.0
0.0
4.0
Heavy metal disappearance (mmol/L)
Cu 1.57 mmol/L
Cd 4.45 mmol/L
Pb 2.41 mmol/L
Zn 7.65 mmol/L

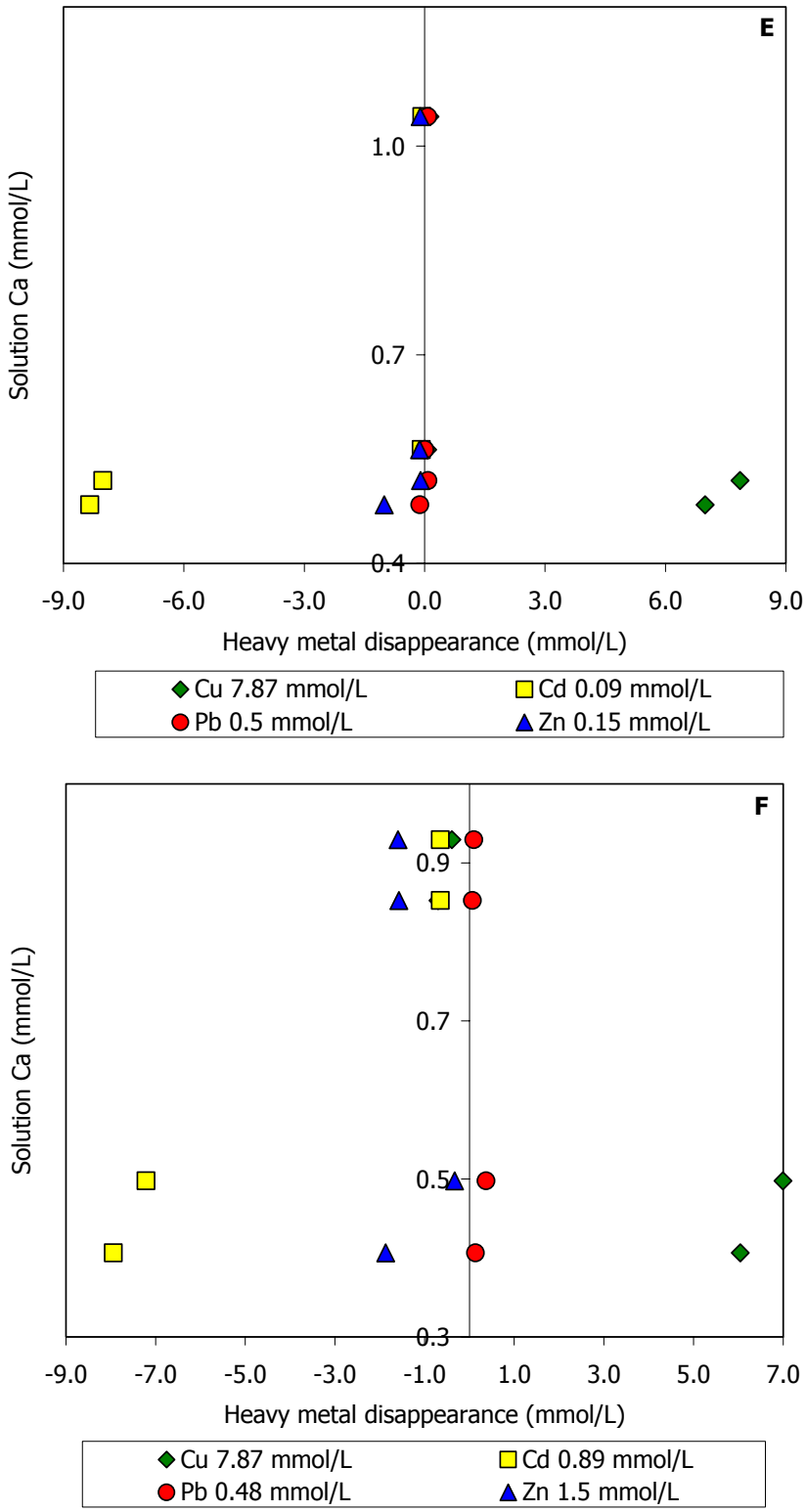

Fig. 9: Relation between Ca in solution (mmol/L) and the amount of heavy metals disappeared (mmol/L) sorbed on MAP surface at the equilibrium in a multi-metal system when Cu is constant. Each initial concentration of the multi-metal system is written in the legend. - Fig. 9: Relazione tra il quantitativo di Ca in

soluzione (mmol/L) e di ciascun metallo pesante adsorbito (mmol/L) nel sistema multi-metal quando Cu è costante. La concentrazione iniziale di ogni elemento del sistema multi-metal è in leggenda.

P concentration ranges from < b.d.l. to 0.3 mmol/g (Fig. 10 A, B, C, D, E and F). These low P values suggest a non-stoichiometric dissolution of MAP and P deposition during the precipitation of the non-crystalline phase.

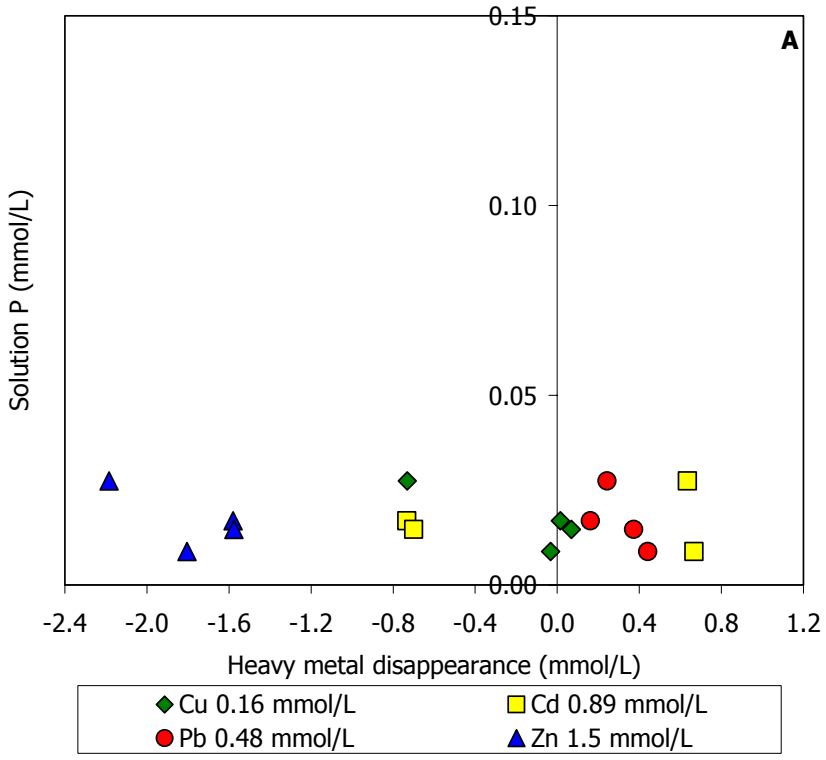

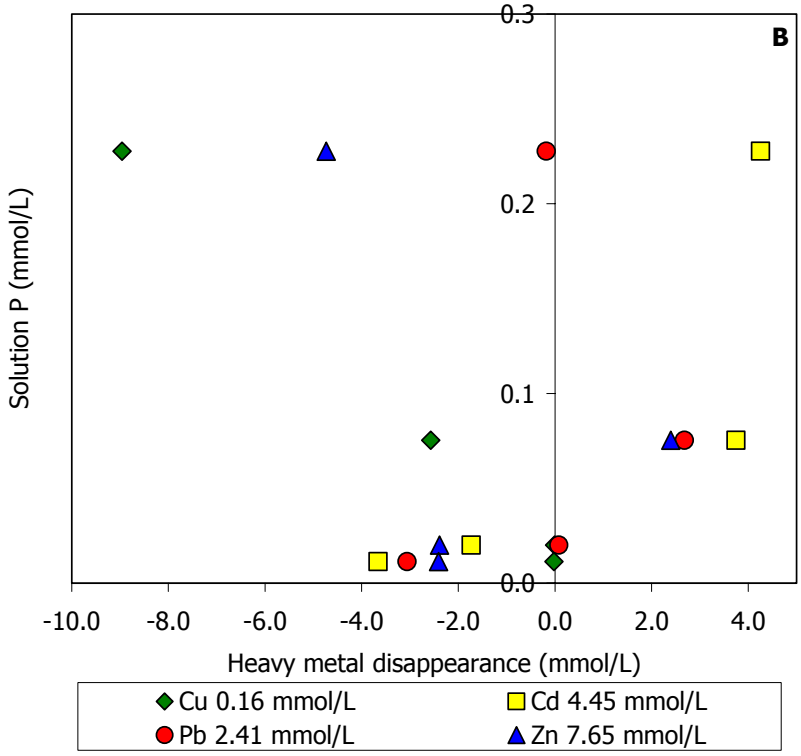
B
0.3
0.2
0.1
0.0
Solution P (mmol/L)
-10.0
-8.0
-6.0
-4.0
-2.0
0.0
2.0
4.0
Heavy metal disappearance (mmol/L)
Cu 0.16 mmol/L
Cd 4.45 mmol/L
Pb 2.41 mmol/L
Zn 7.65 mmol/L

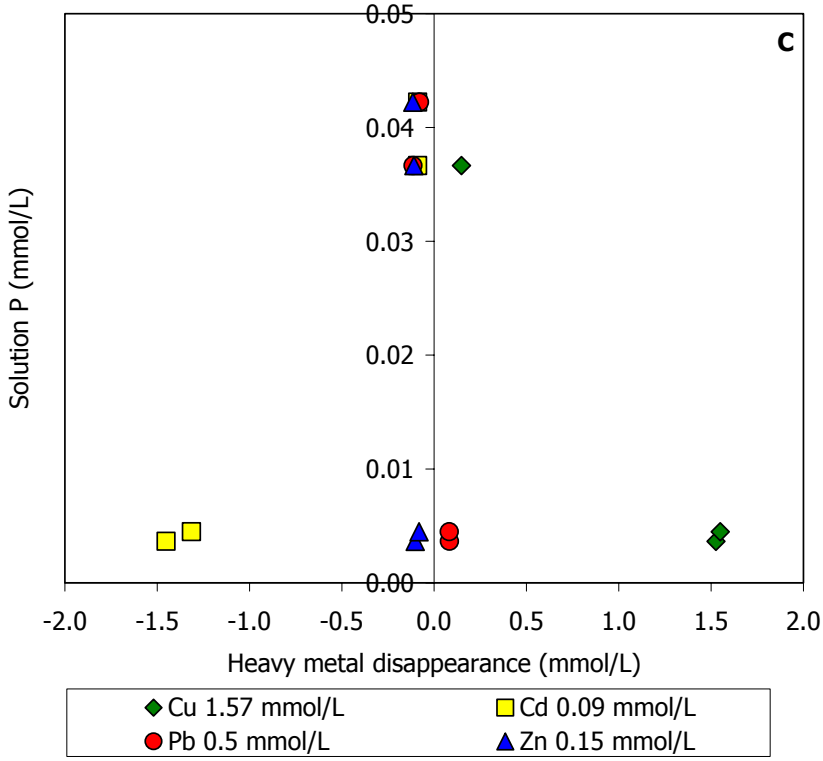
C
0.05
0.04
0.03
0.02
0.01
0.00
Solution P (mmol/L)
-2.0
-1.5
-1.0
-0.5
0.0
0.5
1.0
1.5
2.0
Heavy metal disappearance (mmol/L)
Cu 1.57 mmol/L
Cd 0.09 mmol/L
Pb 0.5 mmol/L
Zn 0.15 mmol/L

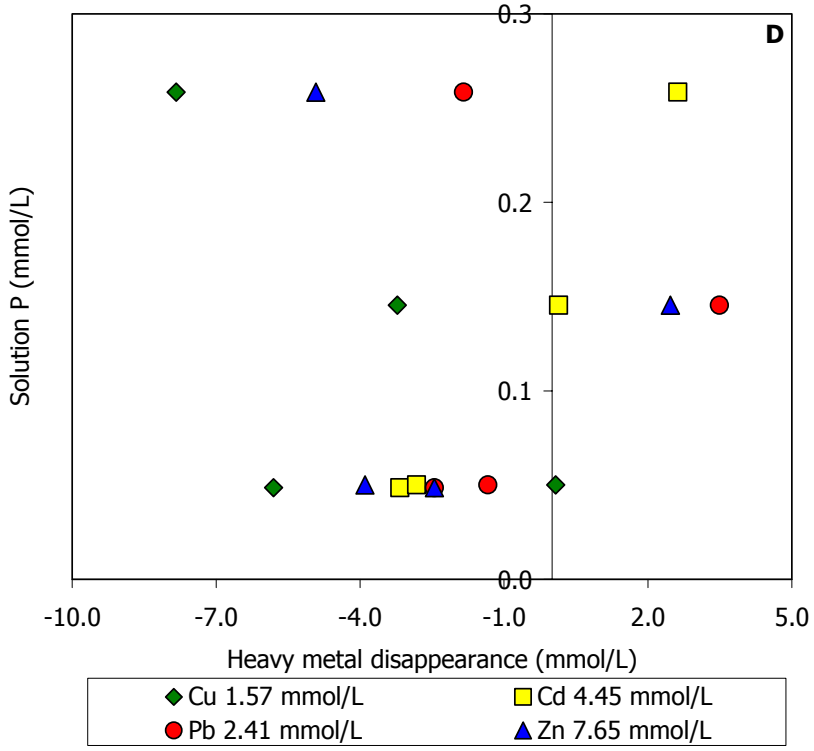
D
0.3
0.2
0.1
0.0
Solution P (mmol/L)
-10.0
-7.0
-4.0
-1.0
2.0
5.0
Heavy metal disappearance (mmol/L)
Cu 1.57 mmol/L
Cd 4.45 mmol/L
Pb 2.41 mmol/L
Zn 7.65 mmol/L

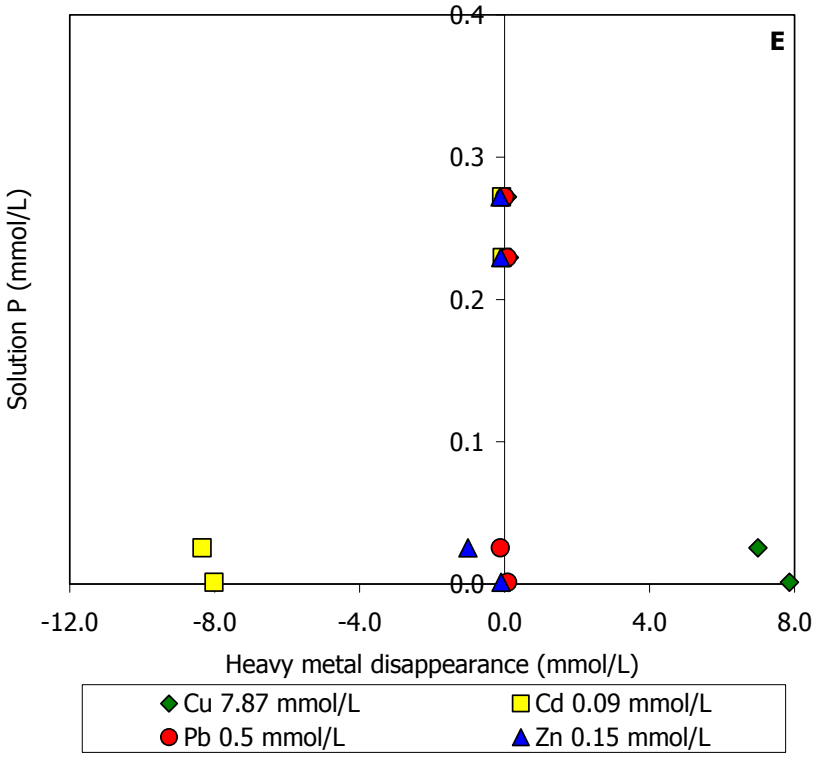
E
0.4
0.3
0.2
0.1
0.0
Solution P (mmol/L)
-12.0
-8.0
-4.0
0.0
4.0
8.0
Heavy metal disappearance (mmol/L)
Cu 7.87 mmol/L
Cd 0.09 mmol/L
Pb 0.5 mmol/L
Zn 0.15 mmol/L

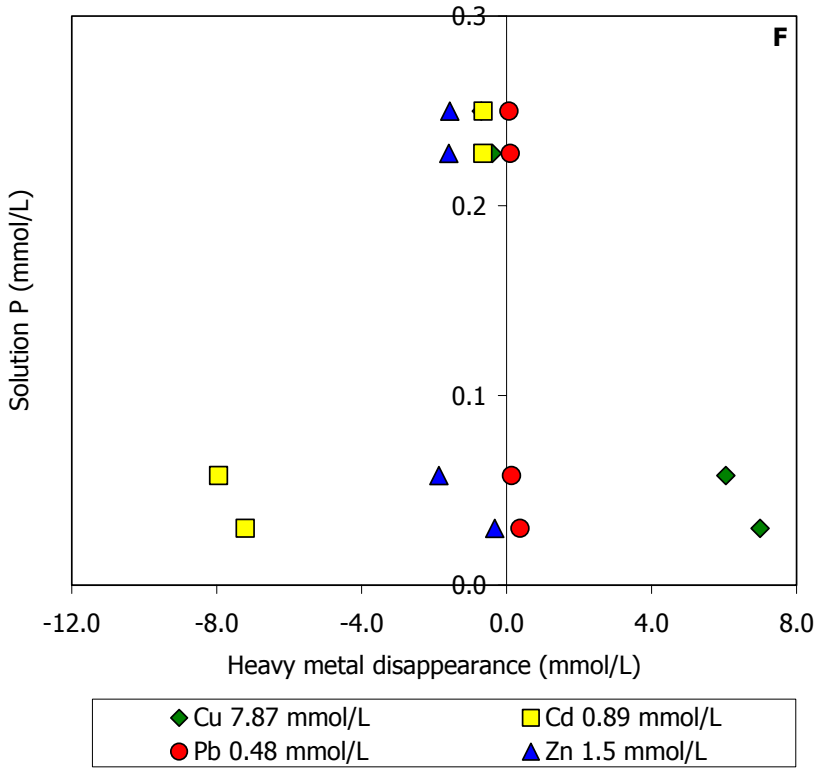

Fig. 10: Relation between P in solution (mmol/L) and the amount of disappeared heavy metals (mmol/L) sorbed on MAP surface at the equilibrium in a multi-metal system when Cu is constant. Each initial concentration of the multi-metal system is written in the legend. - Fig. 10: Relazione tra il quantitativo di P in soluzione (mmol/L) e di ciascun metallo pesante adsorbito (mmol/L) nel sistema multi-metal quando Cu è costante. La concentrazione iniziale di ogni elemento del sistema multi-metal è in leggenda.

In the Pb system (Tab. 6 and Fig. 11 A, B, C, D, E, F, G, H and I) the best immobilization time is generally at 24h and 48h, with only one exception when the concentration of the four metal is 100 mg/L. Two order of immobilization are distinguishable with the increase of the concentration: Pb > Cu > Cd > Zn and Cu > Pb > Zn > Cd. Unfortunately, Cd and Zn are sometimes not well immobilized compared to Cu and Pb. pH values decrease for the firsts two interaction time (2 and 4h) and then always increase after the interaction; the difference between the initial and the final value is from 0.1 – 2 units.

Cd = 10 mg/L	Cu = 10 mg/L	Pb = 10 mg/L	Zn = 10 mg/L
2.097	3.699	3.958	0.860
3.273	3.980	3.832	2.399
3.572	3.993	3.947	3.203
3.883	3.996	3.961	3.878
Cd = 100 mg/L	Cu = 100 mg/L	Pb = 10 mg/L	Zn = 100 mg/L
5.567	20.256	3.386	-2.689
4.851	25.743	3.255	-3.344
2.325	35.350	3.913	-1.569
38.935	38.935	3.987	0.436
Cd = 500 mg/L	Cu = 500 mg/L	Pb = 10 mg/L	Zn = 500 mg/L
44.959	69.495	1.350	-3.497
50.872	95.493	1.673	-0.575
31.145	75.780	3.754	38.652
33.176	79.731	3.935	39.911
Cd = 10 mg/L	Cu = 10 mg/L	Pb = 100 mg/L	Zn = 10 mg/L
0.024	1.871	33.712	-0.469
-0.002	2.090	35.478	-0.582
0.412	2.569	38.400	-0.648
1.236	3.499	39.728	-0.508
Cd = 100 mg/L	Cu = 100 mg/L	Pb = 100 mg/L	Zn = 100 mg/L
1.749	15.606	19.306	-5.930
2.323	18.539	26.248	-5.728
-0.479	36.977	38.400	-2.956
-36.755	-5.495	-30.869	-21.720
Cd = 500 mg/L	Cu = 500 mg/L	Pb = 100 mg/L	Zn = 500 mg/L
21.169	58.268	4.532	-6.716
82.192	111.824	32.478	-1.085
31.960	103.385	28.920	152.593
32.519	130.609	33.766	152.811
Cd = 10 mg/L	Cu = 10 mg/L	Pb = 500 mg/L	Zn = 10 mg/L
-0.923	1.380	34.687	-0.721
-0.909	1.498	58.614	-0.818
-0.737	1.229	55.142	2.913
-0.721	1.508	75.890	2.913
Cd = 100 mg/L	Cu = 100 mg/L	Pb = 500 mg/L	Zn = 100 mg/L
4.682	16.312	41.600	-1.366
6.818	17.709	76.636	0.512
17.679	25.413	73.653	34.322
0.081	13.519	71.632	29.735
Cd = 500 mg/L	Cu = 500 mg/L	Pb = 500 mg/L	Zn = 100 mg/L
65.085	91.473	35.843	23.628
70.458	110.297	116.991	24.498
91.342	163.086	102.661	169.624
25.643	139.557	105.054	151.255

Table 6: Efficiency values for the multi - metal system when Pb has a constant concentration.

Tabella 6: Valori dell'efficienza nell'immobilizzare i metalli pesanti per il sistema multi-metal in cui il Pb mantiene costante le concentrazione.

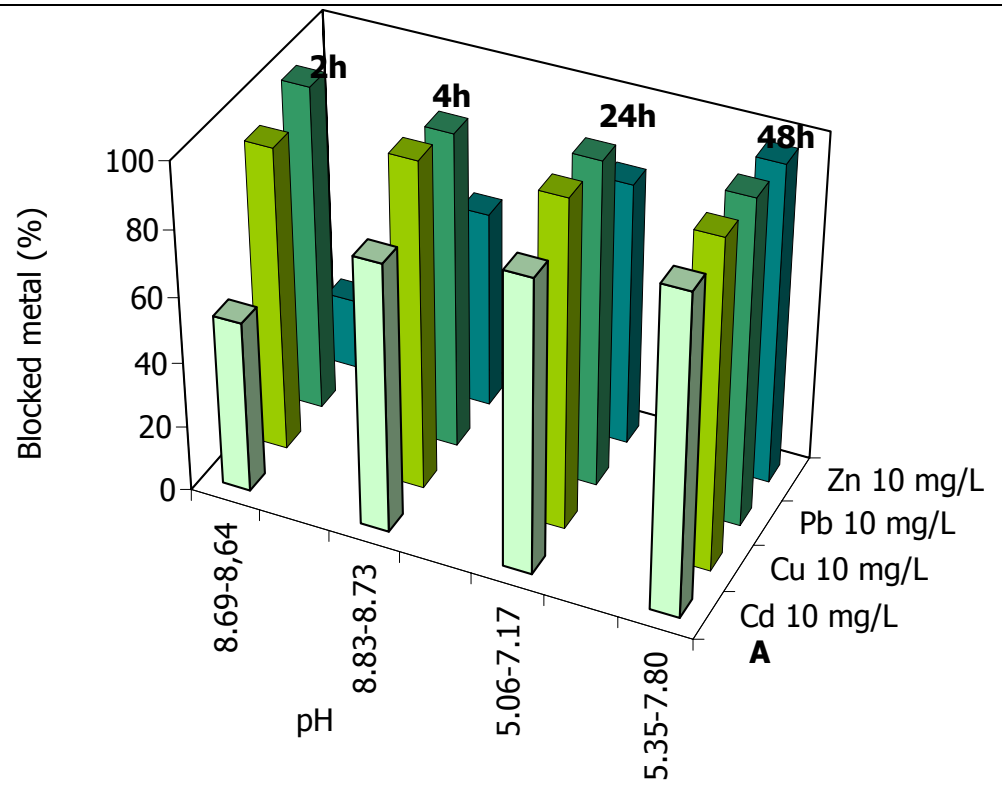
2h
4h
24h
48h
Blocked metal (%)
100
80
60
40
20
0
8.69-8,64
8.83-8.73
5.06-7.17
5.35-7.80
pH
Zn 10 mg/L
Pb 10 mg/L
Cu 10 mg/L
Cd 10 mg/L
A

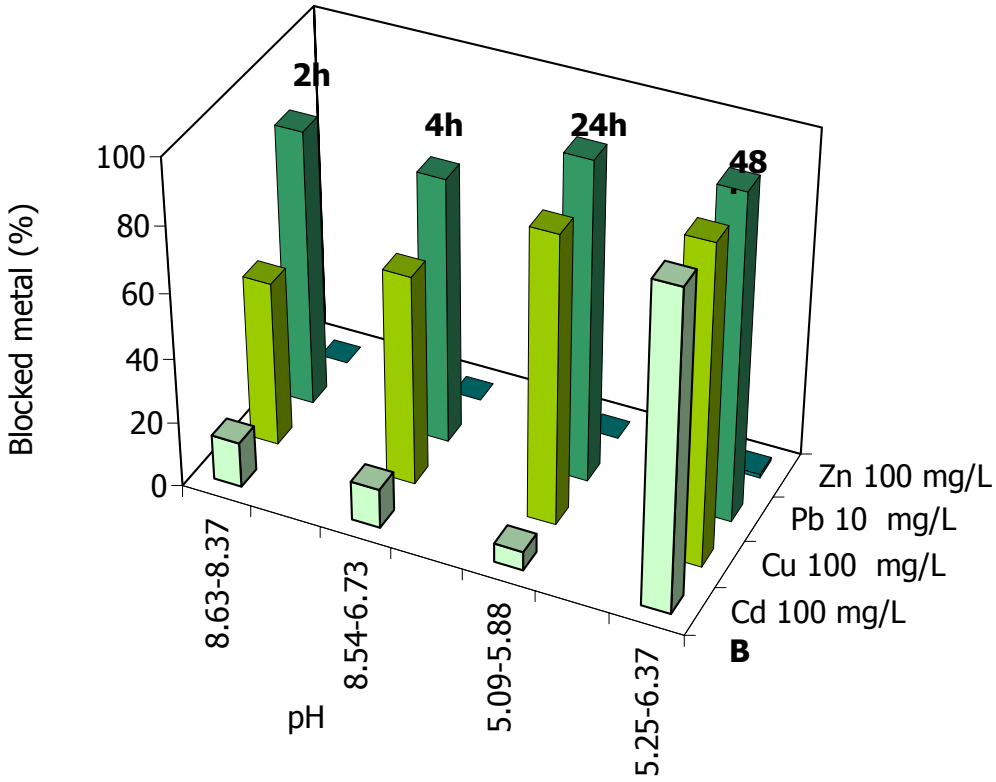
2h
4h
24h
48
Blocked metal (%)
100
80
60
40
20
0
8.63-8.37
8.54-6.73
5.09-5.88
5.25-6.37
pH
Zn 100 mg/L
Pb 10 mg/L
Cu 100 mg/L
Cd 100 mg/L
B

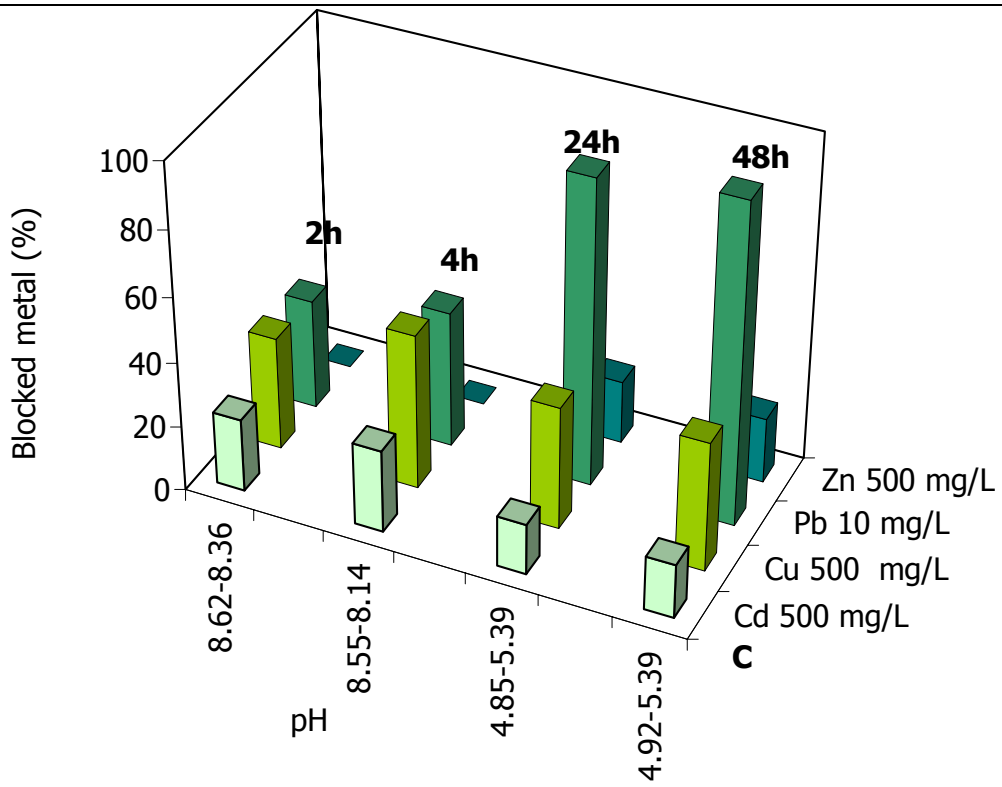
Blocked metal (%)
100
80
60
40
20
0
2h
4h
24h
48h
8.62-8.36
8.55-8.14
4.85-5.39
4.92-5.39
pH
Zn 500 mg/L
Pb 10 mg/L
Cu 500 mg/L
Cd 500 mg/L
C

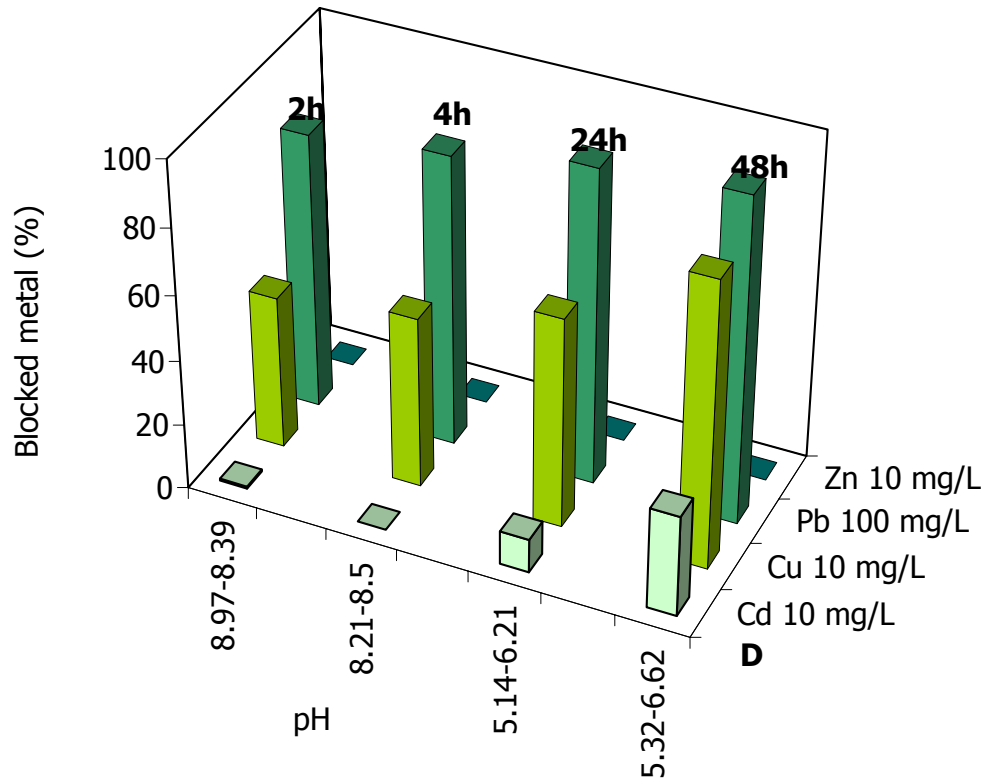
Blocked metal (%)
100
80
60
40
20
0
2h
4h
24h
48h
8.97-8.39
8.21-8.5
5.14-6.21
5.32-6.62
pH
Zn 10 mg/L
Pb 100 mg/L
Cu 10 mg/L
Cd 10 mg/L
D

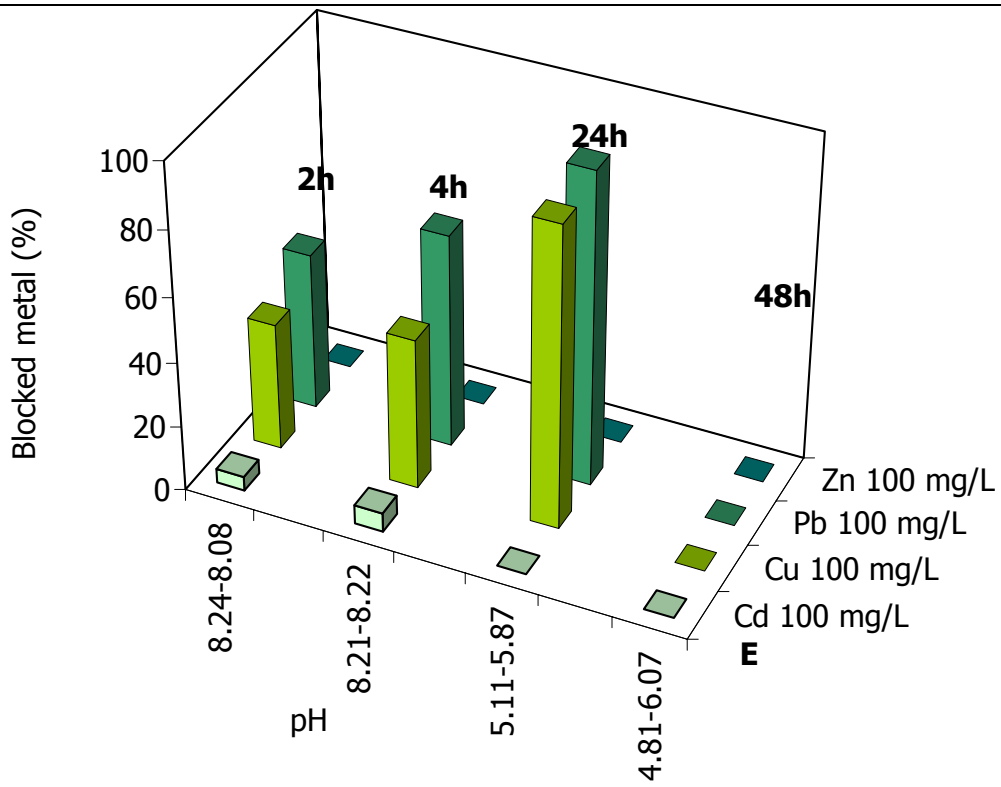
Blocked metal (%)
100
80
60
40
20
0
2h
4h
24h
48h
8.24-8.08
8.21-8.22
5.11-5.87
4.81-6.07
pH
Zn 100 mg/L
Pb 100 mg/L
Cu 100 mg/L
Cd 100 mg/L
E

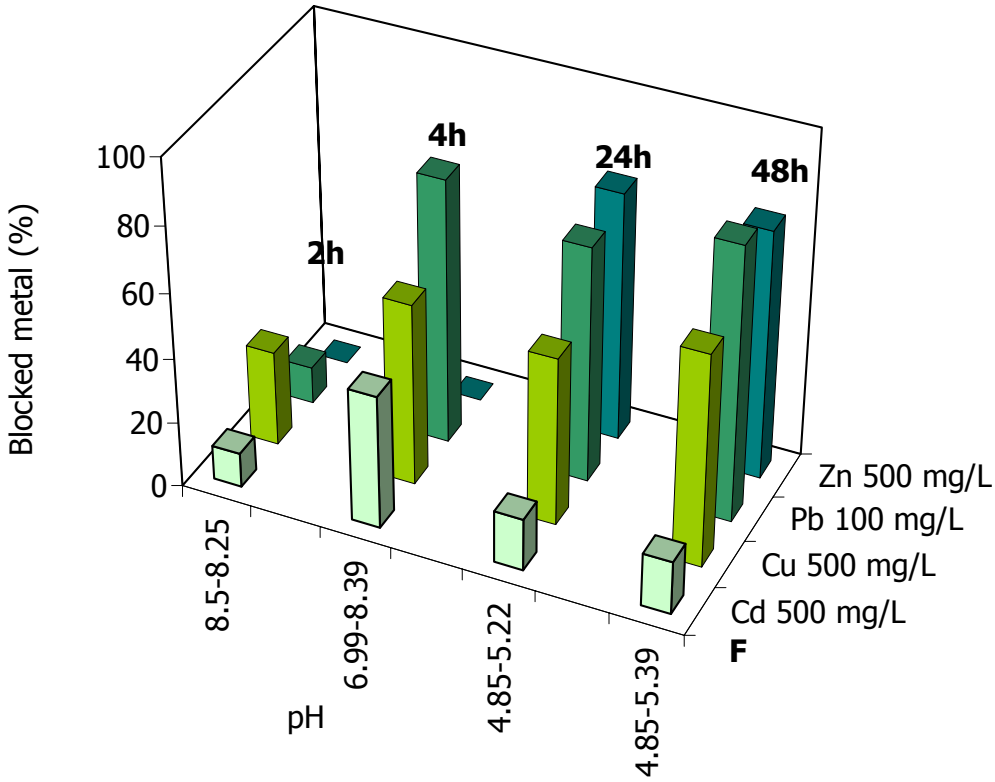
Blocked metal (%)
100
80
60
40
20
0
2h
4h
24h
48h
8.5-8.25
6.99-8.39
4.85-5.22
4.85-5.39
pH
Zn 500 mg/L
Pb 100 mg/L
Cu 500 mg/L
Cd 500 mg/L
F

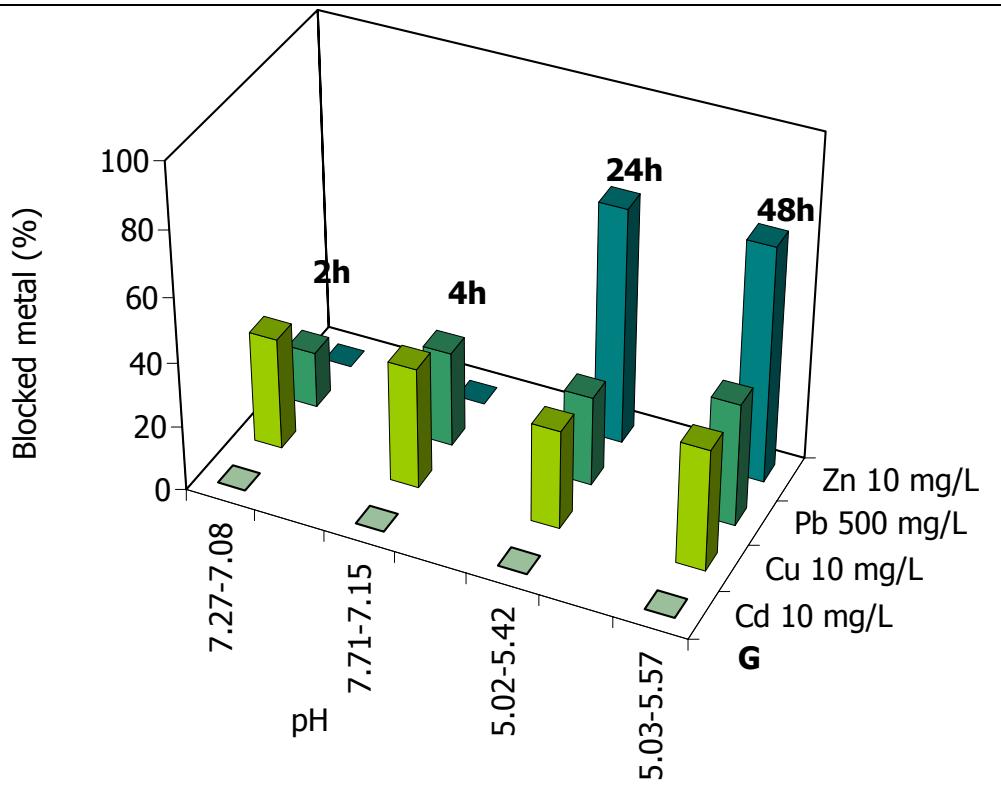
Blocked metal (%)
100
80
60
40
20
0
2h
4h
24h
48h
7.27-7.08
7.71-7.15
5.02-5.42
5.03-5.57
pH
Zn 10 mg/L
Pb 500 mg/L
Cu 10 mg/L
Cd 10 mg/L
G

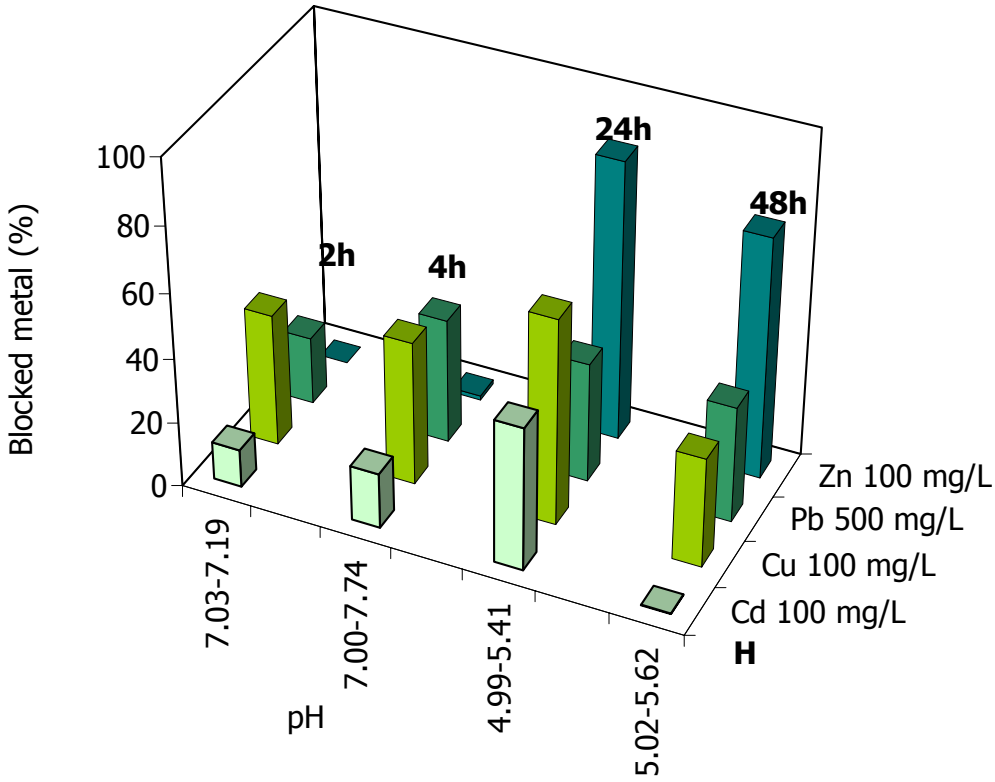
Blocked metal (%)
100
80
60
40
20
0
2h
4h
24h
48h
7.03-7.19
7.00-7.74
4.99-5.41
5.02-5.62
pH
Zn 100 mg/L
Pb 500 mg/L
Cu 100 mg/L
Cd 100 mg/L
H

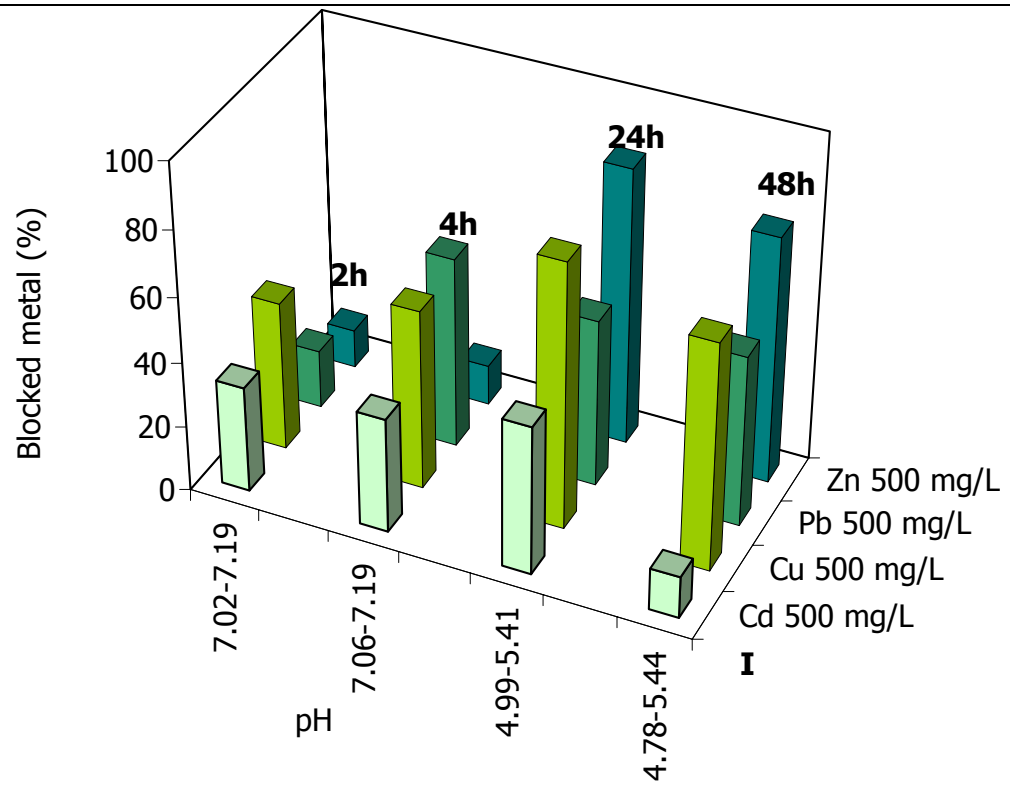

Fig. 11: Variation of the amount of blocked metal with time for the mass of MAP (1 g) in the multi-metal system where Pb is constant. – Fig. 11: Variazione delle percentuali dei metalli immobilizzati in funzione del tempo di interazione per la quantità di MAP (1 g) nel sistema multi-metal in cui Pb è l'elemento costante.

The molar ratio Q_S shows values< 1 when the concentration of the four metals is 10 mg/L (Tab. 7); increasing the concentration of the other three metals to 100 and 500 mg/L, Pb maintains the same molar ratio and Zn shows values >> 1 as Cd and Cu at the higher concentration, whereas Cd and Cu at low concentration have Q_S > 1 for t = 2 and 4h and then it decreases to values < 1. When Pb concentration is 100 mg/L and 10 mg/L for the other heavy metals, Q_S values are lower than 1. When heavy metals concentration is 100 mg/L, Pb shows the same values as before, whereas Cd, Cu and Zn show Q_S > 1. Increasing the concentration of Cd, Cu and Zn to 500 mg/L, for these metals Q_S increases to values >> 1 and Pb shows a Q_S < 1.

Increasing the concentration of Pb to 500 mg/L, Q_S values are >> 1, excepting when the four heavy metals have the highest concentration, in this case Q_S > 1 and for the other three metals Q_S >> 1. When Cd, Cu and Zn concentration is 10 mg/L they have Q_S < 1 and when their concentration is 100 mg/L, they generally have a Q_S> 1.

Cd = 10 mg/L	Cu = 10 mg/L	Pb = 10 mg/L	Zn = 10 mg/L
0.144	0.040	0.002	0.409
0.040	0.002	0.005	0.152
0.021	0.001	0.001	0.066
0.005	0.000	0.001	0.009
Cd = 100 mg/L	Cu = 100 mg/L	Pb = 10 mg/L	Zn = 100 mg/L
1.723	1.748	0.017	3.673
1.442	1.035	0.017	3.058
1.367	0.298	0.002	2.592
0.033	0.058	0.000	2.086
Cd = 500 mg/L	Cu = 500 mg/L	Pb = 10 mg/L	Zn = 500 mg/L
7.558	11.254	0.070	17.057
5.191	6.435	0.044	12.004
7.601	9.891	0.006	12.487
5.302	6.762	0.001	8.748
Cd = 10 mg/L	Cu = 10 mg/L	Pb = 100 mg/L	Zn = 10 mg/L
0.212	0.200	0.181	0.409
0.187	0.158	0.115	0.369
0.185	0.131	0.045	0.413
0.117	0.037	0.006	0.327
Cd = 100 mg/L	Cu = 100 mg/L	Pb = 100 mg/L	Zn = 100 mg/L
2.321	2.618	0.681	4.791
1.639	1.651	0.325	3.420
1.304	0.172	0.028	2.380
3.183	3.337	1.594	4.400
Cd = 500 mg/L	Cu = 500 mg/L	Pb = 100 mg/L	Zn = 500 mg/L
11.827	16.582	1.273	23.506
4.002	5.299	0.139	11.744
6.742	6.857	0.241	3.270
5.527	4.051	0.112	2.678
Cd = 10 mg/L	Cu = 10 mg/L	Pb = 500 mg/L	Zn = 10 mg/L
0.301	0.283	5.481	0.496
0.194	0.175	3.027	0.327
0.289	0.300	4.803	0.114
0.209	0.195	2.979	0.083
Cd = 100 mg/L	Cu = 100 mg/L	Pb = 500 mg/L	Zn = 100 mg/L
2.547	3.021	6.197	5.128
2.065	2.454	4.166	4.226
0.980	1.133	3.009	0.429
1.768	2.075	3.085	0.782
Cd = 500 mg/L	Cu = 500 mg/L	Pb = 500 mg/L	Zn = 500 mg/L
8.869	12.620	5.855	19.934
5.156	6.316	1.792	12.010
3.648	2.192	1.773	1.753
5.281	3.239	1.560	2.539

Table 7: Q_S values for the multi - metal systems when Pb has a constant concentration. Tabella 7: Valori di Q_S per i sistemi multi-metal nei quali la concentrazione di Pb è stata mantenuta costante.

The sorption isotherms are determined for Cu t = 4, 24 and 48h showing a L2 type as sorption isotherm and a C type (horizontal line) (Fig. 12 A, B and C).

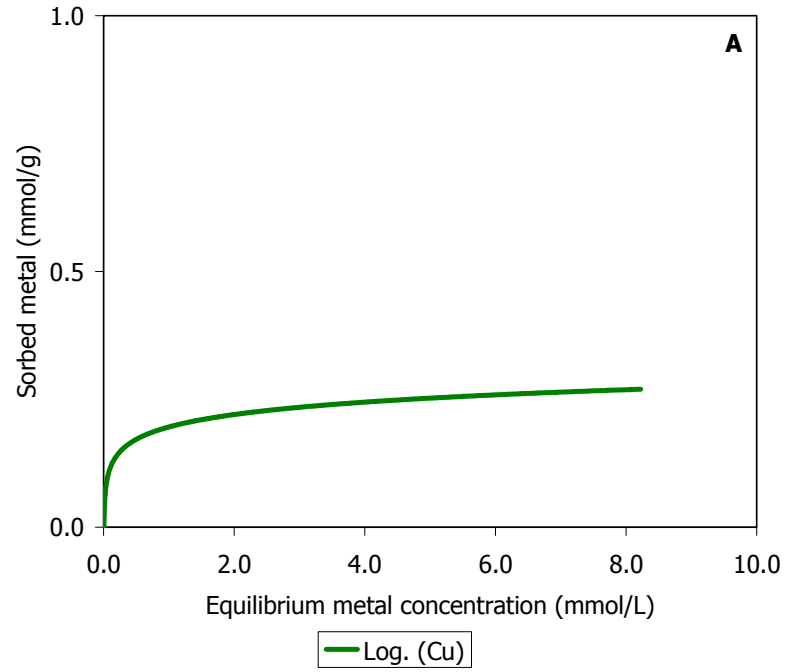

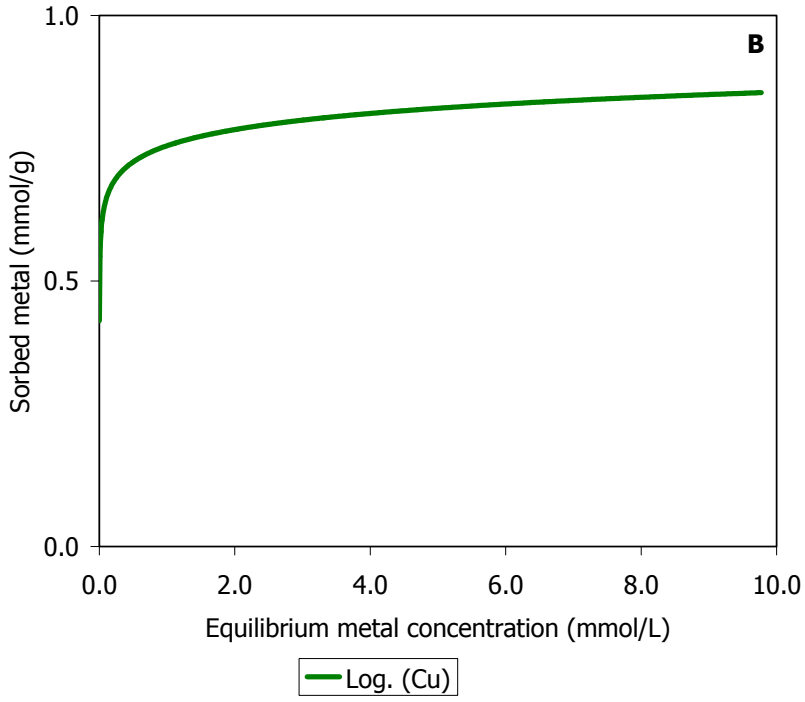

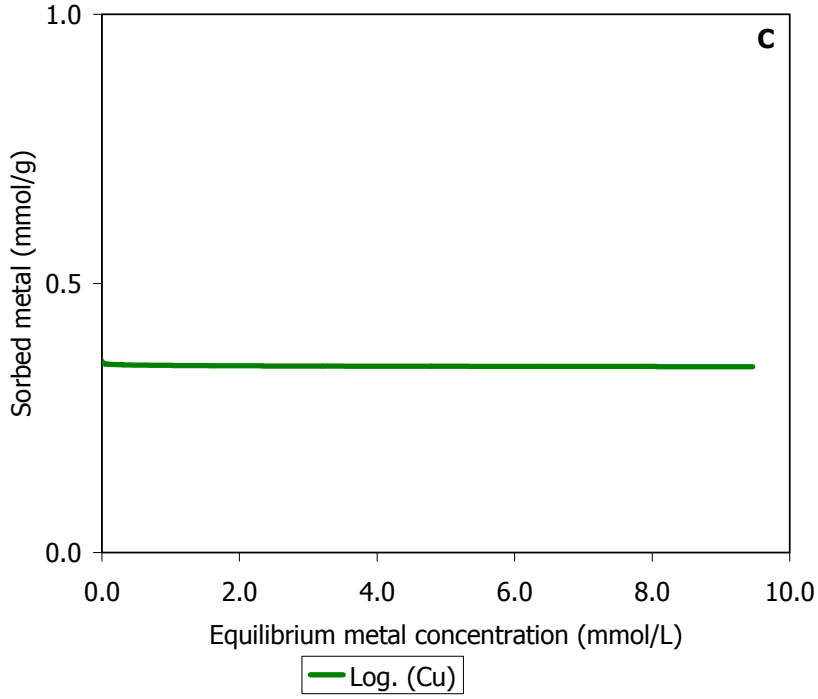

Fig. 12: Sorption isotherms for the multi-metal system where Pb is constant and vs. 1 g MAP. Relation between the metal sorbed (mmol/g) and the final concentration (mmol/L) in solution. A: t = 4h; B: t = 24h; C: t = 48h. – Fig. 12: Curve isotermiche per il sistema multi-metal in cui Pb è costante e vs. 1 g di MAP. Relazione tra il metallo assorbito (mmol/g) e la concentrazione finale (mmol/L) in soluzione. A: t = 4h; B: t = 24h; C: t = 48h.

Ca has a concentration among < b.d.l. – 1.2 mmol/g, almost proportional to the heavy metal concentration at the equilibrium (Fig. 13 A, B, C, D, E, F, G, H and I), not depending on the time as in the previous systems. The amount of desorbed Ca suggests a stoichiometric dissolution of MAP, on the contrary, P concentration at the equilibrium allow to infer a non stoichiometric dissolution (Fig.14 A, B, C, D, E, F, G, H and I). The average of P desorbed is about < 0.4 mmol/g and it doesn't increase with the interaction time.

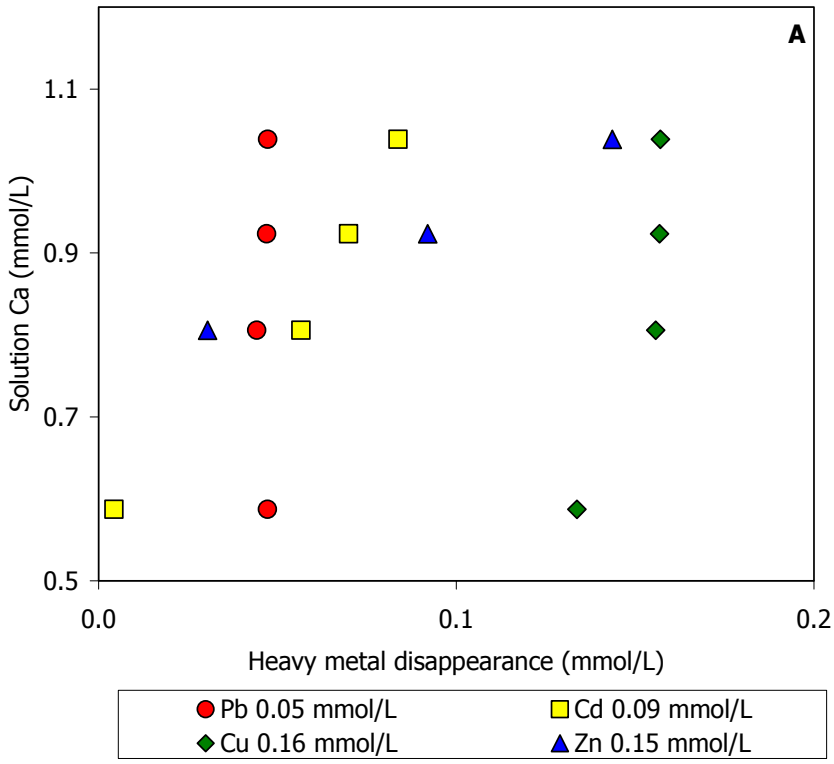
A
1.1
0.9
0.7
0.5
Solution Ca (mmol/L)
0.0
0.1
0.2
Heavy metal disappearance (mmol/L)
Pb 0.05 mmol/L
Cd 0.09 mmol/L
Cu 0.16 mmol/L
Zn 0.15 mmol/L

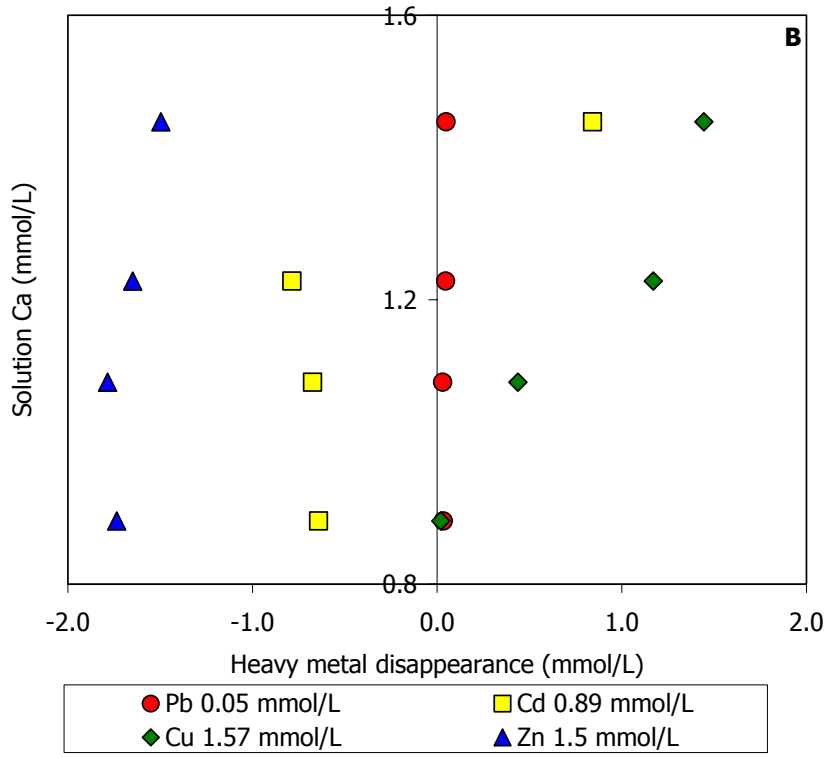
B
1.6
1.2
0.8
Solution Ca (mmol/L)
-2.0
-1.0
0.0
1.0
2.0
Heavy metal disappearance (mmol/L)
Pb 0.05 mmol/L
Cd 0.89 mmol/L
Cu 1.57 mmol/L
Zn 1.5 mmol/L

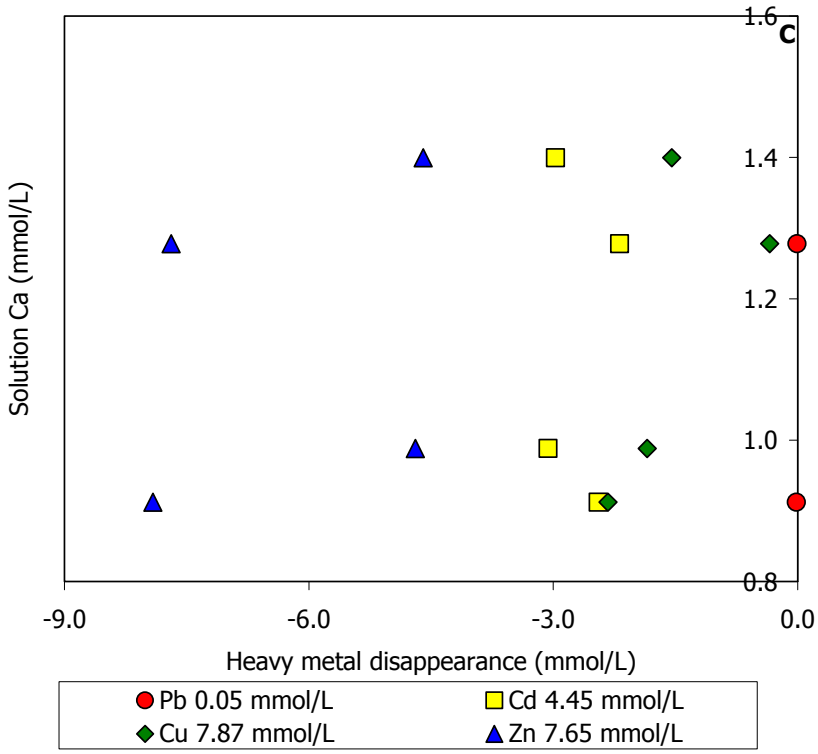
C
1.6
1.4
1.2
1.0
0.8
Solution Ca (mmol/L)
-9.0
-6.0
-3.0
0.0
Heavy metal disappearance (mmol/L)
Pb 0.05 mmol/L
Cd 4.45 mmol/L
Cu 7.87 mmol/L
Zn 7.65 mmol/L

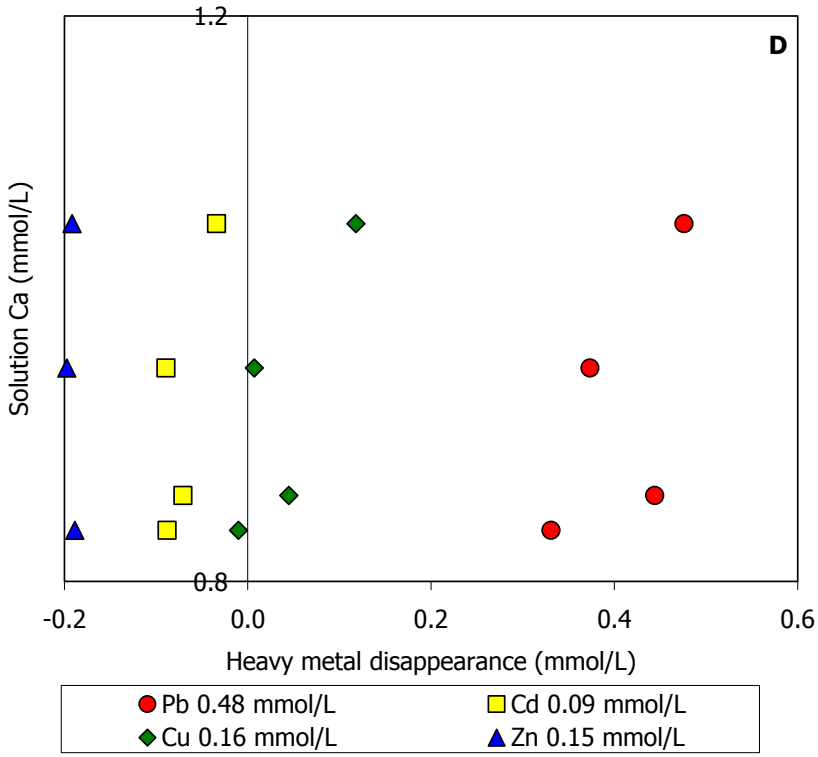
D
1.2
0.8
Solution Ca (mmol/L)
-0.2
0.0
0.2
0.4
0.6
Heavy metal disappearance (mmol/L)
Pb 0.48 mmol/L
Cd 0.09 mmol/L
Cu 0.16 mmol/L
Zn 0.15 mmol/L

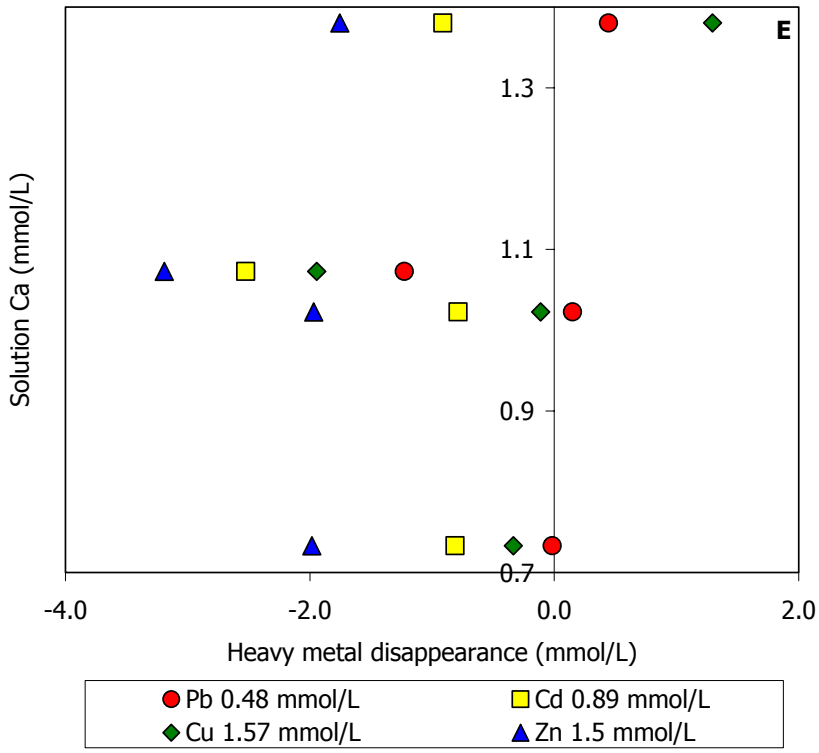
E
1.3
1.1
0.9
0.7
Solution Ca (mmol/L)
-4.0
-2.0
0.0
2.0
Heavy metal disappearance (mmol/L)
Pb 0.48 mmol/L
Cd 0.89 mmol/L
Cu 1.57 mmol/L
Zn 1.5 mmol/L

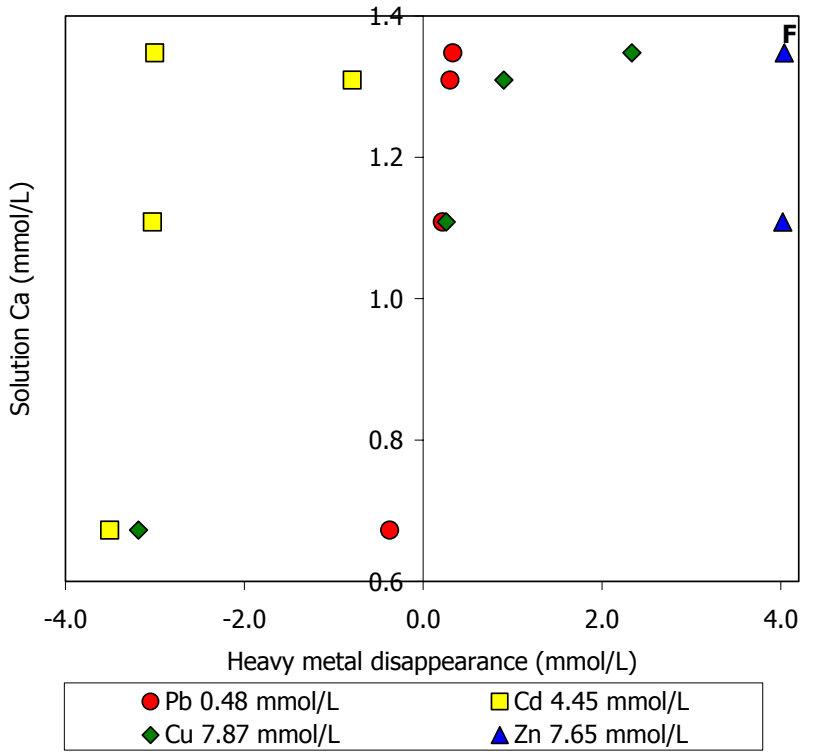
F
1.4
1.2
1.0
0.8
0.6
Solution Ca (mmol/L)
-4.0
-2.0
0.0
2.0
4.0
Heavy metal disappearance (mmol/L)
Pb 0.48 mmol/L
Cd 4.45 mmol/L
Cu 7.87 mmol/L
Zn 7.65 mmol/L

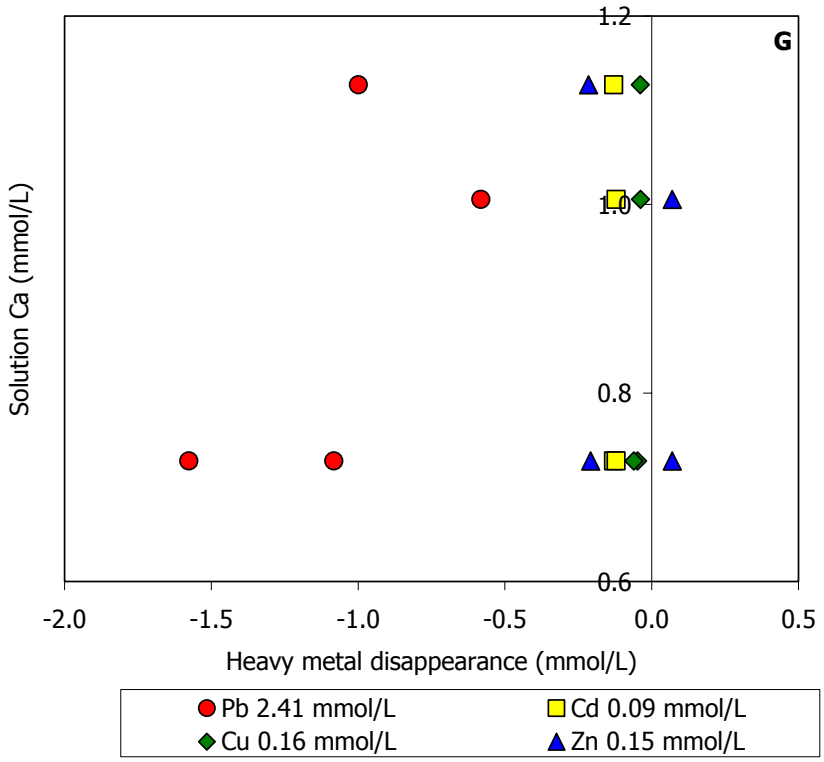
G
1.2
1.0
0.8
0.6
Solution Ca (mmol/L)
-2.0
-1.5
-1.0
-0.5
0.0
0.5
Heavy metal disappearance (mmol/L)
Pb 2.41 mmol/L
Cd 0.09 mmol/L
Cu 0.16 mmol/L
Zn 0.15 mmol/L

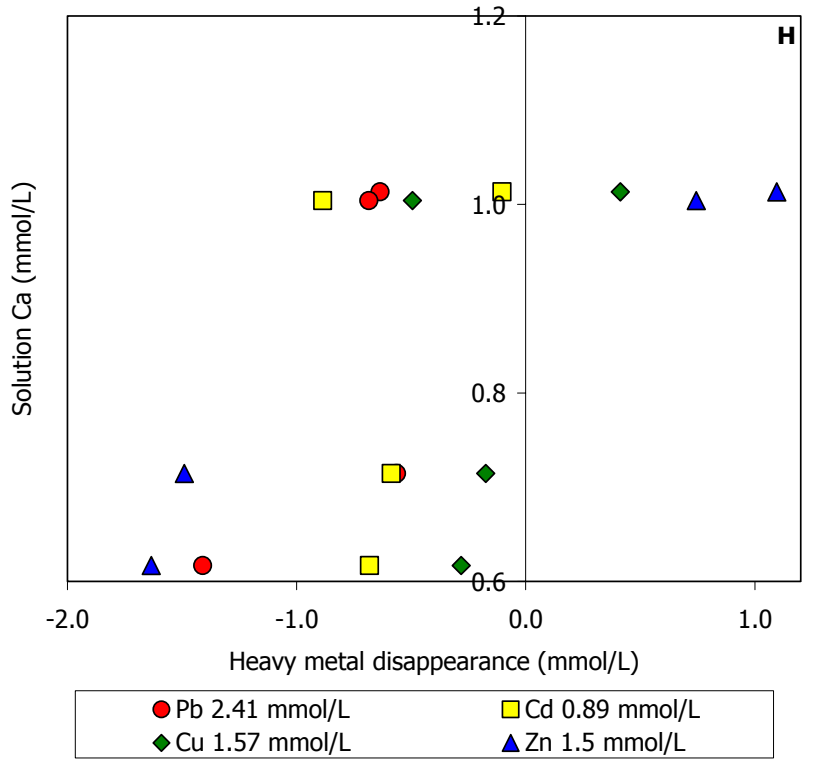
H
1.2
1.0
0.8
0.6
Solution Ca (mmol/L)
-2.0
-1.0
0.0
1.0
Heavy metal disappearance (mmol/L)
Pb 2.41 mmol/L
Cd 0.89 mmol/L
Cu 1.57 mmol/L
Zn 1.5 mmol/L

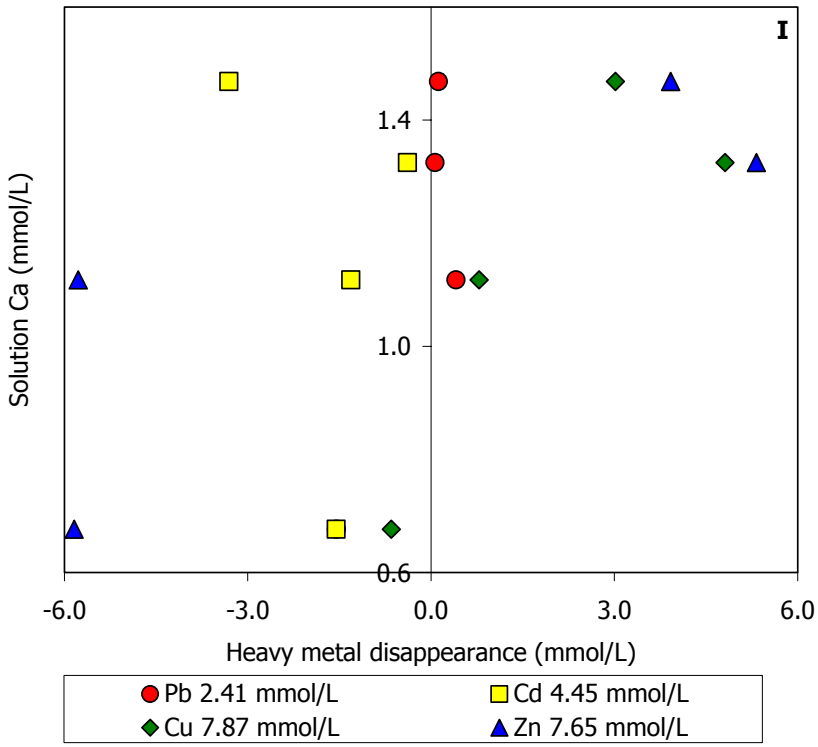

Fig. 13: Relation between Ca in solution (mmol/L) and the amount of heavy metals disappeared (mmol/L) sorbed on MAP surface at the equilibrium in a multi-metal system when Pb is constant. Each initial concentration of the multi-metal system is written in the legend. - Fig. 13: Relazione tra il quantitativo di Ca in soluzione (mmol/L) e di ciascun metallo pesante adsorbito (mmol/L) nel sistema multi-metal quando Pb è costante. La concentrazione iniziale di ogni elemento del sistema multi-metal è in leggenda.

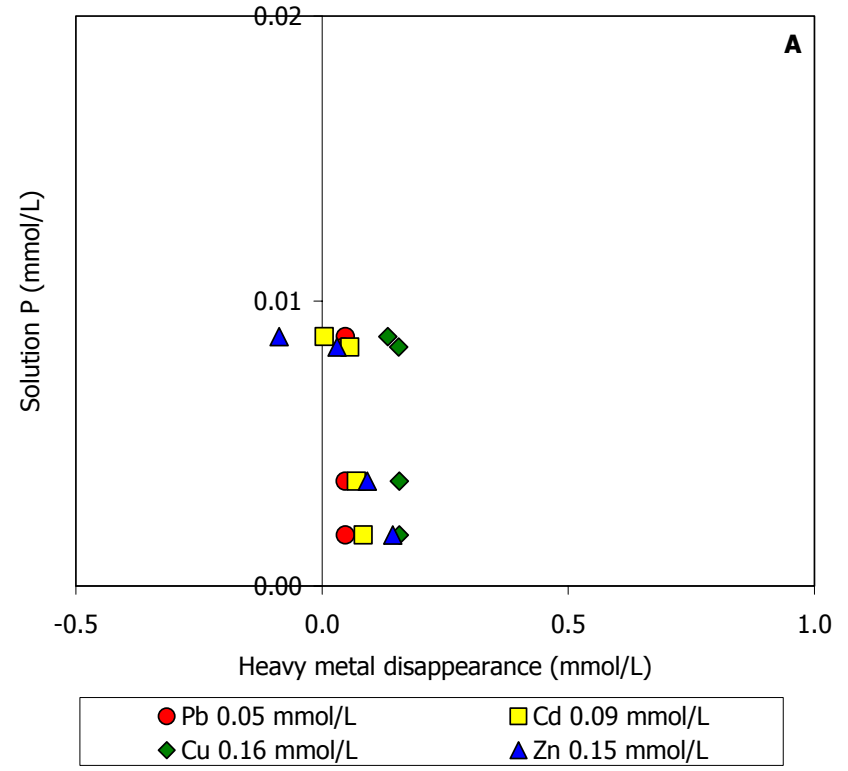
A
0.02
0.01
0.00
Solution P (mmol/L)
-0.5
0.0
0.5
1.0
Heavy metal disappearance (mmol/L)
Pb 0.05 mmol/L
Cd 0.09 mmol/L
Cu 0.16 mmol/L
Zn 0.15 mmol/L

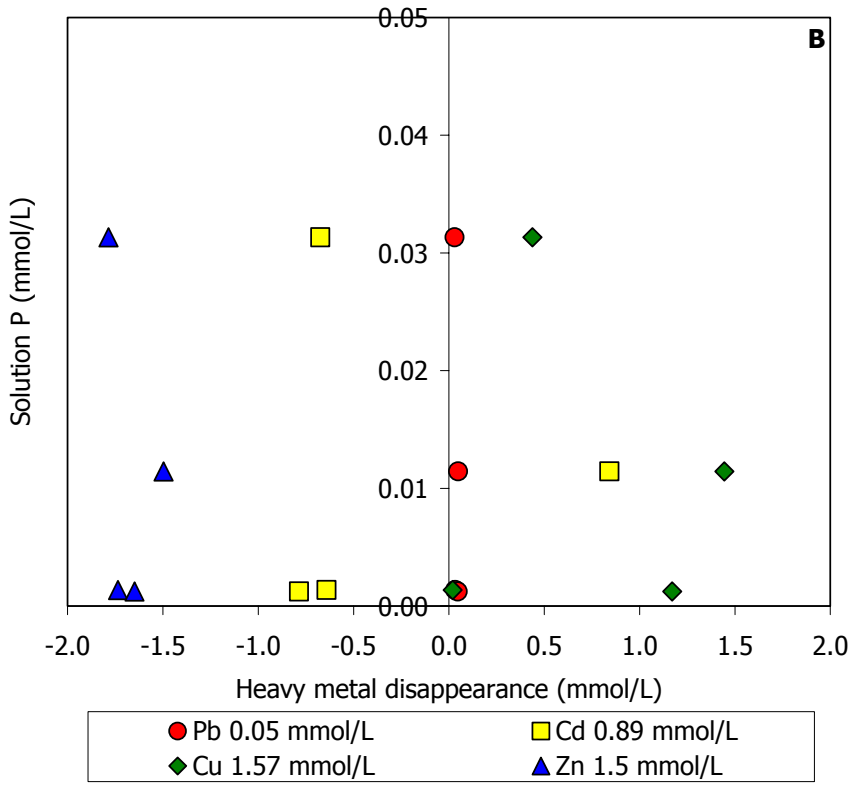
B
0.05
0.04
0.03
0.02
0.01
0.00
Solution P (mmol/L)
-2.0
-1.5
-1.0
-0.5
0.0
0.5
1.0
1.5
2.0
Heavy metal disappearance (mmol/L)
Pb 0.05 mmol/L
Cd 0.89 mmol/L
Cu 1.57 mmol/L
Zn 1.5 mmol/L

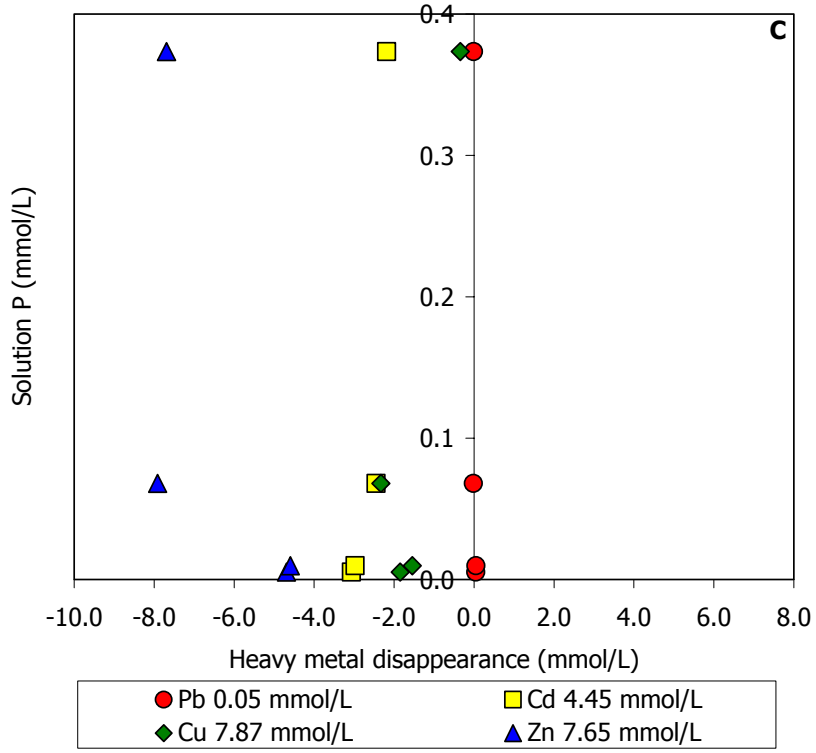
C
0.4
0.3
0.2
0.1
0.0
Solution P (mmol/L)
-10.0
-8.0
-6.0
-4.0
-2.0
0.0
2.0
4.0
6.0
8.0
Heavy metal disappearance (mmol/L)
Pb 0.05 mmol/L
Cd 4.45 mmol/L
Cu 7.87 mmol/L
Zn 7.65 mmol/L

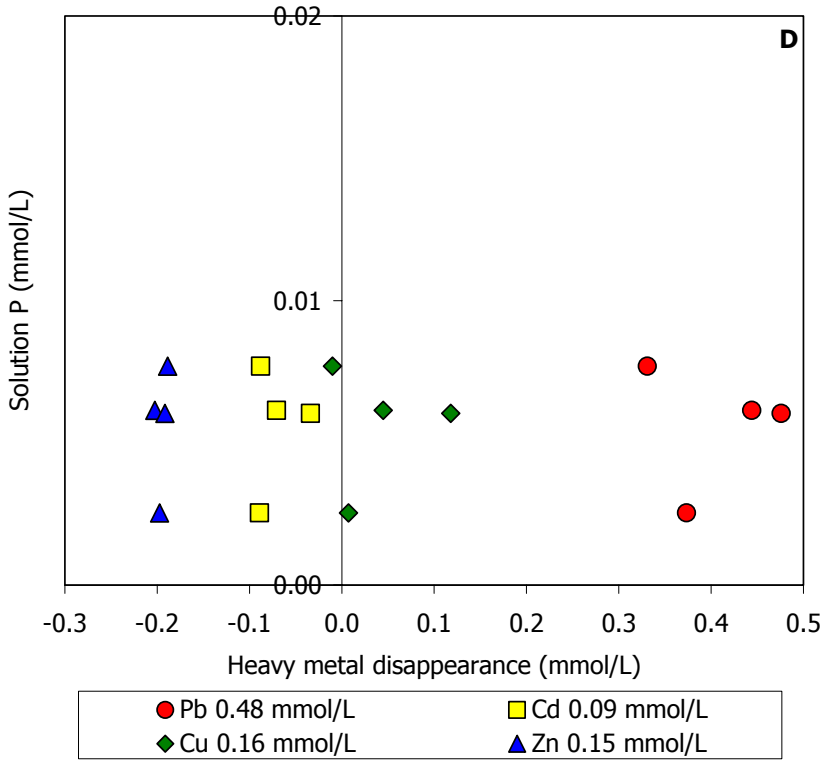
D
0.02
0.01
0.00
Solution P (mmol/L)
-0.3
-0.2
-0.1
0.0
0.1
0.2
0.3
0.4
0.5
Heavy metal disappearance (mmol/L)
Pb 0.48 mmol/L
Cd 0.09 mmol/L
Cu 0.16 mmol/L
Zn 0.15 mmol/L

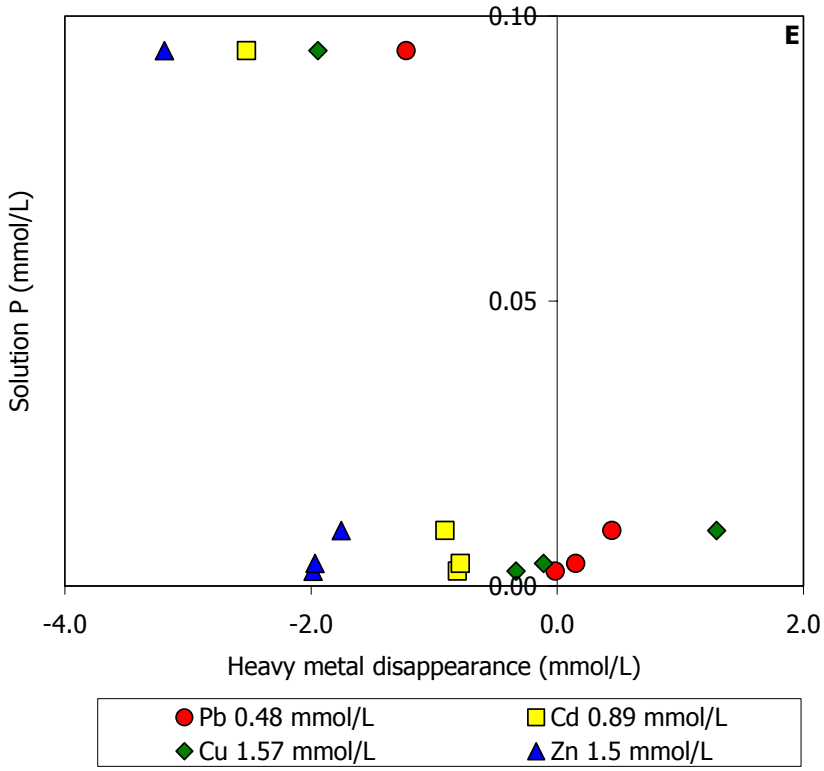
E
0.10
0.05
0.00
Solution P (mmol/L)
-4.0
-2.0
0.0
2.0
Heavy metal disappearance (mmol/L)
Pb 0.48 mmol/L
Cd 0.89 mmol/L
Cu 1.57 mmol/L
Zn 1.5 mmol/L

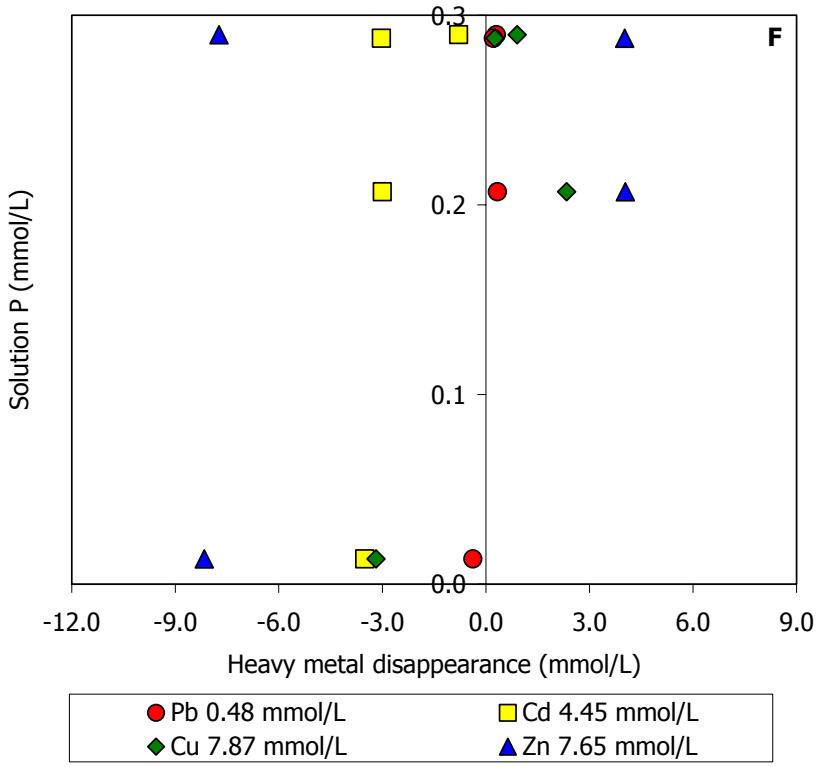
F
0.3
0.2
0.1
0.0
Solution P (mmol/L)
-12.0
-9.0
-6.0
-3.0
0.0
3.0
6.0
9.0
Heavy metal disappearance (mmol/L)
Pb 0.48 mmol/L
Cd 4.45 mmol/L
Cu 7.87 mmol/L
Zn 7.65 mmol/L

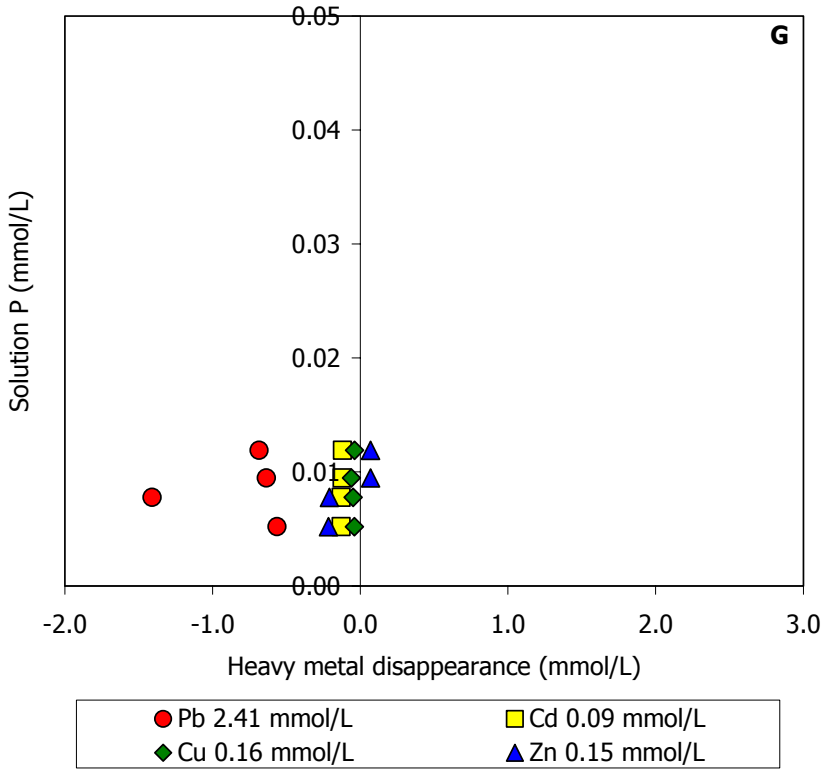
G
0.05
0.04
0.03
0.02
0.01
0.00
Solution P (mmol/L)
-2.0
-1.0
0.0
1.0
2.0
3.0
Heavy metal disappearance (mmol/L)
Pb 2.41 mmol/L
Cd 0.09 mmol/L
Cu 0.16 mmol/L
Zn 0.15 mmol/L

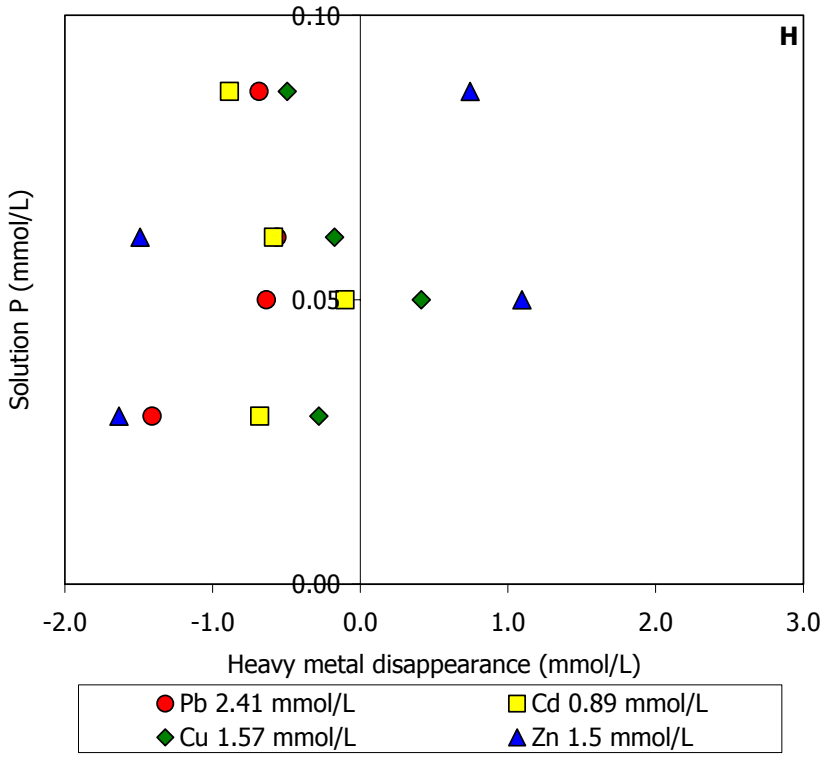
H
0.10
0.05
0.00
Solution P (mmol/L)
-2.0
-1.0
0.0
1.0
2.0
3.0
Heavy metal disappearance (mmol/L)
Pb 2.41 mmol/L
Cd 0.89 mmol/L
Cu 1.57 mmol/L
Zn 1.5 mmol/L

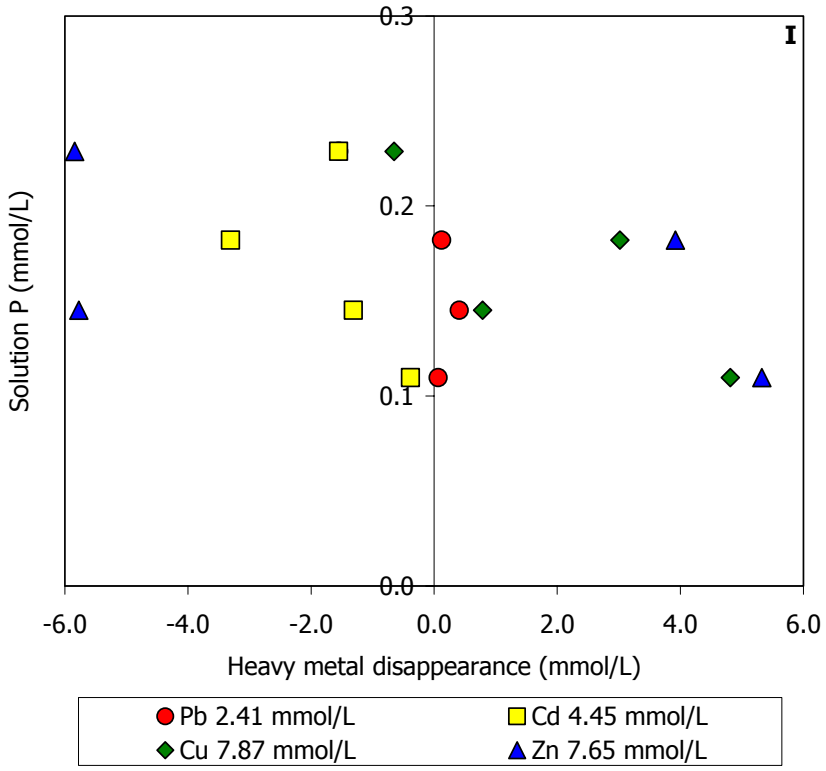

Fig. 14: Relation between P in solution (mmol/L) and the amount of disappeared heavy metals (mmol/L) sorbed on MAP surface at the equilibrium in a multi-metal system when Pb is constant. Each initial concentration of the multi-metal system is written in the legend. - Fig. 14: Relazione tra il quantitativo di P in soluzione (mmol/L) e di ciascun metallo pesante adsorbito (mmol/L) nel sistema multi-metal quando Pb è costante. La concentrazione iniziale di ogni elemento del sistema multi-metal è in leggenda.

In the last system Zn is the constant element (Tab. 8 and Fig. 15 A, B, C, D, E and F), the best immobilization time is 48h, although it is not constant, as it seems to depend on the initial concentration of the heavy metals. The order of immobilization is Pb > Cu > Cd > Zn, independently from the concentration or time. In this system, generally, there are few cases when heavy metal are well sorbed. pH, before and after the interaction, increases or decreases about 0.5.

Cd = 10 mg/L	Cu = 10 mg/L	Pb = 10 mg/L	Zn = 100 mg/L
3.533	3.533	3.533	-0.002
3.836	3.836	3.836	0.139
-62.606	-62.606	-62.606	-24.201
3.709	3.709	3.709	-5.726
Cd = 500 mg/L	Cu = 500 mg/L	Pb = 500 mg/L	Zn = 100 mg/L
35.959	89.262	58.154	-0.046
163.854	181.454	145.501	0.140
100.664	139.339	199.873	-23.613
35.641	80.262	199.850	-42.077
Cd = 10 mg/L	Cu = 10 mg/L	Pb = 10 mg/L	Zn = 100 mg/L
0.135	2.779	3.190	0.733
1.121	3.679	3.448	3.731
-79.370	-55.270	3.231	16.547
0.899	3.076	3.109	39.006
Cd = 500 mg/L	Cu = 500 mg/L	Pb = 500 mg/L	Zn = 100 mg/L
31.195	78.414	51.144	-0.998
33.692	102.841	58.857	0.063
118.910	153.819	194.644	17.332
39.140	120.345	191.727	-4.759
Cd = 10 mg/L	Cu = 10 mg/L	Pb = 10 mg/L	Zn = 500 mg/L
0.391	2.988	1.466	13.866
0.632	3.207	1.586	18.055
-52.901	-28.395	-91.801	184.364
-0.591	1.464	-71.845	198.948
Cd = 100 mg/L	Cu = 100 mg/L	Pb = 100 mg/L	Zn = 500 mg/L
4.175	3.533	3.533	9.524
5.978	3.836	3.836	17.840
0.104	-62.606	-62.606	-11.176
4.823	3.709	3.709	11.496

Tab. 8: Efficiency values for the multi - metal system when Zn has a constant concentration. Tabella 8: Valori dell'efficienza nell'immobilizzare i metalli pesanti per il sistema multi-metal in cui lo Zn mantiene costante la concentrazione

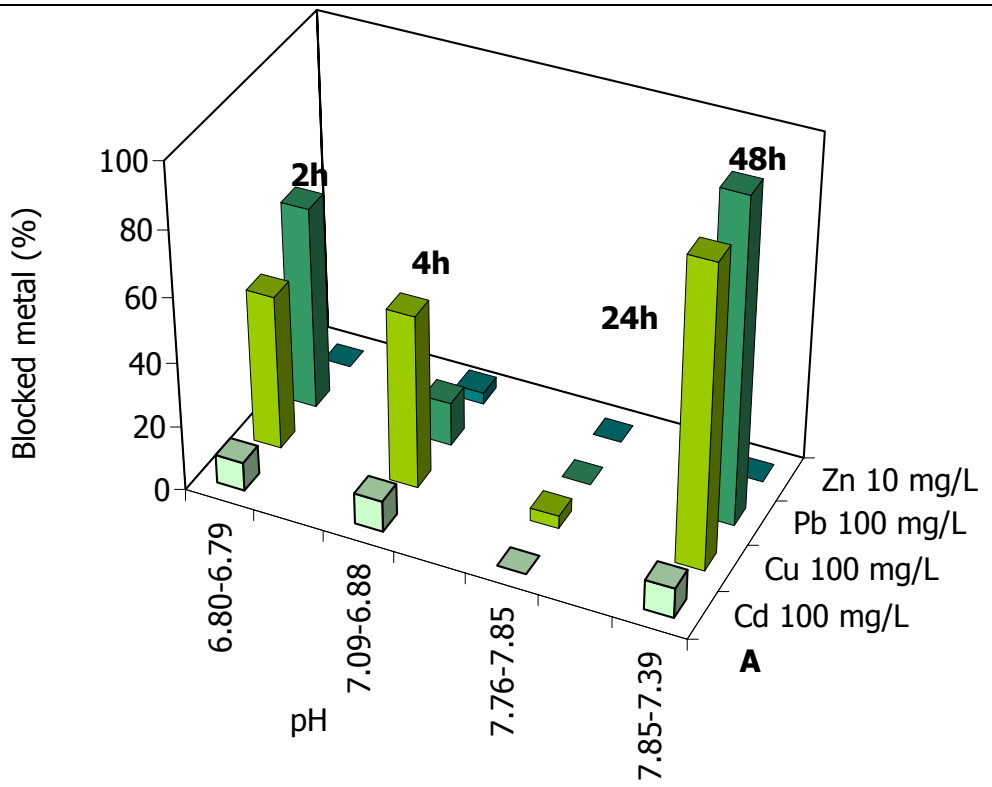
Blocked metal (%)
100
80
60
40
20
0
2h
4h
24h
48h
6.80-6.79
7.09-6.88
7.76-7.85
7.85-7.39
pH
Zn 10 mg/L
Pb 100 mg/L
Cu 100 mg/L
Cd 100 mg/L
A

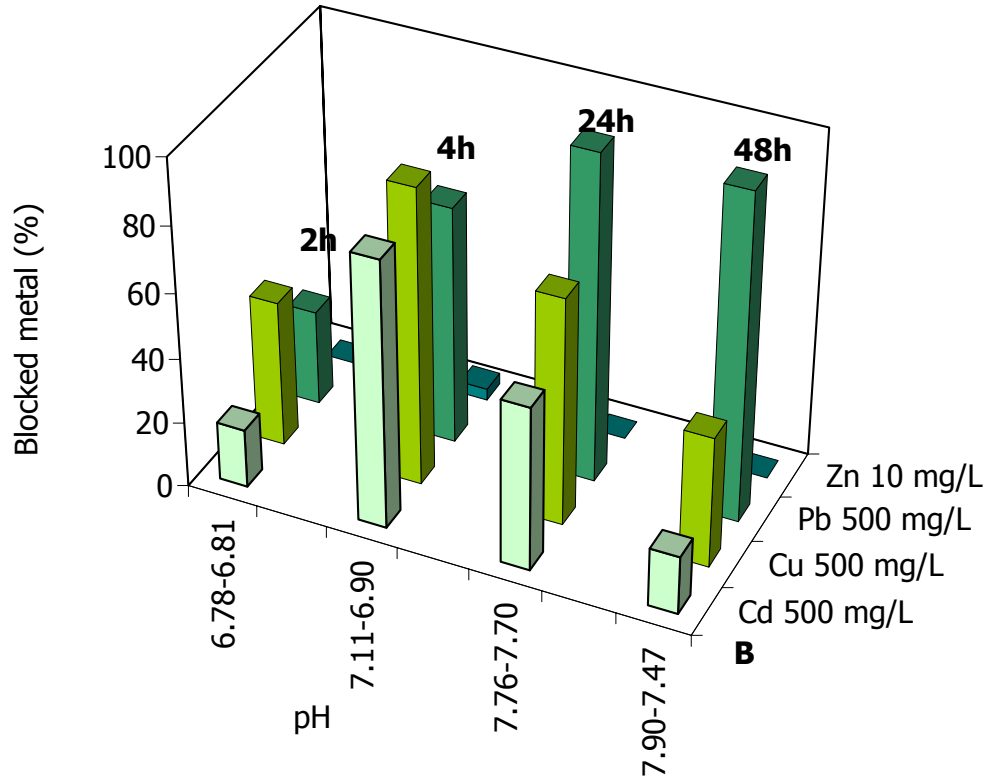
Blocked metal (%)
100
80
60
40
20
0
2h
4h
24h
48h
6.78-6.81
7.11-6.90
7.76-7.70
7.90-7.47
pH
Zn 10 mg/L
Pb 500 mg/L
Cu 500 mg/L
Cd 500 mg/L
B

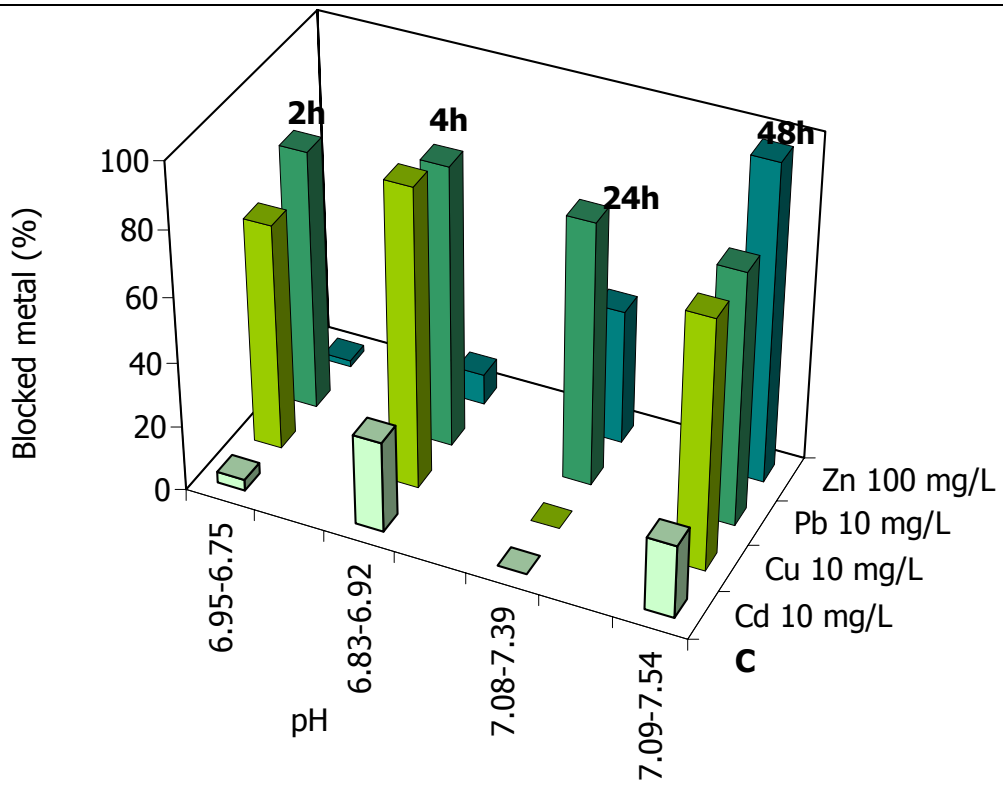
Blocked metal (%)
100
80
60
40
20
0
2h
4h
24h
48h
6.95-6.75
6.83-6.92
7.08-7.39
7.09-7.54
pH
Zn 100 mg/L
Pb 10 mg/L
Cu 10 mg/L
Cd 10 mg/L
C

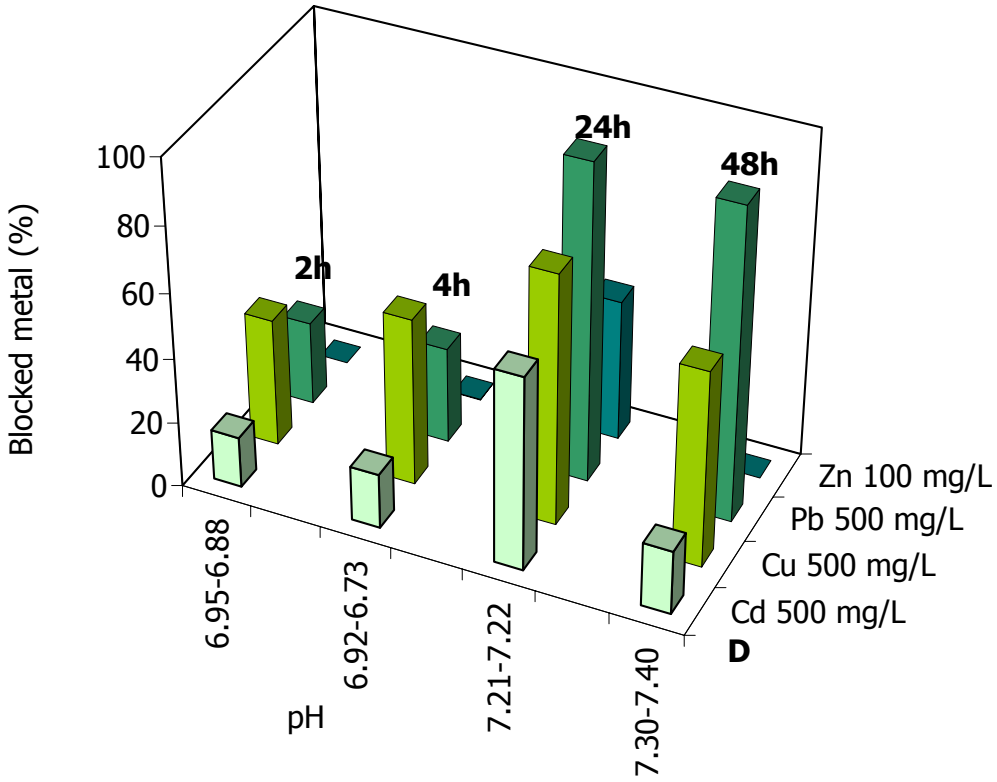
Blocked metal (%)
100
80
60
40
20
0
2h
4h
24h
48h
6.95-6.88
6.92-6.73
7.21-7.22
7.30-7.40
pH
Zn 100 mg/L
Pb 500 mg/L
Cu 500 mg/L
Cd 500 mg/L
D

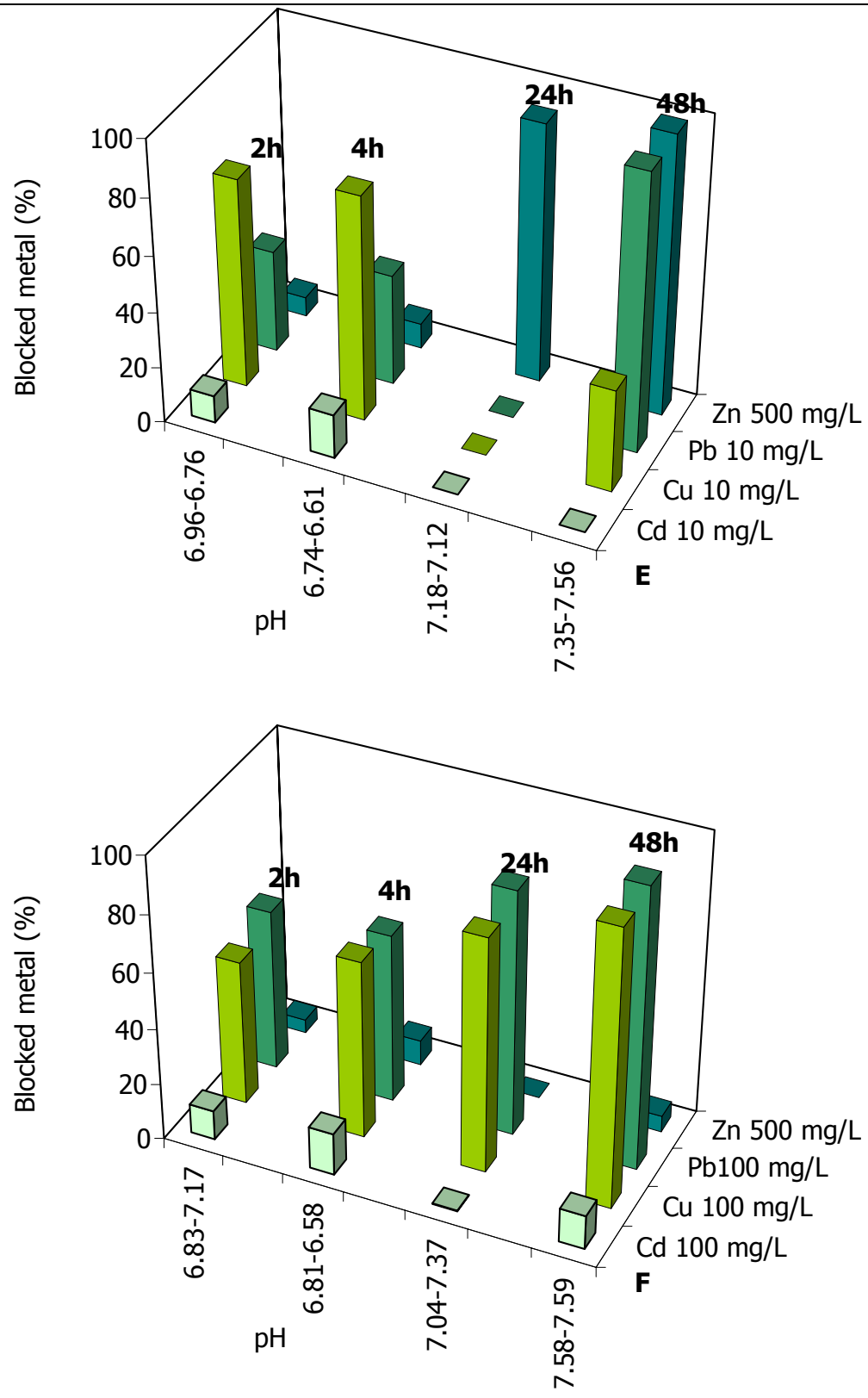

Fig. 15: Variation of the amount of blocked metal with time for the mass of MAP (1 g) in the multi-metal system where Zn is constant.. – Fig. 15: Variazione delle percentuali dei metalli immobilizzati in funzione del tempo di interazione per la quantità di MAP (1 g) nel sistema multi-metal in cui Zn è l'elemento costante.

In this system, the molar ratio are similar to those in the previous systems (Tab. 9), $Q_S < 1$, $Q_S > 1$ and $Q_S >> 1$, inferring two types of sorption mechanism, non-crystalline precipitation and adsorption. The variation of Q_S values seems to depend on the heavy metal concentration and not the contact time. Generally, Q_S values for Pb suggest a non-crystalline amorphous precipitation, whereas for Cd, Cu and Zn the adsorption mechanism.

Cd = 100 mg/L	Cu = 100 mg/L	Pb = 100 mg/L	Zn = 10 mg/L
2.438	2.472	0.544	0.460
2.307	2.094	1.199	0.424
3.927	2.601	1.319	1.856
1.346	0.185	0.001	0.620
Cd = 500 mg/L	Cu = 500 mg/L	Pb =500 mg/L	Zn = 10 mg/L
9.649	11.523	4.527	0.409
2.288	2.077	1.872	0.420
4.102	4.432	0.003	1.961
6.796	8.758	0.003	3.276
Cd = 10 mg/L	Cu = 10 mg/L	Pb = 10 mg/L	Zn = 100 mg/L
0.362	0.202	0.041	6.318
0.159	0.031	0.017	3.453
3.641	4.579	0.018	1.761
0.160	0.085	0.025	0.088
Cd = 500 mg/L	Cu = 500 mg/L	Pb =500 mg/L	Zn = 100 mg/L
10.122	12.897	4.843	4.227
7.260	7.503	3.343	2.997
3.617	3.644	0.130	1.739
6.149	5.386	0.172	2.942
Cd = 10 mg/L	Cu = 10 mg/L	Pb = 10 mg/L	Zn = 500 mg/L
0.219	0.109	0.083	19.420
0.173	0.072	0.067	16.110
2.532	2.550	2.313	1.196
0.242	0.236	2.169	0.095
Cd = 100 mg/L	Cu = 100 mg/L	Pb = 100 mg/L	Zn = 500 mg/L
2.034	1.955	0.529	18.591
1.782	1.369	0.455	16.406
1.367	0.410	0.098	12.438
0.702	0.029	0.002	6.464

Table 9: Q_S values for the multi - metal systems when Zn has a constant concentration. Tabella 9: Valori di Q_S per i sistemi multi-metal nei quali la concentrazione di Zn è stata mantenuta costante.

The sorption isotherm has been determine only for Zn a t= 4h (Fig. 16) and it is a L type suggesting a surface precipitation mechanism.

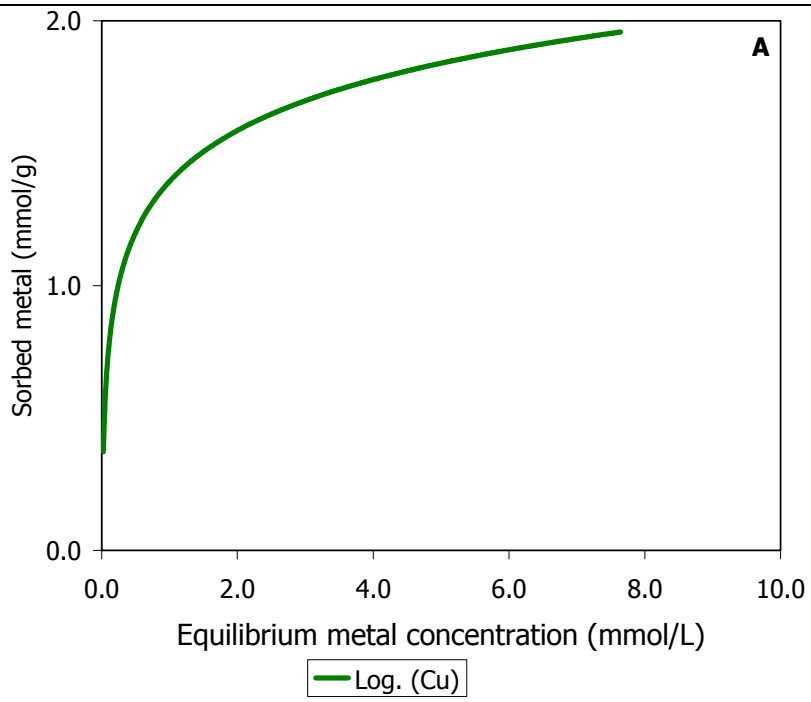

Fig. 16: Sorption isotherms for the multi-metal system where Zn is constant and vs. 1 g MAP. Relation between the metal sorbed (mmol/g) and the final concentration (mmol/L) in solution. A: t = 4h. – Fig. 16: Curve isotermiche per il sistema multi-metal in cui Zn è costante e vs. 1 g di MAP. Relazione tra il metallo assorbito (mmol/g) e la concentrazione finale (mmol/L) in soluzione. A: t = 4h.

The amount of Ca at the equilibrium is proportional to the amount of sorbed heavy metals (Fig. 17 A, B, C, D, E and F). The average values range from < b.d.l. to 1 mmol/g. Desorbed Ca concentration doesn't increase with time.

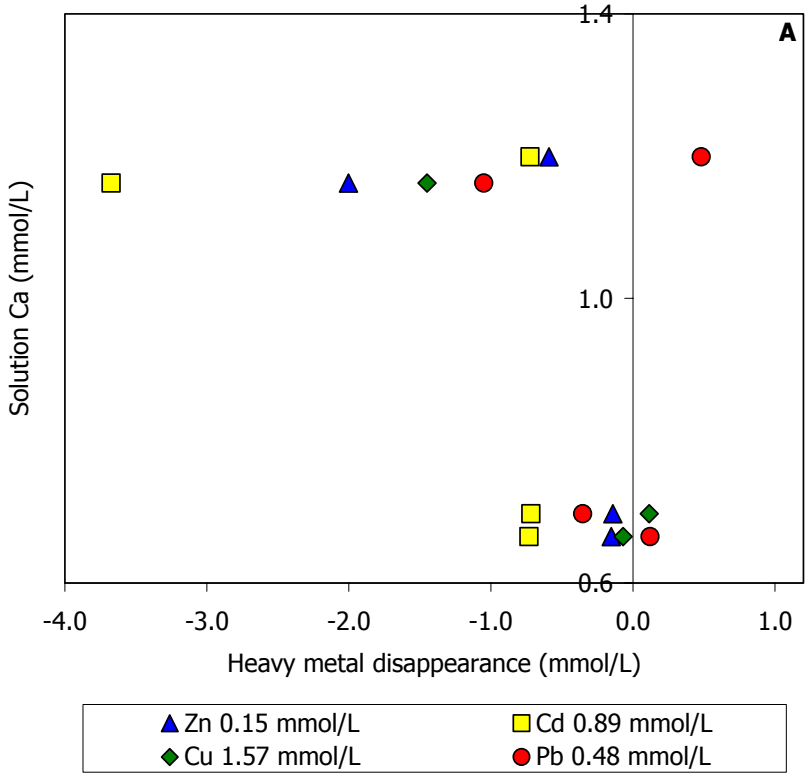
A
1.4
1.0
0.6
Solution Ca (mmol/L)
-4.0
-3.0
-2.0
-1.0
0.0
1.0
Heavy metal disappearance (mmol/L)
Zn 0.15 mmol/L
Cd 0.89 mmol/L
Cu 1.57 mmol/L
Pb 0.48 mmol/L

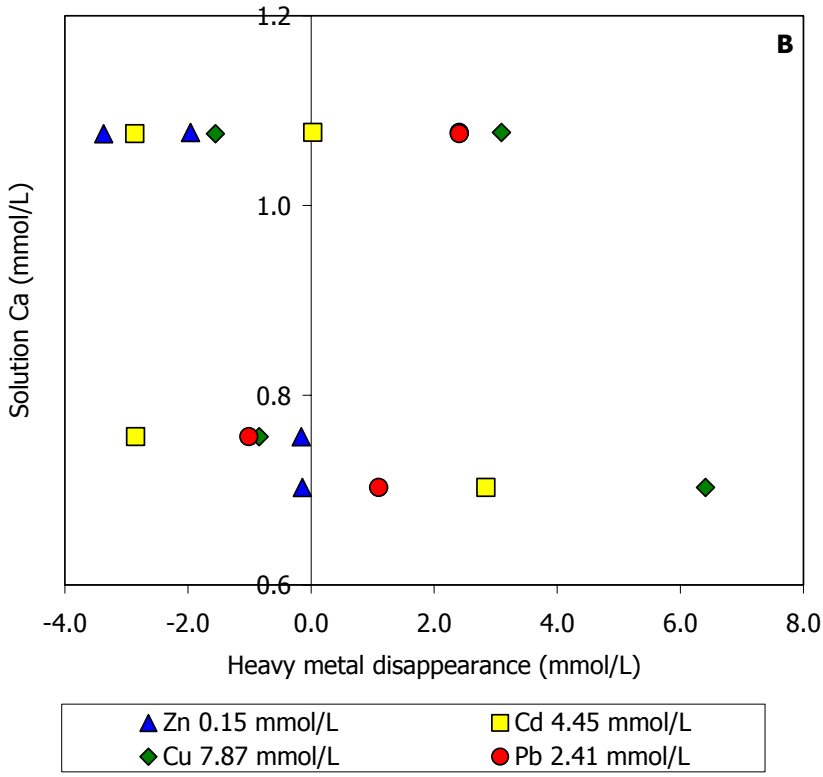
B
1.2
1.0
0.8
0.6
Solution Ca (mmol/L)
-4.0
-2.0
0.0
2.0
4.0
6.0
8.0
Heavy metal disappearance (mmol/L)
Zn 0.15 mmol/L
Cd 4.45 mmol/L
Cu 7.87 mmol/L
Pb 2.41 mmol/L

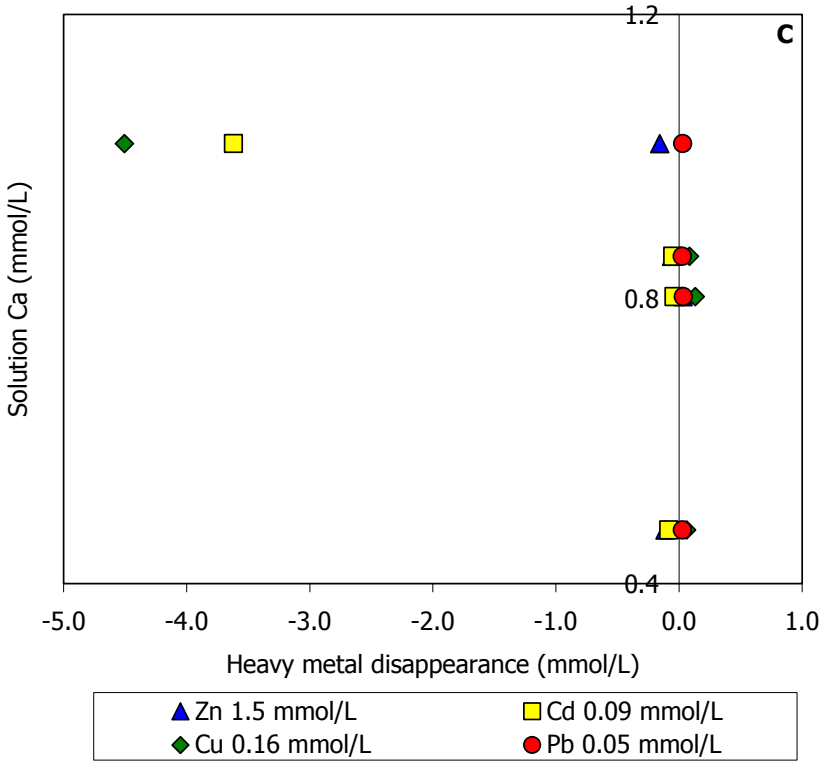
C
1.2
0.8
0.4
Solution Ca (mmol/L)
-5.0
-4.0
-3.0
-2.0
-1.0
0.0
1.0
Heavy metal disappearance (mmol/L)
Zn 1.5 mmol/L
Cd 0.09 mmol/L
Cu 0.16 mmol/L
Pb 0.05 mmol/L

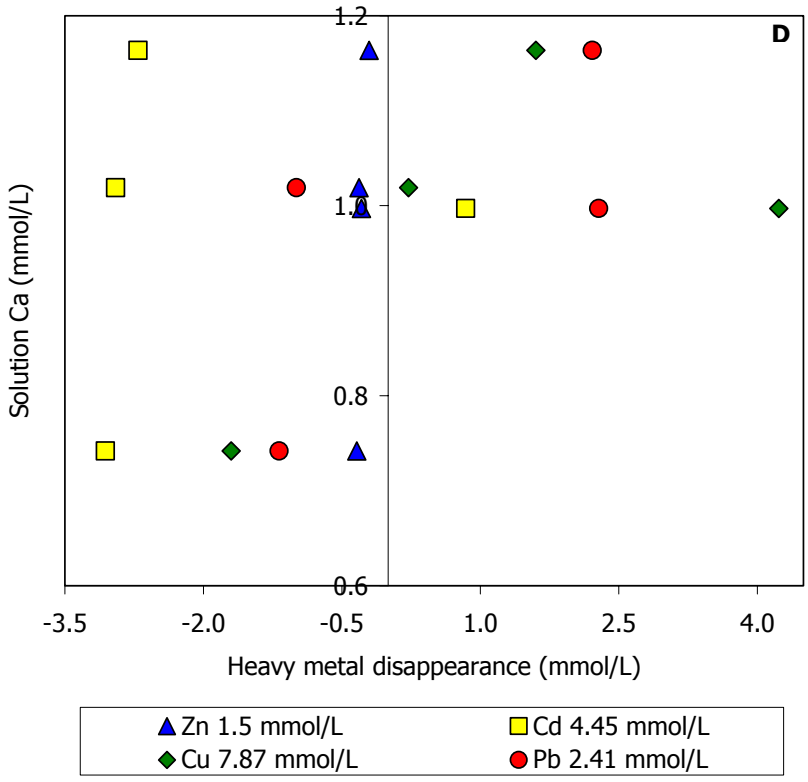
D
1.2
0.8
0.6
Solution Ca (mmol/L)
-3.5
-2.0
-0.5
1.0
2.5
4.0
Heavy metal disappearance (mmol/L)
Zn 1.5 mmol/L
Cd 4.45 mmol/L
Cu 7.87 mmol/L
Pb 2.41 mmol/L

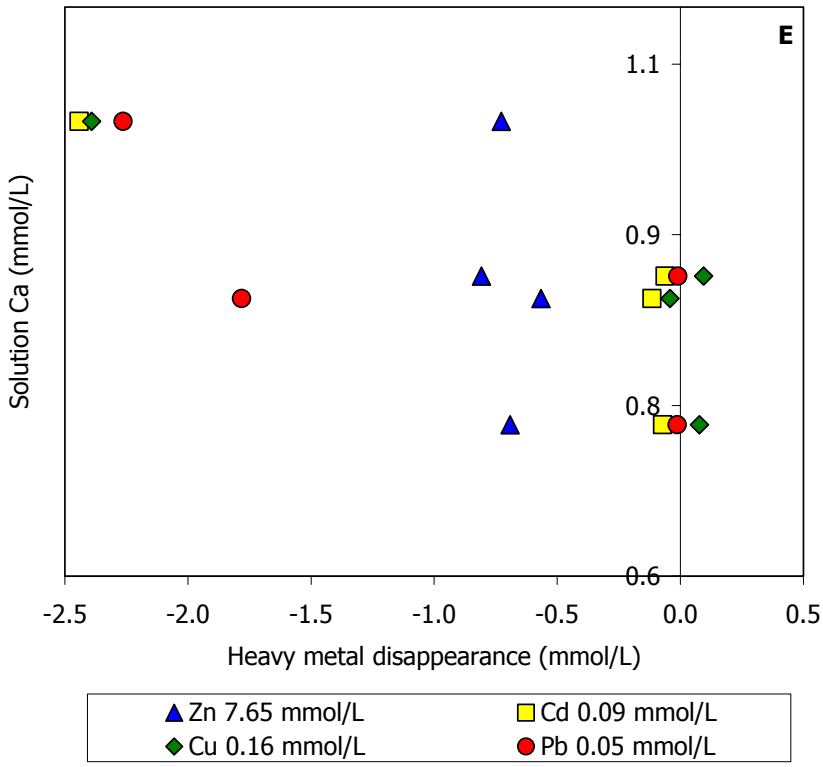

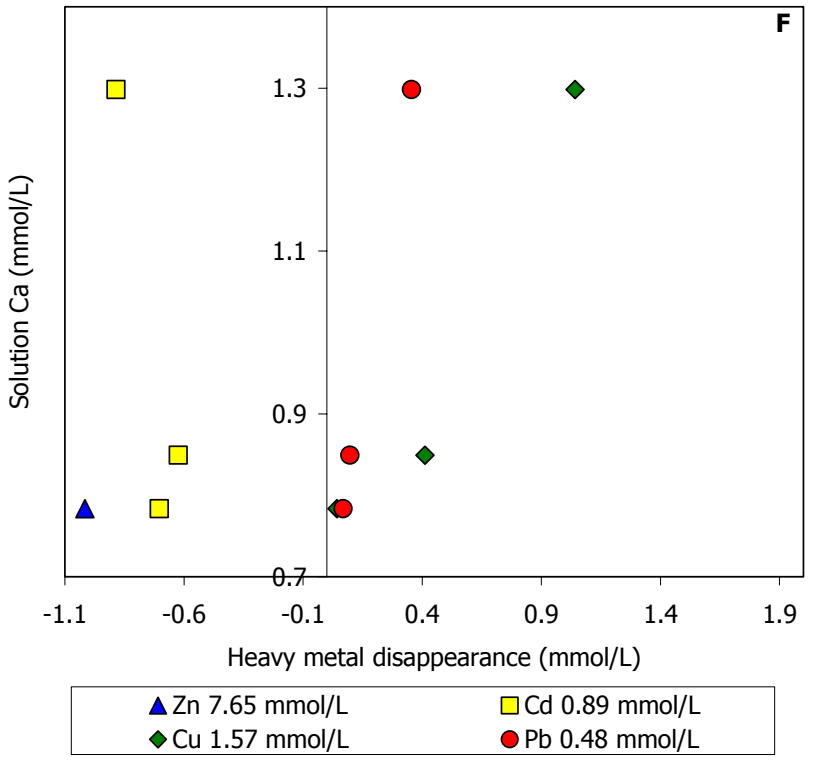

Fig. 17: Relation between Ca in solution (mmol/L) and the amount of heavy metals disappeared (mmol/L) sorbed on MAP surface at the equilibrium in a multi-metal system when Zn is constant. Each initial concentration of the multi-metal system is written in the legend. - Fig. 17: Relazione tra il quantitativo di Ca

in soluzione (mmol/L) e di ciascun metallo pesante adsorbito (mmol/L) nel sistema multi-metal quando Zn è costante. La concentrazione iniziale di ogni elemento del sistema multi-metal è in leggenda.

P concentration at the equilibrium is always low (Fig. 18 A, B, C, D, E and F), it runs from < b.d.l. to 0.4 mmol/g, whereas the sorbed heavy metals concentration is from < b.d.l. to 8 mmol/g. Therefore, it is probable a stoichiometric dissolution of MAP in case of Ca and a non-stoichiometric dissolution for P.

The proportional Ca concentration to the sorbed heavy metal concentration suggest a copreciptation process, on the other hand the low P concentration confirm the amorphous precipitation process as a sorption mechanism, in particular for Pb.

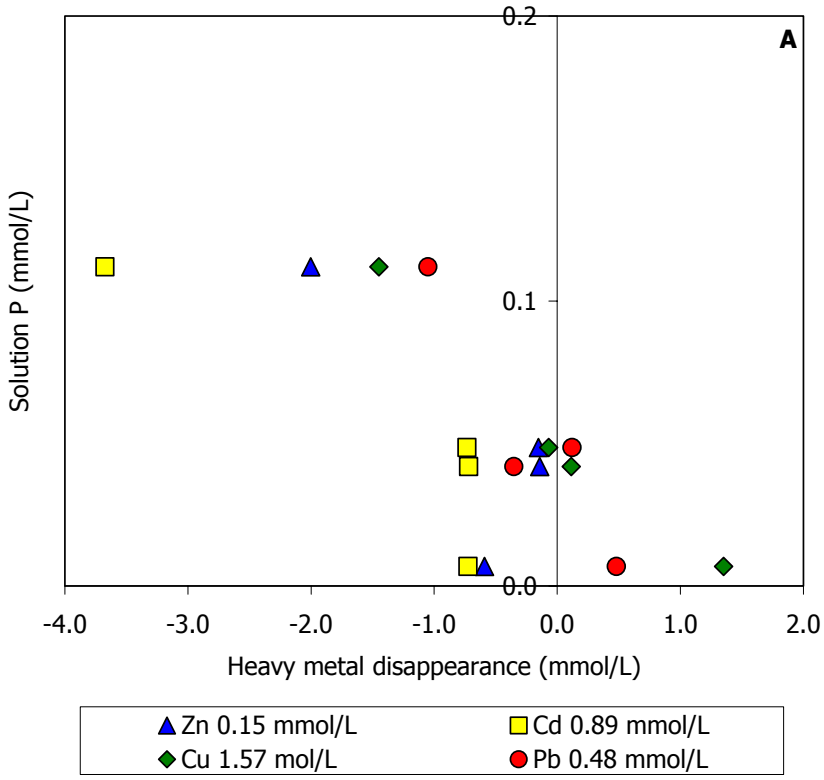

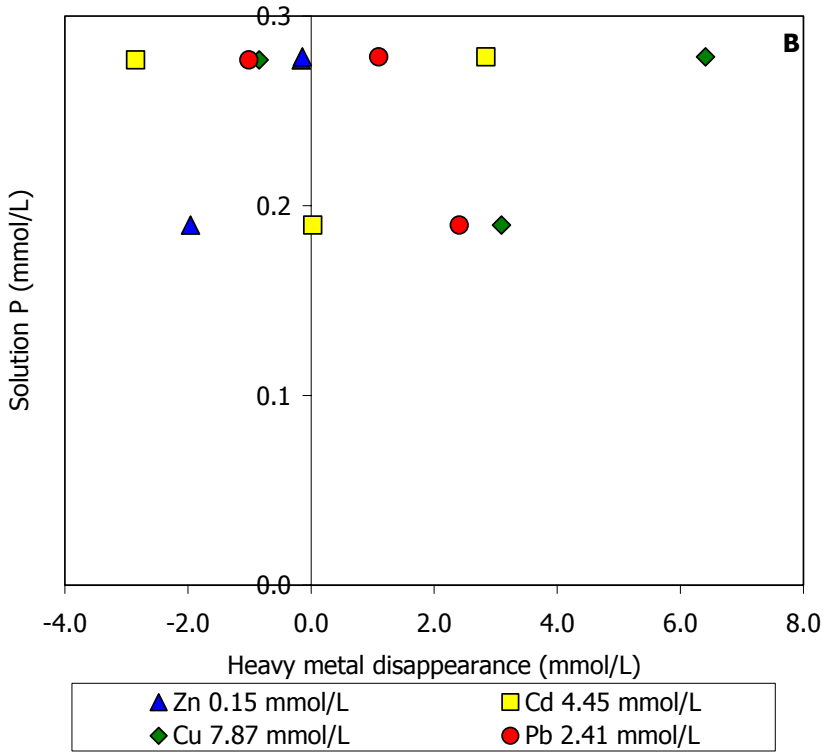
B
0.3
0.2
0.1
0.0
Solution P (mmol/L)
-4.0
-2.0
0.0
2.0
4.0
6.0
8.0
Heavy metal disappearance (mmol/L)
Zn 0.15 mmol/L
Cd 4.45 mmol/L
Cu 7.87 mmol/L
Pb 2.41 mmol/L

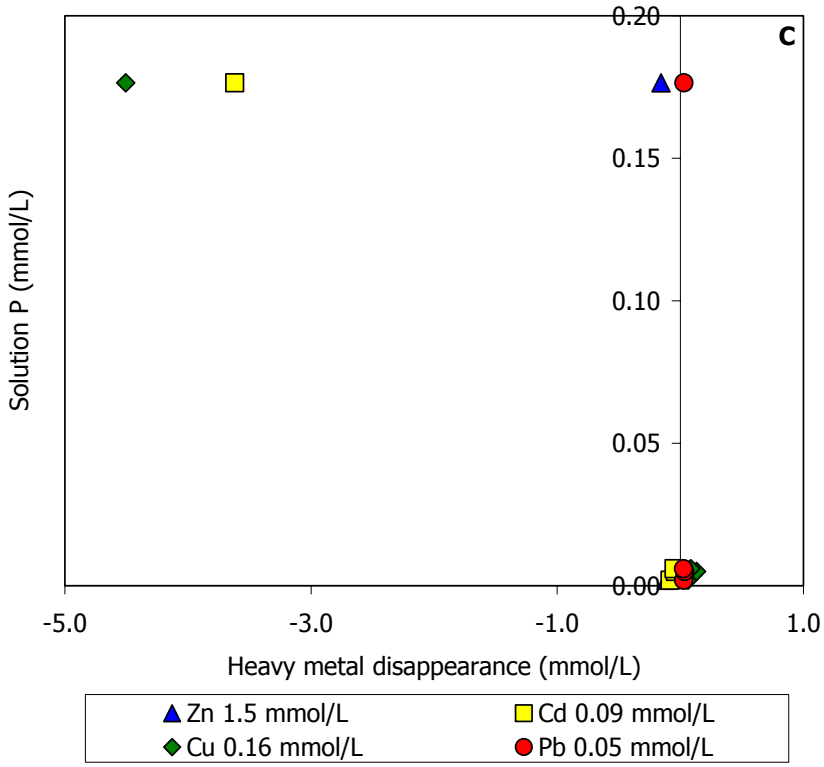
C
0.20
0.15
0.10
0.05
0.00
Solution P (mmol/L)
-5.0
-3.0
-1.0
1.0
Heavy metal disappearance (mmol/L)
Zn 1.5 mmol/L
Cd 0.09 mmol/L
Cu 0.16 mmol/L
Pb 0.05 mmol/L

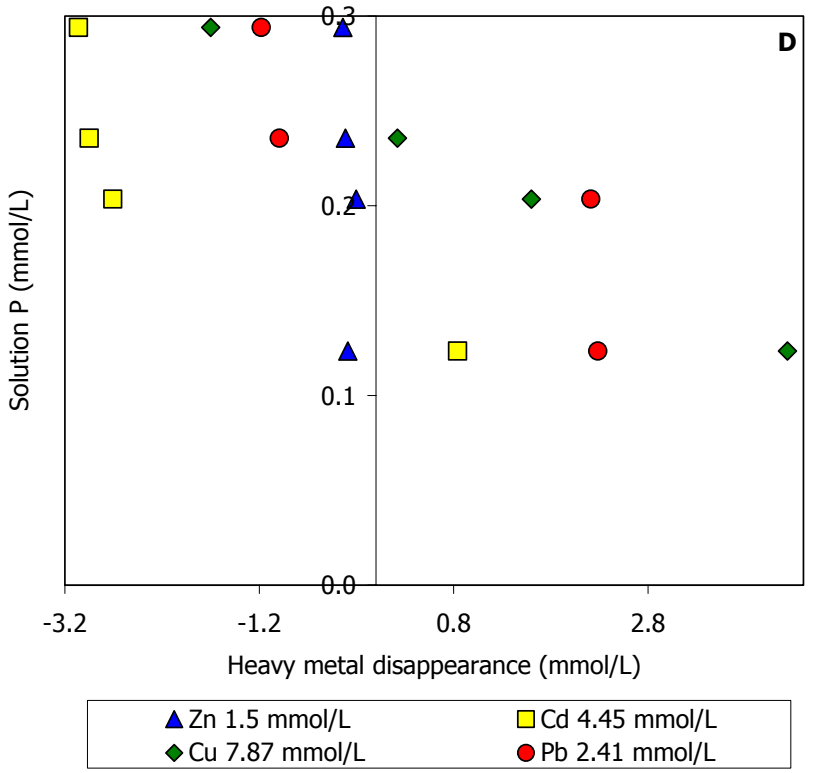
D
0.3
0.2
0.1
0.0
Solution P (mmol/L)
-3.2
-1.2
0.8
2.8
Heavy metal disappearance (mmol/L)
Zn 1.5 mmol/L
Cd 4.45 mmol/L
Cu 7.87 mmol/L
Pb 2.41 mmol/L

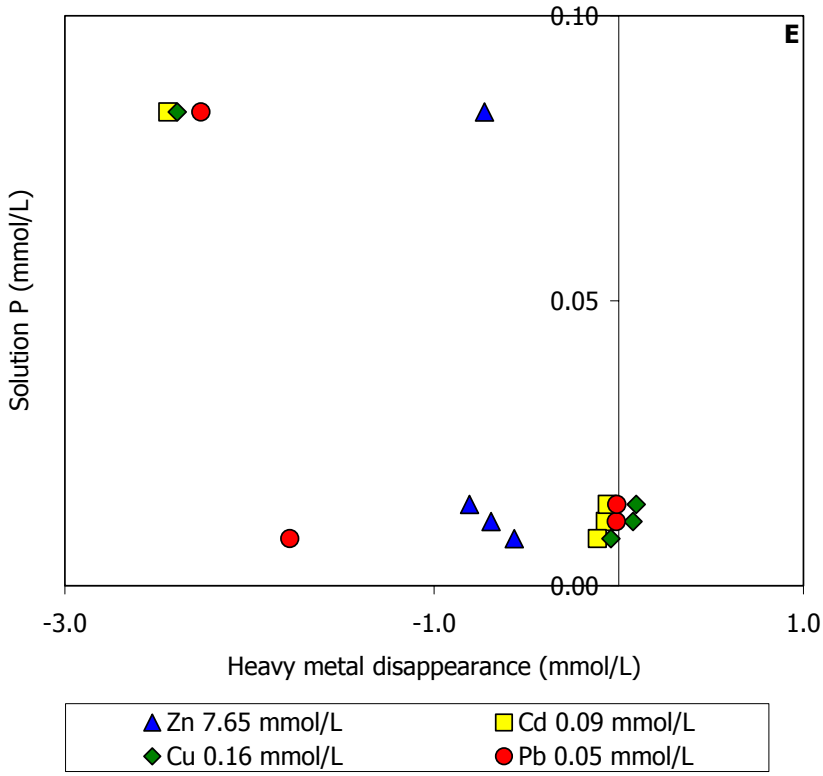
E
0.10
0.05
0.00
Solution P (mmol/L)
-3.0
-1.0
1.0
Heavy metal disappearance (mmol/L)
Zn 7.65 mmol/L
Cd 0.09 mmol/L
Cu 0.16 mmol/L
Pb 0.05 mmol/L

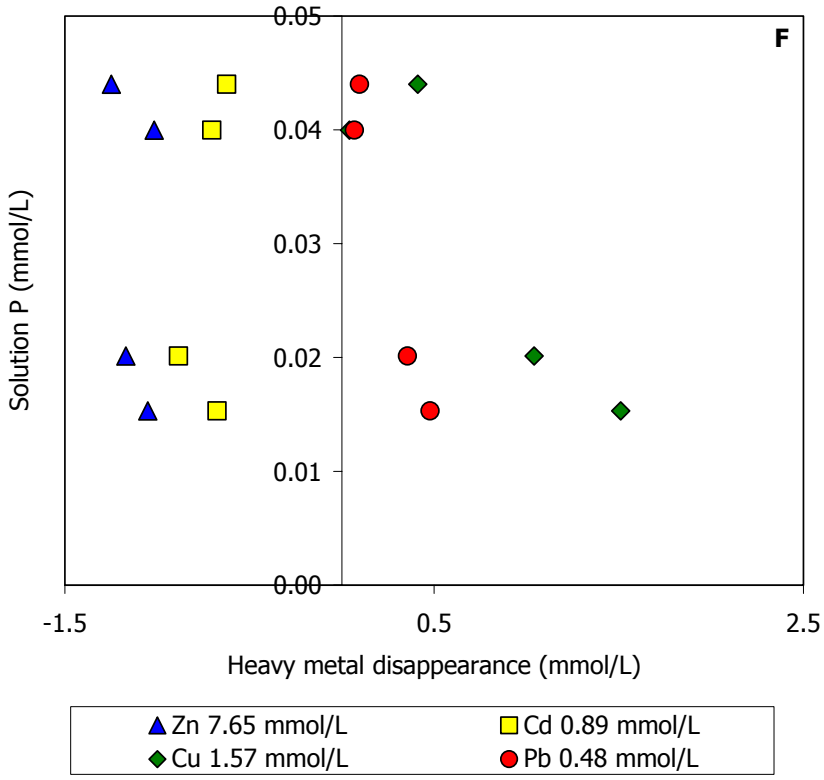

Fig. 18: Relation between P in solution (mmol/L) and the amount of disappeared heavy metals (mmol/L) sorbed on MAP surface at the equilibrium in a multi-metal system when Zn is constant. Each initial concentration of the multi-metal system is written in the legend. - Fig. 18: Relazione tra il quantitativo di P in soluzione (mmol/L) e di ciascun metallo pesante adsorbito (mmol/L) nel sistema multi-metal quando Zn è costante. La concentrazione iniziale di ogni elemento del sistema multi-metal è in leggenda.

7 DISCUSSION ON AQUEOUS SOLUTIONS

7.1 XRD ANALYSES

XRD analyses were conducted on the single metal and multi-metal system sorbed on HA. XRD patterns did not detect new crystalline phase in the solid materials, even in those reacted with the solution at highest heavy metal concentration

According to the results of previous studies (e.g. Singh et al. *(135)*), we can suggest a non to poorly crystalline precipitation of heavy metal-phosphates. However, based only on XRD data, we were unable to confirm whether a non or poorly crystalline phase is formed during the interaction with HA. This is stated also by Hartmann et al.

(64), as an amorphous phase precipitated on HA surface produces a structured diffuse X-ray background hard to analyze and the only crystalline phase detected by XRD is HA.

The minimum reduction in the intensity of HA peaks observed in our XRD spectra might be an indication of HA dissolution and it, also, could indicate an increase in metals sorption on HA. The reduced peak intensity due to from the metal sorption on HA surfaces causes an increase of mass absorption coefficient of X-rays upon adsorption of metals (McKenzie *(104)*). The two distinctive shoulders at 2.76 and 2.78 Å from the peak of 2.79 Å could be an indication of coprecipitation of HA with other metals (Bigi et al. *(12)*; and Hettiarachchi et al. *(69)*)

Comparing the values of lattice parameters, *a* and *c* from our solid materials with these of the starting HA, we observed, generally, an increase in *a* values and a decrease in *c* values, even though few of the analyzed solid materials show the opposite situation depending on the increasing of the original heavy metal concentration as observed also by Fedoroff et al. *(53)*. We can only infere that the little differences in the crystal lattice parameters between the starting HA and the solid residues implies that heavy metals are present in the latter as suggested also by van der Houwen et al. *(148)*. Brückner et al. *(23)* stated, in case of amorphous Pb precipitation, the metal might substitute for Ca, determining a distortion from the orginal HA at medium (100 mg/L) Pb concentration, with Pb^{2+} preferably occupying site (2) and Ca^{2+} ion site (1); on the other hand, at higher Pb concentrations (500 mg/L) the enlargement and the distorsions of the unit cell doesn't appear, and the structure of the Pb-hydroxyapatite is similar to that of the original HA. Moreover, Suzuki et al. *(142)*, stated that Pb ions in solutions are easily ion-exchanged with Ca occupying both the sites with no distinction from their refinement study, even though the ionic radius of Pb (1.20 Å) is larger than that of Ca (0.99 Å).

On the other hand, elements such as Cd can substitute for Ca (2) and increasing the concentration and the temperature (75°C) the metal can occupy both Ca (1) and Ca (2) sites *(53)*. Similar statement for batch experiments sorption was from Mc Grellis et al. *(103)*, as at room temperature Cd is found in Ca (2) and increasing the temperature (72°C) there are more Cd in Ca (2) sites. In case of slow introduction experiment, the distribution is inverted and the observed decrease of the cell parametres is caused by the occupancy of Ca (1) sites. In particular, in case of calcium - cadmium – hydroxyapatite precipitation, Ca (2) is more substituted. Moreover, the progressive Cd introduction induce

a greater decrease of *a* than *c*, which explains the deformation of the cell according to Lacout et al. *(80)*.

We, usually, observed a decrease of *c* parameter for the solid material in both the single metal and multi-metal systems, but the *a* parameter shows either an increase and a decrease, and the initial metal concentration seems not to be the key factor. The difference in the lattice parameters we observed are likely caused by the impurities, with a destabilizing effect. In particular, the decrease of the *c*-axis parameter in the solid material with respect to the starting HA allows to suppose substitutions on OH positions in channels along *c*-axis, combined with the presence of $(HPO_4)^{2-}$, CO_3^{2-} and associated charge-balancing calcium affecting the cell properties as suggested by van der Houwen *(148)*.

We might infer that the interaction with the heavy metals cause small changes, notwithstanding the PO_4^{3-} tetrahedron is closer to the one of the starting HA. Moreover, we didn't observe an increase in the peak intensity as in Cao et al. *(25)*, but we detected peaks at 2.96 and 3.19 Å which may represent mixed Ca-heavy metal phosphates in agreement with Cotter-Howells and Thorton *(35)* and Laperche et al. *(82)*.

7.2 FTIR ANALYSES

In general, the FTIR spectra of the precipitates formed both in single- and multi-metal systems are comparable to those of the original HA, suggesting no other phases formed during the heavy metal sorption.

In particular, amorphous calcium phosphate gives a broad and symmetrical single absorption band in the region 500-600 cm^{-1}, while the anisotropic crystalline apatite partially splits the degeneracy of this absorption band into a well-defined doublet. Some of the absorption bands (630 cm^{-1}) are interpreted as a shoulder indicating a poorly crystalline phase *(146)* and in our FTIR spectra only the single band is visible, nor the split.

The ν_1 phosphate band is a small one attributed to P-O-P groups linked with large metaphosphate rings and this one is indicative of crystalline calcium phosphate *(136)*. It appears as a shoulder on the ν_3 phosphate band.

Xu et al. *(152)* suggested that the identical IR spectra argued against the dominance of coprecipitation at the end of the sorption reaction; in this view, on the basis

of our data it might be possible to infer the adsorption and/or the superficial complexation as probable sorption mechanisms.

7.3 SEM ANALYSES

From SEM images it is possible to infer the absence of pyromorphite, in fact the classical esagonal shape *(89)* of HP is not visibile, but EDS spectra confirm the presence of ions.

Observing the solid materials from the interaction with HA, particles presents a spherical shape as HA, not showing the features resembling needles which were commonly found when Pb reacted with HA. The same morphological characters are reported from the solid materials interacted with FAP and MAP. Any kind of different features is found from the original phosphates and the solid materials after the interaction. The SEM micrographs from FAP and MAP show edge particles, either before and after the interaction.

Generally, the solid material showed white spots spread on the phosphates, corresponding to the heavy metals adsorbed on the surface and confirmed from the EDS spectra as reported also by McGrellis et al. *(103)*.

In contrast with the findings of Lower at al. *(89)* our SEM data don't suggest sample ageing effects, that is the length and width of the particles are almost similar for the four different times, there is no a decreasing in the dimensions of the shape which would mean a transformation to a more stable morphology, which is in contrast from what said by Steefel and Van Cappellen *(137)* increasing the interaction time occurs a gradual increase in the size due to the Ostwald ripening, in our case the size is almost constant. Moreover, we didn't observe the increasing of the particle size according to the pH as Laperche et al. *(82)*; in particular, under acidic and neutral pH, particle dimensions for the three phosphates don't change comparing with the dimensions of the amendant used for the interaction.

Moreover, the saturation is proportional to the concentration of the heavy metals, so at high concentration (500 mg/L) corresponds high saturation state and a rapid precipitation of numerous small nuclei, at intermediate concentration (100 mg/L) well defined crystall might precipitate, decreasing the concentration the precipitation is slow till the heterougenous precipitation. In this case, it is not possible to be certain about the HP

precpitation, but heterogenous Pb-phosphate phase on phosphate amendants might have crystallized (Lower et al. *(89)*). In particular, increasing the initial concentration of the heavy metals, after the interaction with the phosphates, the initial shape is always present. It may suggests that the original structure of the phosphate host exerts a controll on the nucleation process and also the microtopography, in effect the particles are on the surface features, probably defects can help the dissolution/precipitation mechanism providing sites with a decreased adsorption energy (Manecki et al. *(100)*). No particular orientation was observed after the interaction, which could suggest the way the particles grew, probably the direction is toward the source of the heavy metals as phosphate anions were consumed from the phosphate dissolution. Generally the growth is perpendicular to the *c* axis leading to an undersaturated state respect the phosphate and consequently the phosphate dissolution continue till the heavy metals were not removed from solution (Lower et al. *(90)*).

According to Lower at al. *(89)*, the presence of round edges, on the surface of HA particles suggests bulk-transport controlled dissolution. The absence of the hesagonal shape might make think that the dissolution and precipitation phenomenon didn't happen or only poorly - to - amorphous phase is precipitated. The non-needle shape indicates an heterogeneous precipitation of HP on HA. Furthermore, Ma et al. *(94)* stated that the precipitation of the non-crystalline phase or the absorption, which occurred near the phosphate surface, it is due to the constant solubility of the heavy-metal minerals was probably exceeded due to locally high P concentration.

Perhaps from our solutions at room temperature and low concentration the precipitated amorphous phase is the form ACP1 (amorphous calcium phosphate) with a spherical morfology. The flakes might indicate a poor crystalline phase, this difference is possibly due to the solution composition and especially pH which controlls the speciation as stated from Abbona and Baronnet *(1)*.

From the SEM micrographs we could infer a precipitation mechanism of a non crystalline HP or heavy-metal phosphate, but, also other mechanism are important like ion exchange, surface complexation and adsorption.

7.4 AFM ANALYSES

Atomic Force Microscopy (AFM) was used to decipher the uptake mechanism of heavy metals, as it allows imaging mineral surfaces in aqueous solutions to a molecular scale, thus enabling us to observe the formation of any new phase on the unit cell scale.

The solid materials, show always rounded particles not showing any features resembling needles, characteristic of the HP, neither the absence of etch pits on the surface suggesting a bulk-transport controlled dissolution *(11 and 89)*.

In particular, the FAP images show a different shape compared to the SEM micrographs, probably because SEM was unable to achieve high enough resolution to detect the FAP rounded surface imaged with AFM.

However, collecting stable images, the surface of HA and FAP particles revealed crystallographic indistinct features, suggesting that HP didn't precipitate, in agreement with the results from XRD and SEM-EDS analyses, but in contrast with other studies *(89, 90 and 100)*. Therefore other sorption mechanisms are involved in the sequestration of heavy metals from the solutions, confirming the type of phosphate, exerts a control on the sorption process and the sorption capacity can vary according to different experimental conditions, sample preparation as stated from Manecki et al. *(100)* and Da Rocha et al. *(37)* and the characteristics of the phosphate itself *(93)*.

From the Qs values and the isotherm curves it is possible to hypothesize a non-crystalline precipitation of a new phosphatic phase so that upon the nucleation HA or FAP particles in the solution would become temporarily depleted in the heavy metals and phosphate, the process can be based on the heavy metal immobilization and the P diffusion from the HA or FAP dissolution, subsequently a combination of the phosphate with the heavy metals. Probably the precipitation can terminate because of an isolating un-reacted HA core (Valsami –Jones et al. *(147)*).

7.5 EFFECT OF SORBENT AMOUNT

The amendants were the HA, FAP and MAP and all of them reduced the concentration of the heavy metals in the solutions or their bio available fraction in the soils.

Concerning the use of HA to immobilize heavy metal in the aqueous solutions, with the increase in the amount (0.1 and 0.2 g), the amount of sorbed heavy metal also

increases. HA was effective in removing heavy metals, in particular for Zn as previously observed by Ma et al. *(95)*, while the effectiveness of HA is slightly lower in reducing Cd and Cu with their increasing initial concentrations.

In case of the multi-metal system, all metal concentrations in solution decreased after the reaction with HA and each heavy metal was highly immobilized. Contrarily from what stated by Ma et al. *(94)*, the presence of more heavy metals in the same solution didn't inhibit the immobilization of the cations, except few cases already described in chapter 6. The effectiveness in the immobilization can be reduced in both systems by the competitive effects: internal competition, competition with H^+ and competition with each other for the adsorption sites and for precipitation (Corami et al. *(33)*).

The effectiveness of the two phosphate rocks (FAP and MAP) in reducing heavy metals varied considerably.

As expected, FAP was effective in retaining the four heavy metals in the single-metal system; the only exception is Zn retention at highest concentration, where a desorption phenomenon is observed, due to the Zn content in the FAP itself. On the other hand, in the multi-metal system, where the concentration of Pb and Zn are constant, the retention of the four heavy metals decreased with respect to HA results because of the original contents of the heavy metals in the FAP. This phenomenon can be explained taking into account the competitive sorption for the adsorption sites among the ions of the heavy metals and H^+.

The lower removal efficiency of FAP compared to HA can be attributed to its lower solubility and purity. The phosphate rock from Morocco, MAP, was more effective than FAP in immobilizing the heavy metals in a multi-metal system.

Comparing the chemical composition of FAP and MAP, we observed the amounts of P_2O_5 are almost similar, whereas the concentrations of the four heavy metals are really different. MAP shows a major amount of these heavy metals, and, notwithstanding the high concentration of the cations, the retention is better than FAP. If one of the main factors affecting the sorption properties is the specific surface areas (SSA) (Peld et al. *(122)*), MAP must have a bigger SSA than FAP so that MAP is more effective in the immobilization than FAP.

The solubility is the other factor which influences the immobilization, more the amendant is soluble and more P is released to immobilize the heavy metals.

According to Ma et al. *(96)* and Saxena et al. *(132)* with the increase in the amount of added phosphate rock the percent adsorption of metal ions also increases. From our data it is possible to infer that also time is a control factor besides P content. In particular, at the equilibrium P concentration in the solution is generally low, suggesting that part of P can be used for the precipitation of a new phosphate and/or heavy metals are sorbed on the phosphate surface and it is not possible further phosphate dissolution and the precipitation of the new phase.

7.6 EFFECT OF INITIAL METAL CONCENTRATION

Concerning the single metal system vs. HA and FAP, the initial concentration seems to be the main parameter only for Zn retention. In particular, as already seen, at the highest concentration Zn is better immobilized by HA *(95)*, whereas Zn is not immobilized by FAP at the highest concentration. In the multi-metal system vs. HA only in two cases Cd is not well immobilized due to the competitive sorption rather than its initial concentration (10 mg/L), whereas the multi-metal system vs. FAP and MAP the initial heavy metal concentration is more incisive for the immobilization, moreover competitive sorption is proportional to the initial heavy metal concentration as Basta and Tabatabai *(8)* suggested.

7.7 EFFECT OF CONTACT TIME

Time seems to be an important factor for the immobilization in the single system vs. HA, but Pb. In fact the reaction among HA and Pb is very fast as already said (Ma et al. *(93)*), less than two hours. Increasing the heavy metal concentration, the long interaction time (24h and 48h) is more successful for sorption, as Ma et al. *(96)* observed that a smaller increase in heavy metal removal was obtained by increasing the time. This is not true for the single system which has interacted with FAP where the time is more important, that is increasing the time it is achieved a high percentage of immobilization. For the multi-metal system vs. HA, contact time is not a decisive factor, in the other two multi-metal systems (vs. FAP and MAP), time is fundamental to achieve a good immobilization of the four heavy metals, suggesting a stable equilibrium is achieved (Ma, *(97)*).

It is observed also that heavy metal concentrations increase in some aqueous suspensions, either single metal and multi-metal system, then the concentration decreases, this can be explained considering heavy metal extractability; therefore increasing the contact time the metals were transformed to less extractable fractions after long incubation (Ma et al. *(98)*).

7.8 EFFECT OF pH

In order to simulate the true environmental conditions in case of the remediation of polluted water and soil, where the pH control is either not applicable, or not necessary or hard to be realized (e.g. Raicevic et al. *(127)*)., in the present study no effort was made to modify the solution pH during the experiments and no ionic strength was imposed. The initial pH of the metal solutions and final pH of the filtrate at adsorption equilibrium were measured for each metal concentration.

Generally, the sorption mechanism is pH dependent and in particular, the quantity and crystallinity of the products, from the interaction between the solution and the amendant, decreases with the increasing of pH (Chen et al. *(30)*). Moreover, the solubility of the phosphate is pH dependent, showing low solubility at high pH (Cao et al. *(24)*) and Chen et al. *(30)*), and the pyromorphite which could be formed is also pH dependent (Chen et al. *(29)* and Hettiarachchi et al. *(68)*).

Our pH values usually range from 6-7 in all the multi-metal systems, showing a variation less than ± 1 unit (about 0.5-0.7 unit) from the initial value to the final one, in contrast with other results where a significant decrease of pH values was observed (about 1.5 unit) as in Cao et al. *(26)* and Xu et al. *(152)*.

These high pH values suggest a low solubility of the phosphates. Nevertheless, HA shows high values of immobilization, and also for FAP and MAP, except in the two multi-metal systems where Pb and Zn are constant, the immobilization is generally good. Because of the low solubility, it could be possible the dissolution/precipitation is a rare sorption mechanism than the surface complexation and the ion exchange process, confirming the results of Boisson et al. *(15)* showing more HP is formed at pH 5 than at pH 6 or 7.

7.9 SORPTION ISOTHERM

Sorption isotherms suggests information about the sorption mechanism and the strength by which the sorbate is held onto the phosphate (Morera et al. *(110)*).

Generally, the isotherms for the single-metal systems and the multi-metal systems are the L type subtype 2, the subtype means the theoretical monolayer has been completed as defined from Echeverria et al. *(49)*. This isotherm is characterized by a steep initial slope that level off as the equilibrium concentration of metal increases, giving rise to a plateau or a linear section of positive slope. According to Giles et al. *(62)* the L2 type occurs probably in the majority of cases of adsorption from a dilute solution. The initial slope depends on the rate of change of site availability with increase in solute adsorbe. As more solute is taken up, there is usually progressively less chance that a bombarding solute molecule will find a suitable site on which it can be adsorbed.

Implying either that the adsorbed solute molecule is not vertically oriented or that there is not strong competition from the solvent.

Furthermore, there are also two particular curves, the H type and the C type. The former is a special case of L curve. The solute has such high affinity that in dilute solutions it is completely adsorbed, or at least there is no measurable amount remaining in solution. The initial part of the isotherm is therefore vertical. The conditions for this particular curve are a substrate with region of different degree of crystallinity, a solute with higher affinity for the substrate than the solvent has and a better penetrating power into the crystalline region of the substrate. The linearity shows the number of sites for adsorption remains constant, as more solute is adsorbed, more sites must be created. The process stops when more highly crystalline region of the substrate are reached (Giles et al. *(62)*). The latter curve suggests a constant partition of solute between solution and substrate, right up to the maximum possible adsorption, where an abrupt change to a horizontal plateau occurs. The isotherm usually do change direction to give the horizontal plateau, the solute is penetrating regions inaccessible to the solvent (linear isotherm). The shape of the L2 isotherm suggests as a sorption mechanism the surface precipitation and the adsorption according to Stumm *(139)*. The H sorption isotherm suggest a phenomenon of precipitation according to Echeverria et al. *(49)* confirming what Ma proposed for Pb (Ma

et al.*(93, 94 and 95)*). However precipitation phenomenon takes place also for the other heavy metals in the multi-metal systems, either vs. HA and MAP.

7.10 MOLAR RATIO

The molar ratio (Q_S) is the ratio of the bound cations to the cations released from the amendant. In particular, the values of the ratio can be $Q_S = 1$, that is ion exchange between the cations of the amendant and of the solution; $Q_S > 1$ suggesting a surface complexation mechanism, filling the vacancies in the amendant and finally $Q_S < 1$ suggesting the dissolution and precipitation mechanism (Peld at al. *(121 and 122)*).

Our data show a Q_S ranging from a value < 1 and > 1, and in some cases >> 1. The phenomenon of dissolution and precipitation occurs at low initial metal concentration in the single-metal system, for the multi-metal system vs. HA and for the other two multi-metal systems in few cases, whereas the adsorption mechanism prevails in the multi-metal system. Discerning the right sorption mechanism is difficult because the different mechanisms may occur simultaneously, as in the multi-metal system. Peld et al. *(122)* stated that if the mechanism of dissolution/precipitation implies the precipitation of a solid with a structure like the original amendant (eg. our HA), the mechanism cannot be distinguish only on the basis of Q_S. In particular, the ion exchange mechanism is the more probable confirmed by the results of our XRD and FTIR analyses, in fact the solid materials retain the same structure as the amendant used for the immobilization, in agreement with Peld et al. *(121)*.

Although the same experimental conditions have been used the same for single- and multi-metal system the sorption mechanism is different according the chemical characteristics of the phosphate, so we distinguish the dissolution/precipitation and the surface complexation mechanism.

7.11 SORPTION MECHANISMS

From the sorption isotherms, the molar ratio (Q_S) and the results of XRD and SEM analyses it is possible to infer the suitable sorption mechanism for each heavy metals in the two systems.

Our results suggest that Cd immobilization by phosphate (HA, FAP and MAP) involved two different processes that occurred simultaneously (Peld et al. *(121)*),

complicating the main sorption mechanism's identification. In particular, when the initial metal concentration was low, the Q_s values suggest that Cd removal depended mainly on phosphate dissolution and precipitation of a new phosphate phase. As XRD analysis did not detect any new crystal phase in the solid residues, we could propose that in our experiments the formation of an amorphous Cd-containing phase occurred, in agreement with other experimental findings (Lusvardi et al. *(92)*). On the contrary, for high initial metal concentration Q_s values indicate that Cd immobilization is mainly due to non-stoichiometric sorption on the phosphate surface. These conclusions are supported also by the results of FTIR analysis as the spectra of the blanks and the solid residues are identical and OH and PO_4 peaks well overlapped with the same HA peaks (Farmer *(52)*).

According to Raicevic et al. *(127)*, the overall removal of Cd by phosphate appears to be due to a two-step mechanism. The first step involves the dissolution of phosphate and the formation of a new stable Cd-apatite on the phosphate surface. In the second step, the diffusion of Cd ions inside the phosphate crystal lattice through the ion exchange occurs. Fedoroff et al. *(53)* have shown that ion exchange leads to the formation of a (Cd-Ca) solid solution. However, true exchange equilibrium is certainly not achieved during the time intervals usually used in standard sorption experiments. Further support to the two-step mechanism involving also ion exchange is provided by our XRD results showing a significant broadening in the X-ray diffraction peaks, suggesting Ca/Cd exchange as showed by Bigi et al. *(13)*.

The shape of the sorption isotherms for Cu, either in single- and binary-metal systems, suggests surface adsorption or complexation mechanisms (Echeverria et al. *(49)*; Cao et al. *(26)*), whereas Q_S values suggest the dissolution/precipitation process for low initial concentration and then the values increase indicating the surface adsorption or complexation as sorption mechanisms. Our data are consistent with the conclusions of previous studies (Xu et al. *(152)*; Echeverria et al. *(49)*; Cao et al. *(26)*), suggesting that the most important sorption mechanism for Cu involved surface complexation and coprecipitation with Ca into the phosphate structure instead of formation of new metal phosphates.

The substitution of Ca by other cations in phosphate crystal structure is well known in natural apatites (Xu et al. *(152)*). However, LeGeros and LeGeros *(86)* concluded that cations with ionic radii smaller than Ca^{2+} (0.99 Å) may be incorporated in the apatite

structure to a lesser extent than cations of larger ionic radii. Therefore, Cu^{2+} (0.81 Å) coprecipitation with Ca could be unlikely. This explanation is consistent with our results as Q_s values are usually > 1, indicating that the main sorption mechanism was surface complexation. The XRD analyses did not detect any new mineral formation in the solid residues arguing against the hypothesis of ion exchange mechanism as, if we assume that all the amount of Cu removed from the solutions was incorporated in phosphate through ion exchange, this could determine a significant broadening in the X-ray diffraction peaks, as Bigi et al. *(13)* showed. Therefore, when aqueous Cu is mixed with phosphate, surface complexation on the phosphate surface is the main mechanism.

Pb sorption isotherm are either the L2 type and the H type, the former being characteristics in the multi-metal systems and in the single-metal system vs. FAP; on the contrary, only the single-metal system vs. HA shows the H isotherm. The H type isotherm suggests the dissolution/precipitation mechanism. According to Ma et al. *(93 and 96)*, this type of sorption process is the main mechanism for the immobilization of Pb through phosphate, also as natural rock. However, if the solutions contains other cations, there is the possibility of other sorption mechanisms rather than the precipitation (Ma et al. *(95)*), and the precipitated hydroxypiromorphite, could be a poor- to crystalline phase (Ma et al. *(95)* and Lower et al. *(89)*). From our XRD and SEM data it wasn't possible to determine the precipitation of a crystalline product, and therefore, in case of the single-metal system vs. HA, it is possible to suggest the precipitation of a poor-crystalline product. Our Q_S data confirm this phenomenon for low Pb concentration (10 mg/L), and increasing the metal concentration Q_S values suggest other mechanisms such as the surface complexation and the adsorption. Moreover, previous studies suggested that ion exchange and adsorption were responsible for sorption of this metal on HA (e.g. Suzuki et al. *(141 and 142)*; Takeuchi and Arai *(143*). In any case, it is still unknown to what extent these processes can be involved in the immobilization of Pb by HA. As already said, it is difficult to quantify the relative contribution from each of the mechanism that is responsible for metal removal and it could be probable the mechanisms may work together.

Like Cu, the shape of the sorption isotherms for Zn suggests surface adsorption or complexation mechanisms. These processes are also suggested by the analysis of molar ratios values. Our Q_s > 1 are consistent with the conclusions of previous studies (Xu et al.

(152 and Echeverria et al. *(49)*), suggesting that the main sorption mechanism is surface complexation and coprecipitation with Ca into the phosphate.

Moreover, taking into account the conclusion of LeGeros and LeGeros *(86)* Zn^{2+} (0.83 Å) coprecipitation with Ca could be unlikely.

According to Xu et al. *(152)* and Wu et al. *(150)* when aqueous Zn was mixed with phophate, surface complexation occurred on its surface, displacing partially the H^+ ions and resulting in pH reduction. With Zn in solution, the following reactions may occur:

$$\equiv POH + Zn^{2+} = \equiv POZn^{+} + H^{+} \quad (1)$$

$$\equiv PO^{-} + Zn^{2+} = \equiv POZn^{+} \quad (2)$$

According to Wu et al. *(150)*, the eq. 1 should dominate over the experimental pH range, with contribution from reaction 2 for lower pH values of the range.

In this view, the critical mechanism of overall removal of Zn from solutions involved surface complexation with phosphate functional groups.

Anyway, more information about the sorption mechanism can be obtained from the amount of Ca and P in solution. Generally, their concentration is not proportional to the amount of the retained heavy metal, suggesting a non-stoichiometric phosphate dissolution, which confirms the surface complexation or adsorption mechanisms.

8 DESORPTION

In order to determine the stability of the heavy metal sorption by phosphates (HA, FAP and MAP), desorption experiments were carried out. Three extracting solutions at different pH (4, 5, 6) diluting concentrated HNO_3 and HCl were used. This pH values correspond to regularly leaching tests and open CO_2 leaching system (eg. landfills) as suggested by Crannel et al. *(22)*. The solid residues used in these experiments were those which had reacted with the heavy metals at the highest concentration (500 mg/L) and the desorption tests were carried out for 24h in both single- and multi-metal systems. The slurries were filtered and the solutions analyzed for Pb, Zn, Cu, Cd, Ca and P. pH was measured before the filtration.

The amount of heavy metal desorbed from phosphates depended on the extracting solutions (Tab. 1 and 2). Heavy metals were not desorbed significantly in the single- and multi-metal systems by both type of solutions showing very low values or even below the ICP-AES detection limits, indicating the stability of the sorption in aggressive leaching environment. Therefore, phases, formed during the sorption process, result insoluble and geochemically stable.

	HNO_3			**HCl**		
	pH = 4	*pH = 5*	*pH = 6*	*pH = 4*	*pH = 5*	*pH = 6*
Cd vs. HA	0.18	0.34	0.17	0.18	< 0.1	< 0.1
Cd vs. FAP	0.18	0.46	< 0.1	0.09	0.16	0.05
Cu vs. HA	0.02	0.29	< 0.1	0.04	< 0.1	< 0.1
Cu vs. FAP	0.16	0.19	< 0.1	0.10	< 0.1	< 0.1
Pb vs. HA	< 0.1	< 0.1	< 0.1	< 0.1	< 0.1	< 0.1
Pb vs. FAP	< 0.1	< 0.1	0.05	< 0.1	< 0.1	< 0.1
Zn vs. HA	< 0.1	0.12	0.13	0.24	0.08	0.15
Zn vs. FAP	0.01	< 0.1	< 0.1	0.08	0.01	0.03

Table 1: Amount (%) of desorbed heavy metals from the phosphate after the interaction with solution at different pH for some of the solid materials from the single-metal system.– Tabella 1: Percentuali dei metalli pesanti rilasciati dai fosfati dopo l'interazione con soluzioni a diverso pH per alcuni materiali solidi del sistema a metallo singolo.

	HNO_3				**HCl**			
pH = 4	Cd	Cu	Pb	Zn	Cd	Cu	Pb	Zn
Cd, Cu, Pb and Zn = 500 mg/L vs. HA	< 0.1	< 0.1	< 0.1	< 0.1	< 0.1	< 0.1	< 0.1	< 0.1
Cd, Cu, Pb and Zn = 500 mg/L vs. MAP	< 0.1	< 0.1	< 0.1	0.11	< 0.1	0.10	0.24	0.02
Cd, Cu, Pb and Zn = 500 mg/L vs. FAP	< 0.1	0.03	< 0.1	< 0.1	< 0.1	< 0.1	< 0.1	< 0.1
pH = 5	Cd	Cu	Pb	Zn	Cd	Cu	Pb	Zn
Cd, Cu, Pb and Zn = 500 mg/L vs. HA	< 0.1	< 0.1	< 0.1	< 0.1	< 0.1	< 0.1	< 0.1	< 0.1
Cd, Cu, Pb and Zn = 500 mg/L vs. MAP	< 0.1	< 0.1	< 0.1	< 0.1	< 0.1	0.16	< 0.1	0.05
Cd, Cu, Pb and Zn = 500 mg/L vs. FAP	< 0.1	< 0.1	< 0.1	< 0.1	< 0.1	< 0.1	< 0.1	< 0.1
pH = 6	Cd	Cu	Pb	Zn	Cd	Cu	Pb	Zn
Cd, Cu, Pb and Zn = 500 mg/L vs. HA	< 0.1	< 0.1	< 0.1	0.06	< 0.1	< 0.1	< 0.1	< 0.1
Cd, Cu, Pb and Zn = 500 mg/L vs. MAP	< 0.1	< 0.1	< 0.1	0.05	< 0.1	< 0.1	< 0.1	0.01
Cd, Cu, Pb and Zn = 500 mg/L vs. FAP	< 0.1	< 0.1	< 0.1	0.07	< 0.1	< 0.1	< 0.1	< 0.1

Table 2: Amount (%) of desorbed heavy metals from the phosphate after the interaction with solution at different pH for some of the solid materials from the multi-metal system.– Tabella 1: Percentuali dei metalli pesanti rilasciati dai fosfati dopo l'interazione con soluzioni a diverso pH per alcuni materiali solidi del sistema multi-metal.

Zn desorption increased with the pH of HNO_3 solution either in the single- and multi metal system, probably because an amount of the metal is weakly bound onto the phosphate as already seen for the batch experiments vs. FAP and MAP, where an increase in its concentration is observed at the equilibrium.

Cd desorption increased with pH of HNO_3 solution in the single-metal system, whereas its concentration in the solution is always below the detection limit for the multi-metal system. Cu desorption increased with pH of HCl solution in the single-metal system and its amount in the solution is almost below the detection limit for the multi-metal system. Pb desorbed is usually under the detection limit suggesting, even though Pb was not chemisorbed by precipitating as pyromorphite, it was adsorbed or complexed on the surface and strongly bound.

In particular, heavy metal behaviour is different for the HCl solution in the single-metal system, they show an increase in the desorption at pH = 5, as described in Peld et al. *(122)*, suggesting desorption depending on the anionic composition of the aqueous medium so that different processes are involved. Furthermore, Boisson et al. *(16)*, also confirmed that the use of HCl results in a greater desorption phenomenon compared to HNO_3.

The solid materials were analyzed by SEM-EDS, showing a shape of the particles close to the shape before the desorption experiments (Fig. 1 A and B), Moreover, EDS spectra confirmed the presence of the heavy metals (Fig. 2 A and B) in the solid materials. Our results are in contrast to what Xu et al. *(152)* and Cao et al. *(26)* stated, that is the amount of heavy metal desorbed increases with the decrease of pH, confirming heavy metals are strongly bound on the amendant we used for the sorption.

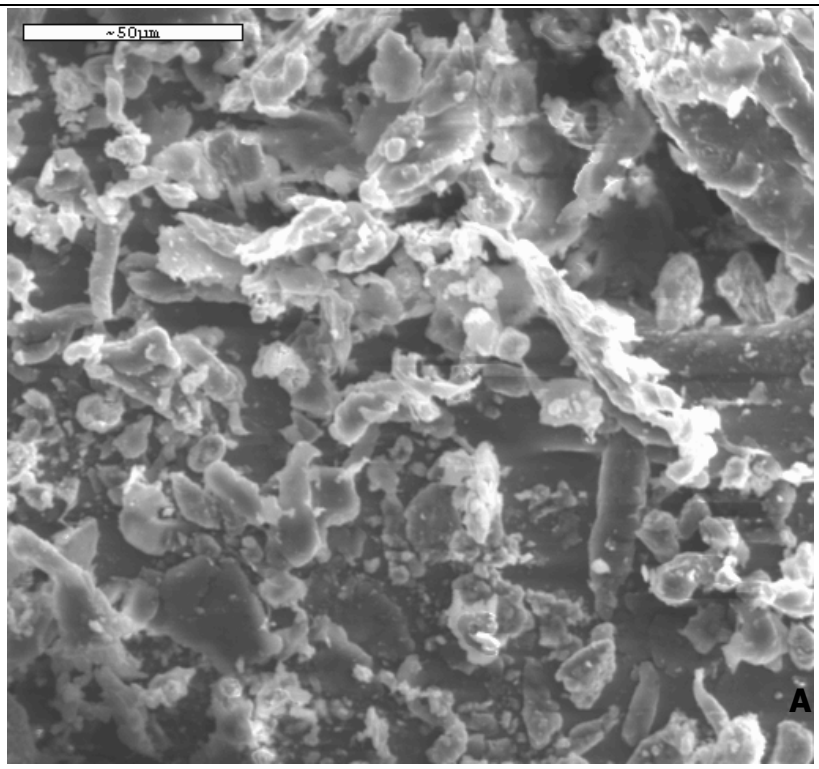

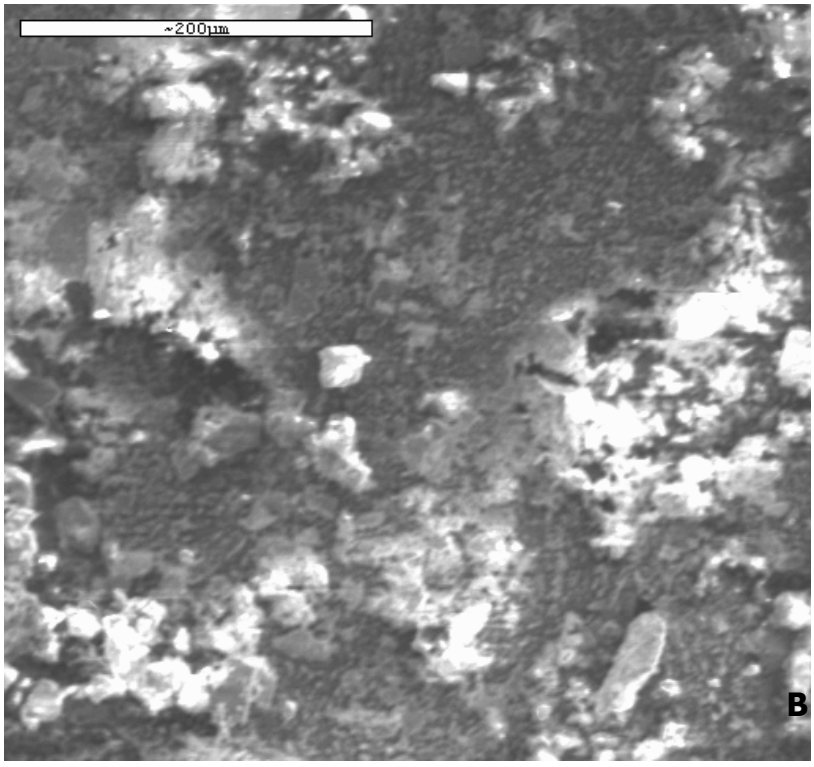

Fig. 1 SEM micrographs of solid materials from desorption experiments: A = Cd, Cu, Pb and Zn = 500 mg/L vs. MAP t = 24h pH = 4; B = Cd, Cu, Pb and Zn = 500 mg/L vs. FAP t = 24h pH = 5. - Fig. 1 Immagini al SEM dei materiali sottoposti alle prove di desorption A = Cd, Cu, Pb and Zn = 500 mg/L vs. MAP t = 24h pH = 4; B = Cd, Cu, Pb and Zn = 500 mg/L vs. FAP t = 24h pH = 5.

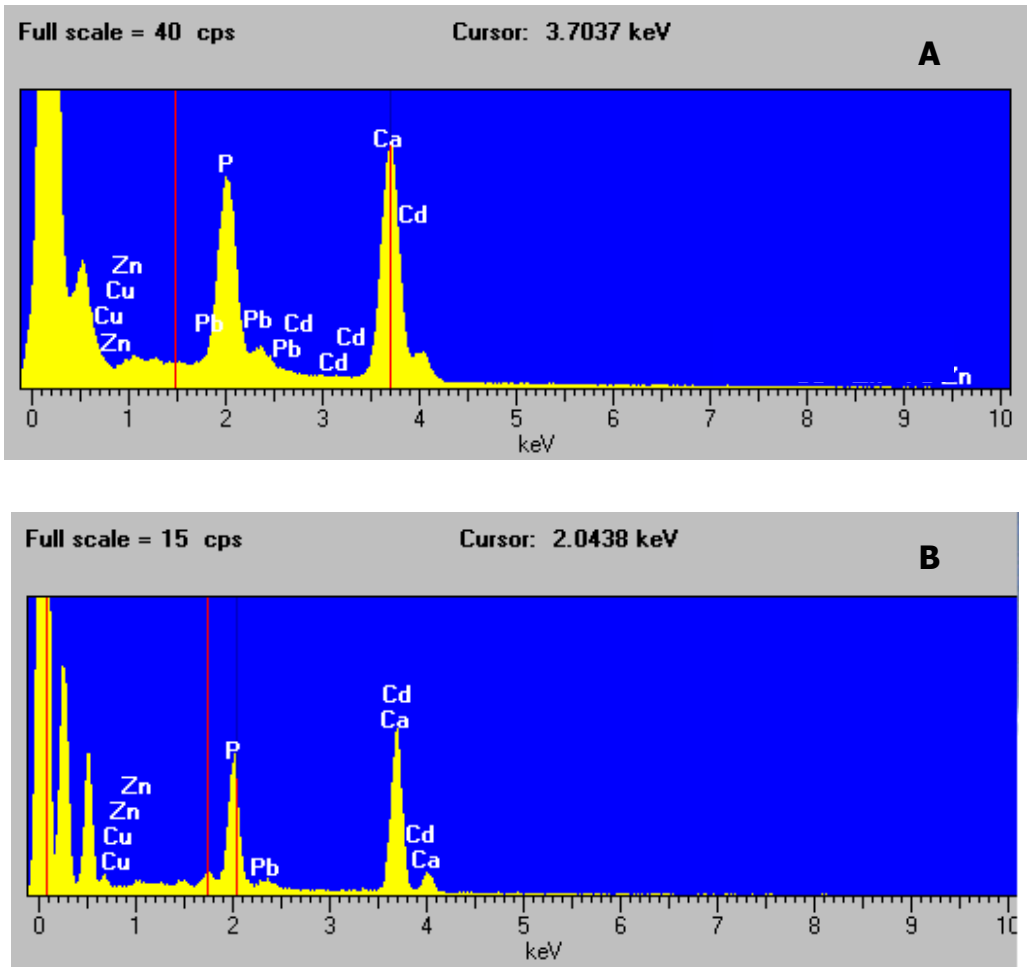

Fig. 2 EDS spectra of the SEM micrographs in Fig. 1. – Fig. 2 Spettri EDS delle immagini al SEM della Fig. 1.

9 SOILS

9.1 XRD

The starting soils are mainly composed by pyrite, chalcopyrite, sphalerite, galena, calcite, dolomite, feldspar and clay minerals.

The X-ray diffraction spectra (Fig. 1) of the soils after the sorption tests were very similar to those of the original samples, that is no other solid phase were detected. However, according to Laperche et al. *(83)* the presence of two peaks 2.87 and 3.19 Å might suggest the newly formation of Ca-heavy metal phosphate. Furthermore, multi-

metal phosphates can be formed with unknown peaks, or peaks broadening obscuring the identification of peak position as stated by Hettiarachchi et al. (69). In this view, Ma et al. *(95)* speculated that precipitation of amorphous to poorly crystalline metal phosphate can occur.

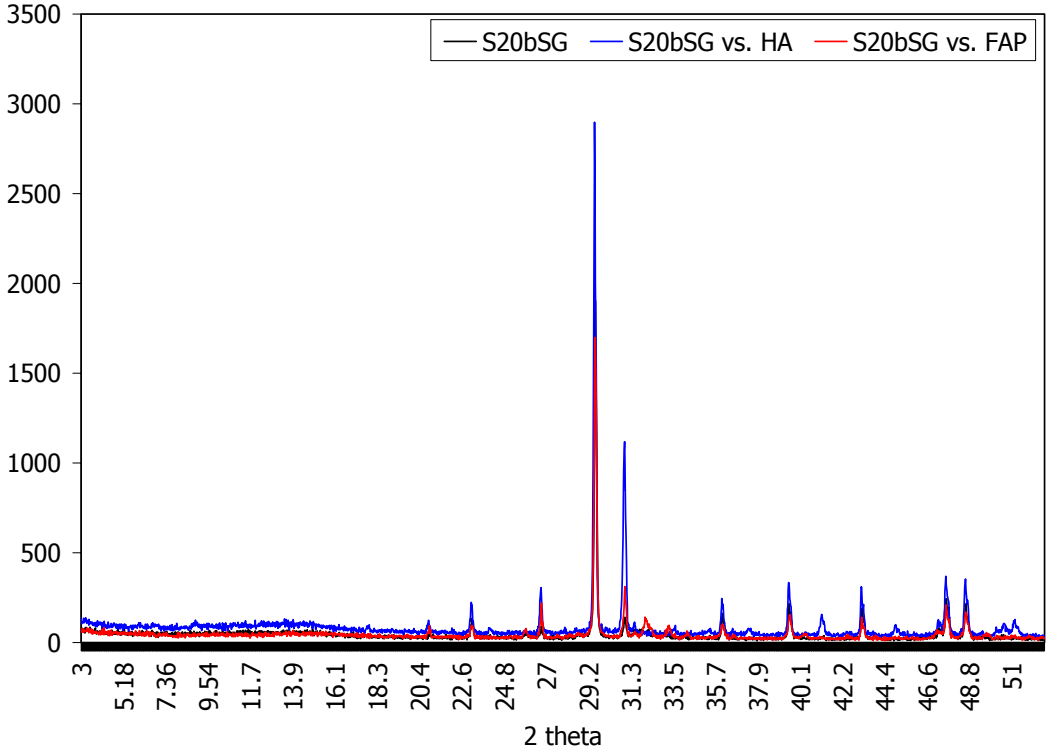

Fig. 1: Examples of XRD patterns of the starting sample soil (S20bSG) and after the interaction vs. HA and FAP. – Fig. 1: Esempio di un diffrattogramma di un suolo (campione S20bSG) prima e dopo l'interazione con HA e FAP.

9.2 ICP-AES ANALYSES

The efficiency of phosphates in immobilizing the heavy metals in the soils is generally very high (> 80%) (Fig. 2 A, B, C, D, E, F, G and H) and it doesn't depend on the amendant (Table 1 and 2). In only few cases some exceptions occurred. A particular situation is represented by a sample from Campo Pisano (S18aCP) after the interaction with FAP probably because the reaction of Pb and Zn immobilization was terminated and there was a desorption phenomenon of the metals.

Samples from Sardinia are from two depths (0 and 60 m) to determine if there could be a difference in the heavy metal concentration with the depth. Heavy metal concentration usually diminish with depth, whereas only one sample (S19bMP from

Monteponi mine) shows an increase in the metal concentration (see Table 3 in Materials). Finally the immobilization efficiency was high either using the synthetic HA either the FAP. The application of phosphates was found to reduce efficiently the extractable fractions of the heavy metals. P treatment was able to modify the partitioning of the heavy metals from the potential available fraction to the less available fraction as suggested by Melamed et al. *(105)*.

It is reasonable to assume that a possible sorption mechanism is the adsorption on the surface of the phosphate, in fact the XRD spectra, before and after the interaction, doesn't show any difference, suggesting deposition of new phosphate did not occur.

	Cd	Cu	Pb	Zn
S1G vs. HA	97.66	99.41	69.26	86.48
S2G vs. HA	98.56	99.72	98.40	98.97
S3G vs. HA	99.78	99.98	99.73	99.97
S5Gc vs. HA	96.06	99.96	99.74	99.61
S6Gc vs. HA	97.09	99.57	99.86	99.32
S7N vs. HA	96.14	99.66	98.51	95.24
S10N vs. HA	94.79	98.92	99.48	83.41
S11N vs. HA	94.04	99.80	99.27	99.35
S12N vs. HA	92.33	99.08	97.86	76.09
S13N vs. HA	96.23	98.81	99.14	96.85
S14B vs. HA	96.45	95.29	99.49	88.67
S18aCP vs. HA	97.48	94.43	-453.94	-173.51
S18bCP vs. HA	98.51	95.37	99.62	99.06
S19aMP vs. HA	99.25	93.99	99.94	99.75
S19bMP vs. HA	99.88	99.95	99.94	99.98
S19bMP vs. HA	99.89	98.66	97.47	88.41
S20aSG vs. HA	99.82	99.72	99.51	99.97
S20bSG vs. HA	99.69	99.37	99.87	99.97
S21FG vs. HA	99.98	99.85	99.96	99.94
S22MA vs. HA	99.95	99.99	99.58	100.00

Table 1: HA efficiency (%) of the heavy metal's immobilization in soils. – Tabella 1: Efficienza dell'immobilizzazione (%) dei metalli pesanti nei suoli da parte dell'HA.

	Cd	Cu	Pb	Zn
S1G vs. FAP	99.71	99.97	99.65	99.88
S5Gc vs. FAP	96.11	99.33	99.79	98.37
S6Gc vs. FAP	99.20	95.58	99.24	96.86
S7N vs. FAP	97.34	97.35	95.69	89.30
S11N vs. FAP	94.91	99.27	99.94	99.38
S14B vs. FAP	97.43	4.75	95.84	42.79
S18aCP vs. FAP	99.78	99.74	99.67	97.03
S18bCP vs. FAP	92.15	64.38	96.45	95.52
S19aMP vs. FAP	99.21	93.50	98.97	92.00
S20aSG vs. FAP	99.70	99.08	99.86	98.02
S20bSG vs. FAP	99.59	98.09	99.72	98.25
S21FG vs. FAP	96.37	98.09	2.64	84.99
S22MA vs. FAP	99.33	99.94	96.70	90.95

Table 2: FAP efficiency (%) of the heavy metal's immobilization in the soils. – Tabella 2: Efficienza dell'immobilizzazione (%) dei metalli pesanti nei suoli da parte della FAP.

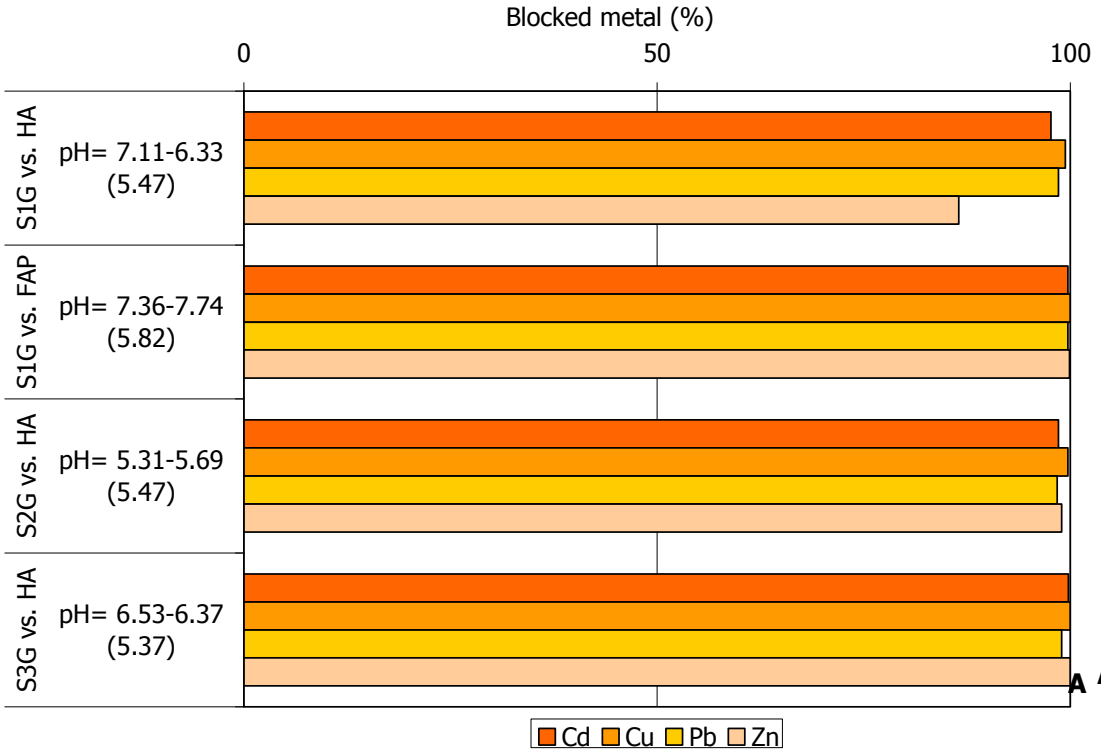

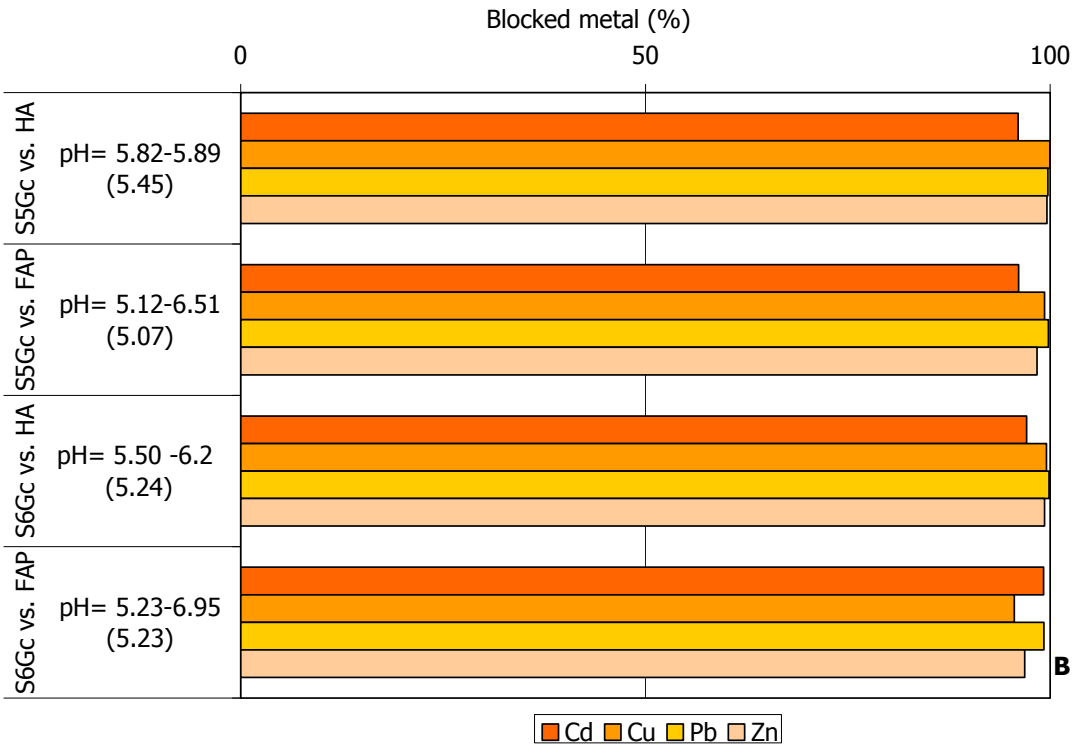

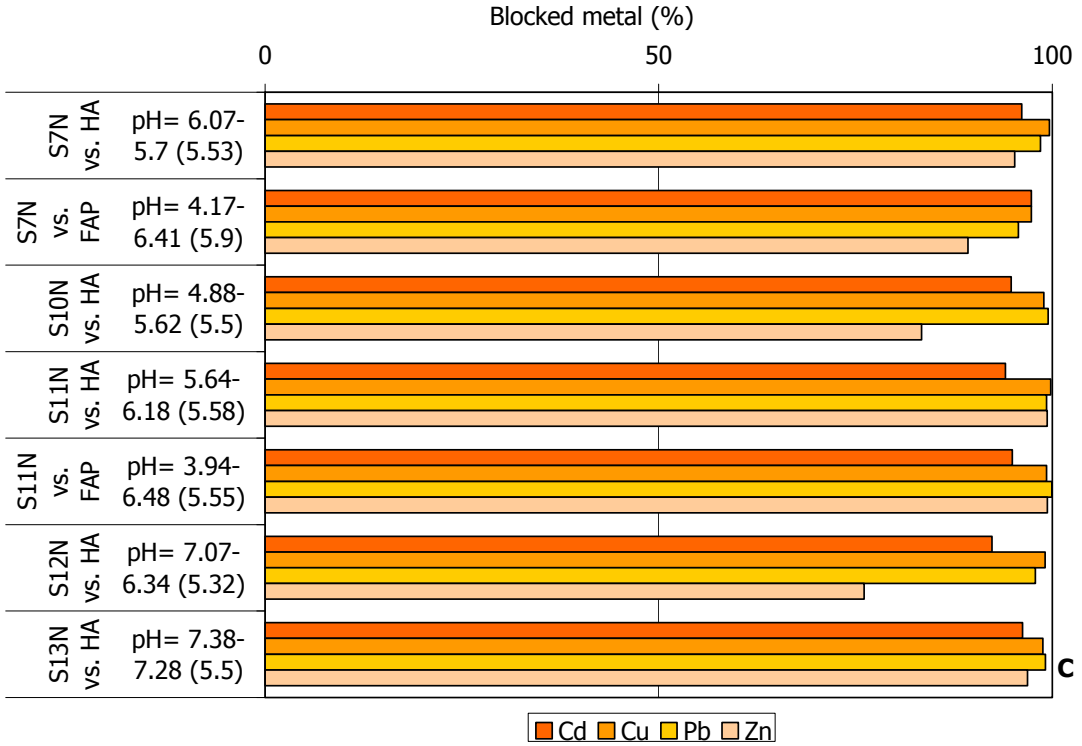
Blocked metal (%)
0
50
100
S7N vs. HA
pH= 6.07-5.7 (5.53)
S7N vs. FAP
pH= 4.17-6.41 (5.9)
S10N vs. HA
pH= 4.88-5.62 (5.5)
S11N vs. HA
pH= 5.64-6.18 (5.58)
S11N vs. FAP
pH= 3.94-6.48 (5.55)
S12N vs. HA
pH= 7.07-6.34 (5.32)
S13N vs. HA
pH= 7.38-7.28 (5.5)
C
Cd Cu Pb Zn

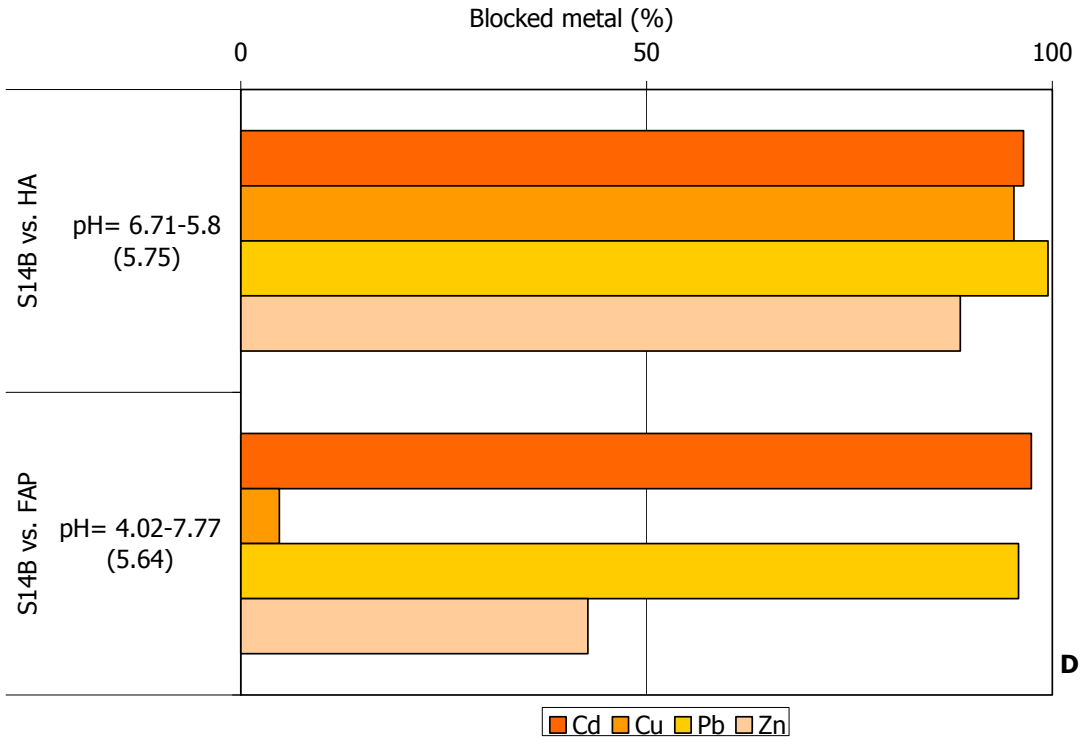
Blocked metal (%)
0
50
100
S14B vs. HA
pH= 6.71-5.8 (5.75)
S14B vs. FAP
pH= 4.02-7.77 (5.64)
D
Cd Cu Pb Zn

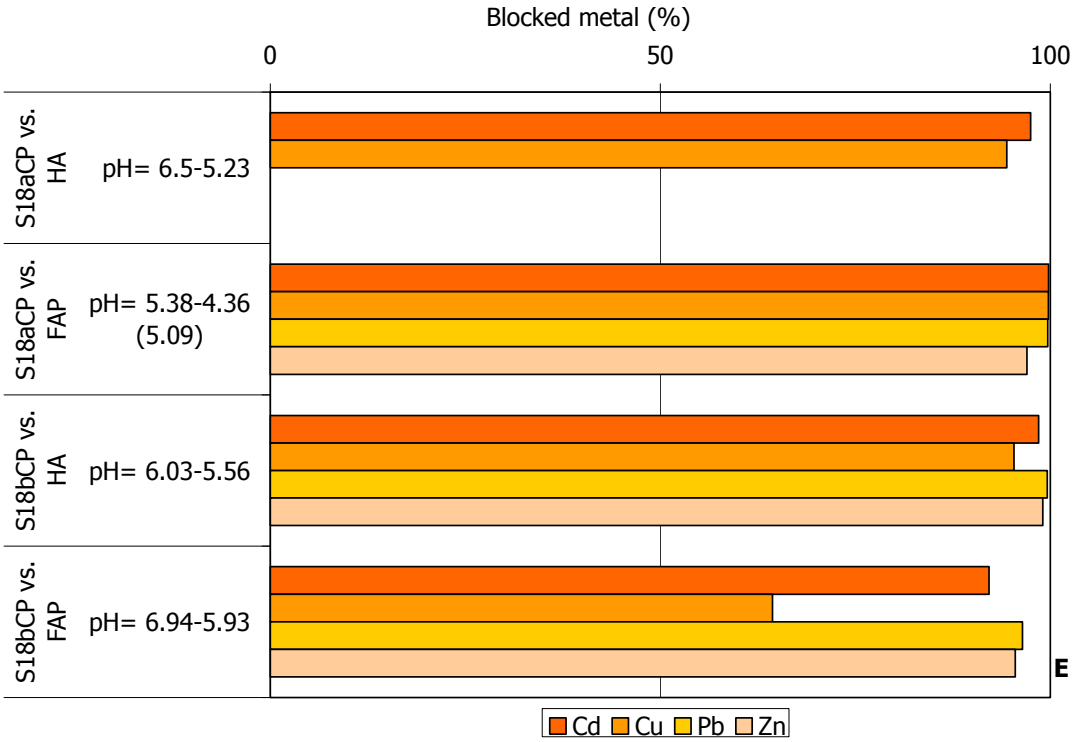
Blocked metal (%)
0
50
100
S18aCP vs. HA
pH= 6.5-5.23
S18aCP vs. FAP
pH= 5.38-4.36 (5.09)
S18bCP vs. HA
pH= 6.03-5.56
S18bCP vs. FAP
pH= 6.94-5.93
Cd Cu Pb Zn

E

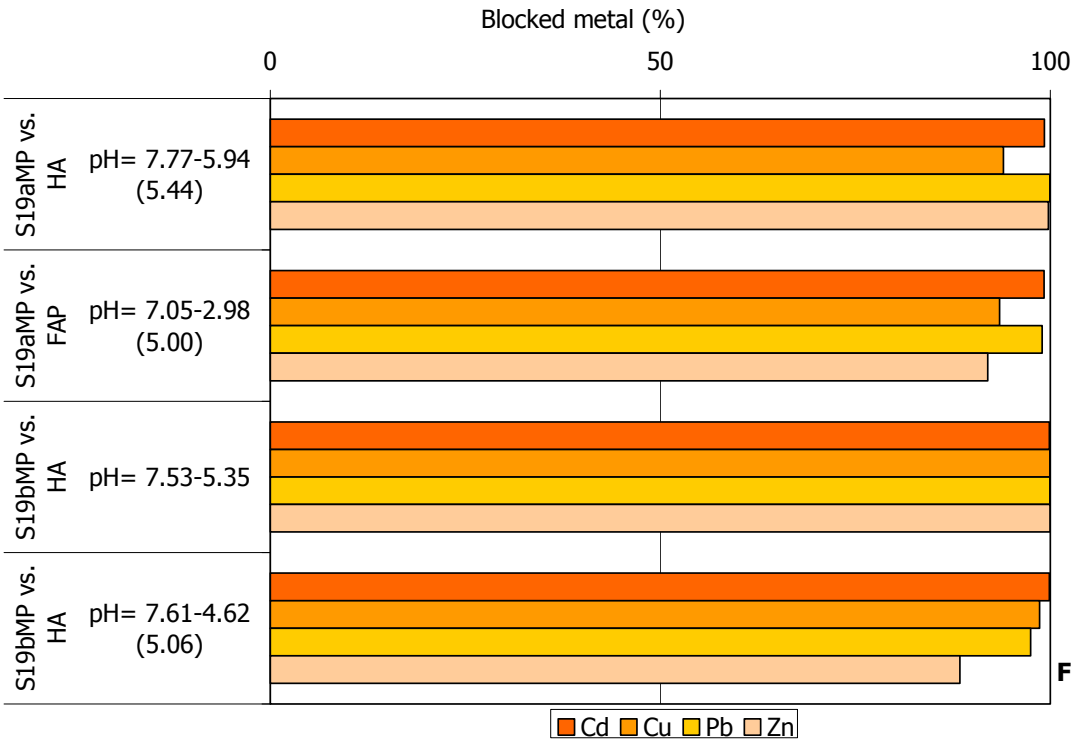
Blocked metal (%)
0
50
100
S19aMP vs. HA
pH= 7.77-5.94 (5.44)
S19aMP vs. FAP
pH= 7.05-2.98 (5.00)
S19bMP vs. HA
pH= 7.53-5.35
S19bMP vs. HA
pH= 7.61-4.62 (5.06)
Cd Cu Pb Zn

F

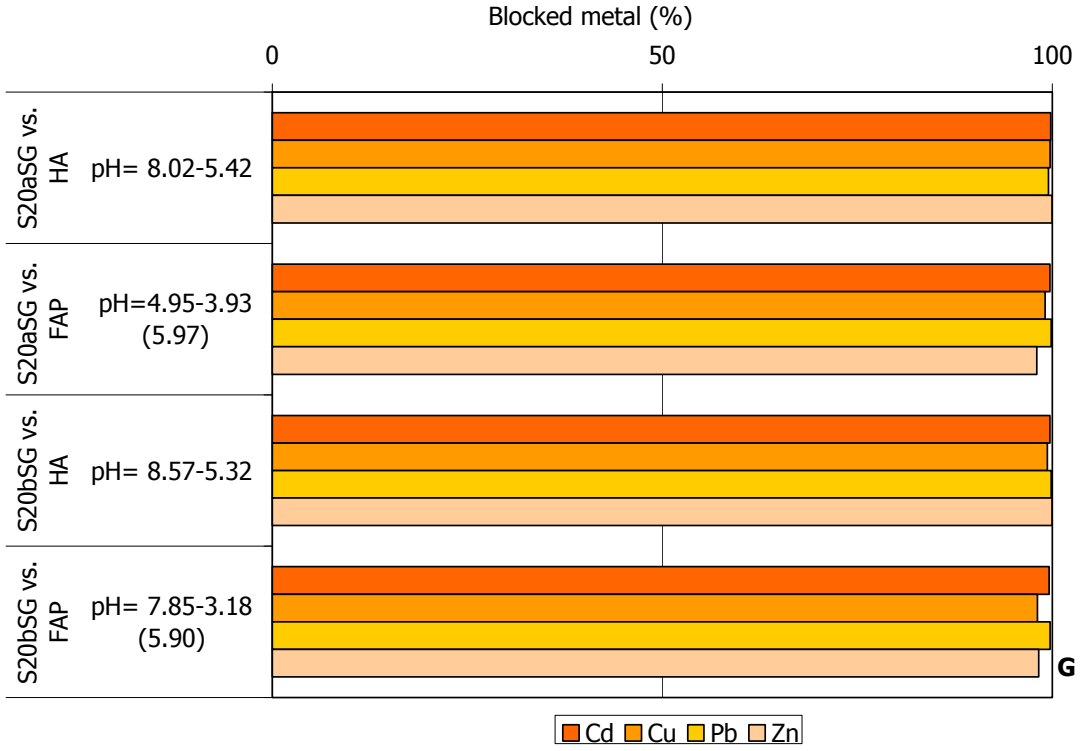

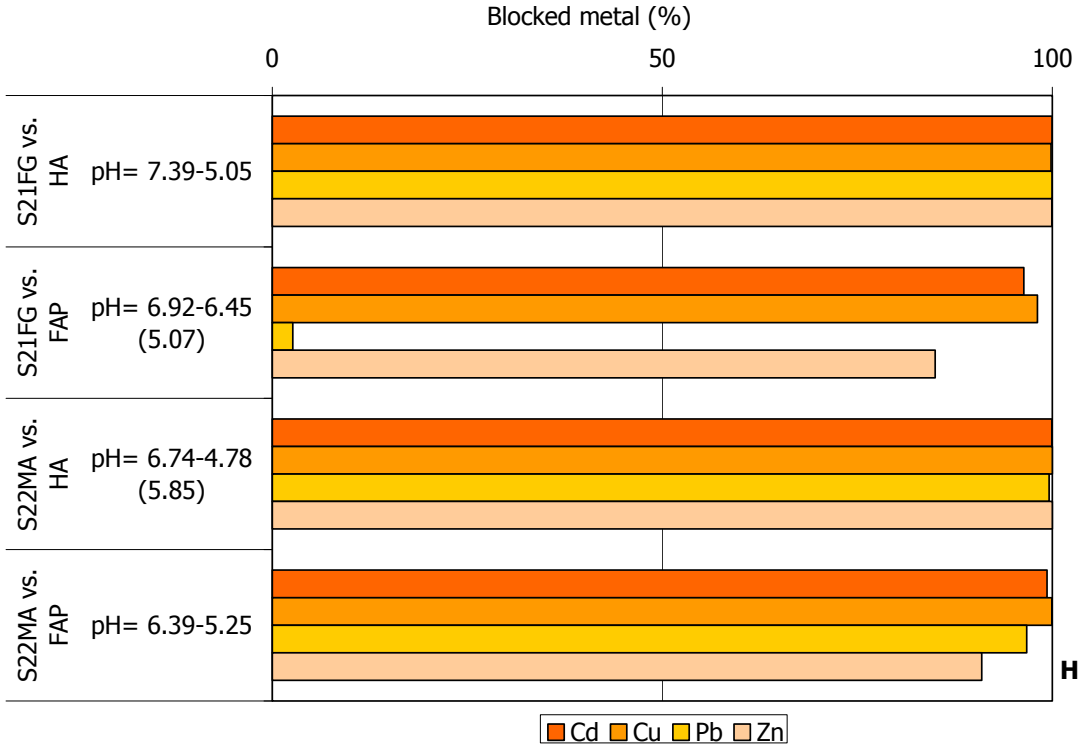

Fig. 2: Heavy metal immobilization efficiency. pH values are the initial and the final one, in bracket it has been adjusted. Tuscany: A = Gavorrano; B = Campiano; C = Niccioleta and D = Boccheggiano; Sardinia: E = Campo Pisano; F = Monteponi; G = San Giovanni and H = Monte Agruxau. - Fig. 2: Efficienza dell'immobilizzazione dei metalli pesani. I valori di pH sono quello iniziale e finale, tra parentesi il valore finae

se è stato tamponato. Toscana: A = Gavorrano; B = Campiano; C = Niccioleta and D = Boccheggiano; Sardegna: E = Campo Pisano; F = Monteponi; G = San Giovanni e H = Monte Agruxau.

CONCLUSIONS

The goal of this work was to study the effectiveness of synthetic and natural phosphate in removing different heavy metal ions from aqueous solutions and contaminated soils. P amendment is efficient in transforming the bio-available heavy metals in a less-bio-available form. Effective remediation technology entails minimizing both leaching and bio-availability. In fact the extractable concentration of the heavy metals at the equilibrium are usually lower than the regulatory limits.

The results of the laboratory treatment allow to determine if this remediation is efficient and in which way. In particular, the percentage of the immobilization is always higher using as amendant the synthetic hydroxyapatite, whereas the natural phosphate rock might seem less efficient, instead this lower efficiency is due to the non-stoichiometric P amount. The values of the immobilization are from the 90-99 %, either for the single- and the multi-metal system, whereas for the two natural rocks the percentage ranges from the 25 to 50 %. Therefore, HA reduce the heavy metal concentration below the limit stated from the law. FAP and MAP are less effective than HA, so that increasing the P amount it is possible to increase the immobilization value, as already observed from the literature. Even though P concentration is low, the two phosphate rocks resulted good as amendant except few cases, in particular for Zn immobilization. In fact each metal behaves in a different way, for examples Pb is always immobilized better than the others metals.

The reason for the different sorption values is the internal competition, which is among the same ions and the different ions of the heavy metals and the H^+ for the sorption sites in every single cases, in fact the initial concentration of the heavy metal is less fundamental for the sorption than the competition; for example Zn is better immobilized in a single metal system at high concentration rather than at low concentration.

However, HA, FAP and MAP have aptitude for heavy metal retention. Considering the retention capacity per gram of material, HA is more efficient than FAP and MAP

because its specific surface area is bigger than the SSA of the other two phosphatic rocks. Therefore, increasing the concentration of natural rock and the contact time the effectiveness in the immobilization increases. In particular, the type and rate of P amendment, and the appropriate application management to be utilized require careful scrutiny. On the other hand, the use of a natural phosphate is a cost effective remediation process.

Other aim was to determine the sorption mechanism in the single- and multi-metal system and therefore to propose the most suitable one. According the experimental condition and the type of phosphate we could suggest the adsorption and surface complexation as sorption mechanism, either in the aqueous solution and soil. Two types of data can give this information, the shape of the sorption isotherm and the molar ratio values. The sorption isotherm are the ratio among the amount of the heavy metal sorbed and the amount in solution of the heavy metal. The shape of the sorption isotherm suggests the sorption mechanism, our data mainly show the L2 curve characterised by a steep vertical line, a knee and then a plateau which means the metal is at the equilibrium. In particular this type of isotherm is characteristics either for the single- and the multi-metal systems.

The initial slope depends on the rate of change of site availability with increase in solute adsorbe. As more solute is taken up, there is usually progressively less chance that a bombarding solute molecule will find a suitable site on which it can be adsorbed. Implying either that the adsorbed solute molecule is not vertically oriented or that there is not strong competition from the solvent.

This isotherm refers to the two previous mechanisms, even though in some case the curve is the H type (vertical line) and the C type (horizontal line). The first one (L2 type) occurs in the majority of cases of adsorption from a dilute solution, the H isotherm is a particular case, a solute with higher affinity for the substrate than the solvent and C type suggests a constant partition of solute between solution and substrate. In particular the H type suggests a dissolution/precipitation process.

Moreover, the molar ratio (Q_S), that is the ratio of the cations bound to the cations released from the amendant, confirms the results from the sorption isotherm. Generally, Q_S values are > 1 confirming the two sorption processes before mentioned. In few cases Q_S < 1 which indicates the precipitation phenomenon. Furthermore, increasing the initial

concentration of the heavy metals vs. the two phosphatic rock in the multi-metal system, Q_S become >>1 suggesting that the Ca amount in solution is low compared to the heavy metal amount at the equilibrium, so that the suitable sorption process is the surface complexation. In particular, $Q_S < 1$ is characteristic for the low initial concentration of the heavy metals and for the systems vs. HA rather than the systems vs. FAP and MAP.

Another datum which can help in understanding the sorption mechanism is the amount of Ca and P at the equilibrium. Generally, the amount of Ca at the equilibrium is not proportional to the amount of the heavy metal sorbed, suggesting there is not a stoichiometric dissolution of the phosphate and the precipitation of the new phase. P concentration at the equilibrium is very low suggesting that P can be used for the precipitation of a new phase or there is the non-stoichiometric dissolution as for the Ca concentration in solution. Ca and P dissolution also depends on the solubility of the amendant and these three phosphates, used in this study, are less soluble than other phosphates used in literature.

The contact time is another factor which can control the amount of the heavy metal sorbed. The contact time was from 2h to 48h, considering the adsorption equilibrium is obtained in less than one hour for lead. This study shows that 24h is the suitable time for the heavy metals in the single- and in the multi-metal system. Increasing the P concentration and the contact time it is possible to achieve higher immobilization values than the obtained values, in particular, this is true when natural phosphatic rocks are used.

In order to simulate the true environmental conditions in case of the remediation of polluted water and soil, where the pH control is either not applicable, or not necessary or hard to be realized, in the present study no effort was made to modify the solution pH during the experiments and no ionic strength was imposed. The initial pH of the metal solutions and final pH of the filtrate at adsorption equilibrium were measured for each metal concentration.

Our pH values usually range from 6-7 in all the multi-metal systems, showing a variation less than ± 1 unit (about 0.5-0.7 unit) from the initial value to the final one. These high pH values suggest a low solubility of the phosphates. Nevertheless, HA, FAP and MAP show high values of immobilization. Because of the low solubility, it could be

possible the dissolution/precipitation is a rare sorption mechanism than the surface complexation and the ion exchange process.

To confirm the results from the sorption isotherms and the molar ratio, the solid materials have been studied by XRD and SEM-EDS analyses. From the XRD pattern it was observed that they well overlapped the XRD pattern of the original material, indicating that there isn't the formation of a new phase. Successively the values of lattice parameters of some solid materials and the starting HA were compared, the results suggest that heavy metals are present, inferring the precipitation of a heavy metal-phosphate. In particular, the peaks at 2.96 and 3.19 Å were detected which may represent mixed Ca-heavy metal phosphates These results allow to infer that, probably, a phosphatic phase from poorly crystalline to non-crystalline precipitates, so that from XRD analyses is not possible to determine the precipitation of this phase, probably because the amount of this new phase is less than 1% (XRD detection limit) or is poorly crystalline.

The SEM analyses confirm the XRD results, the shape of the particles are identical to the original materials (HA, FAP and MAP). It may suggests that the original structure of the phosphate host exerts a control on the nucleation process and also the micro-topography, in effect the particles are on the surface features, probably defects can help the dissolution/precipitation mechanism providing sites with a decreased adsorption energy.

The white spots, spread on the phosphates, corresponds to the heavy metals adsorbed on the surface and confirmed from the EDS spectra are indicative of the presence of the heavy metals. the length and width of the particles are almost similar for the four different times, suggesting the absence of the ageing effect, there isn't the decreasing in the dimensions of the shape meaning the transformation to a more stable morphology, in our case the size is almost constant. Any kind of orientation is absent after the interaction, probably the growing direction is toward the source of the heavy metals as phosphate anions were consumed from the phosphate dissolution. It is also absent the characteristic hexagonal shape of the HP, which might make think that the dissolution and precipitation phenomenon didn't happen or only poorly - to - amorphous phase is precipitated. The precipitation of the non-crystalline phase or the absorption, which occurred near the phosphate surface, it is due to the constant solubility of the heavy-metal, minerals was probably exceeded due to locally high P concentration.

AFM analyses confirm the results from XRD and SEM, the particles show always the shape similar to the original one of the phosphate. In particular, the FAP images show a different shape compared to the SEM micrographs, probably because SEM was unable to achieve high enough resolution to detect the FAP rounded surface imaged with AFM.

AFM images didn't reveal crystallographic features suggesting as a probable mechanism the surface complexation and adsorption rather than the dissolution/precipitation, suggesting the type of phosphate, exerts a control on the sorption process and the sorption capacity can vary according to different experimental conditions

In particular, the ion exchange mechanism is the more probable confirmed by the results of XRD and FTIR spectra, in fact the solid materials retain the same structure as the amendant used for the immobilization. The same IR spectra argued against the dominance of coprecipitation at the end of the sorption reaction; in this view, on the basis of our data it might be possible to infer the adsorption and/or the superficial complexation as probable sorption mechanisms.

In conclusion, the removal of Cd appears depending on the initial concentration, if it is low, the Q_s values suggest that Cd removal depended mainly on phosphate dissolution and precipitation of a new phosphate phase and we might propose the formation of an amorphous Cd-phosphate, whereas for high initial metal concentration Q_s values indicate that Cd immobilization is mainly due to non-stoichiometric sorption on the phosphate surface and it is probable a two-step mechanism, dissolution of phosphate and the formation of a new stable Cd-apatite on the phosphate surface and later the diffusion of Cd ions inside the phosphate crystal lattice through the ion exchange occurs.

The sorption mechanism for Cu and Pb involved surface complexation and coprecipitation with Ca into the phosphate structure instead of formation of new metal phosphates.

The substitution of Ca by other cations in phosphate crystal structure is well known in natural apatites and generally, cations with ionic radii smaller than Ca^{2+} (0.99 Å) can substitute it, according Cu ionic ray this is not possible. On the contrary, from the Q_s values > 1 it is possible to infer as sorption mechanism the surface complexation. The XRD analyses did not detect any new mineral formation in the solid residues arguing

against the hypothesis of ion exchange mechanism Therefore, when Cu is mixed with phosphate, surface complexation on the phosphate surface is the main mechanism.

Concerning Pb sorption, the isotherm are either the L2 type and the H type which suggests the dissolution/precipitation mechanism. From our XRD and SEM data it wasn't possible to determine the precipitation of a crystalline product, so that when this process occurred there is the precipitation of a poor-crystalline product. Increasing the metal concentration, Q_S values suggest other mechanisms, surface complexation and the adsorption.

When Zn was mixed with phosphate, surface complexation occurred on its surface, displacing partially the H^+ ions, so that the mainly mechanism for Zn removing from solutions is surface complexation with phosphate functional groups; whereas coprecipitation with Ca could be unlikely because of the dimension of ionic ray, too big for the substitution as Cu before.

Furthermore mechanisms are characteristics for each heavy metals, that is it is more probable that the sorption mechanisms work together so that it can be difficult to quantitatively estimate the proportions of the immobilization for a specific mechanism. From our data it is possible to infer the formation of Heavy-Metal-Ca-phosphate, rather than the pyromorphite precipitation. The solid materials, obtained after the interaction, should provide long-term reductions in metal solubility and transport, even though they are poorly crystalline.

Although there is not the precipitation of pyromorphite, less soluble than the apatite, the heavy-metal phosphate phase is stable. In fact desorption tests were carried out to determine the stability of the solid materials obtained from the interaction. The solid materials are from the interaction among the aqueous solution at the highest concentration and at 24h which is considered the suitable time for a good immobilization for every experimental condition. Data from desorption tests confirm that the solid materials are also stable in an acidic environment, even though the sorption process is surface complexation or adsortion and nor the precipitation which would have to be the precipitation of a less soluble phase (e.g. HP). In particular, the amount of the metals released are usually below the detection limits or less than 1%.

Further investigations are necessary to optimize P application rates and the ratio between phosphate rock and soluble P sources, in order to develop an environmentally sound in situ heavy metal remediation technology.

Similar results were obtained from the interaction among the contaminated soil from the mines and HA and FAP. The interaction was slightly different from that one of the aqueous solutions, the time was only 20 minutes and pH was adjusted to 5, after ten minutes and at the end of the interaction. The results confirm the effectiveness of the two type of phosphate in immobilizing the bio-available amount of the heavy metals, reducing the limit below the limit from the law. From the XRD pattern it is observed the absence of any new phases, spectra are overlapped in both cases (HA and FAP) suggesting the adsorption mechanism or the precipitation of a poorly crystalline phase.

Finally, this remediation technology is effective in immobilizing the heavy metals in different systems (water and soils). In particular, it is fundamental the type of the amendant and successively the amount of the amendant. Secondly it is important the contact time and the initial concentration of the heavy metals.